



Nrf2 in metabolic related inflammation in the brain

By

Mary Katherine Liddell

Thesis submitted for the degree of Doctor of Philosophy

University of Dundee

September 2015

TABLE OF CONTENTS

<i>TABLE OF FIGURES</i>	V-VIII
<i>LIST OF TABLES</i>	IX
<i>ABBREVIATIONS AND ACCRONYMS</i>	X-XIII
<i>ACKNOWLEDGEMENTS</i>	XIV-XV
<i>DECLARATION</i>	XVI
<i>SUMMARY</i>	XVII
1 Introduction	1
1.1 Dementia and Alzheimer Disease	2
1.1.1 Tau Protein and Pathology	5
1.1.2 The Amyloid Precursor Protein Processing Pathway and A β	6
1.1.3 Genetic Factors in AD.....	14
1.2 Oxidative Stress and Neurodegeneration	17
1.2.1 Mitochondrial Dysfunction	17
1.2.2 Brain Hypometabolism	18
1.2.3 Targeting the antioxidant system as treatment of OS	20
1.3 Nrf2 Antioxidant Response Element	22
1.3.1 Nrf2-ARE Discovery and Structure	22
1.3.2 Nrf2 Mechanisms of Repression and Activation	23
1.3.3 Nrf2-ARE and the CNS	27
1.4 Glial Cells and Neuroprotection.....	28
1.4.1 Astrocytes.....	28
1.4.2 Microglia.....	30
1.5 AD and the Immune System Response.....	32
1.5.1 Innate vs Adaptive Immune Response.....	32
1.5.2 Neutrophils, natural killer cells, B Cells and T Cells; the contribution of the blood born immune cells	33
1.5.3 The Role of Chemokines and Other Signalling Molecules in the Immune Pathway.....	34
1.5.4 The Complement Immune System.....	38
1.5.5 The Immune System and Its Response to Infection.....	39
1.5.6 The Immune System and Disease	40
1.6 Lifestyle Related Risk Factors for AD.....	41
1.6.1 Hypertension and Vascular Dysfunction	42
1.6.2 Obesity and Inflammation.....	43
1.6.3 Diabetes Mellitus and Insulin Resistance	45

1.7	Nrf2 in Disease pathology.....	46
1.7.1	Cancer	46
1.7.2	Metabolic Syndrome and NASH	47
1.7.3	Role of Nrf2 in Cardiovascular Disease and Ischaemia.....	49
1.7.4	Role of Nrf2 in Neurodegeneration and Alzheimer’s Disease.....	50
1.8	Project Aims.....	51
2	Materials and Methods.....	53
2.1	Materials.....	54
2.1.1	Chemicals.....	54
2.1.2	Machines	54
2.2	Animals	54
2.2.1	Animal maintenance and housing conditions	54
2.2.2	Generation of <i>Nrf2</i> KO mice.....	55
2.2.3	Generation of <i>hAPP_{swe}</i> mice	55
2.2.4	Generation of a novel AD mouse line.....	56
2.2.5	Genotyping of mouse lines.....	56
2.3	<i>In Vivo</i> Studies	60
2.3.1	High Fat Metabolic Study	60
2.3.2	Peripheral Infection Study.....	63
2.4	Biochemistry	68
2.4.1	Tissue Collection.....	68
2.4.2	Tissue lysis	69
2.4.3	Gene Expression using Real-Time qPCR	69
2.4.4	Protein Expression by Western Blotting.....	72
2.4.5	Quantification of Protein Carbonylation.....	75
2.4.6	Amyloid protein expression	76
2.4.7	Immunohistochemistry.....	77
2.5	Statistical analysis	80
3	The Role of Nrf2 in High Fat Feeding Induced Inflammation	81
3.1	Introduction	82
3.2	Nrf2 and APP Are Expressed Throughout the Murine Brain	87
3.3	Overexpression of <i>hApp_{swe}</i> and Loss of Functional <i>Nrf2</i> Have Opposing Effects on Adiposity Following Prolonged High Fat Feeding	91
3.4	<i>Nrf2</i> ^{-/-} Mice Maintain Insulin Sensitivity Even After Long-Term High Fat Feeding.....	93
3.5	Peripheral Effects of Long-Term High Fat Feeding	96
3.6	Effect of <i>Nrf2</i> ^{-/-} and a High Fat Diet on Ageing Cognition	99
3.7	The Effect of High Fat Feeding and <i>Nrf2</i> ^{-/-} on Inflammation and Protein Carbonylation Markers in the Mouse Brain	103

III

3.8	Diet and Genotype Affect Glial Cell Activation in Aged Mouse Brains	110
3.9	The Effect of High Fat Feeding on Expression of Proteins Commonly Associated With AD.	120
3.10	The Effect of <i>Nrf2</i> loss on Akt Signalling and Downstream NF-Kb Signalling	126
3.11	No Change in in a Marker of The Glutathione Detoxifying Pathway Following Long-Term High Fat Feeding.....	128
3.12	A Role For Stress-Activated MAPK Enzymes In High Fat Induced Rescue Of The <i>Nrf2</i> ^{-/-} Phenotype In Brain Tissue	130
3.13	<i>Nrf2</i> Depletion Drives Alterations in Mouse Brain Mitochondria....	141
3.14	Discussion	143
3.14.1	Long-Term HF Feeding Has Contrasting Effects on Glucose Management and Body Weight in <i>Nrf2</i> ^{-/-} and <i>hApp_{swe}</i> Mice	143
3.14.2	Mice Lacking <i>Nrf2</i> Have Increased Locomotor Activity in Early Adulthood Following High Fat Feeding	148
3.14.3	High Fat Feeding and Inflammation Following Loss of <i>Nrf2</i> and a Role for Contrasting Organ Specific Effects	150
3.14.4	High Fat Feeding Increased AD Related Proteins in the Brains of Aged Mice	156
3.14.5	HF Feeding and Other Stress Activated Proteins.....	157
3.14.6	Mitochondrial Impairment Following Loss of <i>Nrf2</i>	160
3.14.7	Conclusions	162
4	The Role of Nrf2 in Infection-Induced Inflammation.....	165
4.1	Introduction.....	166
4.2	Repeated IP LPS Induces Weight Loss In Aged Adult Mice	171
4.3	Knocking Out Nrf2 Impairs Short Term Spatial Location Memory In Mice As Shown By Object Location	172
4.4	Low Dose IP LPS Significantly Impairs The Ability Of Mice To Perform Short Term Novel Object Recognition	177
4.5	Low Dose IP LPS Does Not Affect The Ability Of Mice To Spontaneously Alternate	180
4.6	Low Dose Repeated IP LPS Induces A Peripheral Inflammatory State	180
4.7	Peripheral IP LPS Drives a Mild Increase in Inflammatory State in The Brains of Adult Mice	184
4.8	<i>Nrf2</i> Plays an Important Role in the Modulation of Glial Cell Responses to Perceived Cellular Insults	193
4.9	Short-Term Repeated IP LPS Affects Synaptic Health in the Cortex of the Murine Brain.....	196
4.10	Repeated Peripheral LPS Administration Selectively Affects Key AD Related Proteins.....	198

4.11	Repeated IP Injections of LPS Does Not Impact on the PI-3K-Dependent Pathway in the Mouse Brain.....	203
4.12	Repeated IP LPS Fails to Impact the Glutathione Pathway in The Brains of Adult Mice.....	205
4.13	Repeated IP LPS Induces Brain Region Specific Induction of Key MAPK Members.....	207
4.14	LPS and <i>Nrf2</i> ^{-/-} Significantly Impact on Brain Derived Mitochondrial Health in Adult Mice.....	211
4.15	Discussion.....	214
4.15.1	The Effects of <i>Nrf2</i> ^{-/-} and LPS-Induced Inflammation on Behaviour May Highlight a Hippocampal-Dependent Memory Impairment.....	214
4.15.2	Inflammation and Cytokine Expression May Suggest a Role for Immune Cell Priming and Inflammasome Activation.....	217
4.15.3	Seven Day LPS Exposure Induced Little Change in AD-Related Proteins	220
4.15.4	Loss of Nrf2 Causes Dysregulation of Members of the MAPK Family	221
4.15.5	Loss of Nrf2 Impacts on Mitochondrial Function Following LPS-Induced Inflammation.....	222
4.15.6	Conclusions.....	224
5	Final Conclusions and Further Work.....	226
5.1	Mouse models in AD: breakthroughs, shortfalls and the amyloid cascade	227
5.2	Loss of Nrf2 and the altered response to DIO and pathogen associated inflammation.....	228
5.3	Loss of Nrf2 and the impact this may have on age related cognitive decline	230
5.4	A Role for Nrf2 in the Regulation of MAPK Signalling and Its Impact in AD	232
5.5	Mitochondria, ER stress and their importance in further AD research	234
5.6	Study Limitations.....	235
5.7	Physiological relevance.....	236
6	References.....	238
7	Appendices.....	278
7.1	Appendix I - Solutions.....	279
7.2	APPENDIX II – Behavioural Task Objects.....	281
7.3	APPENDIX III – Taqman Probes.....	282
7.4	APPENDIX IV – Western Blotting Antibodies.....	283
7.5	APPENDIX V – Preliminary Data.....	285

TABLE OF FIGURES

Figure 1.1 Anatomical progression of AD related pathology in the human brain.....	2
Figure 1.2 Histopathology image depicting the hallmark protein deposits of A β and neurofibrillary tangles used as the gold standard of disease diagnosis for AD (Van Leuven, 2013)	3
Figure 1.3 Domain structure and homology of the APP protein family	7
Figure 1.4 Schematic representation of the pro-amyloidogenic and non-amyloidogenic pathways of APP processing.....	9
Figure 1.5 Sequence localisation of a selection of well-known APP mutations.....	15
Figure 1.6 Simplified pictorial representation of the TCA cycle and electron transport chain and relevant proton exchanges.	19
Figure 1.7 Overview of the antioxidant mechanisms of key endogenous small antioxidant molecules.....	21
Figure 1.8 Domain structures of human Nrf2 and Keap1	23
Figure 1.9 Nrf2 regulation by Keap1 under stressed and basal conditions.....	25
Figure 1.10 Summary of preferred cysteine binding sites for a selection of commonly referred to Nrf2 activators	26
Figure 1.11 Simplified overview of complement system activation and its key physiological outputs	38
Figure 2.1 Example image of PCR products produced by genotyping of <i>Nrf2</i> ^{-/-} mice...58	58
Figure 2.2 Example image of PCR products produced by genotyping of <i>hAPP</i> _{swe} mice59	59
Figure 2.3 Pictorial representation of the elevated plus maze behavioural apparatus	62
Figure 2.4 Time-line for the peripheral infection study, depicting the order in which behavioural tasks and relevant habituation were performed.....	63
Figure 2.5 Pictorial representation of the object-based behavioural apparatus and related tasks.....	66
Figure 3.1 <i>Nrf2</i> is expressed throughout the mouse brain.	88
Figure 3.2 APP expression is found throughout the mouse brain.....	90
Figure 3.3 Long-term HF feeding causes a time and genotype dependent divergent change in weight gain in <i>Nrf2</i> ^{-/-} and <i>hAPP</i> _{swe} transgenic mice.	92
Figure 3.4 Knocking out <i>Nrf2</i> and overexpressing <i>hAPP</i> _{swe} have opposing effects on glucose tolerance in aged high fat fed mice.	95

Figure 3.5 HF feeding further impacts on changes in key physiological organs driven by the loss of <i>Nrf2</i> ^{-/-} .	98
Figure 3.6 A time-dependent impairment in spontaneous alternation is seen in all groups whilst <i>Nrf2</i> ^{-/-} / <i>hAPP</i> _{swe} decline more rapidly than WT and <i>Nrf2</i> ^{-/-} mice.	101
Figure 3.7 HF feeding significantly increases activity in young and middle-aged mice lacking <i>Nrf2</i> without impairing their ability to SA.	102
Figure 3.8 Loss of <i>Nrf2</i> drives a hippocampal dominant increase in pro-inflammatory markers in the brain that is rescued by HF feeding.	105
Figure 3.9 Pictorial representations of oxyblot assays performed in the hippocampus and cortex of adult RC or HF fed animals.	106
Figure 3.10 HF feeding prompts an amelioration in cortical protein carbonylation state in aged mice lacking <i>Nrf2</i> .	108
Figure 3.11 Loss of <i>Nrf2</i> drives predominantly cortical increases in anti-inflammatory and complement system markers.	109
Figure 3.12 Loss of <i>Nrf2</i> drives increases in macrophage expression that is partially mimicked by astrocyte activation.	112
Figure 3.13 <i>Nrf2</i> ^{-/-} mice show a trend for increased chemokine gene expression in the brains of aged adults.	114
Figure 3.14 Pictorial representation of hippocampal sub-regions of the mouse brain.	115
Figure 3.15 Removal of <i>Nrf2</i> in the brains of mice increases astrocyte branching, which is further amplified by addition of <i>hAPP</i> _{swe} in the hippocampus.	116
Figure 3.16 <i>Nrf2</i> ^{-/-} mice show increased microglial staining following HF feeding with little change in the added presence of <i>hAPP</i> _{swe} in the hippocampus.	117
Figure 3.17 An greater impact on synaptic SYP expression is seen in the hippocampus than the cortex following loss of <i>Nrf2</i> and HF feeding.	119
Figure 3.18 HF feeding increases AD related APP and BACE1 in a brain region specific manner in WT and <i>Nrf2</i> ^{-/-} mice.	121
Figure 3.19 HF feeding has no effect on the production of soluble murine A β ₁₋₄₂ in cortical tissue of aged WT and <i>Nrf2</i> ^{-/-} mice.	124
Figure 3.20 HF feeding of <i>hAPP</i> _{swe} mice increases protein expression of total tau with diet and <i>Nrf2</i> ^{-/-} also impacting on tau phosphorylation.	125
Figure 3.21 PI-3k driven changes in Akt are not responsible for the protective effects of HF feeding in <i>Nrf2</i> ^{-/-} mice, and only small changes in the related NF-kB stress response pathway are induced.	127

Figure 3.22 No change is seen in the rate limiting glutathione pathway GCLC enzyme in brain tissue as a result of HF feeding.....	129
Figure 3.23 HF feeding of <i>Nrf2</i> ^{-/-} mice activates the JNK pathway increasing phosphorylation of JNK in brain homogenates.....	131
Figure 3.24 Aged transgenic mouse models lacking <i>Nrf2</i> have increased ERK 1 and 2 MAPK phosphorylation, which is further enhanced by HF feeding.....	134
Figure 3.25 Loss of <i>Nrf2</i> and HF feeding impact significantly on the gene expression of important MAPK DUSP proteins.	137
Figure 3.26 Loss of <i>Nrf2</i> and HF feeding impact significantly on both MEK1/2 and important ERK-related DUSP proteins in the hippocampus of aged mice.....	139
Figure 3.27 Loss of <i>Nrf2</i> and HF feeding both impact on mitochondrial health and mitophagy markers.....	142
Figure 3.28 Simplified pictorial summary of some of the main long-term HF diet-driven alterations described in the brains of WT (A) and <i>Nrf2</i> ^{-/-} (B) mice	164
Figure 4.1 Repeated IP LPS induces acute weight loss in aged adult mice irrespective of genotype.....	173
Figure 4.2 Neither genotype nor treatment affect exploration or object preference during the sample phase of the OL task.	175
Figure 4.3 Both repeated LPS administration and loss of <i>Nrf2</i> inhibit the ability of mice to perform a short term OL task.....	176
Figure 4.4 Neither genotype nor treatment affect exploration or object location preference during the sample phase of the NOR task.....	178
Figure 4.5 Repeated IP LPS in adult mice impedes their ability to perform a short term NOR task.....	179
Figure 4.6 Neither repeated LPS administration nor loss of <i>Nrf2</i> prevent mice spontaneously alternating in a closed arm elevated plus maze.....	181
Figure 4.7 Repeated administrations of IP LPS induce changes in both liver and spleen tissues irrespective of genotype.	183
Figure 4.8 Peripheral LPS administration induces a predominantly <i>IL1β</i> driven pro-inflammatory environment in the brains of adult mice.....	185
Figure 4.9 Pictorial representations of oxyblot assays performed in the hippocampus and cortex of adult saline or LPS treated animals.....	187
Figure 4.10 Loss of <i>Nrf2</i> drives increases in protein carbonylation in both the hippocampus and cortex of adult mice.	188

VIII

Figure 4.11 Repeated peripheral LPS treatment prompts a predominantly cortical induction of anti-inflammatory markers with mild escalation following loss of Nrf2.	190
Figure 4.12 Loss of <i>Nrf2</i> and LPS both impact on the activation of the complement immune pathway.	192
Figure 4.13 Loss of <i>Nrf2</i> and LPS both modulate markers of glial cell activation and recruitment.	194
Figure 4.14 Repeated peripheral LPS administration induces a small loss of cortical synapses in <i>Nrf2</i> ^{-/-} mice.	197
Figure 4.15 Administration of repeated IP LPS reduces BACE1 protein expression in the cortex of adult mice with no effect on APP expression.	199
Figure 4.16 Modest changes in phosphorylated and total tau can be seen following LPS treatment of <i>Nrf2</i> ^{-/-} mice.	202
Figure 4.17 Repeated IP LPS has little effect on PI3-K driven Akt phosphorylation or IκBα degradation in the hippocampus and cortex of adult <i>Nrf2</i> ^{-/-} and mice.	204
Figure 4.18 Repeated IP LPS does not significantly affect expression of the rate limiting glutathione pathway GCLC enzyme in brain tissue.	206
Figure 4.19 <i>Nrf2</i> ^{-/-} and WT mice show a mild induction of SAPK/JNK in the cortex following repeated IP LPS injections.	208
Figure 4.20 Transgenic mouse models lacking <i>Nrf2</i> show a trend towards increased ERK 1 and 2 MAPK phosphorylation with brain region dependent responses to peripheral LPS treatment.	210
Figure 4.21 Loss of <i>Nrf2</i> and repeated LPS injections both impact on mitochondrial health and mitophagy markers.	212
Figure 5.1 Simplified pictorial summary of some of the principle biochemical alterations observed in completion of this project.	233
Figure 7.1 Pictorial representation and pairing of objects used in behavioural tasks.	281
Figure 7.2 Portrayal of changes in astrocyte number resulting from genotype or dietary intervention as depicted by GFAP staining in the hippocampus	285

LIST OF TABLES

Table 1.1 Summary of commonly quoted chemokines, their receptors and their main physiological functions in relation to AD.	37
Table 2.1 List of PCR primers and their sequences used for <i>Nrf2</i> ^{-/-} mouse line.....	57
Table 2.2 Heat cycling PCR programme for genotyping of <i>Nrf2</i> ^{-/-} earnotches	57
Table 2.3 List of PCR primers and their sequences used for <i>hAPP</i> _{swe} mouse line	58
Table 2.4 Heat cycling PCR programme for genotyping of <i>hAPP</i> _{swe} earnotches.....	59
Table 2.5 Details of tissue lysis volumes used for protein analysis.....	69
Table 2.6 Heat cycling PCR programme for TaqMan RT-qPCR analysis	71
Table 2.7 List of IR dye linked secondary antibodies for use with the Odyssey scanner	74
Table 2.8 List of secondary antibodies for final processing by HRP-ECL reaction.....	75
Table 2.9 List of antibodies used for immunohistochemistry of brain sections	79
Table 2.10 Specifications of confocal lasers used	80
Table 7.1 Table of content of common solutions used for protein elucidation.....	279
Table 7.2 Constituents of self-poured Acrylamide gels.....	280
Table 7.3 Table of content of common solutions used for immunohistochemistry.....	280
Table.7.4 Table of content of other frequently used solutions.....	280
Table 7.5 List of RT-PCR TaqMan probes – Prof. M.L.J. Ashford lab	282
Table 7.6 List of RT-PCR TaqMan probes – Prof. S.M. Keyse lab	282
Table.7.7 List of primary antibodies used for protein elucidation by Western blotting – Prof. M.L.J. Ashford Lab (*denotes gifts)	284
Table 7.8 List of primary antibodies used for protein elucidation by Western blotting – Keyse Lab.....	284

ABBREVIATIONS AND ACRONYMS

%SA	Percentage spontaneous alternation
A.U.	Arbitrary units
AD	Alzheimer's disease
ADAM	A disintegrin and metalloproteinase
AICD	Amyloid precursor protein intracellular domain
ALID	Amyloid precursor protein-like intracellular domain
ALS	Amyotrophic lateral sclerosis
ANOVA	Analysis of variance
APLP1	Amyloid precursor protein-like protein 1
APLP2	Amyloid precursor protein-like protein 2
ApoE	Apolipoprotein E
APP	Amyloid precursor protein
ARE	Antioxidant response element
Arg1	Arginase-1
ARUK	Alzheimer's Research U.K.
ATP	Adenosine triphosphate
A β	Amyloid- β protein
BACE	β -site amyloid precursor protein cleaving enzyme
BBB	Blood brain barrier
BMDM	Bone marrow derived macrophages
BMI	Body mass index
bp	Base pair
BSA	Bovine serum albumin
bZip	basic-region leucine zipper
CCR	C-C chemokine receptor
cDNA	Complementary deoxyribonucleic acid
CMR	Cerebral metabolic rate
CMR _g	Cerebral metabolic rate of glucose
CMR _{O₂}	Cerebral metabolic rate of oxygen
CNS	Central nervous system
COX IV	Complex IV of the electron transport chain
CR	Caloric restriction
CRL ^{Keap1}	Keap1-Cullin 3-RING –box 1 E3 ubiquitin ligase complex
CST	Cognitive stimulation therapy
CTF	Carboxy terminal fragment
Cul	Cullin
CVD	Cardiovascular disease
D3	Discrimination index
DAMP	Danger associated molecular pattern molecules
DC	Dendritic cells
DIO	Diet-induced obesity
DNA	Deoxyribonucleic acid
dNTP	Deoxy-nucleotide triphosphates
DS	Down's syndrome
DUSP/MKP kinase phosphatase	Dual specificity protein phosphatase/Mitogen-activated protein kinase phosphatase
EDTA	Ethylene diamine tetraacetic acid
EGTA	Ethylene glycol tetraacetic acid
ER	Endoplasmic reticulum

ERC	Entorhinal cortex
ERK	Extracellular-signal-regulated kinases
ETC	Electron transport chain
F4/80	aka Emr1 in humans (EGF-like module-containing mucin-like hormone receptor-like 1)
FACS	Fluorescence-activated cell sorting
FAD	Familial Alzheimer's disease
FTD	Frontotemporal dementia
GCLC	Glutamate cysteine ligase catalytic subunit
GFAP	Glial fibrillary acidic protein
GlcNAc	β -N-acetyl-glucosamine
GLUT	Glucose transporter
GPX	Glutathione peroxidase
GSH	Glutathione
GSK3	Glycogen synthase kinase 3
H ₂ O ₂	Hydrogen peroxide
<i>hAPP</i> _{swe} mutation	Human amyloid precursor protein containing the Swedish mutation
HF	High fat
HIF-1	Hypoxia inducible factor-1
HMOX	Haem oxygenase
HRP	Horseradish Peroxidase
Iba1	Allograft inflammatory factor-1 aka AIF1
ICV	Intracerebroventricular
IDE	Insulin degrading enzyme
IF	Immunofluorescence
IGF-1	Insulin-like growth factor-1
IGTT	Intraperitoneal glucose tolerance test
IL	Interleukin
iNOS	Inducible nitric oxide synthase
IP	Intraperitoneal
IR	Infrared
ITT	Insulin tolerance test
I κ B α inhibitor α	Nuclear factor of κ light polypeptide gene enhancer in B-cells
JNK	c-Jun N-terminal kinase
KD	Knock down
Keap1	Kelch-like ECH-associated protein 1
KGDH	α -ketoglutarate dehydrogenase
KO	Knockout
KPI	Kunitz proteinase inhibitor
lacZ	β -galactosidase
LPS	Lipopolysaccharide
M1	Pro-inflammatory macrophage phenotype
M2	Anti-inflammatory macrophage phenotype
Maf	Musculoaponeurotic fibrosarcoma protein
MAP	Microtubule associated proteins
MAPK	Mitogen-activated protein kinase
MASP	Mannose-binding lectin-associated serine protease
MBL	Mannose-binding lectin
MCI	Mild cognitive impairment
MCP-1	Monocyte chemotactic protein- 1 aka CCL2

XII

MEK	Mitogen-activated protein kinase kinase
MHC	Major histocompatibility complex
MIP-1 α	Macrophage inflammatory protein-1 α aka CCL3
MRC1	Mannose receptor 1
mtDNA	Mitochondrial deoxyribonucleic acid
MTL	Medial temporal lobe
MW	Molecular weight
MWM	Morris water maze
NAFLD	Non-alcoholic fatty liver disease
NASH	Non-alcoholic steatohepatitis
Neh	Nrf2-ECH homology domains
NFT	Neurofibrillary tangle
NF- κ B	Nuclear factor κ -light-chain-enhancer of activated B cells
NK	Natural killer cells
NLR proteins	nucleotide-binding domain, leucine-rich repeat containing
NOR	Novel object recognition
NQO1	NAD(P)H quinone oxidoreductase 1
Nrf	Nuclear factor (erythroid-derived 2)-like
OL	Object location
OS	Oxidative stress
PAGE	Polyacrylamide gel electrophoresis
PAMP	Pathogen-associated molecular pattern molecules
PBS	Phosphate buffered saline
PBST	Phosphate buffered saline with Triton TM -X
PBS-T	Phosphate buffered saline with Tween [®] 20
PCR	Polymerase chain reaction
PD	Parkinson's disease
PDGF- β	platelet-derived growth factor- β
PDH	Pyruvate dehydrogenase
PFA	Paraformaldehyde
PHF	Paired helical filaments
PI	Preference index
PI3-K	Phosphoinositide 3-kinase
PMSF	Phenylmethylsulphonyl fluoride
PPAR γ	Peroxisome proliferator-activated receptor γ
PrP	Prion protein promoter
PRR	Pattern recognition receptor
PSEN	Presenilin
PUFA	Polyunsaturated fatty acid
qPCR	Quantitative polymerase chain reaction
RANTES	Regulated on activation, normal T cell expressed and secreted aka
CCL5	
RBX1	RING-box 1
RC	Regular chow
RI	Recognition index
RNA	Ribonucleic acid
RNS	Reactive nitrogen species
ROS	Reactive oxygen species
RT	Real-Time
SA	Spontaneous alternation
SAMP	Senescence-accelerated prone mouse

XIII

SAMR	Senescence-accelerated resistant mouse
sAPP	Soluble amyloid precursor protein
SDS	Sodium dodecyl sulphate
SFN	Sulforaphane
SYP	Synaptophysin
TAE	Tris-acetate-EDTA
<i>t</i> BHQ	<i>tert</i> -Butylhydroquinone
TBST	Tris-buffered-saline-Tween [®] 20
TCA	Tricarboxylic acid cycle
TEMED	Tetramethylenediamine
Tg	Transgenic
T1D	Type I diabetes
T2D	Type II diabetes
TIMP	Tissue inhibitors of metalloproteinases
TLR	Toll-like receptor
TNF- α	Tumour necrosis factor- α
TRX	Thioredoxin
UV	Ultraviolet
VaD	Vascular dementia
VDAC1	Voltage dependent anion channel 1
WAT	White adipose tissue
WHO	World Health Organisation
WT	Wild type
YM1	aka chitinase-3-like protein-3 (Chi3l3)
β -TrCP	β -transducin repeat-containing protein

ACKNOWLEDGEMENTS

I would first like to thank Prof. Mike Ashford for giving me the opportunity to partake in this PhD and for providing support throughout. Thanks also to the Alzheimer's Society for making this PhD possible and Alzheimer Research U.K. for a pilot grant that helped to keep the project moving forward. I would like to thank past and present members of the Ashford and McCrimmon labs for all their help and support in carrying this project to fruition. I would like to thank John Sharkey, Marie and Sharon for all their help and assistance, especially when it came to working the cryostat. Thanks also to Prof. Steve Keyse and his PhD student Andrew for their help and collaboration with the DUSP work performed.

I would like to extend a very special thank you to Alison McNeilly, without whom this project would never have gotten this far. Her knowledge of all things mouse-related and her help with behavioural tasks were invaluable, whilst her willingness to read over countless thesis drafts when already very busy was very much appreciated. I would like to extend heartfelt thanks to my fellow final year PhD students Susan, Geoff and Lauren for the opportunity to vent and air the worries associated with a PhD; and for encouraging me and giving the occasional shove in the right direction when required. Thesis boot camp made completing this thesis that little bit easier to endure and gave a useful outlet for all the stress related baking that ensued.

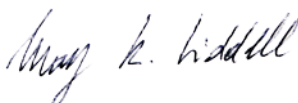
Thank you to the Swans (Susan, Arun, Moneeza, Abi and Fiona) who provided many occasions of joy and laughter throughout this PhD; and to the members of the Fine Dining Club (Susan, Arun, Cyrielle, David, Fiona and Abi) and my co-chef Moneeza for the afternoons of good food and great company as we pursued culinary success of ever more exotic cuisines. Thanks to Arun for the carefree instances of 'Childhood Regression', to Abi for the encouragement and volunteering to read thesis drafts, to Susan for putting up with me from day one and weathering the PhD storm together, and to Cyrielle for the French, the cheese, the ice-cream trips and so much more. Finally, thanks to Monzo for always teasing me, dragging me places in search of good food, watching Disney movies on the bad days even though she doesn't like them, and for being her own amazing self. I can't wait for all of you to come and visit; waffles and chocolate galore!

Finally I would like to thank my friends from back home for their support, phone-calls and spare rooms when I couldn't make it to the family for holidays. I would like to thank my family who have been nothing but supportful throughout this journey despite the numerous ups and downs along the way. Lastly, I would like to dedicate this work to my Grandfather, whose love of learning inspired so many people in his life and whose curiosity and excitement about all things new were instrumental in setting me on this journey in the first place. I'm sure he would have been overjoyed to see this project through to completion.

DECLARATION

I declare that this thesis is based on results obtained from investigations which I have personally carried out in the Division of Cardiovascular and Diabetes Medicine part of the School of Medicine at the University of Dundee from October 2011 to September 2015 using funding provided by the Alzheimer Society and an additional pilot grant from Alzheimer's Research U.K. I declare that the entire thesis is my own composition. Any work other than my own is clearly stated in the text and acknowledged with reference to any relevant investigators or contributors. This thesis has never been presented previously, in whole or in part, for the award of any higher degree. I have consulted all the references cited within the text of this thesis.

Signed



Date ...28.09.2015...

I confirm that Mary Katherine Liddell has spent the equivalent of at least 9 terms in the Division of Cardiovascular and Diabetes Medicine, School of Medicine, University of Dundee, and that she has fulfilled the condition of the University of Dundee, thereby qualifying her to submit this thesis in application for the degree of Doctor of Philosophy.

Signed



Date ...28.09.2015...

SUMMARY

Novel approaches are required to address Alzheimer's disease (AD) in our ageing population, with recent interest focused on inflammation and oxidative stress (OS). Disruption of NF-E2-related factor 2 (Nrf2) signalling increases OS and promotes AD. Amyloid precursor protein (APP) is intimately linked with AD, with the Swedish mutation (*hAPP_{swe}*) used in numerous transgenic models. Furthermore, increasing importance has been placed on the suggested link between nutritional status and AD. To assess Nrf2 as a potential target in AD, we examined the effect of metabolic stress, by chronic high fat (HF) feeding or acute lipopolysaccharide (LPS) treatment on the brains of aged WT, *Nrf2*^{-/-}, *hAPP_{swe}* and *Nrf2*^{-/-}/*hAPP_{swe}* mice.

Nrf2^{-/-} mice displayed impaired entorhinal cortex-dependent cognition, with raised basal hippocampal inflammation. The inflammatory state was attenuated by chronic HF feeding, whilst maintaining insulin sensitivity. In contrast, *hAPP_{swe}* did not display an inflammatory response to HF feeding, but demonstrated impaired insulin signalling; in line with AD-associated insulin resistance. Additionally, *Nrf2*^{-/-} mice display increased glial cell activation and activation of mitogen activated protein kinases and mitochondrial impairment. These may be indicative of OS-induced cellular dysfunction and is supported by an aggravated response to LPS, which potentiates IL-1 β production. Furthermore, despite an attenuated LPS response following the induction of tolerance, *Nrf2*^{-/-} mice maintain glial cell activation following treatment which may be suggestive of a primed immune environment within the brain.

In conclusion, these data indicate altered glucose homeostasis in both *Nrf2*^{-/-} and *hAPP_{swe}* mice, as previously reported. Further, we advocate that Nrf2 plays a key role in mitochondrial function and health and may be important for the ameliorative effects of HF feeding. Taken together, mitochondrial dysregulation and associated OS may help explain the development of cognitive impairment in *Nrf2*^{-/-} mice. This may be relevant for AD given the age-dependent decline in Nrf2 expression in humans.

1 INTRODUCTION

1.1 DEMENTIA AND ALZHEIMER DISEASE

Alzheimer Disease (AD) is the most prevalent cause of dementia in both developed and developing countries. Dementia itself is not a disease but a syndrome associated with deterioration of memory, thinking and behaviour; all of which impact on day to day living. Three further diseases are associated with the development of dementia; these are vascular dementia (VaD), dementia with lewy bodies and frontotemporal dementia (FTD). AD affects approximately 60-70% of the 850,000 dementia sufferers in the U.K. (Alzheimer's Research U.K. (ARUK), 2015), and it is estimated that 47.5 million people suffer from a form of dementia worldwide (World Health Organisation (WHO), 2015a). A progressive and irreversible neurodegenerative disorder, AD is associated with widespread neuronal cell death resulting in gradual cognitive decline centred round memory loss. Strongly correlated with ageing, the risk of developing AD almost doubles every 5 years from the age of 65 (Qiu *et al.*, 2009). It is currently believed that AD pathology is initiated at least 10 years prior to the development of symptoms and subsequent clinical diagnosis of dementia.

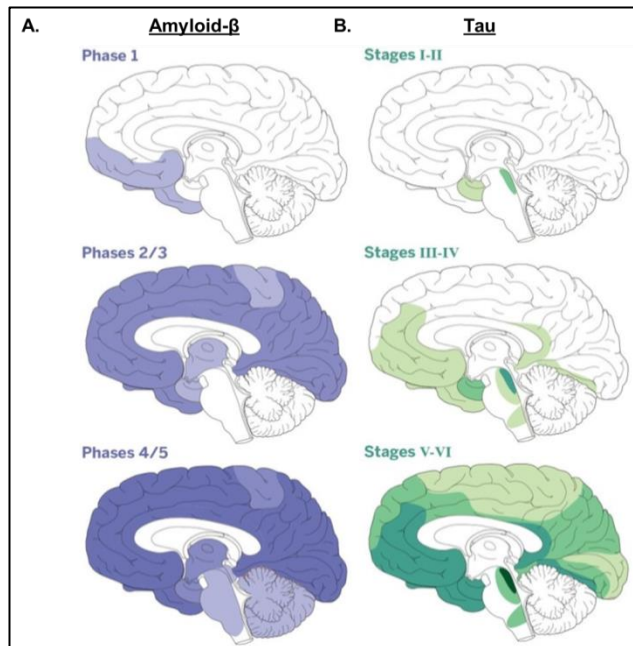


Figure 1.1 Anatomical progression of AD related pathology in the human brain

Pictorial representation of the pathological spread of Amyloid- β protein aggregates (A) and tau neurofibrillary inclusions (B) throughout the development of AD in the human brain. Adapted from Goedert (2015)

Propagating from subregions of the medial temporal lobe (MTL), the entorhinal (ERC) and parahippocampal cortices, AD spreads into the hippocampus causing cell death related shrinkage (See Figure 1.1; Didic *et al.*, 2011).

This neuronal damage continues to unfold, moving into the cerebral cortex where progressive impairment is reflected by a mild to moderate AD diagnosis. Increasing overall brain shrinkage due to cell death eventually results in the

diagnosis of severe AD that correlates with acute cognitive impairment. AD was first described

by Dr. Aloysius 'Alois' Alzheimer

in 1906 following his long-term clinical following of a 51 year old woman, Auguste D.,

who presented with very particular symptoms including short-term memory loss and disorientation (Alzheimer *et al.*, 1995). Post-mortem analysis enabled the discovery of two major AD pathologies: extracellular fibrous plaques primarily made up of β -amyloid ($A\beta$) protein, and intracellular neurofibrillary tangles (NFTs) made up of hyperphosphorylated microtubule tau protein aggregates (Figure 1.2; Karran *et al.*, 2011). Despite their requirement for a confirmed

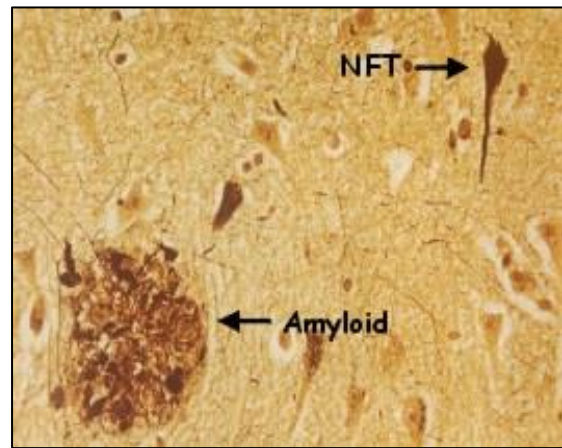


Figure 1.2 Histopathology image depicting the hallmark protein deposits of $A\beta$ and neurofibrillary tangles used as the gold standard of disease diagnosis for AD (Van Leuven, 2013)

diagnosis, the exact role of these pathologies in AD progression remains unclear and hotly debated (Castellani & Smith, 2011). Recent research has indicated that the upregulation of $A\beta$ may be a cellular coping mechanism to protect neurons from unmanageable levels of oxidative stress (OS; Bonda *et al.*, 2010).

The rate of incidence of AD is predicted to continue increasing, with incidences of dementia diagnoses expected to broach 70 million worldwide by 2030 (WHO, 2015a). Much of the estimated increase in disease diagnosis will be largely attributable to rising numbers of patients being reported in low and middle income countries. However, the lack of curative treatment options severely hampers the successful management of the disease, resulting in long-term treatment and care costs currently estimated at over £20 billion per year to the National Health Service (NHS; ARUK, 2015). Whilst the most common current treatments include the glutamate receptor antagonist memantine and acetylcholine esterase inhibitors, such as donepezil, these are largely symptomatic treatments with minimal impact on the underlying disease progression. Many clinical treatments are now being combined with non-invasive interventions such as cognitive stimulation therapy (CST). CST makes use of a range of stimulating social activities and group exercises and has been shown to provide improved maintenance of cognitive function when compared to standard treatment alone (Aguirre *et al.*, 2013). Additional non-pharmacological approaches in use to aid in the management of AD include interventions such as music therapy and sensory stimulation, both of which have been suggested to aid with symptoms of dementia such as agitation. In addition, the co-medication of commonly associated conditions such as depression, anxiety and agitation may help improve patient's quality of life. As yet,

there are no diagnostic tests or screening tools available for diagnosis of AD at a pre-symptomatic disease stage. Disease diagnosis of sporadic AD is still only provided upon presentation with cognitive or behavioural impairment, with definitive confirmation supplied by post-mortem pathology examinations to confirm the presence of plaques and tangles. In addition, given the nature of AD and its often slow progression rate, the cause of death for many patients is attributed to acute causes of mortality such as pneumonia and diseases of the circulatory system (Brunnström & Englund, 2009). This can act as a confounding factor when analysing clinical data; as well as highlighting the importance and complexities of long-term clinical care for patients suffering from dementia.

Novel research has ascribed roles for alternative targeting mechanisms such as metal ion chelators to reduce the spread of reactive oxygen species (ROS) and A β vaccines or A β binding molecules to prevent the build-up of A β (Salomone *et al.*, 2011). However, in order to improve patient outcome, treatments targeted at earlier stages of disease progression are required. These are dependent on establishing a more in depth knowledge of the mechanisms of disease initiation and early progression. In addition, the development of relevant biomarkers for use in clinical diagnosis is of particular importance. These include reliable markers of early stage AD development, potentially preventing the onset of much of the irreversible cell loss associated with AD, and disease stage dependent markers to aid in assessing the most appropriate treatment interventions. From a therapeutic perspective, consistent biomarkers that allow confirmation of treatment efficacy would allow for the tailoring of any necessary pharmacological intervention. Biomarkers currently linked with early cognitive dysfunction, in both humans and animal models, include reductions in brain glucose utilisation as measured by fluorodeoxyglucose positron emission tomography resulting in altered energy homeostasis. In addition, both decreased insulin in the brain as well as insulin resistance, and an increased prevalence of OS which most closely tracks AD development are also used as biomarkers in AD (de la Monte, 2009; Mosconi *et al.*, 2009; Yao *et al.*, 2009; Bonda *et al.*, 2010). This alteration in insulin signalling and energy homeostasis may be a key factor in gaining further understanding of AD. Diabetes UK describes insulin resistance as the prolonged presence of elevated insulin in the body leading to insulin desensitisation resulting in an impaired response to the hormone's signalling pathway (DiabetesUK, 2015). Moreover, whilst essential for the subsequent development of diabetes, it is also associated with increased inflammation which may long-term be important in further dysregulation of the energy balance as is

suspected to occur in AD. Finally, AD has more recently been linked with central insulin signalling impairment leading to insulin resistance, with A β thought to have a detrimental impact on insulin receptor activity and localisation (Xie *et al.*, 2002; Zhao & Townsend, 2009; Moloney *et al.*, 2010). This in turn may play a role in the subsequent development of cognitive impairment.

In order to better understand the processes occurring during the progression of AD, much of the early research performed in the field concentrated on the characterisation and classification of the two key AD associated pathologies of A β and phosphorylated tau aggregation. These hallmark pathologies, first described by Alois Alzheimer at the turn of the twentieth century, remain essential for confirmation of AD diagnosis following posthumous tissue analysis. Over the years, a variety of disease-linked mutations have been discovered in both of these dysregulated protein pathways. The mutations in A β are largely associated with the early onset familial form of AD (FAD), whilst those associated with tau protein have been linked with the spectrum of diseases covered by FTD. Work performed using these mutations have helped further our understanding of the potential function of the relevant proteins in health and disease.

1.1.1 Tau Protein and Pathology

Accumulation of tau protein has been cited as playing important roles in many neurodegenerative diseases including FTD and AD, but also neurodegenerative disorders such as Parkinson's disease (PD) and amyotrophic lateral sclerosis (ALS). Tau protein belongs to the family of proteins known as microtubule-associated proteins (MAP). Discovered simultaneously by Nunez and colleagues in France and Kirschner and colleagues in the U.S.A. in 1977 (Cleveland *et al.*, 1977a; Cleveland *et al.*, 1977b; Fellous *et al.*, 1977), its cellular role centres around regulating and managing microtubule formation (Avila *et al.*, 2004). It is primarily found in neurons, although can on occasion be found in certain glial cells, and is heavily post-translationally modified. It is these post-translational modifications that regulate tau's role in assembling and stabilising microtubules (Iqbal *et al.*, 2005). The most studied of these secondary modifications is phosphorylation. Phosphorylation of tau has been reported to be assisted by a multitude of different kinases, including such ubiquitously expressed enzymes as glycogen synthase kinase 3 (GSK3), cyclin-dependent kinase 5 and members of the mitogen-activated protein kinase (MAPK) family (Mandelkow & Mandelkow, 2012).

AD NFTs are made up of a combination of paired helical filaments (PHF) and straight filaments. Research has shown that tau is the primary protein present in the PHFs. This has led to the coining of the term ‘tauopathies’ to define neurodegenerative diseases in which pathological aggregation of tau protein is observed. Other examples of tauopathies include PD, where aggregates are largely localised in the substantia nigra pars compacta region of the brain and associates with other PD protein aggregates such as Lewy bodies, and many others including ALS and those disorders encompassed by the umbrella term of FTD (Spires-Jones *et al.*, 2009; Lei *et al.*, 2010). It is aberrant processing of the post-translational modifications of tau, such as phosphorylation, glycosylation and the addition of β -N-acetyl-glucosamine (GlcNac) by O-GlcNAcylation, which are largely to blame for its pathology associated toxicity. Specifically, hyperphosphorylation has been found to be a precursor to the formation of PHFs and NFTs in AD. However, formation of PHFs is not solely associated with the development of AD NFTs and an accumulation of PHF formations can also be found in other known tauopathies. More recently, as increasing research goes into better understanding other post-translational modifications, it has been suggested that a balance between the different modifications possible for tau is necessary for maintaining correct cell function. Aberrant glycosylation of tau *in vitro* has been shown to facilitate its subsequent phosphorylation whilst inhibiting its dephosphorylation by protein phosphatases, thereby promoting increasing the ratio of phosphorylated to non-phosphorylated tau (Liu *et al.*, 2002a; Liu *et al.*, 2002b). Additionally modification of tau protein *via* O-GlcNAcylation has been shown to negatively regulate protein phosphorylation with *in vitro* and rodent *in vivo* evidence suggesting a role for decreased O-GlcNAcylation in AD pathology development (Liu *et al.*, 2004; Yuzwa *et al.*, 2012). This may reflect a link between the alterations seen in brain metabolism and the aberrant processing of tau seen in the brains of AD patients.

1.1.2 The Amyloid Precursor Protein Processing Pathway and A β

In 1987, eighty years after the original discovery of A β protein plaques by A. Alzheimer, several independent laboratories identified A β proteins as cleavage products of a large transmembrane precursor protein, subsequently named amyloid precursor protein (APP) (Thinakaran & Koo, 2008; Figure 1.3). APP is a ubiquitously expressed type 1 membrane glycoprotein and is the product of the *APP* gene found on chromosome 21, the same chromosome responsible for Down’s syndrome (DS). DS, which is caused by the presence of an extra copy of chromosome 21 and therefore an

additional copy of *APP*, is characterised by both physical and cognitive deficits. Individuals diagnosed with DS as a result of a full chromosomal replication go on to develop early onset AD and many of these show clinical signs of AD-type dementia (Millan Sanchez *et al.*, 2012). In addition, a patient presenting with only segmental trisomy of chromosome 21 and lacking the region coding for APP showed no signs of dementia development (Prasher *et al.*, 1998), further supporting an important role for APP in AD development.

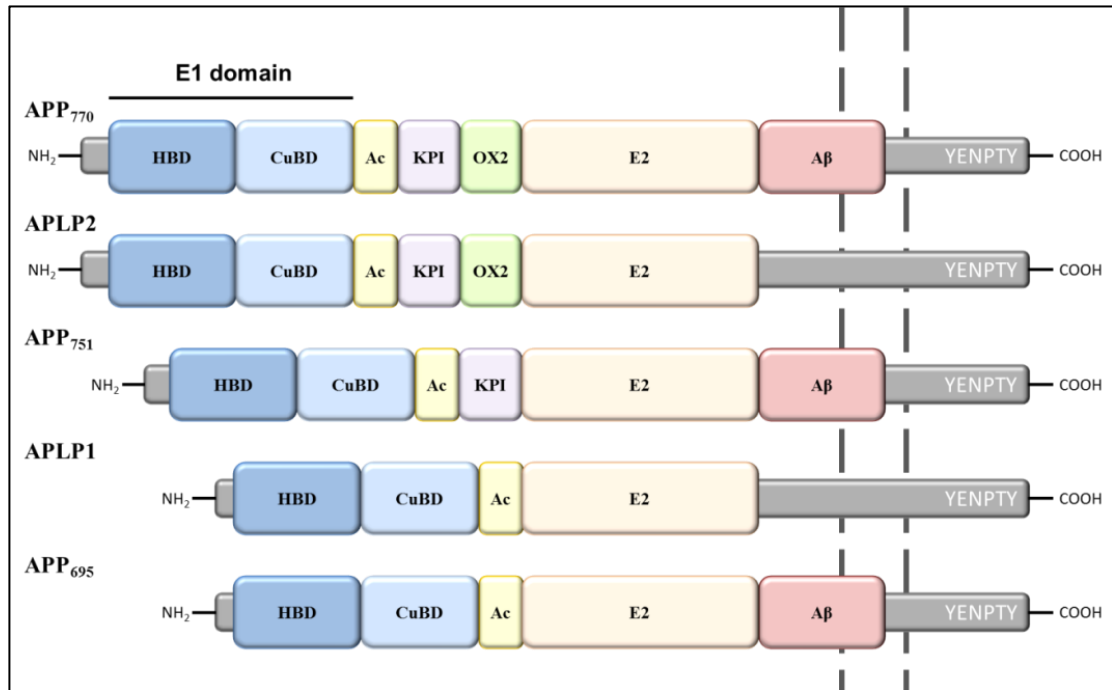


Figure 1.3 Domain structure and homology of the APP protein family

In total, three major isoforms of APP are known to be formed as a result of alternative splicing of *APP*, namely *APP*₆₉₅, *APP*₇₅₁, *APP*₇₇₀ (Figure 1.3). Named after their total amino acid content both *APP*₇₅₁, the predominant peripheral isoform, and *APP*₇₇₀ are widely expressed. They are similar in that they both contain a serine protease inhibitor domain called the Kunitz proteinase inhibitor (KPI) domain. In contrast, the principle neuronal isoform of APP is *APP*₆₉₅ which lacks the exon 7 located KPI domain (Ling *et al.*, 2003). Recent research has implicated the KPI domain in the control of protein dimerization, trafficking and processing; suggesting it in turn may be dysregulated in disease pathogenesis (Ben Khalifa *et al.*, 2012). Additional mammalian members of the APP protein family include APP-like protein 1 and 2 (APLP1 and APLP2 respectively), with APLP1 more closely resembling the domain composition of *APP*₇₇₀ whilst APLP2 is most similar to *APP*₆₉₅. Whilst the A β domain is unique to APP, other conserved regions are present across all three proteins including the so

called E1 and E2 domains (Figure 1.3). Moreover, although both APP and APLP2 are ubiquitously expressed APLP1 is solely expressed within the brain, giving further indications that despite their structural similarity there may be functional differences between these protein homologs.

Further investigation uncovered APP processing pathways dependent on the action of three protein secretases, namely α -, β - and γ - secretase, responsible for the processing of APP down two focal signalling cascades (Figure 1.4). Whilst cleavage of APLP1 appears independent of β -secretase activity, unlike APLP2, both APLP proteins have been shown to generate intracellular fragments (termed ALIDs) in a γ -secretase dependent manner (Eggert *et al.*, 2004) indicating at least partial processing conservation between these proteins. With a variety of proposed physiological roles, members of the APP family are largely accepted to have dominant trophic roles in neurons and at the synapse. The essential role played by the APP family in neuronal development was confirmed by the development of knock-out (KO) models for each protein. Ablation of more than one family member such as APP/APLP2, APLP1/APLP2 or APP/APLP1/APLP2 all prove lethal shortly after birth. This indicates a key physiological role for APLP2 in particular, with a certain degree of inbuilt redundancy amongst the remaining family members (for review of known physiological functions see Müller & Zheng, 2012).

Despite their similarity in structure to APP, there has been less research performed investigating the roles of the APLP proteins. However, research into the mechanisms driving the lethality of the double KO model of APP/APLP2 implicated dysfunctional management of the insulin system, suggesting a potentially important functional role of the APP protein family in glucose and insulin homeostasis (Needham *et al.*, 2008). Subsequent work utilising the information that both insulin and insulin-like growth factor-1 (IGF-1) are capable of activating α -secretase cleavage has indicated that whilst α -cleavage of APP and APLP2 are both activated as a result of IGF-1 this occurs via two different enzymes, namely ‘a disintegrin and metalloproteinase’ (ADAM) 10 and ADAM17 (aka tumor necrosis factor- α converting enzyme (TACE); Jacobsen *et al.*, 2010). This suggests that whilst these proteins are similar in structure they may yet have subtly different downstream effects following similar stimuli. Although APP, APLP1 and APLP2 can all be cleaved by similar enzymes (α -, β -, γ -secretases) the resulting products vary in length, further supporting a role for analogue

specific signalling abilities resulting from the same initial cleavage pathways (Shariati & De Strooper, 2013).

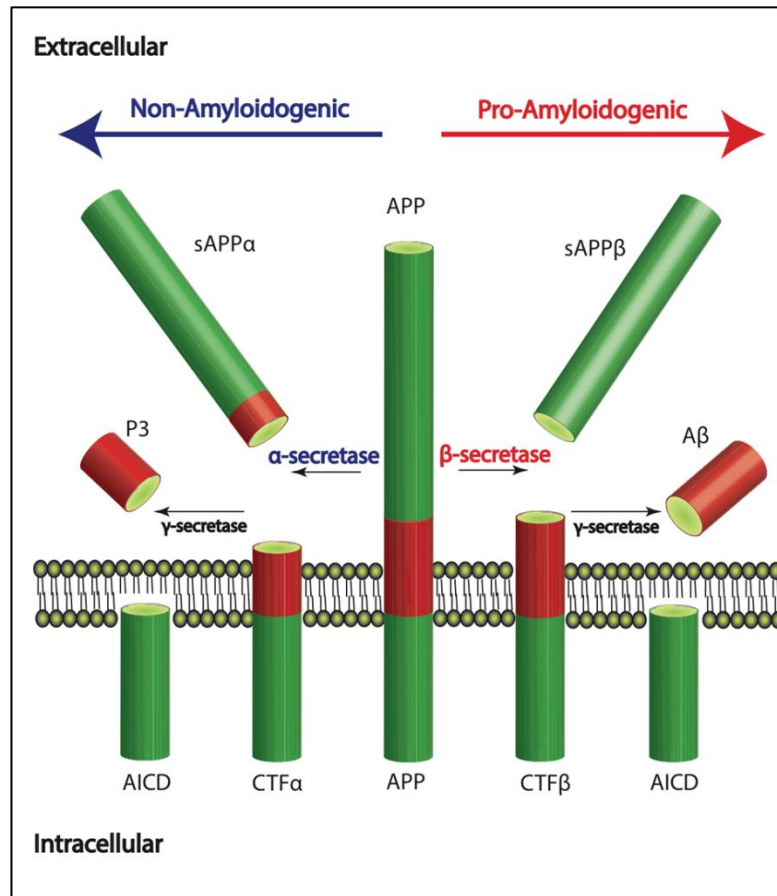


Figure 1.4 Schematic representation of the pro-amyloidogenic and non-amyloidogenic pathways of APP processing.

Where α -secretase represents enzymes such as ADAM 10 and 17, β -secretase represents the β -site APP cleaving enzyme 1 and 2 (BACE1 and 2)

Despite these findings, to date there has been little indication that either APLP1 or APLP2 produce toxic cleavage products that contribute to the development of AD. However, structural analysis has supported the physiological presence of not only homodimers within the APP family but also heterodimers combining multiple APP family members. Furthermore, this dimerization has been suggested to be influential not only for correct protein action at the synapse, but also for the channelling of APP down either amyloidogenic or non-amyloidogenic cleavage (Baumkötter *et al.*, 2012). It has since been suggested that homodimerisation of APP may promote the amyloidogenic processing of APP, whilst heterodimerisation with APLP1 or APLP2 has been suggested to decrease the affinity of APP for cleavage by BACE1 thereby attenuating the production of A β (Kaden *et al.*, 2012). Therefore, whilst not directly required for

production of A β , dysfunctional alterations in APLP levels or the ratio of homo- and hetero- dimerization of APP may be influential in the development and progression of AD.

1.1.2.1 Amyloidogenic cascade

The amyloidogenic pathway is responsible for the production of the toxic A β peptide found in aggregated plaques in AD. Initiated by β -secretase cleavage of APP within its luminal domain, the amyloidogenic pathway sees shedding of a large percentage of the soluble ectodomain of APP (sAPP β). Release of the sAPP fragment leaves a membrane associated carboxy terminal fragment (β -CTF) behind. It is this membrane associated β -CTF fragment that is cleaved within its transmembrane domain by a second secretase enzyme, γ -secretase, to form the A β fragments now so commonly associated with AD (Figure 1.4). The main toxic species of A β , namely A β ₁₋₄₀ and A β ₁₋₄₂, can both be produced by this cleavage and coincide with the release of an APP intracellular domain (AICD) fragment that varies in size according to the γ -secretase cleavage site. A β ₁₋₄₂ being a more hydrophobic molecule has an increased predisposition towards fibril formation and, therefore, is largely responsible for driving the production of the insoluble plaques seen in AD despite accounting for only a small percentage of total amyloid produced (Zhang *et al.*, 2011). A β peptides are released into the extracellular environment and the AICD is released into the cytoplasm where it most often relocates to the nucleus following stabilisation by binding of members of the Fe65 scaffolding/adaptor protein family (Turner *et al.*, 2003). Once in the nucleus, it can act as a transcription factor reportedly upregulating genes such as GSK3 β and the A β -degrading enzyme neprilysin (Kim *et al.*, 2003; Pardossi-Piquard *et al.*, 2005). Highly labile in nature, AICD can be rapidly degraded by insulin degrading enzyme (IDE), especially when not stabilised by Fe65 (Müller *et al.*, 2008).

The enzymes that perform the initial cleavage of APP at the β -site, instigating the amyloidogenic pathway cascade, have since been identified as aspartic proteases, BACE1 and BACE2 respectively. Their discovery has prompted investigations into their potential use as therapeutic targets, with research predominantly targeted at BACE1. This may in part be due to the expression profiles of BACE1 and BACE2, with BACE1 being shown to have a higher expression in the central nervous system (CNS) and brain regions than BACE2, which is more widely expressed in the periphery (Cole & Vassar, 2007). In addition, subsequent work using *BACE1*^{-/-} mouse models has

highlighted it as the predominant β -secretase responsible for the production of A β (Luo *et al.*, 2001).

BACE1, which was first identified by Citron and colleagues in 1999, is known to be expressed both in neurons and astrocytes (Vassar *et al.*, 1999; Roßner *et al.*, 2005). It is predominantly localised to the Golgi apparatus and cellular endosomes within the cell cytosol from which A β peptides are produced, and is described as the rate limiting step in A β production (Vassar, 2001). It is worth noting that APP is not the sole substrate processed by BACE1, with other substrates ranging from APLP2 to more recent reported hits such as various members of the neuroligin family and insulin-like growth factor-binding protein 2 (Kuhn *et al.*, 2012). Induction of BACE1 activity is strongly influenced by a variety of both environmental and cellular stressors including OS, hypoxia, inflammation and metabolic challenges such as obesity and impaired insulin/leptin signalling (Cole & Vassar, 2007). *BACE1*^{-/-} mouse models fed a high fat diet are protected against diet-induced obesity (DIO) and have enhanced insulin sensitivity compared to *BACE1*^{+/+} controls (Meakin *et al.*, 2012). In addition, BACE1 activity positively correlates with ageing in both human and mouse brains (Fukumoto *et al.*, 2004); and has been implicated in the management of energy homeostasis with BACE1 expression being increased following energy inhibition, a chronic state in AD development (Velliquette *et al.*, 2005).

Recent research has shown the BACE1 promoter region to harbour functional binding sites for a number of well-known stress activated transcription factors such as peroxisome proliferator-activated receptor γ (PPAR γ), nuclear factor κ -light-chain-enhancer of activated B cells (NF- κ B) and hypoxia inducible factor-1 (HIF-1) many of which are also associated with other AD risk factors such as obesity and stroke (Sastre *et al.*, 2006; Bourne *et al.*, 2007; Zhang *et al.*, 2007; for comprehensive review see Chami & Checler, 2012). Further work has suggested that BACE1 cleavage products, such as A β , may act as danger-associated molecular pattern molecules (DAMP), capable of initiating and perpetuating immune responses in the absence of other infectious agents (Heneka *et al.*, 2014). The action of DAMPs contrasts with those of pathogen-associated molecular pattern molecules (PAMPs) which partake in a similar role but require the presence of an initiating infectious factor such as lipopolysaccharide (LPS). However, both DAMPs and PAMPs are important in the management of the immune system and the resolution of cellular damage.

1.1.2.2 *Non-Amyloidogenic Cascade*

The alternative, non-amyloidogenic, APP processing pathway (Figure 1.4) involves an initial cleavage by α -secretase within the A β sequence, which causes shedding of the ectodomain (sAPP α) leaving behind a membrane bound α -CTF. The placement of the α -secretase cleavage within the A β site prevents the production of A β by subsequent γ -secretase cleavage. Instead, transmembrane γ -cleavage produces a smaller p3 protein as well as the previously mentioned AICD. Although the molecular identity of α -secretase remains to be fully established, the most commonly quoted are zinc-metalloproteinases that show increased APP cleavage when overexpressed. Of these the three most frequently named are ADAM 9, 10 and 17, part of the disintegrin and metalloproteinase ADAM family (Boseman-Roberts *et al.*, 1994; Turner *et al.*, 2003; Zhang *et al.*, 2011).

Members of the ADAM family have been linked with a variety of roles including cell growth and migration, cell-cell communication and both intra- and extra-cellular signalling. Divided into two groups, catalytically active and inactive, both ADAM 10 and 17 fall into the cluster of zinc containing catalytically active enzymes (Edwards *et al.*, 2008). ADAM activity is known to be regulated by specific tissue inhibitors of metalloproteinases (TIMPs), with Amour and colleagues showing that ADAM10 interacts with both TIMP1 and TIMP3 (Amour *et al.*, 2000). Contrasting with BACE1 cleavage which occurs largely in endosomes and the Golgi apparatus, α -secretase cleavage of APP occurs at the plasma membrane (Thinakaran & Koo, 2008). In addition to APP, ADAMs have been shown to share many substrates in common with both BACE1 and γ -secretase including Notch related ligands as well as E-cadherin (Six *et al.*, 2003; Maretzky *et al.*, 2005). And whilst both ADAM 9 and 17 have been implicated in APP processing, it is ADAM10 that appears to be the constitutively active α -secretase enzyme with *in vitro* knockdown models suggesting neither ADAM9 nor ADAM17 are able to compensate fully for its loss (Kuhn *et al.*, 2012). In addition, work done in ADAM10 overexpressing mouse models show increased sAPP α and decreased A β production which is reversed in models overexpressing a mutated inactive form of ADAM10 (Postina *et al.*, 2004). Moreover, improvements were also seen in Morris water maze performance in ADAM10 overexpressing mice suggesting an improvement in cognitive function following increased α -secretase cleavage. These effects may in part be associated with the neuroprotective and neurotrophic roles suggested for the sAPP α cleavage product, which also includes inhibition of common stress related pathways such as the MAPK known as c-jun N-terminal kinase (JNK) (Copanaki *et al.*,

2010; for review on ADAMs see Vingthdeux & Marambaud, 2012). Taken together, current research suggests targeting of both α - and β - secretase pathways may provide beneficial therapeutic avenues for pharmacological intervention.

1.1.2.3 APP processing and disease

Under healthy physiological conditions, the non-amyloidogenic α -secretase pathway cleaves 90% of APP. Little is known about the induction mechanisms involved in the overproduction of $A\beta$ by BACE1 in the sporadic form of AD, which is the most common; although much research has centred on this area of research in recent years (see below). It is also worth noting that the detrimental effects associated with AD cannot be entirely attributed to an increase in production of $A\beta$. Other factors such as tau related toxicity and vascular damage, including an increase in microinfarcts in AD brains and alterations to the blood brain barrier (BBB), have been associated with damaging effects in conjunction with those attributed to $A\beta$ (Kalaria, 2010). Indeed, $A\beta$ deposition within the brain microvasculature has been recorded with a predominance of $A\beta_{1-40}$ as opposed to the $A\beta_{1-42}$ more strongly associated with plaque deposition. This has been further supported by data from the both the Dutch (APP_{E693Q}) and Italian (APP_{E693K}) FAD mutations that have an increased production of $A\beta_{1-40}$ and consistently develop hereditary cerebral amyloid angiopathy and subsequently hereditary cerebral haemorrhage with amyloidosis, strongly linking the alterations occurring in AD with those of VaD (Agyare *et al.*, 2013). In addition, hypoxia-induced damage as a result of vascular impairment has been suggested to increase the expression of APP, which may be of importance in the initiation of the amyloidogenic cascade and AD (Wang *et al.*, 2002).

As previously mentioned, the different forms of $A\beta$ are not produced equally. Similar to the ratio of amyloidogenic to non-amyloidogenic processing of APP, a change in the ratio of $A\beta_{1-42}/A\beta_{1-40}$ peptides produced has been described in forms of both FAD and sporadic AD, with increased production of $A\beta_{1-42}$ to $A\beta_{1-40}$ associated with enhanced amyloidogenic damage (Yoshiike *et al.*, 2003; Hellström-Lindahl *et al.*, 2009; Kuperstein *et al.*, 2010). Experimental models have also demonstrated altered APP metabolism can occur as a result of various cerebral insults including synaptic damage and altered energy metabolism. Acute mouse models of energy inhibition such as described by Velliquette and colleagues (2005), where impairment of brain energy metabolism resulted in increased BACE1, sAPP β and $A\beta$, supports more recent work in a type I model of diabetes (T1D). In the described model of T1D, streptozotocin-induced

insulin-deficient diabetes further diminished cognitive performance in a mouse model of AD whilst increasing the severity of AD pathological markers and GSK3 activity (Jolivald *et al.*, 2010). In addition, rodent models of metabolic stress including feeding of high fat/cholesterol diets, which in turn leads to impaired insulin signalling, has been shown to increase BACE1 expression whilst *BACE*^{-/-} mice are protected from weight gain and maintain normal metabolic signalling (Meakin *et al.*, 2012; Wang *et al.*, 2013b). In conjunction with rodent models, human studies have also reported links between AD and altered metabolic state with reports linking brain hypometabolism as well as obesity with the development of AD (Blass *et al.*, 2000; Marchesi, 2011). Moreover, a growing body of evidence supports a central role of OS as an early event in AD and also as a major factor in the alteration of APP processing (Mohammad Abdul *et al.*, 2006; Karuppagounder *et al.*, 2009; Choudhry *et al.*, 2012).

Although the mechanisms responsible for altering BACE1 activity are still uncertain, what is clear is that a variety of stressors are capable of inducing the altered activity including inflammation, OS, hypoxia and metabolic dysregulation. One suggested pathway linked with increased amyloidogenic processing of APP via BACE1 is through the interaction of stress-induced MAPK proteins such as JNK. It has been shown that under pro-oxidant conditions, BACE1 expression is upregulated through activation of JNK *in vitro* (Tamagno *et al.*, 2005; Tamagno *et al.*, 2009). Further investigations have revealed that a similar stress-induced activation of γ -secretase by JNK is observed in neuroblastoma cell lines stably expressing human APP₆₉₅ (Shen *et al.*, 2008; Quiroz-Baez *et al.*, 2009). This upregulation in β - and γ - secretase activity has been associated with contemporaneous impairment of endogenous antioxidant enzymes such as Cu/Zn-superoxide dismutase activity implying inhibitory or damaging effects to the endogenous neuroprotective system (Schuessel *et al.*, 2005). Inhibition of JNK activity has been shown to negatively impact on A β production, attenuating the progression of AD in animal models by preventing the phosphorylation of APP by JNK (Mazzitelli *et al.*, 2011). However, as with many facets of this disease it is unlikely to be the sole responsibility of one signalling cascade, and a combination of a multitude of factors taken together that are more likely at fault.

1.1.3 Genetic Factors in AD

Following on from its initial discovery, AD is now separated into two different forms. FAD, which is known to be primarily linked to genetic mutations in a subset of genes, occurs earlier in life (often before the age of 65) and accounts for a very small

number of cases each year. Whereas late onset or sporadic AD, whose aetiology remains unknown, is the predominant form of AD and is more common in those over the age of 65. Sequencing of full length APP followed on from that of A β , providing the genetic data necessary to identify a variety of mutations in families presenting with FAD across multiple generations (Weggen & Beher, 2012). This sequencing revealed multiple mutations in the APP gene (Chartier-Harlin *et al.*, 1991; Goate *et al.*, 1991; Figure 1.5), as well as subsequently highlighting the importance of mutations within the catalytic subunit of the γ -secretase enzyme through the identification of the presenilins (PSEN1 and PSEN2; Sherrington *et al.*, 1995). A full list of the mutations associated with AD can be found at a variety of databases, such as the ‘AD & FTD mutation database’ (Cruts *et al.*, 2012), and the number of known mutations has increased exponentially since those initial discoveries in the early 1990s.

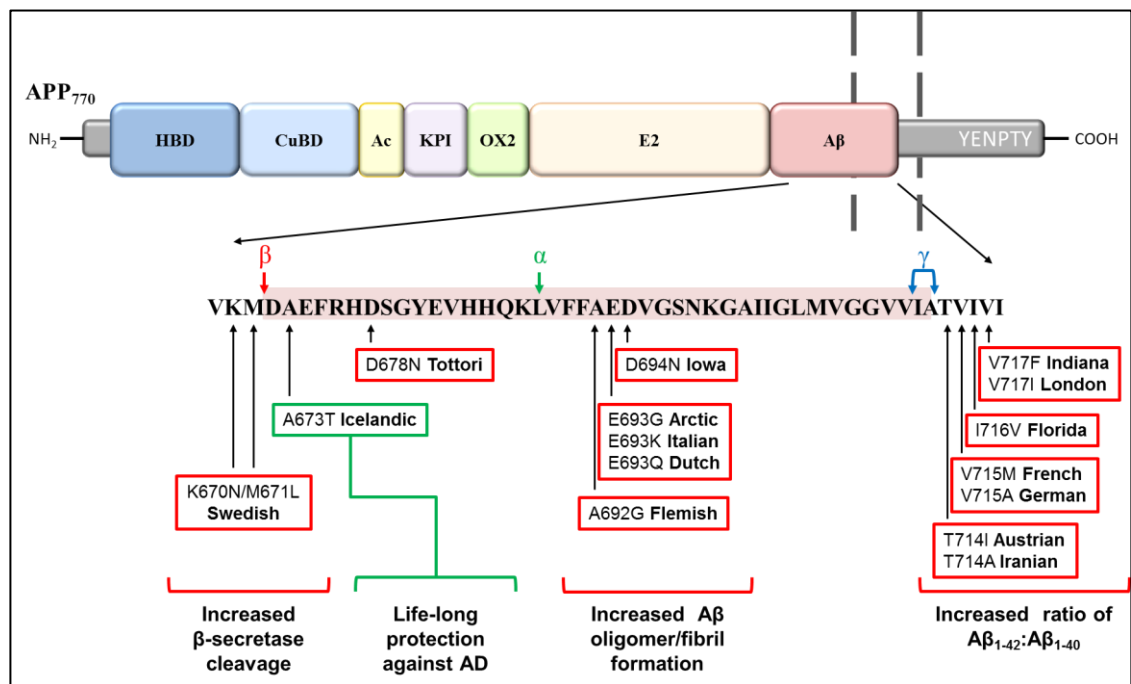


Figure 1.5 Sequence localisation of a selection of well-known APP mutations.

Where red boxes depict detrimental mutations and green depict protective mutations.

Despite the boom in number of newly described mutations, their localisation has remained restricted to a small subset of proteins, namely APP, PSEN1 and PSEN2 in the case of AD, all of which are involved in the amyloid pathway. Mutations found within the catalytic subunit of γ -secretase, either PSEN 1 or 2, increase the ratio of the more toxic A β ₁₋₄₂/A β ₁₋₄₀ produced (Figure 1.5). In a similar manner, mutations found within the γ -secretase cleavage region of APP, such as the Indiana (*APP*_{V717F}) and London (*APP*_{V717I}) mutations, also alter the ratio of amyloid produced in favour of the

1-42 isoform (Figure 1.5). And whilst a number of APP regions have been linked with FAD related mutations, all occur within or surrounding the A β region of APP, with mutations found within A β , such as the Dutch (*APP*_{E693Q}) and Arctic (*APP*_{E693G}), increasing the number of A β fibrils produced (Hall & Roberson, 2012).

Worthy of particular note is the APP related mutation first highlighted in two Swedish families with histories of FAD in 1992; and subsequently prompting the coining of the term *hAPP*_{swe} (Mullan *et al.*, 1992). This mutation was found to occur at exon 16 of the APP gene within the A β coding region and caused by a double nucleic base transversion (G to T and A to C) at codons 670 and 671 (Figure 1.5). This prompts the substitution of two amino acids, namely lysine (K) to asparagine (N) and methionine (M) to leucine (L). In turn this alters the affinity of APP for cleavage by β -secretase, and the cellular localisation at which the cleavage occurs changes from the endosome to Golgi-derived vesicles, eliminating the need for reinternalization and recycling of APP prior to cleavage by BACE1 (Felsenstein *et al.*, 1994; Haass *et al.*, 1995). This change in APP processing pathway alters the ratio of non-amyloidogenic/amyloidogenic processing resulting in an increased production of A β compared to the wild type (WT) APP. Incorporation of the double Swedish mutation into rodents was one of the first successful transgenic models to replicate at least in part the pathologies seen in AD patients (Reaume *et al.*, 1996). This sparked the development of a multitude of different transgenic animal models used in aiding ongoing research in the field; and many of these models today still incorporate the Swedish *APP*_{K670N/M671L} alone or in combination with other AD related mutations. In stark contrast to the number of detrimental mutations now documented, a single mutation has thus far been linked with a protective phenotype towards AD. The so called 'Icelandic mutation' (*APP*_{A673T}; Figure 1.5), only recently identified by Jonsson and colleagues (2012), occurs adjacent the BACE1 cleavage site on APP resulting in ~ 40% reduction in amyloidogenic compounds *in vitro* and preventing the advent of cognitive decline in the elderly. The discovery of the Icelandic mutation therefore raises a crucial point suggesting a limited reduction in BACE1 regulated APP cleavage is sufficient to provide a protective environment. This then advocates a role for partial BACE1 inhibition as a pharmaceutical target for treatment of AD.

Finally, whilst cases of mutation driven FAD remain rare in comparison to late onset AD, geneticists hypothesised the likely presence of genes which though not directly causative would predispose individuals to develop AD. This was proven to be

correct when, in 1993, a correlation between apolipoprotein E (ApoE) isoform and AD was demonstrated in both FAD and sporadic AD cohorts (Roses, 1996). Three isoforms of ApoE exist designated simply $\epsilon 2$, $\epsilon 3$ and $\epsilon 4$. Research has shown that presence of the $\epsilon 4$ isoform significantly increases an individual's risk of developing AD, and also drops the age of diagnosis. Subsequent to this discovery and with the development of genome wide research platforms, further genes have been identified as contributing towards increased risk of developing AD. These include genes such as clusterin and bridging integrator 1, but none have demonstrated as potent an effect as that seen for ApoE (Roses, 1996; Kauwe *et al.*, 2011).

1.2 OXIDATIVE STRESS AND NEURODEGENERATION

OS is caused by an imbalance between the pro-oxidant, ROS and reactive nitrogen species (RNS), and antioxidant systems. Long-term exposure to ROS and RNS, which are by-products of various metabolic pathways, is cytotoxic (Emerit *et al.*, 2004). This can occur by direct injury, such as deoxyribonucleic acid (DNA) damage, or indirectly by causing lipid peroxidation; and results in cell death by necrotic or apoptotic pathways. The brain is particularly sensitive to OS due to high oxygen throughput, high levels of unsaturated lipids and transition metals, including copper (Cu) and iron (Fe), as well as mitochondria. Although scientists have known about OS for a long time, it has more recently been implicated as an early event in AD (Castellani *et al.*, 2001; de Vries *et al.*, 2008; Bonda *et al.*, 2010; Cruz-Sánchez *et al.*, 2010) and other neurodegenerative disorders including PD and ALS.

1.2.1 Mitochondrial Dysfunction

The origins of ROS species associated with AD remain unclear, with both enzymatic (e.g. Cyclophilin D; Borger *et al.*, 2011) and non-enzymatic pathways (e.g. impaired mitochondrial respiration) being implicated. However, it is likely to be largely due to the formation of highly reactive hydroxyl radicals from hydrogen peroxide (H_2O_2), produced in particular by the mitochondria. Overproduction of radical compounds occurs as a result of a breakdown of the endogenous detoxification system and damage to metabolic pathways and organelles. Mitochondria, due to their high level of adenosine triphosphate (ATP) production, are likely to be the largest producers of ROS in the brain. As a result of ageing, mitochondrial function is known to decline which causes an increased production of ROS due to premature electron leakage from the electron transport chain (ETC) and a deterioration in energy metabolism, both of which are exacerbated in AD (Figure 1.6; Swerdlow, 2011). It has been shown that, in

AD, neuronal and astrocytic energy metabolism is widely affected further implicating the mitochondria as primary ROS sources.

Several of the enzyme complexes associated with mitochondrial oxidation of substrates to produce energy have been shown to be disrupted both in early stages of AD and in post-mortem brains. Further work, using primary cultures from a variety of rodent models, has corroborated these findings following administration of A β *in vitro*. Included in those enzymes altered are the pyruvate dehydrogenase (PDH) complex, the α -ketoglutarate dehydrogenase (KGDH) complex of the tricarboxylic acid cycle, and complex IV (COX IV) of the electron transport chain (Figure 1.6; Blass *et al.*, 2000; Casley *et al.*, 2002; Allaman *et al.*, 2010). This is supplemented by recent research implicating earlier A β accumulation in the synaptic mitochondria when compared with their non-synaptic compatriots (Du *et al.*, 2010). This is further supported by work performed in so called ‘cybrid models’ of AD that incorporate patient mitochondrial deoxyribonucleic acid (mtDNA) into cells devoid of mtDNA. Cells derived from AD patients were shown to induce ROS production, reduce ATP and cytochrome c oxidase or COX IV levels when compared to those cells derived from age-matched healthy controls. An increased sensitivity to A β toxicity and worsening bioenergetic function over time were also seen in cells derived from AD patients contrary to those from controls (Cardoso *et al.*, 2004; Trimmer *et al.*, 2004).

1.2.2 Brain Hypometabolism

A role for alterations in brain metabolism leading to a hypometabolic state as part of AD progression has been documented since the 40’s and 50’s (Blass *et al.*, 2000). As mitochondria are the energy powerhouses of the cell, it is not unreasonable to assume that mitochondrial dysfunction may go hand in hand with adaptations in the metabolic profile of the brain. Indeed, this appears to be the case in AD with the advent of a multitude of new imaging techniques, more accurate and versatile, revolutionising the field. Many recent publications have been able to highlight the importance of decreased central glucose metabolism in AD patients, in some cases prior to cognitive changes commonly associated with the disease stage seen at diagnosis (De Santi *et al.*, 2001; Mosconi *et al.*, 2008a; Mosconi *et al.*, 2008b; Mosconi *et al.*, 2009; Chen *et al.*, 2011). Decreases of ~25% in the cerebral metabolic rate (CMR) of glucose (CMR_g) are seen in AD, and are often accompanied by changes in the metabolic rate of oxygen (CMR_{O₂}) when compared to controls (Blass *et al.*, 2000; Cunnane *et al.*, 2011).

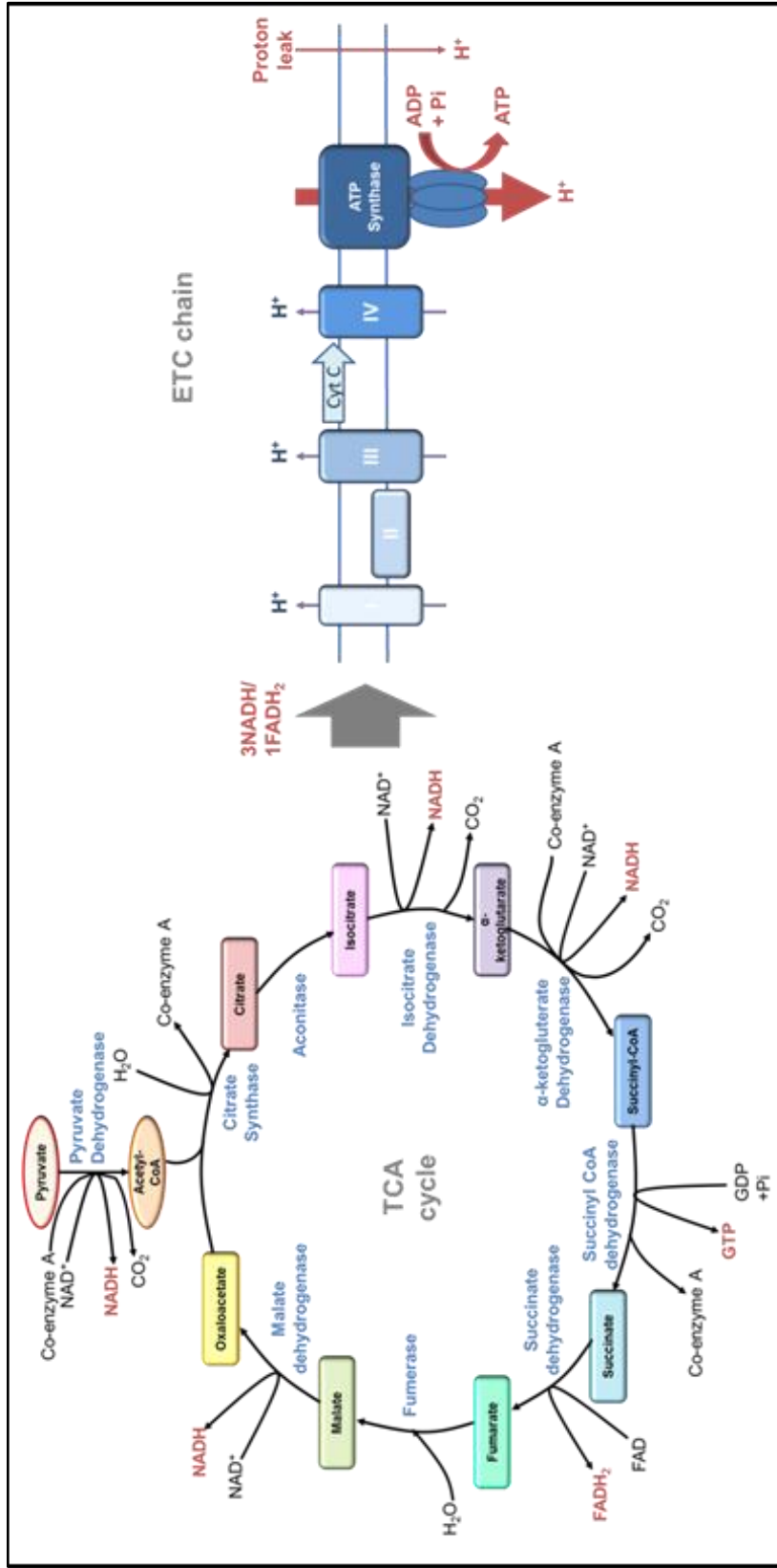


Figure 1.6 Simplified pictorial representation of the TCA cycle and electron transport chain and relevant proton exchanges.

Where TCA = tricarboxylic acid cycle, NAD/NADH = nicotinamide adenine dinucleotide, FADH = flavin adenine dinucleotide, GDP = Guanosine diphosphate, GTP = guanosine triphosphate, ADP= adenosine diphosphate and ATP= adenosine triphosphate. H+ is represents ion flux across the mitochondrial membrane, and I, II, III, IV denote the main complexes of the ETC.

Although it is still not entirely clear on how far these changes affect other metabolic substrates, Bubber and colleagues demonstrated a strong correlation of decreased CMR_g with key decarboxylase dehydrogenase enzymes, in particular PDH and KGDH, of the tricarboxylic acid cycle (TCA). These findings were supported by changes in both succinate dehydrogenase and malate dehydrogenase, increased activity of which is supportive of a change to an alternative energy metabolism pathway to bypass the blocks apparent in the TCA cycle (Bubber *et al.*, 2005). Corroborating the importance of these enzymes in AD, work *in vitro* and *in vivo* using mouse models of AD and isolated cell samples from patients has shown a co-localisation of amyloid within the mitochondria. In addition, the accumulation of mitochondrial amyloid appears to parallel that of other AD-type pathologies. This deposition was subsequently shown to have detrimental effects on mitochondrial respiration with decreased activity of both complex III (succinate-cytochrome c reductase) and COX IV (Caspersen *et al.*, 2005). Supporting these findings, a cortical proteome analysis performed by Chou and colleagues (2011) using a triple transgenic mouse model of AD, highlighted the dysregulation of many of the above mentioned enzymes, alongside members of other key mitochondrial processes such as fatty acid oxidation and ketone body metabolism. In light of this, the alterations in glucose transport receptors within the CNS during the progression of AD may have an amplified effect. A decrease in the levels of glucose transporter (GLUT) 1 and GLUT3 have been shown in AD patients when compared to controls, with decreases in the regulatory factor HIF-1 also observed (Liu *et al.*, 2008). Impairment of the glucose transport system and energy metabolism in AD has also raised the possibility of alteration of the insulin signalling pathway (See for full reviews Blass *et al.*, 2000; Mamelak, 2012).

1.2.3 Targeting the antioxidant system as treatment of OS

Possibly due to a lack of BBB penetration, trials of excess antioxidant administration to AD patients have been unsuccessful. Modified antioxidants with improved BBB permeation have been put forward as novel forms of pharmacological intervention, such as the mitochondrial targeted antioxidant, MitoQ. MitoQ combines the endogenous antioxidant ubiquinone with a triphenylphosphonium cation, allowing it to cross the BBB and accumulate inside the mitochondria as a result of its altered ionic state. Compounds such as MitoQ are being trialled in animal models of AD with some success, although it is too early to predict effects in humans (McManus *et al.*, 2011). Other therapeutic avenues include the upregulation of endogenous antioxidant systems

consisting of enzymes such as thioredoxin (Trx; Figure 1.7), glutathione peroxidase (GPX; Figure 1.7) and haem oxygenases (HMOX). The antioxidant response element (ARE) is an enhancer element that is responsible for the regulation of many constitutive and induced antioxidant enzymes and the control of cellular redox homeostasis. As such, it has strong therapeutic potential for oxidative stress related neurodegeneration and this has prompted further research into its regulation under stressed and non-stressed conditions. The ARE is activated through binding of the transcription factor, nuclear factor-erythroid 2 p45-related factor 2 (Nrf2) which itself is regulated by repressor proteins such as Kelch-like ECH-associated protein 1 (Keap1).

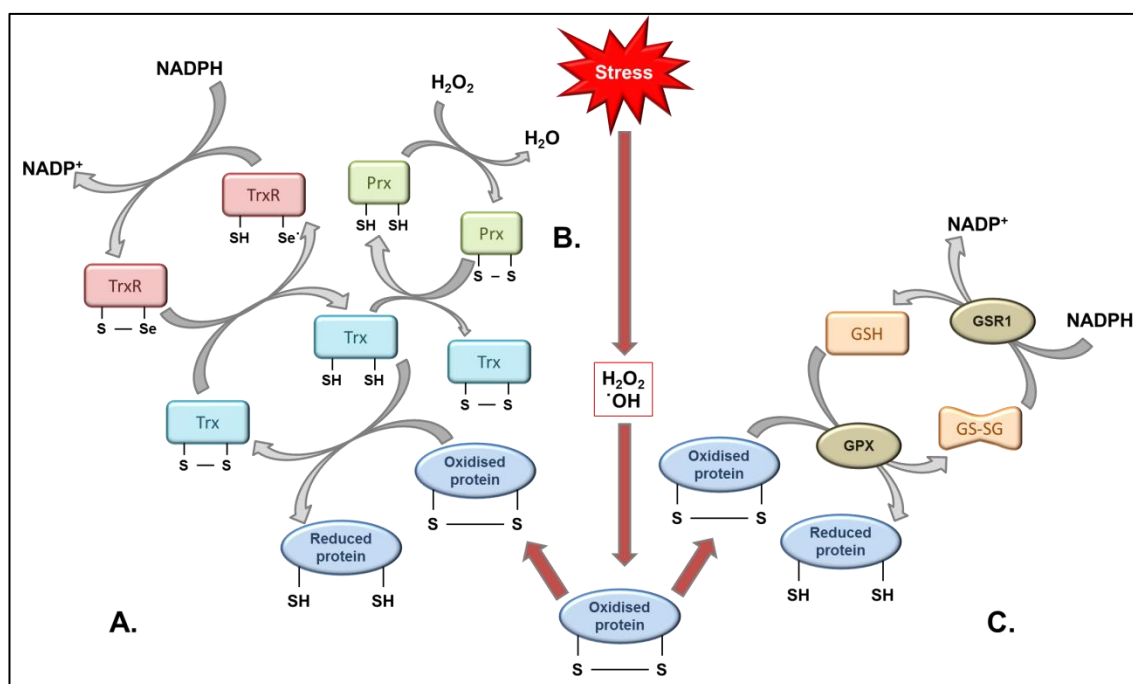


Figure 1.7 Overview of the antioxidant mechanisms of key endogenous small antioxidant molecules.

(A) Direct mechanism of action of the Trx redox system in detoxifying oxidized proteins after a stress event. Reduced Trx catalyses the reduction of disulfides (s-s) within damaged oxidized proteins. Trx is detoxified through reduction by thioredoxin reductase (TrxR), which relies on NADPH turnover for electron donation. (B.) Trx can also act indirectly by fuelling the turnover of peroxiredoxin (Prx), which acts to detoxify ROS such as H_2O_2 directly. (C) Glutathione (GSH) may also be oxidized by ROS and oxidized proteins, generating a s-s bridge between two glutathione molecules and catalyzed by glutathione peroxidase (GPX), forming GSSG. The GSSG can be reduced back to two GSH molecules by the action of glutathione reductase 1 (GSR1), and utilizing NADPH as the electron donor.

1.3 NRF2 ANTIOXIDANT RESPONSE ELEMENT

1.3.1 Nrf2-ARE Discovery and Structure

Nrf2 belongs to the basic-region leucine zipper (bZip) protein family, and at least three Nrf members are currently known and have been sequenced, namely Nrf1, Nrf2 and Nrf3. Nrf2 was originally isolated and localised by Yuet Kan and collaborators in the mid-90s where they were subsequently able to show that unlike Nrf1 it did not appear to have a role in murine growth and development (Moi *et al.*, 1994; Chan *et al.*, 1995; Chan *et al.*, 1996). The cytoprotective role of Nrf2 against oxidative or electrophilic stress was first described by Venugopal & Jaiswal in 1996, when they investigated the role of Nrf2 in ARE mediation of NAD(P)H quinone oxidoreductase 1 (NQO1) gene expression (Venugopal & Jaiswal, 1996). They were able to show that in the presence of xenobiotics Nrf1 and Nrf2 upregulated the expression and induction of NQO1. This was corroborated by the development of *Nrf2*^{-/-} mice that failed to induce the production of phase II detoxifying enzymes such as NQO1 (Itoh *et al.*, 1997). It is now well accepted that Nrf2 controls an array of over 200 genes under both basal non-stressed homeostatic conditions as well as following induction by redox perturbation (McMahon *et al.*, 2001; Chanas *et al.*, 2002; Thimmulappa *et al.*, 2002). Whilst many of these genes have actions directly related to cytoprotection, as had initially been suggested, others have more varied cellular actions. These hits include links with lipid and carbohydrate metabolism and regulation of chemokine receptor binding implicating a direct link with Nrf2 to the immune system response (Chartoumpekis *et al.*, 2013).

Nrf2 has since been shown to contain a number of distinct regions known as Nrf2-ECH homology (Neh) domains, and to date seven Neh domains have been described each with their own functional relevance (Figure 1.8 A). The C-terminal Neh3 domain is involved in the transcriptional activation of Nrf2 and has been shown to interact directly with binding to CHD6 (a chromo-ATPase/helicase DNA binding protein) during Nrf2 transcription. This in turn suggests a role for the Neh3 domain in particular as a transactivation domain enabling increased gene transcription to occur (Nioi *et al.*, 2005). The N-terminal domain Neh2, on the other hand, is crucial in the negative regulation of Nrf2's activity.

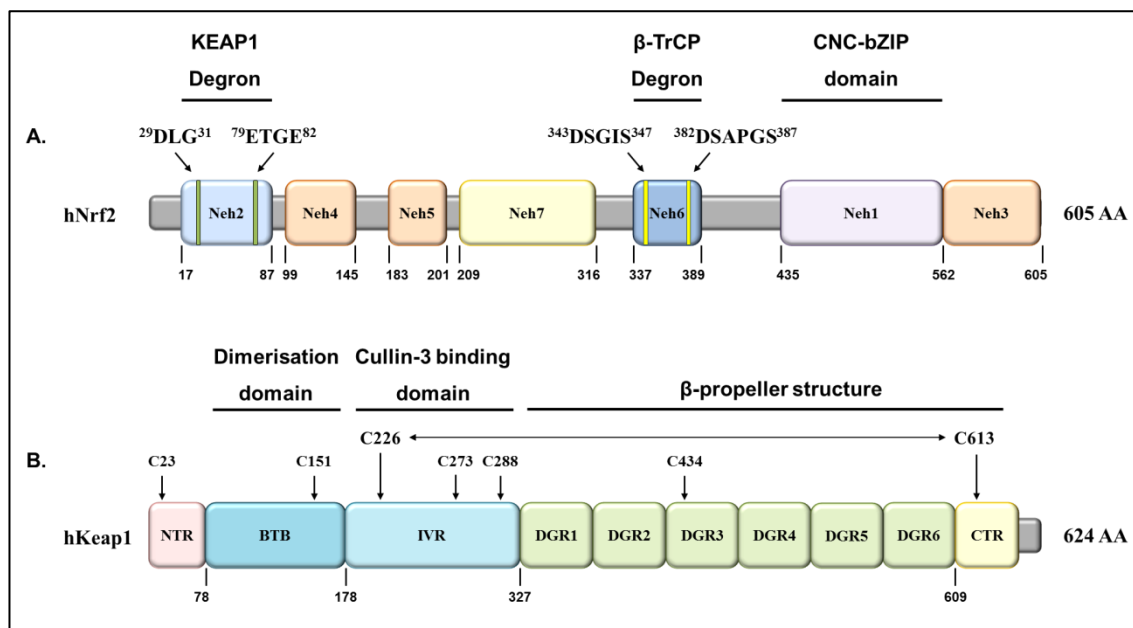


Figure 1.8 Domain structures of human Nrf2 and Keap1

(A) Nrf2 contains six well-conserved domains, from Neh1 to Neh7. Neh2 is essential for Keap1 complex formation and Neh1 is notably involved in the dimerization of Nrf2 with small Mafs, whilst more recently Neh6 has been shown to be important in β -TrCP binding. (B) In Keap1, the bric-a-brac, tramtrack, broad-complex/Poxvirus Zinc finger (BTB/POZ) domain contributes to homodimerisation. IVR is essential for interaction with Cullin 3 (Cul3), whilst the Kelch repeat domain (β -propeller structure) is essential for interaction with Nrf2.

Following on from the discovery of Keap1 in 1999, and its identification as an electrophile regulated suppressor of Nrf2 activity, the Neh2 domain was found to be vital in successful binding of Keap1 to Nrf2 (Itoh *et al.*, 1999; Katoh *et al.*, 2005). Electrophiles are described as molecules or ions that are electron deficient in some form, with these ranging from compounds with an overt positive charge (e.g. H^+), through those with a partial positive charge (δ^+ ; HCl), to those who fail to satisfy the octet rule (e.g. Borane). Further research showed it was possible for the Keap1 Kelch region to bind specifically to the Nrf2 amino terminal, which was antagonised by the presence of the electrophilic compounds diethylmaleate and catechol (Figure 1.8; Itoh *et al.*, 1999). Research has since elucidated a clearer view of the most likely mechanism of action and regulation of the Nrf2-Keap1 complex as well as the importance of the remaining Neh domains (Kobayashi *et al.*, 2002; McMahon *et al.*, 2003; McMahon *et al.*, 2004; Kobayashi & Yamamoto, 2006; McMahon *et al.*, 2006; Wang *et al.*, 2013a).

1.3.2 Nrf2 Mechanisms of Repression and Activation

Nrf2 is tightly regulated by Keap1 homodimers and the response initiated by the various stimuli is mainly down to destabilisation of the Nrf2-Keap1 complex. Although

originally believed to have a relatively passive cytosolic tethering action, further research indicates that Keap1 exerts a more dynamic role in Nrf2 repression and degradation. Keap1 is known to homodimerize and disruption of this dimerization greatly diminishes its ability to bind Nrf2 (Zipper & Timothy Mulcahy, 2002). Crystal structure analysis showed that the repeat sequence in the Kelch domain contains six structurally similar β -propeller blades. One of these blades binds to a conserved hairpin motif at the C-terminus end of the Neh2 Nrf2 domain prompting further binding of the Neh2 domain already described by also binding at the DLG motif thereby enhancing stabilisation of the complex (Kensler *et al.*, 2007). Keap1 aids in the targeting of Nrf2 for ubiquitylation by acting as a substrate adaptor protein for the cullin-3 (Cul3) RING-box 1 (RBX1) E3 ubiquitin ligase complex (CRLKeap1; Figure 1.9; Kobayashi *et al.*, 2004; Zhang *et al.*, 2004). In this way, Keap1 is able to quickly channel Nrf2 down a proteasomal degradation pathway, maintaining only low basal levels of antioxidant activity under normal physiological conditions.

More recent work has highlighted an alternative Keap1-independent regulatory pathway of Nrf2. It is through this pathway that the Neh6 domain of Nrf2 exerts its role (McMahon *et al.*, 2004). Two conserved peptide motif regions, DSGIS and DSAPGS, within the Neh6 domain are recognised by the β -transducin repeat-containing protein (β -TrCP). Phosphorylation of the DSGIS motif of β -TrCP by GSK3 increases its ability to repress Nrf2 activity allowing further control of Nrf2 regulation (Rada *et al.*, 2011; Rada *et al.*, 2012; Chowdhry *et al.*, 2013). It is worth noting that the Neh6 domain, unlike the better-described Neh2 domain, is redox insensitive thereby separating the roles of the two repression pathways known to exist for Nrf2 management. This opens the door for other mechanisms of regulation which may include indirect modulation through the insulin signalling pathway by influencing GSK3 activity through Akt regulated inhibitory phosphorylation. Furthermore, this may provide another link between altered Nrf2 activity and the progression of AD given the reported elevation in GSK3 activity in AD, confirmed by attenuation of amyloid pathology following GSK3 inhibition (Avrahami *et al.*, 2013).

Nrf2 activation occurs largely as a result of redox or inflammatory stress exposure. Upon cellular stress stimulation the ability of Keap1 to present bound Nrf2 for degradation is inhibited by modulation of cysteine residues present on Keap1. This modulation results in failure to induce proteasomal degradation of the CNC-bZIP factor on Nrf2, in turn allowing for a build-up of unbound newly translated Nrf2 to occur. Free

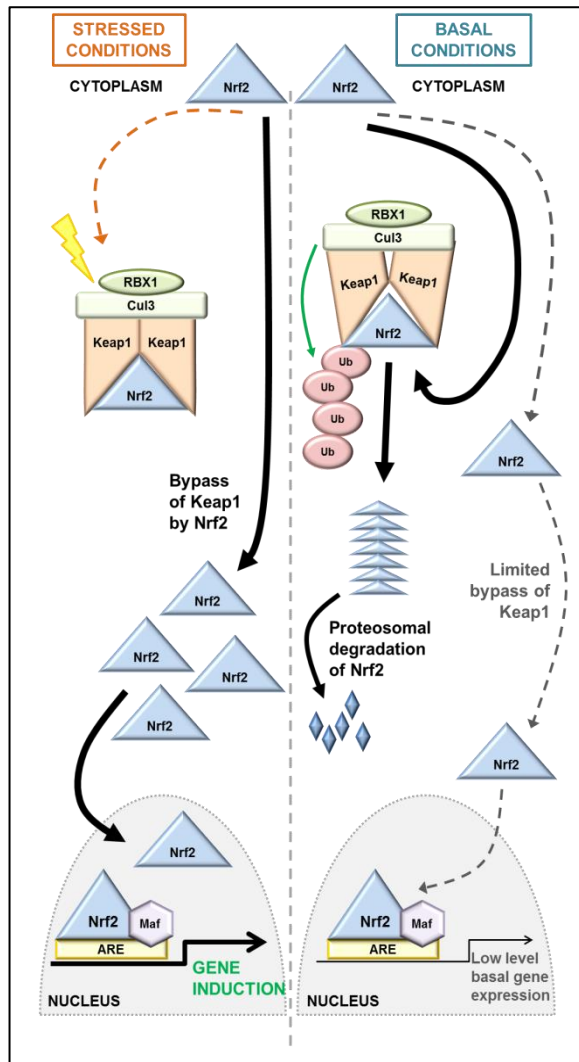


Figure 1.9 Nrf2 regulation by Keap1 under stressed and basal conditions.

Basal: Newly synthesized Nrf2 is rapidly sequestered in the cytoplasm by Keap1. Once bound it is targeted for proteasomal degradation following the formation of the CRLKeap1 complex. Rapid ubiquitylation and degradation of Nrf2 releases the Keap1 homodimer leaving it free to bind Nrf2 and repeat the process. A small percentage of Nrf2 evades Keap1 binding, translocates to the nucleus, heterodimerizes with small Maf proteins and maintains low level transcription of ARE-driven genes. Stressed: Keap1-Nrf2 complexes undergo a conformational modification that prevents the CRLKeap1 driven ubiquitylation of Nrf2. Unable to release Nrf2, Keap1 is prevented from curtailing further Nrf2 turnover, allowing newly synthesized Nrf2 to bypass Keap1 binding and translocate directly to the nucleus where it heterodimerizes with small Maf proteins and induces increased target gene transcription by binding to ARE sequences.

Nrf2 is then able to bypass the Keap1 complex and cross out of the cytoplasm into the nucleus, whereupon it can bind to so called small musculoaponeurotic fibrosarcoma (Maf) proteins forming dimers (Figure 1.9). Three Maf proteins have currently been characterised, namely MafF, MafG and MafK. This dimerization in turn prompts the binding of Nrf2 to ARE and thereby induces increased gene transcription by Nrf2 (Kobayashi & Yamamoto, 2006).

Of note is the ability of different electrophiles, including reactive metals, to induce the alteration of different stress sensors on the Keap1 motif; indicating the ability to specifically manipulate Keap1 inhibition targeting depending on the stress pathway present. This is in large part due to the relatively cysteine rich make up of Keap1. Targeting of diverse reactive cysteines within the Keap1 makeup by electrophiles usually results in the stabilisation of the Nrf2-Keap1 complex, as mentioned above. In particular, Cys-273 and Cys-288 are essential in maintaining the normal cellular turnover of Nrf2 (Yamamoto *et al.*, 2008); whilst Cys-434 also targeted by innate electrophiles such as NO-induced 8-nitroguanosine-3',5'-cyclic monophosphate causes Nrf2 induction by S-guanylation of Keap1 (Figure 1.10;

Fujii *et al.*, 2010). More recently studies have investigated the potential therapeutic role of other electrophiles, such as *tert*-butylhydroquinone (*t*BHQ) and sulforaphane (SFN), in the treatment of neurodegenerative disorders including PD and AD. Both *t*BHQ and SFN have been shown to interact with Cys-151 within the BTB domain of Keap1 alongside the stress-induced cell signal response NO (Figure 1.10; McMahon *et al.*, 2010). Studies have since suggested potentially beneficial roles for SFN/*t*BHQ activation of Nrf2 using transgenic mouse models of AD that demonstrated increased clearing of amyloid following administration of *t*BHQ and protective effect for SFN on dopaminergic neuron toxicity in a model of PD (Akhter *et al.*, 2011; Morroni *et al.*, 2013). Nrf2 interacts with both exogenous and endogenous compounds, such as SFN and nitric oxide (NO) which is predominantly produced through the activity of nitric oxide synthases (NOS). In addition, the transcriptional activity of Nrf2 can also be induced by a number of reactive metal(loid)s including Zn^{2+} , Cd^{2+} and Se^{4+} . Reactive metals differ from many other Nrf2 activators in their simultaneous use of two reactive cysteine sites on the Keap1 residue, namely Cys226 and Cys613 (Figure 1.10). Zn^{2+} , the most likely physiological reactive metal candidate, along with other metals non-covalently interacts with these cysteins which form a transient disulphide bridge in the presence of H_2O_2 (Fourquet *et al.*, 2010; McMahon *et al.*, 2010).

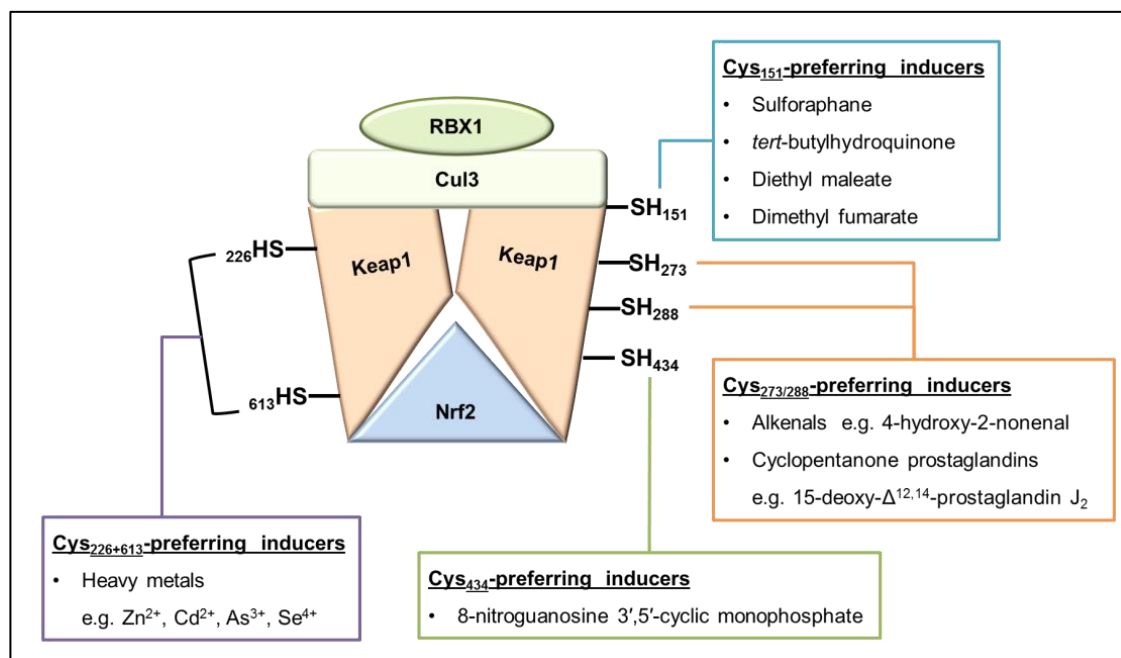


Figure 1.10 Summary of preferred cysteine binding sites for a selection of commonly referred to Nrf2 activators

Recent research in single cells has elucidated that one of the mechanisms behind the Keap1 modulatory inhibition results from increased strength of binding via the

ETGE and DLG motifs. Using fluorescence imaging live microscopy, it has been possible to identify two distinct conformations of the Nrf2 complex combining either a single or dimerised form of Keap1. Inducers promote the accumulation of the ‘closed’ Keap1 dimerised Nrf2 complex preventing the proper cycling of Nrf2 and sequestering Keap1 molecules inhibiting them from binding further Nrf2 (Baird *et al.*, 2013). Implications of this would place the emphasis on changes within the RBX1-Cul3-Keap1 setup instead of on Keap1-Nrf2 binding to alter the susceptibility of the complex to ubiquitination. Indeed, alterations in conformation of the RBX1-Cul3-Keap1 towards prevention of ubiquitination are supported by a lack of evidence towards activators of Nrf2 being capable of inducing release of the bound Nrf2 (Eggler *et al.*, 2005).

As the discovery of the second known modulator for Nrf2, β -TrCP, occurred only recently; its mechanism of action is less well characterised. Two isoforms of β -TrCP are known to exist, referred to simply as β -TrCP1 and β -TrCP2. As previously alluded to, degradation of Nrf2 by β -TrCP targeting is aided by GSK3 phosphorylation. β -TrCP has been shown, like Keap1, to bind to a Cul-RBX complex known as SCF ^{β -TrCP}. In addition to the RBX1 protein, members of the SCF family of E3 ubiquitin ligases each consist of the adapter protein Skp1, the scaffold protein Cul1 and an F-box substrate receptor protein, the identity of which is dependent on the substrate to be ubiquitinated (Wu *et al.*, 2003). GSK3, known to be constitutively active unlike the majority of other kinases, can be negatively regulated by the phosphoinositide 3-kinase (PI3-K)/Akt insulin-signalling pathway (see above). Research has suggested a link between alterations in insulin and changes in Nrf2 signalling (Loh *et al.*, 2009; Chowdhry *et al.*, 2010). Therefore, it is possible this alternative repression pathway is partly responsible for these changes. However, more work is needed to fully characterise β -TrCP and its role in Nrf2 regulation as well as potential roles outside of the Nrf2 pathway. For a comprehensive and exhaustive review, it is worth referring to work in press from our collaborators (Tebay *et al.*, 2015).

1.3.3 Nrf2-ARE and the CNS

Nrf2 is ubiquitously expressed, with high levels expressed in many of the major organs such as the heart, lungs, liver and brain. In relation to the distribution of Nrf2 within the CNS certain discrepancies exist, with studies reporting Nrf2 to be present in neurons, glial cells or neurons and glial cells (Hong *et al.*, 2010; Tanaka *et al.*, 2011). Some of these discrepancies may be linked with the manner of Nrf2 activation and the individual stressors administered. However, it is now well accepted that both glial cells

and neurons can express Nrf2 within the brain and this expression increases following trauma (Dang *et al.*, 2012). In general it is thought that glial cells have increased activation of the Nrf2 pathway following trauma, in no small part due to their important roles regarding management and resolution of inflammation and other damaging events (de Vries *et al.*, 2008; Johnson *et al.*, 2008). Research using known inducers of the Nrf2 pathway, such as sulforaphane, have been shown to improve resolution of trauma related damage and diminish detrimental toxic effects of ROS such as protein carbonylation (Hong *et al.*, 2010). Activation of the Nrf2-ARE pathway in astrocytes has been shown to promote astrocyte cellular survival when exposed to stresses (Lee *et al.*, 2003; Shih *et al.*, 2003). And with the preponderance of research supporting a role for OS, inflammation and ROS it is maybe not surprising that Nrf2 has become, in recent years, a target for research within the neurodegeneration field.

1.4 GLIAL CELLS AND NEUROPROTECTION

Cells falling under the umbrella term of glia incorporate a variety of subtypes including oligodendrocytes, astrocytes, microglia and Schwann cells. Previously, many glial cells were believed to play only a limited role in maintaining healthy brain function. However, it is now understood that they are equally as important as their neuronal counterparts in many cases, and partake in a wide variety of intra and inter-cellular processes. Of particular interest and of relevance to AD are the astrocyte family, which are known to be important in direct interactions with their surrounding neurons including such roles as energy homeostasis and maintaining healthy neuronal signalling profiles. Another of the key cell types believed to be of importance in AD and neurodegenerative disorders are the microglia, so called resident macrophages of the CNS.

1.4.1 Astrocytes

A star-shaped sub-type of glial cells, astrocytes are interspersed among neurons in the brain using their extensive processes to form organised domains with little overlap observed between adjacent cells. The specialisation of the processes put out by the astrocytes promotes their ability to affect a wide range of pathways within the brain (Verkhatsky *et al.*, 2010). This ranges from close interaction with neurotransmitters released into neuronal gap junctions prompting the coinage of the term tripartite synapse (replacing the previously accepted solely neuronal bipartite synapse), to the endfeet processes that link with intraparenchymal blood vessels (Bélanger *et al.*, 2011; Tremblay *et al.*, 2011). This complex network of processes, along with their unique

architectural and phenotypic features, enables them to play a vital role in neuronal homeostasis as well as contributing to neuronal function and promoting neuronal survival through the release of intrinsic factors. Astrocytes have been shown to have a role in neuronal energy metabolism playing a part in glucose, insulin and glutamate pathways. The so-called astrocyte-neuron lactate shuttle model is initiated by glutamate-induced astrocytic activation. Although initially contested, further research appears to support the theory that subsequent lactate production by astrocytes is released into the extracellular space allowing for its potential use as an energy source by neurons, either at a basal level or as a result of cellular activation (Loaiza *et al.*, 2003; Kasischke *et al.*, 2004; Serres *et al.*, 2004; Magistretti, 2006; Erlichman *et al.*, 2008; Wyss *et al.*, 2011). Other known astrocytic roles include ion and water homeostasis, tissue repair and defence against OS (Allaman *et al.*, 2010; Bélanger *et al.*, 2011).

In order to maintain healthy cerebral function, it is important that the symbiotic relationship between astrocytes and neurons is correctly maintained. The dysregulation of this relationship has been shown to play an important role in many neurodegenerative disorders including Alexander disease, caused by a primary dysfunction of astrocytes and characterised by the presence of intracellular protein aggregates (Rosenthal fibres), PD, ALS and AD (Verkhatsky *et al.*, 2010; Wang *et al.*, 2011; Yoshida & Nakagawa). As mentioned previously, OS has been linked with early stage neuronal damage in numerous neurodegenerative disorders. Overwhelming the astrocytic OS defensive system and/or affecting its protection mechanisms leads to neuronal impairment, as a result of disruption to the symbiotic relationship mentioned above as well as the damaging production of ROS. However, OS has also been shown to cause a glial reaction that results in the production of activated microglia and astrogliosis which can prompt the subsequent release or activation of potentially detrimental mediators such as the NF- κ B pathway, NO and glutamate (Hamby *et al.*, 2006; Sofroniew, 2009). Astrogliosis is characterised by hypertrophy of the cell, changes in gene expression and alterations in the expression of the cytoskeleton intermediate filaments, glial fibrillary acidic protein (GFAP) and vimentin (Barreto *et al.*, 2011). The presence of astrogliosis has been noted as part of the post mortem pathology associated with AD, with some located within the A β plaques. Further studies have shown that when A β is administered in culture, astrocytes are able to internalize and degrade the A β fragments. However, this causes metabolic changes to the astrocytes, which can be detrimental especially at higher doses of A β (Allaman *et al.*, 2010). This posits an important role for astrocytes in the metabolism and removal of A β in both healthy and AD brains. Recent research

suggests that the upregulation in A β and resultant changes in astrocytes could be the result of a protective mechanism to allow neurons to survive under much higher levels of OS (Smith *et al.*, 2002; Hayashi *et al.*, 2007; Nakamura *et al.*, 2007; Nunomura *et al.*, 2010). In view of the above, the investigation of astrocytes and endogenous antioxidant mechanisms as targets for AD becomes all the more essential.

1.4.2 Microglia

Microglia are a form of glial cell termed the resident macrophages of the CNS and as a result are one of the frontlines of immune defence within this system. The idea of resident macrophage cells within the brain and CNS was first suggested in the early parts of the 20th century by Pio del Rio-Hortega and his key hypotheses still hold true today (Kettenmann *et al.*, 2011). However, it wasn't until the 1960s with work performed by Kreutzberg using his novel facial nerve lesion model that microglial research really started to take off. The novel lesion model allowed the study of microglia injury responses without disrupting the BBB and with the added benefit of being able to separate out the role of microglia from invading monocytes (Kettenmann *et al.*, 2011). Following on from Kreutzberg's work, the introduction of an efficient technique for isolating large numbers of microglia from rodent brains by Giulian and Baker (1986), allowed more detailed *in vitro* studies of microglia to be undertaken. Microglia have since been shown to exist in a distinct 'resting' state, associated with healthy tissue. However, they are armed with the ability to rapidly and profoundly alter their cell morphology, gene expression and functional behaviour in response to traumatic or detrimental alterations in tissue conditions. This alteration from the typical resting state has since been termed microglial activation, and enables microglia to return to a more mobile phenotype allowing them to migrate to sites of damage or infection by following a chemotactic gradient. Tissue damage can also induce an increase in microglial cell proliferation, with microglial cells playing a crucial role in the coordination of the CNS immune response but also in the subsequent re-establishment and maintenance of a healthy tissue environment and cellular population.

More recent research has overturned the long-term belief that microglial cells present within a healthy brain environment were quiescent and functionally dormant. Scientists have now indicated that even under optimal environmental conditions microglial cells are constantly scanning their surroundings, with resting motility of cellular projections occurring in as little as a couple of minutes (Davalos *et al.*, 2005; Nimmerjahn *et al.*, 2005). It has also been demonstrated that microglia are capable of

communicating directly with neurons even whilst maintaining their so-called ‘resting state’ (Tremblay *et al.*, 2010; Li *et al.*, 2012). This may in turn suggest a role for the constant microglial adjustment in aiding microglia to respond rapidly to perceived threats.

The activation of microglial cells can, in a similar manner to classical macrophages, be subdivided into two predominant phenotypes defined by their chemical profiles as either pro-inflammatory (M1) or anti-inflammatory (M2). Although not always mutually exclusive, as some cytokines such as interleukin (IL)-6 can have both pro- and anti-inflammatory roles, a subset of well-established inflammatory mediators are often used to ascribe either an M1 or M2 phenotype to macrophages and microglial cells. Characterisation of an M1 phenotype is often confirmed through the presence of cytokines including IL-1 β , tumour necrosis factor- α (TNF- α) and high levels of IL-12, in combination with other cell markers, such as chemokines, and activation of stress-induced pathways including NF- κ B (Martinez & Gordon, 2014). In contrast, an M2 phenotype is more often attributed in the presence of high levels of IL-10 combined with low IL-12, increased expression of transforming growth factor- β (TGF- β) and, in mice, heightened expression of markers such as YM1 (aka chitinase-3-like protein-3; Chi3l3) and arginase-1 (Arg1). However, what is becoming increasingly clear is the complex ability of the stimuli-response interaction to define the resulting macrophage response; preventing the absolute categorisation of many of the subsequently expressed signalling molecules.

Recent work has suggested a potential priming ability of microglial cells, exemplified by a heightened response to any secondary stimuli. This usually results in an increased M1 like phenotype with an amplified release of known pro-inflammatory markers. Ageing has been suggested as one of the factors capable of inducing a priming effect in microglial cells (Dilger & Johnson, 2008), with studies using animal models suggesting an important role for ageing in altering the manner in which the immune system responds to challenges (Luo *et al.*, 2010). Ageing being the biggest risk factor for many neurodegenerative conditions it is maybe not surprising that microglial priming and alterations in both microglial and astrocytic responses have been associated with not only AD but also PD, Prion’s disease and ALS amongst others (Li *et al.*, 2004; Cunningham *et al.*, 2005; Purisai *et al.*, 2007; Schilling & Eder, 2011; Ramaglia *et al.*, 2012). It is also worth making note of the association of infection related immune insults in the aged and a propensity for increased development of neurodegenerative

diseases including direct effects on immune related cells such as microglia and astrocytes (Butovsky *et al.*, 2005; Henry *et al.*, 2009; Hughes *et al.*, 2010; Sy *et al.*, 2011). For more information and a thorough and exhaustive review on microglial physiology and function, one should refer to the work published by Kettenmann and colleagues (2011).

1.5 AD AND THE IMMUNE SYSTEM RESPONSE

Along with OS, a role for alterations in the immune system has been suggested as being influential in the development of AD. In particular an increased presence of inflammation and associated markers has been reported in patients diagnosed with AD. However, the immune response is a highly intricate and diverse system with multiple potential points of activation and some of these responses will be affected by the relatively isolated status occupied by the brain. This is largely due to the bodies additional protective barriers placed around this potentially highly vulnerable organ which include such shielding measures as the BBB.

1.5.1 Innate vs Adaptive Immune Response

Two main forms of immune response exist in humans and are largely conserved throughout the mammalian kingdom. These are the innate and adaptive immune response and they each have key roles in the adaptation of the body to detrimental events such as infections and trauma (Parkin & Cohen, 2001). The innate immune system is responsible for any immediate reaction to a perceived threat. It does not differentiate between specific pathogens and instead relies on the recognition of conserved features of pathogens by its arsenal of cells to induce an activation cascade capable of destroying the threat. Activation of the innate immune pathway can lead to two main outcomes, which are inflammation and phagocytosis. Included in the cells that are involved in phagocytosis are the macrophages such as the microglia of the CNS described previously. As they can also be present in permanent resident form, they are some of the first immune cells to respond to an insult and therefore play an important role in the initiation of the immune response cascade both releasing and being targeted by many of the important signalling compounds involved in the orchestration of the immune response.

On the other hand, as the name suggests the adaptive immune system relies on building up a library of previous pathogen exposures, allowing it to produce specific immune responses targeted to individual pathogens following any re-exposure. This

tends to be a slower process than the innate immune response and is reliant on information from prior exposure to function. However, it is worth noting that many immune cells will not exclusively be activated by either immune pathway and cells including the likes of macrophages can be activated by both the innate and acquired immune pathways through differing mechanisms (Davies & Taylor, 2015). By this stage, it is clear that the immune system comprises a highly complex network of reaction cascades as well as cell types, all of which are capable of catering to specific components of a toxic insult or injury.

1.5.2 Neutrophils, natural killer cells, B Cells and T Cells; the contribution of the blood born immune cells

Balancing factors from both the innate and adaptive immune system, blood born immune cells play a crucial role in the response to immune challenges. Participants in the innate immune response such as neutrophils and natural killer (NK) cells are able to rapidly respond to novel immune threats. Neutrophils, the most abundant type of white blood cell in the majority of mammals, are rapidly released from the bone marrow into the blood upon immune activation and react to cytokines and chemokines in order to orient themselves towards the target site (Parkin & Cohen, 2001). They are one of the hallmark cells in the acute phase response of the innate immune system and have just recently been suggested to play a more active role in the development of hallmark pathologies related to AD (Zenaro *et al.*, 2015).

Believed to be involved in obesity-related peripheral inflammation, B-cells, T-cells and NK cells are all lymphocytes, with both B- and T- cells playing central roles in the adaptive immune response (Seijkens *et al.*, 2014). B-cells are primarily responsible for the production of an immune antibody response and are activated and released from the spleen having migrated there from the bone marrow. Furthermore, memory B-cells circulate in the blood stream and enable the rapid response to previously detected antigens typical of the adaptive immune system. T-cells, which mature in the thymus instead of the spleen, are split into different sub-families according to their physiological role, and include T helper cells and natural killer T cells. Whilst T-helper cells aid other members of the immune response as the name suggests, natural killer T cells help bridge the gap between the innate and adaptive immune response by recognising glycolipid rather than major histocompatibility complex (MHC) molecules. Finally, NK cells are critical to the innate immune system instead of the adaptive immune response, providing backup to the neutrophil response they differ from other

lymphocytes as they do not require MHC markers and antibodies in order to detect stressed cells, thereby filling a niche role within the immune system (Parkin & Cohen, 2001). The role of many of the key blood born immune cells in the inflammatory response in neurodegenerative disorders, such as AD, was for many years deemed minimal, with the majority of the immune response triggered in AD believed to be driven and regulated by resident immune cells such as microglia (Heneka *et al.*, 2015). However, recent work has supported a role for peripherally derived immune cells in the promotion of AD pathology and may coincide with impairment of the BBB and amyloid deposition in the vasculature (Togo *et al.*, 2002; Baik *et al.*, 2014; Zenaro *et al.*, 2015).

1.5.3 The Role of Chemokines and Other Signalling Molecules in the Immune Pathway

As was described previously, it is already understood that resident immune cells such as microglia can undergo differentiation or priming to promote either of two different cell profiles. These are described as either a pro-inflammatory M1 profile or a resolution state designated as M2. Key to distinguishing these two differentiation states is the individual signalling molecule profile associated with them. Signalling molecules such as cytokines and chemokines are essential in aiding the orchestration of the immune system's response to a perceived threat. They also play a role in identifying potentially relevant downstream pathways for further investigation as the presence of specific molecules may predominantly favour the activation of particular downstream signalling.

1.5.3.1 Pro-inflammatory Signalling

Key members of the pro-inflammatory signalling pathway, which as the name indicates promotes the maintenance of an inflammatory state, are well characterised and include cytokines such as IL-1 β , TNF- α , and interferon- γ (Mosser & Edwards, 2008). Other pro-inflammatory signals include the likes of inducible nitric oxide synthase (iNOS), which is primarily driven by the presence of an oxidative environment. Markers such as IL-6, as mentioned previously, are capable of acting in either a pro- or anti-inflammatory manner depending on the context of the exposure. Release of pro-inflammatory signals, as well as instigating the activation of many pathways within the immune system such as the activation and/or recruitment of immune cells, can also initiate subsequent downstream signalling leading to changes in both gene and protein markers. An example can be made of IL-1 β , which subsequent to cleavage by caspase 1

can impact on numerous cellular processes including cell differentiation and targeting of cells for apoptosis.

IL-1 is a small family of cytokines comprising to date eleven members, with the two well most well-known and best-characterised isoforms known simply as IL-1 α and IL-1 β (Palomo *et al.*, 2015). Products of two separate genes present on chromosome 2, both IL-1 α and IL-1 β are produced as precursor proteins requiring cleavage to present their mature form (Patel *et al.*, 2003). And whilst pro-IL-1 α is active prior to cleavage, although its activity is significantly enhanced following cleavage; pro-IL-1 β requires activation by the converting enzyme, caspase 1. Cleavage of IL-1 β by caspase 1 occurs upon activation of the inflammasome, which is integral to caspase-1 activation. Initiation of inflammasome production is an important part of the innate immune response when challenged with PAMPs (e.g. LPS) and DAMPs (e.g. A β) and its composition includes several pattern recognition receptor (PRR) families such as nucleotide-binding domain, leucine-rich repeat containing protein receptors (NLRs) and the absent in melanoma 2-like receptors, both of which are present in the human and mouse complex (Takeuchi & Akira, 2010).

Upon stimulation, relevant members of these families can oligomerise and form a caspase-1-activating scaffold whereby inactive pro-caspase-1 is recruited and as a result of oligomerisation is autoproteolytically cleaved to its active form. Although some stimuli dependent variations are observed in inflammasome make-up and activity, in general their role remains very similar with the majority combining to form a variation on a caspase-1 scaffold. NLRP3 inflammasome, so called after the predominant protein used to construct it, responds to the widest array of stimuli and these can include those such as mitochondrial ROS production, release of cathepsin B from ruptured lysosomes and the translocation of NLRP3 to the mitochondria (Guo *et al.*, 2015). In the majority of cell types, NLRP3 must be primed, an example of which is through lipopolysaccharide binding to the PRR toll-like receptor-4 (TLR4). In addition, breaking research has shown that inflammasomes may play a key role in the propagation of inflammation from cell to cell (Franklin *et al.*, 2014). Furthermore, activation of IL-1 β signalling as a result of inflammasome formation and activity has now been linked with the development of not only AD, but also some of the other known risk factors for AD, such as type II diabetes (TIID), as well as other forms of neurodegenerative disease including PD (Hook *et al.*, 2008; Stienstra *et al.*, 2011; Vandanmagsar *et al.*, 2011; Yan *et al.*, 2015).

1.5.3.2 Anti-Inflammatory Signalling

As for the pro-inflammatory signalling molecules, interleukins can also play an important role in the so-called anti-inflammatory or resolution pathway. Molecules involved in the termination of an inflammatory or immune response are most commonly engaged in roles such as the down-regulation of pro-inflammatory signals (including those mentioned above), enhancing removal of cellular debris and dysfunctional cells, as well as promoting healthy cellular regrowth where necessary. In other words, following activation of the inflammatory pathway and recruitment of immune cells by inflammatory markers, under normal conditions the anti-inflammatory signalling promotes the resolution of the immune response and a return to a healthy tissue environment. One of the most characterised anti-inflammatory cytokines is another member of the interleukin family, IL-10. Although first described as a T helper 2 (TH2)-type cytokine, expression of IL-10 has since been shown to be much more widespread than a single cell type within the adaptive immune system. Expression of IL-10 is now known to be associated with many immune cell types including a variety of different adaptive immune cells, such as T-cells and B-cells, as well as cells forming part of the innate immune response, such as myeloid dendritic cells (DC), macrophages, NK cells and neutrophils (Saraiva & O'Garra, 2010). IL-10 has been shown to play an active role in the suppression of pro-inflammatory cytokines such as many of those listed above and has been shown to be decreased in chronic inflammatory diseases such as multiple sclerosis. However, interleukins are not the only signalling molecules capable of attenuating an inflammatory state. Molecules such as Arg1, YM1 and mannose receptor 1 (MRC1) are just some of the other commonly represented anti-inflammatory markers in the literature (Mosser & Edwards, 2008).

1.5.3.3 Chemokine Signalling

Chemotactic cytokines, better known as chemokines, are a group of small signalling molecules secreted from cells that act as chemoattractants and activate both immune and non-immune cells in the periphery as well as the CNS. With the first chemokine identified in 1977 (platelet factor 4 aka CXCL4), the understanding of the importance and variety of roles performed by these small chemokines has greatly increased. Due to the size the chemokine family has reached in current times, it has been subdivided into four families based on the number and spacing of the conserved cysteine residues in the N-terminal position. These families are labelled CXC, CC, CXC3 and C, and are named according to the systematic nomenclature. However, as many compounds were only later identified as having chemokine activity; many

chemokines have two nomenclatures still in regular use. A list of some of the chemokines more frequently associated with neurodegenerative diseases can be found in Table 1.1; and whilst many are widely expressed due to their key role in recruitment of immune cells, a small subset has been suggested as being dysregulated in AD (McLarnon, 2012).

Signalling through members of the G-protein coupled receptor family, chemokines are believed to largely induce downstream inductions through the $G_{\alpha i}$ pathway (Ransohoff, 2009). Alternative pathways, however, also include activation of MAPK enzymes, such as the insulin sensitive extracellular-signal-regulated kinases (ERK) 1/2 MAPK. Although many chemokines can be produced and released by circulating immune cells, they have also been shown to be expressed in resident regulatory cells such as the astrocytes and microglia of the CNS, and more recently in neuronal cell populations (Rostène *et al.*, 2011). They are important modulators of the immune response throughout the body, however, they are particularly crucial within the CNS and the brain where there is often an altered immune response in comparison to that observed in the periphery (Ransohoff, 2009). Recent work has also indicated an endocrine role for some of the chemokines expressed natively in the brain. This may be of importance with regards to alterations in hormonal and immune response during disease (Callewaere *et al.*, 2007).

Chemokine	Chemokine Receptor	Cell recruitment and function
MCP-1 (aka CCL2)	CCR2	Phagocyte infiltration and microglial accumulation
MIP-1 α (aka CCL3)	CCR1, CCR5	Accumulation of activated glial cells and T cells, migration of immune cells from blood to brain
RANTES (aka CCL5)	CCR1, CCR3, CCR5	Migration of peripheral immune cells, potential induction of alternative microglial immune response
IL-8 (aka CXCL8)	CXCR2, likely CXCR1	Potent chemoattractant for activated microglia and neutrophils
SDF-1 (aka CXCL12)	CXCR4	Attracts both brain and peripheral immune cells, anti-inflammatory
Fractalkine (aka CX3CL1)	CX3CR1	Suppression of microglia activation, neuroprotective

Table 1.1 Summary of commonly quoted chemokines, their receptors and their main physiological functions in relation to AD.

Where MCP-1 is monocyte chemotactic protein-1, MIP-1 α is macrophage inflammatory protein-1 α , RANTES is ‘regulated on activation, normal T cell expressed and secreted’ and SDF-1 is stromal cell-derived factor-1. See Azizi *et al.* (2014), Lee *et al.* (2012a) and Bose & Cho (2013), McLarnon (2012) for further information.

1.5.4 The Complement Immune System

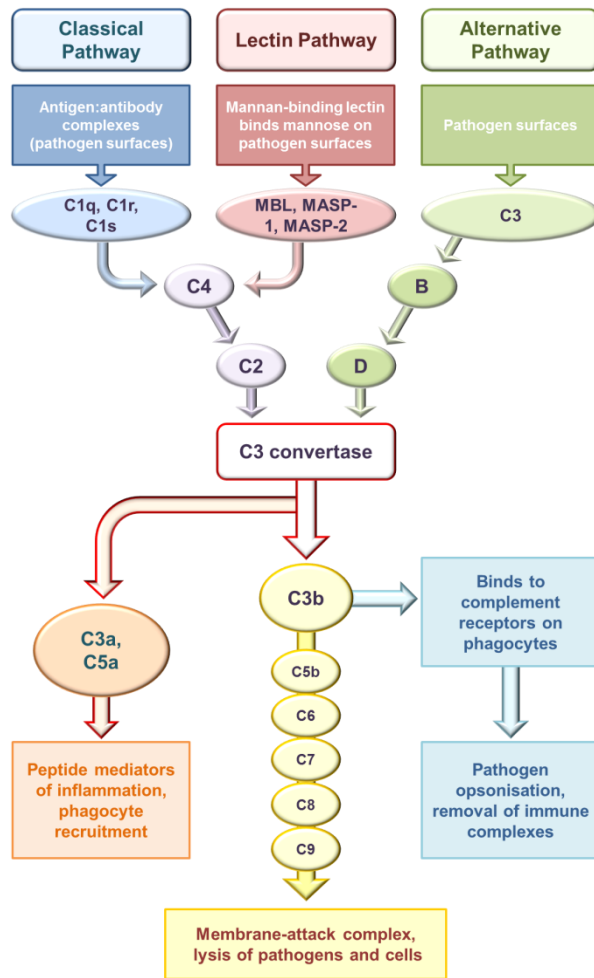


Figure 1.11 Simplified overview of complement system activation and its key physiological outputs

certain specific protein motifs including fibrillar amyloid (Veerhuis *et al.*, 2011). Activation of the pathway prompts the cleavage of C3 to form C3b which plays a key role in targeting molecules for phagocytosis. Working via an approach termed as opsonisation, C3b is deposited on the outer membrane of microbes with its presence targeting those molecules for phagocytosis and increasing the rate at which pathogens are neutralised.

Induction of the alternative pathway dispenses with the need for activators, relying instead on spontaneous hydrolysis of the internal thioester bond of circulating C3 to form so called ‘C3b-like C3’ which in turn binds with a second factor, factor B. This is itself cleaved to form C3 convertase initiating the cascade. As no outside initiator is required, the alternative pathway provides a constant turnover and

Members of the complement immune system stem largely from the liver, and can be found circulating within the blood stream and the extracellular fluid within tissues. They are a family of distinct plasma proteins, many of which are proteases that are themselves activated by proteolytic cleavage, and are responsible for the activation of the complement cascade which promotes the phagocytosis and/or lysis of pathogens. Although three activation pathways exist for the complement cascade, namely classical, lectin and the alternative pathway, they all combine to produce the same end function (Figure 1.11). The classical pathway is activated through exposure to activators, and these can include factors such as immune complexes, microbes and even

availability of the key opsonising C3b molecule of the complement system through tight balance of regulatory factors. Finally, the lectin pathway responds to PAMPs by recognition of mannose-binding lectin (MBL). MBL binds repeated carbohydrate patterns on the surface of pathogens and specific protease members of the complement cascade (MBL-associated serine protease; MASPs) recognise MBL initiating activation of the system (Bonifati & Kishore, 2007). Following activation, the individual strands of the complement system coalesce to activate cleavage of the focal C3 protein. It is this fragmentation of the C3 protein that drives the immune system response, allowing for cascading cleavage of subsequent complement proteins and induction of the inflammatory, phagocytic and lysis responses associated with the complement immune system.

In recent years, research has indicated a role for the complement system in AD along with alterations in a multitude of other immune related proteins. Increased gene expression of complement related proteins have been shown in the brains of AD patients (Yasojima *et al.*, 1999; Strohmeyer *et al.*, 2000). Whilst later work has linked progression of AD, as measured by the well described Braak stage scale, with progressive alterations in the particular subset of complement proteins demonstrating the highest degree of expression (Veerhuis *et al.*, 2011). Recent work using AD animal models has also supported a role for the complement system in AD (Chakrabarty *et al.*, 2010), although mouse models of AD may not prove to be the optimal system to investigate changes in complement induction (Reichwald *et al.*, 2009).

1.5.5 The Immune System and Its Response to Infection

Infection, which is a common activator of our immune system from birth, has also been implicated in neurodegenerative conditions. Susceptibility to infectious agents is correlated with aging once past infancy. In addition, an increased presence of infection related markers such as LPS or endotoxins have been associated with disorders demonstrating chronic low-grade inflammation such as obesity, T1D, atherosclerosis, *etc.*

Of particular importance in many infection-related responses are the TLRs, members of the PRR family. Present on most residential immune cells, TLRs are a key part of the innate immune system recognising structurally conserved microbial molecules. In humans, there are ten known forms of TLRs with additional and alternative receptors identified in rodents. TLRs share common motifs with the

interleukin-1 receptors and many interleukin cytokines will target TLRs during an immune response. Through the use of genetically modified mouse strains, it has been established that each individual TLR is responsible for the response to a specific subset of molecules. In the case of LPS, found in the outer membrane of gram negative bacteria such as those responsible for meningitis and meningococcal disease, activation is through the TLR4 receptor and is one of the better documented TLR pathways. Known to be present to varying degrees in even so called healthy individuals, LPS is commonly used as an infection-inducing agent in research in areas including metabolism, immunology and drug development. Studies have previously demonstrated the presence of an increased endotoxin load under conditions of DIO (Cani *et al.*, 2007). More recent studies have also indicated a potential role for LPS in the development of insulin resistance and resulting metabolic disruption, indicating it may have a more specific role to play in energy metabolism related disorders than simply aiding in the maintenance of a chronic inflammatory state (Lassenius *et al.*, 2011; Pussinen *et al.*, 2011). Whilst interest of late has also lighted on a potential role for systemic infections in the development of certain neurodegenerative diseases including AD (Sly *et al.*, 2001; Sheng *et al.*, 2003; Cunningham *et al.*, 2009; Krstic *et al.*, 2012), mutation of the TLR4 receptor has been shown to impact on A β pathology in a mouse model of AD, increasing pathology and negatively impacting on cognition (Song *et al.*, 2011). Finally, the impact of LPS on the ageing system in AD may be of particular importance given the potentiating effect observed when PAMPs and DAMPs are present in the same environment (Heneka *et al.*, 2014).

1.5.6 The Immune System and Disease

Designed to protect the body from perceived damaging exposures such as infection and trauma; the immune system as a whole, like other pathways, is still open to dysregulation. In fact, dysregulation of the immune system is the primary cause of diseases of the autoimmune variant such as ALS, and altered immune responses have been associated with long-term chronic inflammation such as occurs in obesity. It is now well established that increased inflammatory responses and activation of the immune system occur in many forms of neurodegenerative disease and AD is no exception. Links have been shown between increased inflammatory markers such as IL-1 β and TNF- α , alterations in chemokine profiles and increased activation of resident regulatory glial cells often inducing increased infiltration of immune cells such as peripherally derived macrophages and neutrophils. Increased expression of molecules

such as the chemokines MCP-1, fractalkine, MIP-1 α , MIP-1 β , RANTES and interferon- γ induced protein-10 (IP-10/CXCL10) in reactive astrocytes have all been linked with AD pathology *in vitro* (Johnstone *et al.*, 1999; Xia *et al.*, 2000). And whilst many patient cohort studies have failed to consistently report changes in specific circulating cytokines as measures of disease progression, it is well accepted that there is a localised presence of inflammatory cytokines occurring during neurodegeneration.

Another avenue down which dysfunctional activation of the immune system has been linked with neurodegenerative diseases, such as AD, is through the presence of increased markers of peripheral microbial infection such as LPS. *In vitro* studies have indicated that LPS is capable of interacting with amyloid production and its metabolism, with ICV LPS accelerating the rate of amyloid pathology in mice modelling the human APP Indiana (*APP*_{V717F}) mutation (Qiao *et al.*, 2001). Furthermore, IP LPS has been suggested to increase amyloid deposition and the ratio of A β ₁₋₄₂:A β ₁₋₄₀ in WT ICR mice, with cognitive impairment also associated with LPS treatment of these mice (Lee *et al.*, 2008). Moreover, phagocytosis and LPS-driven inflammation have been reported to increase the expression of both APP and A β from mononuclear phagocytes, providing a direct connection between LPS driven inflammation, activation of immune cells and increased amyloidogenic processing of APP (Spitzer *et al.*, 2010). And there are indications of heightened levels of LPS in the plasma of patients presenting with either mild cognitive impairment (MCI) or AD despite being termed free of active infection when bloods were taken (Zhang *et al.*, 2009). Finally in the elderly, these detrimental impacts from the immune system response occur in an environment also impaired by decreased levels of Nrf2 as a result of its natural age related decline.

1.6 LIFESTYLE RELATED RISK FACTORS FOR AD

As has been previously described there are no causative genetic mutations associated with sporadic AD, unlike the early onset FAD. The strongest risk factor is, in fact, simply age. Accordingly, research has been on-going to identify further risk factors with strong correlations to AD in order to aid in the targeting of new treatments and in the identification of potential early disease mechanisms. As might be expected, a selection of known health risks have now also been correlated with increased risk of developing AD including factors such as smoking, hypertension, obesity and TIID.

1.6.1 Hypertension and Vascular Dysfunction

Hypertension is itself a risk factor for cardiovascular events as well as being one of the triad contributing to metabolic syndrome, the other two being T1D and obesity. However, long-term hypertension is not limited to a detrimental effect on the periphery and is also a risk factor for cerebral events such as stroke. As a result, it is more commonly associated with VaD. As the name suggests, VaD results from impaired blood supply to the brain such as may occur following a series of small strokes, or may result from small vessel disease impairing blood flow in the microvasculature of the brain. The cerebral microvasculature encompasses the network of capillaries within the brain, but also the small arterioles and venules that support the capillary bed. It is damage to this vital supply network along with parts of the microvasculature that have been used to describe the vascular damage seen in both AD and VaD. More specifically, A β deposition has been shown to impact on vessel health through a reduction in vessel density, increases in the number of fragmented vessels present and changes in vessel diameter amongst others that have been used to describe the vascular changes observed in both AD and VaD (Zlokovic, 2005). Although VaD is classified as a separate form of dementia, a proportion of all dementia sufferers are diagnosed with so called mixed dementia, which is most often described as a combination of both AD and VaD pathologies. However, in more recent years this distinction has been questioned and the lines between AD and cerebrovascular disease, of which VaD is a form, have blurred with hallmark pathologies crossing the divide from both sides (Smith & Greenberg, 2009; Kalaria, 2010).

Changes in hypertension, as well as cholesterol and obesity, are known to be relatively complex in persons who go on to develop dementia. Patients presenting with AD have been shown to have lower blood pressure, cholesterol and body mass index (BMI) despite high levels of all of these factors in mid-life being associated with AD development. Recent research suggests AD driven impairment of the hypothalamus, mediated by increased inflammation and endoplasmic reticulum (ER) stress, may be the driving factor behind this switch in presenting phenotype (Ishii *et al.*, 2014; Clarke *et al.*, 2015). A β deposits have been shown to occur in the vasculature, and some groups suggest that lesions within the microvasculature may be some of the early symptoms of AD (Marchesi, 2011). It is now thought that the majority of A β vessel damage starts in the leptomeningeal and cortical cerebral vessels, before spreading to the subcortical layers and beyond (Viswanathan & Greenberg, 2011). A β is deposited on the outer

walls of vessels, where impaired clearance results in protein aggregation which works to undermine the vessels outer wall through the destruction of smooth muscle cells, leading to vessel weakening (Thal *et al.*, 2008). Furthermore, vascular deposition of amyloid is associated with increased inflammation, increased risk of cerebral angiopathy and impaired blood flow leading to increased risk of hypoxic damage (Agyare *et al.*, 2013). A β -related vascular damage continues spread inwards through the lamina following the disruption of the smooth muscle cells within the damaged vessels (Grinberg *et al.*, 2012). Although it is worth noting that limited structural damage to the subsequent endothelial layer has been reported, suggestions of functional impairment have been made, with administration of A β inducing endothelial constriction (Park *et al.*, 2011). It is thought that increased deposition of damaging proteins and damage to the vasculature resulting from conditions such as hypertension, promote a detrimental environment towards the maintenance of healthy vascular function and contribute to both AD and VaD (Smith & Greenberg, 2009; Sosa-Ortiz *et al.*, 2012). In addition it has also been suggested that key proteins believed to be involved in the transport of A β into the circulation, such as low-density lipoprotein receptor-related protein 1 (LRP1) in smooth muscle cells and CD36 in the endothelium, may be downregulated and/or impaired in AD (Park *et al.*, 2011; Kanekiyo *et al.*, 2012). These may prove to be useful alternative targets for future treatment initiatives.

1.6.2 Obesity and Inflammation

It is well established that there is an obesity epidemic spreading across both developed and developing countries; driven at least in part by our more sedentary lifestyle and increased consumption of refined food products marked by increased dietary consumption of fats and sugars. Incidences of obesity have more than doubled since 1980 according to the WHO, with almost 40% of the world's adults overweight in 2014 and 13% obese (WHO, 2015b). Obesity is defined as abnormal or excessive fat accumulation that may impair health and is directly caused by a positive energy imbalance resulting from increased energy consumption *versus* energy expenditure in an individual. Alteration of this energy balance results in a plethora of effects on both hormonal and metabolic pathways such as reduced respiratory quotient, hyperinsulinaemia, glucose intolerance and low grade inflammation (Lee, 2011). This imbalance is what leads to the subsequent hypertrophy and hyperplasia of white adipose tissue (WAT; de Ferranti & Mozaffarian, 2008). However, it is worth noting that WAT is not solely made up of adipocytes with other components including fibroblasts,

resident macrophages and monocytes playing just as important a role (Vázquez-Vela *et al.*, 2008).

The obesity driven storage of excessive lipids and subsequent adipocyte dysfunction combine to enable excess circulation of free fatty acids. The release of pro-inflammatory mediators from dysfunctional WAT, combine with changes in other important tissues including the liver and the CNS, to induce the establishment of a pro-inflammatory state following a high fat (HF) diet. Adipose derived factors, such as TNF- α , IL-6, IGF-1, are known to be increased in the circulation of people diagnosed with obesity, along with crucial hormones responsible for managing energy homeostasis, such as leptin and resistin (Vázquez-Vela *et al.*, 2008). These factors combine to bring about a state of both central and peripheral leptin and insulin resistance and lead to glucose intolerance (Arnold *et al.*, 2014; Davis *et al.*, 2014). A secondary consequence of the change in cytokine output is an alteration of the resident WAT macrophages from the traditional M2 profile associated with healthy WAT, to the classically activated M1 profile. This in turn promotes the recruitment and M1 differentiation of further macrophages, propagating and maintaining the inflammatory state whilst obesity persists (Balistreri *et al.*, 2010). More recently data has indicated a role for central insulin and leptin signalling impairment in AD leading to insulin and leptin resistance in the brain. Central insulin resistance in AD has been suggested to be linked to insulin receptor relocation with a diminished presence of downstream insulin signalling products (Zhao & Townsend, 2009; Moloney *et al.*, 2010). In addition, mouse models of AD have been shown to present with attenuated levels of leptin in the brain which may be linked to impaired hypothalamic signalling and an inhibition of leptin signalling following accumulation of leptin receptor within NFT (Pérez-González *et al.*, 2011; Bonda *et al.*, 2014; Ishii *et al.*, 2014; Perez-Gonzalez *et al.*, 2014).

As mentioned previously, obesity in midlife has been associated with increased risk of AD despite AD itself being associated with a consistent decrease in bodyweight over time (Marchesi, 2011). Of particular relevance to AD, are the chronic inflammatory state induced by obesity along with the alterations in insulin and leptin signalling. Studies performed in rodents have shown associations between HF diet-induced obesity and memory impairment in a variety of tasks, strengthening the potential link between obesity and AD (Granhölm *et al.*, 2008; White *et al.*, 2009; Morrison *et al.*, 2010; Pistell *et al.*, 2010; Freeman *et al.*, 2011). Many of the other disorders that commonly accompany obesity have also been intimated as risk factors in

their own right for AD, and these include hypertension (see 1.6.1), TIID (see 1.6.3), chronic activation of immune cells and elevated presence of infectious agents such as LPS (see 1.5.6; Cani *et al.*, 2007; de La Serre *et al.*, 2010; Lee, 2011; Oliveira *et al.*, 2011; Nakarai *et al.*, 2012).

1.6.3 Diabetes Mellitus and Insulin Resistance

Diabetes mellitus of the type II variant, otherwise known simply as TIID, results from a dysfunction of the body's use of the insulin it produces along with chronic elevation of circulating glucose. It is far more common than the earlier onset type I variant, accounting for approximately 80% of cases, and is strongly associated with previously described risk factors for AD such as hypertension and obesity. The pathophysiological factors behind TIID are limited to dysfunction of the insulin pathway. Twofold, they are described as deteriorating function of the insulin secreting β -cells of the pancreas, and the diminished effect of insulin on its various target tissues which has since been termed insulin resistance (Correia *et al.*, 2012).

Insulin resistance is linked with increased levels of OS and mitochondrial dysfunction, promoting cell death; all of which are also markers associated with late-onset AD. Furthermore, patients under treatment for TIID that are given insulin have the highest chance of going on to develop dementia (van der Heide *et al.*, 2006). However, this should be balanced by the increased severity of the disease, which is usually associated with insulin prescription. Insulin itself has been shown to accelerate APP metabolism to $A\beta$ by increasing the rate at which $A\beta$ is trafficked from the Golgi and trans-Golgi network to the plasma membrane. Insulin also promotes secretion of $A\beta$ and prevents degradation once released, by inhibiting the insulin-degrading enzyme. It would also appear that once present at a high enough concentration, $A\beta$ can further deregulate insulin signalling by acting as a competitive inhibitor to insulin binding (van der Heide *et al.*, 2006; de la Monte, 2009; Cholerton *et al.*, 2011). This is supported by research from our lab showing that inhibition of BACE1 in animal models increases insulin sensitivity and decreases circulating glucose levels (Meakin *et al.*, 2012). BACE1 inhibition in particular, as well as insulin sensitisation, could have beneficial effects on preventing AD development.

In addition to the functional changes mentioned above, insulin has also been linked with alterations in learning and memory. Studies of acute insulin administration consistently show improvements in spatial memory formation through hippocampal site

activation (Park *et al.*, 2000; Zhao *et al.*, 2004; Haj-ali *et al.*, 2009). Furthermore, mouse models of AD presenting with induced impaired insulin sensitivity have shown aggravated disease pathology (Ho *et al.*, 2004; Devi *et al.*, 2012). Clinical trials using acute insulin treatment have also been performed, most commonly with intranasal insulin administration. These appear to replicate other acute trials performed in rodents, with many showing improved cognition following treatment (Craft *et al.*, 2012). It is clear therefore from the complex and sometimes contradictory effects of chronic vs acute insulin administration and its relationship with ageing and AD that insulin is intimately linked with many aspects of AD pathology. What is still unclear is whether these alterations are part of the causative process aiding in initiation of the disease or whether they occur as a result dysfunction within alternative pathways.

1.7 NRF2 IN DISEASE PATHOLOGY

The ubiquitous expression profile of Nrf2, in combination with the large number of genes under its control, has lent it to be a subject of interest in a variety of disease pathologies. Links have been established between Nrf2 and degenerative diseases as diverse as various forms of cancer, obesity and associated non-alcoholic steatohepatitis (NASH), kidney disease and more recently neurodegenerative disorders such as PD and AD.

1.7.1 Cancer

Despite being the most heavily researched function of Nrf2 to date, the role of Nrf2 in cancer remains unclear, appearing to play a role at both ends of the spectrum. As previously explained, too little Nrf2 heightens ROS production and impacts cellular health and protection. Concurrently, heightened Nrf2 expression is present in many forms of cancer, often as a result of somatic mutation-induced constitutive activation attenuating cellular apoptosis and promoting tumour propagation (Wang *et al.*, 2008; Hayes & McMahon, 2009). As a result, although Nrf2 is clearly important both in its ability to prime an environment for pre-cancerous changes it is also capable of aiding established tumour growth and progression. Taken together, current research warrants further work in this field to establish the intricacies of the role Nrf2 is clearly able to play. Further research is also necessary to establish any potential for Nrf2 as a therapeutic target for cancer, and whether its usefulness will be overly limited by its opposing roles. Furthermore, this knowledge can serve as a cautionary tale regarding the duplicitous and complex role played by Nrf2 in disease development.

1.7.2 Metabolic Syndrome and NASH

Whilst the relationship between metabolic syndrome and AD has been portrayed earlier, the role of Nrf2 has yet to be described. In order to better understand the varied and vital roles that Nrf2 appears to play within diverse disease progressions, it is important to demonstrate the intricate and varied effects such a ubiquitously expressed protein is capable of exerting. This is well exemplified by the complexities of Nrf2 involvement within the different symptoms of the metabolic syndrome.

1.7.2.1 T1D and obesity

As discussed previously, there have been numerous publications linking obesity and T1D with development of AD. In turn there have been roles suggested for Nrf2 in the progression of obesity and in T1D development; although this is a relatively new area of research with regards to Nrf2. Nrf2 has been implicated in the development of insulin resistance, lipogenesis and adipogenesis (Seo & Lee, 2013). However, the described relationship of Nrf2 with obesity is not clear-cut as has been demonstrated by some of the studies published in recent years. In order to further dissect the potential role of Nrf2 in metabolic disease, researchers have proceeded down one of two routes: through increased Nrf2 activity by pharmacological activation or through the use of Keap1 knock down (KD) and/or Nrf2 knockout (*Nrf2*^{-/-}) animal models of Nrf2 dysregulation.

Gene expression studies have confirmed the multitude of genes regulated in an Nrf2 dependent manner, and have enabled scientists to classify them broadly into two different groups (Abdullah *et al.*, 2012; Chartoumpekis *et al.*, 2013). Those are: 1) Shared antioxidant genes present across different tissues analysed and largely involved in the tissues defence against damaging factors such as oxidants and electrophiles; and 2) tissue specific families of genes that are relevant to particular correct management of functions essential to the tissues in question. Of particular relevance to the impact of Nrf2 on metabolic syndrome, is the subset of genes found to be specifically regulated by Nrf2 within the liver. These genes are largely linked with the management of lipid homeostasis and more specifically the metabolism of fatty acids and other lipids. The fact that these genes are primarily repressed by Nrf2 has been confirmed recently in an expression study using *Nrf2*^{-/-} mice (Chartoumpekis *et al.*, 2013). These discoveries suggest a potentially important link between Nrf2 activity and the development of aspects associated with metabolic syndrome such as T1D and obesity, both of which are associated with energy imbalances and alterations in the management and roles of

lipids, triglycerides and their metabolism. Linking in with the suggested role of Nrf2 in lipid processing, altered lipid management is also seen in AD with isoforms of ApoE, important in the management of triglyceride-rich lipoprotein constituents, known to alter a person's risk of developing AD.

Consequently, studies using genetic or pharmacological activation of Nrf2 have demonstrated reductions in lipid levels within the liver, as well as in other tissues such as the white adipose tissue (Tanaka *et al.*, 2008; Shin *et al.*, 2009). This suggests that Nrf2 is intimately involved in lipogenesis and therefore obesity. However, it has been noted that ablation of Nrf2 does not, as might have been expected, induce an increase in adiposity although there are noted alterations in key lipid metabolism components including those related to the production of triglycerides (Shin *et al.*, 2009; Pi *et al.*, 2010). Instead, it is likely that dual activity is exerted by Nrf2, whereby increased activation of Nrf2 beyond a basal level provides some beneficial effects on obesity but ablation of Nrf2 inhibits alternative adipogenic pathways. Indeed, further investigation of Nrf2 showed it to play a role in the regulation of PPAR- γ ; a known adipogenic transcription factor (Tanaka *et al.*, 2008; Pi *et al.*, 2010). It is also of note that the particulars of the diet in use can affect the alteration in Nrf2 related activity with recent work by Milder and Patel (2012) demonstrating an alternative induction of Nrf2 in response to administration of a ketogenic as opposed to HF diet.

1.7.2.2 NAFLD and NASH

Fatty liver disease is characterised by abnormal retention of triglycerides within liver cells, otherwise known as steatosis of the liver. Non-alcoholic fatty liver disease (NAFLD) describes the variant of fatty liver disease resulting from mediators other than excessive chronic alcohol abuse, which falls under the alternative categorisation simply named alcoholic liver disease. Non-alcoholic steatohepatitis, or NASH, is a more severe progression of fatty liver disease where patients have progressed beyond the reversible NAFLD disease state. The condition is associated with disorders that influence the body's fat metabolism pathways, and as a result, can be a consequence of metabolic syndrome. It is of interest with regards to Nrf2, given the evidence just portrayed promoting the importance of Nrf2 in the healthy regulation of fat metabolism and the potential for dysregulation of this control when subjected to challenges such as HF feeding. In support of its role in lipogenesis mentioned earlier, *Nrf2*^{-/-} mice have an increased predisposition towards the development of NAFLD and NASH when challenged with a diet high in fat, which is overturned by Nrf2 activation (Tanaka *et al.*,

2008; Chowdhry *et al.*, 2010; Sugimoto *et al.*, 2010; Zhang *et al.*, 2010). This promotes Nrf2 as a potential target in the management of these aspects of the metabolic syndrome, whilst advocating a certain degree of caution due to the obvious multi-faceted role Nrf2 plays within the body as advocated by the long list of known regulated genes.

1.7.3 Role of Nrf2 in Cardiovascular Disease and Ischaemia

Cardiovascular disease (CVD) is already cited as a risk factor for AD, as previously mentioned, with initial epidemiology studies reporting an increased presence of CVD within a population diagnosed with dementia in comparison to those not presenting with dementia (Newman *et al.*, 2005). Upon further investigation, and similar to its role in cancer, Nrf2 has been shown to have a complex relationship with cardiovascular associated pathologies. Loss of functional Nrf2 has been implicated in the accelerated and aggravated response of murine hearts to models of haemodynamic stress such as occurs through the implementation of transverse aortic constriction (Li *et al.*, 2009). Furthermore, disruption of Nrf2 increases the susceptibility of the heart to succumb to the ROS produced following periods of acute exercise (Muthusamy *et al.*, 2012). In addition, Nrf2 has also been implicated in diabetes related cardiomyopathies with the T1D *db/db* mouse model displaying depleted arteriole levels of Nrf2 in comparison to their non-diabetic controls along with impaired vessel constriction and elevated ROS (Velmurugan *et al.*, 2013). This phenotype was rescued following administration of the Nrf2 activator SFN.

Nrf2 has further been implicated in ischaemia/reperfusion injury, important not only in cardiovascular diseases but also other disorders such as chronic kidney disease, T1D and cerebrovascular diseases. Similar to the beneficial arteriole effects described by Velmurugan and colleagues, preconditioning of *db/db* hearts through the use of hydrogen sulphide activates Nrf2 and downstream ERK, protecting the tissue from subsequent ischaemia/reperfusion injury (Peake *et al.*, 2013). In addition, treatment of mice with dimethyl fumarate induced the activation of Nrf2, providing a protective environment against periods of cardiac ischaemia which was abolished in mice lacking Nrf2 (Ashrafian *et al.*, 2012). This may be of particular interest given dimethyl fumarates recent clinical approval by the FDA for the treatment of recurrent MS, making it a potential candidate for repurposing. Furthermore, loss of Nrf2 in an STZ-induced diabetic nephropathy mouse model results in a significant worsening of pathology when compared to mice expressing Nrf2 (Jiang *et al.*, 2010), whilst activation

of Nrf2 has been suggested to be protective against cerebral ischaemia/reperfusion injury following post-treatment with an Nrf2 inducer (Peng *et al.*, 2013). This would indicate that the beneficial effects of Nrf2 activation with regards to ischaemia/reperfusion injury are not tissue specific, and may be of therapeutic interest.

1.7.4 Role of Nrf2 in Neurodegeneration and Alzheimer's Disease

Due to the widespread presence of high levels of OS in many metabolic and neurodegenerative diseases, Nrf2 has been implicated as a therapeutic target for multiple disorders including neurodegenerative conditions such as AD. Nrf2 has only recently been investigated as a possible therapeutic target in AD and more specifically in glial cells. As mentioned previously, Nrf2 is expressed in astrocytes and the presence of functioning Nrf2 provides a neuroprotective effect to astrocytes in situations of cellular stress. In neuron-astrocyte co-cultures, this neuroprotective effect spreads to include the neurons and improves cell survival over neurons cultured alone (Johnson *et al.*, 2008). It should also be noted that insulin/IGF1 regulated neuroprotection is in part dependent on the PI-3k pathway (van der Heide *et al.*, 2006). When inhibited, this pathway also disrupts Nrf2 regulated neuroprotection implying possible links between changes in energy homeostasis and insulin, dysregulation of Nrf2, increases in oxidative stress and the role of astrocytes and the immune system in AD (Nakaso *et al.*, 2003; Beyer *et al.*, 2008). Astrocytes are able to internalise A β and, when subsequently co-cultured with neurons, the astrocytic metabolic changes associated with A β internalisation appear detrimental to neuronal survival with increased neuronal death compared with controls (Allaman *et al.*, 2010). Use of *t*BHQ, a known Nrf2-ARE activator, in Ntera2/D1 neuron-like cells (NT2N) neuronal cells inhibited the formation of A β after exposure to H₂O₂. Co-culturing the NT2N neurons with astrocytes increased the neuroprotective effect of *t*BHQ, with higher levels of Nrf2 in both neurons and astrocytes, as well as lower levels of A β formation (Eftekharzadeh *et al.*, 2010). Finally, significant improvement in spatial learning of aged *APP/PSEN1* mice was observed after the administration of a lentiviral vector encoding human *Nrf2*. This was linked with an increase in insoluble A β vs. soluble A β with no increase in overall A β burden, and a drop in the amount of inflammatory astrogliosis present (Kanninen *et al.*, 2009). Furthermore, the only clinical application of an Nrf2 activator (dimethyl fumarate) to date is for the treatment of relapsing-remitting forms of MS and occasionally for the treatment of psoriasis). It is believed that activation of the Nrf2 system aids in targeting the associated inflammation and OS that occurs during MS, aiding in protecting and

potentially slowing the nerve damage that occurs as the disease progresses (Linker *et al.*, 2011; Venci & Gandhi, 2013). Given that a similar issue is being targeted in AD, this may support a role for treatments such as dimethyl fumarate in AD in the future.

However, despite more being known about potential mechanisms behind alterations in key AD proteins than ever before; scientists are little closer to understanding the intricacies of its development than they were fifty years ago. The heightened inflammatory response previously reported in *Nrf2*^{-/-} mice suggest it may be of benefit in the further study of AD given the increasing body of knowledge implicating dysregulation of the immune system response and age related decreases in cellular response strategies. In particular, the links already suggested between Nrf2 and changes in neurodegenerative conditions support the *Nrf2*^{-/-} model as a potentially useful model for research into modelling of an early disease stage paradigm.

1.8 PROJECT AIMS

Taken together these data suggest an important role for the loss of antioxidant regulating Nrf2 in the development of a pro-AD environment. In particular, it implicates Nrf2 in the dysregulation of inflammation and cellular damage associated with the occurrence of obesity, a risk factor for developing AD.

With this in mind, the main aim of this project was to assess the effect of Nrf2 loss in the brains of animals targeted with DIO or systemic infection, both believed to impact on the development of the metabolic syndrome. This was assessed by examining brain tissue following either long-term feeding of a HF diet, or short term repeated IP administration of LPS. Moreover, to further assess the potential involvement of Nrf2 loss in the development of a pro-amyloidogenic environment, a novel double transgenic model was developed. To make the assessment more physiologically relevant, all studies were performed in aged adult mice, allowing for the incorporation of an ageing interaction not normally seen in studies of metabolic disease.

In order to assess the effects of genotype along with those of the different stressors administered (HF diet or peripheral LPS), a range of gene and protein expressions were assessed along with *in vivo* measurements and cognitive evaluations. We concentrated our efforts on those genes and proteins associated with markers of inflammation (e.g. IL-1 β , YM1), resident glial cell activation and migration (e.g. GFAP, Iba1, MCP-1) and pathways commonly associated activation as a result of elevated stress (e.g. NF- κ B, MAPK). Further to this, we also investigated the effect the

interventions mentioned above had on proteins associated with known AD pathology (e.g. APP, BACE1), in addition to markers of mitochondrial dysfunction (e.g. Mitofusin 2) given the growing evidence of links between mitochondrial dysfunction and AD. In this way we could chronical the alterations caused by impaired antioxidant defence, and therefore increased ROS and RNS, on AD promoting factors following a metabolic syndrome intervention.

2 MATERIALS AND METHODS

2.1 MATERIALS

2.1.1 Chemicals

Ammonium persulphate (APS), benzamidine HCl, bovine serum albumin (BSA), Bradford reagent, citric acid, ethylene diamine tetraacetic acid (EDTA), ethylene glycol tetraacetic acid (EGTA), ethidium bromide, glycerol, β -mercaptoethanol, paraformaldehyde (PFA), Phenylmethylsulphonyl fluoride (PMSF), Ponceau S, sodium dodecyl sulphate (SDS), sodium orthovanadate, tetramethylethylenediamine (TEMED), TrisAcetate, Triton X-100 and Tween[®]-20 were purchased from Sigma Aldrich. Ethanol, glycine, hydrochloric acid, methanol, sodium chloride, sodium hydroxide, sodium pyrophosphate (NaPPi) and sucrose came from VWR International. Bromophenol blue and tris(hydroxymethyl)aminomethane (TRIS) base were from Fisher Scientific. Agarose was purchased from Bioline. Nuclease free H₂O was from Life Technologies.

2.1.2 Machines

7500 and 7900HT real-time PCR system (96 well plate) and relevant software (Applied Biosystems/Life Technologies), OTF 5040 microtome cryostat (Bright Instrument Company Ltd.), GeneFlash (Syngene bioimaging) acrylamide gene visualiser with Pulnix lens and Mitsubishi p93 thermal printer, TCS SP5 Confocal microscope with LAS AF software (Leica), NanoDrop ND-8000 with Nanodrop 8000 v. 2.3.2 software (Thermo Scientific), Odyssey infrared (IR) Western blot imager (Li-Cor Biosystems) with Odyssey (v. 3.0) and Image Studio (v. 4.0) Software, EnVision 2104 multilabel reader spectrophotometer (PerkinElmer), Veriti thermal PCR cycler (96 well) and an SRX-101A X-ray film developer (Konica-Minolta).

2.2 ANIMALS

2.2.1 Animal maintenance and housing conditions

All animal procedures performed were approved by the British Home Office Animal Scientific procedures act (1986) under the project licence number 60/4280 held by Professor Michael L.J. Ashford and with approval of the University of Dundee Animal Ethics Committee. Mice were maintained on a 12 h light/dark cycle with an environmental temperature of 20-23°C, *ad libitum* access to food and water, and bedding material to allow nests to be built. Mice were maintained on the RM1 standard diet (RC; 7.5 % fat, 75.75 % carbohydrate and 17.5 % protein by energy (801151,

Special Diet Services)) unless part of the high fat (HF) feeding study. HF fed mice were maintained on a diet containing 45% fat (45% fat, 35% carbohydrate, 20% protein (824053, Special Diet Services)).

All mice were maintained in standard size cages in groups of between two and five animals of the same sex. Exceptions were made for one mouse each in the *Nrf2*^{-/-}/*hAPP*_{swe} Saline and LPS groups, which had been housed singly, due to the very limited number overall of animals available from this genotype. All cages were given a shelter which was either a red tube or u-shaped roof. All mice undergoing behaviour tasks were given the same type of shelter in their cages to maintain uniform environmental factors across the different cages. Mice from a cage where only some animals were assigned to behaviour tasks were maintained in their full social group throughout until the animals were taken for tissue to minimise any impacts on social environment during the study. No additional environmental enrichment was provided for the duration of the studies.

2.2.2 Generation of *Nrf2* KO mice

Whole body *Nrf2* KO (*Nrf2*^{-/-}) mice were gifted by Professor J.D. Hayes (University of Dundee). This model of *Nrf2*^{-/-} mice was first introduced by Itoh *et al.* (1997). The authors made use of the targeting vector SV40 nuclear localisation signal- β -galactosidase (lacZ) recombinant gene to replace the b-Zip region of the *Nrf2* gene; resulting in a model displaying non-functional, disrupted *Nrf2* expression. These mice were previously backcrossed onto the C57Bl/6 background for 8 generations by Professor J.D. Hayes lab and mice were maintained by homozygotic breeding on the same background strain. It is generally accepted that 6 generations of backcrossing is an acceptable number in order to develop a majority genetic consistency.

2.2.3 Generation of *hAPP*_{swe} mice

*hAPP*_{swe} transgenic (Tg) mice were obtained from Jackson Laboratories (Strain: B6.129-Tg(APP^{swe})40Btla/Mmjax). This mouse line, also known as the R1.40 mouse owing to the R1 embryonic stem (ES) cells used when producing the line, was originally generated and further characterised by Lamb *et al.* (1997; 1999). They express the full length human *APP* gene sequence containing the well documented Swedish mutation (*APP*_{K670N/M671L}) under the control of the murine *APP* promoter. The murine *APP* promoter is expressed ubiquitously with different *APP* isoforms demonstrating some isoform specific tissue localisation. *hAPP*_{swe} animals were backcrossed for more than 20 generations on a C57Bl/6 background strain and were

subsequently maintained on this genetic background, with Tg carriers bred to WT mice due to reported increased mortality in young homozygous animals (JacksonLaboratories, 2015). Hemizygous Tg carrier mice were used for the relevant studies undertaken and are still reported to produce 7-8x the level of brain A β ₁₋₄₂ protein at 3-4 months of age although no plaque deposition is reported until much older (24-26 months; Lamb *et al.*, 1999).

2.2.4 Generation of a novel AD mouse line

A novel double transgenic mouse line was developed using the two existing mouse lines mentioned above. Mice from the *Nrf2*^{-/-} line were bred with hemizygous *hAPP*_{swe} expressing mice. This cross produced a mouse line delineated by the combination of ubiquitous *Nrf2*^{-/-} and hemizygotic *hAPP*_{swe} expression driven through the murine *APP* promoter. This line has subsequently been referred to as *Nrf2*^{-/-}/*hAPP*_{swe} for simplicity. This novel mouse line, with a C57Bl/6 background strain, was subsequently maintained by crossing *Nrf2*^{-/-}/*hAPP*_{swe} mice with transgenic mice from the *Nrf2*^{-/-} colony.

2.2.5 Genotyping of mouse lines

Following weaning, mice were ear notched for identification, using a well-established notch number and localisation protocol, and the collected ear punch biopsy was used for genotyping analysis. DNA was extracted using the Extract-N-AMP Tissue polymerase chain reaction (PCR) kit. In short, 100 μ l of extraction solution (E7526, Sigma-Aldrich) was mixed with 25 μ l of tissue preparation solution (T3073, Sigma-Aldrich) and added to the tissue. Samples were briefly centrifuged, ensuring the tissue notches were submerged in the solution, prior to being incubated at room temperature for 10 min. The samples were vortexed and incubated for a further 3 min at 95°C. Lastly, 100 μ l of neutralisation buffer (N3910, Sigma-Aldrich) was added to each sample, and these were stored at 4°C. The PCR was performed using the Novagen[®] KOD Hot Start polymerase kit (71086, Merck Millipore) and optimised for each primer/genotype combination. Relevant controls were run on a regular basis including known positive and negative samples, as well as samples lacking DNA. Individualised PCR primer and cycling information is detailed below, with all primers being synthesised by Sigma-Aldrich. *Nrf2*^{-/-} mice were genotyped by Dr. Paul Meakin, with remaining mice being genotyped by Dr. P. J. Meakin, postdoctoral PhD student S. M. Jalicy or myself. All notching was performed by licensed practitioners.

2.2.5.1 *Nrf2*^{-/-}

Due to the design of the *Nrf2*^{-/-} model, a combination of three primers was used. A generic *Nrf2* forward coding primer, a reverse primer coded to recognise the original WT mouse *Nrf2* sequence and a second reverse primer designed to recognise the LacZ disruption thereby signifying a knockout genotype (Table 2.1).

Primer	Sequence 5' → 3'	Primer Type	Primer Sequence Origin
1516	ACA AGC AGC TGG CTG ATA CTA CC	Generic <i>Nrf2</i> forward	Dr. C. J. Henderson, University of Dundee
1517	CAC TAT CTA GCT CCT CCA TTT CCG AG	WT <i>Nrf2</i> reverse	
1518	TGG GAT AGG TTA CGT TGG TGT AGA TGG	β-gal <i>Nrf2</i> reverse	

Table 2.1 List of PCR primers and their sequences used for *Nrf2*^{-/-} mouse line

Individual PCR reaction mixtures included 5 µl of genomic DNA and final concentrations of 0.6 µM forward primer and 0.3 µM each of the reverse primers, and were combined with the elements of the Novagen[®] KOD Hot Start polymerase kit. This resulted in absolute concentrations of 1x KOD hot start buffer, 1.5 mM MgSO₄, 0.2 mM dNTPs, and 1 U KOD hot start DNA polymerase made up to a final volume of 50 µl with nuclease free PCR grade H₂O. Samples were placed in the thermal PCR cycler and run under the conditions detailed in Table 2.2.

Step N°	Step	Temperature (°C)	Duration (s)
1	Polymerase Activation	94	120
2	Denaturation	94	20
3	Annealing	62	15
4	Elongation	70	7
5	Repeat steps 2-4 35x		
6	Hold	4	∞

Table 2.2 Heat cycling PCR programme for genotyping of *Nrf2*^{-/-} earnotches

The manufactured PCR products were mixed with 6x loading dye (G2101, Promega) to ease sample loading and visualise sample gel migration. Samples were run alongside a 100 base pair (bp) PCR reference marker (G1881, Promega) on a 1% agarose gel containing ethidium bromide (Appendix I; see chapter 7.1, Table 7.4) at 120 V in Tris-acetate-EDTA (TAE) buffer (Appendix I; see chapter 7.1, Table 7.4) for 40 min at room temperature. The gel was viewed by exciting the ethidium bromide stained DNA with ultraviolet (UV) light in a GeneFlash imaging machine and an image captured for record purposes using a p93 Mitsubishi high resolution thermal printer.

Primer design countenances the visualisation of WT and *Nrf2*^{-/-} band in a single reaction. The LacZ motif insertion increases the size of the recognised PCR product from 537 bp (WT) to 684 bp for the LacZ disrupted *Nrf2* gene (Figure 2.1). Presence of solely the larger product confirms the homozygotic genotyping of *Nrf2*^{-/-} mice.

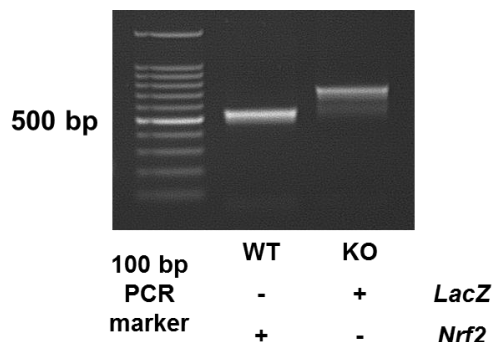


Figure 2.1 Example image of PCR products produced by genotyping of *Nrf2*^{-/-} mice

2.2.5.2 *hAPP*_{swe}

Owing to the similarity in weight of the PCR end products, two separate reactions were run in order to genotype the *hAPP*_{swe} mouse line. One reaction with forward and reverse primers designed to recognise the murine APP sequence (oIMR8744 and oIMR8745), and a second reaction containing the primers coding for the human transgene (oIMR6938 and oIMR6939; Table 2.3).

Primer	Sequence 5' → 3'	Primer Type	Primer Sequence Origin
oIMR6938	CTT CAC TCG TTC TCA TTC TCT TCC A	Transgene forward	Jackson Laboratory
oIMR6939	GCG TTT TTA TCC GCA TTT CGT TTT T	Transgene reverse	
oIMR8744	CAA ATG TTG CTT GTC TGG TG	Internal +ve control forward	
oIMR8745	GTC AGT CGA GTG CAC AGT TT	Internal +ve control reverse	

Table 2.3 List of PCR primers and their sequences used for *hAPP*_{swe} mouse line

Individual PCR reaction mixtures included 1 µl of genomic DNA and final concentrations of 0.8 µM forward and reverse primers for each reaction once combined with the elements of the Novagen[®] KOD Hot Start polymerase kit. This resulted in absolute concentrations of 1x KOD hot start buffer, 1.5 mM MgSO₄, 0.2 mM dNTPs, and 1 U KOD hot start DNA polymerase made up to a final volume of 25 µl with nuclease free PCR grade H₂O. Samples were placed in the thermal PCR cyclor and run under the conditions detailed in Table 2.4.

Step N°	Step	Temperature (°C)	Duration (s)
1	Polymerase Activation	95	180
2	Denaturation	95	30
3	Annealing	67	30
4	Elongation	72	30
5	Repeat steps 2-4 35 x		
6	Terminal elongation	72	300
7	Hold	4	∞

Table 2.4 Heat cycling PCR programme for genotyping of *hAPP_{swe}* eartnotches

As for the *Nrf2*^{-/-} genotyping described above, the manufactured PCR products were mixed with 6x loading dye and samples were run alongside a 100 bp PCR marker ladder on an 2% agarose ethidium bromide gel (Appendix I; chapter 7.1, Table 7.4) at 120 V in TAE buffer for 40 min at room temperature. The gel was viewed by exciting the ethidium bromide stained DNA with UV light and an image captured. PCR products were examined from the two individual reactions. The internal positive control reaction produces a band at a molecular weight of \approx 200 bp in all samples and can therefore also serve as a sample quality control confirming the extraction of DNA from the ear notch. The second PCR reaction, isolating a product at a molecular weight of 84 bp, enabled the identification of the transgenic animals (Figure 2.2). However, presence of non-specific band close to that demarking the Tg *APP* band (see Figure 2.2 WT column) caused genotyping issues that resulted in mice being falsely allocated the Tg genotype. Subsequent to this being found, PCR gels were run for longer to ensure full separation, PCR products were run separately in case of cross-PCR primer contamination and positive and negative controls were run on every gel. However, this resulted in much reduced group sizes in our double transgenic line, resulting from re-allocation of false positive animals and a decrease in the number of available correctly genotyped animals.

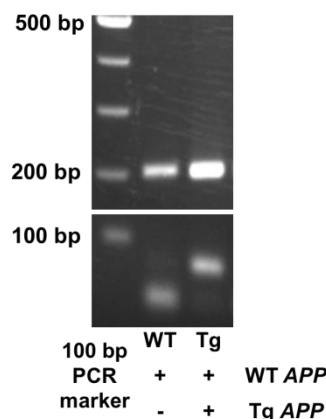


Figure 2.2 Example image of PCR products produced by genotyping of *hAPP_{swe}* mice

2.3 *IN VIVO* STUDIES

2.3.1 High Fat Metabolic Study

Adult mice from three transgenic genotypes, namely *Nrf2*^{-/-}, *hAPP*_{swe} and *Nrf2*^{-/-}/*hAPP*_{swe}, were used alongside appropriate WT controls. Mice were placed on the study for a period of 14 months, with some additional mice being used for the purposes of the behaviour work carried out. Total numbers of mice used in each group, including those for the behaviour task were as follows: WT RC = 47, WT HF = 20, *Nrf2*^{-/-} RC = 29, *Nrf2*^{-/-} HF = 37, *hAPP*_{swe} RC = 11, *hAPP*_{swe} HF = 12, *Nrf2*^{-/-}/*hAPP*_{swe} RC = 10, *Nrf2*^{-/-}/*hAPP*_{swe} HF = 12. Animals harvested for this study were then split into two groups, one for biochemistry (tissue was flash frozen) and the other for immunohistochemistry (tissue was perfuse fixed).

2.3.1.1 Feeding

All mice were weaned onto a standard rodent diet (RM1). At 8-10 weeks of age, mice were allocated to either the RC control arm of the study or the HF treatment arm of the study. This gave rise to 8 separate experimental groupings. Mice in the HF study arm were placed on a 45% fat diet (see chapter 2.2.1) with 1 week dietary crossover period. Mice were weighed weekly once the diet change had commenced. Both male and female mice were used for the purposes of this study.

2.3.1.2 Intraperitoneal Glucose Tolerance Test

Peripheral glucose tolerance was assessed by intraperitoneal (IP) glucose tolerance test (IPGTT) at 15 months of age following 55-57 weeks of dietary intervention. Although not as deemed to be as accurate as the gold standard measurement associated with clamp studies, IPGTTs were deemed to be more appropriate given the long-term nature of the study and remain more accurate measurements than the more basic HOMA (homeostatic model assessment) or FIRI (fasting insulin resistance index).

All IPGTTs were performed by Dr. A.D. McNeilly, postgraduate PhD student S.M. Jality and Dr. P.J. Meakin in accordance with the standard protocol. In brief, following overnight starvation fasted blood glucose measurements were taken using ~1 µl of tail vein blood placed on a glucose strip and the glucose concentration quantified using a glucometer (Gluco Rx Nexus TD-4277 glucose meter and compatible strips). Following basal measurements, glucose was injected IP at a concentration of 1 g/Kg

(25% solution in PBS) and whole blood glucose levels were measured at 15, 30, 60, 90 and 120 min post injection, using the same method as described above.

2.3.1.3 IP Insulin tolerance test

Peripheral insulin tolerance was assessed by IP insulin tolerance test (ITT) at 16 months of age following 59-61 weeks of dietary intervention. After a 4 h starvation period fasted blood glucose measurements were recorded as described above. Following basal measurements, insulin was injected IP with a solution of insulin consisting of 0.75 U/Kg of recombinant human insulin (Actrapid[®], Novo Nordisk). Blood glucose levels were again measured at 15, 30, 60, and 90 post IP injection as previously described. All ITT experiments were performed by Dr. A.D. McNeilly, postgraduate PhD student S.M. Jaliczy and Dr. P.J. Meakin.

2.3.1.4 Spontaneous alternation behavioural task

Spontaneous alternation (SA) utilises rodents' natural tendency to investigate novelty. It has previously been suggested to test spatial working memory, although other forms of memory have since been suggested for it instead such as dead reckoning, self-movement cues and/or response strategies (McNay *et al.*, 2000; Lennartz, 2008; Vorhees & Williams, 2014). It can be performed in a variety of maze shapes, such as T, Y, +. This behavioural paradigm is considered to be largely hippocampal independent when performed without spatial localisation cues (egocentrically). However, some researchers maintain there is still a role for hippocampal centred learning even under egocentric conditions with the deposition of olfactory cues or the acquisition of spatial cues not noticeable by the tester (Lennartz, 2008).

The successful completion of the task revolves around entry into as many alternative arms as possible based on the animal's previous arm entry. The outcome measurement is described as a percentage alternation indicating the degree to which the animal has successfully completed arm alternations out of the total possible number of alternations based on the number of arm entries performed by any single animal. Measures of memory performance in the plus maze format used in this study are standardly reported as percentage 4/5 alternation (McNay *et al.*, 2000). In brief, this means that within any consecutive five arm entries the animal must have entered every possible arm for it to count as a positive alternation (N, S, E and W). Therefore the total number of alternations possible equals the total number of arm entries performed minus four, allowing a percentage alternation value to be obtained (see chapter 3.6 for the formula).

An elevated plus maze was used to measure changes in SA in WT, *Nrf2*^{-/-}, and *Nrf2*^{-/-}/*hAPP*_{swe} mice (see Figure 2.3). In order to measure SA instead of anxiety, the closed arm model of the maze was used. The same experimental room was used for all testing and within that room, the base of the maze was placed in the same position for each behaviour session as was the video camera tripod to ensure no localisation related interference. All sessions were videoed (HDR-XR260VE, Sony) and a second screen

used during testing to allow real-time monitoring of the task.

All elements of the maze (4x removable black Plexiglas arms, 1x elevated base with adjustable feet (Figure 2.3)) were cleaned prior to the start of any assessment sessions with disinfectant surface wipes (Citroxx Bio[®]) to remove any potential olfactory cues. Mice were placed in the centre of the maze intersections and arm entries were recorded for a total of 10 min. Between mice, the whole apparatus was again cleaned and dried before the next mouse was recorded. Mice were measured following consumption of either RC or HF diets and a selection of ages were assessed. Age intervals investigated were: 2.5 to 4.5 months, 5.5 to 7.5 months, 9.5 to 11.5 months, and 13 to 15 months.

For ease of reference, these groups will now be referred to as 3 months, 6 months, 10 months and 14 months respectively.

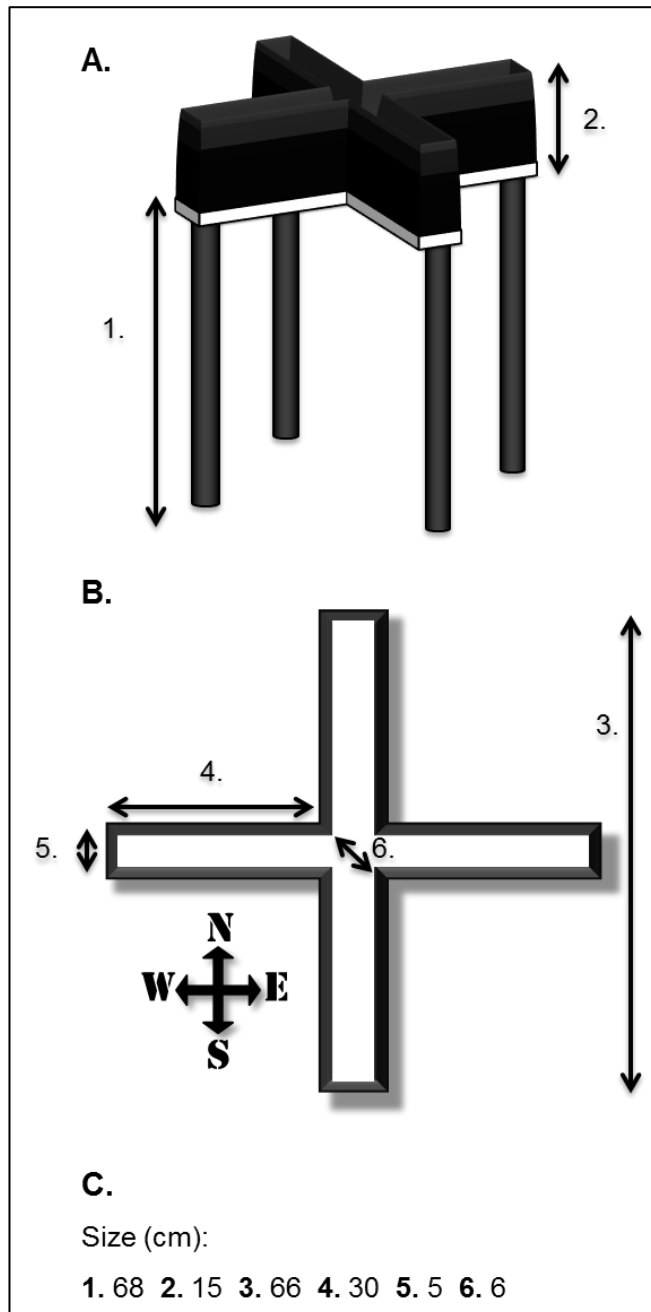


Figure 2.3 Pictorial representation of the elevated plus maze behavioural apparatus

Where (A) depicts a side on view of the apparatus and (B) an aerial view. (C) describes the dimensions of the apparatus used for the cohorts in question.

Additional assistance for the behavioural work on this project was provided by Dr. A.D. McNeilly with contributions from undergraduate students S. Garner, R. Convery and D. Cavellini, who were awarded summer studentship project grants and aided in the recording of SA assessments and bodyweight measurements.

2.3.2 Peripheral Infection Study

Adult male (M) and female (F) mice from the transgenic $Nrf2^{-/-}$ and $Nrf2^{-/-}/hAPP_{swe}$ lines were used alongside appropriate WT controls. Mice were randomly subdivided into groups of between 11 and 14 for the WT and $Nrf2^{-/-}$ genotypes according to availability (WT saline = 14, WT LPS = 11, $Nrf2^{-/-}$ saline = 13, $Nrf2^{-/-}$ LPS = 12), and in addition only 4 saline-treated and 3 LPS-treated $Nrf2^{-/-}/hAPP_{swe}$ due to the aforementioned genotyping issues (see Chapter 2.2.5.2). Genders were split evenly across genotypes and treatments as much as possible. Mice were placed on the study for a period of seven days and followed the study plan outlined in Figure 2.4.

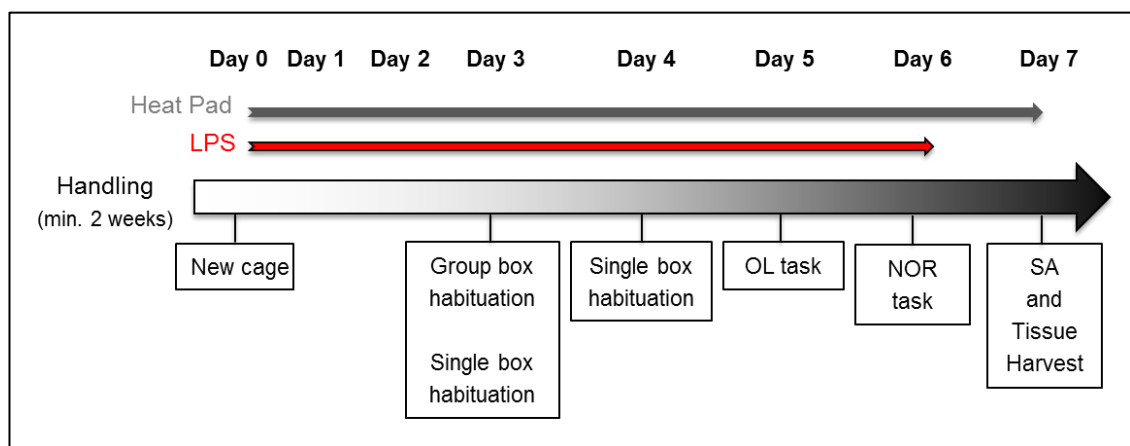


Figure 2.4 Time-line for the peripheral infection study, depicting the order in which behavioural tasks and relevant habituation were performed

Where NOR = novel object recognition and OL = object location.

2.3.2.1 *In vivo* LPS treatment

Adult mice were randomly allocated to either the saline or LPS study arm ensuring a comparable gender and genotype allocation across groups where possible. Mice were administered LPS via IP daily for a period of seven days. After reviewing relevant literature and taking into account the age of the animals in question a set dose of 2.5 μg of LPS in saline solution per mouse was used with a final dosage volume of 100 μl or an equivalent volume of saline for the controls. Prior to initiating the programme, mice were placed in fresh cages and no further cage changes were performed throughout the duration of the study in order to minimise disruption to the

animals as this might have impacted on bodyweight and recovery. Injections were undertaken at the same time every day between the hours of 9.00 and 10.00 at which time daily weights were also recorded. Subsequent to initial injections, all mice were maintained in a quiet room on heat pads, and fresh softened RM1 diet was made available on a daily basis post IP injection. All IP injections in this study were performed by either Dr. A.D. McNeilly, postgraduate PhD student S.M. Jaliczy or Dr. P.J. Meakin.

2.3.2.2 *Animal Behaviour*

Mice were handled daily for a minimum of two weeks prior to the commencement of the study, following which they were allocated to a treatment group. Behaviour tasks used included two object based tasks, namely the novel object recognition task (NOR) and the object location task (OL), as well as the previously described SA assessment (see 2.3.1.4). Both the NOR and the OL tasks rely on the innate rodent response to novelty resulting in investigative behaviour. Therefore, these tasks make a basic assumption tailored around the ability of rodents to recognise previously observed objects as familiar. Once this theory is established the tasks can be used to evaluate the animal's ability to respond to (i) a simple introduction of novelty to an experimental paradigm (NOR) dependent on the perirhinal cortex, or (ii) alterations in the localisation of the familiar by incorporating the use of spatial queues (OL). Both of these tasks have been previously used in the behavioural evaluation of animal models of AD as they are considered to reflect, at least in part, other assessment paradigms used in both human and non-human primate models (Leger *et al.*, 2013; Webster *et al.*, 2014).

At the beginning of the study in each individual cohort mice were randomly assigned a running order, alternating treated and control animals in addition to object pairings and locations. For all tasks performed, mice were left for a minimum of 2 h post IP injection prior to any task participation. All mice were maintained on a heat pad when not undergoing behavioural testing and had access to both fresh softened chow and standard RC as well as water throughout. Furthermore, at the beginning and end of testing, as well as between each mouse or mouse group, any apparatus or objects in use were cleaned and dried in order to minimise any transfer of olfactory cues. All testing was filmed using either a fixed overhead video-camera (OL and NOR) or a video-camera attached to a tripod (SA) but placed far enough away to not adversely affect the task being carried out.

2.3.2.2.1 Habituation

Mice were habituated to the experimental room on a minimum of two occasions during the initial handling period prior to any task habituation occurring. A polystyrene box coated in wood effect sticky back plastic with two object grips was used for all behaviour tasks (Figure 2.5 A) and mice were first habituated to the experimental box on day 3 with their cage-mates for a total of 10 min per cage. The empty experimental box was placed in a designated location on a bench surface with spatial location queues in the top right and top left corners. Following group habituation, a further period of habituation was performed on the same day. The mice were placed in the experimental box in the same order as for the group habituation, but this time they were habituated individually for a total of 8 min per mouse. This allowed all animals to have a break period between habituation sessions.

A further individual habituation session was performed on day 4 for a total of 10 min per mouse. For any single cohort of mice both the NOR and OL tasks were performed using the same experimental box, dispensing with any requirements for separate habituation for the secondary object task. In addition, object pairings were used that had been previously established to engender the same degree of interest to aid in minimising object-based bias in either of these tests. All sessions were videoed and a second screen used during testing to allow real-time monitoring of the task. The assessment of SA, as described in 2.3.1.4, does not require any prior habituation to the apparatus, therefore no additional habituation was performed for this task.

2.3.2.2.2 OL Task

Mice were randomly assigned a running order, alternating treated and control animals, and object pairings and locations. On day 5 of the study, each mouse was placed individually in the test box previously used for habituation in the presence of two never-seen-before different objects (sample phase) for a duration of 10 min. Mice were placed in the behavioural box facing the south wall on every presentation in order to prevent inadvertent bias resulting from direct presentation of the mice to the objects in use. During the sample phase, the time spent investigating each object was measured and total time spent exploring was recorded following 10 min from placement in the test box. Mice were then removed from the test box and placed in an opaque holding box for 10 min, bedded down with standard shavings which were renewed at the beginning of each day of testing.

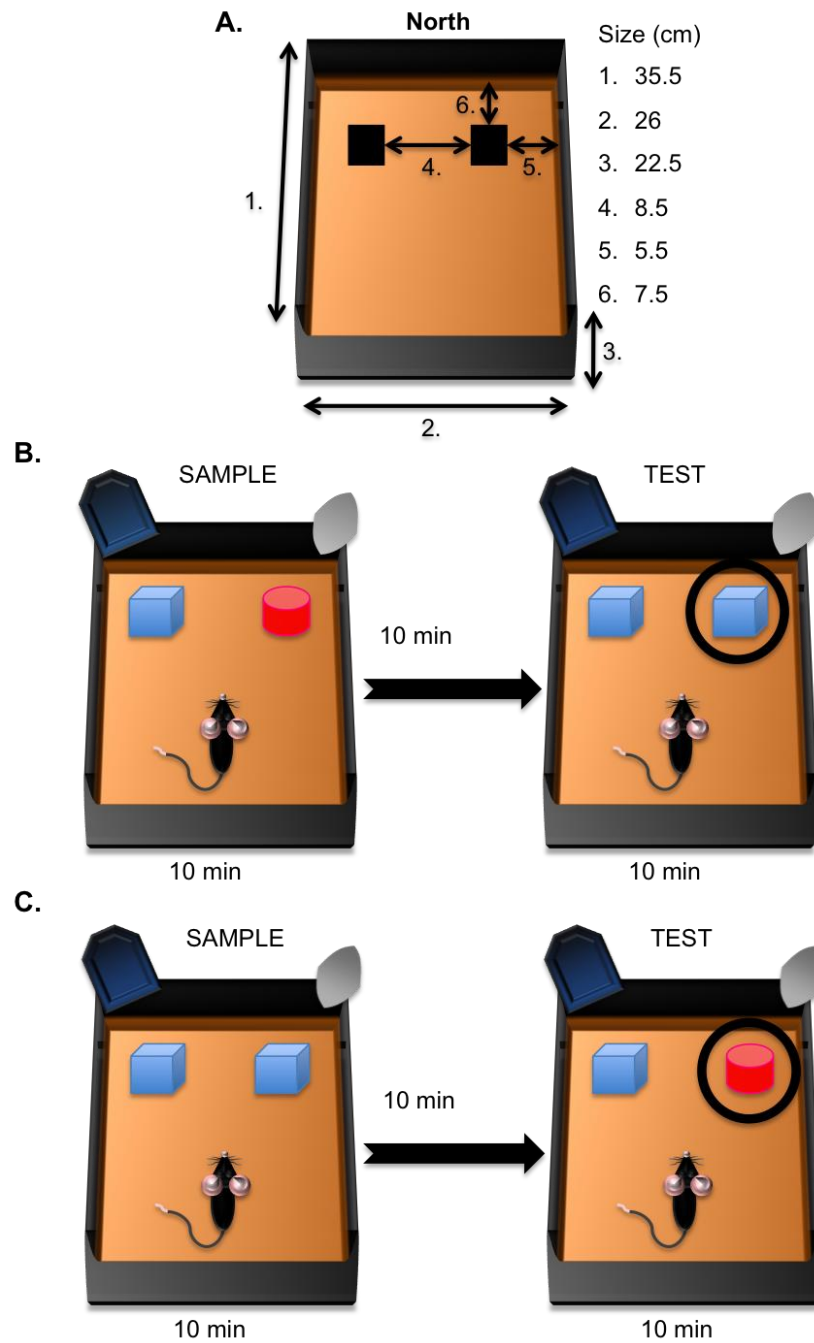


Figure 2.5 Pictorial representation of the object-based behavioural apparatus and related tasks.

Where (A) depicts the specifications of the apparatus, (B) demonstrates the task undertaken in the OL assessment where the novel object is identified by a circle in the test phase, and (C) demonstrates a basic replica of the NOR task where the novel object is again depicted by a circle in the test phase analogy.

Whilst the mouse was in the holding box, the test box and objects were cleaned and a new pairing of objects was placed in the test box. For OL, two replicas of one of the objects seen in the sample phase were used with a novelty of location associated with one of the objects (see Figure 2.5 B). At the end of the holding phase, mice were placed again in the test box, facing the south wall of the box and now in the presence of the new object pairing. Individual object investigation was measured and noted following 10 min within the test box (test phase). Additional descriptions of objects utilised can be found in Appendix II (chapter 7.2).

2.3.2.2.3 NOR Task

On day 6 of the study, each mouse was placed individually in the test box previously used for habituation and facing the south wall (sample phase). In the presence of two copies of a novel object the time spent investigating each object and total time spent exploring for each mouse were recorded following a period of 10 min. Mice were then removed from the test box and placed in an opaque holding box for 10 min, bedded down with standard shavings which were renewed at the beginning of each day of testing. During the holding time, the test box and objects were cleaned and a new pairing of objects was placed in the test box. For NOR, one object is a replica of an object seen in the sample phase and one object is entirely novel (Figure 2.5 C). At the end of the holding phase, mice were placed in the test box again in the presence of the new object pairing and individual object and total investigation were measured and noted at the end of 10 min (test phase). Additional descriptions of objects utilised can be found in Appendix II (see chapter 7.2).

2.3.2.2.4 SA task

Refer to chapter 2.3.1.4 for task setup. For the purposes of this study WT, *Nrf2*^{-/-}, and *Nrf2*^{-/-}/*hAPP*_{swe} mice were assessed following either repeated IP of saline or LPS (see Figure 2.3 for apparatus description). All testing occurred the morning after the final IP procedure on the 7th and final day of the study. Subsequent to this task, mice were sacrificed and tissue harvested as described below.

2.4 BIOCHEMISTRY

2.4.1 Tissue Collection

2.4.1.1 *Frozen Tissue*

Mice were killed by cervical dislocation and the head was removed to allow blood to be captured. Brains were excised from the skull by performing a sagittal incision in the skin exposing the skull. Excess spinal cord and brain stem were cut away and small snips made at the base of the skull. The skull was then cut sagittally and peeled away to either side to allow access to the brain. Taking care to ensure no pieces of meninges were still lying across the brain, a rounded small spatula was used to remove the brain from the skull in one piece. Once out the brain was placed in ice-cold PBS to remove excess blood, facilitate dissection, and slow down tissue degradation by cooling the tissue. Dissection was performed on ice with the brain being divided sagittally and one half being used for protein analysis whilst the other half was set aside for RNA processing. Relevant brain regions excised were the hypothalamus, cerebellum, cortex and hippocampus. It is worth noting that in the case of the cortical tissue an effort was made to excise the same region each time.

2.4.1.2 *Perfuse Fixed Tissue*

Mice were placed in a CO₂ box individually and deep narcosis induced using a gradual increase in CO₂ levels, which precedes euthanasia following an overdose of CO₂. An incision was made down their front to expose the rib cage. The sternum and front of the rib cage were cut away to expose the still-beating heart. A 10 ml syringe with a 1.1 mm gauge needle filled with ice-cold PBS was inserted in the posterior end of the left ventricle of the heart. A cut was made on the opposite side, permitting the PBS to be flushed through the vascular system and clear the blood from the animal. The empty syringe was replaced with a 10 ml syringe filled with ice-cold 4%-paraformaldehyde (PFA) taking care to leave the needle in place. 4%-PFA was flushed through the cardiovascular system in order to achieve whole body fixation. The appearance of fixation tremors indicated both the true time of fixation and confirmed successful fixation had occurred. Desired organs were then dissected out whole, and placed in 4%-PFA for a further 24 h post-fixation to ensure full tissue fixation had occurred. After 24 h tissue was dehydrated by placing it in a sucrose solution (30% sucrose in PBS) at 4°C to minimise the chance of ice crystal formation upon subsequent freezing of the tissue.

2.4.2 Tissue lysis

2.4.2.1 Protein

Snap frozen tissue was placed in a 1 ml dounce glass homogeniser mortar and standard Triton X-100 cell lysis buffer (Appendix I; see chapter 7.1, Table 7.1), with freshly added inhibitors, was added to the mortar using tissue specific volumes as detailed in Table 2.5. A tight 1 ml glass pestle was used to homogenise the tissue, with the combination of the vacuum seal and abrasion of glass against glass enabling tissue and cell shearing. Once homogenised and no further tissue being observed, the sample was placed in an eppendorf tube at -20°C correctly labelled with genotype, diet, mouse ID and tissue type. For long-term storage samples were migrated to a -80°C freezer.

Tissue Type	Tissue amount	Species	Lysis buffer (µl)
Cerebellum	½	Mouse	500
Cortex	½	Mouse	500
Hippocampus	½	Mouse	500
Hypothalamus	½	Mouse	100

Table 2.5 Details of tissue lysis volumes used for protein analysis

2.4.2.2 RNA

Snap frozen tissue stored at -80°C was placed in a 1 ml dounce glass homogeniser mortar. For all brain tissue types, 1 ml of TRI reagent was used to isolate RNA and a tight 1 ml pestle used to homogenise the tissue. Once fully homogenised, the sample was placed in eppendorf tubes designated solely for RNA use and stored in -20°C freezer until required. Assistance in tissue extraction of samples from the metabolic study was provided by D. Cavellini as part of a summer studentship.

2.4.3 Gene Expression using Real-Time qPCR

2.4.3.1 RNA extraction

Tissue homogenised in TRI reagent as per manufacturer's instructions. Briefly, tissue was defrosted and left at room temperature for 5 min to ensure complete lysis. The extraction was initiated by the addition of 0.2 ml chloroform to each sample. Samples were shaken vigorously for 15 s each before being left to stand at room temperature for 15 min, followed by a 15 min centrifugation in a refrigerated (4°C) centrifuge at 12000g. The centrifugation enabled the separation of the samples into layers largely divided into protein, DNA and RNA. The top layer of supernatant from each sample was removed and placed in fresh eppendorf tubes. The solution was mixed

using gentle inversion following the addition of 0.5 ml of isopropanol. Samples were again left to stand at room temperature for 10 min prior to centrifugation at 12000 g for 10 min at 4°C, resulting in the accumulation of an RNA pellet at the base of the tube. The supernatant was removed with particular care taken to not disturb the pellet and a final wash was performed through the addition of 1 ml of 75% ethanol to the pellet. Samples were vortexed in order to dislodge and disrupt the pellet, followed immediately by centrifugation at 4°C for 5 min at 12000 g. Taking care to not disturb the pellet, as much of the supernatant was removed as possible prior to air-drying inside an extractor hood for 7.5 min. Samples were solubilised in 30 µl of RNase-free water before being heated at 58°C for 15 min prior to being stored on ice for immediate use or at -80°C until required.

2.4.3.2 Nanodrop

RNA purity and concentration were evaluated using a NanoDrop ND-8000 machine and software (Nanodrop 8000 v. 2.3.2). This Nanodrop spectrophotometer is equipped as a high throughput machine capable of analysing 8-samples at any one time. The pedestals were cleaned with 5 µl water a minimum of twice, prior to loading a water control. They were wiped down and cleaned again before loading the relevant vehicle control, in this case purified RNase-free water. 1.5µl per sample was loaded and the RNA concentration (ng/µl) was measured at 260 nm and used to calculate the volumes of sample required to form 1 µg complementary DNA (cDNA).

2.4.3.3 cDNA synthesis

First strand cDNA synthesis was performed using the SuperScript™ II reverse transcriptase setup from Invitrogen as per manufacturer's instructions. Briefly, a blend of 1 µl random primers (48190-011; Invitrogen), 1 µl 10 mM dNTP (18427-013; Invitrogen) and 1 µg extracted RNA were combined in nuclease free Eppendorf tubes and made up to a volume of 13 µl with RNase-free water. The mixture was heated at 65°C in a heat block for 5 min and then briefly chilled on ice prior to being pulse centrifuged to collect the solution at the bottom of the tube. A combination of 4 µl 5x first strand buffer and 2 µl 0.1 M DTT (18064-014; Invitrogen) were added and the solution was gently mixed before being incubated at 25°C for 2 min. Following this, 1 µl of SuperScript™ II (18064-014; Invitrogen) was added, bringing the final volume of solution to 20 µl, and the samples were gently mixed. Reactions were incubated at 25°C for a further 10 min prior to being heated at 42°C for 50 min, allowing the reaction to

take place. Termination was achieved by heating the samples at 70°C for 15 min and the resulting synthesised cDNA was stored at -20°C until required.

2.4.3.4 *Real-Time qPCR*

TaqMan® assays are one of the most commonly used methodologies for real-time quantitative PCR (qPCR) detection. TaqMan® gene expression arrays specifically target desired genes using a fluorogenic probe. In brief, the reaction contains a combination of forward and reverse DNA polymerase with a sequence specific primer. The primer incorporates a fluorescent reporter dye (in this case 5'-fluorescein) and a non-fluorescent quencher (in this case 3'-minor groove binder). When the probe is intact, close proximity of it to the quencher prevents emissions from the reporter dye by utilising fluorescence resonance energy transfer. During the extension cycle of the PCR if the probe has bound the target sequence, the 5' activity of the Taq DNA polymerase cleaves the reporter dye from the primer sequence. This releases the dye into the solution allowing it to emit its characteristic fluorescence as it is no longer in repressed by the quencher, with this fluorescence recorded by the detection instrument of the RT-qPCR system.

For the purposes of our experiments a PCR reaction mix was prepared for each sample with final concentrations equating to 1x TaqMan® Universal PCR Mastermix, no AmpErase® (4324020; Applied Biosystems/Life Technologies), 1x primer/probe assay mix (Life Technologies; Appendix III chapter 7.3 for list of individual probes used) and 12.5 ng cDNA diluted in RNase-free water. The final volume for each reaction of 20 µl was loaded into a 96-well optical reaction plate in duplicate (or triplicate for the work done in collaboration with Prof. S.M. Keyse) and briefly centrifuged to spin the solution down in each of the wells. The plate was placed in the RT-qPCR system (Applied Biosystems/Life Technologies) and the PCR reaction run as per Table 2.6. The cycle threshold values (Ct) were analysed via the Δ Ct methodology with actin as the endogenous housekeeping control gene.

Step N°	Step	Temperature (°C)	Duration (s)
1	Polymerase activation	50	120
2	Initiation	95	600
3	Denaturation	95	15
4	Annealing	60	60
5	Repeat steps 3 and 4 40 x		

Table 2.6 Heat cycling PCR programme for TaqMan RT-qPCR analysis

2.4.4 Protein Expression by Western Blotting

2.4.4.1 Protein Content Determination

Protein content from cell lysates was determined using a Bradford protein assay (Bradford, 1976), which utilises the change in absorbance of Coomassie Blue G-250 from 465 nm to 595 nm upon protein binding to quantify protein content in unknown samples. Sterile 96-well plates were utilised and samples run in triplicate to minimise effects of potential pipetting error. 1 μ l of sample lysate was diluted in 9 μ l of dH₂O, after which 250 μ l of room temperature Bradford reagent (B6916, Sigma) was added to every well and the plate left for 15 min at room temperature. A standard curve was produced using increasing known concentrations of BSA (0, 0.25, 0.5, 1, 2, 5 mg/ml; Pierce Albumin Standard 23209, Thermo Scientific) diluted in dH₂O, whilst lysis buffer was used as a blank for the samples. If required, samples were appropriately further diluted prior to addition to the plate to ensure all values fell within the parameters of the standard curve. Following a brief plate shake, the plate was read using a spectrophotometer set to 595 nm, replicates averaged and protein concentrations extrapolated from the standard curve for each sample.

2.4.4.2 Western Blotting

2.4.4.2.1 SDS-polyacrylamide gel electrophoresis (SDS-PAGE)

The anionic detergent SDS is capable of dissolving hydrophobic molecules resulting in the production of protein complexes with a constant charge-to-mass ratio. Disrupting the proteins hydrophobic region breaks down secondary and tertiary structures linearising molecules coated in a uniform negative charge. This therefore allows the separation of proteins based solely on their molecular weight (MW) with no structural or charge dependent interference. The use of polyacrylamide gel acts to hinder the progression of proteins as they are driven by the electric current in a size dependent manner, with smaller molecules travelling faster down the gel towards the anode than those with larger MW. Standardised markers with known MWs are utilised to enable identification of the MW of the proteins being targeted.

2.4.4.2.2 Bio-Rad self-poured SDS-PAGE setup

Samples were made up to equivalent protein concentrations and SDS-containing sample buffer (Appendix I; see chapter 7.1, Table 7.1) was added. Samples were boiled for 5 min at 95°C and then cooled ready for running on Western blots. Proteins were resolved on self-poured SDS-PAGE tris-glycine gels using the Mini-Protean Tetra

electrophoresis system (Bio-Rad). Gels were cast in Bio-Rad casting stands and frames using 1.0 mm Bio-Rad glass spacer plates. 10% or 15% resolution gel solutions were poured depending on the proteins being probed for and gels left to polymerise. A 4% stacking gel was then poured and left to polymerise with a comb to produce the requisite number of wells (Appendix I; see chapter 7.1, Table 7.2 for gel constituents). Ultrapure Tris/Glycine/SDS running buffer (National Diagnostics; Appendix I; see chapter 7.1 Table 7.1) was used for electrophoresis at a constant voltage of 150 V for approximately 1h15.

2.4.4.2.3 Nitrocellulose membrane protein transfer

Following electrophoresis, proteins were transferred onto Amersham™ Protran™ 0.45 µM nitrocellulose membranes (GE Healthcare Life Sciences) using the aforementioned Bio-Rad Mini-Protean Tetra electrophoresis system, or Immobilon-FL membranes (Millipore) for the work done in collaboration with Prof. S.M. Keyse lab. The application of an electric current drives the negatively charged proteins out of the gel and onto the membrane ready for probing with the desired antibody.

For transfer purposes the stacking gel was removed and transfer sandwiches were prepared from the cathode side as follows: a fibre blotting-pad, a sheet of filter paper, the polyacrylamide gel, a nitrocellulose membrane, a sheet of filter paper and a final fibre blotting-pad. Filter papers, pads and membranes were pre-soaked in transfer buffer (Appendix I; see chapter 7.1, Table 7.1). Proteins were transferred via electrophoresis in transfer buffer for 1 h at 100 V. Subsequent to transfer, the membranes were briefly placed in Ponceau S stain to ensure even transfer had occurred. Membranes were then rinsed using distilled water and cut where necessary prior to being rinsed with Tris-buffered-saline-Tween® 20 (TBS-T; Appendix I, see chapter 7.1 Table 7.1).

2.4.4.2.4 Immunoblotting

To minimise non-specific binding membranes were blocked for 1 h in 10% w/v dried skimmed milk (Marvel™) in TBS-T on a gentle rocker at room temperature. Membranes were incubated overnight on a gentle rocker at 4°C with the relevant primary antibody (Appendix IV; see chapter 7.4 for the list of antibodies used) following a brief TBS-T wash to remove excess blocking agent. Subject to the protein being probed for, blots were either processed for visualisation *via* infrared (IR) fluorescent secondary antibodies for acquisition on the Odyssey machine (Li-Cor); or

via horseradish peroxidase (HRP)-linked secondary antibodies for acquisition on X-ray film.

2.4.4.2.4.1 *Licor Odyssey*

Following removal of the primary antibody, membranes were washed in TBS-T for 3x 10 min, then blocked for 20 min in 5% BSA or milk. Membranes then underwent a quick wash and were probed with specific IR secondary antibodies (Table 2.7) in TBS-T for 1 h at room temperature with gentle rocking. After a further 3x 10 min washes in TBS-T, membranes placed in fresh TBS-T were imaged and densitometry quantified using the Odyssey system as per manufacturer's instructions with relevant software.

Antibody	Supplier Product ID	Dilution in TBS-T	Host	Conjugate
Anti-Rabbit	Rockland Inc. 611-132-122	1:10000	Goat	Alexa Fluor 790 (IR dye 800)
Anti-Mouse	Life Technologies A21057	1:10000	Goat	Alexa Fluor 680 (IR dye 700)

Table 2.7 List of IR dye linked secondary antibodies for use with the Odyssey scanner

2.4.4.2.4.2 *Film development*

Following removal of the primary antibody, membranes were washed in TBS-T for 3x 10 min and blocked for 20 min in 5% BSA/milk. Membranes then underwent a quick wash and were probed with specific HRP-linked secondary antibodies (Table 2.8) for 1 h at room temperature with gentle rocking. Membranes then underwent a further 3x 10 min washes in TBS-T. Whilst the blots were being washed, an enhanced chemoluminescence (ECL) wash (Pierce[®] ECL Western Blotting Substrate, Thermo Scientific) was prepared as per manufacturer's instructions to allow visualisation of the protein-primary antibody-secondary antibody complex. Once washes were complete TBS-T was removed and ECL wash was placed on the blots and left for a minimum of 1 min, ensuring the whole blot was coated. Blots were then placed in X-ray film cassettes inside plastic pockets. Under dark room conditions X-ray film (CL-XPosure[™], Thermo Scientific) was placed into the cassette for a range of times, depending on the protein being probed for. Films were then developed using a SRX-101A developer (Konica-Minolta), and subsequently scanned onto a computer where they were quantified using Aida Image Analyser densitometry software (v.3.28).

Antibody	Supplier Product ID	Dilution	Host	Conjugate	Blocking Agent
Anti-Rabbit	Thermo Scientific 31460	1:5000	Goat	HRP	N/A
Anti-Sheep	Thermo Scientific 31480	1:5000	Rabbit	HRP	N/A
Anti-Chicken	Promega G1351	1:1000	-	HRP	5% Milk

Table 2.8 List of secondary antibodies for final processing by HRP-ECL reaction

2.4.5 Quantification of Protein Carbonylation

Protein carbonylation describes a form of protein oxidation promoted by the presence of ROS resulting in a modification of protein side chains containing methionine, histidine and tyrosine. Protein carbonylation most often refers to the formation of reactive ketone or aldehyde groups on a protein, these can then be used to measure ROS related protein damage. Addition of 2,4-dinitrophenylhydrazine (DNPH) causes the formation of DNP-hydrazones at the location of the aforementioned reactive groups. These hydrazones can then be quantified through the use of a DNP-specific antibody. Protein carbonylation was analysed using the Oxyblot™ protein oxidation detection kit from Merck Millipore (S7150) as per manufacturer's instructions. Briefly, protein lysates were prepared as previously described (chapter 2.4.2.1) and 2x 15 µg of mouse hippocampal or cortical protein lysate were prepared in eppendorfs, allowing for positive (DNPH) and control reactions for each sample. Each aliquot was then denatured with SDS diluted to a final concentration of 6% at room temperature. Samples were derivatised with either 10 µl of 1x DNPH solution or 10 µl of derivatisation-control solution for the control reactions. All tubes were incubated for 15 min at room temperature following gentle mixing, after which the reactions were terminated using 7.5 µl of the provided neutralisation solution. Where necessary, volumes of reagents were adjusted to cater for the more dilute stock protein concentrations of the brain lysates whilst maintaining the same ratio of components within the reaction mix.

Samples were run on 10% SDS-PAGE tris glycine gels. Briefly gels were made up as previously described (chapter 2.4.4.2.2) and 15 µl of sample was loaded per well making sure to alternate control and positive sample preparations, alongside 3 µl of protein standard. Gels were run for 15min at a constant 75V to allow stacking of initial load, and the remainder of the sample solutions were then added and the gels run for a further 15 min at a constant 75V to allow all the solution to enter the stacking gel. Gels

were then run at 100V until the bromophenol blue front from the standard had run off the bottom of the gel. Gels were transferred as previously described onto nitrocellulose paper (Chapter 2.4.4.2.3) and membranes incubated in Oxyblot blocking/dilution buffer (OxyBlock; Appendix I; see chapter 7.1 Table 7.1) for 1 h at room temperature on gentle rocker. Anti-DNP primary antibody stock was diluted into OxyBlock prior to use at a dilution of 1:150, and membranes were incubated for 1 h at room temperature with gentle rocking. After incubation, membranes were briefly rinsed twice in 0.05% PBS-T (Appendix I; see chapter 7.1, Table 7.1), and washed for 1x 15 min in PBS-T followed by 2x 5 min in PBS-T with gentle rocking. Membranes were incubated in rabbit IR secondary antibody in TBS-T (see Table 2.7) for 1 h at room temperature with gentle rocking. Finally, membranes were washed as before and developed as previously described using the Odyssey scanner (chapter 2.4.4.2.4.1).

Proteins differ in their transfer efficiency as well as their degree of carbonylation both of which can affect the immunodetection of the attached DNP moieties. It is also possible that different treatments and the effect of transgenic alterations could affect the ratio of individual protein carbonylation. As we were only interested in changes in overall protein carbonylation and to mitigate any transfer efficiency induced changes, four pre-selected regions were analysed and totalled in order to provide a measurement for protein carbonylation in our samples.

2.4.6 Amyloid protein expression

Triton-X 100 soluble mouse $A\beta_{1-42}$ was measured in cortical lysates from RC and HF fed WT and *Nrf2*^{-/-} mice using an enzyme-linked immunosorbent assay (ELISA) kit (KMB3441, Invitrogen). Lysates were prepared as described in chapter 2.4.2.1 and the protein concentration quantified as described in chapter 2.4.4.1. Samples were diluted 1:10 into the provided Standard Diluent Buffer and the $A\beta_{1-42}$ standard provided was made following manufacturer's instructions. 100 μ l of $A\beta$ standard or sample were loaded in duplicate to wells pre-coated with a monoclonal antibody that recognises the -NH₂ terminus of mouse $A\beta$, the plate was gently mixed by tapping the side, covered with the provided plate cover and incubated for 2 h at room temperature with gentle rocking. The solution was then decanted and wells washed 4x with the provided wash buffer diluted to a 1x concentration. 100 μ l of prepared mouse $A\beta_{1-42}$ specific antibody was added to the wells and the plate gently mixed, covered and incubated for a further 1 h at room temperature with gentle rocking. Wells were again washed 4x and incubated with HRP-tagged secondary antibody for 30 min at room temperature with gentle

rocking. Wells underwent a final wash (4x) before the addition of the stabilized chromogen (100 μ l) which allows visualisation of the bound A β ₁₋₄₂ antibody in the wells. The plate was incubated in the dark at room temperature with gentle rocking for 30 min before terminating the reaction through the addition of 100 μ l of the provided Stop solution. The plate absorbance was read at 450 nm using a spectrophotometer and protein concentrations calculated using the absorbencies of the mouse A β standard curve based on known concentrations of A β protein.

2.4.7 Immunohistochemistry

2.4.7.1 Tissue preparation

Tissue was used from perfuse fixed animals described in chapter 2.4.1.2. Upon initial transfer from fixative, tissue floats in 30% sucrose solution. Therefore, tissue was left for a minimum of 24 h, or the length of time taken for tissue to sink, prior to being used for experimental purposes. Plastic tissue block trays were labelled and a small amount of Shandon M1-Embedding matrix (Thermo Scientific) was placed in the tissue tray. Brains were removed from sucrose solution carefully dried on paper towel and, using a clean scalpel, cut sagittally down the midbrain. Any leftover sucrose solution was dried and hemispheres placed flat-side down in tissue trays and topped up with more M1-Embedding matrix solution until entirely covered. Tissue was quickly frozen using a cooling bath of dry ice/propan-2-ol that averages a temperature of -77°C. Once the embedding matrix was frozen and had turned opaque, trays were temporarily placed in dry ice if more tissue was being processed or stored immediately at -80°C for a minimum of 1 h to ensure tissue was fully frozen.

2.4.7.2 Cryostat sectioning

Tissue was removed from -80°C at least 30 min prior to sectioning and placed in cryostat to equilibrate. The tissue block was then mounted on a ball chuck with the flat side facing the blade using Cryo-M-Bed tissue freezing media (Bright Instrument Company Ltd.). Once set, the chuck was placed in the cryostat holder and the angle of slicing was altered until a whole section was being removed from the tissue block at every pass of the blade, promoting consistent sectioning across tissue blocks. Sections of 30 μ m were taken with on average 4-5 sequential sections being taken followed by an equivalent number being skipped to allow captioning of brain sections across the different regions. Sections were carefully placed in cold PBS until brain was fully

sliced, upon which they were transferred to cryoprotectant solution (Appendix I; see chapter 7.1, Table 7.3) and stored at -20°C if not immediately required.

2.4.7.3 Microscopy Slide Subbing

In order to improve the adhesion of the microscope slides, these were subbed with a chrome-gelatin solution prior to use. A solution of pork gelatin was made up in dH₂O and gently warmed on a magnetic stirrer to aid dissolution. A separate 1% stock solution of chromium (III) potassium sulphate (chrome alum; CrK(SO₄)₂·12H₂O) was prepared in dH₂O and allowed to solubilise at room temperature. Once dissolved chrome alum was added to the pork gelatin solution at a dilution of 1:10. This left a concentrated working subbing solution of 1% pork gelatin and 0.1% chrome alum.

Frosted microscope slides (631-0907; VWR) were laid out on white roll and a small dot placed in the top left corner of the frosted section of each slide to enable differentiation of the subbed from non-subbed face of the slides. A soft paintbrush was used to paint the subbing solution onto the non-frosted upwards facing facet of the new slides. Slides were allowed to dry overnight in a dust free environment before being placed back in their original box ready for use. Subbing solution was made up fresh on the day of use each time as this can easily become infected with micro-organisms. All subsequent immunofluorescence (IF) was performed on subbed slides.

2.4.7.4 Immunofluorescence brain section staining

Free-floating sagittal sections approximating 0.6 mm from the midline were used for the purpose of the IF investigations. Sections were placed in a 24 well plate and rinsed in PBS on orbital shaker prior to commencing staining protocol to ensure removal of any remaining cryo-m-bed or cryoprotectant solution.

2.4.7.4.1 Antigen retrieval

Antigen retrieval is utilised to enable epitope retrieval of proteins when the cross-linking caused by fixation masks protein epitopes, preventing the primary antibody from successfully binding the protein of interest. Several variations of antigen retrieval are currently available with the one described below being one of the mildest. Other antigen retrieval solutions include the likes of formic acid, commonly used when staining for Aβ plaques. Briefly, sections being stained for the microglial/macrophage marker Iba1 were immersed in 10 mM citric acid (pH 6.0; Appendix I; see chapter 7.1, Table 7.3) after rinsing in PBS to remove any cryoprotectant solution. Brain sections were then placed in a pre-heated oven at 80°C for 30 min. The plate was then rapidly

cooled on ice prior to removal of the citric acid solution and proceeding with standard staining protocol detailed below.

2.4.7.4.2 Immunofluorescence staining protocol

All sections were placed in permeabilisation solution (Appendix I; see chapter 7.1 Table 7.3) for 1 h at room temperature with gentle agitation on an orbital shaker. The solution was carefully pipetted off and replaced with blocking solution (Appendix I; see chapter 7.1, Table 7.3) for 1 h on an orbital shaker at room temperature to diminish non-specific antibody binding. Sections were then incubated in primary antibody (see Table 2.9) overnight at 4°C with gentle orbital shaking.

Antibody	Supplier Product ID	Host	Dilution	Conjugate
GFAP	Millipore AB5541	Chicken	1:500	-
Iba1	Millipore MABN92	Mouse	1:250	-
Anti-Mouse	Jackson ImmunoResearch 315-495-044	Rabbit	1:500	DyLight 649
Anti-Chicken	Life Technologies A21449	Goat	1:250	Alexa Fluor 647

Table 2.9 List of antibodies used for immunohistochemistry of brain sections

Sections were then washed for 3x 10 min in permeabilisation solution and incubated in the appropriate fluorophore tagged secondary antibody, as detailed in Table 2.9 for 1 h at room temperature in the dark with gentle orbital shaking. Finally, sections were again washed for 3x 10 min in permeabilisation solution on a gentle orbital shaker at room temperature in the dark and given a final quick wash in PBS. Sections were stored short-term in fresh PBS at 4°C until ready for mounting onto subbed slides. Upon slide mounting excess PBS was removed and slides briefly dried before adding DAPI containing Vectashield mounting medium (Vector Laboratories Inc.) and affixing coverslips and sealing with nail varnish to prevent the slides drying out. Slides were stored in purpose-designed slide boxes at 4°C and later imaged using a TCS SP5 confocal microscope (Leica).

2.4.7.4.3 Confocal imaging setup

Slides were imaged on a TCS SP5 Confocal microscope with associated LAS AF software (Leica). The microscope in question having access to light lasers of multiple wavelengths a list of the lasers used and relevant wavelength parameters for

each laser are detailed in Table 2.10. Slides were imaged using the microscope's oil immersion 40x lens and in order to more accurately compare staining between genotypes and diets, settings were adjusted for the control group (RC fed WT) and maintained consistent throughout the remainder of the slide imaging for each protein of interest. In addition, controls were stained with every staining setup and negative controls were performed by omitting the primary antibody to ensure the fluorescence captured was not the result of auto-fluorescence signalling from the section.

Laser	Colour (spectrum)	Antibody /fluorophore	Fluorophore excitation / emission wavelength peaks (nm)
405	Violet (UV)	- /DAPI	358/461
633	Far-red (visible)	GFAP/AlexaFluor 647	650/668
633	Far-red (visible)	Iba 1/Dylight 649	652/670

Table 2.10 Specifications of confocal lasers used

2.5 STATISTICAL ANALYSIS

Statistical analyses were performed using a variety of tests including t-tests and analysis of variance (ANOVA). Tests were predominantly performed in GraphPad Prism 5/6 software (GraphPad Software). Where analysis were not able to be performed using the aforementioned software, SPSS Statistics 21 software (IBM Corp. ©) was utilised instead enabling multivariate ANOVA to be performed, with where necessary follow up analysis of simple main effects in order to correctly assess terms of interaction. Results from ANOVAs are displayed as described below:

$$F(df_{\text{Between Groups}}, df_{\text{Within Groups}}) = x, p = y$$

Where F is the F value and stands for the ratio of two mean square values and is represented by a value x. The greater the value of x (above 1), the greater the significance of the result observed. Df stands for degrees of freedom which measure either the within or between group variability of the data being analysed. P stands for the significance of the result (or probability value) with y representing the output of the p-value.

**3 THE ROLE OF NRF2 IN
HIGH FAT FEEDING
INDUCED
INFLAMMATION**

3.1 INTRODUCTION

The pathological description of AD was first described at the turn of the 20th century by Alois Alzheimer, highlighting the role of misfolded proteins as defining markers of AD. Over a century later there are still a great many questions left unanswered in relation both to the role played by the hallmark proteins amyloid and tau, but also in reference to the mechanisms driving the development and progression of the disease. Studies involving amyloid and tau processing, as well as the discovery of genetic mutations within these protein pathways, have highlighted the importance of other important proteins such as ApoE and PSEN1/2. Many of these associated proteins have themselves subsequently been linked with detrimental mutations most of which have been associated with the development of FAD; or, as is the case with ApoE, are known risk factors contributing towards the likely development of AD. However, with the advent of genome wide association studies and the increasing collection of epidemiological data from elderly cohorts, other lifestyle risk factors have now been associated with AD. These include disorders such as metabolic syndrome, which incorporates obesity, diabetes, and hypertension, stroke and many risk factors associated with cardiovascular disease such as high blood pressure and high cholesterol. The rise of the worldwide obesity epidemic combined with the concomitant increase in life expectancy across many countries lays the groundwork for an exponential increase in the number of dementia cases diagnosed in the coming decades. However, this has also prompted an increased research interest in the links between these disorders.

As described previously, a fundamental energy imbalance lies at the heart of the development of obesity. The increase in energy intake without a concomitant increase in energy expenditure results in a surfeit of hormonal and metabolic alterations, including many which are linked with alterations to insulin related pathways. Many of these modifications are strongly linked peripherally with changes in adipose tissue (white and brown) and centrally with the hypothalamic region of the brain, known to be important both in connecting the CNS to the endocrine system *via* the pituitary gland but also in the management of hunger and satiety signals. Accordingly, the hypothalamic region has been the primary region of the brain studied with regards to obesity. Subsequent research of this region has prompted the discovery of neuronal populations now known to play important roles in feeding (orexigenic) and satiety (anorexigenic), such as those expressing proteins including agouti-related peptide and cocaine- and amphetamine-regulated transcript, both of which express receptors for leptin and insulin. However,

the key brain regions most often associated with AD are the hippocampus and cortex and it has only been more recently with the links suggested between mid-life obesity and AD that research has begun to emerge on the interaction of these regions with obesity related factors.

Studies using AD related transgenic mouse models, as well as *in vitro* cell work, have implicated obesity as being factorial in alterations of known AD related pathways. HF feeding of WT mice has been shown to prompt increased levels of APP with an aggravated inflammatory response, whilst activation of APP in macrophages *in vitro* prompted the release of pro-inflammatory markers (Puig *et al.*, 2012). In addition, studies performed on middle-aged and aged WT rats using a selection of diets high in factors such as cholesterol and hydrogenated fats demonstrated a clear alteration in immune-reactivity of key glial cells in the hippocampus (Granholt *et al.*, 2008; Freeman *et al.*, 2011). This suggests in turn that, in addition to numerous peripheral alterations, detrimental dietary changes are able to directly impact on brain biochemistry. Furthermore, these changes are not limited to the energy sensitive hypothalamic region of the brain, although alterations in hypothalamic signalling have also been reported (Kohjima *et al.*, 2010). Numerous studies using transgenic mouse models have also suggested an important role for AD related proteins in the dysregulation of insulin signalling (Ho *et al.*, 2004; Jung *et al.*, 2011; Mody *et al.*, 2011; Freeman *et al.*, 2012; Hiltunen *et al.*, 2012). This has led to some researchers coining the term ‘Type III diabetes’ in reference to AD (de la Monte & Wands, 2008), although this is by no means unanimously accepted. Furthermore, studies using models depleting AD related factors such as work produced from our own lab using *BACE1*^{-/-} mice support many of these alterations. *BACE1*^{-/-} mice fed a HF diet have a leaner phenotype in comparison to their WT counterparts, with improved insulin sensitivity and glucose homeostasis (Meakin *et al.*, 2012). Moreover, caloric restriction (CR) in a mouse model of AD has been shown to improve amyloid pathology (Wang *et al.*, 2005), whilst morbidly obese T1D patients have decreased expression of amyloid related markers in their blood following gastric bypass surgery and the subsequent associated CR (Ghanim *et al.*, 2012). When put together, these studies all advocate for altered energy homeostasis playing a pivotal role in the regulation of factors known to be involved in the development and progression of AD.

Although many studies have now demonstrated a role for chronic insulin resistance in the alteration of amyloid pathology, it is worth noting the opposing effect

observed in trials using acute insulin administration. Under these criteria where insulin is administered for a much shorter duration, an argument for favourable neuroprotective effects can be made. Low dose short-term infusion of insulin in TIID patients suppresses APP and PSEN proteins in the blood whilst ameliorating the patient's anti-inflammatory profile (Dandona *et al.*, 2011). As mentioned previously, studies using intranasal insulin administration have been associated with improved cognition in healthy individuals and patients diagnosed with MCI and mild to moderate AD (Benedict *et al.*, 2007; Craft *et al.*, 2012). In addition, rodent studies have also demonstrated enhanced performance in a variety of experimental cognition tasks following central administration of insulin (Park *et al.*, 2000; Zhao *et al.*, 2004; Haj-ali *et al.*, 2009; McNay *et al.*, 2010). However, induction of a TIID model using HF feeding attenuates the beneficial effects of acute insulin administration on cognition whilst promoting an insulin resistant environment (McNay *et al.*, 2010).

In addition to impacting on pathophysiological and metabolic changes in both rodent models and patient cohorts, diets high in fat and other TIID related factors such as cholesterol and sucrose have been shown to negatively impact on cognition. WT mice fed a HF/high cholesterol diet and hypercholesterolemic transgenic mice demonstrated diet and transgene dependent memory impairment with simultaneous activation of the central inflammatory response, whilst hypercholesterolemia in an AD mouse model accelerated amyloid pathology (Refolo *et al.*, 2000; Thirumangalakudi *et al.*, 2008). Intake of high levels of sucrose is of particular relevance to TIID and a study performed using a transgenic mouse model of AD demonstrated that intake of high levels of sucrose was able to induce insulin resistance much like a HF diet. In addition, high sucrose intake exacerbated the amyloid pathology present and impaired memory in cognitive tests indicating that increased intake of fats is not a prerequisite for alterations in cognition (Cao *et al.*, 2007). Moreover, whilst pharmacological treatment of conditions such as TIID and obesity will undoubtedly diminish the risk of subsequently developing dementia, these are by no means the only methods of contributing to an improved physical outcome. Studies in rodent models have suggested the importance of other lifestyle factors in improving cognition and metabolic related health factors. Maesako and colleagues have suggested an important role for exercise in the prevention of HF diet induced A β deposition and cognitive impairment over and above that produced by improved dietary control (Maesako *et al.*, 2012b). Maesako and colleagues have previously demonstrated that addition of environmental enrichment factors for 10 weeks, such as stands and toys, along with a running wheel improved both cognition

and amyloid pathology in HF fed *APP_{Swe/Ind}* mice (Maesako *et al.*, 2012a). This implicated a role both for environmental enrichment through the added access to objects and toys, and for exercise, through the free access to the exercise wheel and greater cage size, in positively impacting on AD-related pathology and symptoms. Subsequent to this, Maesako and colleagues went back and looked at the effects of dietary improvement on the paradigm developed, adding in a return to a RC diet either alone or in combination with the addition of environmental enrichment factors including the running wheel. From this second study they were able to show the beneficial effects associated with the addition of the running wheel and other objects superceded those associated with dietary improvement alone. Mice maintained on a HF diet throughout but given access to the exercise wheels and objects had significantly improved cognitive and pathological profiles when compared with the control group on a HF diet and with those who were switched to a RC diet without objects. Furthermore, there was no additional cognitive or pathological benefit over and above that seen with the objects alone when these were combined with a return to a RC diet (Maesako *et al.*, 2012b).

As has been previously mentioned, the majority of published literature is agreed on there being a role for increased ROS production during development of AD. This has resulted in an increased interest in the role of Nrf2 in neurodegeneration subsequent to its importance in the management and resolution of OS induced damage. In addition, Nrf2 has also been of increasing interest in relation to the study of the metabolic syndrome. Furthermore, expression of Nrf2 is known to negatively correlate with ageing with a concomitant increase in oxidising agents. Despite these revelations, relatively little work has been pursued to further characterise the role of depleted Nrf2 expression in models of neurodegeneration and ageing, with work reported centring instead on the potential for a protective effect following induction of Nrf2 signalling. The majority of *Nrf2^{-/-}* research has concentrated on its potential role in the promotion of NASH and other diet dependent physiological alterations with a flurry of publications to that effect in recent years (Tanaka *et al.*, 2008; Chowdhry *et al.*, 2010; Sugimoto *et al.*, 2010; Zhang *et al.*, 2010).

Due to the complexity of most brain related disorders, it is widely accepted that input from multiple factors come together to provide the environment required to enable diseases initiating changes. As a result, and bearing in mind the lack of overt pathology in the unchallenged *Nrf2^{-/-}* mouse model, a decision was made to incorporate an additional challenge above that of knocking out *Nrf2*. The majority of obesity research

studies using rodent models use a medium-term dietary intervention of typically up to five months. This is usually devised in such a way as to ensure animals reach the required weight category to be qualified as obese, and may be considerably shorter depending on the fat percentage of the diet in use. However, this has meant that few studies look at the long-term effects of HF feeding and the accompanying chronic low grade inflammation in the ageing brain. Therefore, in order to investigate changes in relation to their potential impact on early development of AD, dietary challenges on our mice were pursued for over a year and comparisons made between *Nrf2*^{-/-} mice and those expressing the *hAPP_{swe}* FAD mutation. In addition, a double transgenic mouse model was produced by crossing the aforementioned mouse lines allowing for the elucidation of any synergistic effects. Furthermore, this provided a novel mouse model which incorporates factors thought to be important in the early stages of AD development.

More specifically the aim of this study was to assess the effects of a long-term HF feeding systemic metabolic challenge on the brains of mice with an inflammatory and OS primed brain environment in the presence or absence of a pro-amyloidogenic human mutation. The main hypotheses based on the information available at the commencement of this project were as follows:

- 1) Long-term HF feeding of mice lacking functional Nrf2 will result in an aggravated inflammatory state within the central tissue, similar to that previously described in the liver and proportional to the levels of Nrf2 present in the brains of control animals.
- 2) Loss of Nrf2 when targeted with an environmental stressor leading to systemic inflammation will negatively impact on cognition.
- 3) Loss of Nrf2 when combined with a pro-amyloidogenic APP mutation (*hAPP_{swe}*) and under the increased inflammatory conditions induced by HF feeding will accelerate the development of amyloid related pathology and may further impact on cognition.

In order to try and confirm or disprove these hypotheses, mice from the above described genotypes (WT, *Nrf2*^{-/-}, *hAPP_{swe}*, *Nrf2*^{-/-}/*hAPP_{swe}*) were used. The main output measures for this study were an assessment of cognitive competence through the use of an elevated plus maze model of SA, an evaluation of AD related pathology advancement through protein and RNA assessment of specific AD-related proteins, and an evaluation of the central inflammatory and OS levels through the measurement of

commonly associated cytokines, proteins and support cells at either an RNA or protein level.

In order to achieve this, mice were placed on a HF diet at 8-10 weeks of age and maintained on this diet until termination (see Chapter 2.3.1 for a group number and diet composition breakdown). Cognitive assessments were performed on mice aged 3, 6, 10 and 14 months of age (see Chapter 2.3.1.4), with metabolic related measurements taken at 15 (IPGTT; see Chapter 2.3.1.2) and 16 (IPITT; see Chapter 2.3.1.3) months of age. At 16 months of age tissue was harvested from mice and either processed for biochemical analysis (see Chapters 2.4.1.1, 2.4.2-2.4.6) or immunohistochemistry (see Chapters 2.4.1.2 and 2.4.7). It is important to note that as a result of the genotyping problems that occurred (see Chapter 2.2.5.2) fewer mice than were originally allocated remained in the *hAPP_{swe}* and *Nrf2^{-/-}/hAPP_{swe}* groups. As a result, any power calculations originally evaluated prior to setting up the study, are no longer accurate for these groups. The resultant lower numbers will impact on our ability to confidently confirm significance on smaller biochemical changes recorded within these groups and therefore may prove to be a limiting factor for the interpretation of some of our results.

3.2 NRF2 AND APP ARE EXPRESSED THROUGHOUT THE MURINE BRAIN

In order to verify the expression of *Nrf2*, both in the brain as a whole and in the regions of specific interest for AD, snap frozen samples from WT mice were processed for gene expression analysis. Tissue was used from 4 distinct dissected brain regions: cerebellum, cortex, hippocampus and hypothalamus (Figure 3.1 A), with particular attention focused on the hippocampus and cortex as these are strongly implicated in AD. The hypothalamus is important in energy homeostasis, with altered brain energy metabolism now being cited as an additional marker of neurodegeneration (Wurtman, 2015). The cerebellum is often used as a control brain tissue in the study of AD cases as it is less frequently affected by disease related changes in comparison to other commonly analysed regions.

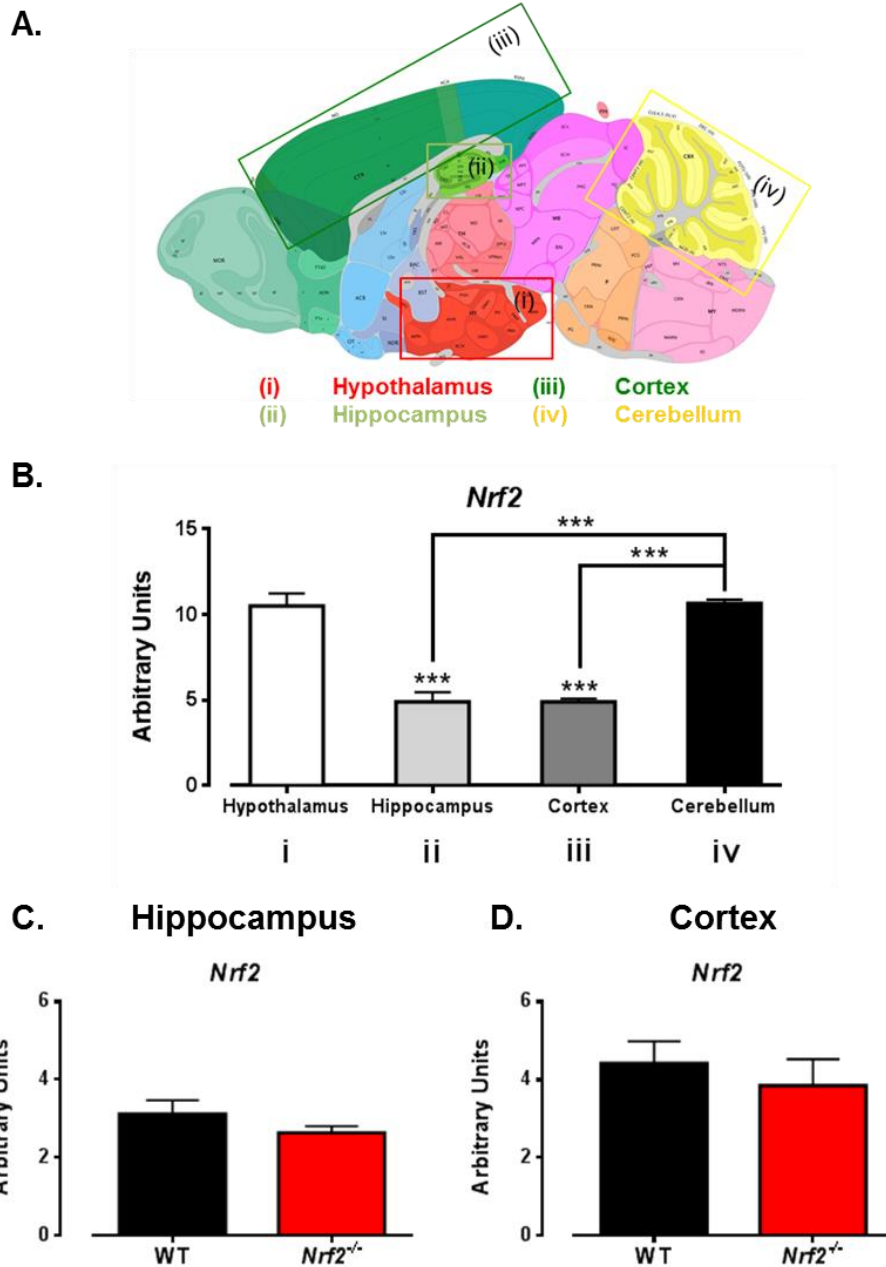


Figure 3.1 *Nrf2* is expressed throughout the mouse brain.

(A) Pictorial representation of a sagittal mouse brain section denoting the four regions dissected for measurement of brain expression levels of relevant genes (adapted from the Allen Brain Atlas). RNA was extracted from aged WT mice and the four brain regions specified in (A) were investigated for expression levels of *Nrf2* (B; n = 6). Relative expression of *Nrf2* measured with commercial primers between WT and *Nrf2*^{-/-} mice is portrayed for the hippocampus (C; n = 6) and the cortex (D; n = 6). Results are displayed as means ± s.e.m with all arbitrary units x1000 for simplicity, and analysed using one-way ANOVA with post hoc Bonferroni or unpaired Student's t-test as appropriate, with ***, p < 0.001.

Analysis indicated a significant difference in *Nrf2* expression between brain regions ($F_{3, 20} = 45.46$, $p < 0.0001$; Figure 3.1 B), with the cortex and hippocampus showing similar levels of expression. The hypothalamus has comparable expression levels to those seen in the cerebellum. However, there is a two fold increase in expression between those seen in the hippocampus/cortex and those seen in the cerebellum/hypothalamus (hippo.: 4.90 A.U. \pm 0.57; cereb.: 10.7 A.U. \pm 0.22; hypo.: 10.5 A.U. \pm 0.73; cortex: 4.89 A.U. \pm 0.21; hippo. vs cereb. $p < 0.001$; hippo. vs hypo. $p < 0.001$; cortex vs cereb. $p < 0.001$; cortex vs hypo. $p < 0.001$; $n = 6$). This confirms the expression of *Nrf2* in the brain regions tested, albeit with region specific degrees of expression. Due to the design of the *Nrf2*^{-/-} model at our disposal, verification of the model was not possible using commercially designed TaqMan primers. Primers would have to specifically recognise the b-Zip region of *Nrf2* as this contains the disruption replacement lacZ motif of the model in question, whilst the remainder of the gene remains intact and therefore recognisable by the majority of commercial primers. This can be seen in Figure 3.1 for both the hippocampus (C; $p > 0.05$) and cortex (D; $p > 0.05$).

Articles delineating the expression of APP in the brain are more prolific than those found for *Nrf2*, in no small part due to its association with AD. Gene expression of murine *APP* (*mAPP*) across the four brain regions described above confirmed its presence in the mouse brain (Figure 3.2 A). The expression of *mAPP* reported is ~100 fold higher than that shown for *Nrf2*, confirming its abundance in the central nervous system. The profile across the four brain regions is very similar to that seen for *Nrf2*, albeit with no significant differences between regions ($p > 0.05$). The *hAPP*_{swe} model chosen for these studies uses the murine *APP* promoter as previously described in the methods section (see chapter 2.2.3). As a result, the expression pattern would be expected to correlate with that shown for *mAPP*. In order to confirm the presence of the human APP variant in the model, human specific gene expression was assessed in the *hAPP*_{swe} and *Nrf2*^{-/-}/*hAPP*_{swe} models with WT mice used as negative controls.

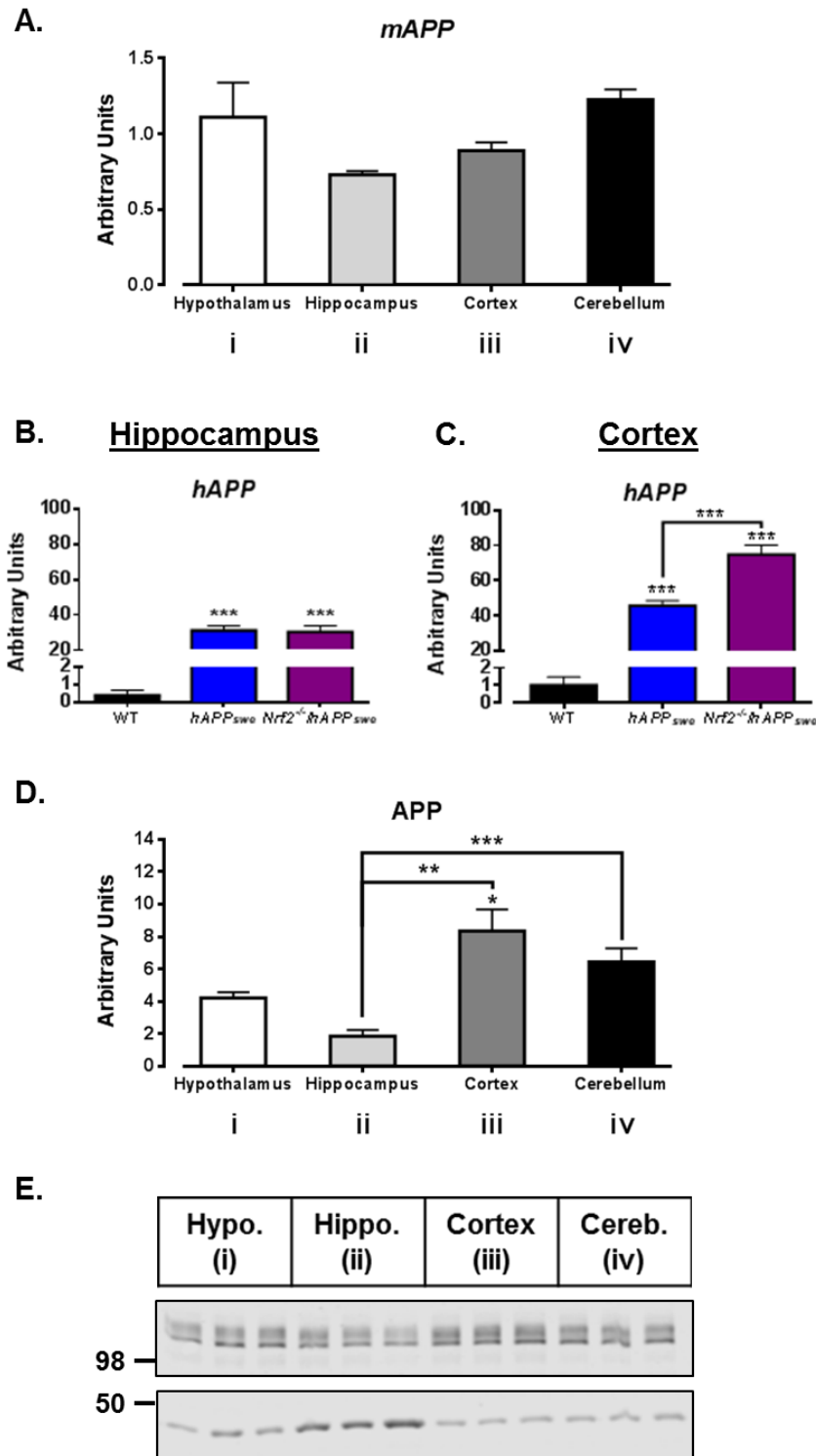


Figure 3.2 APP expression is found throughout the mouse brain.

RNA was extracted from aged WT mice and the four brain regions specified previously were investigated for expression levels of *mAPP* (A; $n = 6$). Expression of human *APP* was used to confirm the presence of the human *APP_{swe}* gene in the single (*hAPP_{swe}*) and double (*Nrf2^{-/-}/hAPP_{swe}*) transgenic mice in the two key brain areas related to AD, the hippocampus (B) and the cortex (C; $n = 4-7$). Following on from this, protein lysates were assessed across the four brain regions of WT mice for total APP expression (D) with exemplar blots in (E; $n = 6$). Results are displayed as means \pm s.e.m, and units for the expression of *hAPP* have been $\times 1000$ for simplicity and analysed using one-way ANOVA with post hoc Bonferroni, where ***, $p < 0.001$.

There is clear expression of *hAPP* observed compared to WT mice in the hippocampus ($F_{2, 13} = 56.86$, $p < 0.0001$), with both *hAPP_{swe}* and *Nrf2^{-/-}/hAPP_{swe}* displaying significantly increased levels (WT: 0.380 A.U. \pm 0.28; *hAPP_{swe}*: 31.1 A.U. \pm 2.8; *Nrf2^{-/-}/hAPP_{swe}*: 30.3 A.U. \pm 3.6; WT vs *hAPP_{swe}* $p < 0.0001$, WT vs *Nrf2^{-/-}/hAPP_{swe}* $p < 0.0001$, $n = 4-6$; Figure 3.2 B), which corresponds to the heterozygotic breeding background with no significant differences between *hAPP_{swe}* and *Nrf2^{-/-}/hAPP_{swe}* mice. Cortical expression of *hAPP* in the *hAPP_{swe}* mice is significant at a little over half that of the equivalent levels of *mAPP* ($F_{2, 13} = 179.9$, $p < 0.0001$) and with both transgenic lines exhibiting significantly increased expression than the WT controls (WT: 1.01 A.U. \pm 0.46; *hAPP_{swe}*: 45.7 A.U. \pm 2.9; *Nrf2^{-/-}/hAPP_{swe}*: 74.7 A.U. \pm 5.5; WT vs *hAPP_{swe}* $p < 0.0001$, WT vs *Nrf2^{-/-}/hAPP_{swe}* $p < 0.0001$, $n = 4-7$; Figure 3.2 C). However, the *Nrf2^{-/-}/hAPP_{swe}* mice have a further significant induction of expression over the *hAPP_{swe}* mice bringing them to similar levels to that seen for *mAPP* (*hAPP_{swe}* vs *Nrf2^{-/-}/hAPP_{swe}* $p < 0.001$, $n = 4-6$). In addition to gene expression, total APP protein levels were assessed in the brains of WT mice. A significant alteration was seen in protein across the brain regions tested ($F_{3, 20} = 11.50$, $p < 0.0001$; Figure 3.2 D), demonstrated by exemplar blots in Figure 3.2 E. The levels of APP protein in the cortex were significantly higher than in the hypothalamus and hippocampus (hypo.: 4.21 A.U. \pm 0.37; hippo.: 1.85 A.U. \pm 0.38; cortex: 8.35 A.U. \pm 1.3; hypo. vs cortex. $p < 0.001$; hippo. vs cortex $p < 0.05$; $n = 6$), whilst hippocampal levels were also significantly lower than the cerebellum (cereb.: 6.44 A.U. \pm 0.84; hippo. vs cereb. $p < 0.01$, $n = 6$).

3.3 OVEREXPRESSION OF *HAPP_{swe}* AND LOSS OF FUNCTIONAL *NRF2* HAVE OPPOSING EFFECTS ON ADIPOSITY FOLLOWING PROLONGED HIGH FAT FEEDING

Having confirmed that *Nrf2* and *APP* are both present across multiple mouse brain regions, we went on to assess the impact of a known AD risk factor, obesity, on our different mouse models. Due to the nature of AD as a disease strongly associated with ageing, mice were placed on a HF diet for longer than would be commonly performed whilst pursuing studies solely investigating the effects of excess nutrient intake on metabolic disease. Age matched mice were placed on a 45% HF diet at 8-10 weeks of age and body weight measured at three different ages, three (Figure 3.3 A), six (Figure 3.3 B) and 14 months (Figure 3.3 C); to assess both the short and long term impact of consumption of a diet high in fats on weight gain across genotypes.

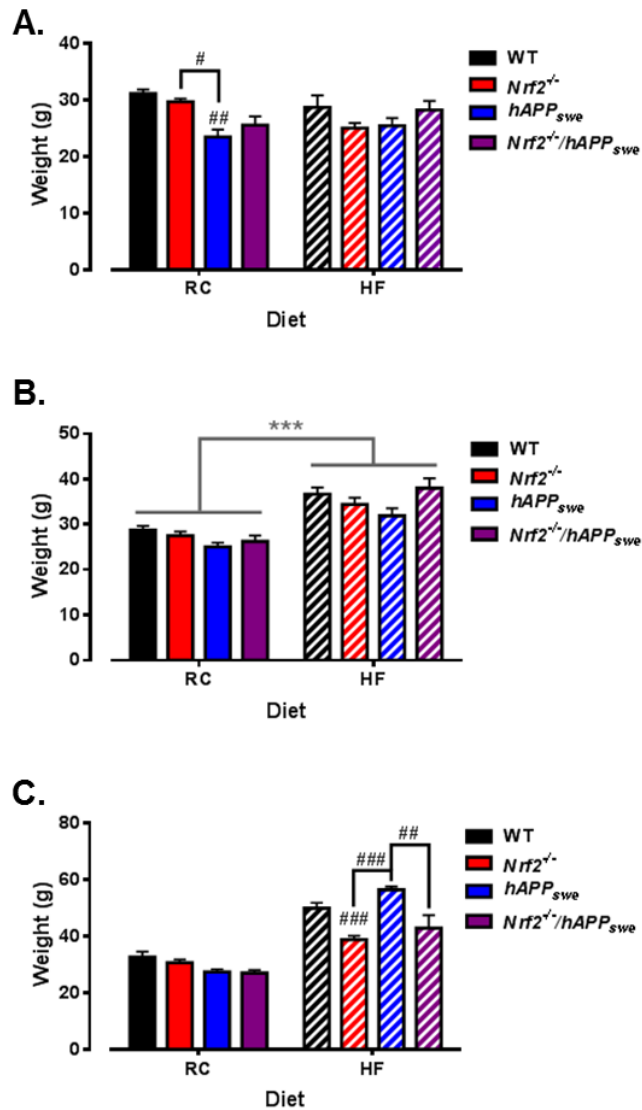


Figure 3.3 Long-term HF feeding causes a time and genotype dependent divergent change in weight gain in *Nrf2*^{-/-} and *hAPP*_{swe} transgenic mice.

Age-matched *Nrf2*^{-/-}, *hAPP*_{swe} and *Nrf2*^{-/-}/*hAPP*_{swe} mice were placed on a RC or HF (45%) diet at 8-10 weeks of age. Mice were handled regularly and body weights recorded at 3 months of age (A), 6 months of age (B) and 14 months of age (C). All data presented as means \pm s.e.m. Changes in body weight were compared between groups at each time interval by two-way ANOVA with factors of genotype and diet, post-hoc Bonferroni used as required. When positive interaction effects were reported, these replaced main effects on graphical representations of data, and were followed up through analysis of simple main effects with post-hoc Bonferroni. * Indicates significantly different main effect (***, $p < 0.001$) and # indicates significant interaction effect (#, $p < 0.05$; ##, $p < 0.01$; ###, $p < 0.001$). 3 months: WT $n = 9-14$, *Nrf2*^{-/-} $n = 12-22$, *hAPP*_{swe} $n = 8$, *Nrf2*^{-/-}/*hAPP*_{swe} $n = 7-10$; 6 months: WT $n = 19-20$, *Nrf2*^{-/-} $n = 20-22$, *hAPP*_{swe} $n = 8$, *Nrf2*^{-/-}/*hAPP*_{swe} $n = 10-12$; 14 months: WT $n = 17-18$, *Nrf2*^{-/-} $n = 21-22$, *hAPP*_{swe} $n = 5-11$, *Nrf2*^{-/-}/*hAPP*_{swe} $n = 5$.

Mice were compared at each individual time point in order to assess the role of the two main factors, namely genotype and diet on total body weight as it is assumed that there will be a significant effect of time on all groups. At three months there is a significant main effect of genotype ($F_{3,96} = 9.11$, $p < 0.0001$) and diet ($F_{1,96} = 131.2$, $p < 0.0001$). However, a significant diet*genotype interaction ($F_{3,96} = 9.78$, $p < 0.0001$) was also observed at three months. Analysis of the diet*genotype interaction using simple main effects described a significantly lower body weight of *hAPP_{swe}* mice compared to both WT and *Nrf2^{-/-}* mice on the RC diet (WT: $31.13 \text{ g} \pm 0.75$; *Nrf2^{-/-}*: $29.70 \text{ g} \pm 0.50$; *hAPP_{swe}*: $23.46 \text{ g} \pm 1.29$; WT vs *hAPP_{swe}* $p < 0.01$, *Nrf2^{-/-}* vs *hAPP_{swe}* $p < 0.05$). By 6 months of age, there is no longer a significant diet*genotype interaction ($p > 0.05$). As would be predicted there is a main effect of diet ($F_{1,109} = 60.28$, $p < 0.0001$) at 6 months of age with HF fed mice having increased body weights compared to their RC fed compatriots. There is no significant effect of genotype on body weight at 6 months ($p > 0.05$).

A final time point was measured at 14 months of age, at which point mice had been on a HF diet for about a year. Upon analysis highly significant main effects of genotype ($F_{3,96} = 9.11$, $p < 0.0001$) and diet ($F_{1,96} = 131.2$, $p < 0.0001$) were seen. However, similar to that previously observed at 3 months, there is a highly significant diet*genotype interaction ($F_{3,96} = 9.78$, $p < 0.0001$) at 14 months of age with genotype-dependent differences in response to long term HF feeding. Further investigation of simple main effects pinpointed a significantly lower weight of HF-fed *Nrf2^{-/-}* mice in comparison to WT control HF-fed mice (WT: $48.32 \text{ g} \pm 2.28$; *Nrf2^{-/-}*: $38.84 \text{ g} \pm 1.39$; WT vs *Nrf2^{-/-}* $p < 0.0001$). *hAPP_{swe}* mice were significantly heavier than both *Nrf2^{-/-}* mice and *Nrf2^{-/-}/hAPP_{swe}* mice with a trend towards but non-significant increase in comparison to WT mice (*hAPP_{swe}*: $56.50 \text{ g} \pm 1.17$; *Nrf2^{-/-}*: $38.84 \text{ g} \pm 1.39$; *Nrf2^{-/-}/hAPP_{swe}*: $42.94 \text{ g} \pm 4.55$; *hAPP_{swe}* vs *Nrf2^{-/-}* $p < 0.0001$; *hAPP_{swe}* vs *Nrf2^{-/-}/hAPP_{swe}* $p < 0.01$).

3.4 *NRF2^{-/-}* MICE MAINTAIN INSULIN SENSITIVITY EVEN AFTER LONG-TERM HIGH FAT FEEDING.

As significant differences in total body weight of long term HF fed mice were observed in a genotype-dependent manner, measures for other markers associated with DIO were pursued. Aged mice from WT, *Nrf2^{-/-}* and *hAPP_{swe}* lines that had been fed either a RC or 45% HF diet from 8-10 weeks of age were put through IPGTT (15 months) and ITT (16 months). This allowed assessment of peripheral glucose clearance

and insulin sensitivity. As has been previously reported, HF fed WT mice on a C57Bl/6 background demonstrate impaired glucose clearance and impaired insulin sensitivity (Fellmann *et al.*, 2013). IPGTT induced changes in blood glucose levels are delineated below for the RC (Figure 3.4 A) and HF (Figure 3.4 D) cohorts.

Analysis of the IPGTT AUC in RC mice showed a significant effect of genotype on glucose disposal ($F_{2,32} = 9.176$, $p < 0.001$; Figure 3.4 B). *Nrf2*^{-/-} mice demonstrate increased sensitivity to a glucose bolus, with significantly better glucose disposal compared with WT mice (WT RC: 1148 ± 40 ; *Nrf2*^{-/-} RC: 889.5 ± 54 ; WT RC vs *Nrf2*^{-/-} RC $p < 0.001$, $n = 12-15$). No significant change was seen in glucose clearance between WT mice and those carrying the *hAPP*_{swe} mutation (*hAPP*_{swe} HF: 1017 ± 35.4 ; WT vs *hAPP*_{swe} $p > 0.05$, $n = 7-18$), with no significant difference in weight seen under RC feeding ($p > 0.05$; Figure 3.4 C).

When fed a HF diet long-term a significant difference in glucose management is seen between genotypes ($F_{2,22} = 6.565$, $p < 0.01$), where both *Nrf2*^{-/-} and *hAPP*_{swe} mice have significantly altered glucose disposal. *hAPP*_{swe} show an impaired ability to dispose of glucose following a bolus injection when compared to WT controls, whilst *Nrf2*^{-/-} mice fed a HF diet maintain an improved clearance profile which is significantly better than that seen in *hAPP*_{swe} mice (WT HF: 1556 ± 117 ; *Nrf2*^{-/-} HF: 1192 ± 152 ; *hAPP*_{swe} HF: 2144 ± 58 ; WT HF vs *Nrf2*^{-/-} HF $p > 0.05$, WT HF vs *hAPP*_{swe} $p < 0.05$, *Nrf2*^{-/-} HF vs *hAPP*_{swe} HF $p < 0.01$, $n = 4-16$; Figure 3.4 E). This occurs despite no longer seeing a significant difference between WT and *Nrf2*^{-/-} mice fed a HF diet ($F_{2,22} = 6.565$, $p < 0.01$; WT HF vs *Nrf2*^{-/-} HF $p > 0.05$, $n = 4-16$; Figure 3.4 F), although this may also be due to low numbers in the *Nrf2*^{-/-} group. However, HF-fed *hAPP*_{swe} mice were found to be heavier than HF-fed WT mice on the day of testing (WT HF: 49.4 ± 2.1 ; *hAPP*_{swe} HF: 55.7 ± 1.3 ; WT HF vs *hAPP*_{swe} HF $p < 0.05$, $n = 5-16$) and therefore received a higher glucose dose as this is administered in a weight-dependent manner. This may prove to be influential in the development of glucose clearance changes displayed here.

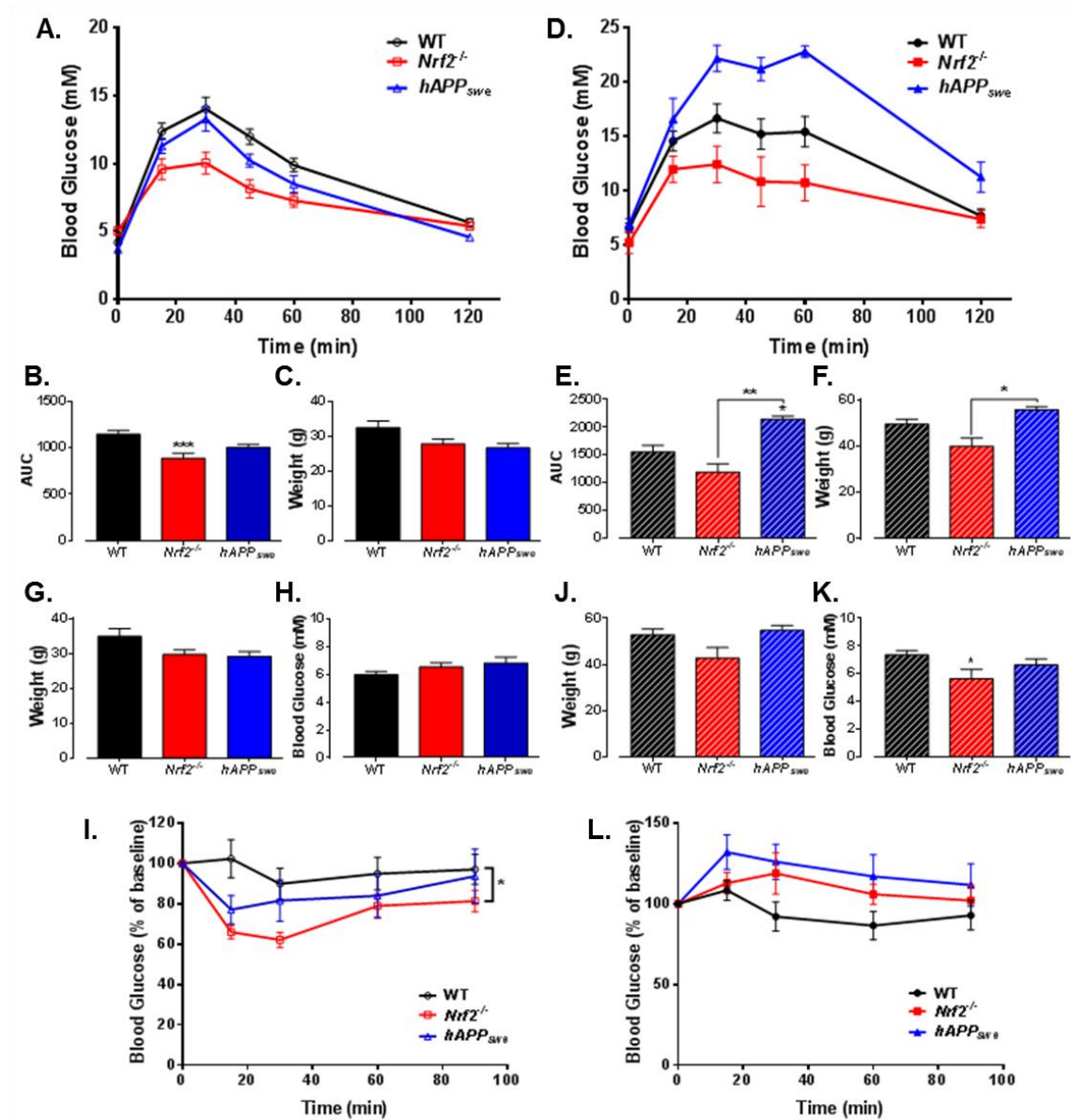


Figure 3.4 Knocking out *Nrf2* and overexpressing *hAPP*_{swe} have opposing effects on glucose tolerance in aged high fat fed mice.

Aged WT, *Nrf2*^{-/-} and *hAPP*_{swe} mice fed a RC or HF diet from 8-10 weeks of age underwent IP glucose and insulin tolerance tests. At 15 months tail vein blood glucose was measured for IPGTT over a period of 120 min in RC (A) and HF (D) fed animals. The area under the curve (AUC) was calculated for each animal and are represented in B and E, whilst body weights on day of testing are presented in C and F respectively (WT n = 15-16; *Nrf2*^{-/-} n = 4-12; *hAPP*_{swe} n = 5-8). ITTs (16 months) were performed using an insulin bolus. Tail vein blood glucose was measured over a period of 90 min for RC and HF fed animals. Body weights on day of testing (G and J) as well as basal fasted blood glucose levels (H and K) are reported for RC and HF fed animals respectively. Changes in blood glucose over time are represented as percentage of baseline values for RC (I) and HF (L) fed respectively (WT n = 13-14; *Nrf2*^{-/-} n = 4-12; *hAPP*_{swe} n = 5-8). All data are represented as means ± s.e.m. AUC and basal glucose concentrations analysed by one-way ANOVA with post hoc Bonferroni, ITT were analysed by dietary group using repeated measures 2-way ANOVA with post-hoc Bonferroni (*, p < 0.05; **, p < 0.01). All experiments were performed and data collected by Dr. A.D. McNeilly, postgraduate PhD student S.M. Jalicy and Dr. P.M. Meakin

ITT were performed to assess insulin sensitivity across genotypes and diet groupings. There were no significant changes in RC fed animals at the time of ITT testing ($p > 0.05$; Figure 3.4 G). Further to this, fasted blood glucose levels showed no significant difference between genotypes on a RC diet with all groups reporting concentrations of $\sim 6\text{mM}$ glucose ($p > 0.05$, $n = 8-14$; Figure 3.4 H). In contrast, $Nrf2^{-/-}$ mice fed a HF diet maintain a similar level of glucose to their RC counterparts whilst both WT and $hAPP_{swe}$ mice have higher circulating glucose levels after HF feeding ($F_{2,19} = 3.656$, $p < 0.05$; WT HF: 7.36 ± 0.31 ; $Nrf2^{-/-}$ HF: 5.63 ± 0.70 ; $hAPP_{swe}$ HF: 6.64 ± 0.44 ; WT HF vs $Nrf2^{-/-}$ HF $p < 0.05$, $hAPP_{swe}$ HF vs WT and $Nrf2^{-/-}$ HF $p > 0.05$, $n = 4-13$; Figure 3.4 K), despite no longer seeing a significant difference in weight ($p > 0.05$; Figure 3.4 J). ITT percentage glucose response curves are reported for RC (Figure 3.4 I) and HF (Figure 3.4 L) groups. From these graphs it is possible to see that, along with maintained glucose clearance, aged $Nrf2^{-/-}$ mice remain more sensitive to an insulin bolus on a RC diet ($F_{2,31} = 3.327$, $p < 0.05$; WT RC vs $Nrf2^{-/-}$ RC $p < 0.05$). However, this effect is lost following long-term HF feeding ($p > 0.05$).

3.5 PERIPHERAL EFFECTS OF LONG-TERM HIGH FAT FEEDING

As well as affecting overall weight gain, consuming a diet high in fat is also linked with detrimental effects on specific peripheral organs. Organs such as the liver, that is responsible for a large percentage of the detoxification and metabolism of external factors, and the spleen, responsible for the production of some of the inflammatory related markers, are both prime targets for obesity driven impairment. Finally, there have been numerous publications linking obesity with cardiac remodelling and hypertrophy. As the animals in this study were placed on a HF diet for upward of a year, longer than many studies looking at obesity, a combination of ageing, diet and incorporation of transgenic mutations could all potentially play a role in altering organ physiology, including heart.

All tissues examined were measured as both raw tissue weight and as a percentage of total body weight in order to tease out the effects of the main genotype and diet factors. There was shown to be a main effect of genotype ($F_{3,72} = 5.69$, $p < 0.01$; $n = 4-20$) but not diet ($p > 0.05$) on total heart weight (Figure 3.5 A), exemplified by significant increases in the heart weights of the $Nrf2^{-/-}/hAPP_{swe}$ mice compared to WT controls (WT: $0.179 \text{ g} \pm 7 \times 10^{-3}$; $Nrf2^{-/-}/hAPP_{swe}$: $0.242 \text{ g} \pm 0.02$; WT vs $Nrf2^{-/-}/hAPP_{swe}$ $p < 0.05$) and both $Nrf2^{-/-}$ and $Nrf2^{-/-}/hAPP_{swe}$ having bigger hearts than the $hAPP_{swe}$ mice ($Nrf2^{-/-}$: $0.209 \text{ g} \pm 0.01$; $hAPP_{swe}$: $0.159 \text{ g} \pm 9 \times 10^{-3}$; $Nrf2^{-/-}/hAPP_{swe}$: 0.242

$g \pm 0.02$; $hAPP_{swe}$ vs $Nrf2^{-/-}$ $p < 0.05$, $hAPP_{swe}$ vs $Nrf2^{-/-}/hAPP_{swe}$ $p < 0.01$). When body weight is accounted for and heart weight is measured as a percentage of bodyweight, a main effect of both genotype ($F_{3,72} = 14.16$, $p < 0.0001$) and diet ($F_{1,72} = 41.86$, $p < 0.0001$) is seen (Figure 3.5 B), with HF feeding leading to a smaller percentage heart weight, which is to be expected. The main effect of genotype is caused by the increased percentage heart weight of both $Nrf2^{-/-}$ and $Nrf2^{-/-}/hAPP_{swe}$ mice over WT and $hAPP_{swe}$ mice (WT: $0.494 \% \pm 0.03$; $Nrf2^{-/-}$: $0.679 \% \pm 0.04$; $hAPP_{swe}$: $0.492 \% \pm 0.03$; $Nrf2^{-/-}/hAPP_{swe}$: $0.762 \% \pm 0.09$; WT vs $Nrf2^{-/-}$ $p < 0.0001$; WT vs $Nrf2^{-/-}/hAPP_{swe}$ $p < 0.001$, $hAPP_{swe}$ vs $Nrf2^{-/-}$ $p < 0.001$, $hAPP_{swe}$ vs $Nrf2^{-/-}/hAPP_{swe}$ $p < 0.001$). No diet*genotype interaction was observed ($p > 0.05$). It is worth noting that all tissue measurements were performed on whole organ weights. As a result, the alterations in cardiac weight observed could be further clarified by dissection of the cardiac tissue to ascertain the occurrence of any region specific alterations in tissue mass that might be indicative of pathological heart remodelling.

Both a main effect of genotype ($F_{3,72} = 8.582$, $p < 0.0001$; $n = 4-18$) and a small but significant main effect of diet ($F_{1,72} = 4.355$, $p < 0.05$) were shown to impact on total liver weight. This is exemplified by a small HF feeding dependent increase in liver weight and significantly lower liver weights in the $Nrf2^{-/-}$ mice compared to WT controls and $hAPP_{swe}$ mice (WT: $1.55 \text{ g} \pm 0.08$; $Nrf2^{-/-}$: $1.107 \text{ g} \pm 0.05$; $hAPP_{swe}$: $1.493 \text{ g} \pm 0.09$; WT vs $Nrf2^{-/-}$ $p < 0.001$, $hAPP_{swe}$ vs $Nrf2^{-/-}$ $p < 0.05$). When looking at liver as percentage of total bodyweight, a main effect of both genotype ($F_{3,71} = 3.343$, $p < 0.05$) and diet ($F_{1,71} = 21.25$, $p < 0.0001$) is seen. However, in this case there is also a significant diet*genotype induced interaction ($F_{3,71} = 3.992$, $p < 0.05$) with $Nrf2^{-/-}$ and $Nrf2^{-/-}/hAPP_{swe}$ mice having smaller livers as percentage of total body weight compared to WT and $hAPP_{swe}$ mice fed a RC but not HF diet (WT: $5.22 \% \pm 0.39$; $Nrf2^{-/-}$: $4.10 \% \pm 0.15$; $hAPP_{swe}$: $5.17 \% \pm 0.26$; $Nrf2^{-/-}/hAPP_{swe}$: $3.25 \% \pm 0.22$; WT vs $Nrf2^{-/-}$ $p < 0.05$, WT vs $Nrf2^{-/-}/hAPP_{swe}$ $p < 0.01$, $hAPP_{swe}$ vs $Nrf2^{-/-}/hAPP_{swe}$ $p < 0.05$).

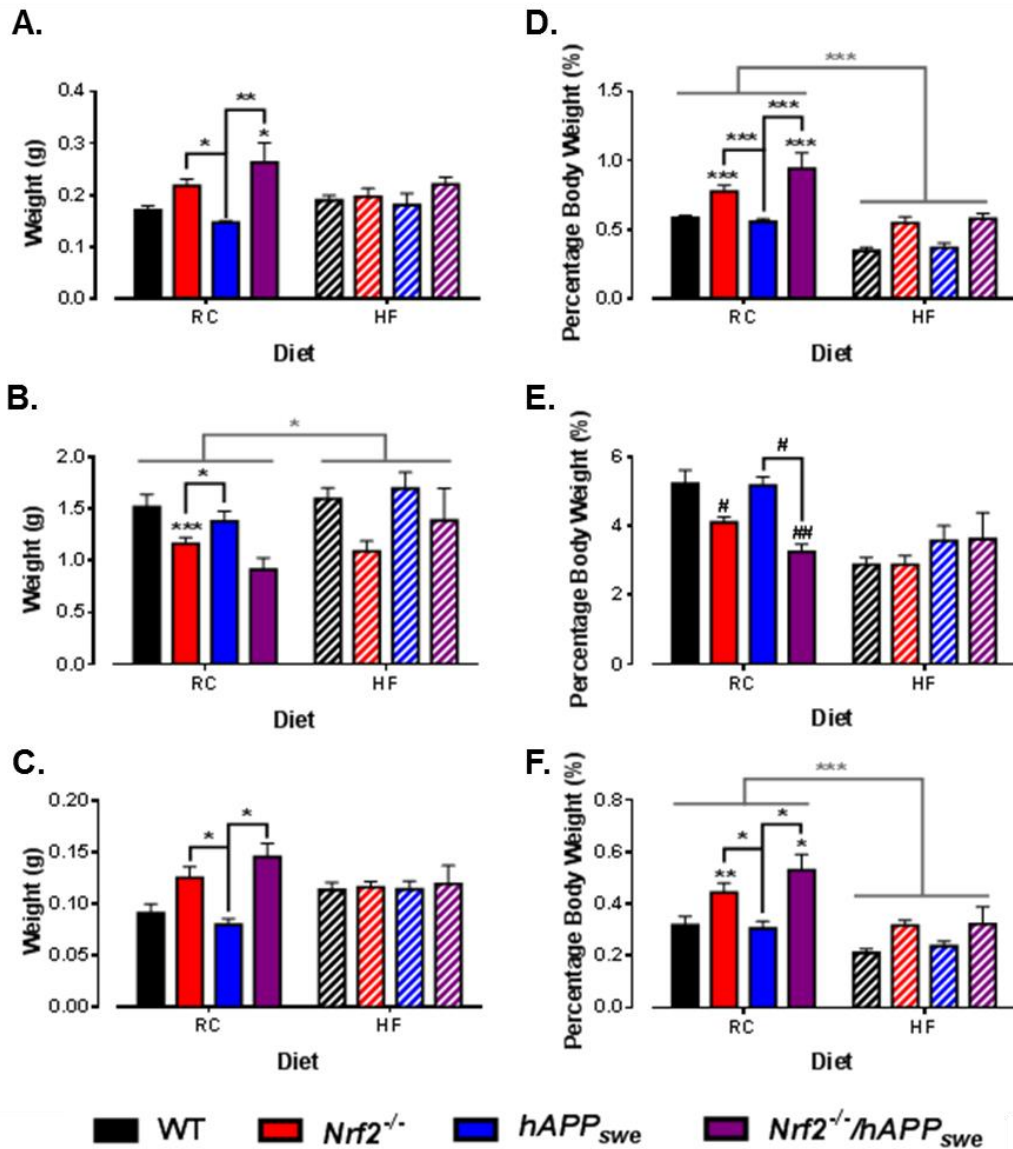


Figure 3.5 HF feeding further impacts on changes in key physiological organs driven by the loss of *Nrf2*^{-/-}.

Tissue was harvested from aged (\pm 16 months) RC and HF fed WT, *Nrf2*^{-/-}, *hAPP*_{swe} and *Nrf2*^{-/-}/*hAPP*_{swe} mice. Organ weights were obtained for hearts (A) after clearing of any remaining blood, livers (B) and spleens (C) to investigate genotype related effects on peripheral tissue health. Organ weights were assessed in relation to total body weight on day of harvest in order to clarify any dietary related changes. These are reported as percentage body weight for the heart (D), liver (E) and spleen (F; WT n = 9-14, *Nrf2*^{-/-} n = 15-20, *hAPP*_{swe} n = 5-9, *Nrf2*^{-/-}/*hAPP*_{swe} n = 4). Data is presented as means \pm s.e.m. and analysed using two-way ANOVA with genotype and diet as designated factors, post-hoc Bonferroni performed as necessary. If positive factor interaction occurred, analysis was followed up by investigation of simple main effects with post-hoc Bonferroni. When positive interaction effects were reported, these replaced main effects on graphical representations of data. * indicates significant main effect of individual factor (*, p < 0.05; **, p < 0.01; ***, p < 0.001), # indicates significant interaction effect (#, p < 0.05; ##, p < 0.01).

Only a main effect of genotype ($F_{3,73} = 3.397$, $p < 0.05$; $n = 4-20$) was seen for total spleen weight. This was illustrated by significantly larger spleens in both the $Nrf2^{-/-}$ and $Nrf2^{-/-}/hAPP_{swe}$ mice compared to $hAPP_{swe}$ mice ($Nrf2^{-/-}$: $0.121 \text{ g} \pm 7*10^{-3}$; $hAPP_{swe}$: $0.092 \text{ g} \pm 6*10^{-3}$; $Nrf2^{-/-}/hAPP_{swe}$: $0.132 \text{ g} \pm 0.01$; $hAPP_{swe}$ vs $Nrf2^{-/-}$ $p < 0.05$, $hAPP_{swe}$ vs $Nrf2^{-/-}/hAPP_{swe}$ $p < 0.05$). Measuring percentage body weight of the spleens showed a main effect of both diet ($F_{1,72} = 16.50$, $p < 0.001$) and genotype ($F_{3,72} = 7.074$, $p < 0.001$) but no significant interaction term ($p > 0.05$). Similar to percentage heart weight, HF feeding decreases the spleens percentage of total body weight. The genotype dependent effect is maintained, however, with $Nrf2^{-/-}$ and $Nrf2^{-/-}/hAPP_{swe}$ mice having larger spleens when compared to WT and $hAPP_{swe}$ mice (WT: $0.273 \% \pm 0.02$; $Nrf2^{-/-}$: $0.392 \% \pm 0.03$; $hAPP_{swe}$: $0.281 \% \pm 0.02$; $Nrf2^{-/-}/hAPP_{swe}$: $0.426 \% \pm 0.06$; WT vs $Nrf2^{-/-}$ $p < 0.01$, WT vs $Nrf2^{-/-}/hAPP_{swe}$ $p < 0.05$, $hAPP_{swe}$ vs $Nrf2^{-/-}$ $p < 0.05$, $hAPP_{swe}$ vs $Nrf2^{-/-}/hAPP_{swe}$ $p < 0.05$).

3.6 EFFECT OF $NRF2^{-/-}$ AND A HIGH FAT DIET ON AGEING COGNITION

Cognitive impairment is often one of the first outward signs of dementia displayed by a patient. Moreover, obesity and TIID have both been associated with impaired cognition in a variety of mouse models (Valladolid-Acebes *et al.*, 2011; Niedowicz *et al.*, 2014; Tucsek *et al.*, 2014) and clinical studies (Smith *et al.*, 2011). Assessment of the effect of genotype along with high fat feeding over time on cognition was done using a model of continuous SA performed in a closed-arm elevated plus maze. In addition to a measure of SA, locomotor activity was assessed by comparing the number of arm entries performed over a set period of time (10 min). Mice fed a RC diet from WT, $Nrf2^{-/-}$ and $Nrf2^{-/-}/hAPP_{swe}$ backgrounds were assessed for alternation in SA at four individual time points, namely 3, 6, 10 and 14 months of age.

There was no main effect of genotype on number of arm entries, indicating no impact on locomotor activity was produced by the loss of $Nrf2^{-/-}$ or addition of $hAPP_{swe}$ at these time points. A main effect of time was observed ($F_{3,133} = 7.055$, $p < 0.001$), with all groups performing significantly fewer arm entries at 14 months than at 6 and 10 months (6 months: 35.4 ± 1.6 ; 14 months: 27.9 ± 1.6 ; 6 months vs 14 months $p < 0.01$, 10 months vs 14 months $p < 0.01$, $n = 34-48$; Figure 3.6 A). Moreover, a similar change is seen in the number of alternations performed. A main effect of time is again seen ($F_{3,133} = 10.818$, $p < 0.001$) with no effect of genotype, exemplified by significantly fewer alternations performed at 14 months than at previous time points for all groups concerned (3 months: 18 ± 1.3 ; 6 months: 17.9 ± 0.81 ; 10 months: 16.2 ± 0.98 ; 14

months: 11.6 ± 0.85 ; 3 months vs 14 months $p < 0.01$, 6 months vs 14 months $p < 0.001$, 10 months vs 14 months $p < 0.01$, $n = 20-48$; Figure 3.6 B).

From the measures determined above, percentage SA (%SA) was calculated with the equation described in Figure 3.6 C and previously described by McNay and colleagues (2000). When analysed, there were both main effects of genotype and time with no interaction seen between these factors on the ability of mice to perform egocentric SA (Genotype: $F_{2,133} = 5.551$, $p = 0.005$; Time: $F_{3,133} = 4.630$, $p = 0.004$). A significant decrease in %SA was seen over time with mice performing fewer successful alternations at 10 and 14 months than at 3 months (3 months: 65.5 ± 2.7 ; 10 months: 52.1 ± 1.8 ; 14 months: 50.7 ± 3.2 ; 3 months vs 10 months $p < 0.01$, 3 months vs 14 months $p < 0.01$, $n = 20-48$; Figure 3.6 D). Furthermore, mice harbouring the novel double mutation ($Nrf2^{-/-}/hAPP_{swe}$) were significantly impaired when compared to both WT and $Nrf2^{-/-}$ mice with no significant difference seen between these two (WT: 58.4 ± 2.0 ; $Nrf2^{-/-}$: 55.8 ± 1.8 ; $Nrf2^{-/-}/hAPP_{swe}$: 45.8 ± 3.6 ; WT vs $Nrf2^{-/-}/hAPP_{swe}$ $p < 0.01$, $Nrf2^{-/-}$ vs $Nrf2^{-/-}/hAPP_{swe}$ $p < 0.05$, $n = 21-74$).

Further to analysing the effect of these mutations on cognition over time, we also compared the effect of HF feeding on cognition and locomotor activity over time in WT and $Nrf2^{-/-}$ mice. When HF feeding is incorporated into the task performance, we see very different profiles for WT and $Nrf2^{-/-}$ mice. Although no significant change is observed in cognition as measured by %SA and no diet*time*genotype interaction was observed, we do see both genotype*diet and time*diet interactions in the number of arm entries (Figure 3.7 A and E) and alternations (Figure 3.7 B and F) performed with HF fed $Nrf2^{-/-}$ mice performing more arm entries and alternations than WT counterparts (genotype*diet: arm entries: $F_{1,139} = 6.531$, $p = 0.012$; alternations: $F_{1,139} = 5.544$, $p = 0.020$. time*diet: arm entries: $F_{1,139} = 6.531$, $p = 0.012$; alternations: $F_{1,139} = 5.544$, $p = 0.020$). Furthermore, although no significant effect of is seen for diet alone, a main effect of genotype is reported for the number of arm entries and alternations performed (arm entries: $F_{1,139} = 9.778$, $p = 0.002$; alternations: $F_{1,139} = 6.393$, $p = 0.013$), whilst there is still a significant effect of time on the number of alternations performed as well as the ability to perform SA (Alternations: $F_{1,139} = 7.145$, $p = 0.001$; SA: $F_{1,139} = 10.090$, $p < 0.001$, Figure 3.7 C and G). This is matched by attenuated weight gain in mice lacking $Nrf2^{-/-}$ fed a HF diet when compared to controls as has been described above (Figure 3.7 D and H, and refer back to Figure 3.4).

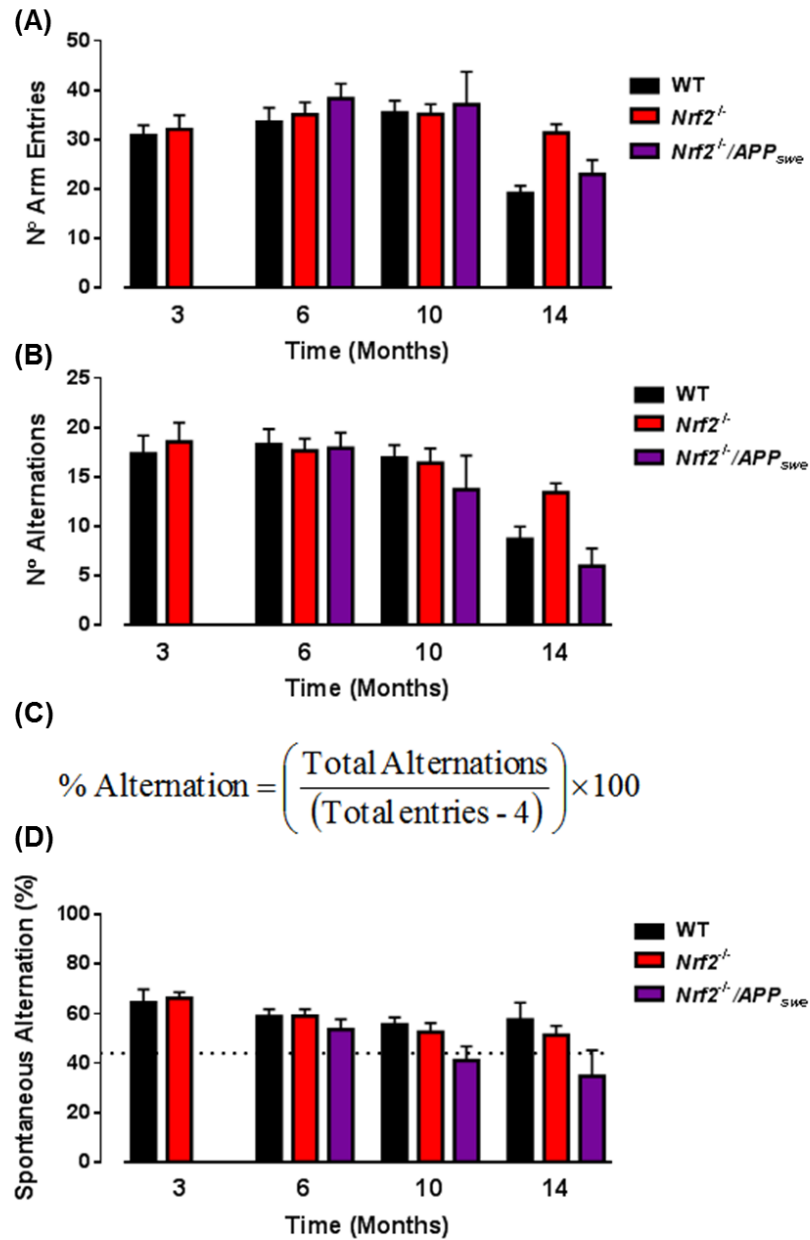


Figure 3.6 A time-dependent impairment in spontaneous alternation is seen in all groups whilst *Nrf2*^{-/-}/*hAPP*_{swe} decline more rapidly than WT and *Nrf2*^{-/-} mice.

Mice from WT, *Nrf2*^{-/-} and *Nrf2*^{-/-}/*hAPP*_{swe} backgrounds were put through the closed arm elevated plus maze at four different ages, namely 3, 6, 10 and 14 months. Measures were taken for total number of arm entries performed (A) and total number of alternations performed (B). These were used to calculate %SA using the equation depicted in C, with results reported in D. All data are presented as means \pm s.e.m. and analysed by ANOVA or MANOVA as appropriate. (3 months: WT: n = 9, *Nrf2*^{-/-}: n = 11; 6 months: WT: n = 14, *Nrf2*^{-/-}: n = 18, *Nrf2*^{-/-}/*hAPP*_{swe}: n = 10; 10 months: WT: n = 19, *Nrf2*^{-/-}: n = 22, *Nrf2*^{-/-}/*hAPP*_{swe}: n = 7; 14 months: WT: n = 7, *Nrf2*^{-/-}: n = 23, *Nrf2*^{-/-}/*hAPP*_{swe}: n = 4).

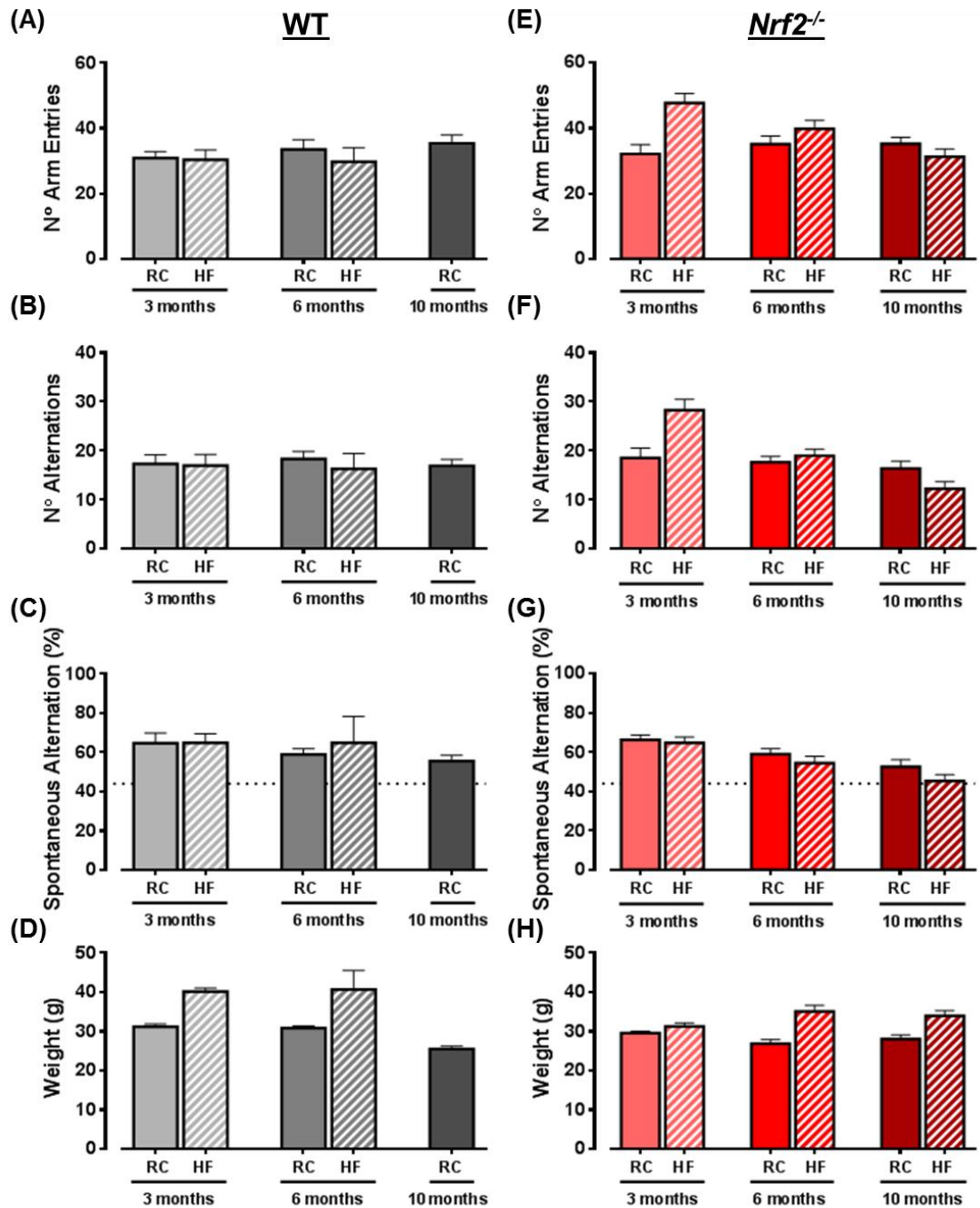


Figure 3.7 HF feeding significantly increases activity in young and middle-aged mice lacking *Nrf2* without impairing their ability to SA.

RC and HF mice from WT and *Nrf2*^{-/-} were put through the closed arm elevated plus maze at three different ages, namely 3, 6, and 10 months. Measures were taken for total number of arm entries performed (A and E) and total number of alternations performed (B and F). These were used to calculate SA (C and G), whilst body weight was also measured on day of testing (D and H). All data are presented as means \pm s.e.m. and analysed by ANOVA or MANOVA as appropriate. (3 months: WT: n = 6-9, *Nrf2*^{-/-}: n = 10-11; 6 months: WT: n = 4-14, *Nrf2*^{-/-}: n = 18-26; 10 months: WT: n = 19, *Nrf2*^{-/-}: n = 11-22).

Analysis revealed a significant diet dependent difference in the number of alternations and arm entries performed at individual time points by HF animals, with HF fed mice performing more arm entries and alternations at 3 months of age but significantly fewer by 10 months of age (3 months: arm entries: RC: 31.5 ± 2.3 ; HF: 39.0 ± 2.7 ; RC vs HF $p < 0.05$; alternations: RC: 17.9 ± 1.4 ; HF: 22.7 ± 1.6 ; RC vs HF $p < 0.05$, $n = 16-20$. 10 months: arm entries: RC: 35.3 ± 1.6 ; HF: 12.3 ± 1.9 ; RC vs HF $p < 0.05$; alternations: RC: 16.7 ± 0.96 ; HF: 12.3 ± 1.9 ; RC vs HF $p < 0.05$, $n = 11-41$). This decrease in locomotor activity, as measured by arm entries, coincides in HF fed *Nrf2*^{-/-} mice with a slower body weight gain. In addition, a significant effect of diet on genotype is observed, with analysis using simple main effects showing that *Nrf2*^{-/-} mice perform more arm entries and alternations when on a HF diet compared to those on RC, an effect not replicated in WT mice (WT RC vs HF $p > 0.05$. *Nrf2*^{-/-}: arm entries: RC: 34.1 ± 1.5 ; HF: 39.6 ± 1.6 ; *Nrf2*^{-/-} RC vs HF $p < 0.05$; alternations: RC: 17.5 ± 0.9 ; HF: 19.9 ± 0.98 ; *Nrf2*^{-/-} RC vs HF $p = 0.078$, $n = 47-51$). Finally the main effects of time are the same as described above and therefore shall not be reiterated here.

3.7 THE EFFECT OF HIGH FAT FEEDING AND *NRF2*^{-/-} ON INFLAMMATION AND PROTEIN CARBONYLATION MARKERS IN THE MOUSE BRAIN

AD had been linked with an increased presence of brain inflammation, particularly in the regions surrounding abnormal protein depositions such as A β plaques. It is, as previously mentioned, also associated with obesity and the metabolic syndrome as well as strokes and cardiovascular events; all of which are linked to an increased presence of inflammation. We have already shown changes in size of some of the key peripheral organs involved in inflammation and metabolite detoxification. In order to assess the potential effect of our models with regards to a role in AD related inflammatory and other associated processes; age-matched aged brain tissue was processed for gene expression analysis by RT-qPCR from mice fed either a RC or 45% HF diet.

A selection of standard pro-inflammatory genes (Mosser & Edwards, 2008) was profiled in the two key AD-associated brain areas, the hippocampus (Figure 3.8 A-D) and cortex (Figure 3.8 E-H). Predominantly, changes in pro-inflammatory markers occur in the hippocampus of *Nrf2*^{-/-} mice fed a RC diet. There is a non-significant trend for an increase in *IL-1 β* in the hippocampus of *Nrf2*^{-/-} mice compared to controls (WT RC: 1.00; *Nrf2*^{-/-} RC: 2.94 ± 0.99 ; WT RC vs *Nrf2*^{-/-} RC $p = 0.08$, $n = 9-10$; Figure 3.8 A) with HF feeding of *Nrf2*^{-/-} causing a mild attenuation of the phenotype (*Nrf2*^{-/-} HF:

1.80 ± 0.36, WT RC vs *Nrf2*^{-/-} HF p = 0.07, n = 7-9). This profile is repeated for the pro-inflammatory *TNF-α* with significant increases seen in RC-fed *Nrf2*^{-/-} (WT RC: 1.00; *Nrf2*^{-/-} RC: 3.02 ± 0.84; WT RC vs *Nrf2*^{-/-} RC p < 0.05, n = 9-10; Figure 3.8 B), and non-significant changes in *IL-6* and *iNOS* (Figure 3.8 C and D respectively). In all three cases, HF feeding of *Nrf2*^{-/-} appears to have an overall attenuating effect on pro-inflammatory markers in the aged mouse hippocampus (*Nrf2*^{-/-} HF *TNF-α*: 0.880 ± 0.18; *Nrf2*^{-/-} RC vs *Nrf2*^{-/-} HF p = 0.06, n = 7-10). When looking at the effect of the presence of *hAPP*_{swe} on pro-inflammatory markers it would appear to have an opposing effect to that seen in the *Nrf2*^{-/-}, with either significant decreases such as that seen with *IL-1β* (*hAPP*_{swe}: 0.773 ± 0.08, WT vs *hAPP*_{swe} p < 0.05, n = 5) or no significant change as seen in the remaining markers *IL-6*, *iNOS* and *TNF-α*. HF-feeding has no significant impact on either *hAPP*_{swe} or WT pro-inflammatory markers in the hippocampus. And although the low number of *Nrf2*^{-/-}/*hAPP*_{swe} hampers analysis they appear to show a profile similar to that seen in the *Nrf2*^{-/-} mice.

In contrast to the hippocampus, the cortex showed very little change in pro-inflammatory gene expression in any group excepting the *hAPP*_{swe} mice. These again show a decreased pro-inflammatory profile across both RC and HF fed groups. This was demonstrated by significantly decreased *IL-1β* (WT RC: 1.00; *hAPP*_{swe} HF: 0.5166 ± 0.0472; WT RC vs *hAPP*_{swe} RC p < 0.001, n = 5-10; Figure 3.8 E), *iNOS* (WT RC: 1.00; *hAPP*_{swe} RC: 0.6370 ± 0.0768; WT RC vs *hAPP*_{swe} RC p < 0.01, n = 6-10; Figure 3.8 G), and *TNF-α* (WT RC: 1.00; *hAPP*_{swe} HF: 0.5822 ± 0.134; WT RC vs *hAPP*_{swe} RC p < 0.05, n = 5-10; Figure 3.8 H), with no change seen in *IL-6* (Figure 3.8 F).

Increases in pro-inflammatory cytokines are not the only marker associated with inflammatory and oxidative damage. In order to assess the role of changes in genotype and diet on protein carbonylation, a marker for protein damage, oxyblot protein assays were performed. Oxyblots utilise the site specific introduction of carbonyl groups following oxidative damage induced molecular modification to measure changes in total protein carbonylation that have occurred in the tissue of interest. Addition of DNP-hydrazone to the protein carbonyl groups, opens them up to visualisation using a DNP-specific HRP tagged secondary antibody. In order to assess the changes in total protein carbonylation, four areas on each positive sample lane were chosen at random and densitometry calculated for each box region. Exemplar blots are depicted with the regions analysed depicted on the control lane for both the hippocampus (Figure 3.9 A) and the cortex (Figure 3.9 B) of RC and HF treated WT and *Nrf2*^{-/-} mice.

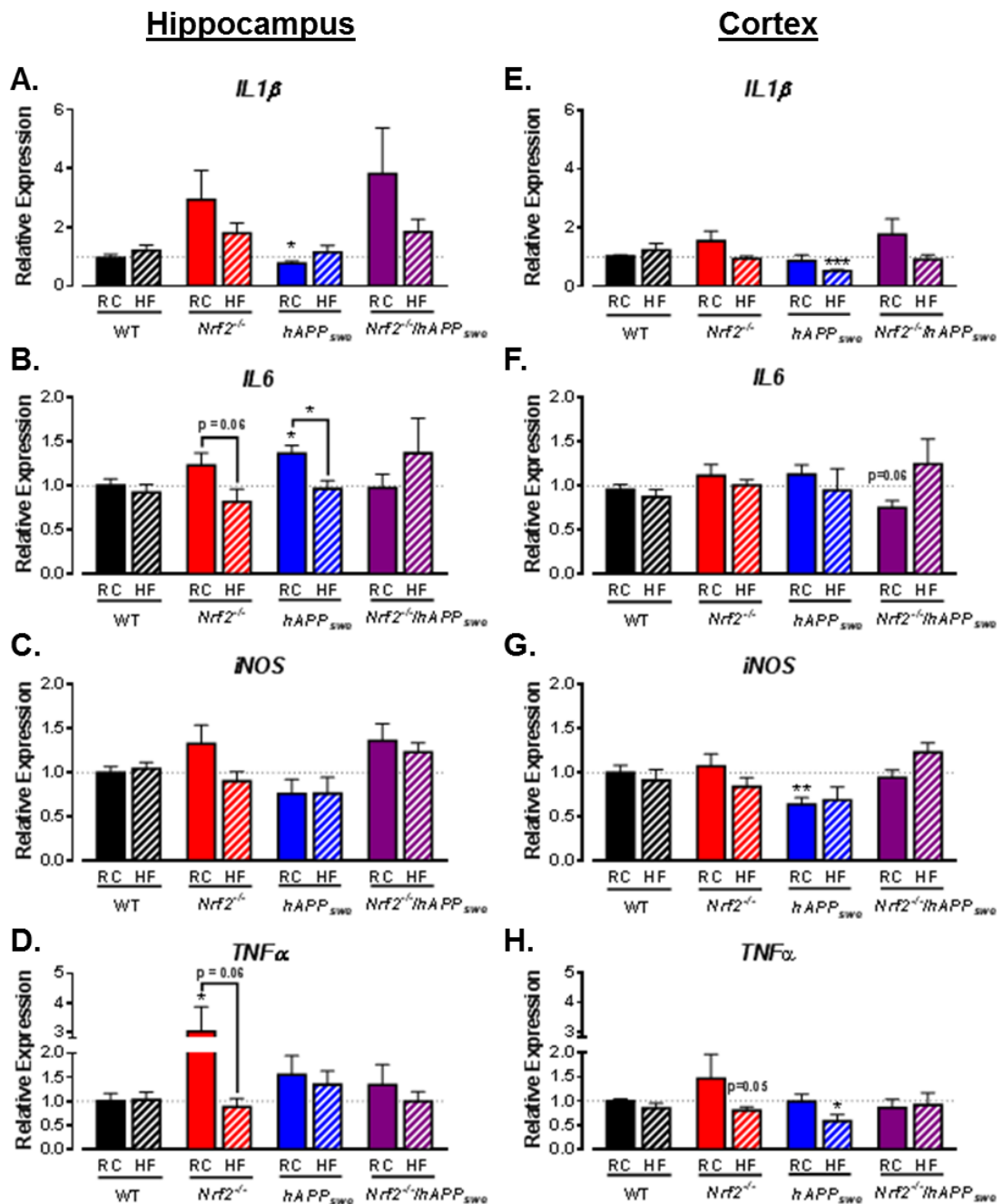


Figure 3.8 Loss of *Nrf2* drives a hippocampal dominant increase in pro-inflammatory markers in the brain that is rescued by HF feeding.

Brains harvested from aged RC and HF fed WT, *Nrf2*^{-/-}, *hAPP*_{Swe} and *Nrf2*^{-/-}/*hAPP*_{Swe} mice were dissected and the hippocampus and cortex were processed for gene expression analysis. A panel of commonly associated pro-inflammatory markers were investigated in all groups in both tissues; namely *IL-1 β* (A + E), *IL-6* (B + F), *iNOS* (C + G) and *TNF- α* (D + H) (WT n = 9-10, *Nrf2*^{-/-} n = 7-10, *hAPP*_{Swe} n = 4-6, *Nrf2*^{-/-}/*hAPP*_{Swe} n = 4). Results are reported as means \pm s.e.m., and analysed by one-sample and unpaired t-test where *, $p < 0.05$; **, $p < 0.01$; ***, $p < 0.001$.

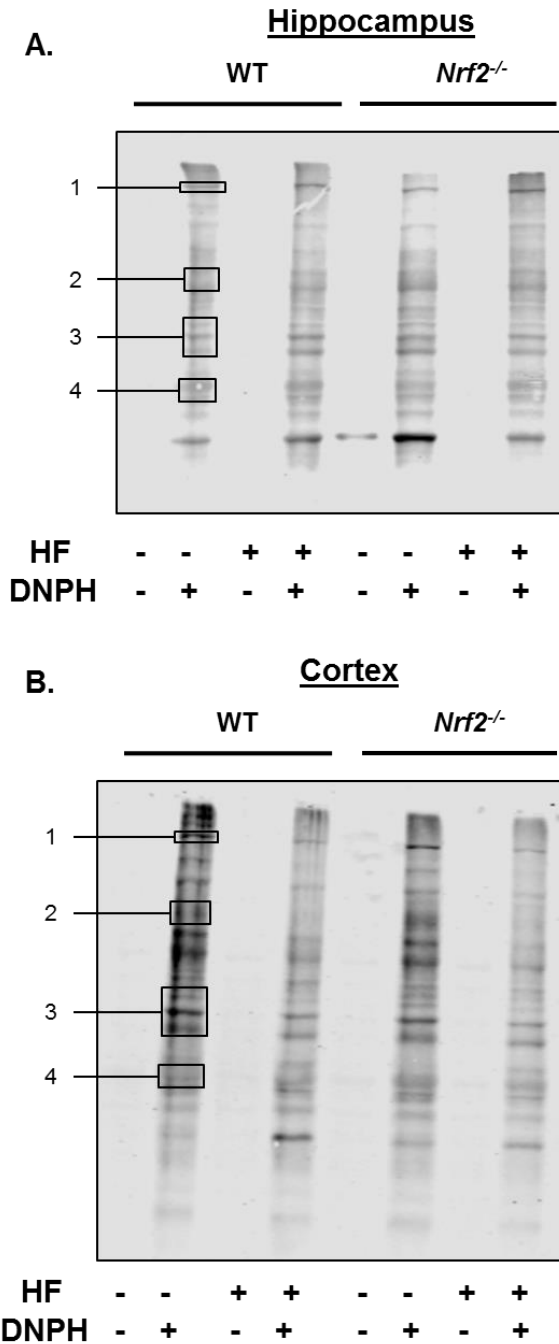


Figure 3.9 Pictorial representations of oxyblot assays performed in the hippocampus and cortex of adult RC or HF fed animals.

Aged adult mice fed either a RC or HF diet were harvested for tissue. Brains were excised and dissected from WT and *Nrf2*^{-/-} and half each of the hippocampus and cortex were lysed for protein. Equal amounts of protein were calculated and samples were run through the oxyblot assay per manufacturer's instructions to assess changes in protein carbonylation. Exemplar blots depicting the hippocampus (**A**) and cortex (**B**) are labelled with regions used for later analysis on the left of the blot.

A total change in carbonylation was assessed using cumulative scores from all of the boxed regions analysed. Tables depicting the means and s.e.m. values for the individual box regions for each mouse group are depicted in Figure 3.10 A for the hippocampus and Figure 3.10 B for the cortex. Values obtained for total carbonylation were assessed for significant effects of genotype from the loss of *Nrf2*^{-/-}, or a diet induced effect following long-term HF-feeding. No significant difference in brain protein carbonylation was seen in the hippocampus of any of the groups analysed ($p > 0.05$; Figure 3.10 C). Significantly less protein carbonylation was seen in the cortex of HF-fed *Nrf2*^{-/-} mice, which was not replicated in HF-fed WT mice (WT RC: 1.00; *Nrf2*^{-/-} HF: 0.595 ± 0.10 ; WT RC vs *Nrf2*^{-/-} HF $p < 0.05$, $n = 4-6$; Figure 3.10 D).

Given the opposing effects observed in the *Nrf2*^{-/-} and *hAPP*_{swe} mice with regards to pro-inflammatory marker profiles, a panel of anti-inflammatory, antioxidant and alternative immune markers was assessed. This allowed an evaluation of markers traditionally associated with inflammatory resolution (Mosser & Edwards, 2008). In contrast to the pro-inflammatory markers investigated the anti-inflammatory markers indicated changes predominantly in the cortical tissue (Figure 3.11 E-H) over hippocampal tissue (Figure 3.11 A-D). No significant changes were seen in anti-inflammatory markers in the hippocampus, although a trend for an effect of HF feeding in WT and *Nrf2*^{-/-} mice can be observed for *Arg 1* (Figure 3.11 A) and trend towards an increase in *YMI* in *Nrf2*^{-/-} mice (Figure 3.11 B). However, in the cortex a trend towards an increase was seen in RC and HF fed *Nrf2*^{-/-} mice for *Arg 1* (WT RC: 1.00; *Nrf2*^{-/-} RC: 2.94 ± 1.3 ; *Nrf2*^{-/-} HF: 1.45 ± 0.13 ; WT RC vs *Nrf2*^{-/-} RC $p > 0.05$, WT RC vs *Nrf2*^{-/-} HF $p < 0.05$, $n = 7$; Figure 3.11 E) and *YMI* (WT RC: 1.00; *Nrf2*^{-/-} RC: 3.49 ± 2.5 ; *Nrf2*^{-/-} HF: 3.81 ± 1.2 ; WT RC vs *Nrf2*^{-/-} RC $p > 0.05$, WT RC vs *Nrf2*^{-/-} HF $p = 0.05$, $n = 6-7$; Figure 3.11 F). HF feeding induced a significant decrease in *Arg 1* expression in HF fed *hAPP*_{swe} mice (*hAPP*_{swe} HF: 0.733 ± 0.0869 ; WT RC vs *hAPP*_{swe} HF $p < 0.05$) with no change in *YMI* from WT control and no significant changes in *Nrf2*^{-/-}/*hAPP*_{swe} mice in either *Arg1* or *YMI*.

A.

CORTEX				
	WT		<i>Nrf2</i> ^{-/-}	
	RC	HF	RC	HF
Box 1	1.00	0.717 ± 0.36	0.703 ± 0.051	0.339 ± 0.046
Box 2	1.00	0.669 ± 0.24	0.848 ± 0.12	0.472 ± 0.061
Box 3	1.00	0.693 ± 0.22	0.795 ± 0.095	0.617 ± 0.12
Box 4	1.00	0.800 ± 0.14	0.876 ± 0.13	0.706 ± 0.061
Total	1.00	0.702 ± 0.21	0.817 ± 0.093	0.595 ± 0.096

B.

HIPPOCAMPUS				
	WT		<i>Nrf2</i> ^{-/-}	
	RC	HF	RC	HF
Box 1	1.00	1.41 ± 0.49	1.27 ± 0.21	1.31 ± 0.29
Box 2	1.00	1.46 ± 0.36	1.42 ± 0.28	1.36 ± 0.34
Box 3	1.00	1.21 ± 0.24	1.24 ± 0.24	0.912 ± 0.20
Box 4	1.00	1.41 ± 0.35	1.36 ± 0.18	1.22 ± 0.26
Total	1.00	1.34 ± 0.32	1.30 ± 0.19	1.12 ± 0.22

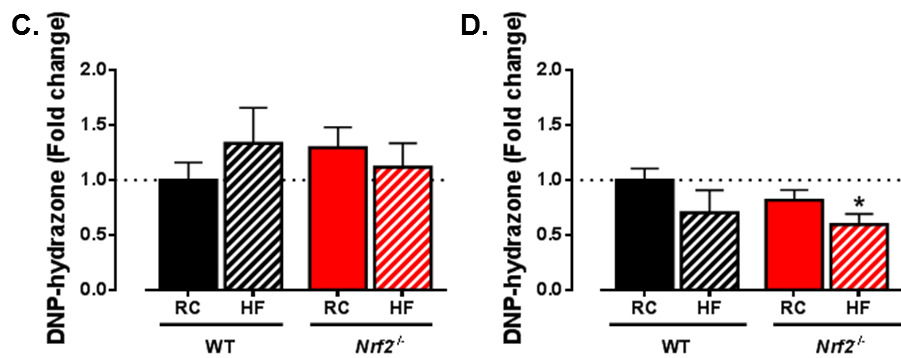


Figure 3.10 HF feeding prompts an amelioration in cortical protein carbonylation state in aged mice lacking *Nrf2*.

Aged adult mice from WT and *Nrf2*^{-/-} backgrounds fed either a RC or HF diet were harvested for tissue. Brains were dissected and hippocampal and cortical tissue were lysed for protein and processed for an oxyblot assay as per manufacturer's instructions. Blots were analysed at pre-selected points and means ± s.e.m. displayed for the individual regions and the averaged total for both the hippocampus (A) and the cortex (B). Analysis of averaged total values is indicated in (C) and (D) respectively for the hippocampus and cortex. All data is displayed as means ± s.e.m., and analyses were performed using one-sample and unpaired t-test where * = $p < 0.05$. (WT: n = 4-6; *Nrf2*^{-/-}: n = 4-5)

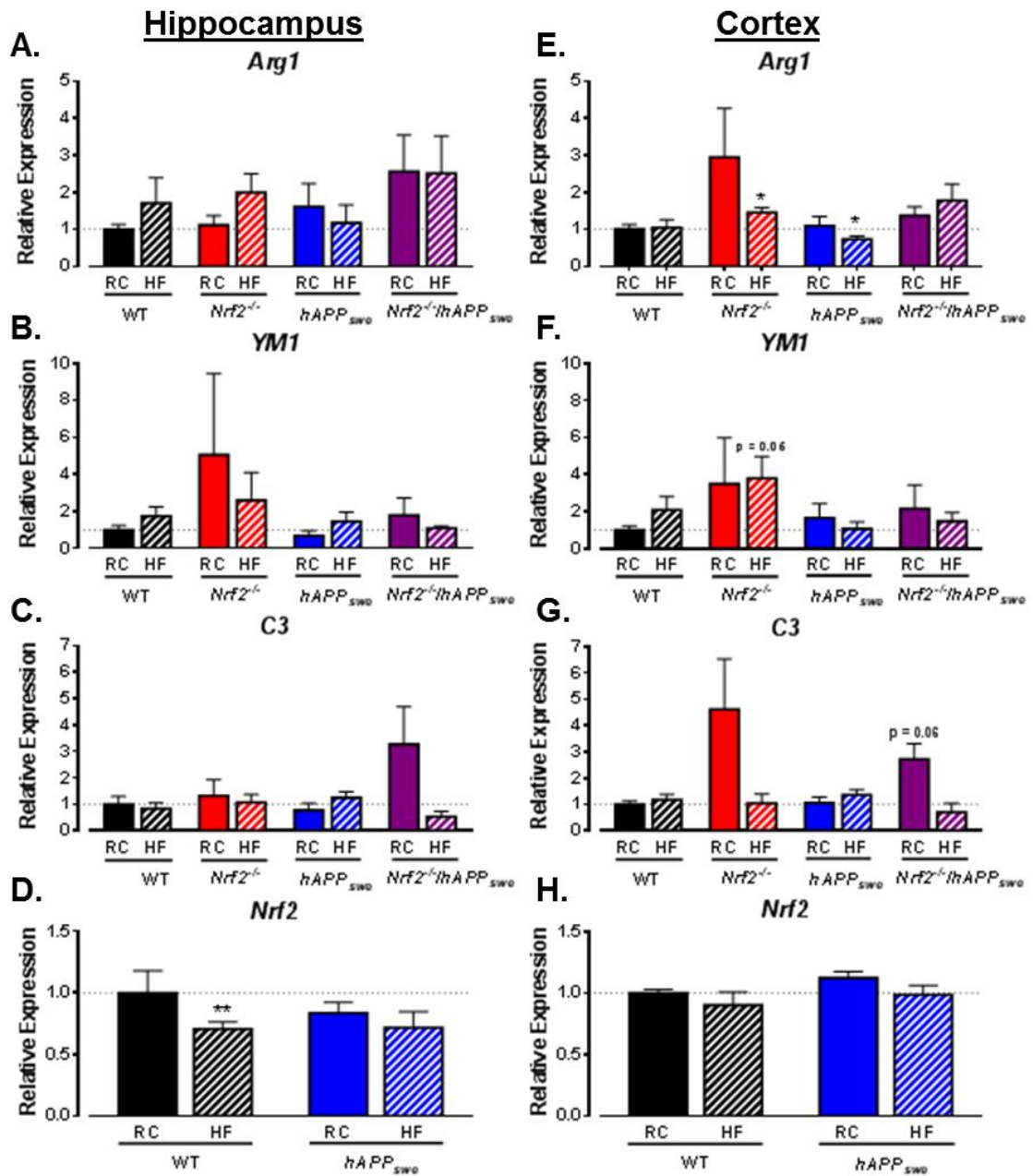


Figure 3.11 Loss of *Nrf2* drives predominantly cortical increases in anti-inflammatory and complement system markers.

Brains harvested from aged RC and HF fed WT, *Nrf2*^{-/-}, *hAPP*_{swe} and *Nrf2*^{-/-}/*hAPP*_{swe} mice were dissected and the hippocampus and cortex were processed for gene expression analysis. Commonly referenced anti-inflammatory markers *Arg1* (A + E) and *YMI* (B + F) were measured alongside a marker for the complement system, *C3* (C + G) part of the alternative immune activation pathway, and *Nrf2*^{-/-} (D + H) that drives transcription of many antioxidant genes (WT n = 6-9, *Nrf2*^{-/-} n = 5-8, *hAPP*_{swe} n = 4-5, *Nrf2*^{-/-}/*hAPP*_{swe} n = 3-4; *Nrf2* only: WT n = 4-6, *hAPP*_{swe} n = 5-6). Results are reported as means ± s.e.m., and analysed by one-sample and unpaired t-test where *, p < 0.05; **, p < 0.01.

C3, a member of the complement immune system cleaved into active forms and essential for complement cascade activation (Noris & Remuzzi, 2013), was assessed to investigate the potential role of alternative immune pathways in the protective effect of HF feeding on *Nrf2*^{-/-}. Similar to the changes observed for the anti-inflammatory markers used, there is no change in C3 expression in the hippocampus of *Nrf2*^{-/-} mice although a trend towards an increase can be observed in the RC fed *Nrf2*^{-/-}/*hAPP*_{swe} mice (Figure 3.11 C). In the cortex there is a trend towards an increase in C3 in both RC fed *Nrf2*^{-/-} and *Nrf2*^{-/-}/*hAPP*_{swe} mice (WT RC: 1.00; *Nrf2*^{-/-} RC: 4.61 ± 1.9; *Nrf2*^{-/-}/*hAPP*_{swe} RC; 2.72 ± 0.59; WT RC vs *Nrf2*^{-/-} RC p > 0.05, WT RC vs *Nrf2*^{-/-}/*hAPP*_{swe} RC p = 0.06, n = 4-7; Figure 3.11 G). No changes are seen in any of the remaining groups.

Nrf2, which as previously described drives the transcription of a large proportion of the antioxidant related genes, was assessed in the WT and *hAPP*_{swe} RC and HF groups in order to investigate the effect of HF-feeding and/or the presence of *hAPP*_{swe} on the basal expression of *Nrf2*. HF-feeding drives a significant decrease in hippocampal *Nrf2* in WT but not *hAPP*_{swe} mice (WT RC: 1.00; WT HF: 0.705 ± 0.06; WT RC vs WT HF p < 0.01, n = 6; Figure 3.11 D). No significant change in *Nrf2* expression was seen in the cortex of WT of *hAPP*_{swe} mice (Figure 3.11 H). In addition, whilst *IL-10* is also a commonly assessed anti-inflammatory cytokine, when a test plate was run the levels of *IL-10* were found to be too low to be consistently measured in these samples and as a result it was not pursued further.

3.8 DIET AND GENOTYPE AFFECT GLIAL CELL ACTIVATION IN AGED MOUSE BRAINS

Combining the changes observed in macrophage infiltration in the WAT and the altered inflammatory profiles described above. A more in depth investigation of two of the dominant support cells present in the brain was performed, namely of the astrocyte glial cells and the brain resident macrophages known as microglia. Cortical and hippocampal brain homogenates from age-matched RC and HF fed mice were processed for both RT-qPCR and protein expression. Gene expression levels of *F4/80*, a macrophage marker, was assessed in WT, *Nrf2*^{-/-}, *hAPP*_{swe} and *Nrf2*^{-/-}/*hAPP*_{swe} mice. *F4/80* was significantly increased in the hippocampi of *Nrf2*^{-/-} and *Nrf2*^{-/-}/*hAPP*_{swe} mice fed a RC diet but not their HF fed compatriots (WT RC: 1.00; *Nrf2*^{-/-} RC: 1.45 ± 0.13; *Nrf2*^{-/-}/*hAPP*_{swe}: 1.70 ± 0.19; WT RC vs *Nrf2*^{-/-} RC p < 0.01, WT RC vs *Nrf2*^{-/-}/*hAPP*_{swe} RC p < 0.05, n = 4-10; Figure 3.12 A). Only the HF fed *hAPP*_{swe} mice showed an

increase in hippocampal *F4/80* with no change seen following RC feeding (*hAPP_{swe}* HF: 1.32 ± 0.09 ; WT RC vs *hAPP_{swe}* HF $p < 0.05$, $n = 5-7$).

Only *Nrf2^{-/-}* and *Nrf2^{-/-}/hAPP_{swe}* mice have increased *F4/80* expression in cortical tissue with no changes seen in WT or *hAPP_{swe}* mice (WT RC: 1.00; *Nrf2^{-/-}* RC: 1.33 ± 0.10 ; *Nrf2^{-/-}* HF: 1.30 ± 0.06 ; *Nrf2^{-/-}/hAPP_{swe}* RC: 1.37 ± 0.14 ; *Nrf2^{-/-}/hAPP_{swe}* HF: 1.25 ± 0.06 ; WT RC vs *Nrf2^{-/-}* RC $p < 0.01$, WT RC vs *Nrf2^{-/-}* HF $p < 0.01$, WT RC vs *Nrf2^{-/-}/hAPP_{swe}* RC $p = 0.07$, WT RC vs *Nrf2^{-/-}/hAPP_{swe}* HF $p < 0.05$, $n = 4-10$; Figure 3.12 C). Furthermore, no changes are observed in the protein levels of the astrocytic marker, GFAP, in the hippocampal tissue of HF fed animals ($p > 0.05$; Figure 3.12 B). In the cortex, long term HF feeding drives a reduction in GFAP across genotypes with *hAPP_{swe}* expressing mice having reduced basal levels of expression (WT RC: 1.00; WT HF: 0.4450 ± 0.0865 ; *Nrf2^{-/-}* HF: 0.4762 ± 0.0856 ; *hAPP_{swe}* HF: 0.3208 ± 0.103 ; *Nrf2^{-/-}/hAPP_{swe}* RC: 0.3769 ± 0.0736 ; *Nrf2^{-/-}/hAPP_{swe}* HF: 0.2852 ± 0.0426 ; WT RC vs WT HF $p < 0.001$, WT RC vs *Nrf2^{-/-}* HF $p < 0.001$, WT RC vs *hAPP_{swe}* HF $p < 0.01$, WT RC vs *Nrf2^{-/-}/hAPP_{swe}* RC $p < 0.01$, WT RC vs *Nrf2^{-/-}/hAPP_{swe}* HF $p < 0.001$, $n = 4-10$; Figure 3.12 D). HF-fed *Nrf2^{-/-}* mice also exhibit a significant reduction in GFAP expression when compared to RC-fed *Nrf2^{-/-}* mice (*Nrf2^{-/-}* RC: 1.770 ± 0.423 ; *Nrf2^{-/-}* RC vs HF $p < 0.01$, $n = 8$). Figure 3.12 E shows representative blots of GFAP protein expression in the hippocampus and the cortex of all eight groups.

Microglia, like peripheral macrophages, are highly motile; much more so than some of the other glial cell population such as astrocytes. As an increased expression of the macrophage/microglial marker *F4/80* was seen in both the hippocampus and cortex of the transgenic mouse models, a decision was made to investigate any changes registering in a sub-selection of chemokines. Chemokines released from resident immune cells, such as microglia and astrocytes, following inflammatory insult are most often chemoattractants that attract further immune cells to the area of damage. MCP-1 and RANTES are both chemokines known to attract monocytes/macrophages. Given the presence of pro-inflammatory markers predominantly in the hippocampus, this is where the majority of markers were pursued.

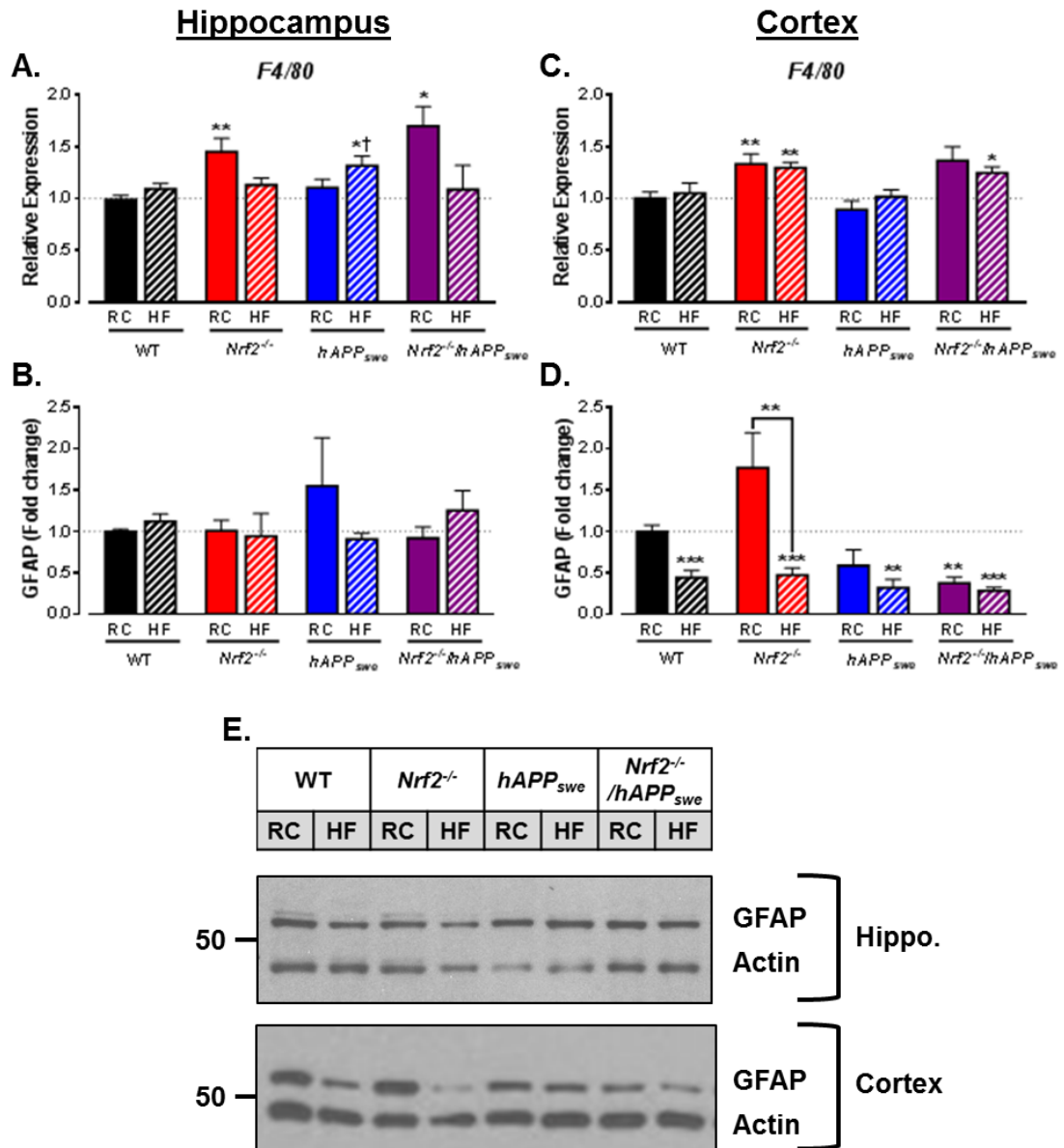


Figure 3.12 Loss of *Nrf2* drives increases in macrophage expression that is partially mimicked by astrocyte activation.

Brains from aged adult mice were harvested, dissected and processed for gene and protein expression. Markers for macrophage activation (*F4/80*; **A + C**) and astrocyte activation (GFAP; **B + D**) were analysed by RT-qPCR or Western blot respectively for changes in expression in the hippocampus (**A + B**) and cortex (**C + D**). Exemplar blots are portrayed for both the cortex and hippocampus where β -actin was used as the protein loading control (**E**). All data portrayed as means \pm s.e.m. and analysed by one-sample and unpaired t-test where * indicates significantly different from WT control and † indicates significantly different from HF fed WT. *, $p < 0.05$; **, $p < 0.01$; ***, $p < 0.001$; †, $p < 0.05$. WT $n = 6-10$, *Nrf2*^{-/-} $n = 6-10$, *hAPP*_{swe} $n = 5-6$, *Nrf2*^{-/-}/*hAPP*_{swe} $n = 4$.

There is no significant change in *MCP-1* expression in the cortex, although a trend towards increased expression is seen in the RC-fed *Nrf2*^{-/-} mice (WT: 1.00; *Nrf2*^{-/-} RC: 3.63 ± 1.9 ; WT RC vs *Nrf2*^{-/-} RC $p > 0.05$, $n = 8-9$; Figure 3.13 A). Hippocampal expression of both *MCP-1* (Figure 3.13 B) and *RANTES* (Figure 3.13 D) show a trend towards increased expression in RC fed *Nrf2*^{-/-} and *Nrf2*^{-/-}/*hAPP*_{swe} mice in addition to a significant increase in expression of *MCP-1* in HF-fed *hAPP*_{swe} mice (*MCP-1*: WT RC: 1.00; *Nrf2*^{-/-} RC: 2.49 ± 1.1 ; *Nrf2*^{-/-}/*hAPP*_{swe} RC: 6.21 ± 3.0 ; *hAPP*_{swe} HF: 2.51 ± 0.45 ; WT RC vs *Nrf2*^{-/-} RC and *Nrf2*^{-/-}/*hAPP*_{swe} RC $p > 0.05$, WT RC vs *hAPP*_{swe} HF $p < 0.05$, $n = 4-7$. *RANTES*: WT RC: 1.00; *Nrf2*^{-/-} RC: 4.32 ± 2.5 ; *Nrf2*^{-/-}/*hAPP*_{swe} RC: 4.94 ± 2.3 ; *hAPP*_{swe} HF: 1.93 ± 0.49 ; WT RC vs *Nrf2*^{-/-} RC and *Nrf2*^{-/-}/*hAPP*_{swe} RC $p > 0.05$, $n = 4-10$).

CCR2, the G-protein coupled receptor for MCP-1, appears to present a similar profile to that seen for hippocampal *MCP-1*, with increases in *Nrf2*^{-/-} and *Nrf2*^{-/-}/*hAPP*_{swe} mice (WT RC: 1.00; *Nrf2*^{-/-} RC: 2.90 ± 1.9 ; *Nrf2*^{-/-} HF: 2.52 ± 0.40 ; *Nrf2*^{-/-}/*hAPP*_{swe} RC: 1.83 ± 0.33 ; *hAPP*_{swe} HF: 2.00 ± 0.34 ; WT RC vs *Nrf2*^{-/-} RC, *Nrf2*^{-/-} HF and *Nrf2*^{-/-}/*hAPP*_{swe} RC $p > 0.05$, WT RC vs *Nrf2*^{-/-}/*hAPP*_{swe} HF $p = 0.06$, $n = 4-10$; Figure 3.13 C). No significant changes are seen in the *RANTES* associated chemokine receptor (*CCR5*; Figure 3.13 E), with only a trend towards decreased expression following HF feeding of *hAPP*_{swe} when compared to RC fed controls (*hAPP*_{swe} RC: 1.31 ± 0.23 ; *hAPP*_{swe} HF: 1.93 ± 0.49 ; *hAPP*_{swe} RC vs *hAPP*_{swe} HF $p = 0.06$, $n = 5-6$). This is a similar trend to that seen for the expression of *CCR2* in *hAPP*_{swe} mice.

The majority of the changes associated with markers of chemokine and glial expression occur in the transgenic mouse lines lacking *Nrf2*. For this reason, these genotypes were taken forward, along with controls, for investigation of morphological changes by immunofluorescence of perfuse-fixed sagittal brain sections. Images were processed for two regions of the hippocampal structure: the adjoining dentate gyrus and hippocampal CA3 area and the upper arc of the hippocampal structure in the CA1 region (Figure 3.14). As previously described, the hippocampal structure is important in correctly integrating and performing a multitude of learning and memory associated tasks. 30 μm sections, situated at ~ 0.6 mm from the midline, were stained for the well-known astrocytic marker GFAP.

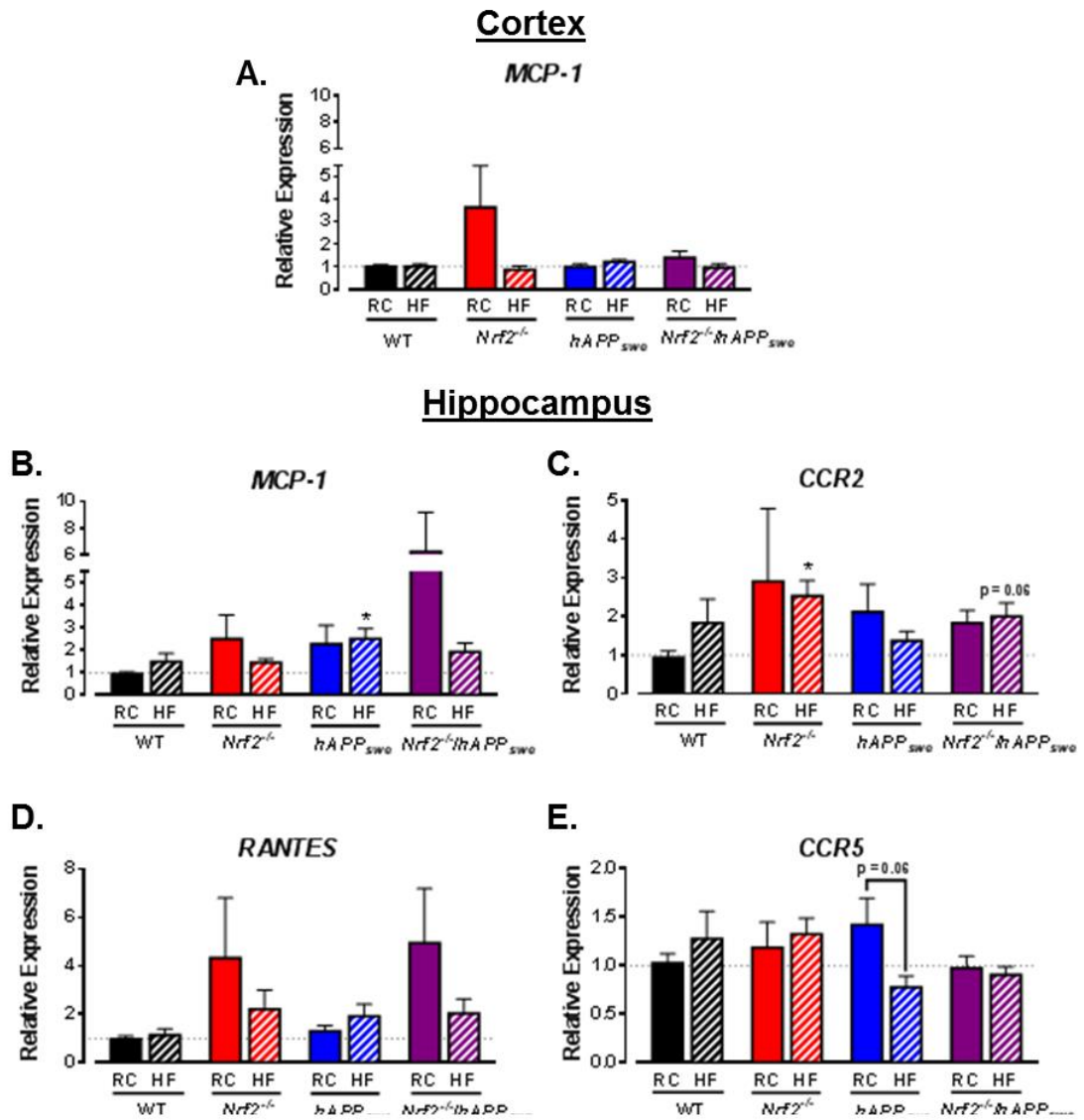


Figure 3.13 *Nrf2*^{-/-} mice show a trend for increased chemokine gene expression in the brains of aged adults.

Brains from aged adult mice were harvested from RC and HF fed WT, *Nrf2*^{-/-}, *hAPP*_{swe} and *Nrf2*^{-/-}/*hAPP*_{swe} mice and hemispheres were dissected. The hippocampus and cortex were processed for gene expression analysis. The chemokine *MCP-1* was investigated in the cortex (A) and hippocampus (B; WT n = 5-8, *Nrf2*^{-/-} n = 5-9, *hAPP*_{swe} n = 5, *Nrf2*^{-/-}/*hAPP*_{swe} n = 4). Expression of further chemokine related genes (*CCR2* (C), *RANTES* (D) and *CCR5* (E)) were concentrated in the hippocampus which showed higher levels of inflammation (WT n = 6-10, *Nrf2*^{-/-} n = 6, *hAPP*_{swe} n = 5, *Nrf2*^{-/-}/*hAPP*_{swe} n = 4). Results are reported as means ± s.e.m., and analysed by one-sample and unpaired t-test where *, p < 0.05.

Overall no change was observed in the morphology of astrocytes in HF fed WT mice, whilst RC fed *Nrf2*^{-/-} mice displayed increased presence of branching (Figure 3.15 A and B respectively). Furthermore, HF feeding of *Nrf2*^{-/-} mice increases astrocytic branching, most obvious in the CA1 region of the hippocampus. Finally and most strikingly, *Nrf2*^{-/-}/*hAPP*_{swe} mice display clear branching under RC conditions, which is increased dramatically following HF feeding. It is also possible to observe astrocytic relocation in the CA1 hippocampal region (Figure 3.15 C; for preliminary cell count data see Appendix V, chapter 7.5).

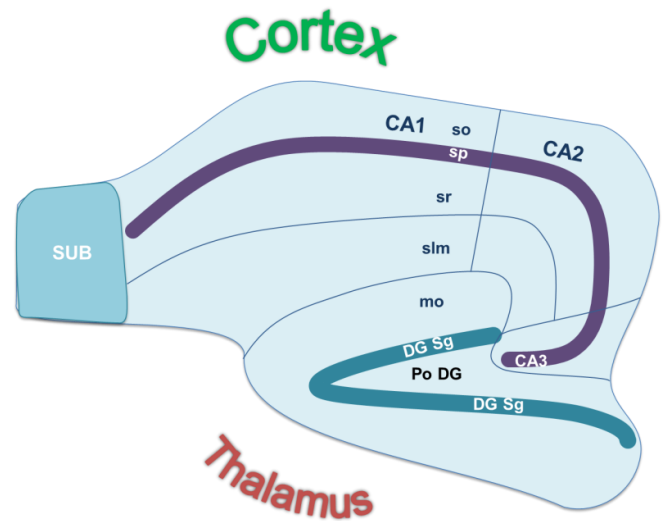
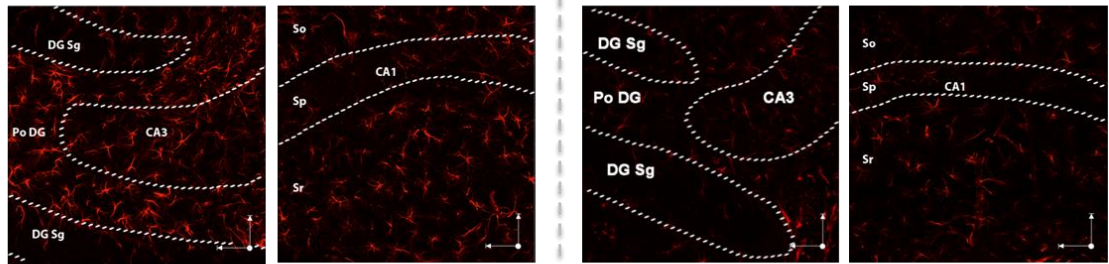
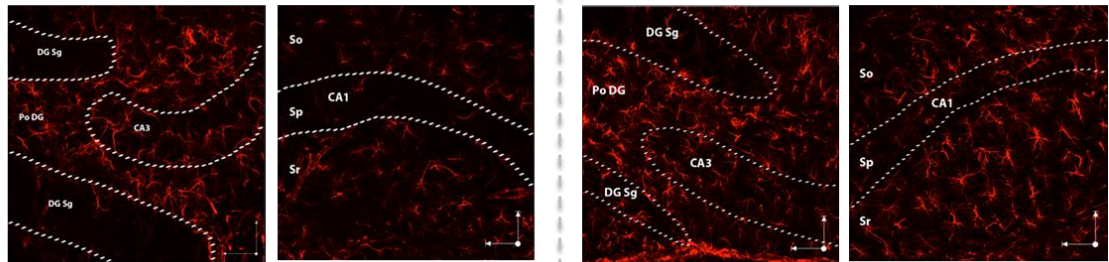
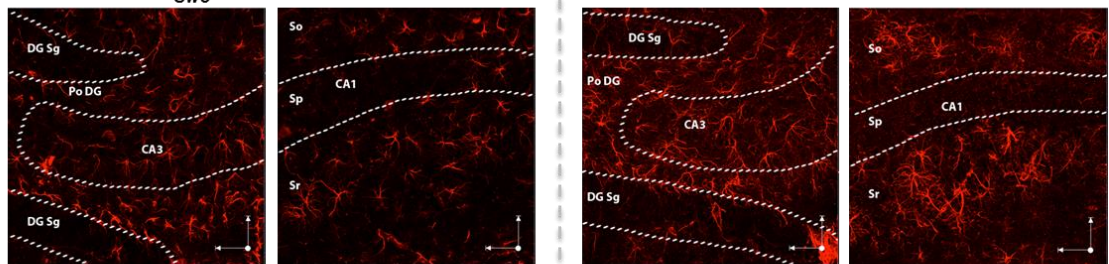


Figure 3.14 Pictorial representation of hippocampal sub-regions of the mouse brain

Where Sub = subiculum, DG Sg = granule cell layer of dentate gyrus, Po DG = polymorph layer of dentate gyrus, So = stratum oriens, Sp = pyramidal layer, Sr = stratum radiatum, slm = stratum lacunosum moleculare, mo = molecular layer of the dentate gyrus, and CA1-3 refer to the different subregions of the hippocampus

Unlike, *F4/80* which is found on different types of immune cells, *Iba1* is found specifically on macrophages and microglia. Therefore, although we cannot rule out the presence of infiltrated peripheral macrophages, the majority of cells picked up by this marker in the brain are likely to be the resident microglial cells. No apparent increase in *Iba1* staining was seen following HF feeding of WT mice (Figure 3.16 A), which is in line with the lack of *F4/80* induction. In addition, whilst it is possible to distinguish a small number of distinct *Iba1* positive cells in RC fed *Nrf2*^{-/-} mice minimal induction is seen under basal conditions (Figure 3.16 B), indicating the change in *F4/80* expression is likely reflecting an additional increase in alternative cell types. HF feeding of *Nrf2*^{-/-} mice causes a noticeable increase in staining, whilst both RC and HF fed *Nrf2*^{-/-}/*hAPP*_{swe} mice present with increased *Iba1* staining in the hippocampus (Figure 3.16 C). In conclusion, whilst the microglial staining is not as dramatic as the morphological changes seen in the astrocytes within the hippocampus both markers indicate alterations in glial cell state in *Nrf2*^{-/-} and *Nrf2*^{-/-}/*hAPP*_{swe} mice, particularly following HF feeding.

A. WT

B. *Nrf2*^{-/-}C. *Nrf2*^{-/-}/*hAPP*_{swe}

RC

HF

Figure 3.15 Removal of *Nrf2* in the brains of mice increases astrocyte branching, which is further amplified by addition of *hAPP*_{swe} in the hippocampus.

Aged WT, *Nrf2*^{-/-} and *Nrf2*^{-/-}/*hAPP*_{swe} mice fed a RC or 45% HF diet from 8-10 weeks of age were perfuse fixed in 4%-PFA. Brains were removed whole and post-fixed for 24 h in 4%-PFA before being placed in 30% sucrose solution. Brains were cut down the midline and frozen in embedding matrix in a propanol/dry ice bath. Hemibrains were sectioned sagittally on a cryostat and 30 μm sections were captured and placed in PBS. Free floating sections were stained for the astrocytic marker GFAP, mounted on gelatin coated slides and imaged on a Leica confocal microscope using a fluorescent secondary antibody. Images of the CA3/Dentate gyrus and the CA1 region of the hippocampus were acquired. Sections were imaged using consistent confocal settings and appropriate software for WT (A), *Nrf2*^{-/-} (B) and *Nrf2*^{-/-}/*hAPP*_{swe} (C) mice (n = 2-3). Where DG Sg = granule cell layer of dentate gyrus, Po DG = polymorph layer of dentate gyrus, CA3 = pyramidal layer of CA3 region of hippocampus, CA1 = pyramidal layer of CA1 region of hippocampus, So = stratum oriens, Sp = pyramidal layer, Sr = stratum radiatum, and scale bars are 50 μm in length.

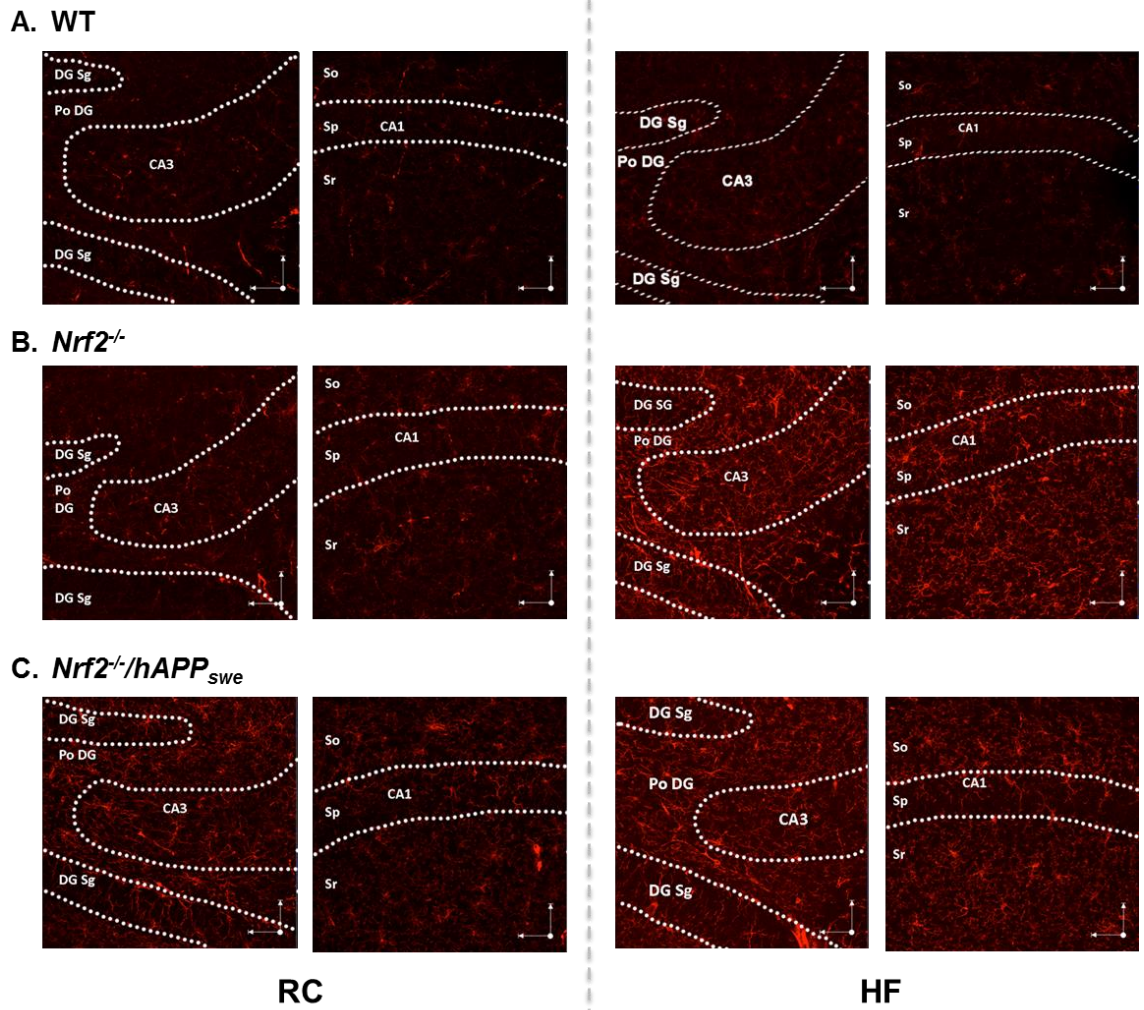


Figure 3.16 *Nrf2*^{-/-} mice show increased microglial staining following HF feeding with little change in the added presence of *hAPP*_{swe} in the hippocampus.

Aged WT, *Nrf2*^{-/-} and *Nrf2*^{-/-}/*hAPP*_{swe} mice fed a RC or 45% HF diet from 8-10 weeks of age were perfuse fixed in 4%-PFA. Brains were removed whole and post-fixed for 24 h in 4%-PFA before being placed in 30% sucrose solution. Brains were processed as for previously described and sectioned on a cryostat at 30 μ m. Free floating sections underwent antigen retrieval with 10 mM citric acid at 80°C for 30 min prior to being stained for the microglial and macrophage marker Iba1. Sections were mounted on gelatin coated slides and imaged on a Leica confocal microscope using a fluorescent secondary antibody. Sections were imaged using consistent confocal settings and appropriate software for WT (**A**), *Nrf2*^{-/-} (**B**) and *Nrf2*^{-/-}/*hAPP*_{swe} (**C**) mice (n = 2-3). Where DG Sg = granule cell layer of dentate gyrus, Po DG = polymorph layer of dentate gyrus, CA3 = pyramidal layer of CA3 region of hippocampus, CA1 = pyramidal layer of CA1 region of hippocampus, So = stratum oriens, Sp = pyramidal layer, Sr = stratum radiatum, and scale bars are 50 μ m in length.

Finally, in order to assess the effect the changes seen in the astrocyte and microglial populations have on neuronal health, protein expression of synaptophysin (SYP) was assessed. SYP, a commonly used synaptic marker that correlates with synaptic health, was measured in the hippocampal and cortical homogenates of aged RC and HF fed mice. RC fed *Nrf2*^{-/-} mice have a significant loss of SYP in the hippocampus (WT RC: 1.00; *Nrf2*^{-/-} RC: 0.659 ± 0.13; WT RC vs *Nrf2*^{-/-} RC p < 0.05, n = 8-10; Figure 3.17 A with blot exemplars depicted in C) when compared to RC-fed WT controls. This hippocampal phenotype is not only rescued by HF-feeding but also further increased above the level of the WT RC control group (*Nrf2*^{-/-} HF: 1.89 ± 0.27; WT RC vs *Nrf2*^{-/-} HF p < 0.05, *Nrf2*^{-/-} RC vs *Nrf2*^{-/-} HF p < 0.001, n = 8-10). Moreover, HF-feeding also increases the level of SYP in the hippocampus of WT mice (WT HF: 1.58 ± 0.22; WT RC vs WT HF p < 0.05, n = 8).

In juxtaposition to both WT and *Nrf2*^{-/-} mice, both *hAPP*_{swe} and *Nrf2*^{-/-}/*hAPP*_{swe} RC-fed mice have elevated levels of SYP in the hippocampus when compared to controls which is unaffected by HF-feeding (*hAPP*_{swe} RC: 1.66 ± 0.26; *Nrf2*^{-/-}/*hAPP*_{swe} RC: 1.73 ± 0.29; *hAPP*_{swe} HF: 1.81 ± 0.27; *Nrf2*^{-/-}/*hAPP*_{swe} HF: 1.68 ± 0.25; WT RC vs *hAPP*_{swe} p = 0.07, WT RC vs *hAPP*_{swe} HF p < 0.05, WT RC vs *Nrf2*^{-/-}/*hAPP*_{swe} RC p = 0.08, WT RC vs *Nrf2*^{-/-}/*hAPP*_{swe} RC p = 0.07, n = 4-8). This suggests the addition of *hAPP*_{swe} may impact on synaptic plasticity.

In contrast to the hippocampus, cortical expression of SYP appears unaffected by loss of *Nrf2*^{-/-} or HF-feeding (p > 0.05; Figure 3.17 B with blot exemplars depicted in C). RC fed *Nrf2*^{-/-}/*hAPP*_{swe} mice show a drop in SYP staining when compared to WT RC in the cortex (WT RC: 1.00; *Nrf2*^{-/-}/*hAPP*_{swe} RC: 0.8031 ± 0.0259; WT RC vs *Nrf2*^{-/-}/*hAPP*_{swe} RC p < 0.01, n = 4-8; Figure 3.17 B). No overt induction in synaptic number is induced by HF feeding, as determined by SYP expression, in fact it induces a further significant depletion in synaptophysin expression in the *Nrf2*^{-/-}/*hAPP*_{swe} mice when compared to RC fed WT or *Nrf2*^{-/-}/*hAPP*_{swe} (*Nrf2*^{-/-}/*hAPP*_{swe} HF: 0.6010 ± 0.0592; WT RC vs *Nrf2*^{-/-}/*hAPP*_{swe} HF p < 0.01, *Nrf2*^{-/-}/*hAPP*_{swe} RC vs *Nrf2*^{-/-}/*hAPP*_{swe} HF p < 0.05, n = 4-8).

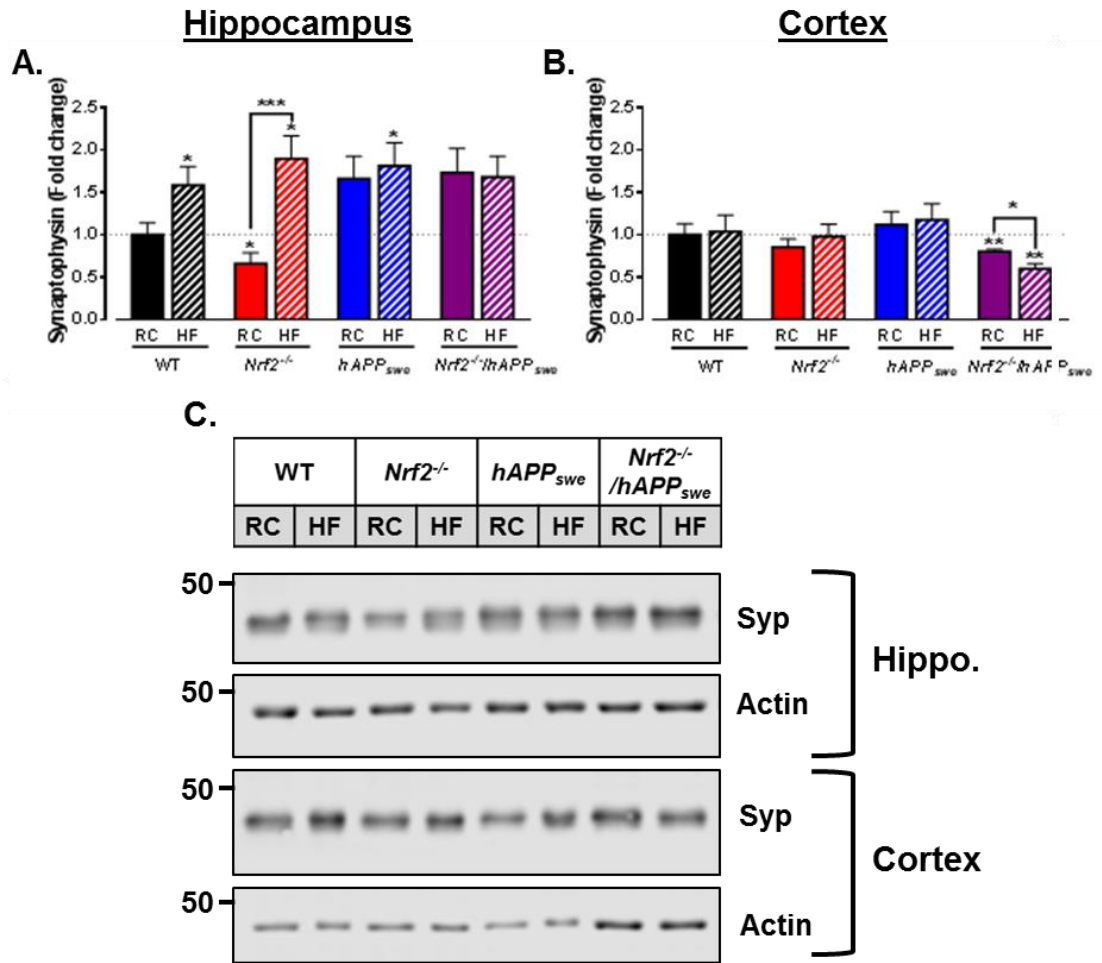


Figure 3.17 A greater impact on synaptic SYP expression is seen in the hippocampus than the cortex following loss of *Nrf2* and HF feeding.

Dissected brain tissue from aged RC and HF fed mice was processed for protein expression and probed for the synapse marker SYP in the hippocampus (A) and cortex (B). (C) Images of exemplar blots for both the hippocampus and cortex, where β -actin was used as the protein loading control. All data portrayed as means \pm s.e.m. and analysed by one-sample and unpaired t-test where * indicates significantly different from RC fed WT control. *, $p < 0.05$; **, $p < 0.01$; ***, $p < 0.001$. WT $n = 7-8$, *Nrf2*^{-/-} $n = 7-10$, *hAPP*_{swe} $n = 5-6$, *Nrf2*^{-/-}/*hAPP*_{swe} $n = 4$.

3.9 THE EFFECT OF HIGH FAT FEEDING ON EXPRESSION OF PROTEINS COMMONLY ASSOCIATED WITH AD.

In order to assess the effect of HF feeding on AD related markers such as APP and BACE1, tissue from aged, age-matched mice were processed for gene and protein expression analysis. There were no significant changes in the hippocampus of WT, *Nrf2*^{-/-} or *hAPP*_{swe} for either *mAPP* (Figure 3.18 A) or *BACE1* (Figure 3.18 B). HF feeding induces a small but significant increase in *mAPP* in *Nrf2*^{-/-}/*hAPP*_{swe} compared to HF fed WT mice (WT HF: 0.945 ± 0.05 ; *Nrf2*^{-/-}/*hAPP*_{swe} HF: 1.22 ± 0.07 ; WT HF vs *Nrf2*^{-/-}/*hAPP*_{swe} HF $p < 0.05$, $n = 4-9$). There was also a significant change in *BACE1* expression in the hippocampus of *Nrf2*^{-/-}/*hAPP*_{swe} mice with a significant decrease in RC animals compared to control that was recovered to control levels by HF feeding (WT RC: 1.00; *Nrf2*^{-/-}/*hAPP*_{swe} RC: 0.603 ± 0.09 ; *Nrf2*^{-/-}/*hAPP*_{swe} HF: 0.904 ± 0.05 ; WT RC vs *Nrf2*^{-/-}/*hAPP*_{swe} RC $p < 0.05$, *Nrf2*^{-/-}/*hAPP*_{swe} RC vs *Nrf2*^{-/-}/*hAPP*_{swe} HF $p < 0.05$, $n = 4-9$).

In the cortex, *Nrf2*^{-/-} mice on a HF diet and *Nrf2*^{-/-}/*hAPP*_{swe} mice are the only groups showing significant changes in *mAPP* (WT RC: 1.00; WT HF: 1.03 ± 0.02 ; *Nrf2*^{-/-} HF: 1.13 ± 0.04 ; *Nrf2*^{-/-}/*hAPP*_{swe} RC: 1.14 ± 0.02 ; *Nrf2*^{-/-}/*hAPP*_{swe} HF: 1.19 ± 0.07 ; WT RC vs *Nrf2*^{-/-} HF $p < 0.05$, WT RC vs *Nrf2*^{-/-}/*hAPP*_{swe} RC $p < 0.01$, WT HF vs *Nrf2*^{-/-}/*hAPP*_{swe} HF $p < 0.05$, $n = 4-10$; Figure 3.18 F). Similar to the hippocampus, the only changes in *BACE1* expression are seen in the *Nrf2*^{-/-}/*hAPP*_{swe} mice with decreased levels in the RC fed animals that are increased by HF-feeding (WT HF: 0.912 ± 0.07 ; *Nrf2*^{-/-}/*hAPP*_{swe} RC: 0.860 ± 0.08 ; *Nrf2*^{-/-}/*hAPP*_{swe} HF: 1.16 ± 0.07 ; *Nrf2*^{-/-}/*hAPP*_{swe} RC vs *Nrf2*^{-/-}/*hAPP*_{swe} HF $p < 0.05$, WT HF vs *Nrf2*^{-/-}/*hAPP*_{swe} HF $p = 0.05$, $n = 4-10$; Figure 3.18 G).

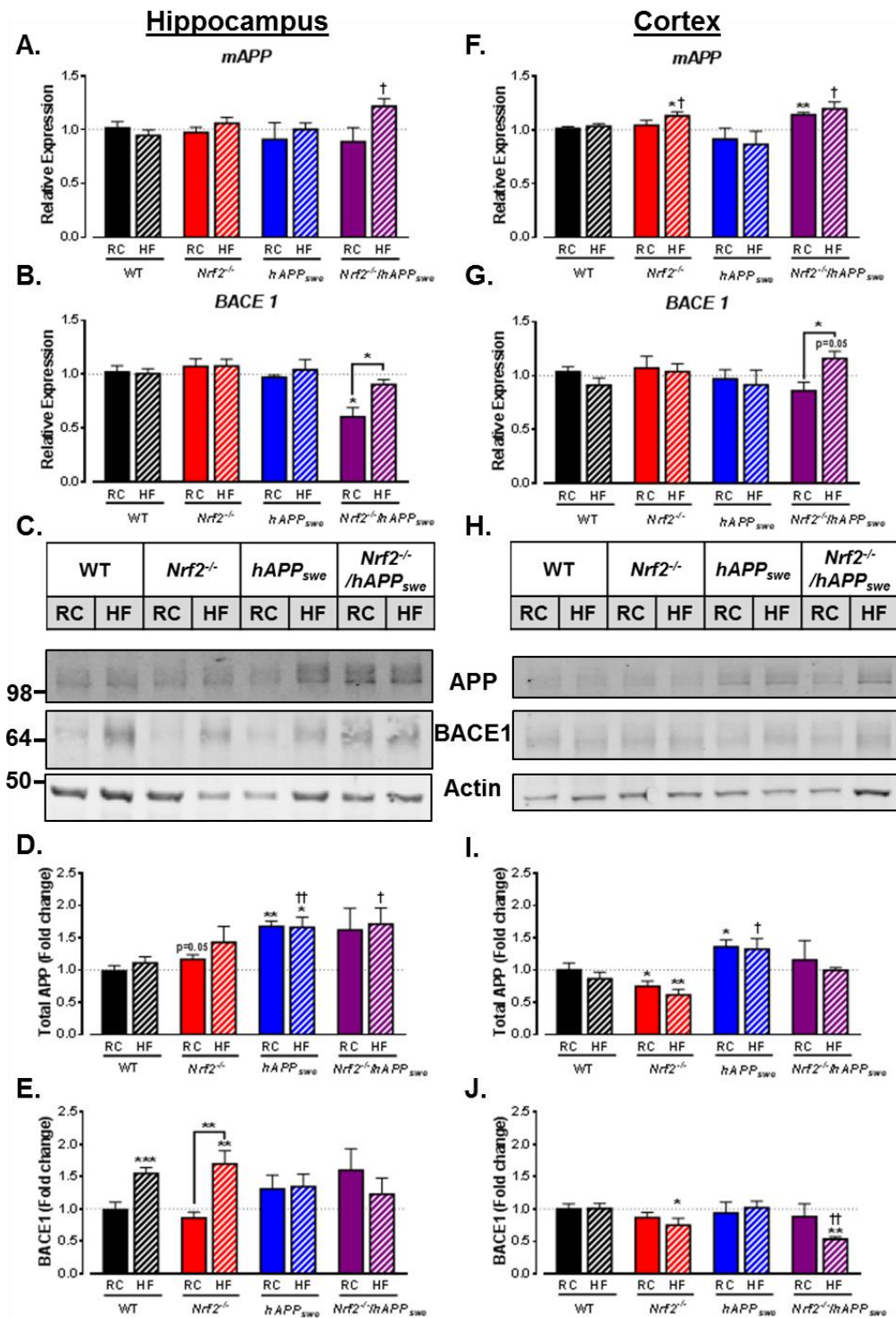


Figure 3.18 HF feeding increases AD related APP and BACE1 in a brain region specific manner in WT and *Nrf2*^{-/-} mice.

Brain tissue collected from aged adult mice was processed for gene and protein expression. Measures were taken for murine *APP* (A + F) and *BACE1* (B + G) gene expression as well as total APP (human and mouse; D + I) and BACE1 (E + J) protein expression, with C and H showing exemplar blots for the hippocampus and cortex respectively, where β -actin was used as the protein loading control. All data portrayed as means \pm s.e.m. and analysed by one-sample and unpaired t-test where * indicates significantly different from RC fed WT control and † indicates significantly different from HF fed WT. *, $p < 0.05$; **, $p < 0.01$; ***, $p < 0.001$; †, $p < 0.05$; ††, $p < 0.01$. WT $n = 9-10$, *Nrf2*^{-/-} $n = 7-10$, *hAPP*_{SWE} $n = 5-6$, *Nrf2*^{-/-}/*hAPP*_{SWE} $n = 4$.

Protein expression was run for total APP and BACE1 in the hippocampus and cortex with representative blots for each being shown in Figure 3.18 C and H respectively. There is a trend towards increased levels of APP in *Nrf2*^{-/-} mice which is concomitant with a decrease in expression in the cortex with no further significant dietary induced change (hippocampus: WT RC: 1.00; *Nrf2*^{-/-} RC: 1.16 ± 0.07; WT RC vs *Nrf2*^{-/-} RC p = 0.05, n = 10; Figure 3.18 D. Cortex: WT RC: 1.00; *Nrf2*^{-/-} RC: 0.745 ± 0.09; *Nrf2*^{-/-} HF: 0.614 ± 0.08; WT RC vs *Nrf2*^{-/-} RC p < 0.05, WT RC vs *Nrf2*^{-/-} HF p < 0.01, n = 10; Figure 3.18 D). In *hAPP*_{swe} mice, increased levels of APP protein are seen in both hippocampal and cortical tissue, which is to be expected as the antibody should pick up both the mouse and human forms of APP (Hippocampus: WT HF: 1.11 ± 0.10; *hAPP*_{swe} RC: 1.68 ± 0.08; *hAPP*_{swe} HF: 1.66 ± 0.16; WT RC vs *hAPP*_{swe} RC p < 0.01, WT RC vs *hAPP*_{swe} HF p < 0.05, WT HF vs *hAPP*_{swe} HF p < 0.01, n = 5-10. Cortex: WT HF: 0.865 ± 0.10; *hAPP*_{swe} RC: 1.36 ± 0.11; *hAPP*_{swe} HF: 1.32 ± 0.17; WT RC vs *hAPP*_{swe} RC p < 0.05, WT HF vs *hAPP*_{swe} HF p < 0.05, n = 5-10). *Nrf2*^{-/-}/*hAPP*_{swe} mice show a mixed profile for APP expression that appears to be controlled by the loss of *Nrf2* with hippocampal levels elevated similar to the *hAPP*_{swe} but cortical expression diminished mirroring the more marked decrease in expression demonstrated by the *Nrf2*^{-/-} mice (hippocampus: *Nrf2*^{-/-}/*hAPP*_{swe} HF: 1.71 ± 0.25; WT HF vs *Nrf2*^{-/-}/*hAPP*_{swe} HF p < 0.05, n = 4-10).

HF feeding induces higher protein expression of BACE1 in both WT and *Nrf2*^{-/-} mice but is not significant in the hippocampus of mice expressing *hAPP*_{swe} (WT RC: 1.00; WT HF: 1.55 ± 0.09; *Nrf2*^{-/-} RC: 0.862 ± 0.09; *Nrf2*^{-/-} HF: 1.70 ± 0.20; WT RC vs WT HF p < 0.001, WT RC vs *Nrf2*^{-/-} RC p < 0.01, *Nrf2*^{-/-} RC vs *Nrf2*^{-/-} HF p < 0.01, n = 9-10; Figure 3.18 E). As seen with total APP expression, cortical expression of BACE1 is inverted with HF feeding decreasing the expression in *Nrf2*^{-/-} mice but no change seen in WT mice fed a HF diet (WT RC: 1.00; *Nrf2*^{-/-} HF: 0.750 ± 0.11; WT RC vs *Nrf2*^{-/-} HF p < 0.05, n = 9-10; Figure 3.18 J). Similar to cortical APP expression, *Nrf2*^{-/-}/*hAPP*_{swe} mice fed a HF diet mimic the pattern seen in the HF fed *Nrf2*^{-/-} animals with decreases in BACE1 protein (*Nrf2*^{-/-}/*hAPP*_{swe} HF: 0.532 ± 0.04; WT RC vs *Nrf2*^{-/-}/*hAPP*_{swe} HF p < 0.01, n = 4-10).

As the AD model used in these studies reflects a much milder pathology than many of the models currently available; no overt plaque deposition was observed in animals irrespective of genotype or diet. In order to assess any changes in soluble amyloid-β (sAβ) induced by the loss of *Nrf2*^{-/-}, a commercially available murine

amyloid- β ELISA kit was run on cortical protein lysates (Figure 3.19). No significant changes in sA β ₁₋₄₂ were seen in WT or *Nrf2*^{-/-} mice irrespective of which diet they were fed when normalised to total protein content ($p > 0.05$, $n = 4-5$; Figure 3.19).

The amyloidogenic pathway is only one of the two main protein misfolding pathways associated with AD. Although the model chosen incorporates a mutation in the amyloidogenic pathway, protein was also run to assess potential changes in the second pathway, namely that of tau. Lysates were run on tissue as previously described and blotted for Ser396 p-tau and total tau protein in both the hippocampus (Figure 3.20 A and B) and the cortex (Figure 3.20 C and D) and exemplar blots portrayed (Figure 3.20 E). No significant increase in tau phosphorylation at the Ser396 site is seen in the hippocampus of these mice, despite a trend for increased phosphorylation in *hAPP*_{swe} mice following HF feeding ($p > 0.05$; Figure 3.20 A). In the cortex, a diet dependent trend towards increased phosphorylation is seen in both the WT and *Nrf2*^{-/-} mice fed a HF diet ($p > 0.05$; Figure 3.20 C). Furthermore, both *hAPP*_{swe} and *Nrf2*^{-/-}/*hAPP*_{swe} mice show a trend towards increased phosphorylation of tau under basal conditions in the cortex ($p > 0.05$) and it is likely low group numbers prevent these becoming statistically significant.

No significant changes are observed in the expression of total tau in hippocampal tissue, with only *hAPP*_{swe} HF animals showing a close to significant trend towards increased tau (WT RC: 1.00; *hAPP*_{swe} HF: 1.37 ± 0.13 ; WT RC vs *hAPP*_{swe} HF $p = 0.06$, $n = 4-9$). The increase in tau expression seen in cortex of the HF fed *hAPP*_{swe} mice, however, does reach significance (WT RC: 1.00; *hAPP*_{swe} HF: 1.23 ± 0.06 ; WT RC vs *hAPP*_{swe} HF $p < 0.05$, $n = 5-10$). The only other change of interest in tau expression occurs in the *Nrf2*^{-/-}/*hAPP*_{swe} HF fed animals that demonstrate a drastic drop in total protein expression when compared to controls (*Nrf2*^{-/-}/*hAPP*_{swe} HF: 0.533 ± 0.02 ; WT RC vs *Nrf2*^{-/-}/*hAPP*_{swe} HF $p < 0.0001$, $n = 4-10$).

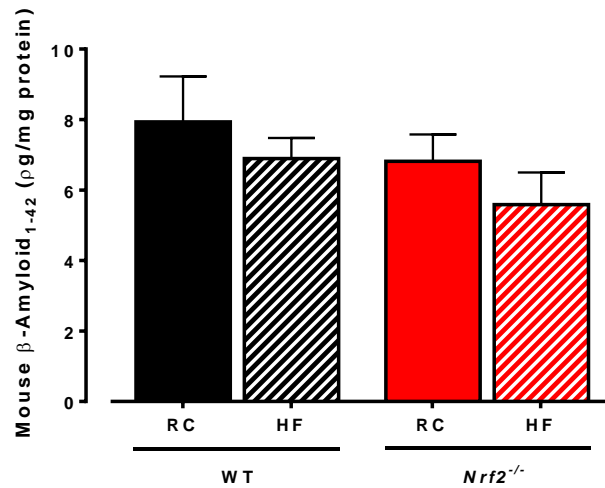


Figure 3.19 HF feeding has no effect on the production of soluble murine Aβ₁₋₄₂ in cortical tissue of aged WT and *Nrf2*^{-/-} mice.

Aged mice fed either a RC or HF diet were sacrificed and brains were dissected and lysed for protein analysis. Soluble mouse Aβ₁₋₄₂ was analysed by ELISA following manufacturer's instructions using prepared protein lysates and values were normalised to total protein concentration obtained from Bradford protein assay. All values are expressed as means ± s.e.m., and analysed by two-way ANOVA. WT n = 5, *Nrf2*^{-/-} n = 4-5

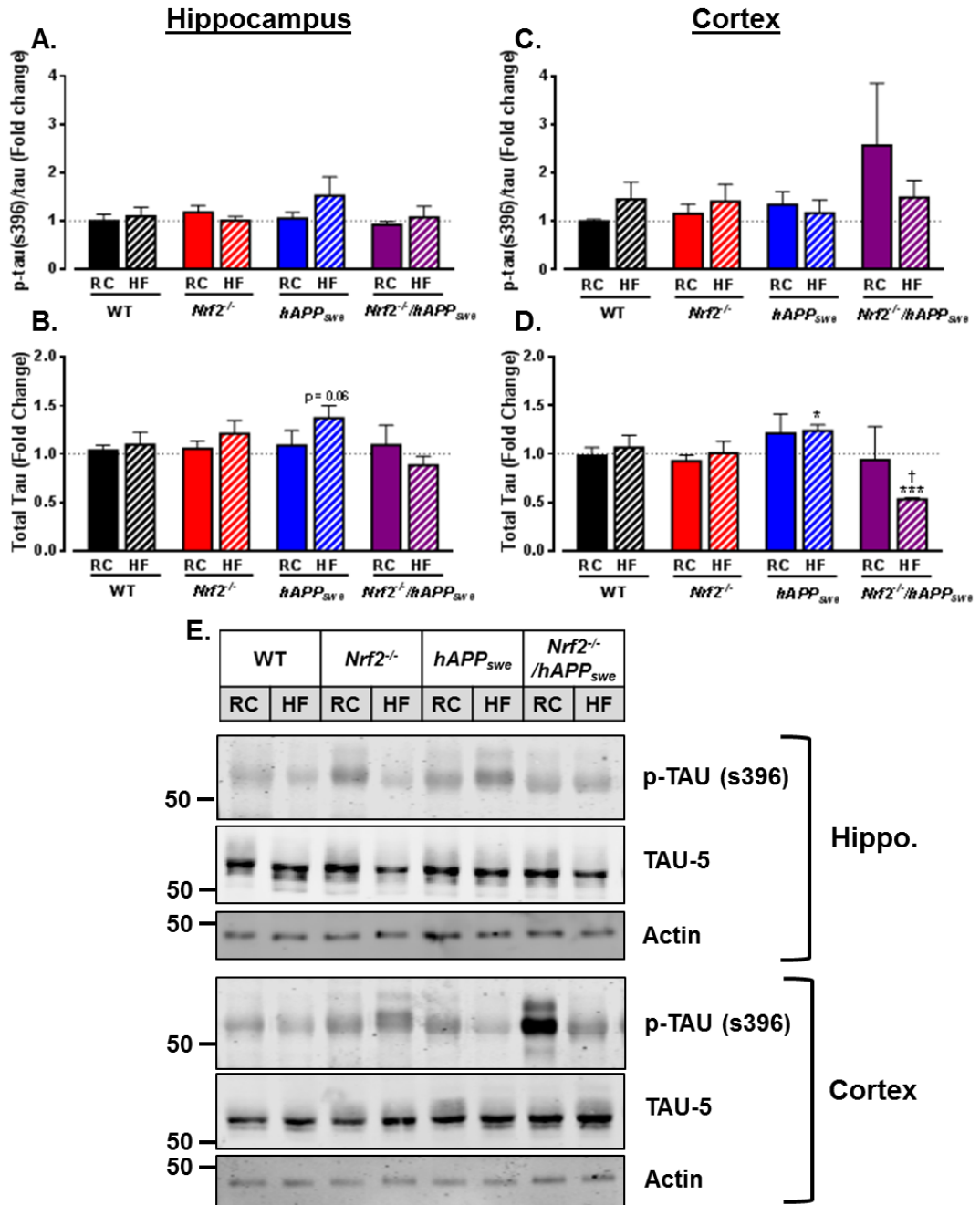


Figure 3.20 HF feeding of *hAPP*_{SWE} mice increases protein expression of total tau with diet and *Nrf2*^{-/-} also impacting on tau phosphorylation.

Brain tissue collected from aged adult mice was processed for protein expression. Measures were taken for p-tau (Ser396) and total tau expression in both the hippocampus (A + B) and cortex (C + D) respectively. (E) displays exemplar blots for both tissues, where β -actin was used as the protein loading control. All data portrayed as means \pm s.e.m. and analysed by one-sample and unpaired t-test where * indicates significantly different from RC fed WT control and † indicates significantly different from HF fed WT. *, $p < 0.05$; ***, $p < 0.001$; †, $p < 0.05$. WT $n = 8-10$, *Nrf2*^{-/-} $n = 8-10$, *hAPP*_{SWE} $n = 4-6$, *Nrf2*^{-/-}/*hAPP*_{SWE} $n = 3-4$.

3.10 THE EFFECT OF *NRF2* LOSS ON AKT SIGNALLING AND DOWNSTREAM NF- κ B SIGNALLING

We previously described changes seen in peripheral glucose disposal and insulin sensitivity both as a result of genotype, with *Nrf2*^{-/-} having improved glucose clearance and diet*genotype responses, where *Nrf2*^{-/-} mice maintained their insulin glucose clearance when HF fed and *hAPP*_{swe} had worsened glucose clearance. Combining this information with the potential protective role reported for insulin signalling, we looked at the role of Akt in the hippocampus and cortex of aged mice fed RC or HF diets long term. No changes were seen in total Akt or Akt phosphorylation at Ser473 in the hippocampus of aged mice (Figure 3.21 A). There is a trend towards increased Akt phosphorylation (Ser473) in the RC fed *Nrf2*^{-/-} mice with no notable changes in any of the other groups examined and no changes in total Akt (WT RC: 1.00; *Nrf2*^{-/-} RC: 1.14 \pm 0.07; WT RC vs *Nrf2*^{-/-} RC $p = 0.08$, $n = 10$; Figure 3.21 B). This is supported by the exemplar blots depicted for both phosphorylated and total Akt (Figure 3.21 E).

Akt signalling is just one of the pathways upstream of NF- κ B capable of affecting its activation. NF- κ B, normally bound to a repressor protein called I κ B α , is released upon activation in order to enter the cell nucleus. As a result, proteasomal degradation of I κ B α can be used as a marker of NF- κ B activation with a decreasing presence of I κ B α indicating increased activity of NF- κ B. I κ B α protein expression was evaluated in the hippocampus and cortex of age-matched, aged mice from RC and HF fed cohorts. A small but significant decrease in I κ B α is seen in the hippocampus of *Nrf2*^{-/-} mice fed a RC diet with no other significant changes seen in this tissue (WT RC: 1.00; *Nrf2*^{-/-} RC: 0.849 \pm 0.06; WT RC vs *Nrf2*^{-/-} RC $p < 0.05$, $n = 10$; Figure 3.21 B). Whilst the cortex shows no change in RC fed animals, a significant drop in I κ B α is seen in both transgenic lines lacking *Nrf2*^{-/-} when compared to RC fed controls (WT RC: 1.00; *Nrf2*^{-/-} HF; 0.845 \pm 0.07; *Nrf2*^{-/-}/*hAPP*_{swe} HF; 0.597 \pm 0.10; WT RC vs *Nrf2*^{-/-} and *Nrf2*^{-/-}/*hAPP*_{swe} HF $p < 0.05$, $n = 4-10$; Figure 3.21 D). Again, representative blots are depicted in Figure 3.21 E alongside those for Akt.

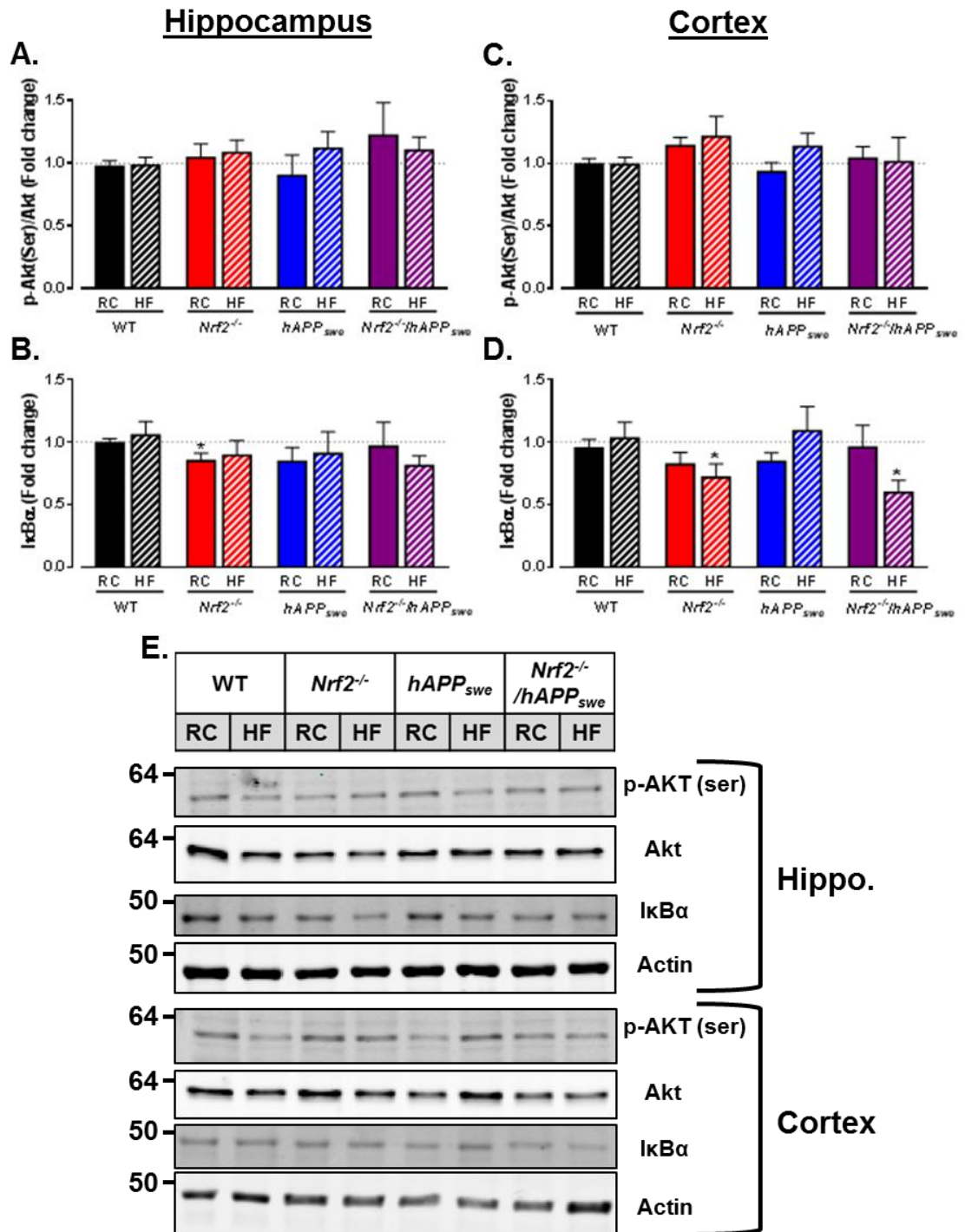


Figure 3.21 PI-3k driven changes in Akt are not responsible for the protective effects of HF feeding in *Nrf2*^{-/-} mice, and only small changes in the related NF-κB stress response pathway are induced.

Brain tissue collected from aged adult mice was processed for gene and protein expression. Measures were taken for relative expression of Akt phosphorylation (Ser473; **A + C**) and IκBα (**B + D**) protein expression, with **E** showing exemplar blots for the hippocampus and cortex respectively, where β-actin was used as the protein loading control. All data portrayed as means ± s.e.m. and analysed by one-sample and unpaired t-test where * indicates significantly different from RC fed WT control and *, $p < 0.05$. WT $n = 9-10$, *Nrf2*^{-/-} $n = 9-10$, *hAPP*_{swe} $n = 5-6$, *Nrf2*^{-/-}/*hAPP*_{swe} $n = 4$.

3.11 NO CHANGE IN IN A MARKER OF THE GLUTATHIONE DETOXIFYING PATHWAY FOLLOWING LONG-TERM HIGH FAT FEEDING

It is well established that *Nrf2*^{-/-} drives the transcription of a multitude of primarily antioxidant genes once activated. Glutathione (GSH) is one of the most well-known of these, acting as a reducing agent in the presence of unstable molecules such as ROS. Following production of GSH via a rate limiting enzyme step, it cycles through active (reduced) and inactive (oxidised) forms following binding of ROS. Here we have looked at the expression of glutamate cysteine ligase catalytic subunit (GCLC), which forms part of the rate-limiting enzyme step in GSH synthesis. No significant changes in GCLC expression were seen in the hippocampus of the RC and HF fed mice. However, a trend towards a HF induced increase in GCLC is seen in WT mice but it fails to reach significance on this occasion (WT RC: 1.00; WT HF: 1.27 ± 0.13; WT RC vs WT HF p = 0.07, n = 10; Figure 3.22 A).

Similar to the hippocampus, there is no significant change in the cortical levels of GCLC in either of the single transgenic mouse models, nor does HF feeding induce a change in the WT mice. The only change in GCLC levels seen is a reduction in the HF fed *Nrf2*^{-/-}/*hAPP*_{swe} double transgenic model with a trend towards a decrease compared to RC fed controls and a significant decrease in comparison to the HF fed WT mice (WT RC: 1.00; WT HF: 1.10 ± 0.10; *Nrf2*^{-/-}/*hAPP*_{swe} HF: 0.643 ± 0.12; WT RC vs *Nrf2*^{-/-}/*hAPP*_{swe} HF p = 0.06, WT HF vs *Nrf2*^{-/-}/*hAPP*_{swe} HF p < 0.05, n = 4-10; Figure 3.22 B). Representative blots have been appended to visualise the changes in expression observed (Figure 3.22 C).

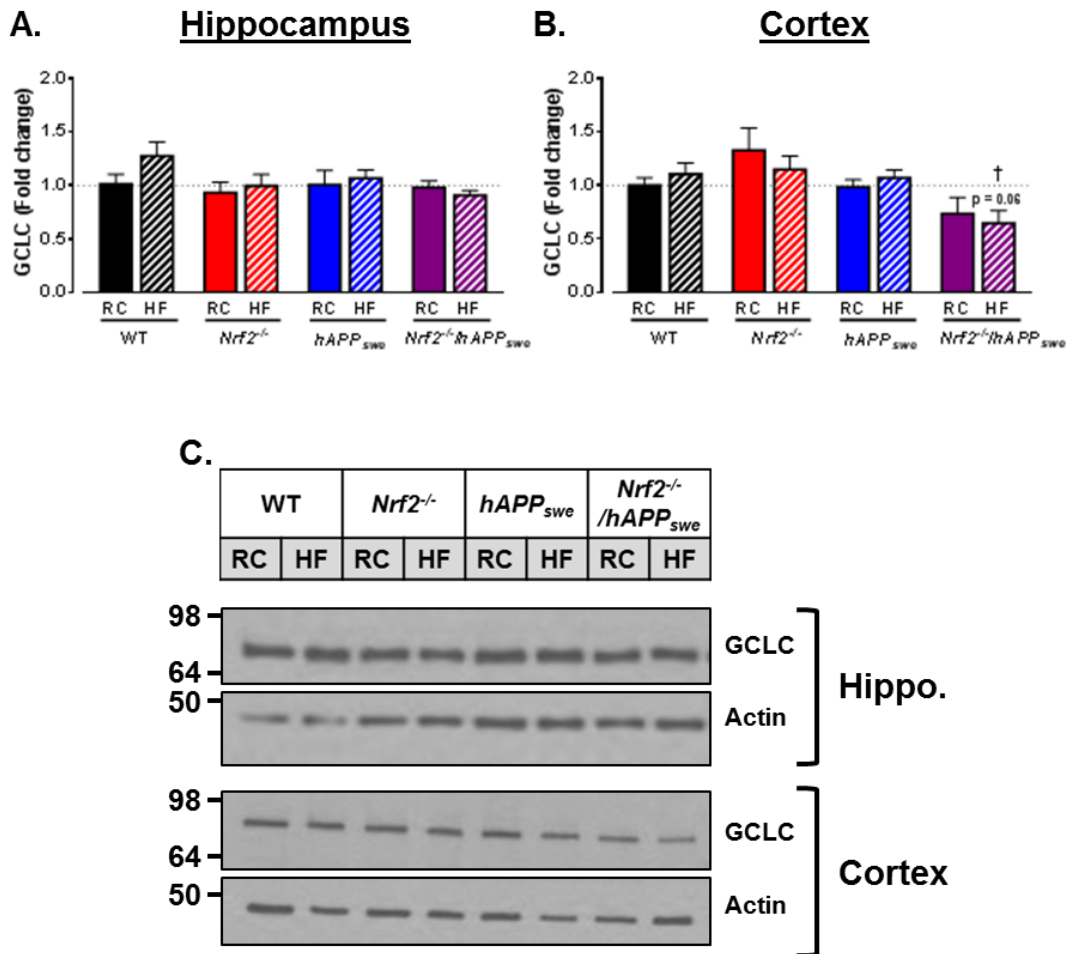


Figure 3.22 No change is seen in the rate limiting glutathione pathway GCLC enzyme in brain tissue as a result of HF feeding.

Brain tissue collected from aged adult mice was processed for protein expression and Western blots were probed for the glutathione pathway enzyme GCLC (A + B). C portrays exemplar blots for the hippocampus and cortex respectively, where β -actin was used as the protein loading control. All data portrayed as means \pm s.e.m. and analysed by one-sample and unpaired t-test where † indicates significantly different from HF fed WT mice and ‡, $p < 0.05$. WT $n = 10$, *Nrf2*^{-/-} $n = 7-11$, *hAPP*_{swe} $n = 5-6$, *Nrf2*^{-/-}/*hAPP*_{swe} $n = 4$.

3.12 A ROLE FOR STRESS-ACTIVATED MAPK ENZYMES IN HIGH FAT INDUCED RESCUE OF THE *NRF2*^{-/-} PHENOTYPE IN BRAIN TISSUE

MAPKs are responsible for processing a diverse array of incoming stimuli including, but not limited to, pro-inflammatory, osmotic stress and insulin. The most commonly investigated MAPK are the JNK MAPK pathway, the p38 MAPK pathway and the pathway associated with ERK 1/2 and its phosphorylation. As these are pathways that can be activated by factors shown to be elevated in some of the models being investigated, JNK and ERK MAPKs were followed up in the hippocampal and cortical brain homogenates of our mice.

Significant increases were seen in phosphorylation of both JNK isoforms in *Nrf2*^{-/-} and *Nrf2*^{-/-}/*hAPP*_{swe} in the hippocampus, with JNK 54 phosphorylation increased significantly both basally and under HF conditions in *Nrf2*^{-/-} and HF fed *Nrf2*^{-/-}/*hAPP*_{swe} when compared to WT mice (WT RC: 1.00; WT HF: 0.867 ± 0.08; *Nrf2*^{-/-} RC: 1.29 ± 0.08; *Nrf2*^{-/-} HF: 1.54 ± 0.12; *Nrf2*^{-/-}/*hAPP*_{swe} HF: 1.67 ± 0.33; WT RC vs *Nrf2*^{-/-} RC and HF p < 0.01, WT HF vs *Nrf2*^{-/-} HF p < 0.001, WT HF vs *Nrf2*^{-/-}/*hAPP*_{swe} HF p < 0.01, n = 4-11; Figure 3.23 A). Furthermore, there is a trend for increased phosphorylation of the JNK 54 isoform basally in *Nrf2*^{-/-}/*hAPP*_{swe} mice (*Nrf2*^{-/-}/*hAPP*_{swe}: 1.59 ± 0.27; WT RC vs *Nrf2*^{-/-}/*hAPP*_{swe} RC p = 0.09, n = 4-10). Similar changes are seen in the phosphorylation of JNK 46 isoform with significantly increased phosphorylation seen in the HF fed *Nrf2*^{-/-} mice as well as the RC and HF fed *Nrf2*^{-/-}/*hAPP*_{swe} mice (WT RC: 1.00; WT HF: 0.871 ± 0.09; *Nrf2*^{-/-} HF: 1.39 ± 0.15; *Nrf2*^{-/-}/*hAPP*_{swe} RC: 1.47 ± 0.14; *Nrf2*^{-/-}/*hAPP*_{swe} HF: 1.59 ± 0.34; WT RC vs *Nrf2*^{-/-} HF p < 0.05, WT HF vs *Nrf2*^{-/-} HF p < 0.01, WT RC vs *Nrf2*^{-/-}/*hAPP*_{swe} RC p < 0.05, WT HF vs *Nrf2*^{-/-}/*hAPP*_{swe} HF p < 0.05, n = 4-10; Figure 3.23 B). Further to this, there is a trend towards increased phosphorylation of the JNK 46 isoform in the RC fed *Nrf2*^{-/-} mice (*Nrf2*^{-/-} RC: 1.15 ± 0.07; WT RC vs *Nrf2*^{-/-} RC p = 0.07, n = 10-11).

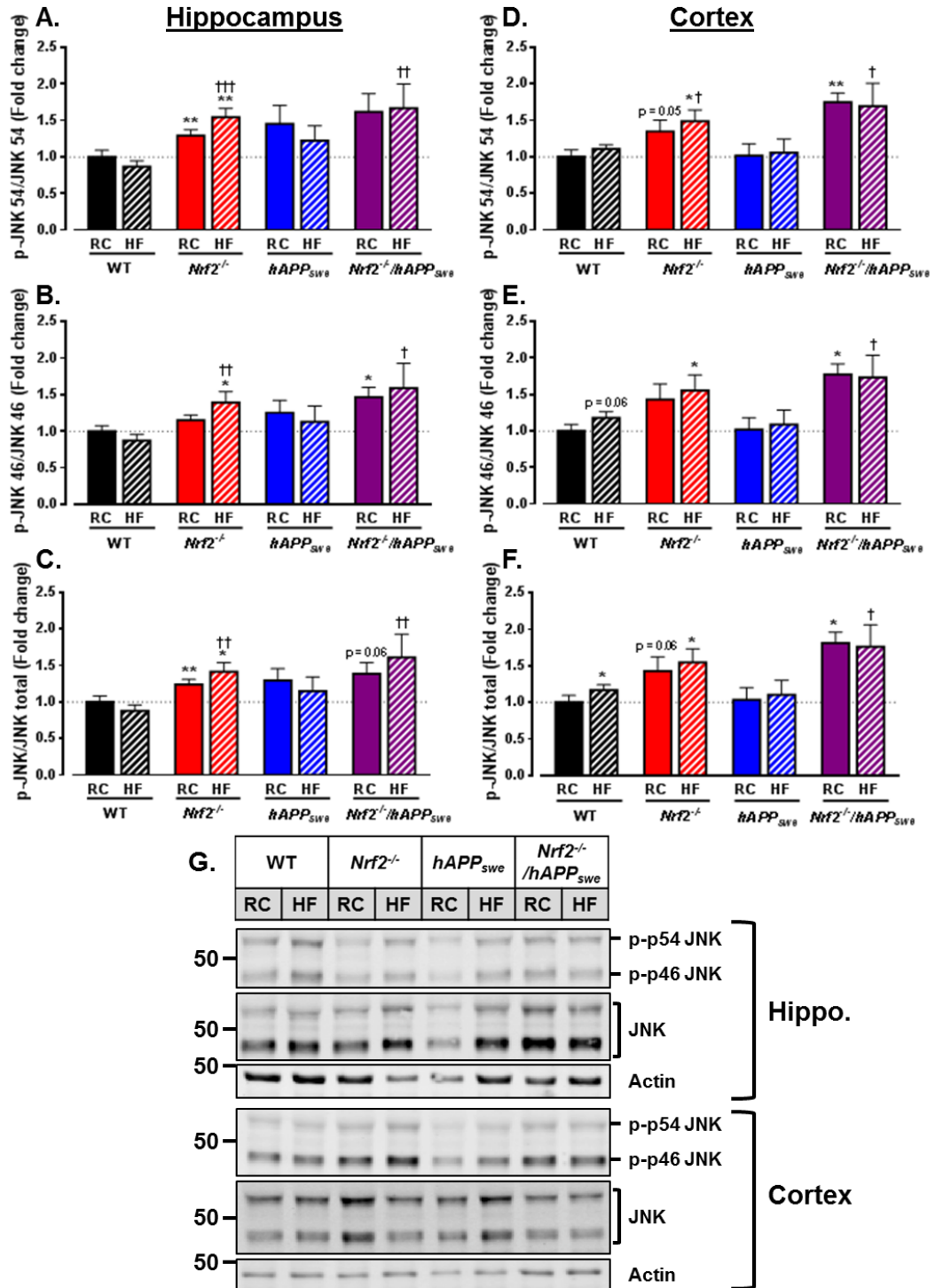


Figure 3.23 HF feeding of *Nrf2*^{-/-} mice activates the JNK pathway increasing phosphorylation of JNK in brain homogenates.

Brain tissue collected from aged adult mice was processed for protein expression and run on Western blots. Membranes were probed for phosphorylated (Thr183/Tyr185) and total JNK. A ratio of phosphorylated to total protein was calculated for JNK 54 (A + D), JNK 46 (B + E) and total JNK (C + F) in hippocampal and cortical homogenates respectively. G portrays exemplar blots for the hippocampus and cortex respectively, where β -actin was used as the protein loading control. All data portrayed as means \pm s.e.m. and analysed by one-sample and unpaired t-test where * indicates significantly different from RC fed WT control and † indicates significantly different from HF fed WT mice. *, $p < 0.05$; **, $p < 0.01$; †, $p < 0.05$; ††, $p < 0.01$; †††, $p < 0.001$. WT $n = 9-10$, *Nrf2*^{-/-} $n = 9-11$, *hAPP*_{SWE} $n = 5-6$, *Nrf2*^{-/-}/*hAPP*_{SWE} $n = 4$.

Total JNK showed an almost 1.5-fold significant induction in phosphorylation in the hippocampus of *Nrf2*^{-/-} mice following HF feeding with increased phosphorylation also seen in the RC fed counterparts (WT RC: 1.00; WT HF: 0.877 ± 0.08; *Nrf2*^{-/-} RC: 1.24 ± 0.07; *Nrf2*^{-/-} HF: 1.41 ± 0.13; WT RC vs *Nrf2*^{-/-} RC p < 0.01, WT RC vs *Nrf2*^{-/-} HF p < 0.05, WT HF vs *Nrf2*^{-/-} HF p < 0.01, n = 9-11; Figure 3.23 C). A trend towards increased induction in total JNK phosphorylation is seen in the RC fed *hAPP*_{swe} mice when compared to WT controls, whilst *Nrf2*^{-/-}/*hAPP*_{swe} mice fed a HF diet have significantly increased JNK phosphorylation when compared to HF fed WT controls (*Nrf2*^{-/-}/*hAPP*_{swe} RC: 1.39 ± 0.15; *Nrf2*^{-/-}/*hAPP*_{swe} HF: 1.61 ± 0.32; WT RC vs *Nrf2*^{-/-}/*hAPP*_{swe} RC p = 0.06, WT HF vs *Nrf2*^{-/-}/*hAPP*_{swe} HF p < 0.01, n = 4-11). Furthermore, no significant changes were seen in the phosphorylation of JNK or either of its isoforms in the hippocampus of *hAPP*_{swe} mice under RC or HF fed conditions (p > 0.05).

A similar profile of JNK phosphorylation induction was seen in the cortical homogenates, with *Nrf2*^{-/-} mice displaying significant increases in JNK 54 phosphorylation when compared to WT mice fed either a RC or HF diet (WT RC: 1.00; WT HF: 1.11 ± 0.06; *Nrf2*^{-/-} RC: 1.35 ± 0.15; *Nrf2*^{-/-} HF: 1.49 ± 0.15; WT RC vs *Nrf2*^{-/-} RC p = 0.05, WT RC vs *Nrf2*^{-/-} HF p < 0.05, WT HF vs *Nrf2*^{-/-} HF p < 0.05, n = 9-10; Figure 3.23 D). A significant induction in JNK 54 phosphorylation is also seen in the cortex of *Nrf2*^{-/-}/*hAPP*_{swe} RC fed mice whilst *Nrf2*^{-/-}/*hAPP*_{swe} mice fed a HF diet have significantly increased JNK 54 phosphorylation when compared to HF fed WT mice (*Nrf2*^{-/-}/*hAPP*_{swe} RC: 1.75 ± 0.13; *Nrf2*^{-/-}/*hAPP*_{swe} HF: 1.69 ± 0.32; WT RC vs *Nrf2*^{-/-}/*hAPP*_{swe} RC p < 0.01, WT HF vs *Nrf2*^{-/-}/*hAPP*_{swe} HF p < 0.05, n = 4-10). No changes in cortical JNK phosphorylation were induced by HF feeding of the control WT mice (p > 0.05), as can be seen in Western blot exemplars (Figure 3.23 G), nor were there any significant alterations in JNK 54 phosphorylation in *hAPP*_{swe} mice (p > 0.05).

Again phosphorylation of the JNK 46 isoform in the cortex presents a very similar profile to that seen for the JNK 54 isoform described above. *Nrf2*^{-/-} HF fed mice describe a significant increase in JNK 46 phosphorylation when compared to RC fed WT controls whilst a trend towards increased phosphorylation is also reported basally in *Nrf2*^{-/-} mice (WT RC: 1.00; *Nrf2*^{-/-} RC: 1.43 ± 0.21; *Nrf2*^{-/-} HF: 1.55 ± 0.21; WT RC vs *Nrf2*^{-/-} RC p = 0.08, WT RC vs *Nrf2*^{-/-} HF p < 0.05, n = 9-10; Figure 3.23 E). Furthermore, a trend towards increased phosphorylation of the JNK 46 isoform is seen in HF fed controls which is not apparent in the JNK 54 analysis (WT HF: 1.18 ± 0.09; WT RC v WT HF p = 0.06, n = 10). A significant induction in JNK 46 phosphorylation

is also seen in the cortex of *Nrf2*^{-/-}/*hAPP*_{swe} RC fed mice whilst *Nrf2*^{-/-}/*hAPP*_{swe} mice fed a HF diet have significantly increased JNK 46 phosphorylation when compared to HF fed WT mice (*Nrf2*^{-/-}/*hAPP*_{swe} RC: 1.78 ± 0.14; *Nrf2*^{-/-}/*hAPP*_{swe} HF: 1.73 ± 0.31; WT RC vs *Nrf2*^{-/-}/*hAPP*_{swe} RC p < 0.05, WT HF vs *Nrf2*^{-/-}/*hAPP*_{swe} HF p < 0.05, n = 4-10). In contrast, there were no significant alterations in JNK 46 phosphorylation in *hAPP*_{swe} mice under either diet (p > 0.05).

Finally, and given the matching profiles of both JNK isoforms, total JNK phosphorylation in the cortex was found to be increased in both *Nrf2*^{-/-} and *Nrf2*^{-/-}/*hAPP*_{swe} mice irrespective of diet fed (WT RC: 1.00; *Nrf2*^{-/-} RC: 1.43 ± 0.20; *Nrf2*^{-/-} HF: 1.55 ± 0.19; *Nrf2*^{-/-}/*hAPP*_{swe} RC: 1.81 ± 0.15; *Nrf2*^{-/-}/*hAPP*_{swe} HF: 1.76 ± 0.30; WT RC vs *Nrf2*^{-/-} RC p = 0.06, WT RC vs *Nrf2*^{-/-} HF p < 0.05, WT HF vs *Nrf2*^{-/-} HF p > 0.07, WT RC vs *Nrf2*^{-/-}/*hAPP*_{swe} RC p < 0.05, WT RC vs *Nrf2*^{-/-}/*hAPP*_{swe} HF p = 0.08, WT HF vs *Nrf2*^{-/-}/*hAPP*_{swe} HF p < 0.05, n = 4-10; Figure 3.23 F). Furthermore, a small increase in total JNK phosphorylation was seen in HF fed WT mice, whilst there was no significant change in JNK phosphorylation overall in *hAPP*_{swe} mice (WT HF: 1.17 ± 0.07; WT RC v WT HF p < 0.05, n = 10). This indicates an alteration in JNK phosphorylation driven by loss of *Nrf2*, with little further potentiation by HF feeding.

When ERK MAPKs were analysed they were split into ERK 1 and ERK 2 as well as measuring the combined change observed. This is because the changes in an individual ERK are not always entirely comparative, with ERK 1 commonly less strongly expressed than ERK 2. Therefore this helped ensure the most accurate measurement of any changes that may occur. There is an almost three-fold induction in phosphorylation of hippocampal ERK 1 following HF feeding of *Nrf2*^{-/-} mice that is also seen in HF fed *Nrf2*^{-/-}/*hAPP*_{swe} mice when compared to both WT RC and HF fed mice (WT RC: 1.00; WT HF: 0.919 ± 0.07; *Nrf2*^{-/-} HF: 2.84 ± 0.75; *Nrf2*^{-/-}/*hAPP*_{swe} HF: 3.37 ± 0.28; WT RC and WT HF vs *Nrf2*^{-/-} HF p < 0.05, WT RC vs *Nrf2*^{-/-}/*hAPP*_{swe} HF p < 0.01, WT HF vs *Nrf2*^{-/-}/*hAPP*_{swe} HF p < 0.001, n = 4-11; Figure 3.24 A). The HF induced increase in ERK 1 phosphorylation just fails to meet significance in the *Nrf2*^{-/-} mice when compared to the RC fed controls, likely due to a mild non-significant increase in the RC fed mice (*Nrf2*^{-/-} RC: 1.42 ± 0.07; *Nrf2*^{-/-} RC vs *Nrf2*^{-/-} HF p = 0.06, n = 8-11).

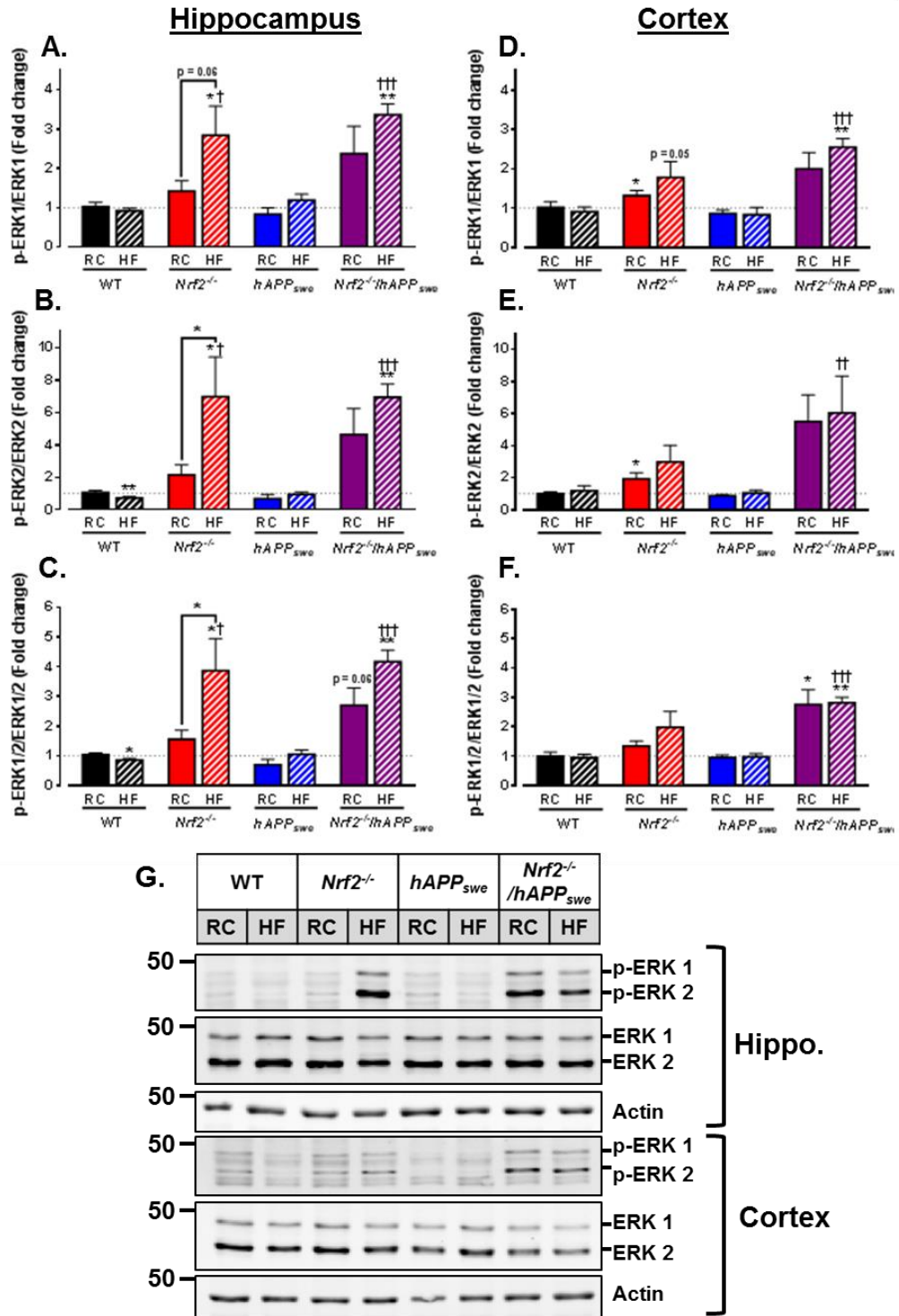


Figure 3.24 Aged transgenic mouse models lacking *Nrf2* have increased ERK 1 and 2 MAPK phosphorylation, which is further enhanced by HF feeding.

Brain tissue was harvested from mice and processed for protein expression by Western blot. Measures were taken for relative expression of phosphorylated (Thr202/Tyr204) and total ERK 1 (A + D), ERK 2 (B + E) and combined ERK 1/2 MAPK expression (C + F) in the hippocampus and cortex of mice, with G showing exemplar blots for the hippocampus and cortex respectively, where β -actin was used as the protein loading control. All data portrayed as means \pm s.e.m. and analysed by one-sample and unpaired t-test where * indicates significantly different from RC fed WT control and † indicates significantly different from HF fed WT. *, $p < 0.05$; **, $p < 0.01$; †, $p < 0.05$; ††, $p < 0.01$; †††, $p < 0.001$. WT $n = 9-10$, *Nrf2*^{-/-} $n = 9-10$, *hAPP*_{SWE} $n = 5-6$, *Nrf2*^{-/-}/*hAPP*_{SWE} $n = 4$.

Hippocampal phosphorylation of ERK 2 show a similar profile to that described for ERK 1, with non-significant increases in RC fed *Nrf2*^{-/-} and *Nrf2*^{-/-}/*hAPP*_{swe} mice and significant increases in ERK 2 phosphorylation in HF fed *Nrf2*^{-/-} and *Nrf2*^{-/-}/*hAPP*_{swe} mice (WT RC: 1.00; WT HF: 0.725 ± 0.08; *Nrf2*^{-/-} RC: 2.14 ± 0.63; *Nrf2*^{-/-} HF: 6.98 ± 2.4; *Nrf2*^{-/-}/*hAPP*_{swe} HF: 6.95 ± 0.81; WT RC and WT HF vs *Nrf2*^{-/-} HF p < 0.05, WT RC vs *Nrf2*^{-/-}/*hAPP*_{swe} HF p < 0.01, WT HF vs *Nrf2*^{-/-}/*hAPP*_{swe} HF p < 0.001, *Nrf2*^{-/-} RC vs *Nrf2*^{-/-} HF p < 0.05, n = 4-11; Figure 3.24 B). The only difference between hippocampal ERK 1 and 2 phosphorylation is the significant decrease in ERK 2 phosphorylation following HF feeding in WT mice (WT RC vs WT HF p < 0.01, n = 10).

When total ERK 1/2 phosphorylation is assessed in the hippocampus it is clear that the dominant changes described previously remain. In addition to these the significant loss of phosphorylation in HF fed WT is present as well as an increase in phosphorylation in the RC fed double transgenic mice that now nears significance (WT RC: 1.00; WT HF: 0.857 ± 0.05; *Nrf2*^{-/-} RC: 1.56 ± 0.31; *Nrf2*^{-/-} HF: 3.87 ± 1.1; *Nrf2*^{-/-}/*hAPP*_{swe} RC: 2.70 ± 0.59; *Nrf2*^{-/-}/*hAPP*_{swe} HF: 4.17 ± 0.38; WT RC vs WT HF p < 0.05, WT RC and WT HF vs *Nrf2*^{-/-} HF p < 0.05, WT RC vs *Nrf2*^{-/-}/*hAPP*_{swe} RC p = 0.06, WT RC vs *Nrf2*^{-/-}/*hAPP*_{swe} HF p < 0.01, WT HF vs *Nrf2*^{-/-}/*hAPP*_{swe} HF p < 0.001, *Nrf2*^{-/-} RC vs *Nrf2*^{-/-} HF p < 0.05, n = 4-11; Figure 3.24 C). Incorporation of the *hAPP*_{swe} mutation does not affect hippocampal ERK phosphorylation even after HF feeding as can be seen from the protein blots (Figure 3.24 G).

Cortical expression of ERK phosphorylation follows a similar pattern to that seen in the hippocampus of aged mice, with no changes seen in either the RC of HF fed WT and *hAPP*_{swe} mice. Loss of *Nrf2* induces phosphorylation of ERK 1 (WT RC: 1.00; *Nrf2*^{-/-} RC: 1.32 ± 0.14; WT RC vs *Nrf2*^{-/-} RC p < 0.05, n = 10; Figure 3.24 D) and 2 (WT RC: 1.00; *Nrf2*^{-/-} RC: 1.93 ± 0.38; WT RC vs *Nrf2*^{-/-} RC p < 0.05, n = 10; Figure 3.24 E), which is further increased by HF feeding and the addition of *hAPP*_{swe} (ERK 1: WT HF: 0.909 ± 0.12; *Nrf2*^{-/-} HF: 1.78 ± 0.41; *Nrf2*^{-/-}/*hAPP*_{swe} HF: 2.55 ± 0.22; WT HF vs *Nrf2*^{-/-} HF p = 0.05, WT RC vs *Nrf2*^{-/-}/*hAPP*_{swe} HF p < 0.01, WT HF vs *Nrf2*^{-/-}/*hAPP*_{swe} HF p < 0.001, n = 4-10. ERK 2: WT HF: 0.9087 ± 0.119; *Nrf2*^{-/-}/*hAPP*_{swe} HF: 2.550 ± 0.218; WT HF vs *Nrf2*^{-/-}/*hAPP*_{swe} HF p < 0.01, n = 4-10.). When analysed together there is a trend towards increased ERK phosphorylation in the *Nrf2*^{-/-} mice that no longer reaches significance, with a significant increase in protein phosphorylation expression seen in the *Nrf2*^{-/-}/*hAPP*_{swe} mice (WT RC: 1.00; WT HF: 0.949 ± 0.11; *Nrf2*^{-/-}

$^{-/-}$ RC: 1.35 ± 0.17 ; $Nrf2^{-/-}/hAPP_{swe}$ RC: 2.76 ± 0.50 ; $Nrf2^{-/-}/hAPP_{swe}$ HF: 2.82 ± 0.19 ; WT RC vs $Nrf2^{-/-}$ RC and HF $p > 0.05$, WT RC vs $Nrf2^{-/-}/hAPP_{swe}$ RC $p < 0.05$, WT RC vs $Nrf2^{-/-}/hAPP_{swe}$ HF $p < 0.01$, WT HF vs $Nrf2^{-/-}/hAPP_{swe}$ HF $p < 0.001$, $n = 4-10$; Figure 3.24 F).

In order to better understand where in the pathway *Nrf2* loss was impacting on the MAPK activation described above, work was undertaken in collaboration with the lab of Prof. S.M. Keyse, who specialise in the dual-specificity MAPK dephosphatases (DUSPs or MKPs) that act to clear phosphorylated MAPKs. It has been shown that whilst dephosphorylation of MAPKs can be performed by different groups of phosphatases, by far the largest family of MAPK-specific phosphatases are the DUSPs (Caunt & Keyse, 2013). DUSPs 6, 7 and 9 are believed to be ERK selective and located in the cellular cytoplasm, whilst 2, 4 and 5 are inducible nuclear variants, specifically regulating the nuclear dephosphorylation and accumulation of ERK. DUSP1, which is also a nuclear inducible DUSP, was analysed although it is known to interact not only with ERK but also with JNK and p38 isoforms. To that effect, hippocampal lysates were assessed for gene expression of some of the key DUSPs associated in particular with regulation of ERK activity.

No effect of long-term HF feeding was seen on gene expression of the promiscuous *DUSP1* in the hippocampus of WT mice ($p > 0.05$; Figure 3.25 A). Loss of *Nrf2* appears to prompt a decrease in gene expression of *DUSP1*, which is rescued by HF-feeding (WT RC: 1.00; $Nrf2^{-/-}$ RC: 0.774 ± 0.05 ; WT RC vs $Nrf2^{-/-}$ RC $p < 0.01$, $n = 6$). In contrast, *DUSP2* expression, which is also located in the nucleus, was significantly depleted by long-term HF feeding (WT RC: 1.00; WT HF: 0.348 ± 0.08 ; $Nrf2^{-/-}$ HF: 0.458 ± 0.09 ; WT RC vs WT HF $p < 0.001$, WT RC vs $Nrf2^{-/-}$ HF $p < 0.01$, $n = 6$; Figure 3.25 B). In addition, a trend towards decreased expression of *DUSP2* was also seen in RC fed $Nrf2^{-/-}$ mice although this failed to reach significance with the numbers analysed ($Nrf2^{-/-}$ RC: 0.662 ± 0.18 ; WT RC vs WT HF $p > 0.05$, $n = 6$). Differing from *DUSP1* and 2, *DUSP4* was not affected by either dietary or genotype changes in the hippocampus of aged mice ($p > 0.05$; Figure 3.25 C). *DUSP5*, the last nuclear DUSP assessed, was decreased significantly by both HF feeding of WT mice and loss of *Nrf2* with no further effect of diet in these mice (WT RC: 1.00; WT HF: 0.252 ± 0.05 ; $Nrf2^{-/-}$ RC: 0.280 ± 0.06 ; $Nrf2^{-/-}$ HF: 0.390 ± 0.10 ; WT RC vs WT HF $p < 0.0001$, WT RC vs $Nrf2^{-/-}$ RC $p < 0.0001$, WT RC vs $Nrf2^{-/-}$ HF $p < 0.01$, $n = 6$; Figure 3.25 D).

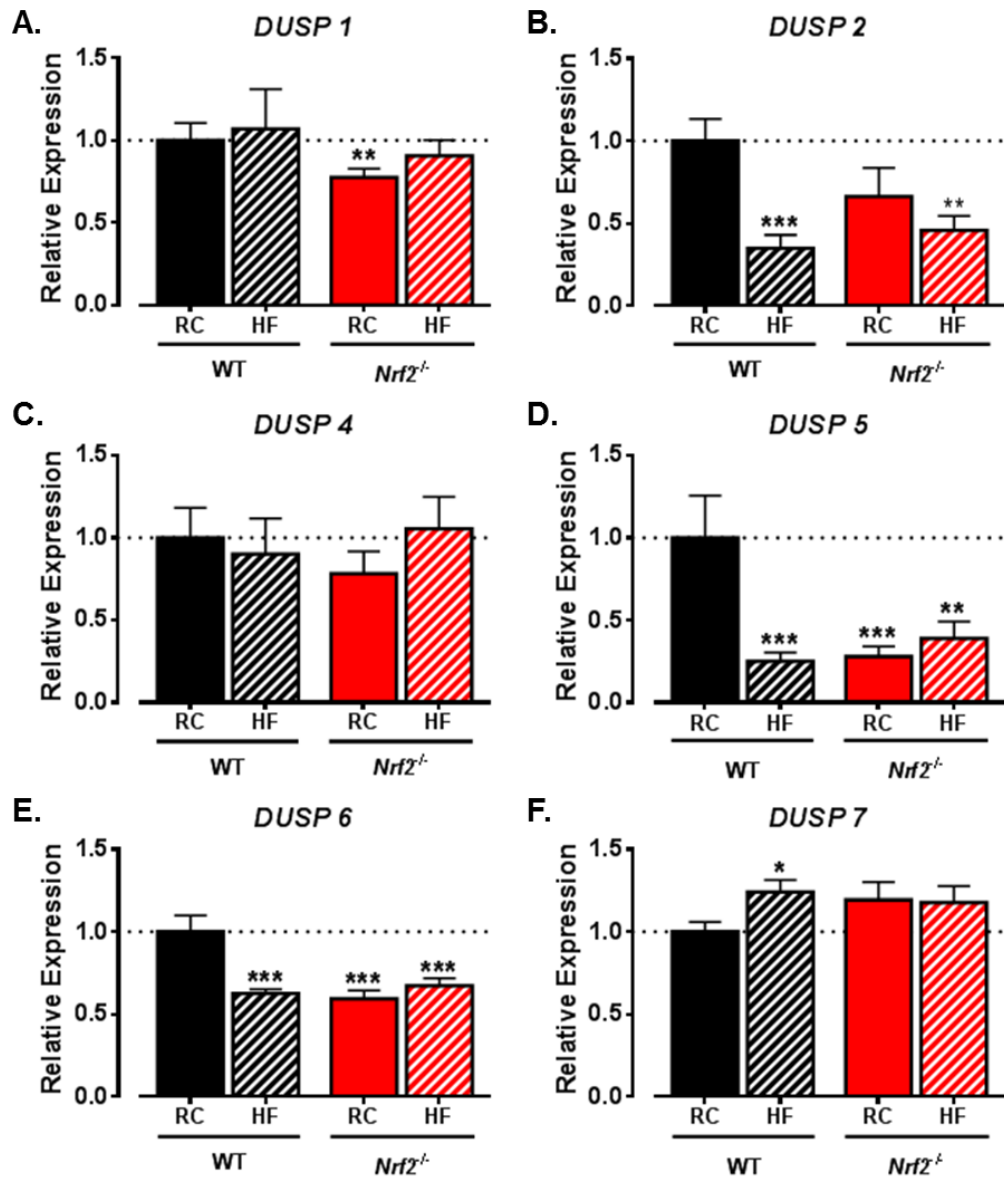


Figure 3.25 Loss of *Nrf2* and HF feeding impact significantly on the gene expression of important MAPK DUSP proteins.

Brain tissue was harvested from mice and processed for gene expression analysis by TaqMan RT-qPCR. Measures were taken for relative expression of *DUSP1* (A), *DUSP2* (B), *DUSP4* (C), *DUSP5* (D), *DUSP6* (E) and *DUSP7* (F) in the hippocampus of aged mice. All data portrayed as means \pm s.e.m. and analysed by one-sample and unpaired t-test where * indicates significantly different from RC fed WT control unless otherwise indicated. *, $p < 0.05$; **, $p < 0.01$; ***, $p < 0.001$. WT $n = 6$, *Nrf2*^{-/-} $n = 6$. Gene expression data captured by PhD student Andrew M. Kidger as part of a collaboration with Prof. Stephen M. Keyse, Division of Cancer Research, University of Dundee.

Of the known ERK-specific cytosolic DUSPs, 6 and 7 were assessed as the expression level of 9 was too variable to be consistently picked up by RT-qPCR machine. The profile of *DUSP6* expression was the same as that seen for the nuclear *DUSP5* with both HF-feeding and *Nrf2* loss impeding expression in the aged hippocampus (WT RC: 1.00; WT HF: 0.625 ± 0.03 ; *Nrf2*^{-/-} RC: 0.593 ± 0.05 ; *Nrf2*^{-/-} HF: 0.672 ± 0.05 ; WT RC vs WT HF $p < 0.0001$, WT RC vs *Nrf2*^{-/-} RC $p < 0.001$, WT RC vs *Nrf2*^{-/-} HF $p < 0.001$, $n = 6$; Figure 3.25 E). Finally, *DUSP7* was the only DUSP measured to be positively affected by HF feeding with WT mice showing a significant increase in expression (WT RC: 1.00; WT HF: 1.24 ± 0.07 ; WT RC vs WT HF $p < 0.05$, $n = 6$; Figure 3.25 F). Furthermore, a trend towards increased expression was also seen in both *Nrf2*^{-/-} RC and HF fed mice, although this failed to reach significance (*Nrf2*^{-/-} RC: 1.19 ± 0.11 ; *Nrf2*^{-/-} HF: 1.18 ± 0.10 ; WT RC vs *Nrf2*^{-/-} RC and HF $p > 0.05$, $n = 6$).

To see if the changes in DUSP gene expression just described were carried through to alterations in protein levels, those DUSPs with functioning Western blotting antibodies were assessed in hippocampal tissue lysates from WT and *Nrf2*^{-/-} RC and HF fed mice. In addition, to assess whether the upregulation in ERK phosphorylation was due to an increase throughout the pathway in combination with alterations of DUSP activity, we looked at protein levels of MEK 1/2 phosphorylation. MAPK kinases, or MEKs, activate the MAPK enzymes by means of phosphorylation. Phosphorylation by MAPK kinase kinase enzymes specifically activates MEK 1/2 to in turn dual phosphorylate and activate ERK 1/2. Despite no significant changes in gene expression, protein levels of DUSP4 were significantly decreased by HF feeding in WT mice (WT RC: 1.00; WT HF: 0.445 ± 0.04 ; WT RC vs WT HF $p < 0.0001$, $n = 6$; Figure 3.26 A). In addition, HF-feeding also impaired DUSP4 protein production in *Nrf2*^{-/-} mice; however, this was significantly attenuated when compared to HF fed WT mice (*Nrf2*^{-/-} HF: 0.722 ± 0.10 ; WT RC vs *Nrf2*^{-/-} HF $p < 0.05$, WT HF vs *Nrf2*^{-/-} HF $p < 0.05$, $n = 6$).

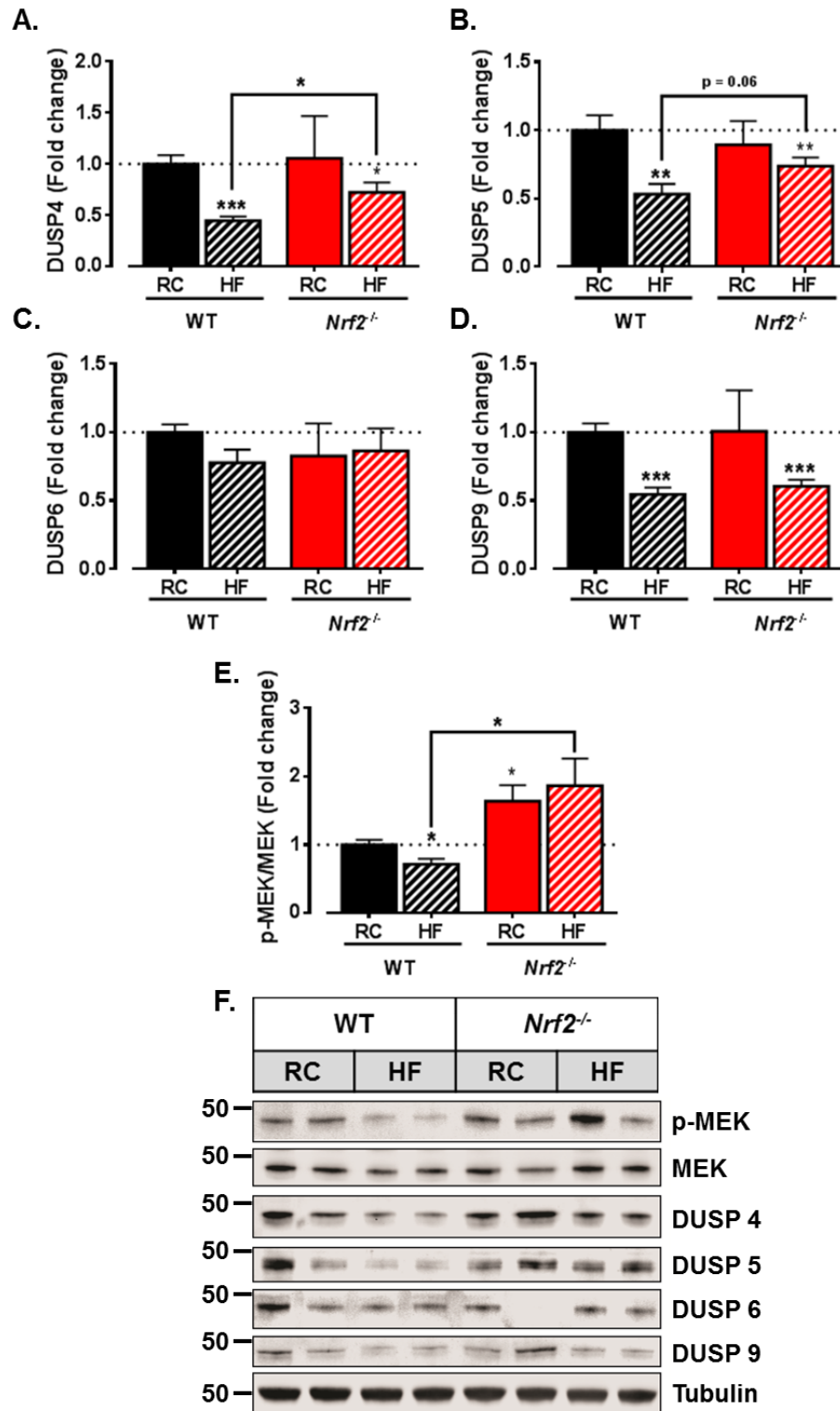


Figure 3.26 Loss of *Nrf2* and HF feeding impact significantly on both MEK1/2 and important ERK-related DUSP proteins in the hippocampus of aged mice.

Brain tissue harvested from WT and *Nrf2*^{-/-} mice was processed for protein expression by Western blotting. Protein levels of DUSP4 (A), DUSP5 (B), DUSP6 (C), DUSP9 (D) and the ERK MAPKK MEK1/2 (E) were calculated by densitometry in the hippocampus of aged mice, where tubulin was used as the protein loading control. All data are portrayed as means \pm s.e.m. and analysed by one-sample and unpaired t-test where * indicates significantly different from RC fed WT control unless otherwise indicated. *, $p < 0.05$; **, $p < 0.01$; ***, $p < 0.001$. WT $n = 6$, *Nrf2*^{-/-} $n = 6$. Protein data captured by PhD student Andrew M. Kidger as part of a collaboration with Prof. Stephen M. Keyse, Division of Cancer Research, University of Dundee.

Repeating a similar profile, DUSP5 protein was significantly affected by HF-feeding with both WT and *Nrf2*^{-/-} mice presenting decreased protein levels following HF feeding (WT RC: 1.00; WT HF: 0.532 ± 0.07; *Nrf2*^{-/-} HF: 0.737 ± 0.06; WT RC vs WT HF p < 0.01, WT RC vs *Nrf2*^{-/-} HF p < 0.01, n = 6; Figure 3.26 B). Moreover, like DUSP4, DUSP5 shows an attenuated response in *Nrf2*^{-/-} HF fed mice although this falls just short of significance (WT HF vs *Nrf2*^{-/-} HF p = 0.06, n = 6). In contrast, despite significantly less gene expression, RC fed *Nrf2*^{-/-} mice reported too much variability in DUSP5 protein levels to report any significant change in comparison to controls. Furthermore, no change in protein level is reported in DUSP6 irrespective of genotype or diet in use (p > 0.05; Figure 3.26 C), but DUSP9 shows a diet dependent decrease in protein level recorded in both WT and *Nrf2*^{-/-} mice (WT RC: 1.00; WT HF: 0.547 ± 0.05; *Nrf2*^{-/-} HF: 0.603 ± 0.05; WT RC vs WT HF p < 0.001, WT RC vs *Nrf2*^{-/-} HF p < 0.001, n = 6; Figure 3.26 D).

Finally, MEK1/2 phosphorylation was assessed in the hippocampus of aged WT and *Nrf2*^{-/-} mice. HF feeding induced a concomitant decrease in MEK phosphorylation alongside those seen in DUSP expression in WT mice (WT RC: 1.00; WT HF: 0.712 ± 0.08; WT RC vs WT HF p < 0.05, n = 6; Figure 3.26 E). However, RC fed *Nrf2*^{-/-} mice report significantly increased levels of MEK phosphorylation in the hippocampus when compared to controls (*Nrf2*^{-/-} RC: 1.64 ± 0.24; WT RC vs *Nrf2*^{-/-} RC p < 0.05, n = 6). Moreover this increase in phosphorylation is maintained following HF feeding in *Nrf2*^{-/-} mice in contrast to WT HF fed mice (*Nrf2*^{-/-} HF: 1.87 ± 0.40; WT RC vs *Nrf2*^{-/-} HF p = 0.08, WT HF vs *Nrf2*^{-/-} HF p < 0.05, n = 6). To summarise the increase in ERK phosphorylation seen in *Nrf2*^{-/-} mice appears to be driven by alterations in both MEK 1/2 and ERK-specific DUSPs. It would appear that under RC-fed conditions the increased ERK phosphorylation is driven primarily by increased activation of the ERK MAPK pathway with increased phosphorylation of MEK. However, on a HF diet this increased MEK phosphorylation is maintained and ERK phosphorylation is potentiated by a decrease in several ERK-specific DUSPs.

3.13 *NRF2* DEPLETION DRIVES ALTERATIONS IN MOUSE BRAIN MITOCHONDRIA

VDAC1 and COX IV are both markers of the outer mitochondrial membrane; with VDAC1 (aka porin), a voltage dependent anion channel protein playing a role in cell metabolism and mitochondrial apoptosis, and COX IV one of the subunits of the final complex in the electron transport chain. RC and HF fed aged mice were analysed for VDAC1 and COX IV expression in whole lysates as shown in the exemplar blots (Figure 3.27 A). HF feeding decreased expression of COX IV in both the hippocampus (WT RC: 1.00; WT HF: 0.340 ± 0.05 ; WT RC vs WT HF $p < 0.0001$, $n = 8$; Figure 3.27 B) and cortex (WT RC: 1.00; WT HF: 0.333 ± 0.71 ; WT RC vs WT HF $p < 0.0001$, $n = 8$; Figure 3.27 D) of WT mice by over 60% relative to RC fed WT mice. HF feeding of *Nrf2*^{-/-} mice also decreases COX IV expression in both the hippocampus (*Nrf2*^{-/-} HF: 0.603 ± 0.11 ; WT RC vs *Nrf2*^{-/-} HF $p < 0.0001$, $n = 8$) and cortex (*Nrf2*^{-/-} RC: 0.974 ± 0.14 ; *Nrf2*^{-/-} HF: 0.250 ± 0.04 ; WT RC vs *Nrf2*^{-/-} HF $p < 0.0001$, *Nrf2*^{-/-} RC vs *Nrf2*^{-/-} HF $p < 0.001$, $n = 8$). However, in the hippocampus COX IV expression remains significantly higher than that seen in HF fed WT mice (WT HF vs *Nrf2*^{-/-} HF $p < 0.05$, $n = 8$).

Similar to levels of COX IV, HF feeding decreased VDAC1 protein in both the hippocampus (WT RC: 1.00; WT HF: 0.466 ± 0.05 ; WT RC vs WT HF $p < 0.0001$, $n = 8$; Figure 3.27 C) and cortex (WT RC: 1.00; WT HF: 0.652 ± 0.03 ; WT RC vs WT HF $p < 0.0001$, $n = 8$; Figure 3.27 E) of WT mice relative those on a RC diet. HF feeding of *Nrf2*^{-/-} mice also decreased VDAC1 in the cortex with a trend towards a significant decrease seen in the hippocampus when compared to RC fed animals (hippocampus: *Nrf2*^{-/-} RC: 1.31 ± 0.16 ; *Nrf2*^{-/-} HF: 0.757 ± 0.21 ; *Nrf2*^{-/-} RC vs *Nrf2*^{-/-} HF $p = 0.05$, $n = 8$. Cortex: *Nrf2*^{-/-} RC: 1.31 ± 0.15 ; *Nrf2*^{-/-} HF: 0.425 ± 0.03 ; WT RC and *Nrf2*^{-/-} RC vs *Nrf2*^{-/-} HF $p < 0.0001$, $n = 7-8$). However, in the cortex VDAC1 expression drops significantly compared to HF fed WT mice in *Nrf2*^{-/-} mice fed a HF diet (WT HF vs *Nrf2*^{-/-} HF $p < 0.0001$, $n = 7-8$). A trend towards increased VDAC1 is seen in the hippocampus and cortex of RC fed mice (Hippocampus: WT RC vs *Nrf2*^{-/-} RC $p = 0.07$, $n = 8$. Cortex: WT RC vs *Nrf2*^{-/-} RC $p = 0.07$, $n = 7-8$).

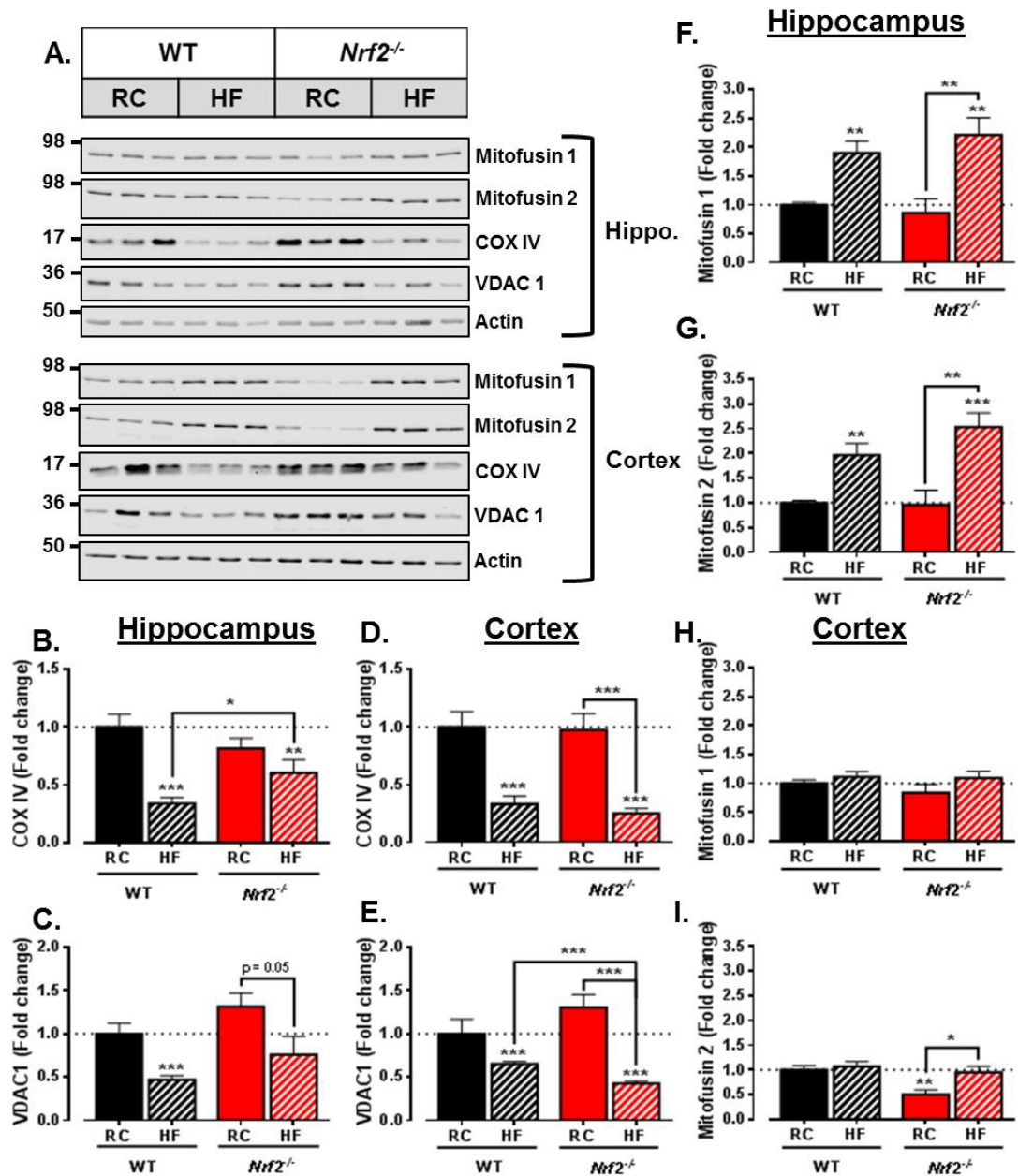


Figure 3.27 Loss of *Nrf2* and HF feeding both impact on mitochondrial health and mitophagy markers.

Brain tissue was harvested from mice and processed for protein expression by Western blot as previously described using whole lysates, with exemplars shown in **A** where β -actin was used as the protein loading control. Measures were taken for relative expression of COX IV (**B** + **C**), VDAC 1 (**D** + **E**), mitofusin 1 (**F** + **G**) and mitofusin 2 (**H** + **I**) in the hippocampus and cortex of RC and HF fed WT and *Nrf2*^{-/-} mice, where β -actin was used as the protein loading control. All data portrayed as means \pm s.e.m. and analysed by unpaired t-test where * indicates significance between groups. *, $p < 0.05$; **, $p < 0.01$, ***, $p < 0.001$. WT $n = 7-8$, *Nrf2*^{-/-} $n = 6-8$.

Changes in mitochondrial proteins can often be associated with a change in mitochondrial number or mitochondrial autophagy, otherwise known as mitophagy. In order to assess this possibility, two key fusion proteins were also analysed (mitofusin 1 and 2). No genotype dependent changes were observed in mitofusin 1 in either the hippocampus (Figure 3.27 F) or cortex (Figure 3.27 H), though there was a significant dietary related induction following HF feeding in the hippocampus (WT RC: 1.00; WT HF: 1.90 ± 0.21 ; *Nrf2*^{-/-} RC: 0.858 ± 0.24 ; *Nrf2*^{-/-} HF: 2.21 ± 0.29 ; WT RC vs WT HF $p < 0.01$; WT RC vs *Nrf2*^{-/-} HF $p < 0.01$, *Nrf2*^{-/-} RC vs *Nrf2*^{-/-} HF $p < 0.01$, $n = 8$).

Mitofusin 2, on the other hand, has opposing expression in the hippocampus and the cortex following HF feeding in *Nrf2*^{-/-} mice. In the hippocampus, expression of mitofusin 2 mimics that seen for mitofusin 1 with HF feeding stimulating expression in both genotypes (WT RC: 1.00; WT HF: 1.96 ± 0.23 ; *Nrf2*^{-/-} RC: 0.956 ± 0.30 ; *Nrf2*^{-/-} HF: 2.53 ± 0.28 ; WT RC vs WT HF $p < 0.01$, WT RC vs *Nrf2*^{-/-} HF $p < 0.001$, *Nrf2*^{-/-} RC vs *Nrf2*^{-/-} HF $p < 0.01$, $n = 8$; Figure 3.27 G). Cortical expression of mitofusin 2 does not change as a result of HF feeding in WT or *Nrf2*^{-/-} mice when compared to WT RC animals. Expression of mitofusin 2 in *Nrf2*^{-/-} RC fed animals, however, is halved compared to WT controls which is recovered to control levels by HF feeding (WT RC: 1.00; *Nrf2*^{-/-} RC: 0.500 ± 0.09 ; *Nrf2*^{-/-} HF: 0.948 ± 0.12 ; WT RC vs *Nrf2*^{-/-} $p < 0.01$, *Nrf2*^{-/-} RC vs *Nrf2*^{-/-} HF $p < 0.05$, $n = 6-8$; Figure 3.27 I).

3.14 DISCUSSION

3.14.1 Long-Term HF Feeding Has Contrasting Effects on Glucose Management and Body Weight in *Nrf2*^{-/-} and *hAPP*_{swe} Mice

Despite its ubiquitous expression, relatively little work has been done on *Nrf2* in the brain in comparison to its study in other areas such as liver and cancer research. Confirmation of the presence of *Nrf2* in the mouse brain was done via gene expression, where it was shown to be present in all four of the brain regions analysed. This was repeated for the APP mouse gene, establishing both of these key proteins as being present in the brain regions of interest. In addition, use of human specific probes permitted us to confirm the presence of the *hAPP* gene in our transgenic carriers, giving confirmation of the model in use. And whilst a small discrepancy was seen in the expression of *hAPP* in the cortex of *Nrf2*^{-/-}/*hAPP*_{swe} mice this did not appear to translate to any significant induction in total APP protein expressed in these mice.

Thereafter, our first aim was to assess the effect long-term HF feeding had on our models. There are a multitude of studies showing HF feeding causes weight gain, insulin resistance and impaired glucose disposal in WT mice on the C57/Bl6 background (Winzell & Ahrén, 2004). The majority of these studies are pursued with a focus on obesity, and in some cases diabetes research. Indeed, transgenic models have been produced that develop a more pronounced disease phenotype such as the leptin deficient *ob/ob* mice and the *db/db* mouse that carries a functional defect in the long form leptin receptor. However, with most studies being centred round obesogenic and diabetic outcomes, very few studies have pursued the effects of HF feeding over a longer period of time. Along with a few other labs (Chartoumpakis *et al.*, 2011; Meher *et al.*, 2012), we have already shown that *Nrf2*^{-/-} mice maintain their insulin sensitivity and glucose disposal when placed on a HF diet for a standard period of 20 weeks (Meakin *et al.*, 2014). Furthermore, a small number of studies have been pursued using AD mouse models which indicate that FAD related mutations may impact on peripheral energy homeostasis, especially when challenged by HF feeding (Kohjima *et al.*, 2010; Mody *et al.*, 2011). This is of particular interest given the reported risks conferred by obesity and T2DM on development of dementia. We were able to show that long-term, *Nrf2*^{-/-} mice maintain their resistance to DIO, remaining significantly lighter than their HF fed WT counterparts at 14 months of age following a year of HF feeding. In addition, loss of *Nrf2*^{-/-} in *Nrf2*^{-/-}/*hAPP*_{swe} appears to counteract the trend for increased body weight seen in mice carrying the *hAPP*_{swe} transgene alone.

We have previously shown that *Nrf2*^{-/-} mice at 28 weeks have the same glucose clearance as WT mice when on a RC diet. However, when these were placed on a HF diet for 20 weeks, *Nrf2*^{-/-} mice demonstrated an improved glucose clearance compared to controls (Meakin *et al.*, 2014). When IPGTTs were performed at 15 months on our aged cohort, we found that mice lacking *Nrf2* had improved glucose clearance, even under RC conditions. In addition, both WT and *hAPP*_{swe} mice had a similar clearance profile. The glucose sensitivity seen in the *Nrf2*^{-/-} correlates with lower total body weight at time of testing, and this may play an important role in the maintenance of glucose sensitivity seen in the HF fed *Nrf2*^{-/-} cohort. Furthermore, *Nrf2*^{-/-} mice fed a RC diet are more insulin sensitive than either WT or *hAPP*_{swe} compatriots as demonstrated by ITT. And despite demonstrating an acute sensitivity to insulin at a younger age following only twenty weeks of HF feeding (Meakin *et al.*, 2014), by 16 months of age *Nrf2*^{-/-} mice on a HF diet report a loss of insulin sensitivity similar to that seen in WT and *hAPP*_{swe} mice. This may suggest a dysregulation of insulin signalling in *Nrf2*^{-/-} mice

fed a HF diet long term and may be linked with damage in the periphery such as is known to occur in the livers of these mice. In order to pursue this further, investigation of circulating insulin levels and analysis of the pancreas may elucidate whether these changes are down to depletion or dysfunction of endogenous insulin, whilst *in vivo* clamp studies may also be important in clarifying the alterations seen in *Nrf2*^{-/-} mice. Furthermore, assessment of hypothalamic tissue for alterations in key metabolic regulators would be important to illuminate the role of central vs peripheral regulation in these changes.

In contrast, whilst *Nrf2*^{-/-} mice maintain their increased glucose sensitivity even after a year of HF feeding, *hAPP*_{swe} mice portray an exacerbated clearance profile following long-term HF feeding even when compared to WT mice on the same diet. This exacerbation appears to occur despite similar body weights to those seen for HF fed WT mice and may indicate an important role for alterations in APP processing on obesity in aging. This is in line with the recent study by Vandal and colleagues (2014) who found that HF feeding of 3x Tg mice (*hAPP*_{swe}, *PS1*_{M146V}, *tau*_{P301L}) was marked by worsened glucose tolerance. In addition, they found that the transgenic model accumulated amyloid in their pancreatic islets whilst HF feeding of these mice caused pancreatic islet degeneration and further exacerbated the cognitive impairment seen under basal conditions. Finally, Vandal *et al.* were able to show an increase in AD-like pathologies following HF feeding which were improved following acute insulin treatment in conjunction with improved cognitive performance. Similarly, another study using the same 3x Tg model demonstrated an increased presence of pathological hallmarks of AD following consumption of a western-style diet supporting the findings of Vandal and colleagues (Julien *et al.*, 2010). In addition, Julien *et al.* suggested a role for the depletion of polyunsaturated fatty acids (PUFA) in the aggravation of AD pathology, with detrimental effects seen when mice were fed a diet low in n-3:n-6 fatty acids either alone or in combination with high levels of fat. Low levels of PUFAs has previously been suggested to be linked with increased risk of developing AD (Morris *et al.*, 2003; Schaefer *et al.*, 2006). This implicates a role for dysfunctional insulin signalling in AD.

Work performed in our lab using the *BACE*^{-/-} mouse may act in support of these findings. We have previously published data showing that *BACE1*^{-/-} mice fail to gain weight following HF feeding and show improved response to both IPGTTs and ITTs. This further supports a potential role for the amyloidogenic pathway in alterations in

insulin signalling. Furthermore, these findings have been replicated using pharmacological inhibitors of BACE1 with similar results. However, contrasting with the findings described by Vandal *et al.*, work performed by Catherine Lawrence's lab showed HF diet induced cognitive impairments in the same 3x Tg model of AD but failed to find significant alterations in pathological markers such as amyloid in the brains of these mice (Knight *et al.*, 2014). Finally, studies on a single mutant model of AD carrying the *hAPP_{swe}* gene inclusion driven by the hamster prion protein promoter showed increased weight gain alongside the alterations in insulin and glucose signalling (Ho *et al.*, 2004). Moreover, in addition to alterations in amyloid production, Ho *et al.* suggested a role for increased γ -secretase activity following HF feeding. However, it is worth noting that under the prion promoter, expression of the *hAPP_{swe}* mutation has been shown to be over five-fold that of normal mouse APP making this a more aggressive model than that used in our studies (Elder *et al.*, 2010). From this it is clear that the animal model used, in addition to the diet administered and the duration of the dietary intervention and age of testing may all play an important role in the outcomes described by the individual studies. In addition, these factors, in particular the prevalence of more aggressive models of AD in many of these studies, may explain why our findings have failed to replicate their work in instances such as the increased presence of pathological markers. What does seem clear is that the interaction between insulin signalling and the APP pathway is intricate and further investigation is required to tease out the actions of the pathways involved.

Further to the alterations in both weight gain and insulin signalling, other key organs were assessed for both genotype and diet induced changes, namely heart, liver and spleen. Increased inflammation, OS and lipogenesis all have the ability to impact on organ morphology. Moreover, it has previously been reported that *Nrf2*^{-/-} mice on a HF diet have an increased risk of developing both steatohepatitis and cirrhosis (Chowdhry *et al.*, 2010; Meakin *et al.*, 2014), which highlights the impact of *Nrf2* loss on liver health. Given the increased duration of this study in comparison to other similar studies performed to date, long term impacts of an obesogenic diet such as cardiac hypertrophy were also assessed in our mouse models. We found that the hearts taken from our *Nrf2*^{-/-} and *Nrf2*^{-/-}/*hAPP_{swe}* mice had undergone tissue hypertrophy by 16 months of age irrespective of the diet being fed. This suggests a role for increased ROS production and OS, through the loss of *Nrf2*, in driving cardiac remodelling, a phenomenon that has been previously described in other models of obesity (Ceylan-Isik *et al.*, 2013). This is further supported by research published by Li and colleagues indicating activation of

Nrf2 aids in counteracting hyperglycaemia-driven cardiac hypertrophy in an STZ-induced diabetic rat model (Li *et al.*, 2015). In addition, activation of Nrf2 has been suggested to protect the murine heart from cardiac hypertrophy and damage resulting from haemodynamic stress, contrasting with the aggravated response observed in Nrf2^{-/-} mice (Li *et al.*, 2009). Furthermore, chemical activation of Nrf2 with well-known Nrf2 activating compounds has attenuated the detrimental cardiac alterations associated with diabetic cardiomyopathy, resulting in renewed interest in Nrf2 activators for the treatment of some cardiovascular complications (Bai *et al.*, 2013; Wang *et al.*, 2013c). As a result, it would be interesting to go back and investigate this further by examining whether the change in heart size is linked with any particular regional alterations of cardiac physiology and whether this is linked with increased ER stress or markers of oxidative damage. This may be of particular interest given the lack of prior information available regarding the effects of long-term HF feeding on the cardiac system of Nrf2^{-/-} mice.

Building on work previously published from ours and others labs, we also found significant decreases in liver size in both our mouse models lacking *Nrf2* expression. This complements previous findings indicating increased fibrosis and liver damage in HF fed *Nrf2*^{-/-} mice both of which are known to negatively impact on liver size. This change in liver size was maintained after accounting for body weight indicating it is not solely as a result of attenuated body weight increase seen in *Nrf2*^{-/-} and *Nrf2*^{-/-}/*hAPP*_{swe} mice. In addition, no further significant impact was seen following the supplementation of *hAPP*_{swe} despite the single transgenic *hAPP*_{swe} mice displaying no alteration in liver size when fed a RC diet. Furthermore, there was an increase in splenic size in both *Nrf2*^{-/-} and *Nrf2*^{-/-}/*hAPP*_{swe} mice. Whilst spleen size is relatively consistent when not challenged by immunoreactive or toxic factors, the change in spleen size seen in our study is likely a result of altered immune cell production. Ongoing research in collaboration with Prof. J. Hayes and his lab has shown that there is no alteration in the ratio of immune cell types produced by the spleen in HF fed *Nrf2*^{-/-} mice, rather there is an overall increase in immune cells. Furthermore, the majority of these cells appear to relocate towards the liver, with a distinct lack of immune cell infiltration seen in the WAT of these mice contrary to HF fed WT controls.

3.14.2 Mice Lacking *Nrf2* Have Increased Locomotor Activity in Early Adulthood Following High Fat Feeding

There has, to date, been very little published work examining the effects of *Nrf2* loss on behavioural phenotype and differences. A paper published by Muramatsu and colleagues (2013) reported no changes in social interaction, open-field and rotarod tests in young *Nrf2*^{-/-} mice. This in turn suggests a lack of impact of *Nrf2* loss on anxiety levels, motor activity and muscle tone when compared to controls at the age tested. However, this does not assess any long-term effects the loss of *Nrf2*^{-/-} may have on cognitive ability. Finally, Muramatsu and colleagues also performed a forced swim test on young *Nrf2*^{-/-} mice that indicated a resistant phenotype of *Nrf2*^{-/-} towards the despair profile associated with acute forced swim stress. However, despite the recent interest in *Nrf2*^{-/-} mice little other cognitive phenotyping has been performed. Furnari performed a battery of behaviour and motor skill related tests on WT and *Nrf2*^{-/-} mice including tasks such as the Morris water maze and the open-arm elevated plus maze model of anxiety (Furnari, 2013; Furnari *et al.*, 2014); however, the majority of the effects seen on cognition resulted from additional treatment alterations as opposed to effects of genotype alone. In addition, similar to the study undertaken by Muramatsu and colleagues, the mice used were all aged younger than six months at time of testing, preventing the assessment of ageing contributions on cognitive performance.

As described, mice were tested at 4 distinct ages using a simple working memory model of a closed arm elevated plus maze where continuous spontaneous alternation was assessed in a non-cued environment. In the first instance we found no effect of genotype on locomotor activity as described by the number of arm entries performed by each group. Furthermore, whilst all groups showed age-dependent attenuation in both the number of arm entries performed as well as the number of alternations performed, these were not further affected by genotypic alterations. In contrast, upon calculation of SA values, which has been previously described by McNay and colleagues (2000), we found both time and genotype dependent effects on performance. A time dependent attrition in SA was seen in all groups, with *Nrf2*^{-/-}/*hAPP*_{swe} mice performing significantly worse than WT and *Nrf2*^{-/-} mice. A similar trend is seen in *Nrf2*^{-/-} mice over time, though this fails to reach significance in comparison to WT controls. However, loss of *Nrf2* may act as a priming force, exacerbating the effects of any additional challenges administered such as the addition of *hAPP*_{swe}. It would be

interesting to pursue this further looking at the effect of Nrf2 loss on cognition over time, especially in light of the negative correlation of Nrf2 with ageing.

The measure of SA measured in a continuous format (in either a Y- or +- maze model) is often linked to a measurement of spatial working memory (Chu *et al.*, 2012; Joshi *et al.*, 2014). Changes in hippocampal glucose consumption and reversal of SA impairment following hippocampal interventions suggests that the continuous SA alternation task may rely at least in part on hippocampal involvement for task completion, even when this task is un-cued (McNay *et al.*, 2000; Krebs & Parent, 2005; McNay *et al.*, 2010). However, the specific regional requirements for successful SA may be heavily influenced by the design setup and as such depending on the availability of external cues, and the type of memory encoding believed to be in use during the task performance this may not be the case (Lennartz, 2008; Vorhees & Williams, 2014; Hargrave *et al.*, 2015). At the very least, it is likely that the hippocampus is not solely responsible in enabling successful task completion, and care should be given in the design and setup of this outwardly simple task as well as the interpretation of the subsequent results. As such, and given the previously described results for our model, it is possible that with an egocentric task design our model reflects a non-hippocampal-dependent task, instead relying more on other brain areas associated with egocentric task completion, such as the dorsal striatum (Vorhees & Williams, 2014). It should be noted, however, that there remains limited research on regional influences for egocentric tasks in comparison to allocentric tasks. Further testing using one of the more strongly correlated hippocampal dependent tasks, such as the MWM, would aid in confirming the presence or lack of hippocampal involvement within this model. Furthermore, in light of the predominantly hippocampal related inflammatory response recorded, tasks that are dependent on this function for successful completion may be of relevance for the characterisation of this model following an ageing intervention.

Further to this, we also assessed the effect of long-term HF feeding on WT and *Nrf2*^{-/-} mice and their ability to SA. Given that obesity and the metabolic syndrome are associated with chronic low grade inflammation as well as alterations in substrate utilisation, it was proposed this might act to challenge the already primed environment of the *Nrf2*^{-/-} mouse. We found that HF feeding had a significant impact on locomotor activity in the *Nrf2*^{-/-} mice as described by increased arm entries performed and this occurred in conjunction with attenuated weight gain following consumption of a 45% HF diet. Moreover, as this increase in activity was matched by an increase in

alternations successfully performed, *Nrf2*^{-/-} mice demonstrated no significant attrition in SA following HF feeding. The increased activity seen in HF fed *Nrf2*^{-/-} mice is supported by activity measures performed during other HF feeding studies, and has also been shown to correlate with an increase in oxygen consumption (Meakin *et al.*, 2014). And whilst the changes reported in behaviour remain relatively mild, this supports further research into the impact of HF feeding on *Nrf2*^{-/-} mice. This may also advocate for the development of a more selective KO model, allowing the roles driven by *Nrf2* in the liver which are clearly important and complex to be separated from potential alterations in central energy regulation.

3.14.3 High Fat Feeding and Inflammation Following Loss of *Nrf2* and a Role for Contrasting Organ Specific Effects

It is now well accepted that inflammation plays a role in many forms of neurodegenerative disorders. In addition, it is a well described presence in both obesity and T2DM, whilst the efficacy of our immune responses is slowly impaired with ageing. It has been shown that consumption of a diet high in fat can affect both peripheral and central tissues, with inflammation previously being reported in brain regions such as the hypothalamus (Thaler *et al.*, 2012). Given the already described significant alterations observed in the livers of *Nrf2*^{-/-} mice, it was originally hypothesised that HF feeding may induce a similar detrimental effect in the brain which would be amplified by HF feeding. We were able to show that, in contrast to the liver, long term HF feeding attenuates the basal inflammatory state present in the aged *Nrf2*^{-/-} mouse brain, with the expression of pro-inflammatory cytokines, such as *IL-1 β* and *TNF- α* , significantly diminished by HF feeding. Furthermore, whilst *Nrf2*^{-/-}/*hAPP*_{swe} mice have a reduced inflammatory profile when compared to *Nrf2*^{-/-} mice, HF feeding is still able to further attenuate this inflammatory response.

In contrast, mice carrying the *hAPP*_{swe} gene fail to replicate the increased pro-inflammatory profile seen in the *Nrf2*^{-/-} mice with many markers appearing at the same expression level or lower than those reported for WT mice. This is maybe surprising in light of other publications which have studied the effects of AD mouse models and mouse models of obesity as many of these report increases in markers related to inflammation (Pistell *et al.*, 2010; Takeda *et al.*, 2010; Ferretti *et al.*, 2012). Still, the majority of the models in use in these studies describe more aggressive AD pathology than is seen in our model. It has been well described that addition of A β can act to induce inflammatory markers (Benito *et al.*, 2012), but we were unable to visualise

plaque deposition in our mouse model. Furthermore, many high fat feeding studies in AD mouse models have failed to quantify changes in inflammatory cytokines, concentrating instead on markers of OS or markers of immune cell activation. And this we have been able to reiterate, with elevation of the microglial marker *F4/80* following HF feeding in the hippocampus of our *hAPP_{swe}* mice (Figure 3.12 A). What we can conclude, therefore, is that *hAPP_{swe}* mice do not require overt pathology to demonstrate altered insulin sensitivity following ageing. However, it is possible that more substantial elevations in amyloid than is likely occurring in the model used here, may be essential in the potentiation of other inflammation related markers that have been shown by groups using alternative mouse models of AD.

Studies performed using HF fed *Nrf2^{-/-}* mice have so far concentrated on the effects of *Nrf2* loss on peripheral organs. However, we can corroborate the improved inflammatory profile seen in the brains of our HF fed *Nrf2^{-/-}* mice with similar apparently protective effects reported in other peripheral organs. It has been previously reported that *Nrf2^{-/-}* fail to gain the same amount weight as WT mice when placed on a HF diet (Meakin *et al.*, 2014). This prompted further investigation into the effects of *Nrf2* loss on lipogenesis, alterations in WAT including impaired adipogenesis and changes in hepatic function following HF feeding. Pi and colleagues (2010) described a role for impaired PPAR- γ activation in vitro through the manipulation of the adipogenic cell line 3T3-L1 and mouse embryonic fibroblasts (MEFs) taken from WT and *Nrf2^{-/-}* mice. Meher and colleagues (2012) took this one step further, combining the use of global *Nrf2^{-/-}* with a novel myeloid cell specific *Nrf2^{-/-}* model to assess the role *Nrf2* loss may play on obesity induced inflammation. Contrary to what might have been expected given the literature available, which demonstrates an aggravated inflammatory response in livers deficient in *Nrf2*, Meher found that whole body *Nrf2^{-/-}* mice had improved WAT inflammatory profiles in addition to continued insulin sensitivity. Their myeloid-specific *Nrf2^{-/-}* was not capable of reproducing these effects although it did show an improved inflammatory profile upon analysis of the stromal vascular fraction from WAT, which contains a high percentage of immune cells.

This robust reduction in obesity associated inflammatory response is similar to that which we have described here in the brain. Moreover, a study performed using a Keap1 KD model, which is characterised by continued increased *Nrf2* activity, demonstrated a potentiation of the standard responses to HF feeding seen in WT mice (More *et al.*, 2013). Keap1 KD mice put on significantly more weight than their WT

counterparts on a HF diet. In addition, HF fed Keap1 KD mice were shown to have significantly increased lipid and triglyceride accumulation in the liver, significantly increased induction in both lipogenic and *Nrf2* target genes in the liver and WAT, along with increased WAT inflammatory markers and further impairment in insulin signalling and glucose sensitivity. Furthermore, unpublished data produced by our collaborators in Prof. J.D. Hayes lab have shown, using fluorescence-activated cell sorting (FACS), that the immune cell profile in the liver and WAT of *Nrf2*^{-/-} mice are in exact opposition to each other. In addition, preliminary data from our lab looking at alterations in inflammation related gene expression suggest a distinct attenuation or prevention in the induction of these genes in the WAT of *Nrf2*^{-/-} mice following HF feeding. Further to this, loss of *Nrf2* is associated with increased fatty acid production within the liver as well as altered triglyceride metabolism; in fact, the liver might almost be suggested to act as a sink for the pro-inflammatory immune responses induced by HF feeding. Therefore, this suggests an important apparently protective role of HF feeding in *Nrf2*^{-/-} mice that comes at a detrimental cost to the liver.

At this stage, it is worth remembering the different profiles of expression seen in the hippocampus and cortex, in particular with relation to the *Nrf2*^{-/-} mice. We have shown region specific alterations in inflammatory profile with the hippocampus reporting an increased presence of pro-inflammatory markers, whilst the cortex demonstrated a more dominant anti-inflammatory profile with increased induction of alternative immune pathways such as that of the complement cascade. This was complemented by a reduction in the formation of protein carbonyl adducts in the cortex of *Nrf2*^{-/-} mice. Furthermore, whilst the anti-inflammatory response is again predominantly induced in the brains of aged *Nrf2*^{-/-} mice, this is still attenuated by HF feeding in a similar manner to that seen for the pro-inflammatory markers. This may indicate the cortex is better able to support resolution of the pro-inflammatory and stress-inducing environment produced by the loss of *Nrf2*^{-/-} than the hippocampus. It would be of interest to assess this further, potentially by using a more aggressive intervention on the model to accelerate the time line. If over time the cortex also succumbs to the damaging effects of *Nrf2* loss, a more complete analysis of important brain regions may be warranted. Further work looking at other brain regions such as the hypothalamus, which plays a crucial role in energy homeostasis, and separate cortical and subcortical regions such as the striatum, important in a variety of memory and reward pathways, may help clarify the regions of the brain most vulnerable to the loss

of *Nrf2*. Furthermore, if there is a distinct progression profile across the brain, this may help clarify the likely role of altered *Nrf2* activity under different disease conditions.

In conjunction with the changes in inflammatory markers described above, alterations in both *F4/80*, a marker found on many macrophage immune cells, and GFAP, a commonly used marker of astrocytic glial cells, were observed. Whilst *F4/80* alone cannot differentiate the type of immune cell being detected without additional tags such as cluster of differentiation molecule 11b, it is found at higher levels in mature macrophages, including brain microglia (van den Berg & Kraal, 2005). Furthermore, GFAP has previously been positively associated with astrocytic activation and is known to play a role in cellular processes important in regeneration and synaptic plasticity (Kamphuis *et al.*, 2012). We found increased expression of *F4/80* in the hippocampus and cortex of both *Nrf2*^{-/-} and *Nrf2*^{-/-}/*hAPP*_{swe} mice whilst a diet dependent increase in expression is seen in the hippocampus of *hAPP*_{swe} mice. It is very difficult to differentiate macrophage phenotype by surface marker alone. However, when taken together with the other inflammatory markers analysed, it is possible to suggest the hippocampal increases in *F4/80* are likely linked to an increase in M1 like macrophages. This is supported by attenuation of *F4/80* expression in the hippocampus of HF fed mice lacking *Nrf2*^{-/-}. In contrast, whilst the basal upregulation in *F4/80* expression may be due to M1 factors, latterly this is likely linked instead with an increase in M2:M1 ratio given the associated increased anti-inflammatory profile present in the cortex. This is further supported by the decreased expression of GFAP in all groups except in the cortex of RC fed *Nrf2*^{-/-} mice whilst no significant change in GFAP expression was seen in the hippocampus.

The increased presence of macrophages within the *Nrf2*^{-/-} and *Nrf2*^{-/-}/*hAPP*_{swe} brain is further supported by increased expression of chemoattractant proteins such as MCP-1 and RANTES. Expression of these chemokines is predominantly present in those mice fed a RC diet and is higher in the hippocampus than the cortex. Chemokines such as MCP-1 and RANTES have been shown to be released from a multitude of cells including resident immune cells such as microglia as well as both astrocytes and endothelial cells (Deshmane *et al.*, 2009). In addition, and in line with the majority of other chemokines identified to date, both MCP-1 and RANTES function in a predominantly immune driven manner. Chemokine receptors were shown to have altered expression in the hippocampus, with in particular CCR2 being elevated in *Nrf2*^{-/-} mice. Microglia, as well as astrocytes, have been shown to express key chemokine

receptors in the brain with a small number of chemokine receptors also expressed by neurons (Liu *et al.*, 2014). This enables the chemokine signalling pathways to conduct elaborate reorganisation of the cells required to resolve an insult in the CNS. Furthermore, chemokine receptors such as CCR2 and CCR5 are known to interact not only with those chemokines analysed here, but a multitude of other commonly found chemokines such as various MIP-1 isoforms, as well as further MCP variants including 2 and 3, further complicating the chemokine signalling cascade.

Using fluorescent confocal microscopy, we were able to show that *Nrf2*^{-/-}/*hAPP*_{swe} mice depicted increased astrocytic branching in both the CA3 and CA1 regions of the hippocampus, which was increased following HF feeding. In addition, astrocytes within the CA1 region of the hippocampus were shown to have aggregated following HF feeding in *Nrf2*^{-/-}/*hAPP*_{swe} mice. Unfortunately, we were unable to visualise any amyloid staining within these sections and therefore it is unclear at this stage what might be causing this spatial relocation. The staining seen in the brain sections from *Nrf2*^{-/-}/*hAPP*_{swe} mice is in contrast to that observed in *Nrf2*^{-/-} mice which show minimal alteration in cell branching when compared to controls in the CA3 region and fail to display a similar aggregation of astrocytes within the CA1 region of HF fed mice. AD has previously been linked with increased gliosis and astrocytes have been shown to congregate around not only aberrant amyloid deposits but also other forms of tissue damage such as is seen following reperfusion injury (Sofroniew, 2009).

Contrary to *F4/80*, *Iba1*, which is thought to be important in calcium homeostasis, is specifically expressed in macrophages including resident microglia, and is believed to be upregulated during activation of these immune cells (Ito *et al.*, 2001). Increased *Iba1* staining is seen in both RC and HF fed *Nrf2*^{-/-}/*hAPP*_{swe} mice along with HF fed *Nrf2*^{-/-} mice in both the CA3 and CA1 regions of the hippocampus. In addition, RC fed *Nrf2*^{-/-} mice show *Iba1* staining which appears more dominant in the CA1 than CA3 region of the hippocampus. Although this profile largely matches the expression of *F4/80* previously described it is likely that the *F4/80* expression also encompasses additional non-macrophage immune cells there to supplement the immune response. Furthermore, whilst we might expect increased activation of glial cells in *Nrf2*^{-/-} mice fed a RC diet given the increase in pro-inflammatory markers described, the lack of inflammation described in the brains of HF fed *Nrf2*^{-/-} mice is perhaps more surprising. However, as *Iba1* is not able to differentiate the different forms of macrophage activation (M1 vs M2) it is possible that following HF feeding the microglia in *Nrf2*^{-/-}

brains are predominantly driven to a more protective M2 phenotype. Further work making use of techniques such as FACS analysis may allow us to clarify if this is the case in the brain following HF feeding.

Furthermore, it would be very interesting to see if even short term HF feeding induces the same changes in microglia and astrocytes staining described here. To date, the only other group to have published work on an AD**Nrf2*^{-/-} mouse model failed to show similar changes in astrocytic and microglial staining (Joshi *et al.*, 2015). Their model consisting of a double AD mutation (*hAPP_{swe}/PSEN1ΔE9*) crossed onto an *Nrf2*^{-/-} background, whilst not challenged by additional stressors such as HF feeding as ours was, demonstrated increased protein expression of both GFAP and Iba1. However, they were unable to show any clear alteration in astrocytic branching in the triple transgenic mice, nor was there any alteration in the spatial localisation of astrocytes across the section presented. They also failed to see any changes in glial expression in their *Nrf2*^{-/-} mice, albeit only measured at 7-8 months of age. In addition, whilst they reported numerous alterations in AD related proteins, which will be expanded on below, they failed to measure any additional markers assessing inflammation. This makes it hard to compare the effects seen in our less aggressive model with those reported in this novel triple transgenic model.

Finally, whilst we have now shown that loss of *Nrf2*, both by itself and in combination with the addition of *hAPP_{swe}*, is capable of inducing an inflammatory effect in addition to inducing activation of key immune cells; we have yet to look at the impact this may have had on the neuronal population. Blotting for the synaptic marker SYP, we showed that aged RC fed *Nrf2*^{-/-} mice showed depleted levels of SYP in the hippocampus, as might be expected given the increased inflammatory presence in this tissue. Contrary to other publications (Unno *et al.*, 2009; Calvo-Ochoa *et al.*, 2014), HF feeding induced an upregulation of hippocampal SYP protein in both WT and *Nrf2*^{-/-} mice whilst mice carrying the *hAPP_{swe}* gene displayed increased levels of SYP protein irrespective of the dietary grouping. Furthermore, these affects appear to be brain region specific with no alteration in SYP in WT, *Nrf2*^{-/-} and *hAPP_{swe}* mice in the cortex and *Nrf2*^{-/-}/*hAPP_{swe}* reporting the opposite effect to that seen in the hippocampus with decreased SYP expression which is further attenuated by HF feeding. It is possible that in the *Nrf2*^{-/-} mice the increase in SYP protein observed following long term HF feeding may result from the improved inflammatory profile seen in these mice in addition to the altered metabolic profile observed. However, from blots alone it is not possible to

discern whether the change in SYP is due to changes in number of functional synapses or whether there is a build of damaged synapses inducing increased synaptic turnover. Further work is required to clarify what may be occurring in these models, although unfortunately the resolution on a standard confocal microscope is not high enough to allow clear visualisation at the synaptic level and therefore primary cultures may be of more use on this occasion.

3.14.4 High Fat Feeding Increased AD Related Proteins in the Brains of Aged Mice

There are now a small number of publications that describe the effects of HF feeding on mouse models of AD, in addition to the effects of HF feeding on AD related proteins in WT mice. Whilst we saw very limited effects of genotype and diet on gene expression levels of both mAPP and BACE, in the hippocampus both WT and *Nrf2*^{-/-} mice reported a significant induction in BACE1 protein following HF feeding. This is in agreement with previous publications demonstrating that BACE1 can be induced by cell stressors including those associated with HF feeding (Meakin *et al.*, 2012; Wang *et al.*, 2013b). It is worth noting that whilst both *hAPP*_{swe} and *Nrf2*^{-/-}/*hAPP*_{swe} mice fail to demonstrate significant increases in hippocampal BACE1, they both sit at higher basal levels of induction than their WT and *Nrf2*^{-/-} compatriots.

In contrast, total APP expression appears to be solely influenced by genotype, with no additional effects being driven by changes in diet. Both the hippocampus and the cortex of our models lacking *Nrf2* show a small increase in hippocampal APP with a concomitant decrease seen in cortical protein, whilst the addition of *hAPP*_{swe} produces elevated APP protein in both brain regions. Furthermore, alterations in *Nrf2*^{-/-}/*hAPP*_{swe} land in between their single transgenic counterparts with hippocampal APP expression remaining high whilst cortical expression is brought down to a similar level to those seen in WT mice. The cortical profile seen for APP protein levels is mimicked by BACE1 protein with both *Nrf2*^{-/-} and *Nrf2*^{-/-}/*hAPP*_{swe} mice describing decreased protein levels whilst WT and *hAPP*_{swe} mice remain constant. In addition, an ELISA assay performed to assess changes in triton-X soluble murine A β ₁₋₄₂ in cortical lysates revealed no significant difference between WT and *Nrf2*^{-/-} mice irrespective of the diet administered. Whilst more aggressive models of AD have reported aggravated amyloid pathology following HF feeding, as previously described, the lack of a prominent change in amyloid pathology in our models may play a key role in explaining the milder phenotype described in other areas such as in cognitive ability. Finally, both HF diet

and loss of *Nrf2* appear to influence mouse tau phosphorylation, with increased phosphorylation seen in both the hippocampus and cortex of mice. Prior publications have shown that along with amyloid pathology, obesity and T1D can also aggravate tau phosphorylation (Jung *et al.*, 2013). This corroborates recent research published on *Nrf2* implicating its activation in the regulation of tau phosphorylation (Jo *et al.*, 2014; Stack *et al.*, 2014).

3.14.5 HF Feeding and Other Stress Activated Proteins

3.14.5.1 NF- κ B and Glutathione Signalling

In addition to the plethora of inflammatory cytokines and other signalling molecules previously described, there exist a variety of other stress induced pathways; many of which work in harmony with the signalling molecules mentioned. One of the most commonly named pathways in relation to the inflammatory response is that of NF- κ B. Like many stress activated kinases, NF- κ B has the ability to be activated by and influence many different pathways and as such it is tightly regulated under basal conditions (Lawrence, 2009). When we analysed blots for the repressor protein I κ B α , we found protein levels were significantly decreased in *Nrf2*^{-/-} and *Nrf2*^{-/-}/*hAPP*_{swe} mice in both the hippocampus and cortex, indicating targeting of I κ B α for degradation and translocation of NF- κ B to the nucleus. The role of NF- κ B in inflammation is complex and multi-faceted. As such, it has been shown to act in both pro- and anti-inflammatory roles, distinguished by the activity of different subsets of proteins which form part of the NF- κ B cascade (Lawrence *et al.*, 2001). In the hippocampus, therefore, the activation of NF- κ B likely coincides with the previously described increase in inflammation, whilst that present in the cortex may play a more complex part, balancing out the remaining anti-inflammatory signalling. In order to clarify the role of the NF- κ B pathway with regards to *Nrf2*^{-/-} mice, further work is required to elucidate the function of other key proteins within this pathway. It has previously been shown that astrocytes lacking *Nrf2* have an increased NF- κ B response to scratch injury than WT cells (Pan *et al.*, 2012), and activation of NF- κ B is known to be induced under inflammatory conditions like those described above.

One of the many antioxidant proteins whose transcription is driven by the *Nrf2*-ARE complex, GSH plays an important role in the management and neutralisation of ROS. GCLC is one of two proteins involved in the first rate limiting step in GSH production. GCLC and other members of the antioxidant GSH pathway have previously

been suggested to be impaired by aging in their response to stress inputs (Chen *et al.*, 2010). In addition, along with downstream GSH, GCLC has previously been shown to be essential for neuronal survival which can be negatively affected by HF feeding (Diaz-Hernandez *et al.*, 2005). When we analysed expression of GCLC, however, we found no significant change in either the hippocampus or cortex of WT, *Nrf2*^{-/-} and *hAPP*_{swe}, with only a small reduction seen in the cortex of *Nrf2*^{-/-}/*hAPP*_{swe} mice. This would indicate that the production of GSH is not directly affected by HF feeding at the age tested. In order to pursue this further a GSH assay ought to be performed allowing for the measurement of the ratio oxidised to reduced GSH present in the tissue. However, the recommended tissue requirement for this assay is around 50-100 mg, which makes it prohibitive given the small amount of tissue available. Finally, whilst insulin has been suggested to have neuroprotective effects, we saw no change in Akt phosphorylation under either RC or HF fed conditions; indicating this is unlikely to be the cause of the improved inflammatory profile seen in HF fed *Nrf2*^{-/-} mice. It may, however, be of interest to pursue this further given that acute insulin treatment may provide a clearer description of the HF induced insulin signalling changes seen in *Nrf2*^{-/-} mice than those seen here under non-stimulated conditions.

3.14.5.2 MAPK Signalling: A Role for Its Dysregulation in *Nrf2*^{-/-} Mice

Stress activated kinases, as the name implies, are activated in response to a variety of different signalling molecules. One of the most well-known families is that of the MAPK proteins, whose best characterised members include isoforms of ERK, JNK and p38. Known to react to factors outside of the immune system such as insulin and osmotic stress, MAPKs have also been shown to interact with A β , with increased JNK expression shown to upregulate both BACE1 and γ -secretase activation (Tamagno *et al.*, 2009; Mazzitelli *et al.*, 2011). When analysed we found a significant increase in JNK phosphorylation compared to WT in both the *Nrf2*^{-/-} and *Nrf2*^{-/-}/*hAPP*_{swe} mice. This increase in protein phosphorylation was present in both the cortical and hippocampal tissue and contrary to many of the other inflammatory and stress markers described up till now, this increased phosphorylation ratio did not disappear following HF feeding indicating that an alternative pathway may be involved to that affecting other inflammatory markers. In contrast, despite showing a trend towards increased phosphorylation in the hippocampus, we saw no significant change in JNK phosphorylation in the *hAPP*_{swe} mice irrespective of dietary group. These changes did appear comparable to the induction in BACE1 seen in the hippocampus of these mice,

which given the supposed activating effect of JNK phosphorylation on BACE1 may be important.

Furthermore, when ERK phosphorylation was assessed we saw a trend towards increased basal phosphorylation of ERK in *Nrf2*^{-/-} and *Nrf2*^{-/-}/*hAPP*_{swe} which was greatly potentiated by HF feeding. Again, the presence of *hAPP*_{swe} alone did not significantly affect ERK phosphorylation, whilst HF feeding of WT mice even induced a reduction in hippocampal ERK phosphorylation. The known sensitivity of ERK to insulin signalling may be of importance in the accentuated signalling described in *Nrf2*^{-/-} mice. All of these facts point towards an *Nrf2* dependent alteration in MAPK phosphorylation. In addition, the discrepancy in phosphorylation of JNK and ERK proteins seen in *hAPP*_{swe} mice may be in relation to the different roles played by these two MAPK. Whilst JNK has previously been described to interact intimately with the pro-amyloidogenic pathway as described previously, activation of various ERK requiring pathways have been shown to attenuate amyloid related detrimental effects (Wang *et al.*, 2012; Zhang *et al.*, 2015).

Upon further examination, and in collaboration with Prof. S. Keyse, we found that under basal conditions mice lacking *Nrf2* have elevated MEK phosphorylation in the hippocampus. Given the amplifying nature of the MAPK cascade, even a small increase in phosphorylation can cause considerable activation of the pathway. However, no further induction of MEK phosphorylation was observed following HF feeding of *Nrf2*^{-/-} mice. This suggested additional means of mediation must be involved to induce the potentiation of MAPK phosphorylation. DUSP enzymes are the largest family of dephosphatases known to act specifically on MAPK proteins. Whilst numerous, these have been classified into different sub groups over the years depending on their cellular localisation (Caunt & Keyse, 2013). Some are constitutively active proteins found in the cytoplasm, whilst others are localised in the nucleus and are termed inducible. Further to this, characterisation work has enabled the identification of the various target MAPKs associated with different DUSPs. We concentrated on those known to interact with ERK, many of which do so specifically. Whilst we found some variance in RNA and protein levels, the predominant change observed was that of a HF diet induced loss of DUSP proteins.

Relatively little work has been published looking at the role of DUSPs in obesity and animal models lacking DUSP expression are only available for a select number of DUSPs. In addition, the data published to date gives contradictory roles for DUSPs and

their involvement in obesity depending on the individual protein studied. DUSP1 (aka MKP1) is being touted as playing an important role in glucose homeostasis with increased liver expression linked with the development of hepatic steatosis (Lawan *et al.*, 2015), whilst DUSP 6 (aka MKP3) has been suggested to play a role in the induction of hyperglycaemia following high fat feeding by increasing hepatic glucose output (Feng *et al.*, 2014). Furthermore, Feng and colleagues found that *DUSP6*^{-/-} mice have attenuated weight gain and altered liver triglyceride content. In addition, overexpression of the nuclear DUSP9 (aka MKP4) has been suggested to be protective against DIO, improving the glucose tolerance and homeostasis in *ob/ob* mice (Emanuelli *et al.*, 2008). Although complex, these findings do in part link in with the phenotype of our model. We saw an increase in DUSP1 in the hippocampus following long-term HF feeding of *Nrf2*^{-/-} mice which may be indicative of their altered insulin sensitivity, although it would be worth pursuing this further in the livers of *Nrf2*^{-/-} mice given their predisposition towards the development of NASH following HF feeding. Furthermore, we saw no change in the expression of DUSP6, which may be surprising given the similar body phenotype described by both *DUSP6*^{-/-} and *Nrf2*^{-/-}. However, these models appear to have opposing actions on triglyceride content indicating they probably function through different mechanisms of action. Finally, we saw diet dependent decreases in DUSP9, which complements its proposed action under WT conditions as decreased DUSP9 may contribute towards impairments in glucose homeostasis. However, we might have expected an increase in expression in the *Nrf2*^{-/-} mice fed a HF diet given their phenotype. This suggests that DUSP9 may not be causative in the improved insulin signalling seen in the *Nrf2*^{-/-} mice although further work will need to be undertaken on key peripheral tissues such as the liver to confirm this. To summarise, therefore, this indicates that *Nrf2*^{-/-} mice have constitutively increased activation of the MAPK pathway, as demonstrated by increased MEK phosphorylation, which when fed a HF diet is combined with a diet dependent decrease in DUSP expression. This contrasts with WT mice which undergo a diet dependent decrease in DUSPs but also have decreased MEK phosphorylation following HF feeding.

3.14.6 Mitochondrial Impairment Following Loss of *Nrf2*

Mitochondria are the powerhouses of the cell; however, as such they are also known to naturally release ROS making them more vulnerable to alterations in the antioxidant capacity of the cell. It has previously been shown that *Nrf2* activation can

attenuate mitochondrial impairment *in vitro* (Miller *et al.*, 2013), whilst there have been links suggested between *Nrf2* loss, mitochondrial impairment and AD (Greco & Fiskum, 2010). When we assessed the effect of *Nrf2* loss on mitochondrial health we found no basal alteration in either the channel protein VDAC1 or the COX IV protein from the electron transport chain. However, both of these were diminished following HF feeding, with *Nrf2*^{-/-} mice showing further impairment when compared to WT mice in the cortex but not the hippocampus where HF feeding has less impact than in the WT cohort. WAT from insulin resistant and HF fed rodents had previously been shown to contain decreased levels of mitochondrial proteins, such as COX IV (Valerio *et al.*, 2006; Sutherland *et al.*, 2008). In contrast, AD has been linked with increasing levels of VDAC1 in the brain further to which it has been suggested that A β and tau may both interact with VDAC1, potentially blocking the mitochondrial pores and driving the rise in VDAC1 expression (Manczak & Reddy, 2012). Furthermore, through its regulation of calcium, VDAC1 is able to regulate the TCA cycle and subsequent ROS production. Given the lack of A β build-up in our model and a potentially attenuating effect from HF feeding, the additional impairment seen in *Nrf2*^{-/-} mice may be as a result of increased ROS production. A slew of recent research in the field of *Nrf2* further supports an important interaction of the *Nrf2* pathway with mitochondrial health and protection (Dinkova-Kostova & Abramov, 2015; Itoh *et al.*, 2015).

Further to these changes, when key fusion proteins mitofusin 1 and 2 were analysed diet dependent increases were seen in the hippocampus of both WT and *Nrf2*^{-/-} mice. However in the cortex *Nrf2*^{-/-} mice have depleted mitofusin 2 expression, which is recovered following HF feeding. Decreased expression of mitofusin proteins has been associated with increased targeting of mitochondria for degradation via mitophagy (Pallanck, 2013). It will be important to pursue this further by assessing key fission proteins, as it is the disconnect between mitochondrial fission and fusion which can prove key in mitochondrial dysfunction. Furthermore, the surge in research supporting an important role for *Nrf2* in mitochondria has also highlighted other organelles prone to targeting by ROS such as the ER. This is maybe even more important in the context of our research given the importance of the ER in lipid metabolism and its increased dysfunction in mice lacking *Nrf2*, but also its influential role in amyloid processing (Pinho *et al.*, 2014).

3.14.7 Conclusions

We have presented here a novel mouse model designed from the outset to try and model an early disease environment of AD. This was done by combining the loss of ROS regulating transcription factor *Nrf2*, which is known to decrease with ageing, with a mild model of FAD containing *hAPP_{swe}* mutation under the mouse *APP* promoter. Although we found some small changes in cognition, the main effects observed through our research indicated a dominant role for the loss of *Nrf2* in defining the responses observed through the double transgenic model. Of interest in the double transgenic model, clear changes in glial cell responses were observed and it would be interesting to pursue this further given the roles suggested for gliosis in AD. Indeed, as demonstrated by Joshi *et al.* (2015), use of a more aggressive AD mouse model may help to elucidate the mechanism occurring behind these changes and help in understanding the interaction occurring between *Nrf2* and the amyloidogenic pathway. In addition, with the mild phenotype of the *hAPP_{swe}* model used and the protective effect HF feeding was found to have in the brains of *Nrf2^{-/-}* mouse brains, our model failed to show the aggravated inflammatory profile that had initially been hypothesized. In light of this, challenging these mice along with the single transgenic *Nrf2^{-/-}* mice with a calorie deficient diet as opposed to a diet containing a calorie surplus may be of even greater interest. This may be even more relevant now, in view of the recent controversial Lancet publication by Quizilbash *et al.* (2015) suggesting that the lower a person's BMI, the greater their risk of developing dementia.

In an attempt to understand the effects of HF feeding on the mouse brain following loss of *Nrf2*, we followed up with further work on this single transgenic model. We were able to show that despite long-term HF feeding, *Nrf2^{-/-}* mice maintain a degree of insulin sensitivity and further we hypothesize this may play a role in the protective effects seen in mice fed a HF diet as demonstrated by dampening of inflammatory markers. Furthermore, these mice displayed altered activity when examined at a young age which slowly diminished over time, advocating further investigation into *Nrf2* loss in an aged mouse model. With no increase in amyloid pathology but changes in tau phosphorylation, research may be better focussed on the role played by attenuated *Nrf2* expression on the development of dysfunctional tau aggregates. The increased presence of ROS, and as we have shown here, altered mitochondrial function may play a role in the induction of disturbed tau processing. Whilst it will be important to also assess whether there are alterations in ER stress given

the links previously reported between amyloid, ER stress and mitochondrial dysfunction.

Finally, we described important alterations in the regulation of MAPK pathways in *Nrf2*^{-/-} mice (see Figure 3.28 for simplified pictorial summary). These were further affected by HF feeding, and given the ability of insulin as well as ROS to interact with the MAPK cascade it would be interesting to pursue this further. MAPK proteins have previously been reported to have both pro- and anti-inflammatory effects. Given the context in which the changes described here are occurring it is possible that maintained MAPK, and more specifically ERK activation, is playing a role in inflammatory resolution and tissue protection. It has previously been shown that proteins such as Ghrelin, the so-called ‘hunger hormone’, activate the ERK signalling pathway resulting in protection of cells such as oligodendrocytes within the CNS (Lee *et al.*, 2011). Furthermore, ERK has also been reported to promote hippocampal neuron survival in a model of excitotoxicity, which itself has been linked with AD and other neurodegenerative diseases such as PD (Ortuño-Sahagún *et al.*, 2014). The attenuated weight gain in *Nrf2*^{-/-} mice would also support a role for this type of signalling pathway. A key step in clarifying what may be occurring in the brain would be to assess the MAPK pathways within the liver, which is known to be highly affected by HF feeding. If the changes presented here are limited to tissues that appear protected by HF feeding in *Nrf2*^{-/-} mice it may advocate a role for this pathway in the differential treatment of tissues lacking *Nrf2* following HF feeding.

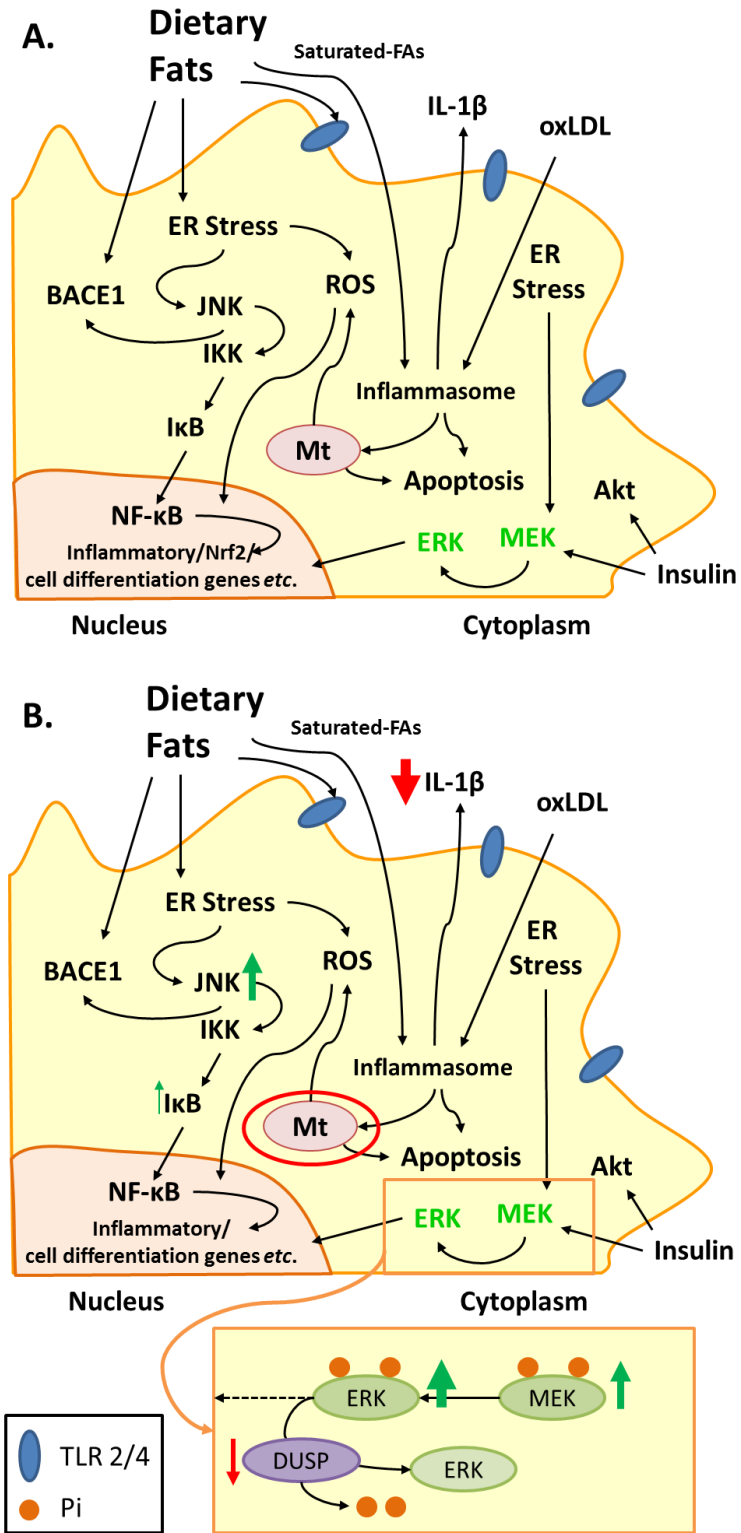


Figure 3.28 Simplified pictorial summary of some of the main long-term HF diet-driven alterations described in the brains of WT (A) and *Nrf2*^{-/-} (B) mice

Where FA = fatty acids, oxLDL = oxidised low-density lipoprotein, Mt = mitochondria and Pi = phosphate.

4 THE ROLE OF NRF2 IN INFECTION-INDUCED INFLAMMATION

4.1 INTRODUCTION

AD, like many neurodegenerative disorders, is a complex combination of elements, only a small percentage of which are currently known to be linked directly with genetic risk factors. A role for neuroinflammation, not only in AD but also in other neurodegenerative diseases, such as PD and ALS to name but a few, has grown in popularity over the last decade (Miklossy *et al.*, 2006; DeLegge & Smoke, 2008; Dibaj *et al.*, 2011; Ferretti *et al.*, 2012). The origins of this inflammation, however, are unclear; as is its place in the disease development timeline. It has been suggested that it may form part of the earlier stages of neurodegenerative development, but no conclusive results have yet been able to tie down its role as being causative or consequential. Inflammation is a key component of the pathological lesions associated with AD and these lesions are often associated with conglomerations of reactive astrocyte and microglial cells. Acutely, activation of the immune system and the initiation of an inflammatory related response in early AD are likely to be of a beneficial nature.

The role of immunological activation is two-fold; to remove cellular debris and necrotised tissue, and to tackle the causative elements behind the damage. This is supported by the ability of protective cells activated by an immune response, such as microglia and astrocytes, to degrade and clear proteins whose dysregulation is associated with AD pathology, such as amyloid (Weldon *et al.*, 1998; Wyss-Coray *et al.*, 2003; Shimizu *et al.*, 2008; Nielsen *et al.*, 2010; Farfara *et al.*, 2011; Pihlaja *et al.*, 2011). However, long-term chronic inflammation is thought to be the dark side of the inflammatory response. Development of chronic inflammation, such as occurs in obesity, as a result of increased markers of infection (e.g. LPS) or as a natural development of ageing, is believed to provide a priming environment for AD development and exacerbate disease progression (Blasko *et al.*, 2000; Mehlhorn *et al.*, 2000; Blasko *et al.*, 2004; Sokolova *et al.*, 2009; Fuller *et al.*, 2010). Scientists have also postulated that the chronic neuroinflammation found associated with neurodegeneration may be factorial in the development of synaptic dysfunction and subsequent cell degeneration (Hauss-Wegrzyniak *et al.*, 2002). Certainly, synaptic dysfunction or loss has shown a high degree of correlation, accurately matching symptomatological disease progression (Shankar & Walsh, 2009). In addition, targeting of immune markers has shown improvement in other associated pathologies of AD such as A β build up and tau phosphorylation (Kitazawa *et al.*, 2011).

Greater understanding of the functions undertaken by cells such as astrocytes and microglia, and how this is altered in relation to ageing, has raised their profile with regards to a potential role for their dysfunction in disease. It has been suggested that microglia, in their role as brain resident macrophages, may undergo a so called 'priming' process. A degree of cell priming is believed to occur as a direct result of ageing. This is supported by age related alterations in response to cellular insults, but it may be further enhanced by other stimuli such as chronic inflammation described previously (Tateda *et al.*, 1996; Kohman *et al.*, 2007; Cunningham *et al.*, 2009; Murray *et al.*, 2012). Largely considered to be pro-inflammatory in basis, priming is not thought to have a significant impact on the basal release of signalling molecules from cells. Cells would therefore appear indistinguishable from non-primed cells under basal conditions. However, upon reaction to insult the response initiated by primed microglia is in acute excess of their non-primed counterparts, inducing an exponential increase in inflammatory response (Cunningham *et al.*, 2005; Cunningham *et al.*, 2009; Henry *et al.*, 2009; Wynne *et al.*, 2009). This could make even minor central challenges into largescale inflammatory events, which long-term could contribute to the accumulation of toxic species and malformed proteins, as well as negatively impacting the clearance mechanisms normally put in place to deal with these events.

LPS, normally found on the outer membrane of gram-negative bacteria, has previously been used acutely in the exploration of sepsis, but also in the manipulation of macrophage responses, including microglia. LPS is frequently used *in vitro* in the induction of macrophage maturation from a basal M0 state to an M1 pro-inflammatory phenotype and an increased LPS presence has been associated with increased obesity and development of metabolic disorders as was alluded to previously (Cani *et al.*, 2007; de La Serre *et al.*, 2010). The role of systemic infection, and in particular LPS, with regards to obesity has evolved over recent years beyond a simple correlation between levels of LPS and weight gain. Indeed, some recent research has suggested a role for LPS in altering insulin signalling and more specifically the development and maintenance of insulin resistance. Animal studies performed by Fei and Zhao (2013) have demonstrated that treatment of germfree mice with bacteria from obese individuals can lead to the development of obesity and insulin resistance. Whilst low grade endotoxemia has been associated with the development of obesity and insulin resistance along with alterations in gut permeability, in particular to lipid soluble molecules such as LPS (Cani *et al.*, 2007; de La Serre *et al.*, 2010). Furthermore, exercise has been

shown to reduce both circulating LPS and activation of its immune receptor TLR4 in DIO rats, whilst concomitantly improving insulin signalling (Oliveira *et al.*, 2011).

Diseases such as obesity, T1DM and metabolic syndrome have long been associated with an increased risk of AD development in old age. Taken alongside the described link between increased systemic infection and development of these disorders including recent studies on clinical cohorts (Lassenius *et al.*, 2011; Pussinen *et al.*, 2011); a logical progression was to investigate the potential role of infection in age-related alterations and neurodegenerative conditions. Indeed, it has been previously described that an increased prevalence of systemic infection is found in the elderly, which is further compounded in patients presenting with neurodegenerative conditions (Holmes *et al.*, 2003; Roubaud-Baudron *et al.*, 2012). Research performed using animal models has implicated chronic inflammation and systemic infection as potentially important players in the development of AD (Sly *et al.*, 2001; Sy *et al.*, 2011; Krstic *et al.*, 2012). Systemic infections, even under short-term conditions, have been shown to exacerbate AD related symptoms including negatively impacting cognition (Erickson *et al.*, 2012; Zhang *et al.*, 2013). Furthermore, the apparent protective effect of long term treatment of other inflammatory diseases such as rheumatoid arthritis have prompted investigations into the use of anti-inflammatory agents for the treatment of AD (McGeer *et al.*, 1996).

Nrf2 is known to play an important role in clearing ROS and preventing a build-up of related cellular damage through activation of the ARE. Subsequent to this role, Nrf2 can also be induced following activation of the immune system and induction of its plethora of signalling molecules. Research has demonstrated a protective role for Nrf2 *in vitro* in the suppression of inflammation-related damage such as is induced through infectious agents like LPS (Wang *et al.*, 2010; Khodagholi & Tusi, 2011; Koh *et al.*, 2011). Furthermore, studies using a rodent model of uveitis have shown that activation of the Nrf2 pathway can reduce the inflammatory response with an altered immune response profile observed in *Nrf2*^{-/-} transgenic mice (Nagai *et al.*, 2009). Finally, Innamorato and colleagues (2008) demonstrated a role for Nrf2 as a potential therapeutic target against brain inflammation. Using an LPS driven acute inflammatory model and *Nrf2*^{-/-} transgenic mice, they showed that *Nrf2*^{-/-} mice had an increased susceptibility to LPS-driven inflammation. Activation of Nrf2 with sulforaphane, which has been shown to cross the BBB, was able to effectively counteract the ROS changes induced by LPS.

In light of the links suggested between AD and systemic infection, such as through LPS, it was decided to further investigate the impact of short-term chronic infection on an antioxidant compromised background. This study was put in place to try and tease out links that may be present between a pro-oxidant environment and systemic inflammation with regards to changes within the brain. However, LPS itself when injected peripherally does not cross the BBB unless impairment of said barrier has occurred. Instead, researchers have suggested that it may exert central immune effects *via* alternative indirect mechanisms (Banks & Robinson, 2010; Mallard, 2012). In light of this, the decision was made to administer LPS through IP injection to maintain a more physiological mechanistic response than would occur through direct ICV injection. Following on from repeated IP LPS injections, behavioural tasks were performed to assess any alterations in cognitive ability. Key factors related to the immune response and AD were also assessed through gene and protein expression in the brain regions most commonly associated with AD, namely the hippocampus and the cortex.

In an attempt to model some of the many facets of AD, a variety of different behavioural tasks have been designed over the decades. Each task attempts to replicate a cognitive facet of AD, which can include examples such as recognition, working and episodic memory. Commonly used behavioural tasks in the study of AD include those such as the Morris water maze (MWM), Barnes maze, T-maze/Y-Maze alternation, NOR and fear conditioning tasks (Puzzo *et al.*, 2014; Webster *et al.*, 2014). The type of learning and memory being assessed will also dictate the brain region required for correct encoding of the task in use. Models, such as NOR in its most basic form, rely on recognition memory which is now believed to require correct functioning of the perirhinal cortex and dentate gyrus with less importance placed on a role for the hippocampus (Langston *et al.*, 2010; Aggleton *et al.*, 2012; Olarte-Sanchez *et al.*, 2014). In contrast, tasks such as the frequently reported Morris water maze and radial arm maze, both of which are more complex in nature, rely on a combination of working and reference memory. Moreover, episodic memory, which is one of the first forms of memory to be affected in AD, is one of the less explored in the context of rodent models of AD. Episodic memory is also one of the more challenging types of memory to model due to its complexity. However, variations on the NOR task, often referred to as the what-where-which model, use the integration of contextual and spatial location information alongside recognition memory (Eacott & Easton, 2010).

The main aim of this study was to assess the effects of a short-term repeated systemic low dose LPS exposure on the brains of mice with an inflammatory and OS primed brain environment in the presence or absence of a pro-amyloidogenic human mutation. The main hypotheses based on the information available at the commencement of this study were as follows:

- 1) Repeated peripheral administration of LPS to mice will result in an aggravated inflammatory state within the central tissue, similar to that seen in previous studies. This will be further aggravated by the loss of Nrf2 and the use of aged adult animals which will impact on the ability of the immune system to respond, mimicking the increased vulnerability of AD patients to infection.
- 2) Loss of Nrf2 when targeted with a commonly used marker and inducer of infection leading to systemic inflammation will negatively impact on cognition.
- 3) Loss of Nrf2 when combined with a pro-amyloidogenic APP mutation (*hAPP_{swe}*) and under the increased inflammatory conditions induced by repeated peripheral LPS will accelerate the development of amyloid related pathology such as has previously been described in other models of AD.

In order to try and confirm or disprove these hypotheses, mice from the previously described genotypes (WT, *Nrf2*^{-/-}, *Nrf2*^{-/-}/*hAPP_{swe}*) were used. The main output measures for this study were an assessment of cognitive competence through the use of three different cognitive tasks, namely the entorhinal cortex-dependent OL task, the perirhinal cortex-dependent NOR task, and the continuous non-cued elevated plus maze model of SA. This was combined with an evaluation of AD related pathology advancement through protein and RNA assessment of specific AD-related proteins, and an evaluation of the central inflammatory and OS levels through the measurement of commonly associated cytokines, proteins and support cells at either an RNA or protein level.

In order to achieve this, adult mice (\pm 1 year) fed a RC diet were handled daily for a minimum of two weeks prior to being randomly allocated to either the vehicle or LPS group (see Chapter 2.3.2 for full group numbers and gender breakdown). Mice were weighed daily in the week prior to and the week of the study, with animals given access to softened food once the course of injections were started. Mice were injected daily starting on day 0 between the hours of 9 and 10 in the morning, for seven days

(see Chapter 2.3.2.1). On days 0-2 no additional activities were done with the mice, and these were left to recover. On day 3, mice were habituated to the box environment required for both the OL and NOR tasks, first in their cage groups then individually (see Chapter 2.3.2.2.1). On day 4, mice were again habituated to the box environment individually, with day 5 allocated for the behavioural assessment of OL (see Chapter 2.3.2.2.2). On day 6 mice underwent NOR assessment (see Chapter 0), with assessment of SA happening on the morning of day 7 (see Chapter 2.3.2.2.4) followed by termination and tissue harvest and processing for biochemistry (see Chapters 2.4.1.1, 2.4.2-2.4.6). For a pictorial representation of the study plan please refer to **Figure 2.4**, chapter 2.3.2. It is important to note that as a result of the genotyping problems that occurred (see Chapter 2.2.5.2), a limited number of mice within the required age bracket were available from the *Nrf2*^{-/-}/*hAPP*_{swe} genotype. As a result, these were deemed too small to include in the behaviour analysis as the small number available may not accurately represent the phenotype, whilst also preventing an even gender allocation. The limited number of animals within the two *Nrf2*^{-/-}/*hAPP*_{swe} groups means any biochemical output should also be interpreted with a degree of caution especially where there is a high degree of variance between animals.

4.2 REPEATED IP LPS INDUCES WEIGHT LOSS IN AGED ADULT MICE

Prior publications have shown that administration of LPS in rodents can have an age dependent effect with older animals proving more susceptible to infection (Tateda *et al.*, 1996; Kohman *et al.*, 2007; Tarr *et al.*, 2011). Aged adult mice (1 year) were used for the purposes of this study in order to better mimic the effects of inflammatory interferences, such as LPS, on an ageing environment. Mice were administered a daily set dose and volume of LPS (2.5 µg in saline) or an equivalent volume of saline vehicle. Research has previously shown an effect of LPS on weight maintenance and mobility, with animals displaying sickness behaviour following acute injection (Bluthé *et al.*, 1999; O'Connor *et al.*, 2008; Bay-Richter *et al.*, 2011). Given the often acute nature of these symptoms, mice were injected daily for seven days and behavioural testing was not performed until day five to bypass the acute sickness and weight loss response. In order to assess the severity of the effect of LPS on the different transgenic mouse lines, weight was recorded daily.

No significant difference was seen in overall weight at the commencement of the study, either between genotypes ($p > 0.05$; Figure 4.1 A) or between treatment groups ($p > 0.05$; Figure 4.1 B). However, when measuring weight change over the duration of the

study, a main overall effect of LPS treatment was observed for all groups, with LPS inducing weight loss (WT saline vs WT LPS $p < 0.001$, *Nrf2*^{-/-} saline vs *Nrf2*^{-/-} LPS $p < 0.001$, *Nrf2*^{-/-}/*hAPP*_{swe} saline vs *Nrf2*^{-/-}/*hAPP*_{swe} LPS $p < 0.05$; $n = 3-14$; Figure 4.1 C, D and E respectively). This effect was observed as early as 24h post initial IP LPS injection. In contrast, there was no main effect of genotype on the rate of weight loss over time in response to LPS injection. By day three, all LPS-treated mice were showing indications of weight gain and/or weight stabilisation, demonstrating the presence of an initial acute phase response to IP LPS at the dosage used. As a result, all behavioural testing was performed in the later phase of the study to minimise the effect of this acute response on the ability of mice to complete the tasks required.

4.3 KNOCKING OUT NRF2 IMPAIRS SHORT TERM SPATIAL LOCATION MEMORY IN MICE AS SHOWN BY OBJECT LOCATION

Total time spent exploring during the sampling phase was measured for three main reasons: 1) to exclude animals that spent insufficient time exploring the objects as these animals may therefore still consider the ‘known object’ as novel in the test phase, 2) to investigate whether there was a genotype-dependent effect on exploration, and 3) to assess whether LPS treatment was negatively impacting overall mobility and therefore biasing the cognitive outputs garnered from the behavioural tests. In addition, any preferences in box location (i.e. left or right) could also be assessed, although box side preferences are controlled for by alternating the placement of the novel object during the test phase as detailed previously (see Chapter 2.3.2.2.2).

No significant effect of genotype or treatment was observed on total exploration time during the sample phase ($p > 0.05$; Figure 4.2 A). Ensuring mice are exploring objects to a similar degree lends confidence to the results obtained during the test phase as differential sample exploration could skew the novelty appreciation of the mouse undergoing the test. In order to investigate any effect of object bias, preference indices (PI1 and PI2) were calculated using the equation described in Figure 4.2 B. There was no significant change in exploration between objects ($p > 0.05$; Figure 4.2 C and D (PI1 and PI2 respectively)). Nevertheless, the localisation and choice of the novel object during the subsequent test phase was routinely alternated to further reduce the potential for any introduced bias in the test phase of the task. Finally, there was no significant difference in total body weight between groups on the day of behavioural testing ($p > 0.05$; Figure 4.2 E).

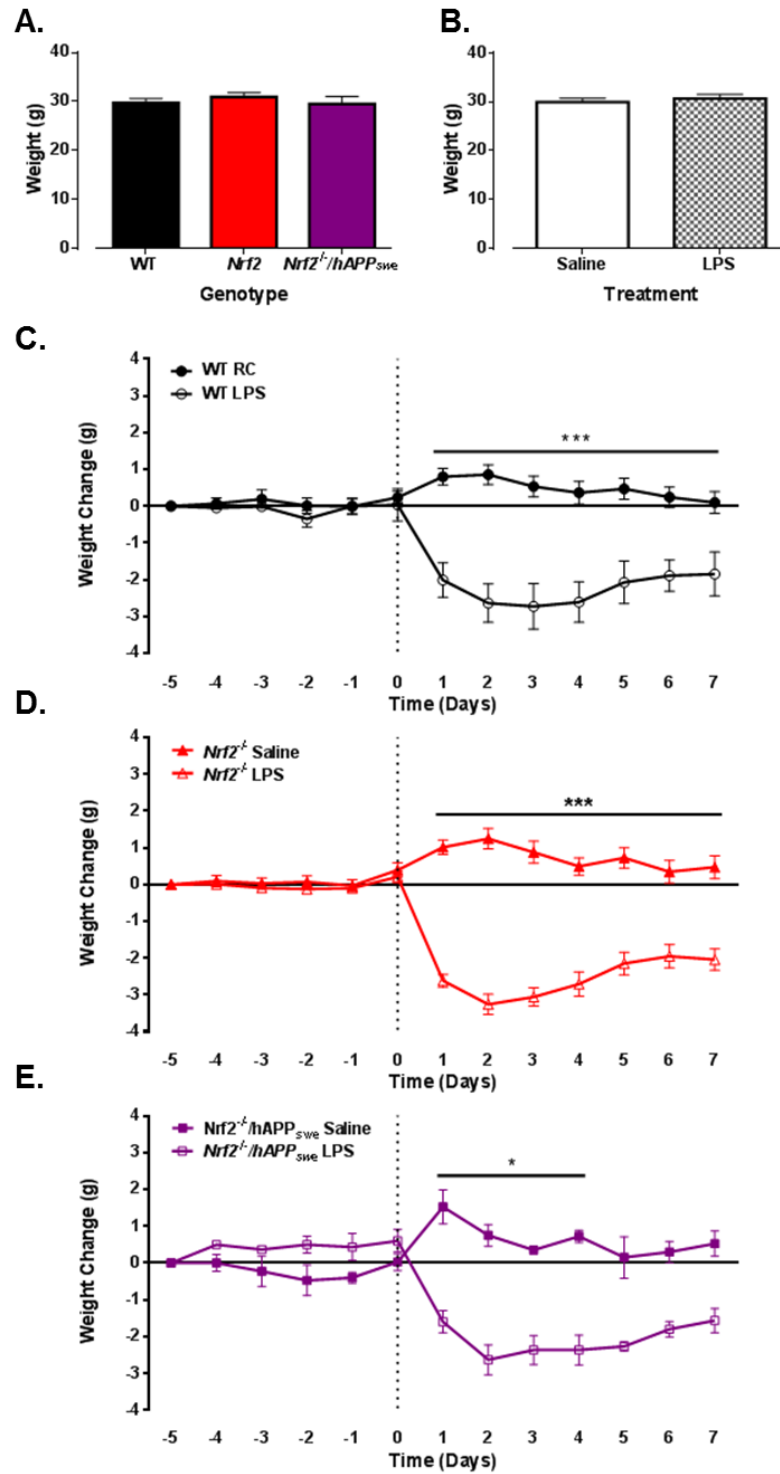


Figure 4.1 Repeated IP LPS induces acute weight loss in aged adult mice irrespective of genotype.

Age matched adult mice from WT, *Nrf2*^{-/-} and *Nrf2*^{-/-}/*hAPP*_{swe} mice were handled for 2 weeks prior to commencing the study. Mice were given 2.5 µg of LPS IP daily for 7 days or a saline vehicle equivalent. Mice were weighed daily from 5 days prior to the initial injection. Net body weight displayed by genotype (A) or treatment (B) is described for day -5. Subsequent graphs depict weight change after treatment for each of the three genotype groups, namely WT (C), *Nrf2*^{-/-} (D) and *Nrf2*^{-/-}/*hAPP*_{swe} (E). All results depicted as means ± s.e.m. Data analysed by ANOVA, Student's t-test or repeated measures ANOVA as appropriate with * p < 0.05, *** p < 0.001. WT n = 11-14; *Nrf2*^{-/-} n = 12-13; *Nrf2*^{-/-}/*hAPP*_{swe} n = 3-4.

Total exploration time was measured during the test phase to ascertain whether the introduction of novelty to the paradigm affected each cohort's tendency for exploration. Exploration of objects during the test phase was comparable to that seen during the sample phase, with no significant differences seen between groups in object exploration ($p > 0.05$; Figure 4.3 A).

Two of the main measurements reported for the analysis of both the OL and NOR task are the discrimination (D3) and recognition indices (RI). The D3 allows for discrimination between the novel and familiar objects in use (see Figure 4.3 C for equation). Values for the D3 are expressed between 1 and -1; values closer to one indicate increased exploration of novelty whereas values closer to -1 indicate an increased exploration of the familiar. The RI is thought to be the main index of retention (Antunes & Biala, 2012) and is usually reported as a percentage; the higher the percentage the greater the exploration of the novel object (see Figure 4.3 E for equation). As these indices can provide slightly different interpretations of the data, both were reported for the purposes of these studies.

After 10 min, a main effect of treatment is observed on D3 ($F_{1, 43} = 18.298$, $p < 0.0001$, $n = 11-12$; Figure 4.3 B) and RI ($F_{1, 43} = 18.314$, $p < 0.0001$, $n = 11-12$; Figure 4.3 D) scores, with LPS impairing the ability of mice to perform the task. A main effect of genotype is also observed that borders on significant for both the D3 ($F_{1, 43} = 4.074$, $p = 0.05$, $n = 11-12$) and RI ($F_{1, 43} = 4.085$, $p = 0.05$, $n = 11-12$) results. However, both of these main effects are superseded by the significant interaction observed between genotype*treatment for both D3 ($F_{1, 43} = 5.162$, $p < 0.05$, $n = 11-12$) and RI ($F_{1, 43} = 5.181$, $p < 0.05$, $n = 11-12$) indices. Further analysis, using simple main effects, shows that loss of Nrf2 alone significantly impairs the ability of mice to perform the task when compared to saline-injected WT mice as measured by both D3 (WT saline: 0.214 A.U. \pm 0.03; *Nrf2*^{-/-} saline: 0.050 A.U. \pm 0.04; WT saline vs *Nrf2*^{-/-} Saline $p < 0.01$, $n = 11-12$) and RI (WT saline: 60.70 % \pm 1.4; *Nrf2*^{-/-} saline: 52.52 % \pm 1.7; WT saline vs *Nrf2*^{-/-} saline $p < 0.01$, $n = 11-12$) indices. No significant further decrease in competency is seen in *Nrf2*^{-/-} mice following repeated LPS administration.

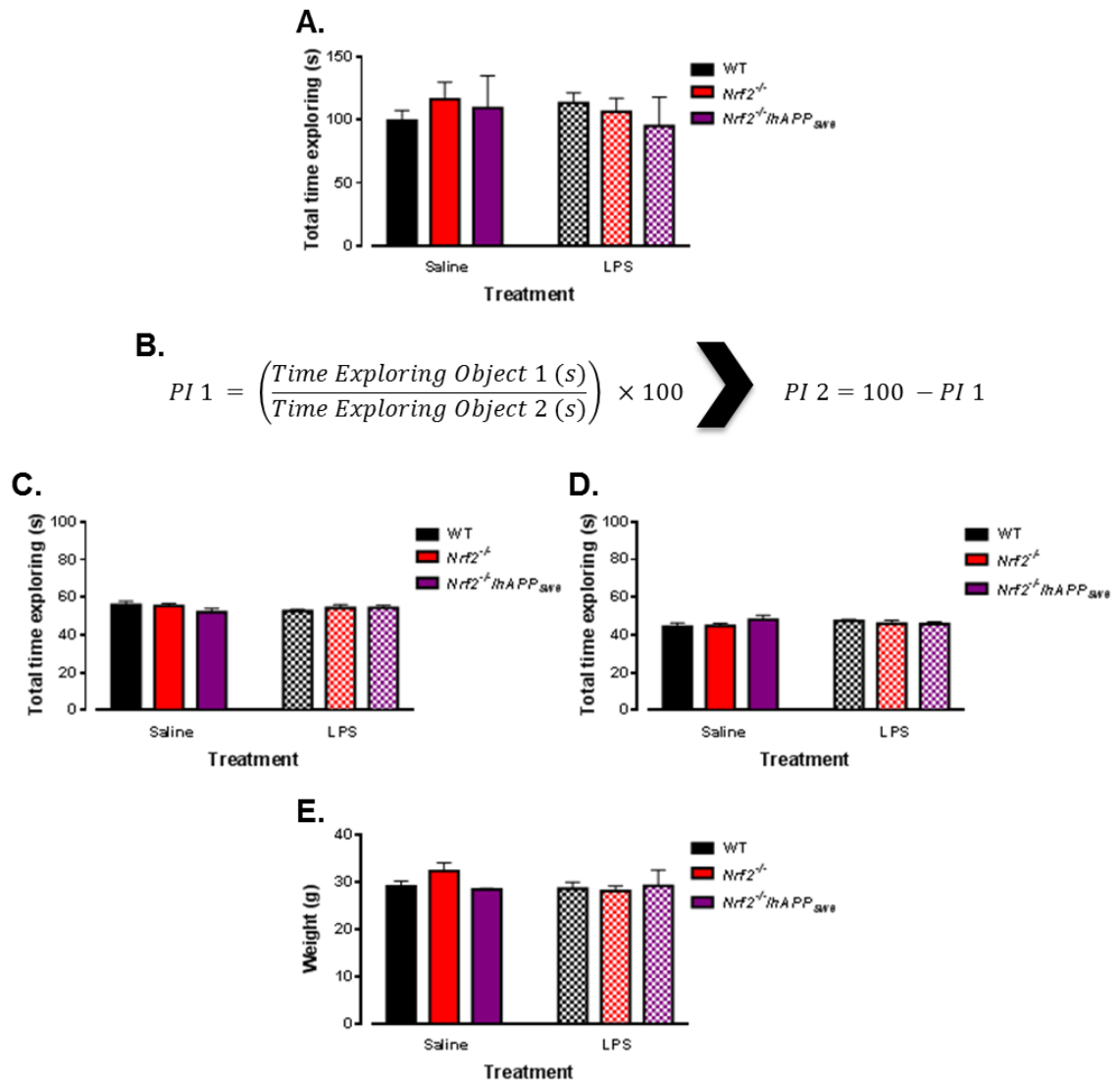


Figure 4.2 Neither genotype nor treatment affect exploration or object preference during the sample phase of the OL task.

Age-matched adult mice were handled for two weeks prior to the starting the study. Mice were given daily IP injections of either 2.5 μ g LPS or equivalent volume of saline for seven days. On day 5 post initial injection, mice were put through a short term OL task. Measures taken during the sample phase included total exploration time (**A**), preference indices for objects (**C** + **D**) calculated using the equation described in (**B**) and body weight on day of behaviour (**E**). All data is presented as means \pm s.e.m. and analysed by ANOVA or MANOVA as appropriate. (WT: n = 8-12; *Nrf2*^{-/-}: n = 9-12, *Nrf2*^{-/-}/*hAPP*_{Swe}: n = 3). Due to low mouse numbers *Nrf2*^{-/-}/*hAPP*_{Swe} mice were not included in behaviour statistical analysis.

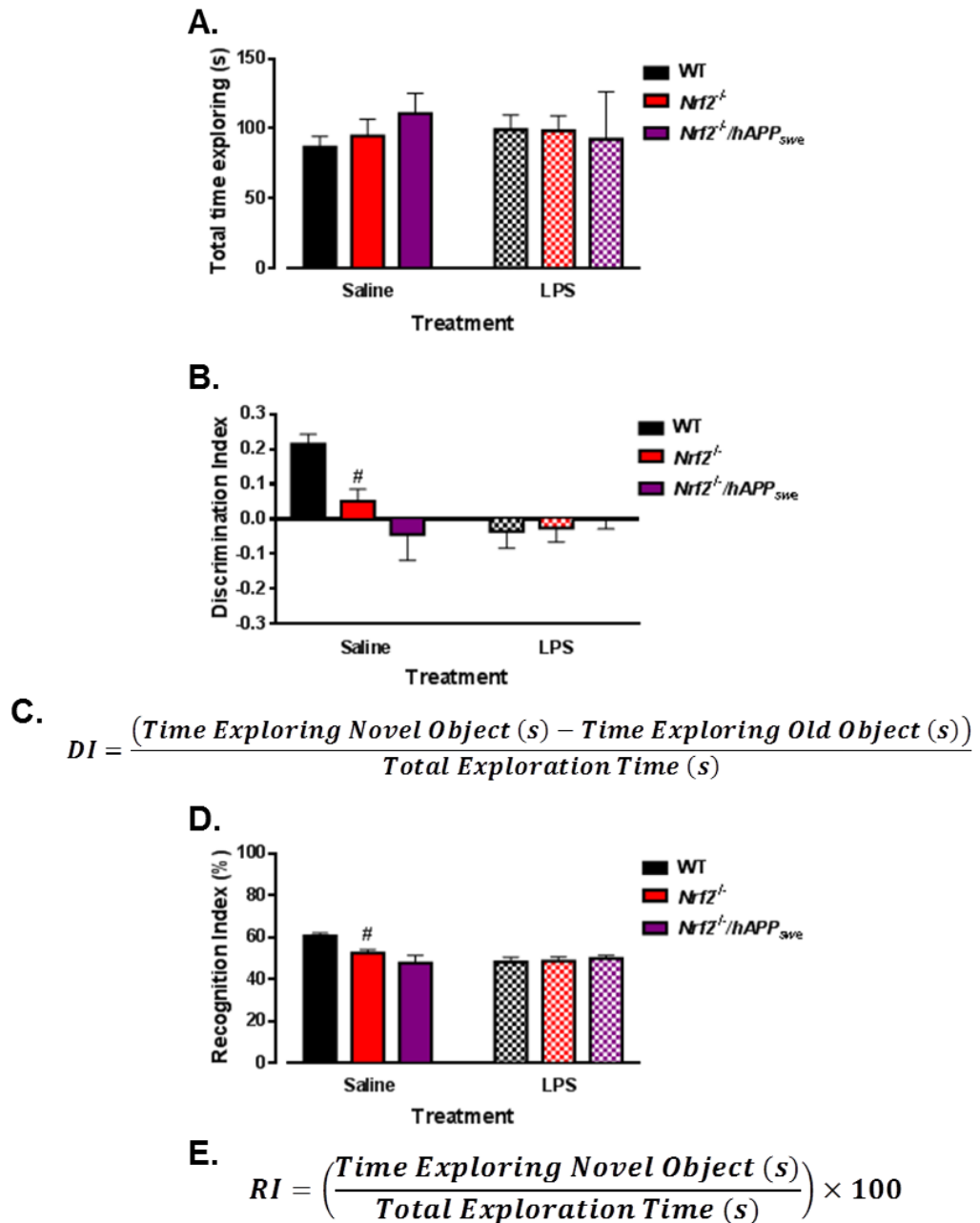


Figure 4.3 Both repeated LPS administration and loss of *Nrf2* inhibit the ability of mice to perform a short term OL task.

Adult mice previously habituated to the behaviour environment were given daily IP injections of either 2.5 µg LPS or equivalent volume of saline for seven days. On day 5 post initial injection, mice were put through a short term OL task (10 min holding time). Measures taken during the test phase included total object exploration time (A), Discrimination indices (B) calculated using the equation described in (C) and Recognition indices (D) calculated using the equation described in (E). All data is presented as means ± s.e.m. and analysed by ANOVA or MANOVA as appropriate. When positive interaction effects were reported, these replaced main effects on graphical representations of data, and were followed up through analysis of simple main effects with post-hoc Bonferroni. # denotes a treatment*genotype interaction effect, # *p* < 0.05. (WT: *n* = 11-12; *Nrf2*^{-/-}: *n* = 12, *Nrf2*^{-/-}/*hAPP*_{swe}: *n* = 3). Due to low mouse numbers *Nrf2*^{-/-}/*hAPP*_{swe} mice were not included in behaviour statistical analysis.

4.4 LOW DOSE IP LPS SIGNIFICANTLY IMPAIRS THE ABILITY OF MICE TO PERFORM SHORT TERM NOVEL OBJECT RECOGNITION

No significant effect of genotype or treatment was observed on total exploration time during the sample phase ($p > 0.05$; Figure 4.4 A). In order to investigate any effect of object localisation, bias preference indices (PI1 and PI2) were calculated. A small but significant main effect of treatment was observed on PI ($F_{1, 41} = 4.225$; $p < 0.05$, $n = 11-12$). A mild preference for objects placed in the top right corner of the box following LPS treatment was observed as shown by the left (Figure 4.4 B) and right (Figure 4.4 C) PI results. To counteract this localisation effect, routine alternation of the localisation of the novel object during the subsequent test phase was performed across groups. As for the OL task, mice were weighed on the day of behaviour. No significant change in body weight was observed between groups ($p > 0.05$; Figure 4.4 D).

During the test phase, total exploration time was again measured with no significant change in exploration observed between groups ($p > 0.05$; Figure 4.5 A). NOR evaluation is commonly assessed using the same tools as for the previously described OL task. As a result, both D3 and RI indices were calculated for the short-term NOR task. When analysed, a main effect of treatment is seen for both the D3 ($F_{1, 44} = 8.672$, $p < 0.01$, $n = 11-13$; Figure 4.5 B) and RI ($F_{1, 44} = 8.697$, $p < 0.01$, $n = 11-13$; Figure 4.5 C) indices. Following LPS treatment, the ability of WT and *Nrf2*^{-/-} mice to perform the NOR task is inhibited in a treatment-dependent manner. There was no main effect of genotype observed on either measurement index ($p > 0.05$), nor was there a significant interaction between genotype*treatment as was seen in the OL task. This indicates that contrary to the OL task, loss of *Nrf2* does not have an impact on adult rodents' ability to recognise the presence of novel objects. LPS treatment, however, significantly impairs the ability of all mice to perform the proposed task. This impairment is not derived from a reduced mobility due to treatment-related sickness, corroborated by the lack of difference in time spent exploring.

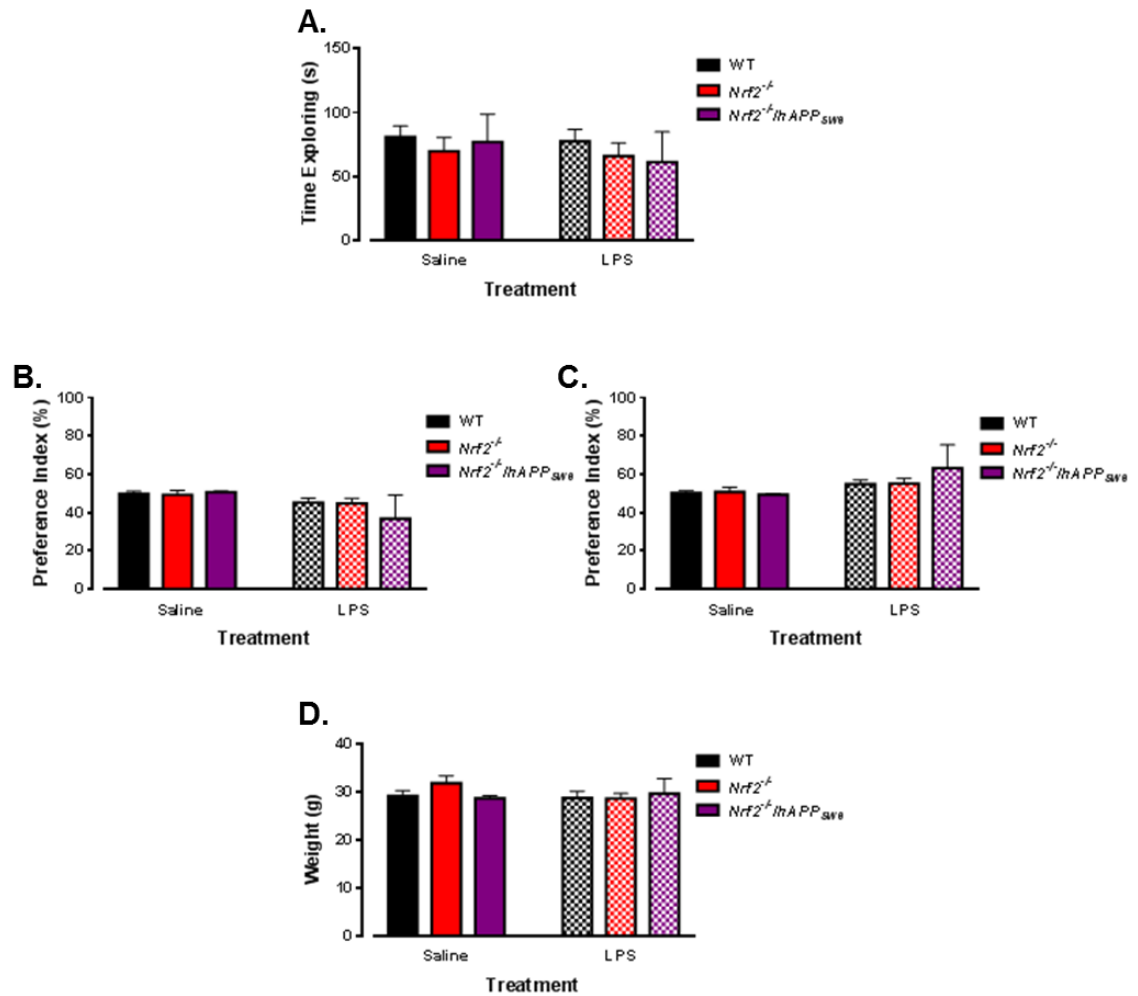


Figure 4.4 Neither genotype nor treatment affect exploration or object location preference during the sample phase of the NOR task.

Age-matched adult mice were handled for two weeks prior to the starting the study, where they were administered daily IP injections of either 2.5 μ g LPS or equivalent volume of saline for seven days. On day 6 post initial injection, mice were put through a short term NOR task. Measures taken during the sample phase included total exploration time (A), preference indices for object location (B + C) and body weight on day of behaviour (D). All data are presented as means \pm s.e.m. and analysed by ANOVA or MANOVA as appropriate. (WT: n = 11-12; *Nrf2*^{-/-}: n = 11, *Nrf2*^{-/-}/*hAPP*_{swe}: n = 3). Due to low mouse numbers *Nrf2*^{-/-}/*hAPP*_{swe} mice were not included in behaviour statistical analysis.

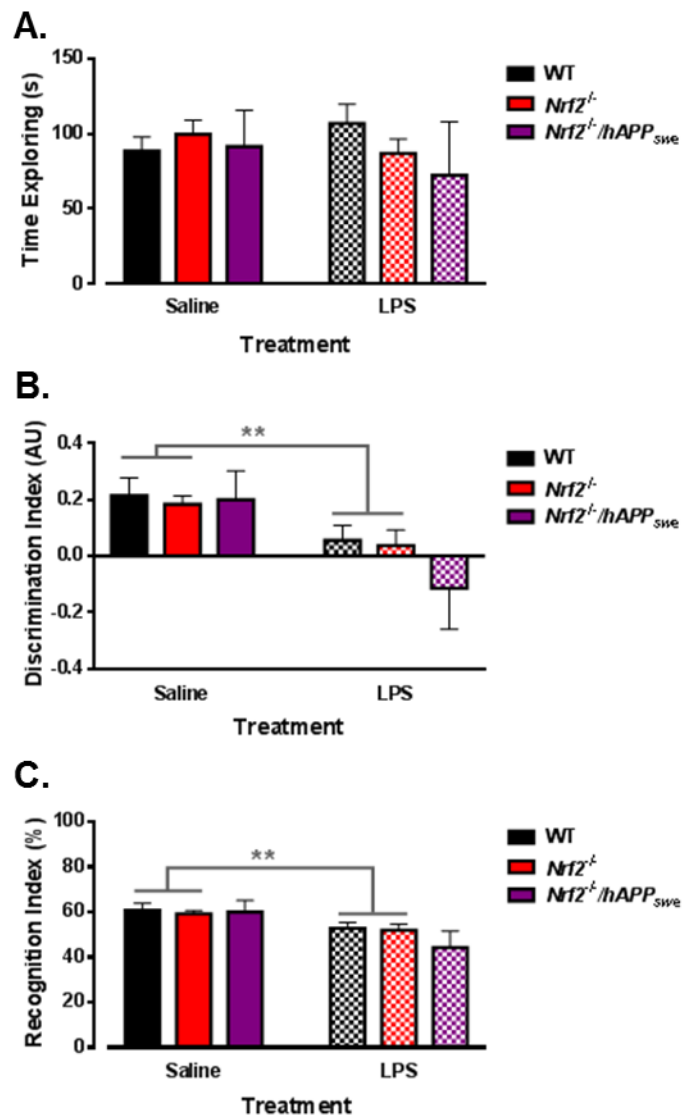


Figure 4.5 Repeated IP LPS in adult mice impedes their ability to perform a short term NOR task.

Adult mice previously habituated to the behaviour environment, were given daily IP injections of either 2.5 μ g LPS or saline for seven days. On day 6 post first injection, mice were put through a short term NOR task (10 min holding time). Measures taken during the test phase included total object exploration time (A), Discrimination indices (B) and Recognition indices (C). All data are presented as means \pm s.e.m. and analysed by ANOVA or MANOVA as appropriate. * denotes a significant main effect, ** $p < 0.01$. (WT: $n = 11-13$; *Nrf2*^{-/-}: $n = 11-13$, *Nrf2*^{-/-}/*hAPP*_{swe}: $n = 3$). Due to low mouse numbers *Nrf2*^{-/-}/*hAPP*_{swe} mice were not included in behaviour analysis.

4.5 LOW DOSE IP LPS DOES NOT AFFECT THE ABILITY OF MICE TO SPONTANEOUSLY ALTERNATE

Finally, to further assess the effect of LPS-induced inflammation on spatial working memory, mice were placed in a closed arm elevated plus maze for a period of 10 min. Measurements were recorded for total number of arm entries and alternations performed, where an alternation is described as entry into all four arms within any rotation of five consecutive arm entries (McNay *et al.*, 2000). The total number of possible alternations is therefore the total number of arm entries minus four. The data acquired from these measures was used to calculate the percentage SA (Figure 4.6 D). There was no significant difference in the number of arm entries performed between WT and *Nrf2*^{-/-} mice, nor was there a difference between treatment groups (Figure 4.6 A). From this, it is also possible to show that there is no change in locomotor ability as assessed by the number of arm entries performed. In line with these results, no significant effect of either genotype or treatment was observed on the total number of alternations performed (Figure 4.6 B). Furthermore, once analysed, the %SA obtained did not vary significantly between groups (Figure 4.6 E) indicating that neither loss of *Nrf2*^{-/-} nor repeated peripheral LPS treatment inhibit the ability of mice to spontaneously alternate at the age tested.

4.6 LOW DOSE REPEATED IP LPS INDUCES A PERIPHERAL INFLAMMATORY STATE

In order to confirm that peripheral inflammation was induced at the dosage of LPS used (2.5 µg/mouse), terminal tissue weights were recorded. More specifically the weights for key organs related to both the metabolism of toxins (liver) and inflammatory status (spleen) as well as the heart; which is thought to be affected by both oxidative stress and shifts in metabolism, were recorded (Purushothaman *et al.*, 2011). Values were analysed both as raw tissue weight and as a percentage of total bodyweight to ensure the effects seen were not solely due to the drop in body weight as a result of LPS treatment. Data obtained from the tissue harvest showed no significant changes in heart weight ($p > 0.05$; Figure 4.7 A) or heart weight as a percentage of total body mass ($p > 0.05$; Figure 4.7 D).

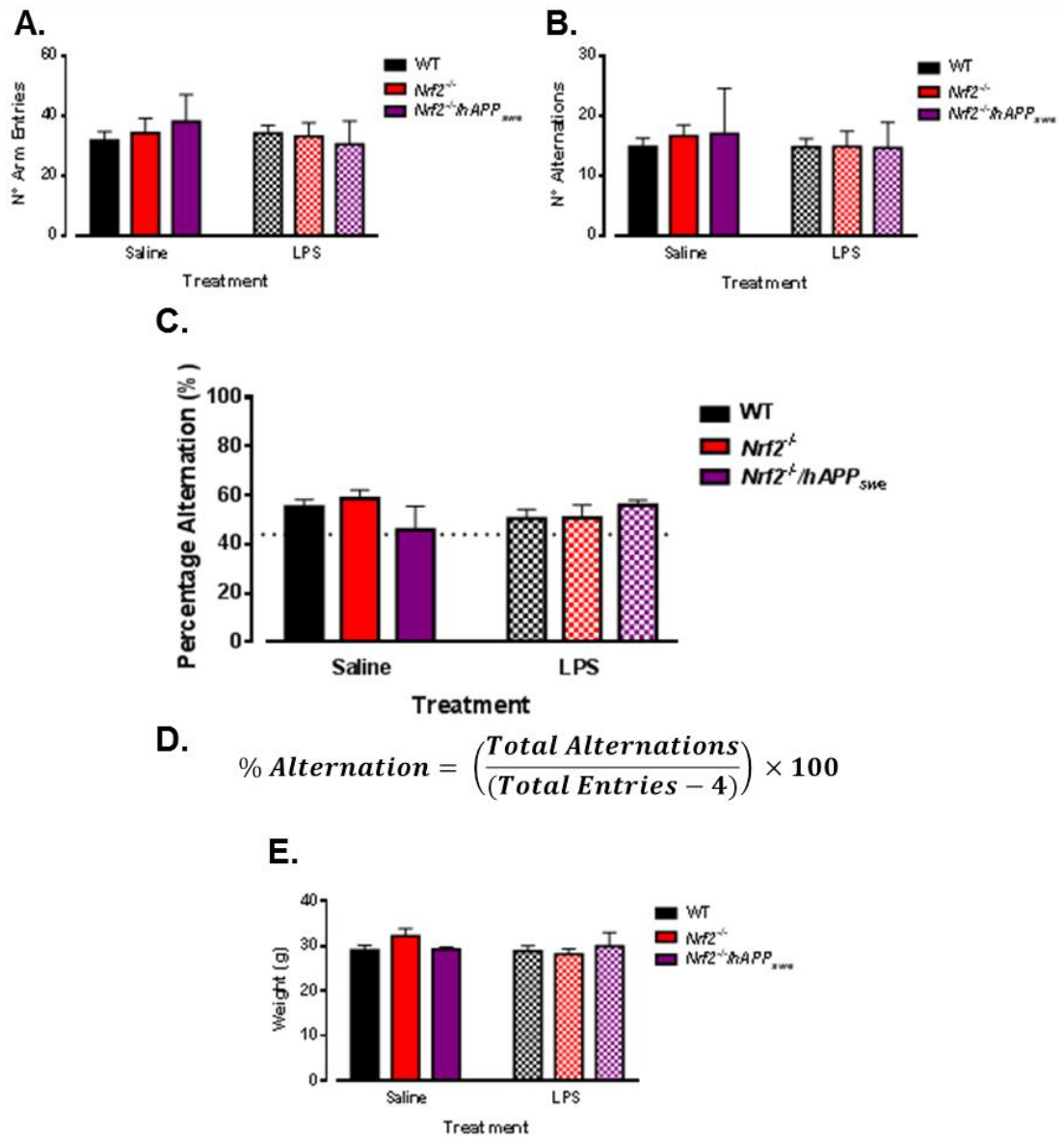


Figure 4.6 Neither repeated LPS administration nor loss of *Nrf2* prevent mice spontaneously alternating in a closed arm elevated plus maze.

Adult mice previously habituated to the behaviour environment were given daily IP injections of either 2.5 μg LPS or equivalent volume of saline for seven days. On day 7 post initial injection, mice were placed in a closed arm elevated plus maze. The number of arm entries (A) and alternations (B) performed were recorded and used to calculate the percentage spontaneous alternation for each mouse (C) using the calculation delineated in (D). Finally, total body weight was also measured (E). All data is presented as means \pm s.e.m. and analysed by ANOVA or MANOVA as appropriate. (WT: n = 11-14; *Nrf2*^{-/-}: n = 11-12, *Nrf2*^{-/-}/*hAPP*_{swe}: n = 3). Due to low numbers *Nrf2*^{-/-}/*hAPP*_{swe} mice were not included in behaviour analysis.

A significant main effect of LPS was seen on total liver weight ($F_{1, 49} = 8.870$, $p < 0.01$, $n = 3-13$), with administration of repeated LPS IP increasing raw liver tissue weight across genotypes. When total body weight was accounted for, a main effect of treatment remained for the measurement of liver as % total weight ($F_{1, 49} = 16.39$, $p < 0.001$, $n = 3-13$; Figure 4.7 E). However, a main effect of genotype is also reported with saline-treated *Nrf2*^{-/-}/*hAPP*_{swe} having significantly smaller livers in comparison to the WT control group ($F_{2, 49} = 4.510$, $p < 0.05$, $n = 3-13$).

A clear change of total spleen weight is observed as a result of LPS treatment ($F_{1, 50} = 98.46$, $p < 0.0001$, $n = 3-14$; Figure 4.7 C), all the more notable due to the lack of variation observed under control conditions. It is generally understood that there is little variation in the ratio of splenic to body weight regardless of age, making changes in this ratio a robust measure of the induction of peripheral inflammation (Cesta, 2006). No main effect of genotype on spleen weight is observed ($p > 0.05$). When expressed as a percentage of total body weight, spleens display a similar profile to that seen for the raw weight, with no effect of genotype but a significant main effect of treatment recorded ($F_{1, 50} = 62.93$, $p < 0.0001$, $n = 3-14$; Figure 4.7 F).

Finally, confirming the weight changes seen over time reported in Figure 4.1, a significant main effect of treatment is seen on the weight change recorded on the final day of the study ($F_{1, 51} = 28.89$, $p < 0.0001$, $n = 3-14$; Figure 4.7 G). Repeated IP LPS at the dosage used causes a significant drop in body weight when compared to the commencement of the study. No effect of genotype is noted when comparing weight change ($p > 0.05$), nor is there an interaction effect between treatment and genotype.

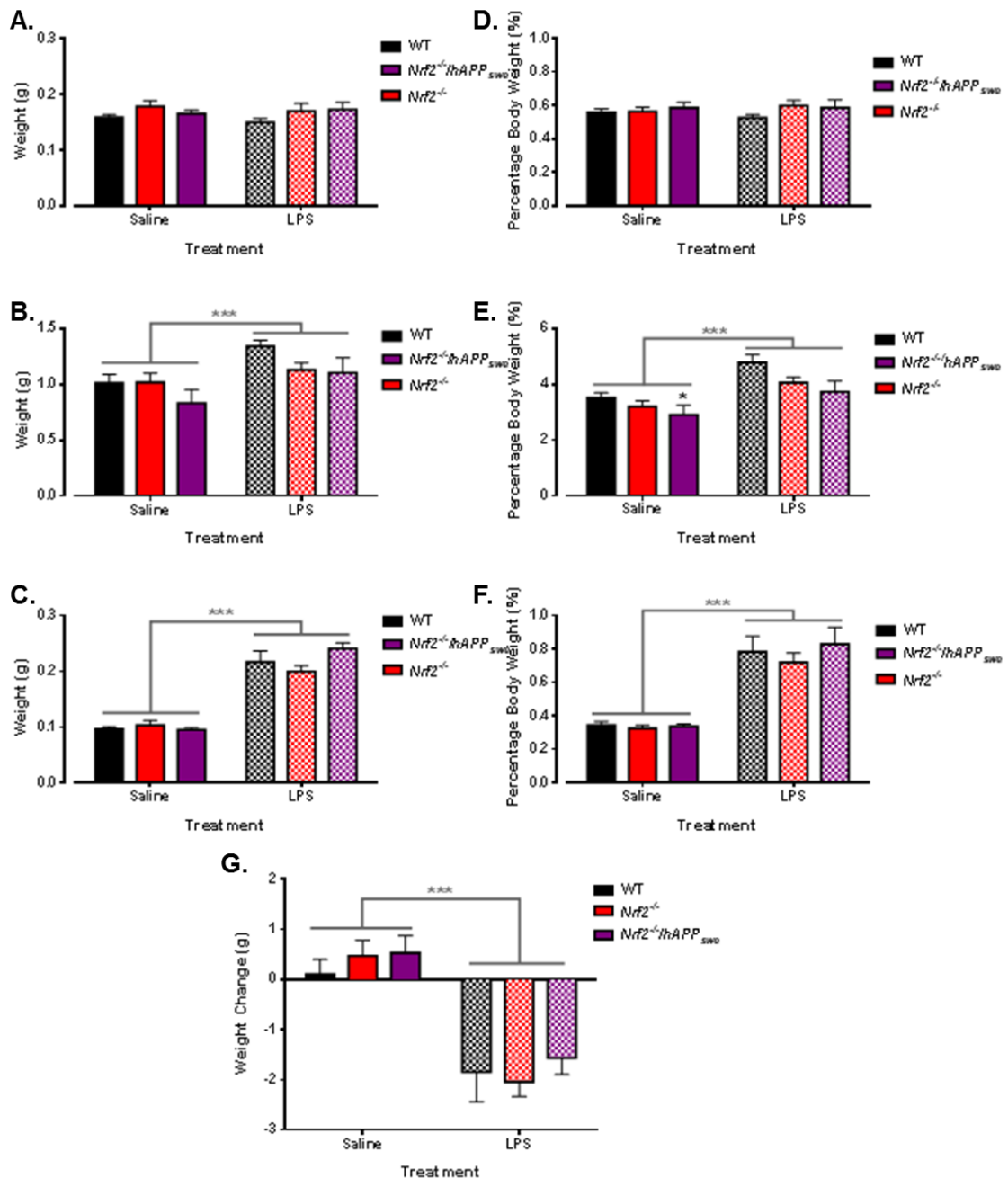


Figure 4.7 Repeated administrations of IP LPS induce changes in both liver and spleen tissues irrespective of genotype.

Tissue was harvested from adult (\pm 11 months) saline or LPS treated WT, *Nrf2*^{-/-} and *Nrf2*^{-/-}/*hAPP*_{SWE} mice. Organ weights were obtained for hearts (A) after clearing of any remaining blood, livers (B) and spleens (C) to investigate genotype-related effects on peripheral tissue health. Organ weight was assessed in relation to total body weight on day of harvest in order to clarify any treatment-related changes resulting from changes in body weight. These are reported as percentage body weight for the heart (D), liver (E) and spleen (F). To assess the effect of repeated LPS on total body weight, the weight change on the final day of the study is also reported (G; WT n = 11-14, *Nrf2*^{-/-} n = 12-13, *Nrf2*^{-/-}/*hAPP*_{SWE} n = 3-4). Data is presented as means \pm s.e.m. and analysed using two-way ANOVA with genotype and treatment as designated factors, post-hoc Bonferroni performed as necessary. * indicates significant main effect of individual factor (*, $p < 0.05$; ***, $p < 0.001$).

4.7 PERIPHERAL IP LPS DRIVES A MILD INCREASE IN INFLAMMATORY STATE IN THE BRAINS OF ADULT MICE

To assess any central inflammation occurring following repeated peripheral LPS insult, a panel of commonly assessed cytokines and related markers were evaluated by RT-qPCR for gene expression. Snap frozen tissue from both the hippocampus and the cortex of saline and LPS-treated mice was assessed following seven days of IP injections. A significant effect of treatment is seen in WT mice with LPS increasing *IL-1 β* in the hippocampus (WT saline: 1.00; WT LPS: 2.15 \pm 0.31; WT saline vs WT LPS $p < 0.01$, $n = 8-9$; Figure 4.8 A). *Nrf2*^{-/-} mice show an effect of genotype with increased basal levels of *IL-1 β* in the hippocampus compared to WT controls, with a further increase observed following LPS treatment (*Nrf2*^{-/-} saline: 2.13 \pm 0.46; *Nrf2*^{-/-} LPS: 4.55 \pm 1.0; WT saline vs *Nrf2*^{-/-} saline $p < 0.05$; WT saline vs *Nrf2*^{-/-} LPS $p < 0.01$, *Nrf2*^{-/-} saline vs *Nrf2*^{-/-} LPS $p < 0.05$, WT LPS vs *Nrf2*^{-/-} LPS $p = 0.06$, $n = 8-10$).

A genotype effect is seen in the cortex of *Nrf2*^{-/-} mice with increased basal expression of *IL-1 β* , whilst a non-significant trend to the same effect is seen in *Nrf2*^{-/-}/*hAPP*_{swe} mice (WT: 1.00; *Nrf2*^{-/-} saline: 1.23 \pm 0.10; *Nrf2*^{-/-}/*hAPP*_{swe} saline: 1.27 \pm 0.09; WT saline vs *Nrf2*^{-/-} saline $p < 0.05$, WT saline vs *Nrf2*^{-/-}/*hAPP*_{swe} saline $p = 0.06$, $n = 3-9$; Figure 4.8 E). Expression of *IL-1 β* is also significantly affected by treatment across all groups, with induction of expression observed following LPS treatment (WT LPS: 1.68 \pm 0.26; *Nrf2*^{-/-} LPS: 1.85 \pm 0.22; *Nrf2*^{-/-}/*hAPP*_{swe} LPS: 1.71 \pm 0.15; WT saline vs *Nrf2*^{-/-} LPS $p < 0.01$, WT saline vs *Nrf2*^{-/-}/*hAPP*_{swe} LPS $p < 0.05$, *Nrf2*^{-/-} saline vs *Nrf2*^{-/-} LPS $p < 0.05$, *Nrf2*^{-/-}/*hAPP*_{swe} saline vs *Nrf2*^{-/-}/*hAPP*_{swe} LPS $p < 0.05$, $n = 3-10$).

No effect of genotype or treatment is seen in the expression of either *IL-6* or *iNOS* in the hippocampus (*IL-6*: $p > 0.05$; Figure 4.8 B. *iNOS*: $p > 0.05$; Figure 4.1 C). A modest effect of genotype is seen in the cortex of *Nrf2*^{-/-}/*hAPP*_{swe} mice with an increase in *IL-6* expression (WT saline: 1.00; *Nrf2*^{-/-}/*hAPP*_{swe} saline: 1.21 \pm 0.07; WT saline vs *Nrf2*^{-/-}/*hAPP*_{swe} saline $p < 0.05$, $n = 4-9$; Figure 4.8 F). However, due to the ability of *IL-6* to perform in both a pro- and anti- inflammatory capacity it is unclear what action it is having on this occasion. There is also no significant change in the expression of cortical *iNOS* ($p > 0.05$; Figure 4.8 G).

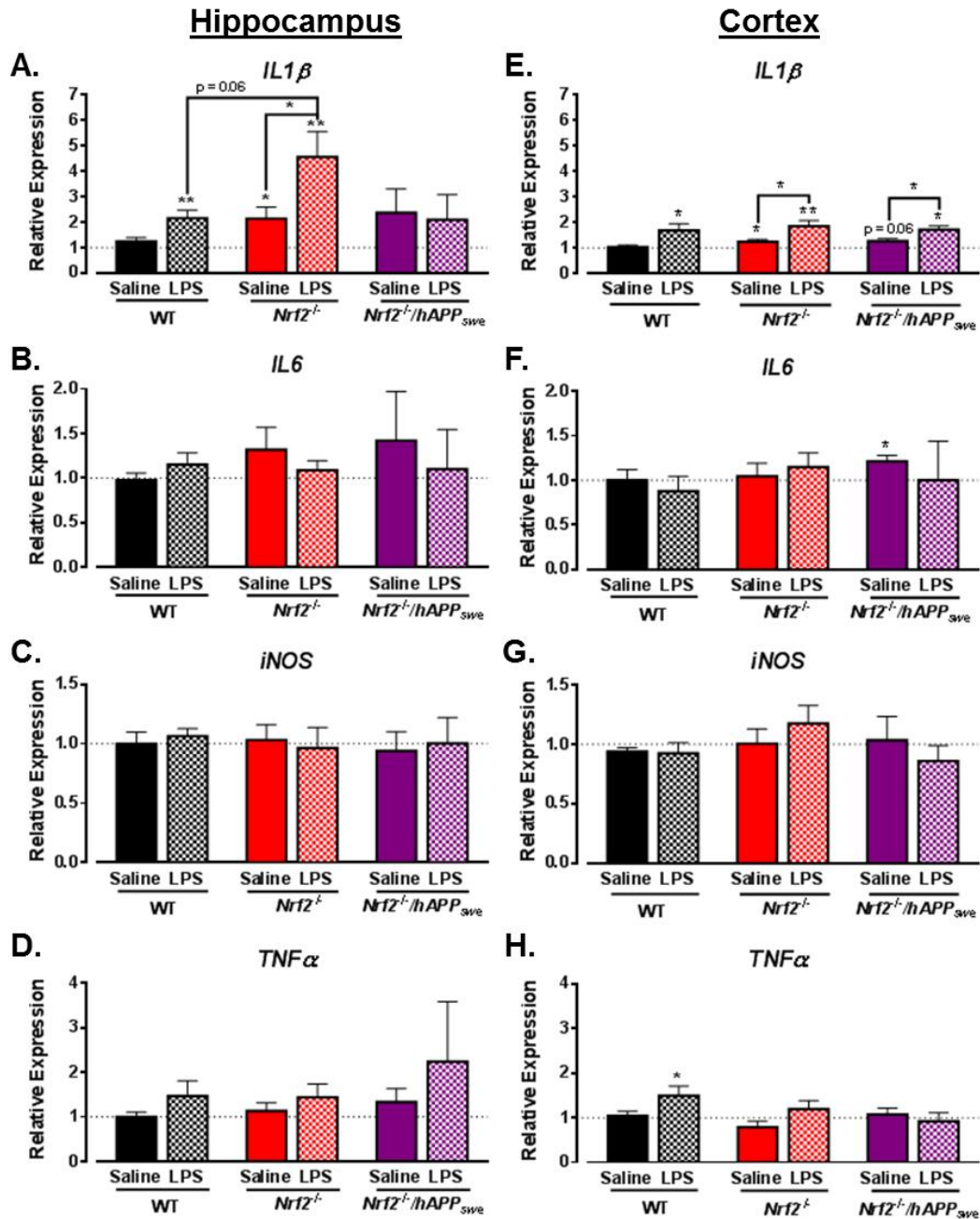


Figure 4.8 Peripheral LPS administration induces a predominantly *IL1β* driven pro-inflammatory environment in the brains of adult mice.

Brains harvested from adult saline or LPS treated WT, *Nrf2*^{-/-} and *Nrf2*^{-/-}/*hAPP*_{swe} mice were dissected and the hippocampus and cortex were processed for gene expression analysis. A panel of commonly associated pro-inflammatory markers were investigated in all groups in both tissues; namely *IL-1β* (A + E), *IL-6* (B + F), *iNOS* (C + G) and *TNF-α* (D + H) (WT n = 8-9, *Nrf2*^{-/-} n = 9-10, *Nrf2*^{-/-}/*hAPP*_{swe} n = 3-4). Results are reported as means ± s.e.m., and analysed by one-way and unpaired t-tests where * p < 0.05.

Finally, expression of the pro-inflammatory cytokine *TNF- α* was examined. A trend for a treatment-induced increase in *TNF- α* expression was seen in the hippocampus of all genotypes; however, this failed to reach significance ($p > 0.05$; Figure 4.8 D). A significant genotype*treatment effect is seen for cortical *TNF- α* with LPS treated WT mice reporting a significant increase when compared to saline-treated controls that is not seen in either *Nrf2*^{-/-} or *Nrf2*^{-/-}/*hAPP*_{swe} mice (WT saline: 1.00; WT LPS: 1.50 ± 0.21 ; WT saline vs WT LPS $p < 0.05$, $n = 9$; Figure 4.8 H). This suggests that repeated peripheral injections of low dose LPS induce a predominantly *IL1- β* driven inflammatory response in the brains of WT, *Nrf2*^{-/-} and *Nrf2*^{-/-}/*hAPP*_{swe} mice.

As inflammatory cytokines are just one of the outputs available to assess stress-related damage, oxyblots were run on protein lysates from hippocampal and cortical samples of brain tissue. Oxyblots, as described previously make use of the site-specific introduction of carbonyl groups following oxidative modification to assess the amount of protein carbonylation occurring. This is used as a marker for oxidative-related protein damage. Derivatisation of the protein carbonyl groups with DNP-hydrazone allows them to be visualised using DNP specific antibodies. To better assess the changes in total protein carbonylation, four areas on each positive sample lane were chosen at random and densitometry calculated for each box region. Exemplar blots are depicted with the regions analysed delineated on the control lane for both the hippocampus (Figure 4.9 A) and the cortex (Figure 4.9 B) in saline and LPS-treated mice.

A total change in carbonylation was assessed using cumulative scores from all of the boxed regions analysed. Tables depicting the means \pm s.e.m. values for the individual box regions for each mouse group are depicted in Figure 4.10 A for the hippocampus and Figure 4.10 B for the cortex. Values obtained for total carbonylation were taken forward and assessed for significant effects of genotype from either the loss of *Nrf2* or presence of *hAPP*_{swe}, or an LPS treatment induced effect following repeated peripheral administration. A significant increase in total carbonylated protein was seen in the hippocampus of saline-treated *Nrf2*^{-/-} mice (WT: 1.00; *Nrf2*^{-/-} saline: 1.63 ± 0.47 ; WT saline vs *Nrf2*^{-/-} saline $p < 0.05$, $n = 5$; Figure 4.10 C). No significant additional effect was observed following peripheral LPS despite a trend towards increased protein carbonylation in LPS treated WT mice ($p > 0.05$). No significant change was seen in *Nrf2*^{-/-}/*hAPP*_{swe} mice which may indicate the addition of *hAPP*_{swe} provides a putative protective effect on protein carbonylation in an environment lacking *Nrf2*.

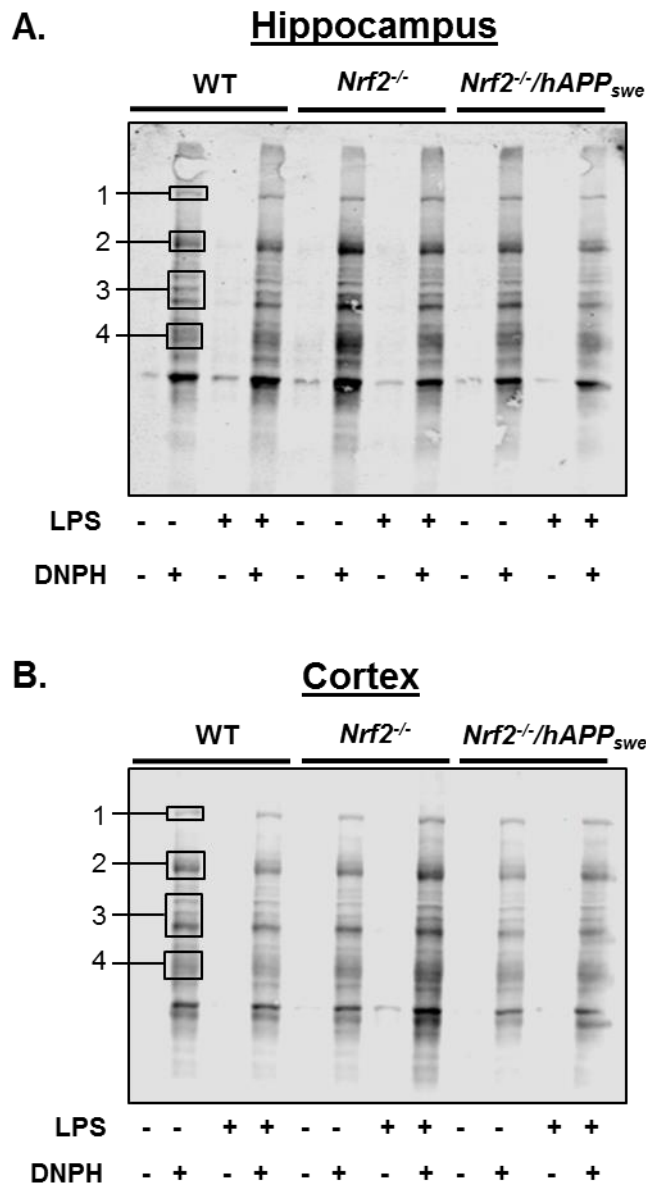


Figure 4.9 Pictorial representations of oxyblot assays performed in the hippocampus and cortex of adult saline or LPS treated animals.

Adult mice given either saline or 2.5 μ g LPS IP for seven days were harvested for tissue. Brains were excised and dissected from WT, *Nrf2*^{-/-} and *Nrf2*^{-/-}/*hAPP*_{swe} mice, and half each of the hippocampus and cortex were lysed for protein. Equal amounts of protein were calculated and samples were run through the oxyblot assay to assess changes in protein carbonylation. Exemplar blots depicting the hippocampus (**A**) and cortex (**B**) are labelled with regions used for later analysis on the left of the blot.

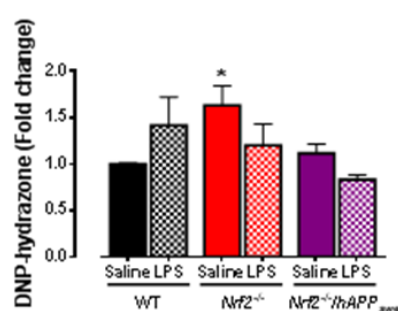
A.

HIPPOCAMPUS						
	WT		<i>Nrf2</i> ^{-/-}		<i>Nrf2</i> ^{-/-} / <i>hAPP</i> _{swe}	
	Saline	LPS	Saline	LPS	Saline	LPS
Box 1	1.00	1.24 ± 0.24	1.34 ± 0.34	1.26 ± 0.33	1.10 ± 0.094	0.75 ± 6*10 ⁻⁸
Box 2	1.00	1.68 ± 1.11	1.65 ± 0.82	1.29 ± 0.83	1.36 ± 0.42	0.81 ± 0.12
Box 3	1.00	1.66 ± 0.90	1.82 ± 0.60	1.41 ± 0.70	1.32 ± 0.24	0.74 ± 0.14
Box 4	1.00	1.34 ± 0.41	1.86 ± 0.57	1.28 ± 0.64	1.07 ± 0.24	1.00 ± 0.068
Total	1.00	1.42 ± 0.68	1.63 ± 0.47	1.20 ± 0.51	1.11 ± 0.20	0.83 ± 0.068

B.

CORTEX						
	WT		<i>Nrf2</i> ^{-/-}		<i>Nrf2</i> ^{-/-} / <i>hAPP</i> _{swe}	
	Saline	LPS	Saline	LPS	Saline	LPS
Box 1	1.00	1.46 ± 0.61	1.51 ± 0.96	1.54 ± 0.22	1.46 ± 0.58	1.31 ± 0.36
Box 2	1.00	1.50 ± 0.75	1.27 ± 0.80	1.23 ± 0.24	1.21 ± 0.59	1.02 ± 0.22
Box 3	1.00	1.42 ± 0.53	1.20 ± 0.60	1.28 ± 0.17	1.08 ± 0.54	0.86 ± 0.19
Box 4	1.00	1.68 ± 0.75	1.48 ± 0.93	1.62 ± 0.37	1.43 ± 0.76	0.936 ± 0.23
Total	1.00	1.52 ± 0.64	1.32 ± 0.77	1.38 ± 0.21	1.24 ± 0.62	0.947 ± 0.21

C.



D.

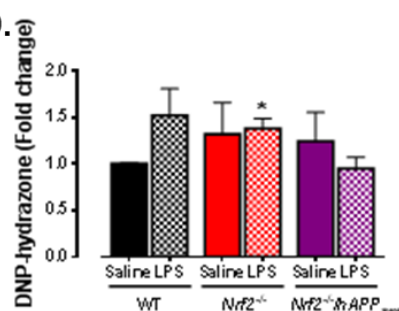


Figure 4.10 Loss of *Nrf2* drives increases in protein carbonylation in both the hippocampus and cortex of adult mice.

Adult mice from WT, *Nrf2*^{-/-} and *Nrf2*^{-/-}/*hAPP*_{swe} backgrounds administered either saline or LPS IP for seven days were harvested for tissue. Brains were dissected and hippocampal and cortical tissue were lysed for protein and processed for an oxyblot assay as per manufacturer's instructions. Blots were analysed at pre-selected points and means ± s.e.m. displayed for the individual regions and the averaged total for both the hippocampus (A) and the cortex (B). Analysis of averaged total values is indicated in (C) for the hippocampus and (D) for the cortex. Data is reported as means ± s.e.m., and analysis was performed using one-sample and unpaired t-test where * = p < 0.05. (WT: n = 5; *Nrf2*^{-/-}: n = 4-5; *Nrf2*^{-/-}/*hAPP*_{swe}: n = 3-4)

When cortical tissue was examined, a significant increase in protein carbonylation of *Nrf2*^{-/-} mice treated with LPS was observed when compared to saline-treated WT controls (WT saline: 1.00; *Nrf2*^{-/-} LPS: 1.38 ± 0.21; WT saline vs *Nrf2*^{-/-} LPS p < 0.05, n = 4-5; Figure 4.10 D). As for the hippocampus, a trend for increased carbonylation following LPS treatment was seen in WT mice but this failed to reach significance (p > 0.05). There were also no significant changes seen in protein carbonylation in *Nrf2*^{-/-}/*hAPP*_{swe} mice. This suggests the loss of *Nrf2*^{-/-} is sufficient to induce increased protein carbonylation, even in tightly regulated tissue such as the brain.

Due to the relatively mild pro-inflammatory response recorded, a selection of anti-inflammatory markers was evaluated to assess the inflammatory resolution capacity of the brain following peripheral LPS dosing. Markers such as *Arg1* and *YMI*, commonly assessed outputs from the alternative microglial activation pathway, were evaluated alongside *MRC1*, which causes the endocytosis of glycoproteins acting in part as a phagocytic receptor for bacteria and other pathogens.

No induction of *Arg1* was seen in the hippocampus of mice irrespective of genotype or treatment group (p > 0.05; Figure 4.11 A). Mice lacking expression of *Nrf2* demonstrated a non-significant increase in cortical expression of *Arg1* (p > 0.05; Figure 4.11 D), which was enhanced following LPS treatment but failed to reach significance (p > 0.05). In addition, no genotype or treatment induced alteration of *Arg1* was seen in either the WT or *Nrf2*^{-/-}/*hAPP*_{swe} mice (p > 0.05). In contrast to *Arg1*, expression of *MRC1* shows an LPS treatment driven effect in both WT and *Nrf2*^{-/-} mice in both the hippocampus (WT saline: 1.00; WT LPS: 1.42 ± 0.14; *Nrf2*^{-/-} saline: 1.16 ± 0.16; *Nrf2*^{-/-} LPS: 1.81 ± 0.25; WT saline vs WT LPS p < 0.05, WT saline vs *Nrf2*^{-/-} saline p < 0.05, *Nrf2*^{-/-} saline vs *Nrf2*^{-/-} LPS p < 0.05, n = 9-10; Figure 4.11 B) and cortex (WT saline: 1.00; WT LPS: 1.64 ± 0.22; *Nrf2*^{-/-} saline: 1.19 ± 0.19; *Nrf2*^{-/-} LPS: 1.74 ± 0.17; WT saline vs *Nrf2*^{-/-} LPS p < 0.01, *Nrf2*^{-/-} saline vs *Nrf2*^{-/-} LPS p < 0.05, n = 9-10; Figure 4.11 E) of adult mice. As for *Arg1*, no significant changes in the *MRC1* expression were seen in the hippocampus or cortex of *Nrf2*^{-/-}/*hAPP*_{swe} mice.

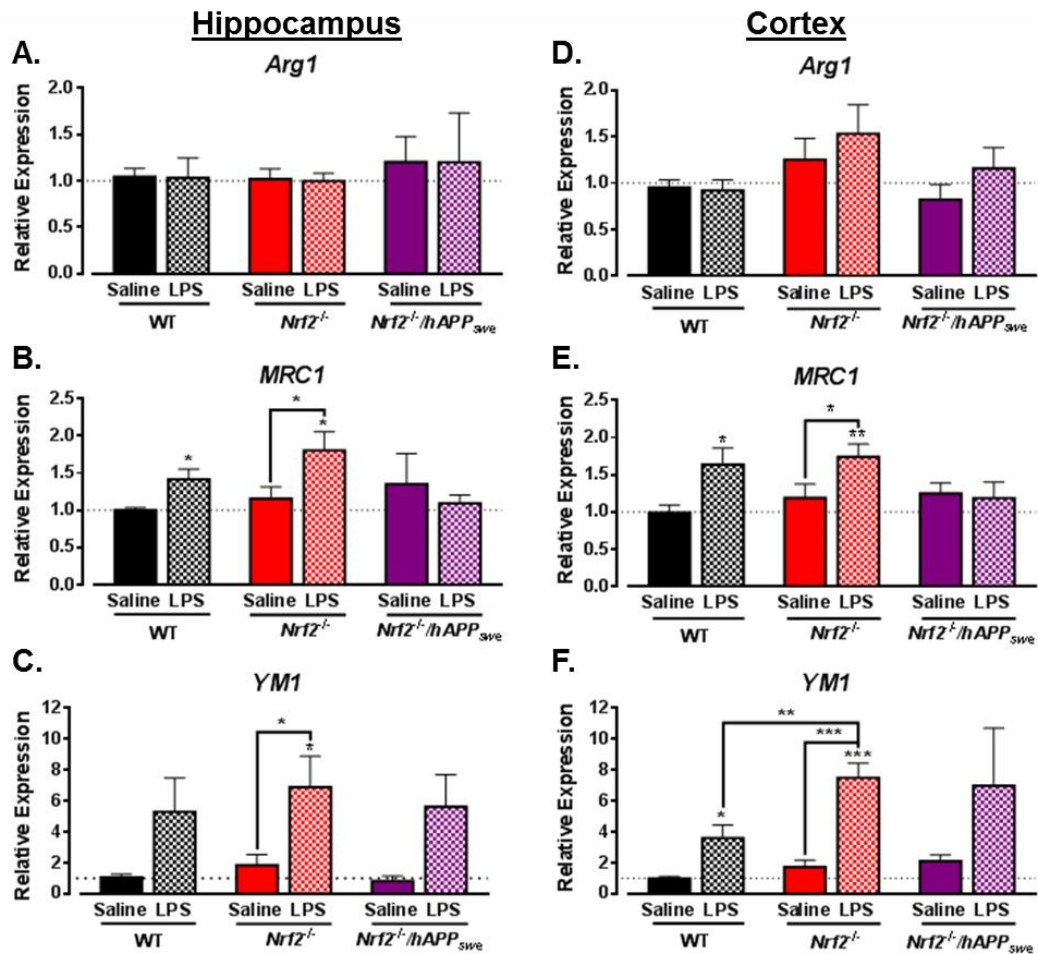


Figure 4.11 Repeated peripheral LPS treatment prompts a predominantly cortical induction of anti-inflammatory markers with mild escalation following loss of Nrf2.

Brains harvested from adult saline and LPS treated WT, *Nrf2*^{-/-}, and *Nrf2*^{-/-}/*hAPP*_{swe} mice were dissected and the hippocampus and cortex were processed for gene expression analysis. Commonly referenced anti-inflammatory markers *Arg1* (A + D), *MRC1* (B + E) and *YM1* (C + F) (WT n = 5-6, *Nrf2*^{-/-} n = 4-7, *Nrf2*^{-/-}/*hAPP*_{swe} n = 3-4). Results are reported as means ± s.e.m., and analysed by unpaired t-test where * indicates a significant change from saline treated WT and † indicates a change from LPS treated WT mice. *, p < 0.05, ** p < 0.01, *** p < 0.001; † p < 0.05.

Lastly, induction of *YMI* expression appears most tightly associated with a treatment driven effect. Increased expression is observed following LPS administration irrespective of genotype or tissue analysed, with both the hippocampus (Figure 4.11 C) and cortex (Figure 4.11 F) exhibiting changes. Although not always achieving statistical significance due to a higher degree of variation, a trend towards increased expression in comparison to saline treatment is observed in the hippocampus of both WT and *Nrf2*^{-/-}/*hAPP*_{swe} mice (WT saline: 1.00; WT LPS: 5.28 ± 2.2; *Nrf2*^{-/-}/*hAPP*_{swe} saline: 0.821 ± 0.33; *Nrf2*^{-/-}/*hAPP*_{swe} LPS: 5.60 ± 2.1; WT saline vs WT LPS p = 0.09, *Nrf2*^{-/-}/*hAPP*_{swe} saline vs *Nrf2*^{-/-}/*hAPP*_{swe} LPS p = 0.09, n = 3-9), whilst a significant induction is observed in LPS-treated *Nrf2*^{-/-} mice (*Nrf2*^{-/-} saline: 1.84 ± 3.4; *Nrf2*^{-/-} LPS: 6.87 ± 2.0; WT saline vs *Nrf2*^{-/-} LPS p < 0.05, *Nrf2*^{-/-} saline vs *Nrf2*^{-/-} LPS p < 0.05, n = 8-10).

Cortical expression outlines a similar profile to that discerned in the hippocampus, with increased expression in *YMI* following repeated peripheral LPS treatment. WT mice demonstrate an almost fourfold induction in gene expression, whilst both *Nrf2*^{-/-} and *Nrf2*^{-/-}/*hAPP*_{swe} are closer to a sevenfold induction following LPS treatment with mildly elevated basal levels (WT saline: 1.00; WT LPS: 3.59 ± 0.85; *Nrf2*^{-/-} saline: 1.72 ± 0.44; *Nrf2*^{-/-} LPS: 7.48 ± 0.93; *Nrf2*^{-/-}/*hAPP*_{swe} saline: 2.10 ± 0.40; 6.97 ± 3.7; WT saline vs WT LPS p < 0.05, WT saline vs *Nrf2*^{-/-} LPS p < 0.0001, *Nrf2*^{-/-} saline vs *Nrf2*^{-/-} LPS p < 0.0001, WT saline vs *Nrf2*^{-/-}/*hAPP*_{swe} saline p = 0.07, WT saline vs *Nrf2*^{-/-}/*hAPP*_{swe} LPS p > 0.05, n = 3-10; Figure 4.11 F). As with the previous study examining the effects of long term HF feeding, the anti-inflammatory response in the brain appears greater in the cortex than the hippocampus of mice, irrespective of genotype analysed.

In contrast, activation of the complement immune system occurs across both brain regions assessed. A trend towards increased hippocampal expression of the C3 complement cascade protein is observed following loss of *Nrf2*^{-/-} (WT saline: 1.00; WT LPS: 1.01 ± 0.15; *Nrf2*^{-/-} saline: 2.22 ± 0.89; *Nrf2*^{-/-} LPS: 2.47 ± 0.79; WT saline vs *Nrf2*^{-/-} saline and LPS p > 0.05, WT LPS vs *Nrf2*^{-/-} LPS p > 0.05, n = 8-10; Figure 4.12 A). No induction is seen following LPS treatment of *Nrf2*^{-/-}/*hAPP*_{swe} mice (p > 0.05) with non-significant increase in basal levels similar to that observed in the *Nrf2*^{-/-} mice (p > 0.05).

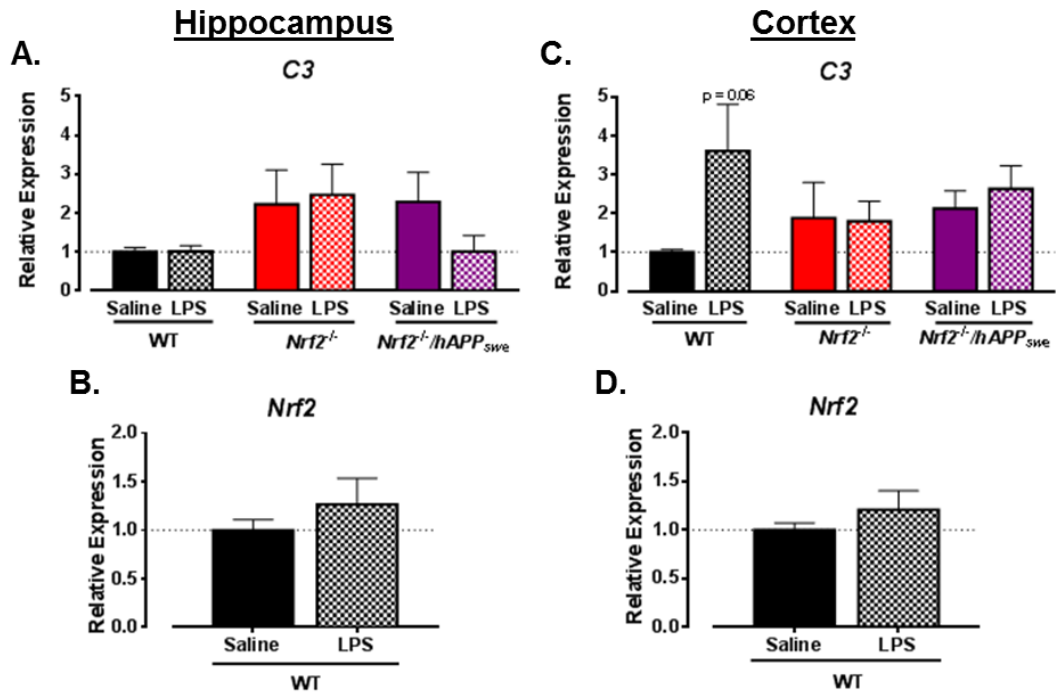


Figure 4.12 Loss of *Nrf2* and LPS both impact on the activation of the complement immune pathway.

The dissected hippocampus and cortex harvested from adult WT, *Nrf2*^{-/-}, and *Nrf2*^{-/-}/*hAPP*_{swe} mice were processed for gene expression analysis. A marker for the alternative complement immune pathway, *C3* (A + C), and the transcription factor controlling the expression of a multitude of antioxidant genes, *Nrf2* (B + D) were analysed for changes in expression following repeated peripheral LPS treatment. (WT n = 5-6, *Nrf2*^{-/-} n = 6-7, *Nrf2*^{-/-}/*hAPP*_{swe} n = 3-4). Results are reported as means ± s.e.m., and analysed by one-way and unpaired t-tests where * indicates a significant change from saline treated WT.

In comparison, cortical expression of *C3* is induced by LPS in WT mice (WT saline: 1.00; WT LPS: 3.61 ± 1.2 ; WT saline vs WT LPS $p = 0.06$, $n = 8-9$; Figure 4.12 C). A trend towards an inducing effect of genotype is seen in both *Nrf2*^{-/-} and *Nrf2*^{-/-}/*hAPP*_{swe} with no additive effect of treatment observed (*Nrf2*^{-/-} saline: 1.89 ± 0.91 ; *Nrf2*^{-/-} LPS: 1.80 ± 0.52 ; *Nrf2*^{-/-}/*hAPP*_{swe} saline: 2.13 ± 0.45 ; *Nrf2*^{-/-}/*hAPP*_{swe} LPS: 2.64 ± 0.59 ; WT saline vs *Nrf2*^{-/-} saline and LPS $p > 0.05$, WT saline vs *Nrf2*^{-/-}/*hAPP*_{swe} saline $p = 0.09$, WT saline vs *Nrf2*^{-/-}/*hAPP*_{swe} LPS $p > 0.05$, $n = 3-10$). Contrary to *C3* expression, LPS does not appear to induce an increased expression of *Nrf2*, a major regulator of the production of antioxidant molecules, in WT mice in either the hippocampus (Figure 4.12 B) or the cortex (Figure 4.12 D).

4.8 NRF2 PLAYS AN IMPORTANT ROLE IN THE MODULATION OF GLIAL CELL RESPONSES TO PERCEIVED CELLULAR INSULTS

As changes in inflammatory response were observed following repeated peripheral LPS administration, markers of activation were analysed for two of the major glial cell populations found in the brain, namely microglia and astrocytes. As previously mentioned, both of these cell populations play an important role in maintaining neuronal cell health. Microglia represent the resident macrophage population of the CNS demonstrating an ability to be polarised into an M1 or M2 state. Astrocytes also play a role in response to trauma and oxidative or inflammatory damage. Furthermore, they are important in nutrient management and neurotransmitter regulation.

F4/80, a marker for microglia, peripheral macrophages and a selection of other immune cells, demonstrated a trend towards a genotype-dependent increase in basal expression driven by the loss of *Nrf2* in the hippocampus (WT saline: 1.00; *Nrf2*^{-/-} saline: 1.28 ± 0.10 ; *Nrf2*^{-/-}/*hAPP*_{swe} saline: 1.43 ± 0.28 ; WT saline vs *Nrf2*^{-/-} saline $p < 0.05$, WT saline vs *Nrf2*^{-/-}/*hAPP*_{swe} saline $p > 0.05$, $n = 4-6$; Figure 4.13 A). All LPS-treated animals showed significant increases in hippocampal *F4/80* expression, with *Nrf2*^{-/-} mice recording a further increase over and above that seen basally (WT LPS: 1.49 ± 0.13 ; *Nrf2*^{-/-} LPS: 1.83 ± 0.16 ; *Nrf2*^{-/-}/*hAPP*_{swe} LPS: 1.41 ± 0.053 ; WT saline vs WT LPS $p < 0.01$, WT saline vs *Nrf2*^{-/-} LPS $p < 0.001$, WT saline vs *Nrf2*^{-/-}/*hAPP*_{swe} LPS $p < 0.05$, *Nrf2*^{-/-} saline vs *Nrf2*^{-/-} LPS $p < 0.05$, $n = 3-10$).

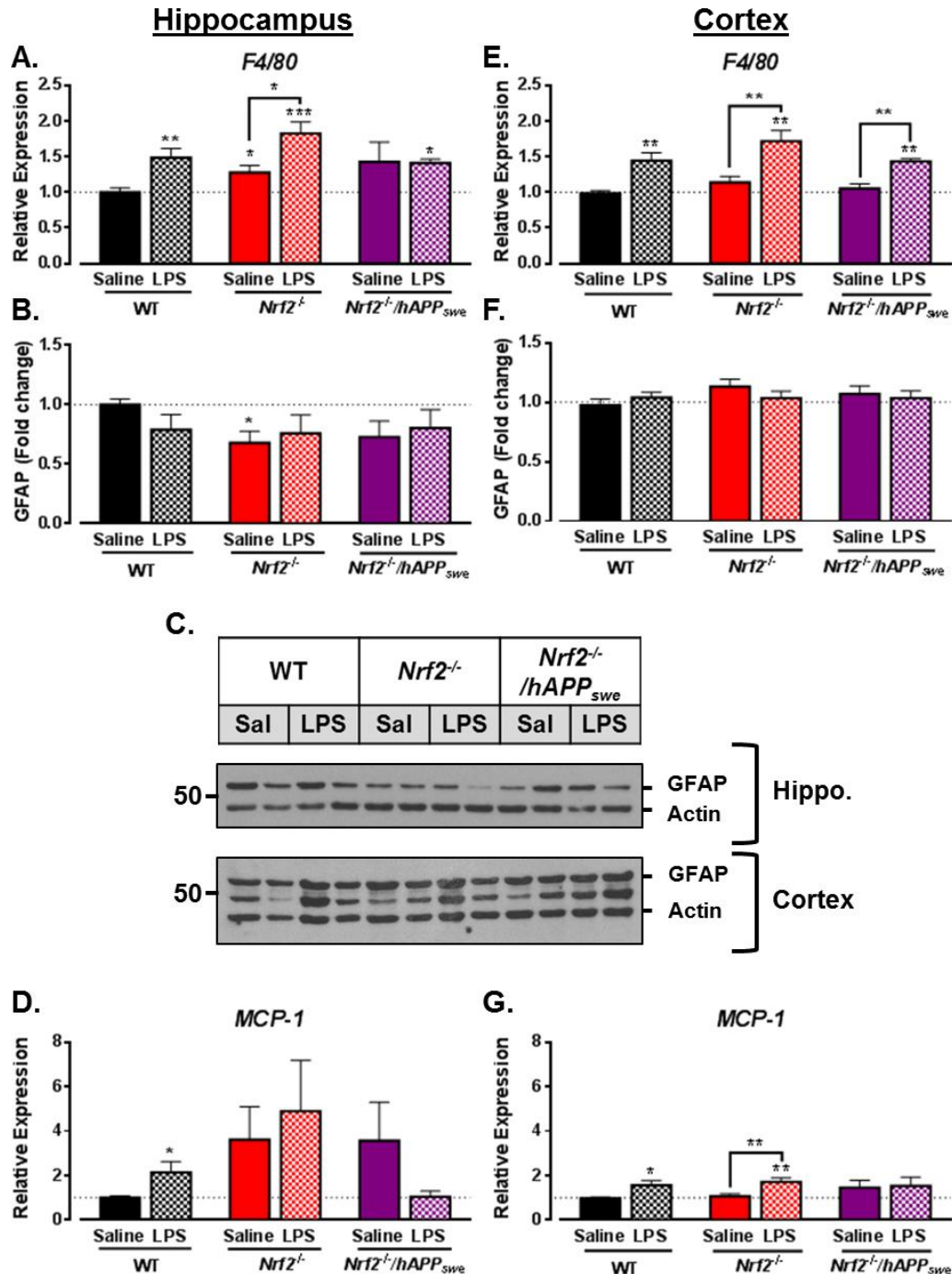


Figure 4.13 Loss of *Nrf2* and LPS both modulate markers of glial cell activation and recruitment.

Brains from adult mice were harvested, dissected and processed for gene and protein expression. Markers for macrophage activation (*F4/80*; **A + E**), astrocyte activation (GFAP; **B + F**) and the chemokine *MCP-1* (**D** and **G**) were analysed by RT-qPCR or Western blot for changes in expression in the hippocampus and cortex regions of the brain. Exemplar blots of GFAP expression are portrayed for both the cortex and hippocampus where β -actin was used as the protein loading control (**C**). The non-specific band seen at 48 kDa has been previously reported as a GFAP derived band, thought to be a degradation product of GFAP. Data portrayed as means \pm s.e.m. and analysed by unpaired t-test where * indicates significantly different from WT control; *, $p < 0.05$; **, $p < 0.01$, *** $p < 0.001$. Genes: WT $n = 8-9$, *Nrf2*^{-/-} $n = 9-10$, *Nrf2*^{-/-}/*hAPP*_{swe} = 3-4; and protein: WT $n = 6$, *Nrf2*^{-/-} $n = 6$, *Nrf2*^{-/-}/*hAPP*_{swe} = 3-4.

In the cortex, a treatment driven increase in expression of *F4/80* was observed with no cross-genotype changes (WT saline: 1.00; WT LPS: 1.44 ± 0.11 ; *Nrf2*^{-/-} saline: 1.14 ± 0.086 ; *Nrf2*^{-/-} LPS: 1.72 ± 0.15 ; *Nrf2*^{-/-}/*hAPP*_{swe} saline: 1.05 ± 0.067 ; *Nrf2*^{-/-}/*hAPP*_{swe} LPS: 1.43 ± 0.037 ; WT saline vs WT LPS $p < 0.01$, WT saline vs *Nrf2*^{-/-} LPS $p < 0.01$, *Nrf2*^{-/-} saline vs *Nrf2*^{-/-} LPS $p < 0.01$, WT saline vs *Nrf2*^{-/-}/*hAPP*_{swe} LPS $p < 0.01$, *Nrf2*^{-/-}/*hAPP*_{swe} saline vs *Nrf2*^{-/-}/*hAPP*_{swe} LPS $p < 0.01$, $n = 3-10$; Figure 4.13 E).

Activation of astrocytes, glial cells that perform a multitude of roles including nutrient transport and neurotransmitter modulation, was assessed using protein changes in GFAP. Hippocampal expression of GFAP was not significantly altered in either WT mice or *Nrf2*^{-/-}/*hAPP*_{swe} mice despite a trend towards lower expression in the LPS-treated WT mice and a genotype-dependent trend towards decreased levels in the double transgenic model (WT saline: 1.00; WT LPS: 0.789 ± 0.13 ; *Nrf2*^{-/-}/*hAPP*_{swe} saline: 0.729 ± 0.13 ; WT saline vs WT LPS and *Nrf2*^{-/-}/*hAPP*_{swe} saline $p > 0.05$, $n = 4-6$; Figure 4.13 B). Loss of *Nrf2* alone appears to decrease hippocampal GFAP expression; this loss is not significantly affected by additional treatment with LPS (*Nrf2*^{-/-} saline: 0.678 ± 0.098 ; WT saline vs *Nrf2*^{-/-} saline $p < 0.05$, $n = 6$). In contrast to the changes observed in hippocampal GFAP, no effect of genotype or treatment is seen on cortical expression in adult mice ($p > 0.05$; Figure 4.13 F).

Increases in expression of glial related markers may indicate an increase in the recruitment of macrophage cells, whether they are residential cells such as the microglia or peripheral macrophages. Chemokines can both be released from and target the different forms of immune cell in order to accrue the selection of cells necessary to resolve the relevant damage. As a result, they are a key mode of communication in the initiation and evolution of the immune cascade response. MCP-1, released from a range of cell types including neurons, targets the recruitment of monocytes and macrophages to the site of injury and has been reported to be involved in the progression of inflammation in AD (Sokolova *et al.*, 2009; McLarnon, 2012; Zhang *et al.*, 2013). A significant increase in *MCP-1* was seen in the hippocampus of LPS-treated WT mice (WT saline: 1.00; WT LPS: 2.15 ± 0.48 ; WT saline vs WT LPS $p < 0.05$, $n = 8-9$; Figure 4.13 D). Whilst *Nrf2*^{-/-} mice show a non-significant increase in basal levels of *MCP-1* expression with little further induction following LPS-treatment (*Nrf2*^{-/-} saline: 3.61 ± 1.48 ; *Nrf2*^{-/-} LPS: 4.89 ± 2.3 ; WT saline vs *Nrf2*^{-/-} saline and LPS $p > 0.05$, $n = 9-10$). *Nrf2*^{-/-}/*hAPP*_{swe} mice mimic the increased basal levels of *MCP-1* in the KO model but show a return to WT saline treated levels of *MCP-1* following LPS treatment (*Nrf2*^{-/-}

/hAPP_{swe} saline: 3.46 ± 1.7 ; WT saline vs *Nrf2^{-/-}/hAPP_{swe}* saline and LPS $p > 0.05$, $n = 3-6$). This altered response in the double transgenic model to LPS may be due to the additional presence of *hAPP_{swe}*.

No effect of genotype is seen on the cortical expression of *MCP-1*, contrary to that seen in the hippocampus (Figure 4.13 G). Peripheral LPS, however, continues to induce expression of *MCP-1* in the cortex of both WT and *Nrf2^{-/-}* mice (WT saline: 1.00; WT LPS: 1.56 ± 0.21 ; *Nrf2^{-/-}* saline: 1.07 ± 0.12 ; *Nrf2^{-/-}* LPS: 1.72 ± 0.18 ; WT saline vs WT LPS $p < 0.05$, WT saline vs *Nrf2^{-/-}* LPS $p < 0.01$, *Nrf2^{-/-}* saline vs *Nrf2^{-/-}* LPS $p < 0.01$, $n = 9-10$). No significant changes in expression of *MCP-1* are observed in the cortex of *Nrf2^{-/-}/hAPP_{swe}* mice ($p > 0.05$). These observations indicate a primarily hippocampus localised pro-inflammatory response following LPS treatment, with increased expression of markers such as *IL-1 β* , *F4/80*, *MCP-1* and protein carbonylation combining with a loss of GFAP. In contrast, a much stronger anti-inflammatory presence is seen in the cortical tissue of the mouse brain with an attenuated pro-inflammatory response in markers such as *IL1- β* and *MCP-1*, when compared to the hippocampus, and an amplified response in anti-inflammatory markers such as *YMI*, *Arg1* and *C3*. It also implicates Nrf2 in the management and amplitude of the response to peripheral LPS administration in the murine brain with an increased basal inflammatory state potentiating the response to peripheral LPS challenge.

4.9 SHORT-TERM REPEATED IP LPS AFFECTS SYNAPTIC HEALTH IN THE CORTEX OF THE MURINE BRAIN

As previously described, SYP is a commonly used marker for the measurement of synaptic density and health. Its exact function is still unclear although putative roles include regulation of synaptic vesicle endocytosis (Kwon & Chapman, 2011). In addition, it has previously been reported that changes in dietary composition can alter SYP expression with increased expression of SYP following a diet with a higher ratio of n-3:n-6 PUFAs (Hajjar *et al.*, 2013). Due to its ubiquitous presence in the synapse, SYP is commonly used to monitor synapse number. Hippocampal lysates obtained from mice given repeated LPS or saline injections IP showed an increase in SYP in *Nrf2^{-/-}* mice under basal conditions with LPS negatively impacting protein levels (WT saline: 1.00; *Nrf2^{-/-}* saline: 1.32 ± 0.14 ; *Nrf2^{-/-}* LPS: 1.01 ± 0.14 ; WT saline vs *Nrf2^{-/-}* saline $p = 0.05$, *Nrf2^{-/-}* saline vs *Nrf2^{-/-}* LPS $p > 0.05$, $n = 9$; Figure 4.14 A). No hippocampal changes in SYP were seen in either WT or *Nrf2^{-/-}/hAPP_{swe}* mice irrespective of treatment.

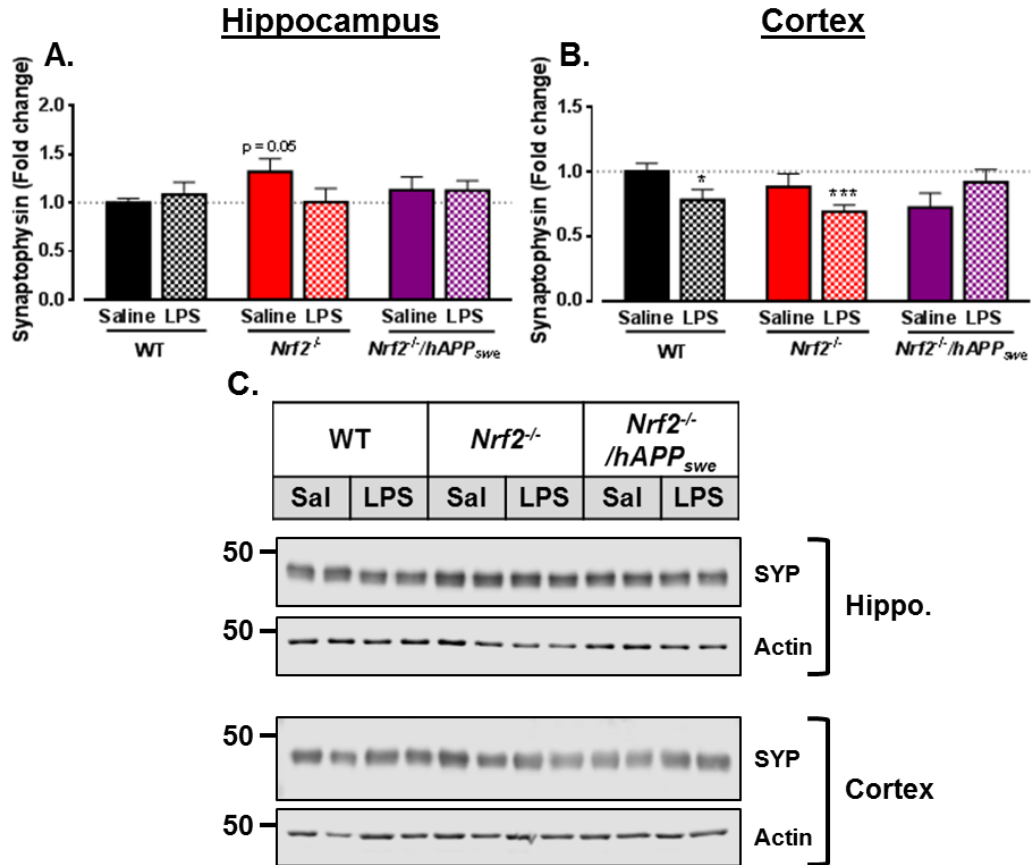


Figure 4.14 Repeated peripheral LPS administration induces a small loss of cortical synapses in *Nrf2*^{-/-} mice.

Dissected brain tissue from adult saline and LPS treated mice was processed for protein expression and probed for the synapse marker SYP in the hippocampus (A) and cortex (B), with (C) showing images of exemplar blots for both the hippocampus and cortex. Data portrayed as means \pm s.e.m. and analysed by one-way and unpaired t-test where * indicates significantly different from RC fed WT control, where *, $p < 0.05$, ***, $p < 0.001$. WT $n = 9$, *Nrf2*^{-/-} $n = 9$, *Nrf2*^{-/-}/*hAPP*_{swe} $n = 3-4$.

When lysates from the cortical region were compared, a significant attenuating effect of treatment was observed in WT mice, with expression levels of SYP decreasing with LPS treatment (WT saline: 1.00; WT LPS: 0.781 ± 0.082 ; WT saline vs WT LPS $p < 0.05$, $n = 9$; Figure 4.14 B). A similar treatment effect is seen in mice lacking *Nrf2*, with a non-significant drop in SYP under basal levels amplified following treatment (*Nrf2*^{-/-} saline: 0.882 ± 0.10 ; *Nrf2*^{-/-} LPS: 0.689 ± 0.052 ; WT saline vs *Nrf2*^{-/-} saline $p > 0.05$, WT saline vs *Nrf2*^{-/-} LPS $p < 0.001$, $n = 9$). A trend for decreased SYP is also seen in the *Nrf2*^{-/-}/*hAPP*_{swe} saline treated mice (*Nrf2*^{-/-}/*hAPP*_{swe} saline: 0.721 ± 0.11 ; WT saline vs *Nrf2*^{-/-}/*hAPP*_{swe} saline $p = 0.09$) with no further effect of treatment. This is visualised by representative blots controlled against loading error by the housekeeping protein β -actin (Figure 4.14 C).

4.10 REPEATED PERIPHERAL LPS ADMINISTRATION SELECTIVELY AFFECTS KEY AD RELATED PROTEINS

Expression of proteins associated with the hallmark pathologies described in AD were analysed for changes in both gene and protein expression in the brains of mice exposed to repeated IP LPS. Environmental stresses, such as those seen from the consumption of diets high in fat content, have been shown to impact on expression levels of AD related proteins such as BACE1 and Tau phosphorylation (Carroll *et al.*, 2011; Meakin *et al.*, 2012). In addition, it has been well established that both APP and BACE1 are strongly expressed in the murine brain (Cole & Vassar, 2007).

Basal levels of *mAPP* were reduced in the hippocampus of *Nrf2*^{-/-}/*hAPP*_{swe} mice (WT saline: 1.00; *Nrf2*^{-/-}/*hAPP*_{swe} saline: 0.880 ± 0.022 ; WT saline vs *Nrf2*^{-/-}/*hAPP*_{swe} saline $p < 0.01$, $n = 4-6$; Figure 4.15 A). Whilst LPS treatment caused a small drop in expression of *mAPP* in WT mice, in *Nrf2*^{-/-}/*hAPP*_{swe} mice an increase in expression was seen bringing levels up to those of saline-treated WT mice (WT LPS: 0.926 ± 0.016 ; *Nrf2*^{-/-}/*hAPP*_{swe} LPS: 0.989 ± 0.038 ; WT saline vs WT LPS $p < 0.05$, *Nrf2*^{-/-}/*hAPP*_{swe} saline vs *Nrf2*^{-/-}/*hAPP*_{swe} LPS $p < 0.05$, $n = 3-6$). Changes in basal expression of *mAPP* were not observed in *Nrf2*^{-/-} mice nor were any changes seen following treatment.

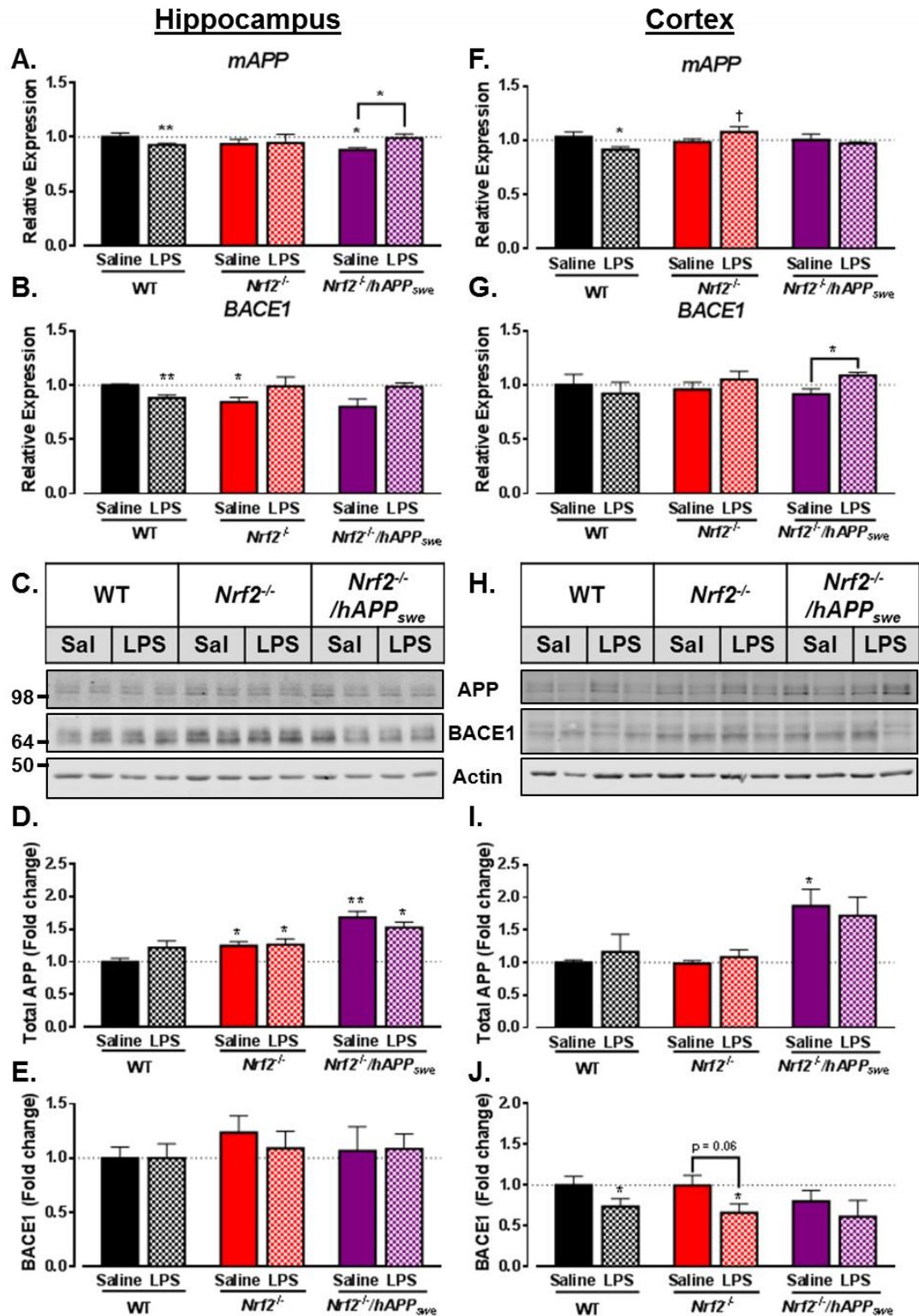


Figure 4.15 Administration of repeated IP LPS reduces BACE1 protein expression in the cortex of adult mice with no effect on APP expression.

Brain tissue collected from adult mice was processed for gene and protein expression. Measures were taken for murine *APP* (A + F) and *BACE1* (B + G) gene expression as well as total APP (human + mouse; D + I) and BACE1 (E + J) protein expression, with C and H showing exemplar blots for the hippocampus and cortex respectively. Data portrayed as means \pm s.e.m. and analysed by one-way and unpaired t-test where * indicates significantly different from saline treated WT control and † indicates significantly different from HF fed WT. *, $p < 0.05$; **, $p < 0.01$; †, $p < 0.05$. WT $n = 6$, *Nrf2*^{-/-} $n = 6-7$, *Nrf2*^{-/-}/*hAPP*_{swe} $n = 3-4$.

The treatment-induced modest decrease in *mAPP* by LPS is maintained in the cortex of WT mice (WT saline: 1.00; WT LPS: 0.914 ± 0.026 ; WT saline vs WT LPS $p < 0.05$, $n = 6$; Figure 4.15 F). As a result, *Nrf2*^{-/-} mice given LPS have a significantly higher level of *mAPP* expression than WT mice given the same treatment with no alteration in basal expression of *mAPP* in *Nrf2*^{-/-} mice (*Nrf2*^{-/-} LPS: 1.08 ± 0.050 ; WT LPS vs *Nrf2*^{-/-} LPS $p < 0.05$, $n = 6-7$). Furthermore, no alteration in expression of cortical *mAPP* was detected in *Nrf2*^{-/-}/*hAPP*_{swe} mice in either treatment group ($p > 0.05$).

With regards to BACE1, basal levels of gene expression in *Nrf2*^{-/-} mice are significantly lower than saline treated WT mice (WT saline: 1.00; *Nrf2*^{-/-} saline: 0.843 ± 0.045 ; WT saline vs *Nrf2*^{-/-} saline $p < 0.05$, $n = 6$; Figure 4.15 B). A similar reduction in *BACE1* is observed in WT mice following treatment with LPS (WT LPS: 0.881 ± 0.029 ; WT saline vs WT LPS $p < 0.01$, $n = 6$). In the cortex, however, no reduction is seen in *BACE1*. Instead, LPS treated *Nrf2*^{-/-}/*hAPP*_{swe} mice show increased expression of *BACE1* in comparison to saline treated mice (*Nrf2*^{-/-}/*hAPP*_{swe} saline: 0.914 ± 0.052 ; *Nrf2*^{-/-}/*hAPP*_{swe} LPS: 1.09 ± 0.030 ; $p < 0.05$, $n = 3-4$; Figure 4.15 G).

When protein expression was evaluated by densitometry from Western blots, as depicted in Figure 4.15 C and H for the hippocampus and cortex respectively; a main effect of genotype was seen in *Nrf2*^{-/-} mice with no additional protein induction following treatment with LPS and no change observed in WT mice (WT saline: 1.00; *Nrf2*^{-/-} saline: 1.25 ± 0.067 ; *Nrf2*^{-/-} LPS: 1.26 ± 0.085 ; WT saline vs *Nrf2*^{-/-} saline $p < 0.05$, WT saline vs *Nrf2*^{-/-} LPS $p < 0.05$, $n = 6$; Figure 4.15 D). *Nrf2*^{-/-}/*hAPP*_{swe} mice had increased levels of total APP in both the hippocampus and the cortex, which is not unexpected and corresponds to the additional expression of the *hAPP*_{swe} protein (hippocampus: *Nrf2*^{-/-}/*hAPP*_{swe} saline: 1.68 ± 0.094 ; *Nrf2*^{-/-}/*hAPP*_{swe} LPS: 1.53 ± 0.085 ; WT saline vs *Nrf2*^{-/-}/*hAPP*_{swe} saline $p < 0.01$, WT saline vs *Nrf2*^{-/-}/*hAPP*_{swe} LPS $p < 0.05$, $n = 3-6$. Cortex: WT saline: 1.00; *Nrf2*^{-/-}/*hAPP*_{swe} saline: 1.87 ± 0.26 ; *Nrf2*^{-/-}/*hAPP*_{swe} LPS: 1.72 ± 0.28 ; WT saline vs *Nrf2*^{-/-}/*hAPP*_{swe} $p < 0.05$, WT saline vs *Nrf2*^{-/-}/*hAPP*_{swe} LPS $p > 0.05$, $n = 3-6$; Figure 4.15 D). Loss of *Nrf2* and treatment with LPS failed to impact on the expression of total APP in the cortex of WT and *Nrf2*^{-/-} mice.

Neither genotype nor treatment altered the levels of BACE1 protein in the hippocampus of adult mice ($p > 0.05$; Figure 4.15). An interesting main effect of treatment was seen in the cortex of LPS treated mice, with treatment significantly attenuating BACE1 protein in both WT and *Nrf2*^{-/-} mice compared to controls (WT saline: 1.00; WT LPS: 0.655 ± 0.12 ; *Nrf2*^{-/-} saline: 0.946 ± 0.15 ; *Nrf2*^{-/-} LPS: $0.536 \pm$

0.099; WT saline vs WT LPS $p < 0.05$, WT saline vs *Nrf2*^{-/-} LPS $p < 0.01$, *Nrf2*^{-/-} saline vs *Nrf2*^{-/-} LPS $p < 0.05$, $n = 6$; Figure 4.15 J). A similar pattern is seen in *Nrf2*^{-/-}/*hAPP*_{swe} mice with a decrease in BACE1 protein, however, this falls short of being statistically significant ($p > 0.05$).

Despite being labelled as the second hallmark pathology for AD and predominantly associated therewith, tauopathies are found in a variety of other dementias and neurodegenerative disorders. A multitude of mutations have been reported for tau; however, even non-mutated tau can be affected by changes in the amyloidogenic pathway. This makes it a worthwhile target to investigate, even when not using a mutant tau transgenic mouse model. Total tau along with a marker for one of its phosphorylation sites were investigated in the hippocampus and cortex of saline and LPS treated mice.

A significant drop in phosphorylation at location Ser396 of tau was seen in *Nrf2*^{-/-} mice under basal conditions, with LPS treatment increasing fold phosphorylation to that of saline-treated controls (WT saline: 1.00; *Nrf2*^{-/-} saline: 0.801 ± 0.068 ; *Nrf2*^{-/-} LPS: 1.03 ± 0.15 ; WT saline vs *Nrf2*^{-/-} saline $p < 0.05$, *Nrf2*^{-/-} saline vs *Nrf2*^{-/-} LPS $p > 0.05$, $n = 9$; Figure 4.16 A). A similar profile was seen for the *Nrf2*^{-/-}/*hAPP*_{swe} mice with lower basal levels of phosphorylation at Ser396 that were increased, albeit non-significantly, following treatment with LPS (WT saline: 1.00; *Nrf2*^{-/-}/*hAPP*_{swe} saline: 0.743 ± 0.063 ; *Nrf2*^{-/-}/*hAPP*_{swe} LPS: 0.885 ± 0.087 ; WT saline vs *Nrf2*^{-/-}/*hAPP*_{swe} saline $p < 0.05$, *Nrf2*^{-/-}/*hAPP*_{swe} saline vs *Nrf2*^{-/-} LPS $p > 0.05$, $n = 3-9$).

However, no significant change is seen in phosphorylation of Tau at Ser396 in the cortex of vehicle or LPS treated mice WT or *Nrf2*^{-/-} mice ($p > 0.05$; Figure 4.16 C). A small drop in tau phosphorylation is still detected in *Nrf2*^{-/-}/*hAPP*_{swe} mice under basal conditions (WT saline: 1.00; *Nrf2*^{-/-}/*hAPP*_{swe} saline: 0.823 ± 0.043 ; WT saline vs *Nrf2*^{-/-}/*hAPP*_{swe} saline $p < 0.05$, $n = 4-9$).

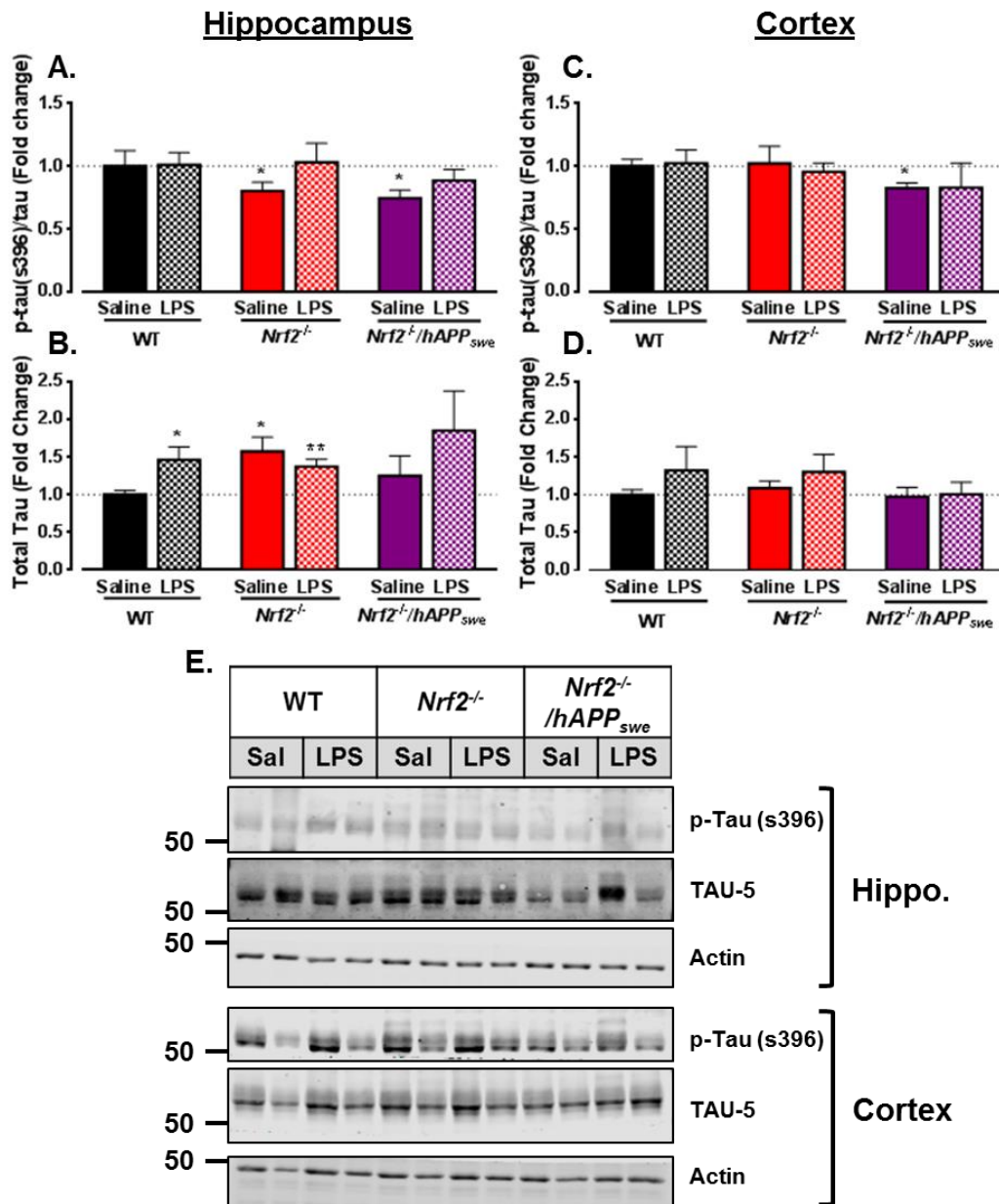


Figure 4.16 Modest changes in phosphorylated and total tau can be seen following LPS treatment of *Nrf2*^{-/-} mice.

Brain tissue collected from adult mice was processed for protein expression. Measures were taken for two tau phosphorylation sites, Ser396 (A and C) and total tau expression (B and D) in both the hippocampus and cortex. E displays exemplar blots for both tissues, where β -actin was used as the protein loading control. Data portrayed as means \pm s.e.m. and analysed by one-way and unpaired t-test where * indicates significantly different from saline treated WT controls. *, $p < 0.05$; **, $p < 0.01$. WT $n = 5-6$, *Nrf2*^{-/-} $n = 6-7$, *Nrf2*^{-/-}/*hAPP*_{swe} $n = 3-4$.

A significant effect of treatment is seen for total tau protein in the hippocampus of WT mice treated with LPS (WT saline: 1.00; WT LPS: 1.46 ± 0.17 ; WT saline vs WT LPS $p < 0.05$, $n = 9$; Figure 4.16 B). Loss of *Nrf2* appears to drive an increase in production of total tau under basal conditions in hippocampal tissue, with little further treatment induced effect from LPS (*Nrf2*^{-/-} saline: 1.57 ± 0.19 ; *Nrf2*^{-/-} LPS: 1.37 ± 0.10 ; WT saline vs *Nrf2*^{-/-} saline $p < 0.05$, WT saline vs *Nrf2*^{-/-} LPS $p < 0.01$, $n = 9$). No significant change in hippocampal total tau protein is seen in *Nrf2*^{-/-}/*hAPP*_{swe} mice, likely hampered by low n-numbers. In contrast, no significant changes are seen in total cortical tau proteins irrespective of genotype and treatment ($p > 0.05$; Figure 4.16 D). This is reflected in the exemplar blots displayed in Figure 4.16 E.

4.11 REPEATED IP INJECTIONS OF LPS DOES NOT IMPACT ON THE PI-3K-DEPENDENT PATHWAY IN THE MOUSE BRAIN

A flurry of recent publications has proposed a role for LPS in the development of obesity and insulin resistance (Cani *et al.*, 2007; Fei & Zhao, 2013), with other work implicating a role for the insulin pathway in AD development and progression (Sly *et al.*, 2001; Sy *et al.*, 2011). We have previously described a link between loss of *Nrf2* and prevention of peripheral diet-induced insulin resistance and dysregulation of glucose management (Meakin *et al.*, 2014). Therefore it was decided to investigate the impact LPS might have on the insulin sensitive PI3-K pathway in hippocampal and cortical brain homogenates. Changes in Akt phosphorylation at the two principle phosphorylation sites were assessed along with the downstream activation of the stress activated NF- κ B pathway. LPS induced no change in phosphorylated protein level at the Ser473 site of Akt in the hippocampus of adult mice in the presence or absence of *Nrf2*, with *Nrf2*^{-/-}/*hAPP*_{swe} mice demonstrating a small but significant drop in phosphorylation of the Ser473 site following LPS treatment (WT saline: 1.00; *Nrf2*^{-/-}/*hAPP*_{swe} LPS: 0.792 ± 0.025 ; WT saline vs *Nrf2*^{-/-}/*hAPP*_{swe} LPS $p < 0.05$, $n = 3-6$; Figure 4.17 A). No significant changes in the level of Ser473 phosphorylated were seen in the cortex, irrespective of genotype and treatment group analysed ($p > 0.05$; Figure 4.17 E).

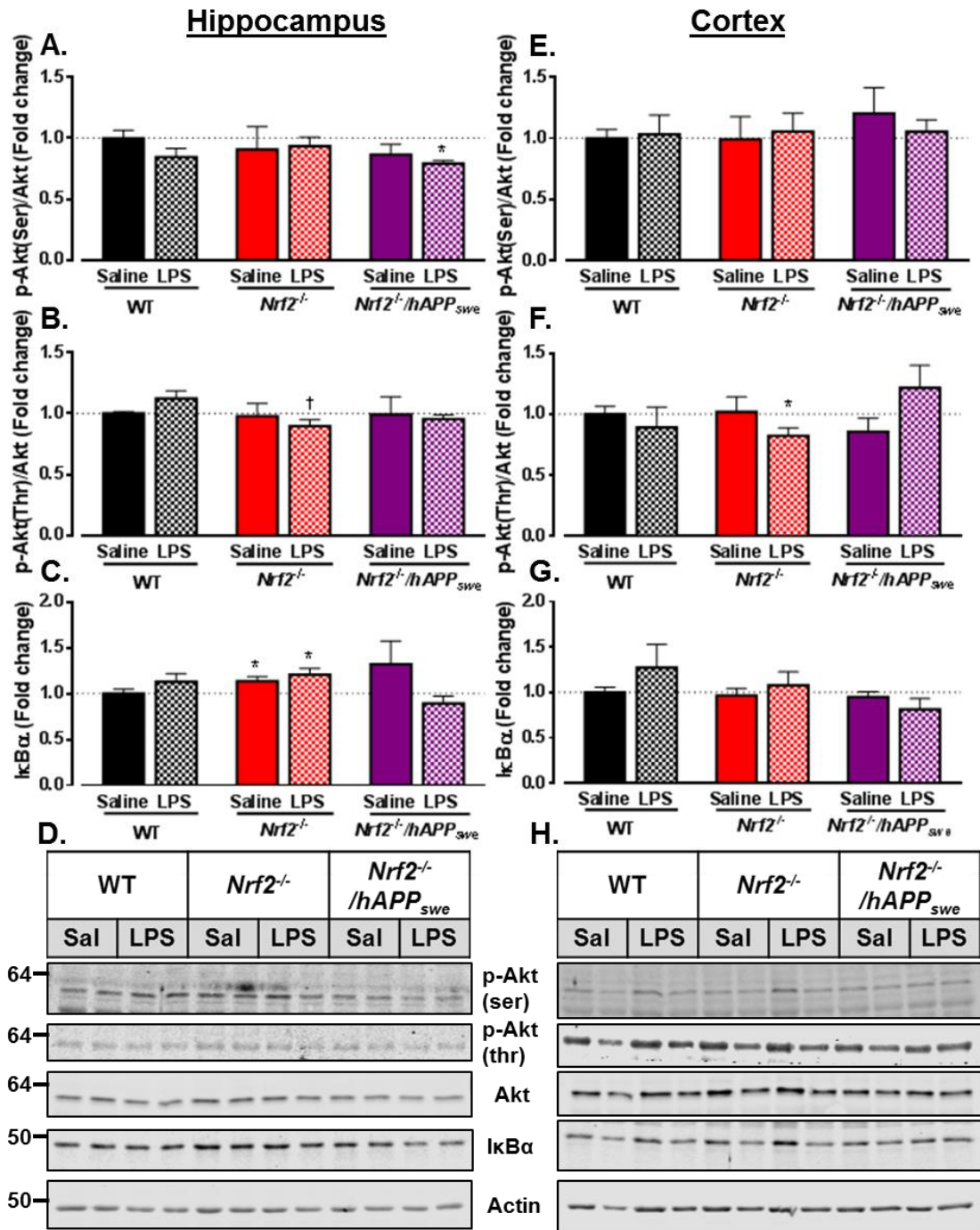


Figure 4.17 Repeated IP LPS has little effect on PI3-K driven Akt phosphorylation or IκBα degradation in the hippocampus and cortex of adult *Nrf2*^{-/-} and mice.

Brain tissue collected from adult mice was processed for gene and protein expression. Measures were taken for relative expression of Akt phosphorylation (Ser473, **A + E**; Thr308, **B + F**), and IκBα (**C + G**) protein expression, with **D** and **H** showing exemplar blots for the hippocampus and cortex respectively. Data portrayed as means ± s.e.m. and analysed by one-way and unpaired t-test where * indicates significantly different from saline treated WT controls and † significantly different from LPS treated WT mice. *, $p < 0.05$, and †, $p < 0.05$. WT $n = 6$, *Nrf2*^{-/-} $n = 4-6$, *Nrf2*^{-/-}/*hAPP*_{swe} $n = 3-4$.

Phosphorylation at the Thr308 site of Akt was assessed, as it can provide an alternative activation pathway. LPS treatment induced a non-significant increase in WT mice when compared to the vehicle group (WT saline: 1.00; WT LPS: 1.12 ± 0.064 ; WT saline vs WT LPS $p > 0.05$, $n = 6$; Figure 4.17 B). A genotype*treatment effect was seen in *Nrf2*^{-/-} mice, with LPS decreasing Akt phosphorylation (Thr308; *Nrf2*^{-/-} LPS: 0.895 ± 0.054 ; WT LPS vs *Nrf2*^{-/-} LPS $p < 0.05$, $n = 6$). A similar phosphorylation decrease was seen in the cortex of LPS-treated *Nrf2*^{-/-} mice (WT saline: 1.00; *Nrf2*^{-/-} LPS: 0.823 ± 0.066 ; WT saline vs *Nrf2*^{-/-} LPS $p < 0.05$, $n = 6$; Figure 4.17 F). Furthermore, in the cortex neither WT nor *Nrf2*^{-/-}/*hAPP*_{swe} mice displayed a significant alteration in the level of phosphorylated Akt (Thr308), irrespective of treatment.

Finally, changes in I κ B α were used as a representation of NF- κ B activation. A small but significant effect of genotype was seen in hippocampal I κ B α in *Nrf2*^{-/-} (WT saline: 1.00; *Nrf2*^{-/-} saline: 1.14 ± 0.052 ; *Nrf2*^{-/-} LPS: 1.21 ± 0.068 ; WT saline vs *Nrf2*^{-/-} saline $p < 0.05$, WT saline vs *Nrf2*^{-/-} LPS $p < 0.05$, $n = 6$; Figure 4.17 C). No further changes were seen in the hippocampus, nor were any significant changes in I κ B α seen in the cortex of saline and LPS treated mice irrespective of genotype ($p > 0.05$; Figure 4.17 G). These changes are depicted in the exemplar blots for both the hippocampus and cortex shown in Figure 4.17 D and H respectively.

4.12 REPEATED IP LPS FAILS TO IMPACT THE GLUTATHIONE PATHWAY IN THE BRAINS OF ADULT MICE

GCLC, a rate-limiting enzyme in the synthesis of GSH, was measured as a means of assessing changes in glutathione production following LPS insult. No change in expression of GCLC was observed in the hippocampus following LPS treatment of WT control mice ($p > 0.05$; Figure 4.18 A). A trend towards decreased production of GCLC was observed in hippocampal lysates from *Nrf2*^{-/-} mice with no significant further effect following injections of LPS (WT saline: 1.00; *Nrf2*^{-/-} saline: 0.756 ± 0.11 ; WT saline vs *Nrf2*^{-/-} saline $p = 0.07$, $n = 6$). Addition of *hAPP*_{swe} demonstrated no further change on GCLC expression upon analysis of *Nrf2*^{-/-}/*hAPP*_{swe} hippocampal lysates ($p > 0.05$). Cortical expression of GCLC showed no alterations in expression in WT or *Nrf2*^{-/-} mice ($p > 0.05$; Figure 4.18 B and C for exemplar blots). Only *Nrf2*^{-/-}/*hAPP*_{swe} mice suggested any change in cortical GCLC expression with a tendency towards lowered GCLC levels following LPS administration (WT saline: 1.00; *Nrf2*^{-/-}/*hAPP*_{swe} LPS: 0.740 ± 0.077 ; WT saline vs *Nrf2*^{-/-}/*hAPP*_{swe} LPS $p = 0.08$, $n = 3-6$).

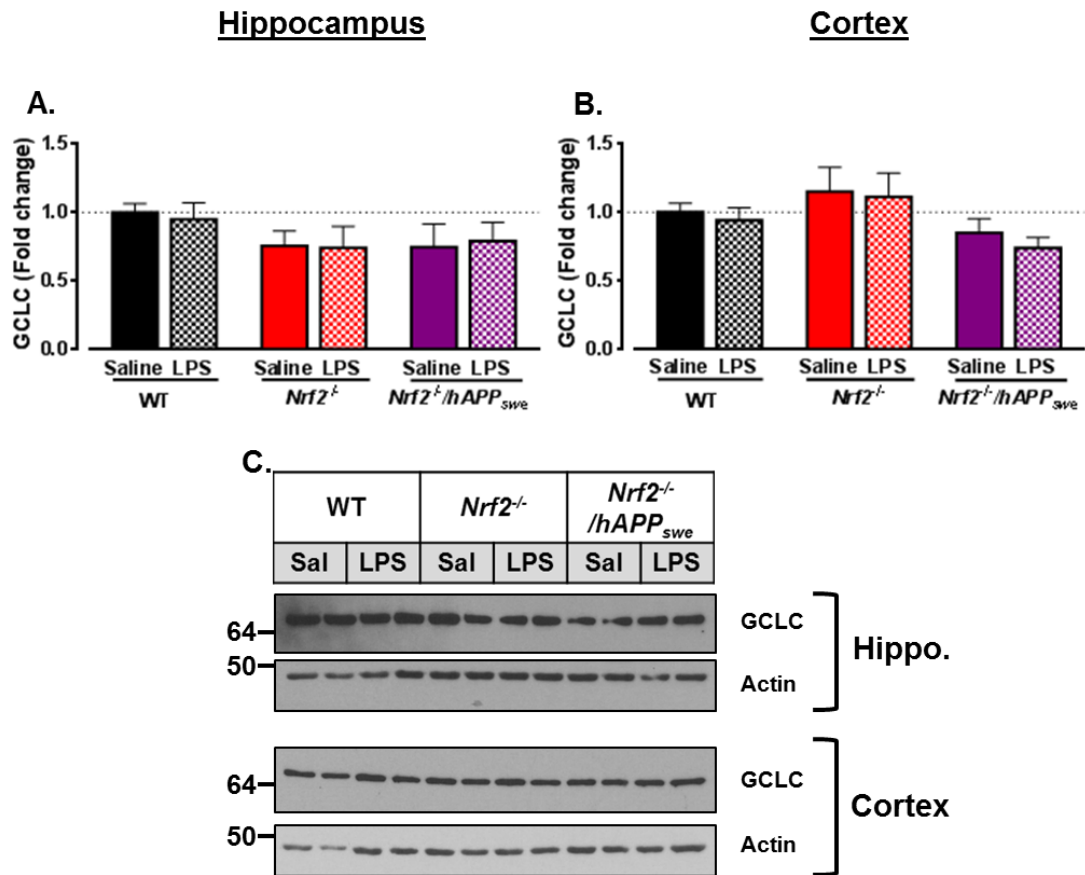


Figure 4.18 Repeated IP LPS does not significantly affect expression of the rate limiting glutathione pathway GCLC enzyme in brain tissue.

Brain tissue collected from adult mice was processed for protein expression and Western blots were probed for the glutathione pathway enzyme GCLC (A + B). C portrays exemplar blots for the hippocampus and cortex respectively. Data portrayed as means \pm s.e.m. and analysed by unpaired t-test. WT n = 6, *Nrf2*^{-/-} n = 6, *Nrf2*^{-/-}/*hAPP*_{swe} n = 3-4.

4.13 REPEATED IP LPS INDUCES BRAIN REGION SPECIFIC INDUCTION OF KEY MAPK MEMBERS

JNK, along with ERK, is one of the most well studied members of the MAPK pathway. It is often induced following activation of common stressor responses, including cytokines. Although there are no known functional difference between the two primary isoforms, JNK46 and JNK54, these were still analysed individually in order to assess whether any isoform specific changes were occurring. A very small but significant decrease in phosphorylation of the JNK54 isoform is seen following treatment of *Nrf2*^{-/-} mice with LPS in the hippocampus with no significant changes seen in the hippocampus of WT or *Nrf2*^{-/-}/*hAPP*_{swe} mice (WT saline: 1.00; *Nrf2*^{-/-} LPS: 0.95 ± 0.020; WT saline vs *Nrf2*^{-/-} LPS *p* < 0.05, *n* = 6; Figure 4.19 A). Furthermore, there was no change from basal phosphorylation of the JNK46 isoform in the hippocampus of any of the cohort groups (*p* > 0.05; Figure 4.19 B). This led to no significant difference in total JNK phosphorylation in the hippocampus in any group (*p* > 0.05; Figure 4.19 C, and G for exemplar blots).

Following analysis of cortical expression, there is a treatment-dependent trend towards increased JNK phosphorylation at the JNK54 isoform in WT and *Nrf2*^{-/-} mice (WT saline: 1.00; WT LPS: 1.49 ± 0.34; *Nrf2*^{-/-} LPS: 1.65 ± 0.36; WT saline vs WT and *Nrf2*^{-/-} LPS *p* > 0.05, *n* = 9; Figure 4.19 D). A non-significant increase in phosphorylation is also seen in *Nrf2*^{-/-}/*hAPP*_{swe} mice given repeated saline injections (*Nrf2*^{-/-}/*hAPP*_{swe} saline: 1.48 ± 0.20; WT saline vs *Nrf2*^{-/-}/*hAPP*_{swe} saline *p* = 0.09, *n* = 4-6). This profile is repeated for the JNK46 isoform in cortical tissue lysates with a trend towards increased p-JNK46 in LPS-treated WT and *Nrf2*^{-/-} mice and increased basal phosphorylation in *Nrf2*^{-/-}/*hAPP*_{swe} mice (*Nrf2*^{-/-}/*hAPP*_{swe} saline: 1.44 ± 0.14; WT saline vs WT and *Nrf2*^{-/-} LPS *p* > 0.05, WT saline vs *Nrf2*^{-/-}/*hAPP*_{swe} saline *p* = 0.05, *n* = 4-9; Figure 4.19 E). LPS treated *Nrf2*^{-/-} and *Nrf2*^{-/-}/*hAPP*_{swe} mice treated with vehicle were both shown to have a trend towards increased levels of total JNK phosphorylation (WT saline: 1.00; *Nrf2*^{-/-} LPS: 1.53 ± 0.30; *Nrf2*^{-/-}/*hAPP*_{swe} saline: 1.44 ± 0.14; WT saline vs *Nrf2*^{-/-} LPS *p* > 0.05, WT saline vs *Nrf2*^{-/-}/*hAPP*_{swe} saline *p* = 0.05, *n* = 4-9; Figure 4.19 F, and G for exemplar blots).

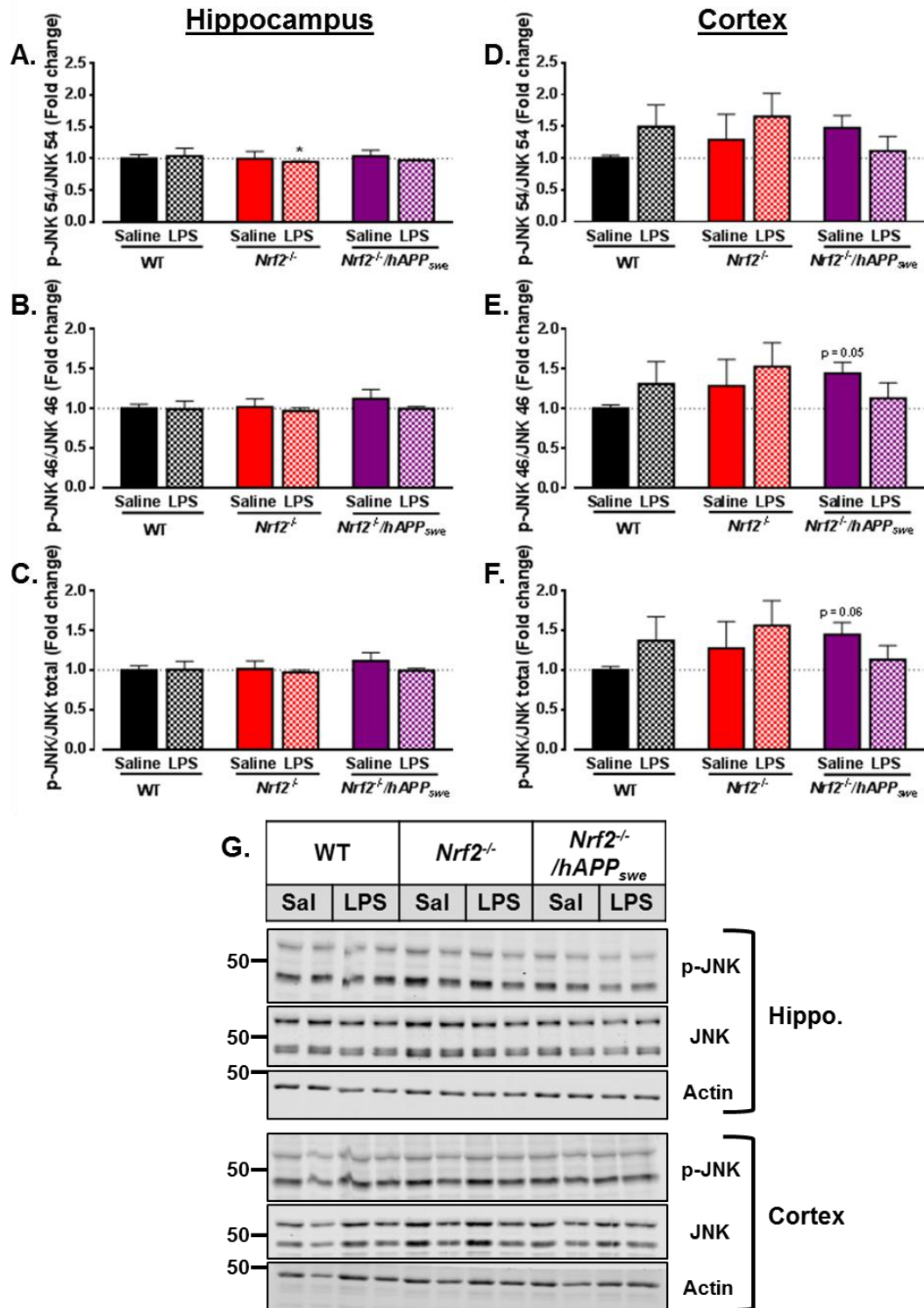


Figure 4.19 *Nrf2*^{-/-} and WT mice show a mild induction of SAPK/JNK in the cortex following repeated IP LPS injections

Brain tissue collected from adult mice was processed for protein expression and run on Western blots. Membranes were probed for phosphorylated (Thr183/Tyr185) and total JNK. A ratio of phosphorylated to total protein was calculated for p54 JNK (A and D), p46 JNK (B and E) and total JNK (C and F) in the hippocampal and cortical protein homogenates. G portrays exemplar blots for both the hippocampus and cortex. Data portrayed as means \pm s.e.m. and analysed by one-way and unpaired t-test. WT n = 6-9, *Nrf2*^{-/-} n = 6-9, *Nrf2*^{-/-}/*hAPP*_{swe} n = 3-4.

Having previously described HF dependent changes in the dual-phosphorylation of the MAPK ERK, we were keen to assess the impact of an alternative stress pathway on MAPK phosphorylation *via* administration of LPS. In the hippocampus, a trend towards a treatment-dependent increase in ERK 1 and ERK 2 phosphorylation was seen in WT mice treated with LPS (ERK 1: WT saline: 1.00; WT LPS: 1.28 ± 0.13 ; WT saline vs WT LPS $p = 0.06$, $n = 9$; Figure 4.20 A. ERK 2: WT saline: 1.00; WT LPS: 1.58 ± 0.27 ; WT saline vs WT LPS $p = 0.06$, $n = 9$; Figure 4.20 B). In addition, *Nrf2*^{-/-} mice revealed significantly increased basal phosphorylation of ERK 1 (*Nrf2*^{-/-} saline: 1.48 ± 0.18 ; WT saline vs *Nrf2*^{-/-} saline $p < 0.05$, $n = 8-9$) which fell just short of significant for ERK 2 (*Nrf2*^{-/-} saline: 1.80 ± 0.36 ; WT saline vs *Nrf2*^{-/-} saline $p = 0.06$, $n = 8-9$).

And finally whilst *Nrf2*^{-/-}/*hAPP*_{swe} mice described what appeared to be a treatment-induced increase in both ERK 1 and ERK 2 phosphorylation, this failed to become significant (ERK 1: *Nrf2*^{-/-}/*hAPP*_{swe} saline: 1.60 ± 0.31 ; *Nrf2*^{-/-}/*hAPP*_{swe} LPS: 1.92 ± 0.44 ; WT saline vs *Nrf2*^{-/-}/*hAPP*_{swe} saline and LPS $p > 0.05$, $n = 3-9$. ERK 2: *Nrf2*^{-/-}/*hAPP*_{swe} saline: 2.16 ± 0.80 ; *Nrf2*^{-/-}/*hAPP*_{swe} LPS: 2.90 ± 0.84 ; WT saline vs *Nrf2*^{-/-}/*hAPP*_{swe} saline and LPS $p > 0.05$, $n = 3-9$). These findings were recapitulated when total ERK 1/2 phosphorylation was assessed with a treatment-dependent increase seen in WT mice and genotype-dependent increases seen in both *Nrf2*^{-/-} and *Nrf2*^{-/-}/*hAPP*_{swe} mice (WT saline: 1.00; WT LPS: 1.48 ± 0.22 ; *Nrf2*^{-/-} saline: 1.72 ± 0.30 ; *Nrf2*^{-/-}/*hAPP*_{swe} saline: 1.99 ± 0.62 ; *Nrf2*^{-/-}/*hAPP*_{swe} LPS: 2.60 ± 0.69 ; WT saline vs WT LPS $p = 0.06$, WT saline vs *Nrf2*^{-/-} saline $p < 0.05$, WT vs *Nrf2*^{-/-}/*hAPP*_{swe} saline and LPS $p > 0.05$, $n = 3-9$; Figure 4.20 C and see G for blot exemplars).

Cortical ERK 1 shows a treatment-dependent increase in phosphorylation in *Nrf2*^{-/-} mice administered LPS (WT saline: 1.00; *Nrf2*^{-/-} LPS: 1.88 ± 0.38 ; WT saline vs *Nrf2*^{-/-} LPS $p < 0.05$, $n = 9$; Figure 4.20 D), with a similar trend seen in WT mice ($p > 0.05$). No significant change is seen in phosphorylation levels of either ERK 1 or ERK 2 in *Nrf2*^{-/-}/*hAPP*_{swe} mice, although there is a trend for increased basal phosphorylation of both (ERK 1: *Nrf2*^{-/-}/*hAPP*_{swe} saline: 1.85 ± 0.35 ; WT vs *Nrf2*^{-/-}/*hAPP*_{swe} saline $p = 0.09$, $n = 4-9$; Figure 4.20 D. ERK 2: *Nrf2*^{-/-}/*hAPP*_{swe} saline: 1.73 ± 0.37 ; WT vs *Nrf2*^{-/-}/*hAPP*_{swe} saline $p > 0.05$, $n = 4-9$; Figure 4.20 E).

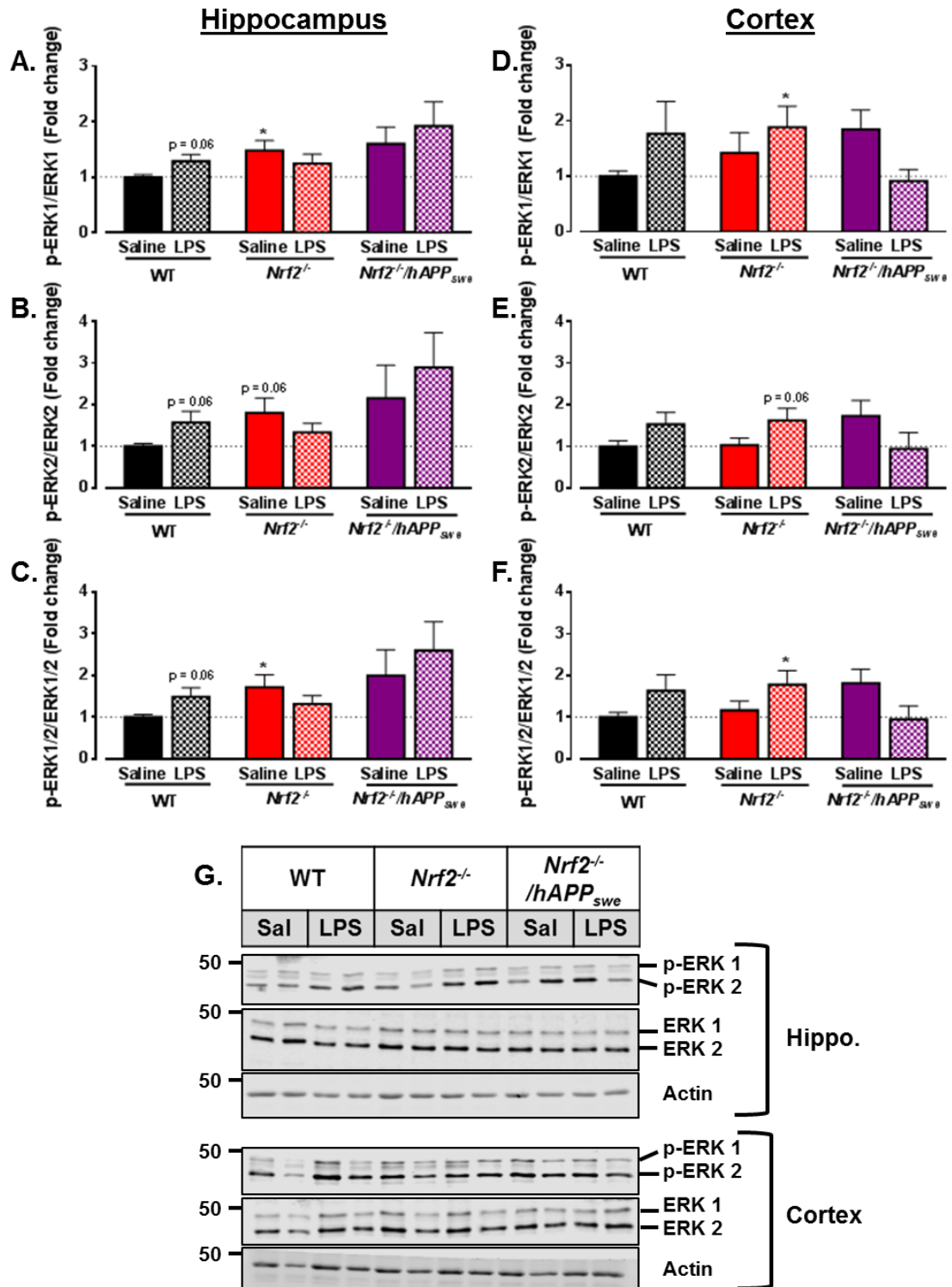


Figure 4.20 Transgenic mouse models lacking *Nrf2* show a trend towards increased ERK 1 and 2 MAPK phosphorylation with brain region dependent responses to peripheral LPS treatment.

Brain tissue was harvested from mice and processed for protein expression by Western blot. Measures were taken for relative expression of phosphorylated (Thr202/Tyr204) and total ERK1 (A + D), ERK2 (B + E) and combined ERK1/2 MAPK expression (C + F) in the hippocampus and cortex of mice, with G showing exemplar blots for the hippocampus and cortex respectively. Data portrayed as means \pm s.e.m. and analysed by one-way and unpaired t-test. WT n = 9, *Nrf2*^{-/-} n = 9, *Nrf2*^{-/-}/*hAPP*_{swe} n = 3-4.

This phosphorylation profile is largely matched by that of ERK 2, with a treatment-dependent induction seen in WT and *Nrf2*^{-/-} mice which falls just short of significance (WT saline: 1.00; WT LPS: 1.53 ± 0.29; *Nrf2*^{-/-} LPS: 1.63 ± 0.29; WT saline vs WT LPS $p > 0.05$, WT saline vs *Nrf2*^{-/-} saline $p = 0.06$, $n = 9$; Figure 4.20 E). With no noteworthy differences in the phosphorylation of ERK 1 and ERK 2, total ERK phosphorylation maintains the same features as those shown for the individual isoforms with a treatment driven effect in WT and *Nrf2*^{-/-} mice and a basal genotype driven increase in *Nrf2*^{-/-}/*hAPP*_{swe} mice (WT saline: 1.00; WT LPS: 1.64 ± 0.38; *Nrf2*^{-/-} LPS: 1.78 ± 0.34; WT saline vs WT LPS $p > 0.05$, WT saline vs *Nrf2*^{-/-} saline $p = 0.06$, $n = 9$; *Nrf2*^{-/-}/*hAPP*_{swe} saline: 1.82 ± 0.33; WT saline vs WT LPS $p > 0.05$, WT saline vs *Nrf2*^{-/-} LPS $p < 0.05$, WT saline vs *Nrf2*^{-/-}/*hAPP*_{swe} saline $p = 0.09$, $n = 4-9$; Figure 4.20 F and see G for exemplar blots).

4.14 LPS AND *NRF2*^{-/-} SIGNIFICANTLY IMPACT ON BRAIN DERIVED MITOCHONDRIAL HEALTH IN ADULT MICE

Previous work has described links between LPS-induced inflammatory responses and increased mitochondrial dysfunction (Nakanishi *et al.*, 2011; Nicholas *et al.*, 2011). In addition, work done by Piantadosi and colleagues (2011) suggests a link between Nrf2 and both mitochondrial biogenesis and mitochondrial response to inflammatory insult in the liver; whilst induction of Nrf2 is protective following induction of mitochondrial stress (Shih *et al.*, 2005). To assess whether peripherally administered LPS could impact mitochondria located within the brain regions of the hippocampus and cortex, commonly utilised markers for mitochondrial health and mitophagy were assessed in WT and *Nrf2*^{-/-} mice repeatedly treated peripherally with LPS or saline.

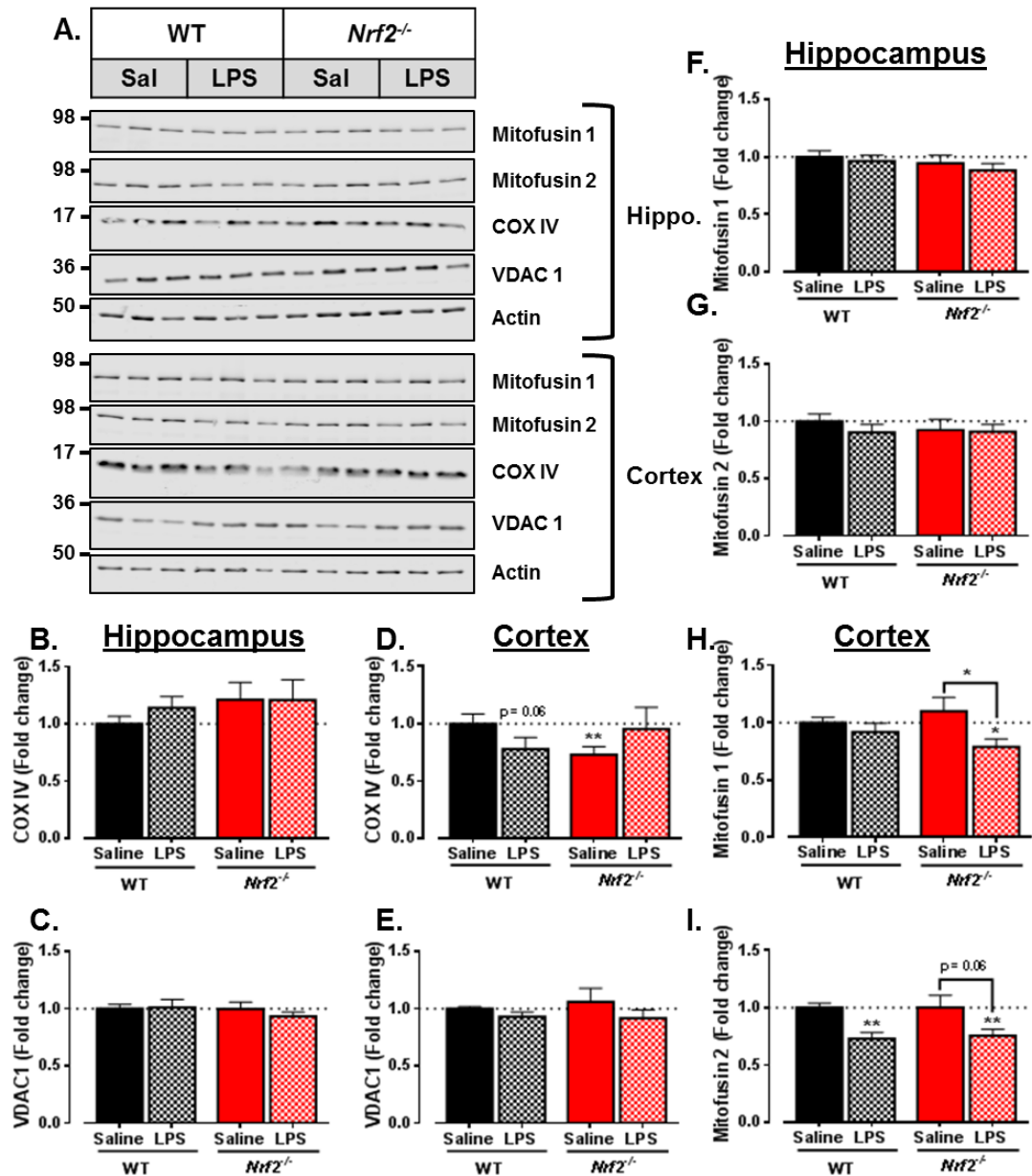


Figure 4.21 Loss of *Nrf2* and repeated LPS injections both impact on mitochondrial health and mitophagy markers.

Brain tissue was harvested from mice and processed for protein expression by Western blot as previously described using whole lysates, with exemplars shown in **A** where β -actin was used as the protein loading control. Measures were taken for relative expression of COX IV (**B** + **C**), VDAC 1 (**D** + **E**), mitofusin 1 (**F** + **H**) and mitofusin 2 (**G** + **I**) in the hippocampus and cortex of RC and HF fed WT and *Nrf2*^{-/-} mice. Data portrayed as means \pm s.e.m. and analysed by one-way and unpaired t-test where * indicates significance between groups. *, $p < 0.05$; **, $p < 0.01$, ***, $p < 0.001$. WT $n = 6$, *Nrf2*^{-/-} $n = 6$.

In the hippocampus, neither of the outer mitochondrial membrane markers, COX IV and VDAC 1, are affected by administration of peripheral LPS ($p > 0.05$; Figure 4.21 B and C respectively and A for exemplar blots). However, *Nrf2*^{-/-} mice demonstrate a trend towards an effect of genotype with increased expression of COX IV in both treatment groups (WT saline: 1.00; *Nrf2*^{-/-} saline: 1.21 ± 0.15 ; *Nrf2*^{-/-} LPS: 1.21 ± 0.18 ; WT saline vs *Nrf2*^{-/-} saline and LPS $p > 0.05$, $n = 9$). An effect of genotype is seen following loss of *Nrf2* in the cortex, with a significant decrease in COX IV (WT saline: 1.00; *Nrf2*^{-/-} saline: 0.730 ± 0.071 ; WT saline vs *Nrf2*^{-/-} saline $p < 0.05$, $n = 9$; Figure 4.21 D). Furthermore, a genotype*treatment effect is observed following repeated peripheral injections with LPS, depicted by a decrease in COX IV levels in WT mice but an increase in those of *Nrf2*^{-/-} mice (WT LPS: 0.781 ± 0.10 ; *Nrf2*^{-/-} LPS: 0.952 ± 0.19 ; WT saline vs WT LPS $p = 0.06$, *Nrf2*^{-/-} saline vs *Nrf2*^{-/-} LPS $p > 0.05$, $n = 9$). Neither genotype nor treatment significantly affects levels of the mitochondrial channel marker VDAC1 ($p > 0.05$; Figure 4.21 E).

Mitofusin proteins are essential in the correct progression of mitochondrial fusion. Increases in mitochondrial fusion can lead to elongation of the mitochondria, whilst decreases can lead to mitochondrial fragmentation through mitochondrial fission. Mitochondrial fission and fusion are key in balancing the dynamic changes in mitochondrial state essential for their proper function (Westermann, 2012). Imbalance in either of these processes can cause cell death, increased ROS production and impaired mitochondrial function. Neither mitofusin 1 nor mitofusin 2, when measured in the hippocampus of WT and *Nrf2*^{-/-} mice, show a significant change in protein levels irrespective of treatment (mitofusin 1: $p > 0.05$, $n = 9$; Figure 4.21 F. Mitofusin 2: $p > 0.05$, $n = 9$; Figure 4.21 G.). Finally, cortical mitofusin 1 is significantly lowered in the lysates of *Nrf2*^{-/-} mice treated with LPS, whilst no change is seen in WT mice even after LPS treatment (WT saline: 1.00; *Nrf2*^{-/-} saline: 1.10 ± 0.12 ; *Nrf2*^{-/-} LPS: 0.790 ± 0.070 ; WT saline vs *Nrf2*^{-/-} LPS $p < 0.05$, *Nrf2*^{-/-} saline vs *Nrf2*^{-/-} LPS $p < 0.05$, $n = 9$; Figure 4.21 H). In contrast, a main effect of treatment is seen for Mitofusin 2, with both WT and *Nrf2*^{-/-} mice treated with LPS displaying a decrease in protein (WT saline: 1.00; WT LPS: 0.730 ± 0.054 ; *Nrf2*^{-/-} saline: 1.00 ± 0.11 ; *Nrf2*^{-/-} LPS: 0.757 ± 0.055 ; WT saline vs WT LPS $p < 0.05$, WT saline vs *Nrf2*^{-/-} LPS $p < 0.05$, *Nrf2*^{-/-} saline vs *Nrf2*^{-/-} LPS $p = 0.06$, $n = 9$; Figure 4.21 I). Previous work has shown Mitofusin 1 and, in particular, Mitofusin 2 to be of importance in the targeting of mitochondria for degradation (Leboucher *et al.*, 2012). As a result, peripheral LPS may be targeting mitochondria for degradation, potentially impacting on brain bioenergetics.

4.15 DISCUSSION

4.15.1 The Effects of *Nrf2*^{-/-} and LPS-Induced Inflammation on Behaviour May Highlight a Hippocampal-Dependent Memory Impairment

LPS is frequently used in research to investigate the effects of inflammation and infection on disease pathways. Given the important role played by the spleen in the production of blood born immune cells in response to an immune challenge, the significant increase in spleen size following LPS treatment is a positive marker of an induction of peripheral inflammation in our mice. In addition treatment-dependent increases in liver size may also be attributable to activation of a peripheral inflammatory state due to the liver's key role in detoxification. Previous work has reported an effect of LPS on weight, with animals administered LPS demonstrating treatment-dependent weight loss (Henry *et al.*, 2008). Examination of weight change in our mouse cohort support this finding, with LPS treated mice showing acute weight loss in response to LPS injections. There was, however, no significant effect of genotype on the degree of weight-loss seen. This would indicate that the effects of LPS on weight loss are not directly related to the altered inflammatory response seen in mice lacking *Nrf2*, but rather on the well documented sickness behaviour often associated with LPS treatment. In addition, a stabilisation in body weight was observed which may be indicative of LPS tolerance. Previous studies have indicated an exacerbated response to LPS with ageing in mouse models (Godbout *et al.*, 2007). The inability of our LPS-treated mice to make a return to baseline weight, as demonstrated by the maintained weight-loss on the final day of the study, may result from this aggravated stimulus response. However, due to the amount of weight-loss recorded, the short duration of the study is likely to have been insufficient to expect those mice treated with LPS to make up the weight deficit.

Memory impairments, sometimes in combination with changes from normal behaviour, are the predominant symptoms that prompt the diagnosis of dementia, with the majority of dementia cases subsequently attributed to AD. As a result of this, tasks assessing learning and memory have played an important role not only in the clinic, where they are used to assess disease progression and the effectiveness of novel therapeutics, but also in the assessment of animal models of dementia and AD. Many rodent behavioural tasks have been designed with the idea of modelling different aspects of cognition known to be affected in AD (see chapter 4.1 for some examples).

These tasks can be subdivided into categories based on the type of memory and behaviour tested and the resultant primary linked brain region.

Much of the AD-related cognition work performed to date has made use of transgenic mice carrying either one or more of the mutations associated with FAD. From these models it has been possible to show that many demonstrate impaired cognitive behaviour over time in a variety of commonly assessed tasks. The case for inflammation-induced cognitive impairment is already well defined with several groups showing alterations in learning following a variety of inflammatory challenges. Some of which, such as LPS, have been shown to worsen cognitive performance with ageing (Kohman *et al.*, 2007). However, despite the recent interest in Nrf2 with regards not only to AD but also to PD and other neurodegenerative disorders and the availability of transgenic knockout mouse models, there is very little published work investigating the impact of Nrf2 loss on cognition. As our interest in the *Nrf2*^{-/-} model is based on the potential role of Nrf2 in AD, we made use of a small selection of tasks to assess any impact on cognition that global loss of Nrf2 may have caused. In addition, we assessed a small number of the novel double transgenic model which incorporated both a loss of *Nrf2* and the addition of *hAPP*_{swe}; unfortunately genotyping issues (see Chapter 2.2.5.2) resulted in insufficient mice in each group to allow for them to be incorporated into the behavioural analysis.

As described previously, NOR is classed as a recognition memory task and is one of the more commonly used tasks. We found that repeated peripheral LPS treatment impaired the ability of mice to successfully differentiate novelty in the NOR test, whilst saline-treated animals performed to a similar capacity irrespective of genotype. This response profile was altered when short-term OL recognition tasks were performed instead of NOR. Here, mice deficient in Nrf2 appeared completely incapable of performing the task under basal conditions in contrast to their saline-treated WT counterparts. This impaired response in the *Nrf2*^{-/-} was similar to that seen in WT mice following peripheral treatment with LPS. This suggests loss of Nrf2 alone is sufficient to negatively impact on important AD related brain regions.

NOR, when lacking additional factors such as place and context, is no longer believed to require a fully functional hippocampus for task completion (Langston *et al.*, 2010) as demonstrated by studies using specific lesion models (Lee *et al.*, 2005). Instead, the recognition memory required for successful participation in the NOR task is believed to be centred in the perirhinal cortex region of the MTL where short-term

memory retention is thought to be seated (Reger *et al.*, 2009). Studies using lesion models of the perirhinal-postrhinal cortex and/or the hippocampus in behavioural paradigms for both spatial memory (Morris water maze, Radial maze, etc.) and spontaneous object recognition (NOR task variants) strongly suggest a distinctive task-related regional involvement. Animals with hippocampal lesions present with intact basic object recognition but severely impaired spatial memory whilst the inverse is observed in those that have undergone perirhinal-postrhinal cortical lesions (Bussey *et al.*, 1999; Winters *et al.*, 2004). Whilst these findings have not been unanimous in nature, it has been suggested that studies implicating the hippocampus in spontaneous object recognition should be evaluated with care. Replication of certain lesion models previously implicating the hippocampus have been reported to occur alongside decreased exploration, which may act as a confounding factor on the evaluation of task completion and falsely implicate the lesioned area as necessary for the successful completion of basic object recognition (Ainge *et al.*, 2006). It is also worth noting there remains some debate regarding long-term NOR, where there is a requirement for recollection that may involve additional brain regions. Studies performed using hippocampal lesion models have both supported and opposed a role for the hippocampus in memory retention (Hammond *et al.*, 2004; Forwood *et al.*, 2005), with some recent research advocating a role for the hippocampus in object recency memory instead (Albasser *et al.*, 2012).

In contrast, OL tasks, which rely on the integration of both recognition memory and spatial orientation, may more heavily involve the hippocampus in their encoding and retention (Barker & Warburton, 2011). However, the variation on OL task described here, sometimes referred to as an object-place task, is currently thought to be centred within the entorhinal cortex (Wilson *et al.*, 2013), further supported by the lack of hippocampal involvement shown by Langston & Wood (2010). As such it may be of particular relevance for the further study of AD models, given that many of the initial pathological changes associated with AD are believed to occur within the entorhinal cortex. In addition, the behavioural pattern recorded here in *Nrf2*^{-/-} mice reflects that seen by Wilson *et al.* in their entorhinal cortex lesion model further supporting a role for entorhinal cortex impairment in these mice. This subtle difference in the brain region believed to play the dominant role in these tasks may help to explain the inability of *Nrf2*^{-/-} mice to fulfil the OL task (entorhinal cortex) whilst maintaining a similar cognitive ability to WT in the NOR task (perirhinal cortex). Furthermore, future research may benefit from specifically dissecting out the entorhinal region of the cortex

instead of the mixed cortical subdivision region overlaying the hippocampus that was dissected here, which will not incorporate the full entorhinal region.

Finally, SA was performed in a closed arm elevated plus maze. This task can provide a different insight into the cognitive capacity of the model under consideration. The SA task, as described previously, has been reported to rely on any of spatial working memory, dead reckoning, self-movement cues and/or response strategies rather than the recognition memory needed for the NOR and OL tasks (McNay *et al.*, 2000; Lennartz, 2008; Hargrave *et al.*, 2015). In addition, it can provide a measure of locomotor ability by quantifying the number of arm entries performed within a finite time period. We saw no significant difference in SA, extrapolated from the continuous spontaneous alternation task, in any of the groups analysed at the time of testing. Furthermore, when tested no significant difference in locomotion was seen as measured by the number of arm entries performed, even following repeated LPS treatment. Joshi *et al.* (2014) also failed to find a difference in SA in a 3x Tg model of AD treated with LPS twice a week for six weeks suggesting this type of task may not be affected following treatment with LPS. Taken together this indicates that aged *Nrf2*^{-/-} mice may have an entorhinal cortex-dependent cognitive impairment demonstrated by their inability to perform the OL task, with no impairment to the perirhinal cortex.

4.15.2 Inflammation and Cytokine Expression May Suggest a Role for Immune Cell Priming and Inflammasome Activation

As predicted, examination of *Nrf2*^{-/-} mice showed an increased central inflammatory response to peripheral LPS treatment in keeping with previous *in vitro* and *in vivo* work using acute LPS stimulation (Thimmulappa *et al.*, 2006). Increased basal expression of pro-inflammatory *IL-1 β* in the hippocampus occurred in conjunction with increased protein carbonylation and increased *F4/80* expression in mice lacking *Nrf2*^{-/-} when compared to the hippocampus of age-matched WT mice. In contrast, the cortex of *Nrf2*^{-/-} mice undergoes less basal inflammatory priming with only a small increase in *IL-1 β* documented. Peripheral activation of the immune system by repeated LPS is able to induce a central inflammatory state in line with other published research (Henry *et al.*, 2009; Bian *et al.*, 2013; Biesmans *et al.*, 2013; Thomson *et al.*, 2014). In the hippocampus this is depicted by increased pro-inflammatory *IL-1 β* as well as anti-inflammatory *MRC1* expression combined with increases in *F4/80* expression as well as the chemokine *MCP-1* in WT mice. Loss of *Nrf2* in the hippocampus results in an aggravated response to a peripheral LPS-induced inflammatory challenge with further

induction of *IL-1 β* and *F4/80* above that displayed basally, combined with an increased presence of anti-inflammatory markers such as *MRC1* and *YMI*. And whilst a small increase in pro-inflammatory markers such as *IL-1 β* and protein carbonylation is seen in the cortex of *Nrf2*^{-/-} mice, this goes hand in hand with an increased anti-inflammatory profile (*Arg1*, *MRC-1*) with *YMI* being increased over and above that seen in WT mice.

It has been previously reported that there can be age-dependent changes in the sensitivity and susceptibility of mice to LPS (Tateda *et al.*, 1996; Kohman *et al.*, 2007; Chen *et al.*, 2008; Henry *et al.*, 2009). Research has indicated this holds true for mouse models of AD, with mice carrying the *hAPP*_{swe} gene driven by the hamster prion protein (PrP) promoter showing increased basal inflammation with ageing combined with an aggravated response to acute LPS (Sly *et al.*, 2001). Work done by Ifuku and colleagues (2012) has since shown a prolonged induction of IL-1 β in combination with TNF- α in both the hippocampus and cortex of C57/Bl6J mice of a similar age to those used in the above cohort which differs from what we have reported here. However, although LPS was administered daily in a similar manner to that described here, the dose of LPS used was more than double that used for our cohort. This alone may account for the altered cytokine profile described.

Limited research has been published to date looking at the changes in inflammation in the brains of mice lacking functional Nrf2. Of this, even less has investigated the effect of an inflammatory stimulus such as LPS on this transgenic background. However, activation of Nrf2 has been suggested as being protective in fighting against LPS-induced damage and inflammation in the brain and purified microglial cells (Lee *et al.*, 2014; Qin *et al.*, 2015). Loss of Nrf2 is implicated in an aggravated immune response to acute LPS treatment both *in vivo* and *in vitro* in isolated immune cells (Innamorato *et al.*, 2008; Kong *et al.*, 2010). It is possible that the lack of significant change in some of the markers commonly associated with inflammation, such as *TNF- α* , may be in part due to the development of a so-called adaptive response or tolerance which has previously been described in chronic models of LPS infection (Morris & Li, 2012). Furthermore, whilst acute activation of astrocytes has been reported in response to LPS administration, repeated LPS treatments have been demonstrated to result in reduced levels of GFAP expression further promoting the potential for a tolerance response (Biesmans *et al.*, 2015). In addition, the duration of time between LPS administration and tissue harvest has been shown to influence the fluctuations in cytokine levels reported, with both acute and variations on repeated

injection models demonstrating time dependent alterations in cytokine profile (Erickson & Banks, 2011). However, it is worth noting that this tolerance effect is not necessarily indicative of an improved state of health as it can be linked with immunosuppressive pathology. With a decrease in synaptophysin in the cortex of LPS-treated mice, it would be foolish to assume that the improved inflammatory profile was indicative of cellular health. Nevertheless, it is clear from the data presented that not all immune signalling has been curbed following chronic administration of LPS as there is clearly a maintained upregulation in IL-1 β signalling in addition to glial cell activation.

IL-1 β signalling, as previously described (see chapter 1.5.3.1), is an important modulator of the body's pro-inflammatory response. It has been shown to activate and be released from a variety of immune cells, including macrophages, in addition to resident brain cells such as astrocytes and microglia under conditions of gliosis (Goshen & Yirmiya, 2009). IL-1 β is capable of activating a multitude of immune-related pathways including the stress-related NF- κ B pathway and members of the MAPK family, such as JNK. Activation of the PRR TLRs by PAMP (e.g. LPS) and DAMP (e.g. A β) compounds is known to induce IL-1 β release through priming of inflammasomes, as is initiation of the complement cascade. Instigation of many of these pathways causes positive feedback enabling further production and transcription of IL-1 β , producing a self-perpetuating state unless interrupted. There are a variety of points at which this signalling can be affected and these can include sequestration of PAMP receptors such as TLR4, activation of 'signal transducer and activator of transcription 3' signalling as well as increased specific DUSP activity downregulating the MAPK stress response. One of the most important mediating factors, however, is the inhibition of inflammasome production as this has recently been shown to promote the propagation of inflammation from cell to cell (Franklin *et al.*, 2014). The presence of inflammasomes has also been corroborated in both *in vitro* and *in vivo* models of AD, whilst post-mortem tissue from AD patients showed elevated cleaved caspase-1 in both the frontal cortex and hippocampus (Heneka *et al.*, 2013; Sheedy *et al.*, 2013). In light of the results described above, it would be of particular interest to see if the exacerbated IL-1 β signalling seen in *Nrf2*^{-/-} mice is down to increased inflammasome production and whether this occurs in an age dependent manner. In support of a role for inflammasome activation, recent work into treatment of rheumatoid arthritis has put forward a role for Nrf2 activation and the subsequent antioxidant gene activation in the suppression of both NLRP3 and NLRC4 inflammasomes in bone marrow derived macrophages (BMDM; Rzepecka *et al.*, 2015). However, decreased expression of *NLRP3* and *NLRC4*

were also seen under basal conditions in the BMDMs derived from *Nrf2*^{-/-} mice, indicating the involvement of a more complex mechanism than may have initially been hypothesised.

4.15.3 Seven Day LPS Exposure Induced Little Change in AD-Related Proteins

A role for inflammation has already been suggested in the development and progression of neurodegenerative disease and a variety of studies have suggested an effect of LPS on amyloid production *in vitro* (Spitzer *et al.*, 2010). We failed to see an increase in BACE1 protein following LPS treatment, with cortical lysates even reporting a drop in BACE1 levels following treatment with LPS. In addition, despite a small reduction in the gene expression of both *mAPP* and *BACE1* in the hippocampus of WT mice treated with LPS, this did not translate to any treatment dependent alteration in protein levels. Activation of BACE1 following the application of common stressors has been established using a variety of different models (Cole & Vassar, 2007). It is possible that the increased anti-inflammatory profile combined with the decrease in protein levels are in accordance with the development of LPS tolerance and an associated move towards resolution of the inflammatory state. This may then be present at a more advanced stage in the cortex than in the hippocampus. In addition, despite a small induction in APP protein levels in the hippocampus of *Nrf2*^{-/-} mice, no effect of treatment was observed in either tissue. Furthermore, although an increase in APP expression is seen in the *Nrf2*^{-/-}/*hAPP*_{swe} this corresponds with the added insertion of *hAPP* and there is no indication of further amplification following LPS treatment. Indeed, a similar BACE1 profile is seen to that of the other groups with a decrease in BACE1 in the cortex following treatment.

In keeping with what we found, a study published by Kitazawa and colleagues (2005) showed no effect of LPS on amyloid-related markers in a 3x Tg AD mouse model but instead reported increased tau phosphorylation, which has since been supported by additional studies (Sy *et al.*, 2011). This is in contrast to work done by Sheng *et al.* (2003), who reported increased APP expression as well as an increase in A β accumulation in twelve month old PrP driven *hAPP*_{swe} transgenic mice. However, with a protocol that consisted of weekly LPS injections for a period of twelve weeks, the increased study duration may be of importance in detecting the changes observed by Sheng *et al.* Moreover, despite LPS treatment causing a significant increase in total tau protein in WT mice, alterations in *Nrf2*^{-/-} mice appear to be driven by genotype with no

further induction following treatment. And although only one of the known tau phosphorylation sites was blotted for, no overt treatment-induced changes were seen. More in depth tau pathology analysis from Frank LaFerla's lab has suggested an effect of LPS on tau pathology in a 3x Tg model of AD (Kitazawa *et al.*, 2005; Sy *et al.*, 2011). This is compounded by a recent publication describing a potential link between Nrf2 loss and aggravated tau pathology, with Nrf2 reportedly aiding in the clearance of phosphorylated tau through the autophagy adaptor protein NDP52 (Jo *et al.*, 2014). Because of this, it may be worth pursuing this avenue further by making use of the markers highlighted in their research to clarify whether our cohort mimics any of these changes. As it stands, the results presented here suggest that the concentration of LPS used for the duration indicated impacted minimally on these AD pathologies.

4.15.4 Loss of Nrf2 Causes Dysregulation of Members of the MAPK Family

We have previously described important impacts of Nrf2 loss on insulin signalling pathway in the liver made more apparent following HF feeding (Meakin *et al.*, 2014). It has been previously established that the insulin pathway can exert protective effects on cell survival, and *in vitro* work has implicated PI3-K in the mediation of key Nrf2 activated antioxidant genes such as HMOX1 (Nakaso *et al.*, 2003). We therefore wanted to assess whether the addition of a well-established alternative stress, LPS, would impact on known insulin activated pathways. However, when we analysed the PI3-K dependent phosphorylation of Akt at Ser473 we saw no change in the levels of phosphorylation in WT and *Nrf2*^{-/-} mice, and only a small drop in Thr308 phosphorylation in the cortex of *Nrf2*^{-/-} mice. This contrasts with recent research that has proposed insulin can attenuate LPS-induced alterations in iNOS and NF-κB signalling in astrocytes *in vitro*, supported by alterations in Akt phosphorylation (Li *et al.*, 2013). In addition, NF-κB, which is known to be affected by a variety of different signalling pathways in response to stress, showed minimal genotype or treatment dependent effects as measured by the levels of the inhibitory IκBα molecule. This may run contrary to initial expectations, with previous studies demonstrating that LPS can induce activation of the NF-κB pathway (Gorina *et al.*, 2011). Moreover, several compounds shown to attenuate LPS-induced inflammation have been suggested to act through manipulation of the NF-κB pathway (Lee *et al.*, 2012b). Furthermore, GCLC which is rate limiting in the synthesis of glutathione also failed to show any significant alteration following either genotypic or treatment manipulation. Although, Nagai and

colleagues (2009) reported an LPS dependent drop in glutamate cysteine ligase modifier subunit (GCLM) gene expression, the other half of the GCL heterodimer, in the retinas of WT mice with *Nrf2*^{-/-} mice recording constitutively lower expression. However, with no measurement of protein these results are not directly comparable to those reported here.

MAPK proteins are activated by a variety of different pathways including various stress related factors such as inflammatory cytokines. Furthermore, LPS has been shown to activate MAPK signalling, and increased MAPK signalling is known to occur in both activated astrocytes and microglia (Kaminska *et al.*, 2009). Able to govern a variety of outputs, MAPK cover a wide range of tasks from cytokine production, to regulation of apoptosis to cell migration and proliferation. We have already shown that high-fat feeding causes a dysregulated MAPK response in *Nrf2*^{-/-} mice, whilst both LPS treatment and Nrf2 induction have been linked with MAPK signalling (Kim *et al.*, 2010). We were therefore interested to see whether the altered MAPK signalling reported in HF-fed mice was replicated under an alternate stressor model. No change in the levels of hippocampal JNK phosphorylation were seen, contrary to the effects reported from long-term HF-feeding; and whilst a trend towards increased cortical phosphorylation was observed in LPS-treated WT mice, *Nrf2*^{-/-} mice and *Nrf2*^{-/-}/*hAPP*_{swe} mice this failed to reach significance. Given that JNK phosphorylation has been linked with LPS treatment as well as being implicated in amyloid processing, a lack of JNK activation may support a state of LPS tolerance. In contrast, ERK MAPK phosphorylation was seen in both the hippocampus and cortex of LPS treated WT mice, with both genotype and treatment driven increases in phosphorylation seen in *Nrf2*^{-/-} mice. Unlike HF feeding, LPS treatment only produced a moderate increase in phosphorylation of both ERK isoforms. However, a recent publication by Bellaver *et al.* (2015) indicated that phosphorylation of MAPK proteins such as p38 and ERK may be detrimental to the resolution of LPS-related inflammation. Therefore whilst phosphorylation of ERK is important for many cellular functions, following LPS treatment it is able to help perpetuate the inflammatory response and therefore may be detrimental in action.

4.15.5 Loss of Nrf2 Impacts on Mitochondrial Function Following LPS-Induced Inflammation

In addition to their important role in energy homeostasis and their susceptibility to ROS, dysfunction of mitochondria is known to increase with ageing and has

previously been linked with neurodegenerative disorders such as PD (Hunter *et al.*, 2007). In conjunction with the alterations in MAPK mentioned above, Emre *et al.* (2007) described a link between altered mitochondrial ROS production and MAPK activity in macrophages following LPS treatment. Uncoupling protein 2, a carrier protein able to negatively regulate mitochondrial ROS production was shown to be downregulated following LPS treatment. Moreover, THP-1 human leukaemia monocytic macrophage cells exposed to mitochondrial extracts underwent a similar response to that seen following LPS administration, with further work supporting the presence of the LPS receptor TLR4 within mitochondria (Nicholas *et al.*, 2011). We found no changes in hippocampal mitochondrial proteins assessed in any of the groups analysed. Furthermore, there was no change in the mitochondrial channel protein VDAC1 in the cortical lysates of any of the mice investigated. However, cortical expression of COX IV was diminished in both LPS-treated WT mice and saline treated *Nrf2*^{-/-} mice. This may implicate changes in the electron chain management of mitochondria following challenge with LPS. It also suggests the loss of Nrf2 may be influential in maintaining mitochondrial health. Moreover, whilst LPS decreased the level of mitofusin 2 in the cortex of WT mice, mitofusin 1 and 2 were significantly decreased in the LPS-treated *Nrf2*^{-/-} mice. This suggests an increase in mitochondrial fission and at the very least would support a drop in mitochondrial fusion.

Changes in mitofusin proteins have been associated with increased mitochondrial dysfunction. Indeed, a reduction in mitofusin proteins is associated with increased targeting of mitochondria for degradation. This is corroborated by recent research demonstrating that low-dose LPS causes a reduction in mitofusin 1 whilst concomitantly promoting mitochondrial fusion through the de-phosphorylation of dynamin-related protein 1 in BMDMs (Baker *et al.*, 2014). These findings are of particular interest in light of recent studies using cybrid cell models which link increased ERK phosphorylation in AD patients with perturbation of mitochondrial fission and fusion markers leading to defects in mitochondrial function (Gan *et al.*, 2014). This supports prior research where analysis of frontal cortex samples from AD patients, with diagnoses ranging from mild to severe, showed a similar disconnect in mitochondrial protein levels (Manczak *et al.*, 2011). Furthermore, whilst not fully replicative, data from a double transgenic *APP/PSEN1* mouse model supported a role for dysregulation of mitochondrial fission/fusion in AD (Wu *et al.*, 2014). Finally, inflammasome activation has been shown to occur as a result of translocation to the mitochondria and through release of mitochondrial ROS (Zhou *et al.*, 2011), both of

which are likely to be increased following impairment in the ability of mitochondria to undergo fission/fusion. When combined, these facts support the importance of further investigation of the mitochondrial-related alterations observed. In particular, this advocates the importance of quantifying crucial fission-related proteins as this will enable us to fully assess the impact of the factors involved in our models on mitochondrial dynamics and may also suggest further mechanisms to pursue.

4.15.6 Conclusions

In addition to LPS-induced cognitive deficits, loss of Nrf2 appears to negatively impact on cognition in entorhinal cortex dependent tasks such as OL. There is limited other published research looking at the behavioural impact of Nrf2 loss to date, with the little available concentrating on mobility driven tasks. Given the changes reported here, in combination with both the detrimental effect of inflammation and the beneficial effect of Nrf2 activation on cognition, this is an avenue worthy of further investigation. Loss of Nrf2 aggravated the inflammatory response to LPS in line with previous research published. However, little alteration was seen in the stress activated pathways of NF- κ B and glutathione, nor was there any change in the insulin sensitive Akt pathway. This may result from the timeframe used for this study as it has been previously established that LPS-activation of the immune system can be prompted into a state of tolerance after repeated exposures. An intriguing avenue of further research would be to investigate the potential alteration in inflammasome production and signalling in light of the increased IL-1 β expression seen in the *Nrf2*^{-/-} mice. A link between these factors may provide important information on the development of inflammation given the age associated decline seen in Nrf2 expression in humans.

We were unable to show any effect of LPS on APP protein levels, whilst BACE1 levels were decreased in the cortex of treated mice in contrast to previous publications which have reported increased processing of APP through the β -secretase pathway. In contrast, both lack of Nrf2 and LPS treatment affect the relative phosphorylation of MAPK proteins JNK and ERK with brain region specific changes observed. This is of interest as MAPK activation has previously been suggested to influence amyloid metabolism. Moreover, ERK MAPK is known to be affected by insulin signalling, which we have previously shown to be altered in *Nrf2*^{-/-} mice. Finally, alterations in MAPK signalling combine with changes in electron transport chain and mitochondrial fusion markers, indicating a potentially important role of mitochondrial dysfunction following LPS-induced inflammation. This dysfunction

appears aggravated by the loss of Nrf2, making the phenotyping of *Nrf2*^{-/-} mitochondria an avenue worth clarifying further. Mitochondrial dysfunction is often associated with increased ROS production, altered energy homeostasis, activation of inflammasomes and increased ER stress; all of which have been linked with AD pathology and progression making it an important target in future AD research.

5 FINAL CONCLUSIONS AND FURTHER WORK

5.1 MOUSE MODELS IN AD: BREAKTHROUGHS, SHORTFALLS AND THE AMYLOID CASCADE

Rodent models have always played an important role in the progression of research; allowing the evolution from biochemistry orientated mechanistic research utilising a vast array of *in vitro* models to more heavily physiologically driven studies incorporating effects of cellular and organ crosstalk. AD is no exception to this rule, indeed given that the greatest predictor of AD is age, the use of rodent models, with their shorter lifespan, is of particular importance. Furthermore, the lack of firm disease aetiology and the failure of rodents to present key disease-associated pathologies, make the modelling of AD both more complex but also crucial to the better understanding of its pathology, progression and treatment. The discovery of the first gene mutation (*hAPP_{swe}*) associated with FAD by Mullan and colleagues (1992) was a major breakthrough in the furthering of understanding of the mechanisms likely to be involved in the development of sporadic AD.

The first transgenic mouse models carrying FAD related mutations were developed by Games *et al.* (*APP_{V717F}*; 1995) and Hsiao *et al.* (*APP_{K670N/M671L}*; 1996). The incorporation of FAD mutations allowing the development of models that demonstrated comparative AD pathology drove an explosion in the development of new animal disease models of AD. By the mid 1990's, the first mouse model carrying mutations on two separate AD related genes had been developed (*PSEN1_{A246E}/APP_{swe}*; Borchelt *et al.*, 1996), whilst the turn of the century saw the development of the first mouse model carrying a double mutation on the APP protein (*APP_{V717F}/APP_{K670N/M671L}*; Mucke, 2000). Animal models presenting tau inclusions have also been developed, furthering understanding of the likely involvement and progression of tau dysregulation in AD. However, the genetic mutations that have so far been found in tau protein are not ones that have been associated with AD, being largely related to tauopathies from a subset of other diseases including FTD. Furthermore, the discovery of mutations within the tau protein has enabled the development of the highly popular triple transgenic mouse model (*hAPP_{K670N/M671L}*, *PSEN1_{M146V}* and *htau_{P301L}*) of AD or 3x Tg model (Oddo *et al.*, 2003). This model was one of the first models able to replicate both amyloid plaque and tau tangle pathology in the same animal, and has also been shown to develop age-dependent cognitive decline and synapse loss (Oddo *et al.*, 2003; Filali *et al.*, 2012). However, it is worth noting that the models described above all require a considerable amplification in the expression of the inserted proteins in order to observe the

pathological changes recorded. Therefore, the physiological relevance of some of these results may be skewed due to the excessive protein production.

In recent years, research interests have spread to incorporate other factors as they have grown in importance and relevance to AD. Our model, combining the depleted antioxidant response with a mild model of FAD was designed in an attempt to model the environment which might be present in the very early stages of AD. It was hypothesised that the loss of Nrf2 might act in a priming manner on key immune cells, such as the microglia and astrocytes in the brain. In addition, increased ROS production and basal inflammation from the imbalance in resolution capacity induced by *Nrf2* loss would lead to a state of chronic low-grade inflammation. Combined with the presence of *hAPP_{swe}* which is more susceptible to cleavage by β -secretase and therefore has increased A β production, low grade inflammation was hypothesised to potentiate the pro-amyloidogenic processing of APP, promoting the cascade of events culminating in AD related pathology. However, the AD model chosen, whilst deliberately picked as one of the more physiologically relevant models available, we now believe may have been too mild to provide sufficient impetus to initiate the cascade of events, especially when maintained on a heterozygotic background. In comparison, the novel model produced by Joshi *et al.* (2015) incorporating a more aggressive *APP_{swe}/PSEN1* AD mouse model, demonstrated clear alterations in amyloid pathology, indicating that this is an avenue that is still worth pursuing.

5.2 LOSS OF NRF2 AND THE ALTERED RESPONSE TO DIO AND PATHOGEN ASSOCIATED INFLAMMATION

Since the development of these early models, many more have been developed, in part, as a result of the increasing number of FAD related mutations that have been discovered. Moreover, models incorporating other risk factors associated with AD have also been created such as those crossing known FAD mutations with human APO-e isoforms, or more recently, models targeting parts of the immune system such as those lacking the fractalkine receptor CX₃CR1, which is located predominantly within the CNS. Following the recent increased interest in inflammation in AD, *CX₃CR1*^{-/-} mice have been crossed with both tau and A β transgenic mouse models with opposite results, indicating the key and complex role played by the immune system in the regulation of pathological factors within AD. Furthermore, and given the importance of age related changes in AD, the development of the senescence-accelerated prone mouse (SAMP) models and their control strains (senescence-accelerated resistant mouse (SAMR)

models) may play a crucial role in incorporating natural ageing factors into the equation. Something that has, to date, been lacking in many models of AD given their accelerated profile of pathology. The complexity of AD development and the growing number of factors believed to be implicated in its progression mean that modelling basic AD pathology is unlikely to be sufficient to recapitulate sufficient disease related factors in order to mimic the environment likely involved in disease initiation. With this in mind we decided to add additional environmental challenges to our models using factors that have previously been linked with AD in human patients.

Two different challenges of HF feeding and pathogen-driven inflammation were used to provide a trigger for the primed environment created by the loss of *Nrf2*. Publications using HF-feeding on mouse models of amyloid pathology have previously indicated a role for altered APP processing in insulin regulation, weight-gain and in some cases increased disease pathology. Even with our mild model we were able to replicate the dysregulation of insulin signalling and the increased weight-gain in our *hAPP_{swe}* model following long-term HF feeding. However, we were unable to record any changes in amyloid production, indicating that the significant build-up of amyloid plaque deposition seen in many of the more aggressive models of AD in use is less likely to be causative in the altered insulin regulation observed. In addition, the lack of detectable plaque deposition in these mice may account for the lack of inflammatory response observed. Further investigation, particularly of the DAMP/PAMP driven inflammasome pathway, which is known to be activated by A β may be crucial in further understanding the responses, or lack thereof, observed in these mice. It is possible that the lack of substantial inflammatory response observed in our mouse model of AD (*hAPP_{swe}*) may correlate with a lack of inflammasome activation, in light of the much lower levels of A β previously reported in this model compared to others currently in use. Furthermore, whilst loss of *Nrf2* has the opposite effect on both insulin signalling and weight-gain, the more surprising outcome was the apparent protective effect exerted by long term HF feeding, which contrasts with that reported for the liver work done on these mice (Sugimoto *et al.*, 2010; Okada *et al.*, 2013; Meakin *et al.*, 2014). This indicates a crucial role for *Nrf2* in the regulation of tissue health in relation to changes in glucose and insulin homeostasis. Crucially this may indicate that a more relevant and important model to test would replace the HF feeding reported here with a calorie restriction model. The steady decrease in *Nrf2* previously recorded in humans following ageing and the link between ageing and declining body weight may suggest this is a more physiologically relevant model in neurodegeneration. In addition, whilst obesity in

midlife has previously associated with increased with the development of AD, a recent study published by Qizilbash *et al.* (2015) has suggested the opposite may actually be true as they reported decreasing risk of AD with every increase in BMI grouping assessed.

Development of obesity has long been linked with the development of a chronic low grade inflammatory response, whilst the ability of our immune system to respond to challenges correlates negatively with ageing, hence the impaired response to infection in aged populations. We have been able to show that following ageing, mice lacking Nrf2 have basally elevated markers of inflammation within the brain which can be further potentiated by administration of an infection related marker such as LPS. With little information available regarding the effects of Nrf2 in the brain it is impossible at this stage to say whether this inflammation is present from a young age or slowly accumulates with ageing. However, the two studies described here suggest that there may be a strong role for ageing in the aggravation of the inflammatory state with basal levels of commonly assessed inflammatory markers increased in mice at 16 months (HF study) when compared to those recorded at 11 months (LPS study). This further enforces the importance of looking at mouse models that incorporate ageing related factors, such as the SAMP models, as key changes may be lacking in mouse models assessed at a younger age even if those models demonstrate relevant pathological alterations associated with AD. In addition, a recent publication using the SAMP8 and SAMR8 mouse lines was able to demonstrate age related decreases in Nrf2 expression in the liver of the SAMP8 but not SAMR8 mice further supporting the potentially important role of Nrf2 loss in ageing related impairments (Tomobe *et al.*, 2012).

5.3 LOSS OF NRF2 AND THE IMPACT THIS MAY HAVE ON AGE RELATED COGNITIVE DECLINE

Following on from the links described above between inflammation and ageing in the *Nrf2*^{-/-} mice, this facet may also be of importance when assessing the impact of different interventions on cognition. It has already been described in various reviews that the design of the AD mouse model chosen can have major implications on the degree of cognitive impairment observed and the behavioural tasks that report the most significant impairments (Webster *et al.*, 2014). Models such as the 3x Tg model may show cognitive deficits as early as 3-5 months of age, whilst the Tg2576 mouse model has shown less consistent behavioural changes with some groups reporting changes as early 5 months and others only seeing changes in more aged mice (King & Arendash,

2002; Westerman *et al.*, 2002). In addition to the inherent differences reported between mouse models, the choice of behavioural task assessed can also have a significant role in whether cognitive impairment is reported or not. Tasks such as the MWM, often referred to as the gold standard for assessment of spatial memory in rodent models, appear to demonstrate consistent impairment in the majority of AD models assessed. Other tasks, such as NOR, have been less consistent in both the age of onset of impairment and even whether any impairment has been recorded. However, it is worth noting that there is often increased variability in the exact set-up and measurements done in the NOR task, and these may impact heavily on the degree of variability reported across publications (Antunes & Biala, 2012).

There are some publications available using the same *hAPP_{swe}* model as what we have described in our results (Subaiea *et al.*, 2013); although these are not as numerous as those for other models with accelerated pathology. However, very little has been published on the effects of Nrf2 loss on cognition, particularly in relation to ageing. What little has been published has suggested there may be a role for depletion of Nrf2 in protection against the forced swim task, and further hypothesises a role for altered neuronal signalling in *Nrf2^{-/-}* mice (Muramatsu *et al.*, 2013). Further to this, Furnari *et al.* (2014) reported a mild impairment in *Nrf2^{-/-}* mice in the MWM, where they had increased latency in locating the visible platform during the test when compared to WT mice. Our novel work in aged *Nrf2^{-/-}* mice suggests that these may develop entorhinal cortex dependent cognitive impairment with ageing, whilst maintaining their ability to partake in tasks that rely more on the perirhinal cortex for successful completion. This further supports the need for more detailed characterisation of the *Nrf2^{-/-}* model with regards to ageing and its potential involvement in neurodegenerative disorders.

It is unlikely that the drop in Nrf2 expression alone would be sufficient to induce the effects seen in the early stages of AD, else it might be expected the number of AD cases reported would be exponentially larger than what is currently observed. Instead, it is more probable that other factors act to tip the scales towards a favourable environment for AD development. This promotes the importance of assessing other environmental factors on the progression of AD like pathology, particularly in more physiologically relevant models. Factors such as obesity and TIID are obvious targets of environmental stress in the study of AD and there is a growing amount of work being devoted to modelling these changes, including the work reported here. However, other effects may prove to be equally important such as the incorporation of factors including

environmental enrichment (Maesako *et al.*, 2012a; Williamson *et al.*, 2012; Barak *et al.*, 2013; Verret *et al.*, 2013), environmental impoverishment and stress (Jeong *et al.*, 2006; Diniz *et al.*, 2010; Perez Nievas *et al.*, 2011), and the potential interaction of long term medications such as statins and non-steroidal anti-inflammatory drugs (Daneschvar *et al.*, 2015); many of which have been suggested to impact on disease development.

5.4 A ROLE FOR NRF2 IN THE REGULATION OF MAPK SIGNALLING AND ITS IMPACT IN AD

The results obtained from our *Nrf2*^{-/-} mouse models also provided novel information regarding the role of MAPK proteins in the brain. We found significant activation of the ERK specific MEK protein in the brains of mice lacking Nrf2, which long-term treatment with HF feeding failed to reduce as was seen in the HF fed WT mice. It has previously been suggested that MAPK enzymes lie upstream of Nrf2 activation in a variety of *in vitro* cell culture models (Correa *et al.*, 2011; Ernst *et al.*, 2011), whilst dendritic cells lacking Nrf2 have been reported to demonstrate a mild increase in ERK and p38 phosphorylation following challenge with LPS (Yeang *et al.*, 2012). Although there is limited research on the role of ERK in *Nrf2*^{-/-} mice, ERK has previously been suggested to have neuroprotective effects. Furthermore, the Nrf2 activator *t*BHQ has been suggested to act in a protective manner via alternative pathways when Nrf2 expression is silenced. Recent work by Li *et al.* (2014) using primary hepatocyte cultures has reported that after silencing of Nrf2, addition of *t*BHQ is still able to produce a protective effect against lipotoxicity. The mechanisms utilised to produce this effect have been suggested to include increased autophagy, increased AMPK phosphorylation and increased phosphorylation of ERK MAPK. Furthermore, a study investigating the protective effects of argon has suggested a protective role for ERK phosphorylation following retinal ischaemia and reperfusion injury (Ulbrich *et al.*, 2015). This was suggested to occur by decreasing both Nrf2 dependent HMOX1 expression and pro-apoptotic caspase-3. Finally, the anti-epileptic drug valproic acid has been hypothesised to exert protective effects over traumatic brain injury via Akt and ERK activating pathways (Zhang *et al.*, 2014).

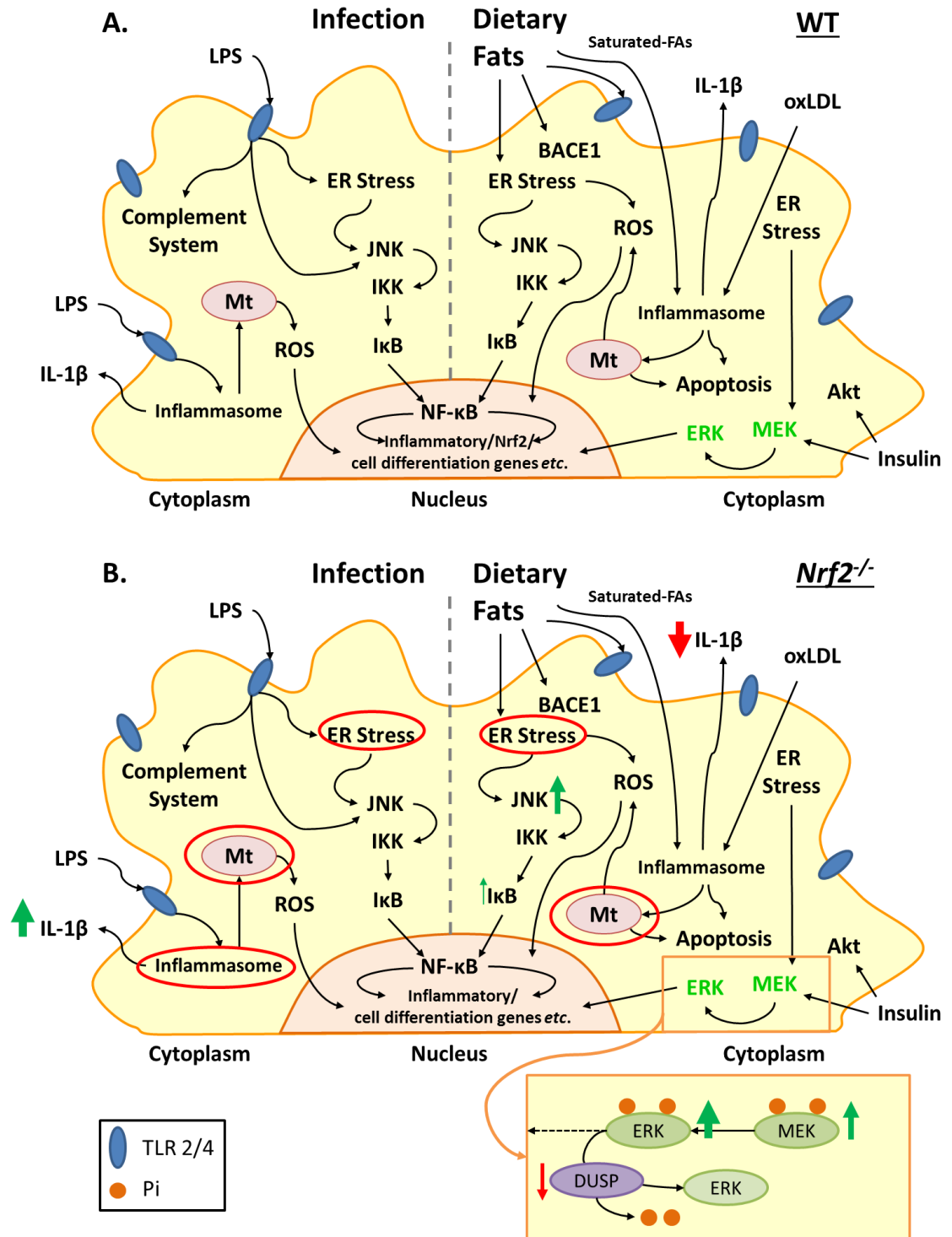


Figure 5.1 Simplified pictorial summary of some of the principle biochemical alterations observed in completion of this project.

The overall effects of long-term HF diet or repeated peripheral LPS driven alterations in the brains of WT (**A**) and *Nrf2*^{-/-} (**B**) mice. Where FA = fatty acids, oxLDL = oxidised low-density lipoprotein, Mt = mitochondria and Pi = phosphate. The red rings depict potential areas of damage or activation that necessitate further investigation in order to achieve a clearer understanding.

Other members of the MAPK enzyme family, such as p38 and JNK, have been suggested to interact with A β , implicating a role for MAPK activity in the propagation of A β pathology (Tamagno *et al.*, 2005; Quiroz-Baez *et al.*, 2009; Tamagno *et al.*, 2009; Mazzitelli *et al.*, 2011). This suggests MAPK enzymes interact in a key manner across multiple pathways and may be important in the switch from neuroprotective effects to amyloidogenic effects. However, further work is required to gain understanding of the mechanisms responsible for these regulations both in the absence of Nrf2, but also in AD models.

5.5 MITOCHONDRIA, ER STRESS AND THEIR IMPORTANCE IN FURTHER AD RESEARCH

Previously associated solely with the turnover of ATP within the cell, mitochondria are being studied increasingly with regard to their ability to interact in a sophisticated manner to their cellular environment. Mitochondria are the primary source of ROS production. In addition, oxidative damage to mitochondrial components has been suggested to occur prior to that of other areas within the cell in the development of neurodegenerative disorders such as AD (Selfridge *et al.*, 2013). Increasingly, research is indicating an important role in altered mitochondrial status in the progression of AD with changes in mitochondrial fusion/fission and membrane potential already having been reported in both mouse models of AD and tissue samples from post-mortem AD brains (Manczak *et al.*, 2011). In addition, it has previously been shown that mitochondria are able to uptake A β , with mitochondria from AD models showing accumulation of A β within the organelle (Pinho *et al.*, 2014). Furthermore, altered mitochondrial functionality can directly impact on energy homeostasis known to be progressively affected in AD and related research models (Yao *et al.*, 2009). This is particularly important in light of the design of our model described here and that described by Joshi *et al.* (2015) given the recent findings that Nrf2 is able to directly regulate mitochondrial bioenergetics by regulating substrate availability (Holmström *et al.*, 2013).

Whilst mitochondrial impairment has been suggested to be involved in AD from as early as the mid 1980's (Selfridge *et al.*, 2013), interest in the interaction between Nrf2 and mitochondria has grown exponentially, particularly in the last few years. The suggested direct interaction between Nrf2 and mitochondrial bioenergetics described by Holmström *et al.* (2013), in combination with the crucial role of Nrf2 in regulating mitochondrial ROS levels (Kovac *et al.*, 2015), and the close link between ER stress

and mitochondrial dysfunction (Marchi *et al.*, 2014; Rainbolt *et al.*, 2014), all combine to implicate an important role for Nrf2 in the regulation and dysregulation of mitochondria during ageing. This supports the early findings we have described in our mouse models. In addition, the strong links now indicated between APP, amyloid, the ER and mitochondria suggest a co-localisation of both the toxic pathology associated with AD alongside regions now believed to be strongly reliant on Nrf2 for maintained functioning. The growing research surrounding the role of mitochondria-associated ER membranes (MAMs) in the development of AD, serves to highlight the importance of further understanding the role of both the ER and mitochondria within AD development (Area-Gomez *et al.*, 2012; Hedskog *et al.*, 2013). This is supported by animal studies that indicate mitochondrial dysfunction has been shown to occur prior to the development of plaque pathology (Wu *et al.*, 2014). Taken together this further supports the need to investigate markers of ER stress in our model detailed here, but also highlights the need for better understanding of the intricate crosstalk occurring between mitochondria, Nrf2, the ER and amyloid pathology; where MAMs may play a crucial linking role between these different components. On a final note, as has been previously suggested here these alterations may also further support a role for the inflammasome pathway, especially given its strong ties not only with mitochondrial dysfunction but also dysregulated APP cleavage and A β production (Salminen *et al.*, 2008; Kapetanovic *et al.*).

5.6 STUDY LIMITATIONS

The main aim of this study was to provide a novel model describing some of the key factors involved in early AD pathology. Although the phenotype was very mild with apparent limited effects, the studies themselves have illuminated some key limitations as to why this may have occurred. One of the key limitations for these studies has been linked to the genotyping issues that occurred (see Chapter 2.2.5.2), resulting in a loss of statistical power as well as reducing the number of mice available carrying either the *hAPP_{swe}* mutation alone or in combination with the disrupted *Nrf2* gene. However, the publishing of a paper by Joshi and colleagues (2015) describing a novel triple transgenic model (*APP/PSEN/Nrf2^{-/-}*) suggests that this avenue may still be worth pursuing further albeit from a slightly different angle.

The second major study limitation was unknown at the time of study commencement given the literature available, and revolves around the role of Nrf2 loss in tissues outside of the liver and WAT. Our attempts to elucidate the importance of the

transcription factor Nrf2 centrally, has subsequently raised some questions about the limitations of using a global *Nrf2*^{-/-} model and the role for alternative compensatory mechanisms. The apparently blunted effects reported here in the brain, in comparison to those previously reported in the liver, have been supported recently by studies in other *Nrf2*^{-/-} tissues. Recent research looking at the effect of ultraviolet radiation on skin in mice either lacking (*Nrf2*^{-/-}) or overexpressing (*Keap1* KD) Nrf2, failed to see the same degree of attenuation of downstream molecules in mice lacking Nrf2 (Knatko *et al.*, 2015). This was also characterized by a much milder phenotype than that previously observed in hepatic studies. Overall, this indicates a potential for markedly differential tissue related effects for this model, which should be used as a marker of caution when designing future experiments.

Finally, some technical limitations were also inherent to our studies, as is the case in most research. Additional behavioural testing would have been very interesting to pursue, in particular some of the commonly used hippocampal dependent tasks (MWM, radial arm maze). In addition, the small size of the mouse limits the volume of dissected cerebral tissue available, which in turn can impact in the number of assays that can be performed using the tissue from any single animal. Some of these problems could soon be addressed by switching to one of the newly developed *Nrf2*^{-/-} rat models, such as that described by Priestley *et al.* (2015), for future experiments. This may also be a beneficial move from a behavioural standpoint, given the increased complexity of tasks that are commonly used when studying rats over mice.

5.7 PHYSIOLOGICAL RELEVANCE

The importance placed on the role of inflammation in the brain of many neurodegenerative disorders has grown in recent years and has led to various clinical trials being put in place. Unfortunately the evidence from these trials is mixed and therefore harder to interpret. Clinical trials in addition to retrospective studies investigating the effects of long-term prescription of drugs such as non-steroidal anti-inflammatory drugs and statins have so far provided evidence both for and against their relevance in the treatment of AD (de Jong *et al.*, 2008; Daneschvar *et al.*, 2015). However, recent research published by researchers from the Gladstone Institute in California suggests that there may yet be potential in this field (Min *et al.*, 2015). Min and colleagues demonstrated a protective effect of the arthritis NSAID drug Salsalate on the propagation of detrimental tau inclusions. In contrast, the mitochondria targeted antioxidant compound, MitoQ, failed to show any amelioration in disease progression

of PD, although improvements were observed in a trial of MitoQ on liver damage resulting from chronic hepatitis C virus (Smith & Murphy, 2010). It should be noted that inflammation remains a hot topic within AD research. This is exemplified by the media coverage surrounding the publication by Olmos-Alonso *et al.* (2016). Their recent research describes the novel attenuating effects of the anti-inflammatory microglial proliferation and differentiation targeting compound GW2580 on the propagation of AD-driven central inflammation, cognitive decline and relevant pathology in a mouse model of AD.

The increasing information surrounding the role of inflammation and ROS in the development of AD suggest an important involvement of these factors in future disease management. Clarification of the chronological relevance of the different immune factors is likely to prove pivotal in the furthering of these factors as clinical targets in disease management (Heneka *et al.*, 2015). Furthermore, combination with other novel targets such as the inhibition of the β -secretase enzyme (Menting & Claassen, 2014) may be required to provide targeting of multiple disease related factors. This in turn may allow for a decrease in the active drug load administered, lessening the risk of drug side effects and promoting the likelihood of disease-fighting effects.

6 REFERENCES

- Abdullah, A., Kitteringham, N. R., Jenkins, R. E., Goldring, C., Higgins, L., Yamamoto, M., Hayes, J. & Park, B. K. (2012). Analysis of the role of Nrf2 in the expression of liver proteins in mice using two-dimensional gel-based proteomics. *Pharmacological Reports* **64**(3): 680-697.
- Aggleton, J. P., Brown, M. W. & Albasser, M. M. (2012). Contrasting brain activity patterns for item recognition memory and associative recognition memory: insights from immediate-early gene functional imaging. *Neuropsychologia* **50**(13): 3141-3155.
- Aguirre, E., Woods, R. T., Spector, A. & Orrell, M. (2013). Cognitive stimulation for dementia: A systematic review of the evidence of effectiveness from randomised controlled trials. *Ageing Research Reviews* **12**(1): 253-262.
- Agyare, E. K., Leonard, S. R., Curran, G. L., Yu, C. C., Lowe, V. J., Paravastu, A. K., Poduslo, J. F. & Kandimalla, K. K. (2013). Traffic Jam at the Blood–Brain Barrier Promotes Greater Accumulation of Alzheimer’s Disease Amyloid- β Proteins in the Cerebral Vasculature. *Molecular Pharmaceutics* **10**(5): 1557-1565.
- Ainge, J. A., Heron-Maxwell, C., Theofilas, P., Wright, P., de Hoz, L. & Wood, E. R. (2006). The role of the hippocampus in object recognition in rats: Examination of the influence of task parameters and lesion size. *Behavioural Brain Research* **167**(1): 183-195.
- Akhter, H., Katre, A., Li, L., Liu, X. & Liu, R.-M. (2011). Therapeutic Potential and Anti-Amyloidosis Mechanisms of Tert-Butylhydroquinone for Alzheimer’s Disease. *Journal of Alzheimer's disease : JAD* **26**(4): 767-778.
- Albasser, M. M., Amin, E., Lin, T.-C. E., Iordanova, M. D. & Aggleton, J. P. (2012). Evidence That the Rat Hippocampus Has Contrasting Roles in Object Recognition Memory and Object Recency Memory. *Behavioral Neuroscience* **126**(5): 659-669.
- Allaman, I., Gavillet, M., Bélanger, M., Laroche, T., Viertl, D., Lashuel, H. A. & Magistretti, P. J. (2010). Amyloid-beta aggregates cause alterations of astrocytic metabolic phenotype: impact on neuronal viability. *J Neurosci* **30**(9): 3326-3338.
- Alzheimer, A., Stelzmann, R. A., Schnitzlein, H. N. & Murtagh, F. R. (1995). An English translation of Alzheimer's 1907 paper, "Über eine eigenartige Erkrankung der Hirnrinde". *Clin Anat* **8**(6): 429-431.
- Amour, A., Knight, C. G., Webster, A., Slocombe, P. M., Stephens, P. E., Knäuper, V., Docherty, A. J. P. & Murphy, G. (2000). The in vitro activity of ADAM-10 is inhibited by TIMP-1 and TIMP-3. *FEBS Letters* **473**(3): 275-279.
- Antunes, M. & Biala, G. (2012). The novel object recognition memory: neurobiology, test procedure, and its modifications. *Cogn Process* **13**(2): 93-110.
- Area-Gomez, E., del Carmen Lara Castillo, M., Tambini, M. D., Guardia-Laguarta, C., de Groof, A. J. C., Madra, M., Ikenouchi, J., Umeda, M., Bird, T. D., Sturley, S. L. & Schon, E. A. (2012). Upregulated function of mitochondria-associated ER membranes in Alzheimer disease. *The EMBO Journal* **31**(21): 4106-4123.
- Arnold, S. E., Lucki, I., Brookshire, B. R., Carlson, G. C., Browne, C. A., Kazi, H., Bang, S., Choi, B.-R., Chen, Y., McMullen, M. F. & Kim, S. F. (2014). High fat diet produces brain insulin resistance, synaptodendritic abnormalities and altered behavior in mice. *Neurobiology of Disease* **67**: 79-87.
- ARUK (2015). About Dementia: Facts and Stats.
<http://www.alzheimersresearchuk.org/about-dementia/facts-stats/>.
- Ashrafian, H., Czibik, G., Bellahcene, M., Aksentijevic, D., Smith, A. C., Mitchell, S. J., Dodd, M. S., Kirwan, J., Byrne, J. J., Ludwig, C., Isackson, H., Yavari, A., Stottrup, N. B., Contractor, H., Cahill, T. J., Sahgal, N., Ball, D. R., Birkler, R.

- I., Hargreaves, I., Tennant, D. A., Land, J., Lygate, C. A., Johannsen, M., Kharbanda, R. K., Neubauer, S., Redwood, C., de Cabo, R., Ahmet, I., Talan, M., Gunther, U. L., Robinson, A. J., Viant, M. R., Pollard, P. J., Tyler, D. J. & Watkins, H. (2012). Fumarate is cardioprotective via activation of the Nrf2 antioxidant pathway. *Cell Metab* **15**(3): 361-371.
- Avila, J., Lucas, J. J., Pérez, M. & Hernández, F. (2004). *Role of Tau Protein in Both Physiological and Pathological Conditions*. edn, vol. 84.
- Avrahami, L., Farfara, D., Shaham-Kol, M., Vassar, R., Frenkel, D. & Eldar-Finkelman, H. (2013). Inhibition of Glycogen Synthase Kinase-3 Ameliorates β -Amyloid Pathology and Restores Lysosomal Acidification and Mammalian Target of Rapamycin Activity in the Alzheimer Disease Mouse Model: IN VIVO AND IN VITRO STUDIES. *Journal of Biological Chemistry* **288**(2): 1295-1306.
- Azizi, G., Khannazer, N. & Mirshafiey, A. (2014). The Potential Role of Chemokines in Alzheimer's Disease Pathogenesis. *Am J Alzheimers Dis Other Demen.*
- Bai, Y., Cui, W., Xin, Y., Miao, X., Barati, M. T., Zhang, C., Chen, Q., Tan, Y., Cui, T., Zheng, Y. & Cai, L. (2013). Prevention by sulforaphane of diabetic cardiomyopathy is associated with up-regulation of Nrf2 expression and transcription activation. *Journal of Molecular and Cellular Cardiology* **57**: 82-95.
- Baik, S. H., Cha, M.-Y., Hyun, Y.-M., Cho, H., Hamza, B., Kim, D. K., Han, S.-H., Choi, H., Kim, K. H., Moon, M., Lee, J., Kim, M., Irimia, D. & Mook-Jung, I. (2014). Migration of neutrophils targeting amyloid plaques in Alzheimer's disease mouse model. *Neurobiology of Aging* **35**(6): 1286-1292.
- Baird, L., Lleres, D., Swift, S. & Dinkova-Kostova, A. T. (2013). Regulatory flexibility in the Nrf2-mediated stress response is conferred by conformational cycling of the Keap1-Nrf2 protein complex. *Proc Natl Acad Sci U S A* **110**(38): 15259-15264.
- Baker, B., Maitra, U., Geng, S. & Li, L. (2014). Molecular and Cellular Mechanisms Responsible for Cellular Stress and Low-grade Inflammation Induced by a Super-low Dose of Endotoxin. *Journal of Biological Chemistry* **289**(23): 16262-16269.
- Balistreri, C. R., Caruso, C. & Candore, G. (2010). The role of adipose tissue and adipokines in obesity-related inflammatory diseases. *Mediators Inflamm* **2010**: 802078.
- Banks, W. A. & Robinson, S. M. (2010). Minimal penetration of lipopolysaccharide across the murine blood-brain barrier. *Brain, Behavior, and Immunity* **24**(1): 102-109.
- Barak, B., Shvarts-Serebro, I., Modai, S., Gilam, A., Okun, E., Michaelson, D. M., Mattson, M. P., Shomron, N. & Ashery, U. (2013). Opposing actions of environmental enrichment and Alzheimer's disease on the expression of hippocampal microRNAs in mouse models. *Transl Psychiatry* **3**: e304.
- Barker, G. R. I. & Warburton, E. C. (2011). When Is the Hippocampus Involved in Recognition Memory? *The Journal of Neuroscience* **31**(29): 10721-10731.
- Barreto, G. E., Gonzalez, J., Torres, Y. & Morales, L. (2011). Astrocytic-neuronal crosstalk: Implications for neuroprotection from brain injury. *Neuroscience Research* **71**(2): 107-113.
- Baumkötter, F., Wagner, K., Eggert, S., Wild, K. & Kins, S. (2012). Structural aspects and physiological consequences of APP/APLP trans-dimerization. *Exp Brain Res* **217**(3-4): 389-395.
- Bay-Richter, C., Janelidze, S., Hallberg, L. & Brundin, L. (2011). Changes in behaviour and cytokine expression upon a peripheral immune challenge. *Behavioural Brain Research* **222**(1): 193-199.

- Bélangier, M., Allaman, I. & Magistretti, P. J. (2011). Differential effects of pro- and anti-inflammatory cytokines alone or in combinations on the metabolic profile of astrocytes. *Journal of Neurochemistry* **116**(4): 564-576.
- Bellaver, B., Souza, D., Bobermin, L., Souza, D., Gonçalves, C.-A. & Quincozes-Santos, A. (2015). Resveratrol Protects Hippocampal Astrocytes Against LPS-Induced Neurotoxicity Through HO-1, p38 and ERK Pathways. *Neurochemical Research* **40**(8): 1600-1608.
- Ben Khalifa, N., Tyteca, D., Marinangeli, C., Depuydt, M., Collet, J.-F., Courtoy, P. J., Renaud, J.-C., Constantinescu, S., Octave, J.-N. & Kienlen-Campard, P. (2012). Structural features of the KPI domain control APP dimerization, trafficking, and processing. *The FASEB Journal* **26**(2): 855-867.
- Benedict, C., Hallschmid, M., Schmitz, K., Schultes, B., Ratter, F., Fehm, H. L., Born, J. & Kern, W. (2007). Intranasal insulin improves memory in humans: Superiority of insulin aspart. *Neuropsychopharmacology* **32**(1): 239-243.
- Benito, C., Tolón, R. M., Castillo, A. I., Ruiz-Valdepeñas, L., Martínez-Orgado, J. A., Fernández-Sánchez, F. J., Vázquez, C., Cravatt, B. F. & Romero, J. (2012). β -Amyloid exacerbates inflammation in astrocytes lacking fatty acid amide hydrolase through a mechanism involving PPAR- α , PPAR- γ and TRPV1, but not CB 1 or CB 2 receptors. *British Journal of Pharmacology* **166**(4): 1474-1489.
- Beyer, T. A., Xu, W., Teupser, D., Auf Dem Keller, U., Bugnon, P., Hildt, E., Thiery, J., Kan, Y. W. & Werner, S. (2008). Impaired liver regeneration in Nrf2 knockout mice: Role of ROS-mediated insulin/IGF-1 resistance. *EMBO Journal* **27**(1): 212-223.
- Bian, Y., Zhao, X., Li, M., Zeng, S. & Zhao, B. (2013). Various roles of astrocytes during recovery from repeated exposure to different doses of lipopolysaccharide. *Behavioural Brain Research* **253**: 253-261.
- Biesmans, S., Acton, P. D., Cotto, C., Langlois, X., Ver Donck, L., Bouwknecht, J. A., Aelvoet, S.-A., Hellings, N., Meert, T. F. & Nuydens, R. (2015). Effect of stress and peripheral immune activation on astrocyte activation in transgenic bioluminescent Gfap-luc mice. *Glia* **63**(7): 1126-1137.
- Biesmans, S., Meert, T. F., Bouwknecht, J. A., Acton, P. D., Davoodi, N., De Haes, P., Kuijlaars, J., Langlois, X., Matthews, L. J., Ver Donck, L., Hellings, N. & Nuydens, R. (2013). Systemic immune activation leads to neuroinflammation and sickness behavior in mice. *Mediators Inflamm* **2013**: 271359.
- Blasko, I., Stampfer-Kountchev, M., Robatscher, P., Veerhuis, R., Eikelenboom, P. & Grubeck-Loebenstein, B. (2004). How chronic inflammation can affect the brain and support the development of Alzheimer's disease in old age: the role of microglia and astrocytes. *Aging Cell* **3**(4): 169-176.
- Blasko, I., Veerhuis, R., Stampfer-Kountchev, M., Saurwein-Teissl, M., Eikelenboom, P. & Grubeck-Loebenstein, B. (2000). Costimulatory effects of interferon-gamma and interleukin-1beta or tumor necrosis factor alpha on the synthesis of Abeta1-40 and Abeta1-42 by human astrocytes. *Neurobiol Dis* **7**(6 Pt B): 682-689.
- Blass, J. P., Sheu, R. K. F. & Gibson, G. E. (2000). Inherent abnormalities in energy metabolism in Alzheimer disease: Interaction with cerebrovascular compromise Vol. 903, pp 204-221.
- Bluthé, R.-M., Castanon, N., Pousset, F., Bristow, A., Ball, C., Lestage, J., Michaud, B., Kelley, K. W. & Dantzer, R. (1999). Central injection of IL-10 antagonizes the behavioural effects of lipopolysaccharide in rats. *Psychoneuroendocrinology* **24**(3): 301-311.

- Bonda, D. J., Stone, J. G., Torres, S. L., Siedlak, S. L., Perry, G., Kryscio, R., Jicha, G., Casadesus, G., Smith, M. A., Zhu, X. & Lee, H.-g. (2014). Dysregulation of leptin signaling in Alzheimer disease: evidence for neuronal leptin resistance. *Journal of Neurochemistry* **128**(1): 162-172.
- Bonda, D. J., Wang, X., Perry, G., Nunomura, A., Tabaton, M., Zhu, X. & Smith, M. A. (2010). Oxidative stress in Alzheimer disease: A possibility for prevention. *Neuropharmacology* **59**(4-5): 290-294.
- Bonifati, D. M. & Kishore, U. (2007). Role of complement in neurodegeneration and neuroinflammation. *Molecular Immunology* **44**(5): 999-1010.
- Borchelt, D. R., Thinakaran, G., Eckman, C. B., Lee, M. K., Davenport, F., Ratovitsky, T., Prada, C.-M., Kim, G., Seekins, S., Yager, D., Slunt, H. H., Wang, R., Seeger, M., Levey, A. I., Gandy, S. E., Copeland, N. G., Jenkins, N. A., Price, D. L., Younkin, S. G. & Sisodia, S. S. (1996). Familial Alzheimer's Disease–Linked Presenilin 1 Variants Elevate A β 1–42/1–40 Ratio In Vitro and In Vivo. *Neuron* **17**(5): 1005-1013.
- Borger, E., Aitken, L., Muirhead, Kirsty E. A., Allen, Zoe E., Ainge, James A., Conway, Stuart J. & Gunn-Moore, Frank J. (2011). Mitochondrial β -amyloid in Alzheimer's disease. *Biochemical Society Transactions* **39**(4): 868-873.
- Bose, S. & Cho, J. (2013). Role of chemokine CCL2 and its receptor CCR2 in neurodegenerative diseases. *Arch. Pharm. Res.* **36**(9): 1039-1050.
- Boseman-Roberts, S., Ripellino, J. A., Ingalls, K. M., Robakis, N. K. & Felsenstein, K. M. (1994). Non-amyloidogenic Cleavage of the beta-Amyloid Precursor Protein by an Integral Membrane Metalloendopeptidase. *Journal of Biological Chemistry* **269**(4): 3111-3116.
- Bourne, K. Z., Ferrari, D. C., Lange-Dohna, C., Roßner, S., Wood, T. G. & Perez-Polo, J. R. (2007). Differential regulation of BACE1 promoter activity by nuclear factor- κ B in neurons and glia upon exposure to β -amyloid peptides. *Journal of Neuroscience Research* **85**(6): 1194-1204.
- Bradford, M. M. (1976). A rapid and sensitive method for the quantitation of microgram quantities of protein utilizing the principle of protein-dye binding. *Analytical biochemistry* **72**: 248-254.
- Brunnström, H. R. & Englund, E. M. (2009). Cause of death in patients with dementia disorders. *European Journal of Neurology* **16**(4): 488-492.
- Bubber, P., Haroutunian, V., Fisch, G., Blass, J. P. & Gibson, G. E. (2005). Mitochondrial abnormalities in Alzheimer brain: Mechanistic implications. *Annals of Neurology* **57**(5): 695-703.
- Bussey, T. J., Muir, J. L. & Aggleton, J. P. (1999). Functionally Dissociating Aspects of Event Memory: the Effects of Combined Perirhinal and Postrhinal Cortex Lesions on Object and Place Memory in the Rat. *The Journal of Neuroscience* **19**(1): 495-502.
- Butovsky, O., Talpalar, A. E., Ben-Yaakov, K. & Schwartz, M. (2005). Activation of microglia by aggregated β -amyloid or lipopolysaccharide impairs MHC-II expression and renders them cytotoxic whereas IFN- γ and IL-4 render them protective. *Mol Cell Neurosci* **29**(3): 381-393.
- Callewaere, C., Banisadr, G., Rostene, W. & Parsadaniantz, S. M. (2007). Chemokines and chemokine receptors in the brain: implication in neuroendocrine regulation. *J Mol Endocrinol* **38**(3): 355-363.
- Calvo-Ochoa, E., Hernandez-Ortega, K., Ferrera, P., Morimoto, S. & Arias, C. (2014). Short-term high-fat-and-fructose feeding produces insulin signaling alterations accompanied by neurite and synaptic reduction and astroglial activation in the rat hippocampus. *J Cereb Blood Flow Metab* **34**(6): 1001-1008.

- Cani, P. D., Amar, J., Iglesias, M. A., Poggi, M., Knauf, C., Bastelica, D., Neyrinck, A. M., Fava, F., Tuohy, K. M., Chabo, C., Waget, A., Delmée, E., Cousin, B., Sulpice, T., Chamontin, B., Ferrières, J., Tanti, J.-F., Gibson, G. R., Casteilla, L., Delzenne, N. M., Alessi, M. C. & Burcelin, R. (2007). Metabolic Endotoxemia Initiates Obesity and Insulin Resistance. *Diabetes* **56**(7): 1761-1772.
- Cao, D., Lu, H., Lewis, T. L. & Li, L. (2007). Intake of Sucrose-sweetened Water Induces Insulin Resistance and Exacerbates Memory Deficits and Amyloidosis in a Transgenic Mouse Model of Alzheimer Disease. *Journal of Biological Chemistry* **282**(50): 36275-36282.
- Cardoso, S. M., Santana, I., Swerdlow, R. H. & Oliveira, C. R. (2004). Mitochondria dysfunction of Alzheimer's disease cybrids enhances A β toxicity. *Journal of Neurochemistry* **89**(6): 1417-1426.
- Carroll, J. C., Iba, M., Bangasser, D. A., Valentino, R. J., James, M. J., Brunden, K. R., Lee, V. M. Y. & Trojanowski, J. Q. (2011). Chronic Stress Exacerbates Tau Pathology, Neurodegeneration, and Cognitive Performance through a Corticotropin-Releasing Factor Receptor-Dependent Mechanism in a Transgenic Mouse Model of Tauopathy. *Journal of Neuroscience* **31**(40): 14436-14449.
- Casley, C. S., Canevari, L., Land, J. M., Clark, J. B. & Sharpe, M. A. (2002). Beta-amyloid inhibits integrated mitochondrial respiration and key enzyme activities. *J Neurochem* **80**(1): 91-100.
- Caspersen, C., Wang, N., Yao, J., Sosunov, A., Chen, X., Lustbader, J. W., Xu, H. W., Stern, D., McKhann, G. & Yan, S. D. (2005). Mitochondrial A β : a potential focal point for neuronal metabolic dysfunction in Alzheimer's disease. *The FASEB Journal* **19**(14): 2040-2041.
- Castellani, R. J., Harris, P. L. R., Sayre, L. M., Fujii, J., Taniguchi, N., Vitek, M. P., Founds, H., Atwood, C. S., Perry, G. & Smith, M. A. (2001). Active glycation in neurofibrillary pathology of Alzheimer disease: N ϵ -(Carboxymethyl) lysine and hexitol-lysine. *Free Radical Biology and Medicine* **31**(2): 175-180.
- Castellani, R. J. & Smith, M. A. (2011). Compounding artefacts with uncertainty, and an amyloid cascade hypothesis that is 'too big to fail'. *The Journal of Pathology* **224**(2): 147-152.
- Caunt, C. J. & Keyse, S. M. (2013). Dual-specificity MAP kinase phosphatases (MKPs). *FEBS Journal* **280**(2): 489-504.
- Cesta, M. F. (2006). Normal Structure, Function, and Histology of the Spleen. *Toxicologic Pathology* **34**(5): 455-465.
- Ceylan-Isik, A. F., Kandadi, M. R., Xu, X., Hua, Y., Chicco, A. J., Ren, J. & Nair, S. (2013). Apelin administration ameliorates high fat diet-induced cardiac hypertrophy and contractile dysfunction. *Journal of Molecular and Cellular Cardiology* **63**: 4-13.
- Chakrabarty, P., Ceballos-Diaz, C., Beccard, A., Janus, C., Dickson, D., Golde, T. E. & Das, P. (2010). IFN- γ Promotes Complement Expression and Attenuates Amyloid Plaque Deposition in Amyloid β Precursor Protein Transgenic Mice. *The Journal of Immunology* **184**(9): 5333-5343.
- Chami, L. & Checler, F. (2012). BACE1 is at the crossroad of a toxic vicious cycle involving cellular stress and beta-amyloid production in Alzheimer's disease. *Molecular Neurodegeneration* **7**(1): 52.
- Chan, J. Y., Cheung, M. C., Moi, P., Chan, K. & Kan, Y. W. (1995). Chromosomal localization of the human NF-E2 family of bZIP transcription factors by fluorescence in situ hybridization. *Human Genetics* **95**(3): 265-269.
- Chan, K., Lu, R., Chang, J. C. & Kan, Y. W. (1996). NRF2, a member of the NFE2 family of transcription factors, is not essential for murine erythropoiesis, growth,

- and development. *Proceedings of the National Academy of Sciences of the United States of America* **93**(24): 13943-13948.
- Chanas, S. A., Jiang, Q., McMahon, M., McWalter, G. K., McLellan, L. I., Elcombe, C. R., Henderson, C. J., Wolf, C. R., Moffat, G. J., Itoh, K., Yamamoto, M. & Hayes, J. D. (2002). Loss of the Nrf2 transcription factor causes a marked reduction in constitutive and inducible expression of the glutathione S-transferase Gsta1, Gsta2, Gstm1, Gstm2, Gstm3 and Gstm4 genes in the livers of male and female mice. *Biochem J* **365**(Pt 2): 405-416.
- Chartier-Harlin, M.-C., Crawford, F., Houlden, H., Warren, A., Hughes, D., Fidani, L., Goate, A., Rossor, M., Roques, P., Hardy, J. & Mullan, M. (1991). Early-onset Alzheimer's disease caused by mutations at codon 717 of the β -amyloid precursor protein gene. *Nature* **353**(6347): 844-846.
- Chartoumpekis, D. V., Ziros, P. G., Psyrogiannis, A. I., Papavassiliou, A. G., Kyriazopoulou, V. E., Sykiotis, G. P. & Habeos, I. G. (2011). Nrf2 Represses FGF21 During Long-Term High-Fat Diet-Induced Obesity in Mice. *Diabetes* **60**(10): 2465-2473.
- Chartoumpekis, D. V., Ziros, P. G., Zaravinos, A., Iskrenova, R. P., Psyrogiannis, A. I., Kyriazopoulou, V. E., Sykiotis, G. P. & Habeos, I. G. (2013). Hepatic Gene Expression Profiling in Nrf2 Knockout Mice after Long-Term High-Fat Diet-Induced Obesity. *Oxidative Medicine and Cellular Longevity* **2013**: 17.
- Chen, C.-n., Brown-Borg, H. M., Rakoczy, S. G., Ferrington, D. A. & Thompson, L. V. (2010). Aging Impairs the Expression of the Catalytic Subunit of Glutamate Cysteine Ligase in Soleus Muscle Under Stress. *The Journals of Gerontology Series A: Biological Sciences and Medical Sciences* **65A**(2): 129-137.
- Chen, J., Buchanan, J. B., Sparkman, N. L., Godbout, J. P., Freund, G. G. & Johnson, R. W. (2008). Neuroinflammation and disruption in working memory in aged mice after acute stimulation of the peripheral innate immune system. *Brain Behav Immun* **22**(3): 301-311.
- Chen, K., Ayutyanont, N., Langbaum, J. B. S., Fleisher, A. S., Reschke, C., Lee, W., Liu, X., Bandy, D., Alexander, G. E., Thompson, P. M., Shaw, L., Trojanowski, J. Q., Jack, C. R., Landau, S. M., Foster, N. L., Harvey, D. J., Weiner, M. W., Koeppe, R. A., Jagust, W. J. & Reiman, E. M. (2011). Characterizing Alzheimer's disease using a hypometabolic convergence index. *NeuroImage* **56**(1): 52-60.
- Cholerton, B., Baker, L. D. & Craft, S. (2011). Insulin resistance and pathological brain ageing. *Diabetic Medicine*: no-no.
- Chou, J. L., Shenoy, D. V., Thomas, N., Choudhary, P. K., LaFerla, F. M., Goodman, S. R. & Breen, G. A. M. (2011). Early dysregulation of the mitochondrial proteome in a mouse model of Alzheimer's disease. *Journal of Proteomics* **74**(4): 466-479.
- Choudhry, F., Howlett, D. R., Richardson, J. C., Francis, P. T. & Williams, R. J. (2012). Pro-oxidant diet enhances β/γ secretase-mediated APP processing in APP/PS1 transgenic mice. *Neurobiology of Aging* **33**(5): 960-968.
- Chowdhry, S., Nazmy, M. H., Meakin, P. J., Dinkova-Kostova, A. T., Walsh, S. V., Tsujita, T., Dillon, J. F., Ashford, M. L. & Hayes, J. D. (2010). Loss of Nrf2 markedly exacerbates nonalcoholic steatohepatitis. *Free Radic Biol Med* **48**(2): 357-371.
- Chowdhry, S., Zhang, Y., McMahon, M., Sutherland, C., Cuadrado, A. & Hayes, J. D. (2013). Nrf2 is controlled by two distinct beta-TrCP recognition motifs in its Neh6 domain, one of which can be modulated by GSK-3 activity. *Oncogene* **32**(32): 3765-3781.

- Chu, J., Giannopoulos, P., Ceballos-Diaz, C., Golde, T. & Pratico, D. (2012). Adeno-associated virus-mediated brain delivery of 5-lipoxygenase modulates the AD-like phenotype of APP mice. *Molecular Neurodegeneration* **7**(1): 1.
- Clarke, J. R., Lyra e Silva, N. M., Figueiredo, C. P., Frozza, R. L., Ledo, J. H., Beckman, D., Katashima, C. K., Razolli, D., Carvalho, B. M., Frazão, R., Silveira, M. A., Ribeiro, F. C., Bomfim, T. R., Neves, F. S., Klein, W. L., Medeiros, R., LaFerla, F. M., Carvalheira, J. B., Saad, M. J., Munoz, D. P., Velloso, L. A., Ferreira, S. T. & De Felice, F. G. (2015). Alzheimer-associated A β oligomers impact the central nervous system to induce peripheral metabolic deregulation. *EMBO Molecular Medicine* **7**(2): 190-210.
- Cleveland, D. W., Hwo, S.-Y. & Kirschner, M. W. (1977a). Physical and chemical properties of purified tau factor and the role of tau in microtubule assembly. *Journal of Molecular Biology* **116**(2): 227-247.
- Cleveland, D. W., Hwo, S.-Y. & Kirschner, M. W. (1977b). Purification of tau, a microtubule-associated protein that induces assembly of microtubules from purified tubulin. *Journal of Molecular Biology* **116**(2): 207-225.
- Cole, S. L. & Vassar, R. (2007). The basic biology of BACE1: A key therapeutic target for Alzheimer's disease. *Curr. Genomics* **8**(8): 509-530.
- Copanaki, E., Chang, S., Vlachos, A., Tschäpe, J.-A., Müller, U. C., Kögel, D. & Deller, T. (2010). sAPP α antagonizes dendritic degeneration and neuron death triggered by proteasomal stress. *Molecular and Cellular Neuroscience* **44**(4): 386-393.
- Correa, F., Ljunggren, E., Mallard, C., Nilsson, M., Weber, S. G. & Sandberg, M. (2011). The Nrf2-inducible antioxidant defense in astrocytes can be both up- and down-regulated by activated microglia: Involvement of p38 MAPK. *GLIA* **59**(5): 785-799.
- Correia, S. C., Santos, R. X., Carvalho, C., Cardoso, S., Candeias, E., Santos, M. S., Oliveira, C. R. & Moreira, P. I. (2012). Insulin signaling, glucose metabolism and mitochondria: Major players in Alzheimer's disease and diabetes interrelation. *Brain Research* **1441**(0): 64-78.
- Craft, S., Baker, L. D., Montine, T. J., Minoshima, S., Watson, G. S., Claxton, A., Arbuckle, M., Callaghan, M., Tsai, E., Plymate, S. R., Green, P. S., Leverenz, J., Cross, D. & Gerton, B. (2012). Intranasal insulin therapy for Alzheimer disease and amnesic mild cognitive impairment: a pilot clinical trial. *Arch Neurol* **69**(1): 29-38.
- Cruts, M., Theuns, J. & Van Broeckhoven, C. (2012). Locus-specific mutation databases for neurodegenerative brain diseases. *Human Mutation* **33**(9): 1340-1344.
- Cruz-Sánchez, F. F., Gironès, X., Ortega, A., Alameda, F. & Lafuente, J. V. (2010). Oxidative stress in Alzheimer's disease hippocampus: A topographical study. *Journal of the Neurological Sciences* **299**(1-2): 163-167.
- Cunnane, S., Nugent, S., Roy, M., Courchesne-Loyer, A., Croteau, E., Tremblay, S., Castellano, A., Pifferi, F., Bocti, C., Paquet, N., Begdouri, H., Bentourkia, M., Turcotte, E., Allard, M., Barberger-Gateau, P., Fulop, T. & Rapoport, S. I. (2011). Brain fuel metabolism, aging, and Alzheimer's disease. *Nutrition* **27**(1): 3-20.
- Cunningham, C., Champion, S., Lunnon, K., Murray, C. L., Woods, J. F., Deacon, R. M., Rawlins, J. N. & Perry, V. H. (2009). Systemic inflammation induces acute behavioral and cognitive changes and accelerates neurodegenerative disease. *Biol Psychiatry* **65**(4): 304-312.
- Cunningham, C., Wilcockson, D. C., Champion, S., Lunnon, K. & Perry, V. H. (2005). Central and Systemic Endotoxin Challenges Exacerbate the Local Inflammatory

- Response and Increase Neuronal Death during Chronic Neurodegeneration. *The Journal of Neuroscience* **25**(40): 9275-9284.
- Dandona, P., Mohamed, I., Ghanim, H., Sia, C. L., Dhindsa, S., Dandona, S., Makdissi, A. & Chaudhuri, A. (2011). Insulin Suppresses the Expression of Amyloid Precursor Protein, Presenilins, and Glycogen Synthase Kinase-3 β in Peripheral Blood Mononuclear Cells. *The Journal of Clinical Endocrinology & Metabolism* **96**(6): 1783-1788.
- Daneschvar, H. L., Aronson, M. D. & Smetana, G. W. (2015). Do statins prevent Alzheimer's disease? A narrative review. *Eur J Intern Med*.
- Dang, J., Brandenburg, L. O., Rosen, C., Fragoulis, A., Kipp, M., Pufe, T., Beyer, C. & Wruck, C. J. (2012). Nrf2 expression by neurons, astroglia, and microglia in the cerebral cortical penumbra of ischemic rats. *J Mol Neurosci* **46**(3): 578-584.
- Davalos, D., Grutzendler, J., Yang, G., Kim, J. V., Zuo, Y., Jung, S., Littman, D. R., Dustin, M. L. & Gan, W.-B. (2005). ATP mediates rapid microglial response to local brain injury in vivo. *Nat Neurosci* **8**(6): 752-758.
- Davies, L. C. & Taylor, P. R. (2015). Tissue-resident macrophages: then and now. *Immunology* **144**(4): 541-548.
- Davis, C., Mudd, J. & Hawkins, M. (2014). Neuroprotective effects of leptin in the context of obesity and metabolic disorders. *Neurobiology of Disease* **72, Part A**: 61-71.
- de Ferranti, S. & Mozaffarian, D. (2008). The Perfect Storm: Obesity, Adipocyte Dysfunction, and Metabolic Consequences. *Clinical Chemistry* **54**(6): 945-955.
- de Jong, D., Jansen, R., Hoefnagels, W., Jellesma-Eggenkamp, M., Verbeek, M., Borm, G. & Kremer, B. (2008). No Effect of One-Year Treatment with Indomethacin on Alzheimer's Disease Progression: A Randomized Controlled Trial. *PLoS ONE* **3**(1): e1475.
- de la Monte, S. M. (2009). Insulin resistance and Alzheimer's disease. *BMB Rep.* **42**(8): 475-481.
- de la Monte, S. M. & Wands, J. R. (2008). Alzheimer's disease is type 3 diabetes-evidence reviewed. *Journal of diabetes science and technology* **2**(6): 1101-1113.
- de La Serre, C. B., Ellis, C. L., Lee, J., Hartman, A. L., Rutledge, J. C. & Raybould, H. E. (2010). *Propensity to high-fat diet-induced obesity in rats is associated with changes in the gut microbiota and gut inflammation*. edn, vol. 299.
- De Santi, S., de Leon, M. J., Rusinek, H., Convit, A., Tarshish, C. Y., Roche, A., Tsui, W. H., Kandil, E., Boppana, M., Daisley, K., Wang, G. J., Schlyer, D. & Fowler, J. (2001). Hippocampal formation glucose metabolism and volume losses in MCI and AD. *Neurobiology of Aging* **22**(4): 529-539.
- de Vries, H. E., Witte, M., Hondius, D., Rozemuller, A. J. M., Drukarch, B., Hoozemans, J. & van Horssen, J. (2008). Nrf2-induced antioxidant protection: A promising target to counteract ROS-mediated damage in neurodegenerative disease? *Free Radical Biology and Medicine* **45**(10): 1375-1383.
- DeLegge, M. H. & Smoke, A. (2008). Neurodegeneration and Inflammation. *Nutrition in Clinical Practice* **23**(1): 35-41.
- Deshmane, S. L., Kremlev, S., Amini, S. & Sawaya, B. E. (2009). Monocyte Chemoattractant Protein-1 (MCP-1): An Overview. *Journal of Interferon & Cytokine Research* **29**(6): 313-326.
- Devi, L., Alldred, M. J., Ginsberg, S. D. & Ohno, M. (2012). Mechanisms Underlying Insulin Deficiency-Induced Acceleration of β -Amyloidosis in a Mouse Model of Alzheimer's Disease. *PLoS ONE* **7**(3): e32792.
- DiabetesUK (2015). Prediabetes and insulin resistance. <http://www.diabetes.co.uk/insulin-resistance.html>.

- Diaz-Hernandez, J. I., Almeida, A., Delgado-Esteban, M., Fernandez, E. & Bolaños, J. P. (2005). Knockdown of Glutamate-Cysteine Ligase by Small Hairpin RNA Reveals That Both Catalytic and Modulatory Subunits Are Essential for the Survival of Primary Neurons. *Journal of Biological Chemistry* **280**(47): 38992-39001.
- Dibaj, P., Steffens, H., Zschüntzsch, J., Nadrigny, F., Schomburg, E. D., Kirchhoff, F. & Neusch, C. (2011). *In Vivo* Imaging Reveals Distinct Inflammatory Activity of CNS Microglia versus PNS Macrophages in a Mouse Model for ALS. *PLoS ONE* **6**(3): e17910.
- Didic, M., Barbeau, E. J., Felician, O., Tramoni, E., Guedj, E., Poncet, M. & Ceccaldi, M. (2011). Which memory system is impaired first in alzheimer's disease? *Journal of Alzheimer's Disease* **27**(1): 11-22.
- Dilger, R. N. & Johnson, R. W. (2008). Aging, microglial cell priming, and the discordant central inflammatory response to signals from the peripheral immune system. *Journal of Leukocyte Biology* **84**(4): 932-939.
- Diniz, D. G., Foro, C. A., Rego, C. M., Gloria, D. A., de Oliveira, F. R., Paes, J. M., de Sousa, A. A., Tokuhashi, T. P., Trindade, L. S., Turiel, M. C., Vasconcelos, E. G., Torres, J. B., Cunnigham, C., Perry, V. H., Vasconcelos, P. F. & Diniz, C. W. (2010). Environmental impoverishment and aging alter object recognition, spatial learning, and dentate gyrus astrocytes. *Eur J Neurosci* **32**(3): 509-519.
- Dinkova-Kostova, A. T. & Abramov, A. Y. (2015). The emerging role of Nrf2 in mitochondrial function. *Free Radical Biology and Medicine*.
- Du, H., Guo, L., Yan, S. Q., Sosunov, A. A., McKhann, G. M. & Yan, S. S. (2010). Early deficits in synaptic mitochondria in an Alzheimer's disease mouse model. *Proceedings of the National Academy of Sciences of the United States of America* **107**(43): 18670-18675.
- Eacott, M. J. & Easton, A. (2010). Episodic memory in animals: Remembering which occasion. *Neuropsychologia* **48**(8): 2273-2280.
- Edwards, D. R., Handsley, M. M. & Pennington, C. J. (2008). The ADAM metalloproteinases. *Molecular Aspects of Medicine* **29**(5): 258-289.
- Eftekhazadeh, B., Maghsoudi, N. & Khodagholi, F. (2010). Stabilization of transcription factor Nrf2 by tBHQ prevents oxidative stress-induced amyloid β formation in NT2N neurons. *Biochimie* **92**(3): 245-253.
- Eggert, S., Paliga, K., Soba, P., Evin, G., Masters, C. L., Weidemann, A. & Beyreuther, K. (2004). The Proteolytic Processing of the Amyloid Precursor Protein Gene Family Members APLP-1 and APLP-2 Involves α -, β -, γ -, and ϵ -Like Cleavages: MODULATION OF APLP-1 PROCESSING BY N-GLYCOSYLATION. *Journal of Biological Chemistry* **279**(18): 18146-18156.
- Eggler, A. L., Liu, G., Pezzuto, J. M., van Breemen, R. B. & Mesecar, A. D. (2005). Modifying specific cysteines of the electrophile-sensing human Keap1 protein is insufficient to disrupt binding to the Nrf2 domain Neh2. *Proc Natl Acad Sci U S A* **102**(29): 10070-10075.
- Elder, G. A., Gama Sosa, M. A. & De Gasperi, R. (2010). Transgenic Mouse Models of Alzheimer's Disease. *The Mount Sinai journal of medicine, New York* **77**(1): 69-81.
- Emanuelli, B., Eberlé, D., Suzuki, R. & Kahn, C. R. (2008). Overexpression of the dual-specificity phosphatase MKP-4/DUSP-9 protects against stress-induced insulin resistance. *Proceedings of the National Academy of Sciences* **105**(9): 3545-3550.
- Emerit, J., Edeas, M. & Bricaire, F. (2004). Neurodegenerative diseases and oxidative stress. *Biomedicine & Pharmacotherapy* **58**(1): 39-46.
- Emre, Y., Hurtaud, C., Nübel, T., Criscuolo, F., Ricquier, D. & Cassard-Doulcier, A.-M. (2007). Mitochondria contribute to LPS-induced MAPK activation via

- uncoupling protein UCP2 in macrophages. *Biochemical Journal* **402**(2): 271-278.
- Erickson, M. A. & Banks, W. A. (2011). Cytokine and chemokine responses in serum and brain after single and repeated injections of lipopolysaccharide: Multiplex quantification with path analysis. *Brain, Behavior, and Immunity* **25**(8): 1637-1648.
- Erickson, M. A., Hartvigson, P. E., Morofuji, Y., Owen, J. B., Butterfield, D. A. & Banks, W. A. (2012). Lipopolysaccharide impairs amyloid beta efflux from brain: altered vascular sequestration, cerebrospinal fluid reabsorption, peripheral clearance and transporter function at the blood-brain barrier. *J Neuroinflammation* **9**: 150.
- Erlichman, J. S., Hewitt, A., Damon, T. L., Hart, M., Kuraszcz, J., Li, A. & Leiter, J. C. (2008). Inhibition of monocarboxylate transporter 2 in the retrotrapezoid nucleus in rats: A test of the astrocyte-neuron lactate-shuttle hypothesis. *Journal of Neuroscience* **28**(19): 4888-4896.
- Ernst, I. M. A., Wagner, A. E., Schuemann, C., Storm, N., Höppner, W., Döring, F., Stocker, A. & Rimbach, G. (2011). Allyl-, butyl- and phenylethyl-isothiocyanate activate Nrf2 in cultured fibroblasts. *Pharmacological Research* **63**(3): 233-240.
- Farfara, D., Trudler, D., Segev-Amzaleg, N., Galron, R., Stein, R. & Frenkel, D. (2011). γ -Secretase component presenilin is important for microglia β -amyloid clearance. *Annals of Neurology* **69**(1): 170-180.
- Fei, N. & Zhao, L. (2013). An opportunistic pathogen isolated from the gut of an obese human causes obesity in germfree mice. *ISME J* **7**(4): 880-884.
- Fellmann, L., Nascimento, A. R., Tibiriça, E. & Bousquet, P. (2013). Murine models for pharmacological studies of the metabolic syndrome. *Pharmacology & Therapeutics* **137**(3): 331-340.
- Fellous, A., Francon, J., Lennon, A. M. & Nunez, J. (1977). Microtubule Assembly in vitro. *European Journal of Biochemistry* **78**(1): 167-174.
- Felsenstein, K. M., Hunihan, L. W. & Roberts, S. B. (1994). Altered cleavage and secretion of a recombinant β -APP bearing the Swedish familial Alzheimer's disease mutation. *Nat Genet* **6**(3): 251-256.
- Feng, B., Jiao, P., Helou, Y., Li, Y., He, Q., Walters, M. S., Salomon, A. & Xu, H. (2014). Mitogen-Activated Protein Kinase Phosphatase 3 (MKP-3)-Deficient Mice Are Resistant to Diet-Induced Obesity. *Diabetes* **63**(9): 2924-2934.
- Ferretti, M. T., Bruno, M. A., Ducatenzeiler, A., Klein, W. L. & Cuellar, A. C. (2012). Intracellular A β -oligomers and early inflammation in a model of Alzheimer's disease. *Neurobiology of Aging* **33**(7): 1329-1342.
- Filali, M., Lalonde, R., Theriault, P., Julien, C., Calon, F. & Planel, E. (2012). Cognitive and non-cognitive behaviors in the triple transgenic mouse model of Alzheimer's disease expressing mutated APP, PS1, and Mapt (3xTg-AD). *Behavioural Brain Research* **234**(2): 334-342.
- Forwood, S. E., Winters, B. D. & Bussey, T. J. (2005). Hippocampal lesions that abolish spatial maze performance spare object recognition memory at delays of up to 48 hours. *Hippocampus* **15**(3): 347-355.
- Fourquet, S., Guerois, R., Biard, D. & Toledano, M. B. (2010). Activation of NRF2 by Nitrosative Agents and H₂O₂ Involves KEAP1 Disulfide Formation. *Journal of Biological Chemistry* **285**(11): 8463-8471.
- Franklin, B. S., Bossaller, L., De Nardo, D., Ratter, J. M., Stutz, A., Engels, G., Brenker, C., Nordhoff, M., Mirandola, S. R., Al-Amoudi, A., Mangan, M. S., Zimmer, S., Monks, B. G., Fricke, M., Schmidt, R. E., Espevik, T., Jones, B., Jarnicki, A. G., Hansbro, P. M., Busto, P., Marshak-Rothstein, A., Hornemann, S., Aguzzi, A., Kastenmuller, W. & Latz, E. (2014). The adaptor ASC has

- extracellular and 'prionoid' activities that propagate inflammation. *Nat Immunol* **15**(8): 727-737.
- Freeman, L. R., Haley-Zitlin, V., Stevens, C. & Granholm, A. C. (2011). Diet-induced effects on neuronal and glial elements in the middle-aged rat hippocampus. *Nutr Neurosci* **14**(1): 32-44.
- Freeman, L. R., Zhang, L., Dasuri, K., Fernandez-Kim, S.-O., Bruce-Keller, A. J. & Keller, J. N. (2012). Mutant Amyloid Precursor Protein Differentially Alters Adipose Biology under Obesogenic and Non-Obesogenic Conditions. *PLoS ONE* **7**(8): e43193.
- Fujii, S., Sawa, T., Ihara, H., Tong, K. I., Ida, T., Okamoto, T., Ahtesham, A. K., Ishima, Y., Motohashi, H., Yamamoto, M. & Akaike, T. (2010). The Critical Role of Nitric Oxide Signaling, via Protein S-Guanylation and Nitrated Cyclic GMP, in the Antioxidant Adaptive Response. *Journal of Biological Chemistry* **285**(31): 23970-23984.
- Fukumoto, H., Rosene, D. L., Moss, M. B., Raju, S., Hyman, B. T. & Irizarry, M. C. (2004). β -Secretase Activity Increases with Aging in Human, Monkey, and Mouse Brain. *The American Journal of Pathology* **164**(2): 719-725.
- Fuller, S., Steele, M. & Münch, G. (2010). Activated astroglia during chronic inflammation in Alzheimer's disease—Do they neglect their neurosupportive roles? *Mutation Research/Fundamental and Molecular Mechanisms of Mutagenesis* **690**(1–2): 40-49.
- Furnari, M. A. (2013). Behavioral, neurochemical, and neuroimmune changes in Nrf2 knockout mice following early postnatal exposure to valproic acid.
- Furnari, M. A., Saw, C. L.-L., Kong, A.-N. & Wagner, G. C. (2014). Altered behavioral development in Nrf2 knockout mice following early postnatal exposure to valproic acid. *Brain Research Bulletin* **109**: 132-142.
- Games, D., Adams, D., Alessandrini, R., Barbour, R., Borthellette, P., Blackwell, C., Carr, T., Clemens, J., Donaldson, T., Gillespie, F., Guido, T., Hagopian, S., Johnson-Wood, K., Khan, K., Lee, M., Leibowitz, P., Lieberburg, I., Little, S., Masliah, E., McConlogue, L., Montoya-Zavala, M., Mucke, L., Paganini, L., Penniman, E., Power, M., Schenk, D., Seubert, P., Snyder, B., Soriano, F., Tan, H., Vitale, J., Wadsworth, S., Wolozin, B. & Zhao, J. (1995). Alzheimer-type neuropathology in transgenic mice overexpressing V717F [beta]-amyloid precursor protein. *Nature* **373**(6514): 523-527.
- Gan, X., Huang, S., Wu, L., Wang, Y., Hu, G., Li, G., Zhang, H., Yu, H., Swerdlow, R. H., Chen, J. X. & Yan, S. S. (2014). Inhibition of ERK-DLP1 signaling and mitochondrial division alleviates mitochondrial dysfunction in Alzheimer's disease cybrid cell. *Biochimica et Biophysica Acta (BBA) - Molecular Basis of Disease* **1842**(2): 220-231.
- Ghanim, H., Monte, S. V., Sia, C. L., Abuaysheh, S., Green, K., Caruana, J. A. & Dandona, P. (2012). Reduction in Inflammation and the Expression of Amyloid Precursor Protein and Other Proteins Related to Alzheimer's Disease following Gastric Bypass Surgery. *The Journal of Clinical Endocrinology & Metabolism* **97**(7): E1197-E1201.
- Giulian, D. & Baker, T. J. (1986). Characterization of amoeboid microglia isolated from developing mammalian brain. *J Neurosci* **6**(8): 2163-2178.
- Goate, A., Chartier-Harlin, M.-C., Mullan, M., Brown, J., Crawford, F., Fidani, L., Giuffra, L., Haynes, A., Irving, N., James, L., Mant, R., Newton, P., Rooke, K., Roques, P., Talbot, C., Pericak-Vance, M., Roses, A., Williamson, R., Rossor, M., Owen, M. & Hardy, J. (1991). Segregation of a missense mutation in the amyloid precursor protein gene with familial Alzheimer's disease. *Nature* **349**(6311): 704-706.

- Godbout, J. P., Moreau, M., Lestage, J., Chen, J., Sparkman, N. L., Connor, J. O., Castanon, N., Kelley, K. W., Dantzer, R. & Johnson, R. W. (2007). Aging Exacerbates Depressive-like Behavior in Mice in Response to Activation of the Peripheral Innate Immune System. *Neuropsychopharmacology* **33**(10): 2341-2351.
- Goedert, M. (2015). Alzheimer's and Parkinson's diseases: The prion concept in relation to assembled A β , tau, and α -synuclein. *Science* **349**(6248).
- Gorina, R., Font-Nieves, M., Márquez-Kisinousky, L., Santalucia, T. & Planas, A. M. (2011). Astrocyte TLR4 activation induces a proinflammatory environment through the interplay between MyD88-dependent NF κ B signaling, MAPK, and Jak1/Stat1 pathways. *Glia* **59**(2): 242-255.
- Goshen, I. & Yirmiya, R. (2009). Interleukin-1 (IL-1): a central regulator of stress responses. *Front Neuroendocrinol* **30**(1): 30-45.
- Granholt, A. C., Bimonte-Nelson, H. A., Moore, A. B., Nelson, M. E., Freeman, L. R. & Sambamurti, K. (2008). Effects of a saturated fat and high cholesterol diet on memory and hippocampal morphology in the middle-aged rat. *J Alzheimers Dis* **14**(2): 133-145.
- Greco, T. & Fiskum, G. (2010). Neuroprotection through stimulation of mitochondrial antioxidant protein expression. *J Alzheimers Dis* **20 Suppl 2**: S427-437.
- Grinberg, L. T., Korczyn, A. D. & Heinsen, H. (2012). Cerebral amyloid angiopathy impact on endothelium. *Experimental Gerontology* **47**(11): 838-842.
- Guo, H., Callaway, J. B. & Ting, J. P. Y. (2015). Inflammasomes: mechanism of action, role in disease, and therapeutics. *Nat Med* **21**(7): 677-687.
- Haass, C., Lemere, C. A., Capell, A., Citron, M., Seubert, P., Schenk, D., Lannfelt, L. & Selkoe, D. J. (1995). The Swedish mutation causes early-onset Alzheimer's disease by β -secretase cleavage within the secretory pathway. *Nat Med* **1**(12): 1291-1296.
- Haj-ali, V., Mohaddes, G. & Babri, S. H. (2009). Intracerebroventricular insulin improves spatial learning and memory in male Wistar rats. *Behav Neurosci* **123**(6): 1309-1314.
- Hajjar, T., Goh, Y. M., Rajion, M. A., Vidyadaran, S., Li, T. A. & Ebrahimi, M. (2013). Alterations in neuronal morphology and synaptophysin expression in the rat brain as a result of changes in dietary n-6: n-3 fatty acid ratios. *Lipids Health Dis* **12**: 113.
- Hall, A. M. & Roberson, E. D. (2012). Mouse models of Alzheimer's disease. *Brain Research Bulletin* **88**(1): 3-12.
- Hamby, M. E., Hewett, J. A. & Hewett, S. J. (2006). TGF- β 1 potentiates astrocytic nitric oxide production by expanding the population of astrocytes that express NOS-2. *Glia* **54**(6): 566-577.
- Hammond, R. S., Tull, L. E. & Stackman, R. W. (2004). On the delay-dependent involvement of the hippocampus in object recognition memory. *Neurobiology of Learning and Memory* **82**(1): 26-34.
- Hargrave, S. L., Davidson, T. L., Lee, T.-J. & Kinzig, K. P. (2015). Brain and behavioral perturbations in rats following Western diet access. *Appetite* **93**: 35-43.
- Hauss-Wegrzyniak, B., Lynch, M. A., Vraniak, P. D. & Wenk, G. L. (2002). Chronic Brain Inflammation Results in Cell Loss in the Entorhinal Cortex and Impaired LTP in Perforant Path-Granule Cell Synapses. *Experimental Neurology* **176**(2): 336-341.
- Hayashi, T., Shishido, N., Nakayama, K., Nunomura, A., Smith, M. A., Perry, G. & Nakamura, M. (2007). Lipid peroxidation and 4-hydroxy-2-nonenal formation

- by copper ion bound to amyloid- β peptide. *Free Radical Biology and Medicine* **43**(11): 1552-1559.
- Hayes, J. D. & McMahon, M. (2009). NRF2 and KEAP1 mutations: permanent activation of an adaptive response in cancer. *Trends Biochem.Sci.* **34**(4): 176-188.
- Hedskog, L., Pinho, C. M., Filadi, R., Rönnbäck, A., Hertwig, L., Wiehager, B., Larssen, P., Gellhaar, S., Sandebring, A., Westerlund, M., Graff, C., Winblad, B., Galter, D., Behbahani, H., Pizzo, P., Glaser, E. & Ankarcona, M. (2013). Modulation of the endoplasmic reticulum–mitochondria interface in Alzheimer's disease and related models. *Proceedings of the National Academy of Sciences* **110**(19): 7916-7921.
- Hellström-Lindahl, E., Viitanen, M. & Marutle, A. (2009). Comparison of A β levels in the brain of familial and sporadic Alzheimer's disease. *Neurochemistry International* **55**(4): 243-252.
- Heneka, M. T., Carson, M. J., Khoury, J. E., Landreth, G. E., Brosseron, F., Feinstein, D. L., Jacobs, A. H., Wyss-Coray, T., Vitorica, J., Ransohoff, R. M., Herrup, K., Frautschy, S. A., Finsen, B., Brown, G. C., Verkhratsky, A., Yamanaka, K., Koistinaho, J., Latz, E., Halle, A., Petzold, G. C., Town, T., Morgan, D., Shinohara, M. L., Perry, V. H., Holmes, C., Bazan, N. G., Brooks, D. J., Hunot, S., Joseph, B., Deigendesch, N., Garaschuk, O., Boddeke, E., Dinarello, C. A., Breitner, J. C., Cole, G. M., Golenbock, D. T. & Kummer, M. P. (2015). Neuroinflammation in Alzheimer's disease. *The Lancet Neurology* **14**(4): 388-405.
- Heneka, M. T., Kummer, M. P. & Latz, E. (2014). Innate immune activation in neurodegenerative disease. *Nat Rev Immunol* **14**(7): 463-477.
- Heneka, M. T., Kummer, M. P., Stutz, A., Delekate, A., Schwartz, S., Vieira-Saecker, A., Griep, A., Axt, D., Remus, A., Tzeng, T.-C., Gelpi, E., Halle, A., Korte, M., Latz, E. & Golenbock, D. T. (2013). NLRP3 is activated in Alzheimer's disease and contributes to pathology in APP/PS1 mice. *Nature* **493**(7434): 674-678.
- Henry, C. J., Huang, Y., Wynne, A., Hanke, M., Himler, J., Bailey, M. T., Sheridan, J. F. & Godbout, J. P. (2008). Minocycline attenuates lipopolysaccharide (LPS)-induced neuroinflammation, sickness behavior, and anhedonia. *Journal of Neuroinflammation* **5**: 15-15.
- Henry, C. J., Huang, Y., Wynne, A. M. & Godbout, J. P. (2009). Peripheral lipopolysaccharide (LPS) challenge promotes microglial hyperactivity in aged mice that is associated with exaggerated induction of both pro-inflammatory IL-1 β and anti-inflammatory IL-10 cytokines. *Brain Behav Immun* **23**(3): 309-317.
- Hiltunen, M., Khandelwal, V. K. M., Yaluri, N., Tiilikainen, T., Tusa, M., Koivisto, H., Krzisch, M., Vepsäläinen, S., Mäkinen, P., Kemppainen, S., Miettinen, P., Haapasalo, A., Soininen, H., Laakso, M. & Tanila, H. (2012). Contribution of genetic and dietary insulin resistance to Alzheimer phenotype in APP/PS1 transgenic mice. *Journal of Cellular and Molecular Medicine* **16**(6): 1206-1222.
- Ho, L., Qin, W., Pompl, P. N., Xiang, Z., Wang, J., Zhao, Z., Peng, Y., Cambareri, G., Rocher, A., Mobbs, C. V., Hof, P. R. & Pasinetti, G. M. (2004). Diet-induced insulin resistance promotes amyloidosis in a transgenic mouse model of Alzheimer's disease. *The FASEB Journal*.
- Holmes, C., El-Okli, M., Williams, A. L., Cunningham, C., Wilcockson, D. & Perry, V. H. (2003). Systemic infection, interleukin 1 β , and cognitive decline in Alzheimer's disease. *Journal of Neurology, Neurosurgery & Psychiatry* **74**(6): 788-789.
- Holmström, K. M., Baird, L., Zhang, Y., Hargreaves, I., Chalasani, A., Land, J. M., Stanyer, L., Yamamoto, M., Dinkova-Kostova, A. T. & Abramov, A. Y. (2013).

- Nrf2 impacts cellular bioenergetics by controlling substrate availability for mitochondrial respiration. *Biology Open* **2**(8): 761-770.
- Hong, Y., Yan, W., Chen, S., Sun, C.-r. & Zhang, J.-m. (2010). The role of Nrf2 signaling in the regulation of antioxidants and detoxifying enzymes after traumatic brain injury in rats and mice. *Acta Pharmacol Sin* **31**(11): 1421-1430.
- Hook, V. Y. H., Kindy, M. & Hook, G. (2008). Inhibitors of Cathepsin B Improve Memory and Reduce β -Amyloid in Transgenic Alzheimer Disease Mice Expressing the Wild-type, but Not the Swedish Mutant, β -Secretase Site of the Amyloid Precursor Protein. *Journal of Biological Chemistry* **283**(12): 7745-7753.
- Hsiao, K., Chapman, P., Nilsen, S., Eckman, C., Harigaya, Y., Younkin, S., Yang, F. & Cole, G. (1996). Correlative memory deficits, Abeta elevation, and amyloid plaques in transgenic mice. *Science* **274**(5284): 99-102.
- Hughes, M. M., Field, R. H., Perry, V. H., Murray, C. L. & Cunningham, C. (2010). Microglia in the degenerating brain are capable of phagocytosis of beads and of apoptotic cells, but do not efficiently remove PrPSc, even upon LPS stimulation. *GLIA* **58**(16): 2017-2030.
- Hunter, R. L., Dragicevic, N., Seifert, K., Choi, D. Y., Liu, M., Kim, H.-C., Cass, W. A., Sullivan, P. G. & Bing, G. (2007). Inflammation induces mitochondrial dysfunction and dopaminergic neurodegeneration in the nigrostriatal system. *Journal of Neurochemistry* **100**(5): 1375-1386.
- Ifuku, M., Katafuchi, T., Mawatari, S., Noda, M., Miake, K., Sugiyama, M. & Fujino, T. (2012). Anti-inflammatory/anti-amyloidogenic effects of plasmalogens in lipopolysaccharide-induced neuroinflammation in adult mice. *Journal of Neuroinflammation* **9**: 197-197.
- Innamorato, N. G., Rojo, A. I., García-Yagüe, Á. J., Yamamoto, M., de Ceballos, M. L. & Cuadrado, A. (2008). The Transcription Factor Nrf2 Is a Therapeutic Target against Brain Inflammation. *The Journal of Immunology* **181**(1): 680-689.
- Iqbal, K., del C. Alonso, A., Chen, S., Chohan, M. O., El-Akkad, E., Gong, C.-X., Khatoon, S., Li, B., Liu, F., Rahman, A., Tanimukai, H. & Grundke-Iqbal, I. (2005). Tau pathology in Alzheimer disease and other tauopathies. *Biochimica et Biophysica Acta (BBA) - Molecular Basis of Disease* **1739**(2-3): 198-210.
- Ishii, M., Wang, G., Racchumi, G., Dyke, J. P. & Iadecola, C. (2014). Transgenic mice overexpressing amyloid precursor protein exhibit early metabolic deficits and a pathologically low leptin state associated with hypothalamic dysfunction in arcuate neuropeptide y neurons. *J Neurosci* **34**(27): 9096-9106.
- Ito, D., Tanaka, K., Suzuki, S., Dembo, T. & Fukuuchi, Y. (2001). Enhanced Expression of Iba1, Ionized Calcium-Binding Adapter Molecule 1, After Transient Focal Cerebral Ischemia In Rat Brain. *Stroke* **32**(5): 1208-1215.
- Itoh, K., Chiba, T., Takahashi, S., Ishii, T., Igarashi, K., Katoh, Y., Oyake, T., Hayashi, N., Satoh, K., Hatayama, I., Yamamoto, M. & Nabeshima, Y. I. (1997). An Nrf2/small Maf heterodimer mediates the induction of phase II detoxifying enzyme genes through antioxidant response elements. *Biochemical and Biophysical Research Communications* **236**(2): 313-322.
- Itoh, K., Wakabayashi, N., Katoh, Y., Ishii, T., Igarashi, K., Engel, J. D. & Yamamoto, M. (1999). Keap1 represses nuclear activation of antioxidant responsive elements by Nrf2 through binding to the amino-terminal Neh2 domain. *Genes and Development* **13**(1): 76-86.
- Itoh, K., Ye, P., Matsumiya, T., Tanji, K. & Ozaki, T. (2015). Emerging functional cross-talk between the Keap1-Nrf2 system and mitochondria. *Journal of Clinical Biochemistry and Nutrition* **56**(2): 91-97.

- JacksonLaboratories (2015). R1.40 mouse strain. <http://jaxmice.jax.org/strain/005300.html>.
- Jacobsen, K. T., Adlerz, L., Multhaup, G. & Iverfeldt, K. (2010). Insulin-like Growth Factor-1 (IGF-1)-induced Processing of Amyloid- β Precursor Protein (APP) and APP-like Protein 2 Is Mediated by Different Metalloproteinases. *Journal of Biological Chemistry* **285**(14): 10223-10231.
- Jeong, Y. H., Park, C. H., Yoo, J., Shin, K. Y., Ahn, S.-M., Kim, H.-S., Lee, S. H., Emson, P. C. & Suh, Y.-H. (2006). Chronic stress accelerates learning and memory impairments and increases amyloid deposition in APPV717I-CT100 transgenic mice, an Alzheimer's disease model. *The FASEB Journal*.
- Jiang, T., Huang, Z., Lin, Y., Zhang, Z., Fang, D. & Zhang, D. D. (2010). The Protective Role of Nrf2 in Streptozotocin-Induced Diabetic Nephropathy. *Diabetes* **59**(4): 850-860.
- Jo, C., Gundemir, S., Pritchard, S., Jin, Y. N., Rahman, I. & Johnson, G. V. W. (2014). Nrf2 reduces levels of phosphorylated tau protein by inducing autophagy adaptor protein NDP52. *Nature communications* **5**.
- Johnson, J. A., Johnson, D. A., Kraft, A. D., Calkins, M. J., Jakel, R. J., Vargas, M. R. & Chen, P.-C. (2008). The Nrf2-ARE Pathway. *Annals of the New York Academy of Sciences* **1147**(1): 61-69.
- Johnstone, M., Gearing, A. J. H. & Miller, K. M. (1999). A central role for astrocytes in the inflammatory response to β -amyloid; chemokines, cytokines and reactive oxygen species are produced. *Journal of Neuroimmunology* **93**(1-2): 182-193.
- Jolival, C. G., Hurford, R., Lee, C. A., Dumaop, W., Rockenstein, E. & Masliah, E. (2010). Type 1 diabetes exaggerates features of Alzheimer's disease in APP transgenic mice. *Experimental Neurology* **223**(2): 422-431.
- Jonsson, T., Atwal, J. K., Steinberg, S., Snaedal, J., Jonsson, P. V., Bjornsson, S., Stefansson, H., Sulem, P., Gudbjartsson, D., Maloney, J., Hoyte, K., Gustafson, A., Liu, Y., Lu, Y., Bhangale, T., Graham, R. R., Huttenlocher, J., Bjornsdottir, G., Andreassen, O. A., Jonsson, E. G., Palotie, A., Behrens, T. W., Magnusson, O. T., Kong, A., Thorsteinsdottir, U., Watts, R. J. & Stefansson, K. (2012). A mutation in APP protects against Alzheimer's disease and age-related cognitive decline. *Nature* **488**(7409): 96-99.
- Joshi, G., Gan, K. A., Johnson, D. A. & Johnson, J. A. (2015). Increased Alzheimer's disease-like pathology in the APP/PS1 Δ E9 mouse model lacking Nrf2 through modulation of autophagy. *Neurobiology of Aging* **36**(2): 664-679.
- Joshi, Y. B., Giannopoulos, P. F., Chu, J. & Praticò, D. (2014). Modulation of lipopolysaccharide-induced memory insult, γ -secretase, and neuroinflammation in triple transgenic mice by 5-lipoxygenase. *Neurobiology of Aging* **35**(5): 1024-1031.
- Julien, C., Tremblay, C., Phivilay, A., Berthiaume, L., Émond, V., Julien, P. & Calon, F. (2010). High-fat diet aggravates amyloid-beta and tau pathologies in the 3xTg-AD mouse model. *Neurobiology of Aging* **31**(9): 1516-1531.
- Jung, H.-J., Kim, Y.-J., Eggert, S., Chung, K. C., Choi, K. S. & Park, S. A. (2013). Age-dependent increases in tau phosphorylation in the brains of type 2 diabetic rats correlate with a reduced expression of p62. *Experimental Neurology* **248**: 441-450.
- Jung, H. J., Park, S. S., Mok, J. O., Lee, T. K., Park, C. S. & Park, S. A. (2011). Increased expression of three-repeat isoforms of tau contributes to tau pathology in a rat model of chronic type 2 diabetes. *Experimental Neurology* **228**(2): 232-241.

- Kaden, D., Munter, L. M., Reif, B. & Multhaup, G. (2012). The amyloid precursor protein and its homologues: Structural and functional aspects of native and pathogenic oligomerization. *European Journal of Cell Biology* **91**(4): 234-239.
- Kalaria, R. N. (2010). *Vascular basis for brain degeneration: faltering controls and risk factors for dementia*. edn, vol. 68.
- Kaminska, B., Gozdz, A., Zawadzka, M., Ellert-Miklaszewska, A. & Lipko, M. (2009). MAPK Signal Transduction Underlying Brain Inflammation and Gliosis as Therapeutic Target. *The Anatomical Record: Advances in Integrative Anatomy and Evolutionary Biology* **292**(12): 1902-1913.
- Kamphuis, W., Mamber, C., Moeton, M., Kooijman, L., Sluijs, J. A., Jansen, A. H. P., Verveer, M., de Groot, L. R., Smith, V. D., Rangarajan, S., Rodríguez, J. J., Orre, M. & Hol, E. M. (2012). GFAP Isoforms in Adult Mouse Brain with a Focus on Neurogenic Astrocytes and Reactive Astroglialosis in Mouse Models of Alzheimer Disease. *PLoS ONE* **7**(8): e42823.
- Kanekiyo, T., Liu, C.-C., Shinohara, M., Li, J. & Bu, G. (2012). LRP1 in Brain Vascular Smooth Muscle Cells Mediates Local Clearance of Alzheimer's Amyloid- β . *The Journal of Neuroscience* **32**(46): 16458-16465.
- Kanninen, K., Heikkinen, R., Malm, T., Roloa, T., Kuhmonen, S., Leinonen, H., Ylä-Herttuala, S., Tanila, H., Levonen, A. L., Koistinaho, M. & Koistinaho, J. (2009). Intrahippocampal injection of a lentiviral vector expressing Nrf2 improves spatial learning in a mouse model of Alzheimer's disease. *Proceedings of the National Academy of Sciences of the United States of America* **106**(38): 16505-16510.
- Kapetanovic, R., Bokil, N. J. & Sweet, M. J. (2015). Innate immune perturbations, accumulating DAMPs and inflammasome dysregulation: A ticking time bomb in ageing. *Ageing Research Reviews*.
- Karran, E., Mercken, M. & Strooper, B. D. (2011). The amyloid cascade hypothesis for Alzheimer's disease: an appraisal for the development of therapeutics. *Nature Reviews Drug Discovery* **10**(9): 698-712.
- Karuppagounder, S. S., Xu, H., Shi, Q., Chen, L. H., Pedrini, S., Pechman, D., Baker, H., Beal, M. F., Gandy, S. E. & Gibson, G. E. (2009). Thiamine deficiency induces oxidative stress and exacerbates the plaque pathology in Alzheimer's mouse model. *Neurobiol Aging* **30**(10): 1587-1600.
- Kasischke, K. A., Vishwasrao, H. D., Fisher, P. J., Zipfel, W. R. & Webb, W. W. (2004). Neural activity triggers neuronal oxidative metabolism followed by astrocytic glycolysis. *Science* **305**(5680): 99-103.
- Katoh, Y., Iida, K., Kang, M. I., Kobayashi, A., Mizukami, M., Tong, K. I., McMahon, M., Hayes, J. D., Itoh, K. & Yamamoto, M. (2005). Evolutionary conserved N-terminal domain of Nrf2 is essential for the Keap1-mediated degradation of the protein by proteasome. *Arch Biochem Biophys* **433**(2): 342-350.
- Kauwe, J. S. K., Cruchaga, C., Karch, C. M., Sadler, B., Lee, M., Mayo, K., Latu, W., Su'a, M., Fagan, A. M., Holtzman, D. M., Morris, J. C., Alzheimer's Disease Neuroimaging, I. & Goate, A. M. (2011). Fine Mapping of Genetic Variants in BIN1, CLU, CR1 and PICALM for Association with Cerebrospinal Fluid Biomarkers for Alzheimer's Disease. *PLoS ONE* **6**(2): e15918.
- Kensler, T. W., Wakabayashi, N. & Biswal, S. (2007). Cell survival responses to environmental stresses via the Keap1-Nrf2-ARE pathway, Cho AK (ed) Vol. 47, pp 89-116.
- Kettenmann, H., Hanisch, U. K., Noda, M. & Verkhratsky, A. (2011). Physiology of microglia. *Physiol Rev* **91**(2): 461-553.

- Khodagholi, F. & Tusi, S. K. (2011). Stabilization of Nrf2 by tBHQ prevents LPS-induced apoptosis in differentiated PC12 cells. *Mol Cell Biochem* **354**(1-2): 97-112.
- Kim, H.-S., Kim, E.-M., Lee, J.-P., Park, C. H., Kim, S., Seo, J.-H., Chang, K.-A., Yu, E., Jeong, S.-J., Chong, Y. H. & Suh, Y.-H. (2003). C-terminal fragments of amyloid precursor protein exert neurotoxicity by inducing glycogen synthase kinase-3 β expression. *The FASEB Journal*.
- Kim, H., Jung, Y., Shin, B. S., Kim, H., Song, H., Bae, S. H., Rhee, S. G. & Jeong, W. (2010). Redox Regulation of Lipopolysaccharide-mediated Sulfiredoxin Induction, Which Depends on Both AP-1 and Nrf2. *Journal of Biological Chemistry* **285**(45): 34419-34428.
- King, D. L. & Arendash, G. W. (2002). Behavioral characterization of the Tg2576 transgenic model of Alzheimer's disease through 19 months. *Physiology & Behavior* **75**(5): 627-642.
- Kitazawa, M., Cheng, D., Tsukamoto, M. R., Koike, M. A., Wes, P. D., Vasilevko, V., Cribbs, D. H. & LaFerla, F. M. (2011). Blocking IL-1 Signaling Rescues Cognition, Attenuates Tau Pathology, and Restores Neuronal β -Catenin Pathway Function in an Alzheimer's Disease Model. *The Journal of Immunology* **187**(12): 6539-6549.
- Kitazawa, M., Oddo, S., Yamasaki, T. R., Green, K. N. & LaFerla, F. M. (2005). Lipopolysaccharide-Induced Inflammation Exacerbates Tau Pathology by a Cyclin-Dependent Kinase 5-Mediated Pathway in a Transgenic Model of Alzheimer's Disease. *The Journal of Neuroscience* **25**(39): 8843-8853.
- Knatko, E. V., Ibbotson, S. H., Zhang, Y., Higgins, M., Fahey, J. W., Talalay, P., Dawe, R. S., Ferguson, J., Huang, J. T.-J., Clarke, R., Zheng, S., Saito, A., Kalra, S., Benedict, A. L., Honda, T., Proby, C. M. & Dinkova-Kostova, A. T. (2015). Nrf2 Activation Protects against Solar-Simulated Ultraviolet Radiation in Mice and Humans. *Cancer Prevention Research* **8**(6): 475-486.
- Knight, E. M., Martins, I. V., Gumusgoz, S., Allan, S. M. & Lawrence, C. B. (2014). High-fat diet-induced memory impairment in triple-transgenic Alzheimer's disease (3xTgAD) mice is independent of changes in amyloid and tau pathology. *Neurobiol Aging* **35**(8): 1821-1832.
- Kobayashi, A., Kang, M. I., Okawa, H., Ohtsuji, M., Zenke, Y., Chiba, T., Igarashi, K. & Yamamoto, M. (2004). Oxidative stress sensor Keap1 functions as an adaptor for Cul3-based E3 ligase to regulate proteasomal degradation of Nrf2. *Mol Cell Biol* **24**(16): 7130-7139.
- Kobayashi, M., Itoh, K., Suzuki, T., Osanai, H., Nishikawa, K., Katoh, Y., Takagi, Y. & Yamamoto, M. (2002). Identification of the interactive interface and phylogenetic conservation of the Nrf2-Keap1 system. *Genes Cells* **7**(8): 807-820.
- Kobayashi, M. & Yamamoto, M. (2006). Nrf2-Keap1 regulation of cellular defense mechanisms against electrophiles and reactive oxygen species. *Advances in Enzyme Regulation* **46**(1): 113-140.
- Koh, K., Kim, J., Jang, Y. J., Yoon, K., Cha, Y., Lee, H. J. & Kim, J. (2011). Transcription factor Nrf2 suppresses LPS-induced hyperactivation of BV-2 microglial cells. *Journal of Neuroimmunology* **233**(1, 2): 160-167.
- Kohjima, M., Sun, Y. & Chan, L. (2010). Increased Food Intake Leads to Obesity and Insulin Resistance in the Tg2576 Alzheimer's Disease Mouse Model. *Endocrinology* **151**(4): 1532-1540.
- Kohman, R. A., Tarr, A. J., Byler, S. L. & Boehm, G. W. (2007). Age increases vulnerability to bacterial endotoxin-induced behavioral decrements. *Physiology & Behavior* **91**(5): 561-565.

- Kong, X., Thimmulappa, R., Kombairaju, P. & Biswal, S. (2010). NADPH Oxidase-Dependent Reactive Oxygen Species Mediate Amplified TLR4 Signaling and Sepsis-Induced Mortality in Nrf2-Deficient Mice. *The Journal of Immunology* **185**(1): 569-577.
- Kovac, S., Angelova, P. R., Holmström, K. M., Zhang, Y., Dinkova-Kostova, A. T. & Abramov, A. Y. (2015). Nrf2 regulates ROS production by mitochondria and NADPH oxidase. *Biochimica et Biophysica Acta (BBA) - General Subjects* **1850**(4): 794-801.
- Krebs, D. L. & Parent, M. B. (2005). The enhancing effects of hippocampal infusions of glucose are not restricted to spatial working memory. *Neurobiology of Learning and Memory* **83**(2): 168-172.
- Krstic, D., Madhusudan, A., Doehner, J., Vogel, P., Notter, T., Imhof, C., Manalastas, A., Hilfiker, M., Pfister, S., Schwerdel, C., Riether, C., Meyer, U. & Knuesel, I. (2012). Systemic immune challenges trigger and drive Alzheimer-like neuropathology in mice. *Journal of Neuroinflammation* **9**.
- Kuhn, P. H., Koroniak, K., Hogg, S., Colombo, A., Zeitschel, U., Willem, M., Volbracht, C., Schepers, U., Imhof, A., Hoffmeister, A., Haass, C., Roßner, S., Bräse, S. & Lichtenthaler, S. F. (2012). *Secretome protein enrichment identifies physiological BACE1 protease substrates in neurons*. edn, vol. 31.
- Kuperstein, I., Broersen, K., Benilova, I., Rozenski, J., Jonckheere, W., Debulpaep, M., Vandersteen, A., Segers-Nolten, I., Van Der Werf, K., Subramaniam, V., Braeken, D., Callewaert, G., Bartic, C., D'Hooge, R., Martins, I. C., Rousseau, F., Schymkowitz, J. & De Strooper, B. (2010). *Neurotoxicity of Alzheimer's disease Aβ peptides is induced by small changes in the Aβ42 to Aβ40 ratio*. edn, vol. 29.
- Kwon, S. E. & Chapman, E. R. (2011). Synaptophysin regulates the kinetics of synaptic vesicle endocytosis in central neurons. *Neuron* **70**(5): 847-854.
- Lamb, B. A., Bardel, K. A., Kulnane, L. S., Anderson, J. J., Holtz, G., Wagner, S. L., Sisodia, S. S. & Hoeger, E. J. (1999). Amyloid production and deposition in mutant amyloid precursor protein and presenilin-1 yeast artificial chromosome transgenic mice. *Nat Neurosci* **2**(8): 695-697.
- Lamb, B. T., Call, L. M., Slunt, H. H., Bardel, K. A., Lawler, A. M., Eckman, C. B., Younkin, S. G., Holtz, G., Wagner, S. L., Price, D. L., Sisodia, S. S. & Gearhart, J. D. (1997). Altered Metabolism of Familial Alzheimer's Disease-Linked Amyloid Precursor Protein Variants in Yeast Artificial Chromosome Transgenic Mice. *Human Molecular Genetics* **6**(9): 1535-1541.
- Langston, R. F., Stevenson, C. H., Wilson, C. L., Saunders, I. & Wood, E. R. (2010). The role of hippocampal subregions in memory for stimulus associations. *Behavioural Brain Research* **215**(2): 275-291.
- Langston, R. F. & Wood, E. R. (2010). Associative recognition and the hippocampus: differential effects of hippocampal lesions on object-place, object-context and object-place-context memory. *Hippocampus* **20**(10): 1139-1153.
- Lassenius, M. I., Pietiläinen, K. H., Kaartinen, K., Pussinen, P. J., Syrjänen, J., Forsblom, C., Pörsti, I., Rissanen, A., Kaprio, J., Mustonen, J., Groop, P.-H., Lehto, M. & Group, o. b. o. t. F. S. (2011). Bacterial Endotoxin Activity in Human Serum Is Associated With Dyslipidemia, Insulin Resistance, Obesity, and Chronic Inflammation. *Diabetes Care* **34**(8): 1809-1815.
- Lawan, A., Zhang, L., Gatzke, F., Min, K., Jurczak, M. J., Al-Mutairi, M., Richter, P., Camporez, J. P. G., Couvillon, A., Pesta, D., Roth Flach, R. J., Shulman, G. I. & Bennett, A. M. (2015). Hepatic Mitogen-Activated Protein Kinase Phosphatase 1 Selectively Regulates Glucose Metabolism and Energy Homeostasis. *Molecular and Cellular Biology* **35**(1): 26-40.

- Lawrence, T. (2009). The Nuclear Factor NF- κ B Pathway in Inflammation. *Cold Spring Harbor Perspectives in Biology* **1**(6).
- Lawrence, T., Gilroy, D. W., Colville-Nash, P. R. & Willoughby, D. A. (2001). Possible new role for NF- κ B in the resolution of inflammation. *Nat Med* **7**(12): 1291-1297.
- Leboucher, Guillaume P., Tsai, Yien C., Yang, M., Shaw, Kristin C., Zhou, M., Veenstra, Timothy D., Glickman, Michael H. & Weissman, Allan M. (2012). Stress-Induced Phosphorylation and Proteasomal Degradation of Mitofusin 2 Facilitates Mitochondrial Fragmentation and Apoptosis. *Molecular Cell* **47**(4): 547-557.
- Lee, D.-S., Ko, W., Yoon, C.-S., Kim, D.-C., Yun, J., Lee, J.-K., Jun, K.-Y., Son, I., Kim, D.-W., Song, B.-K., Choi, S., Jang, J.-H., Oh, H., Kim, S. & Kim, Y.-C. (2014). KCHO-1, a Novel Antineuroinflammatory Agent, Inhibits Lipopolysaccharide-Induced Neuroinflammatory Responses through Nrf2-Mediated Heme Oxygenase-1 Expression in Mouse BV2 Microglia Cells. *Evidence-Based Complementary and Alternative Medicine* **2014**: 11.
- Lee, E. B. (2011). Obesity, leptin, and Alzheimer's disease. *Ann N Y Acad Sci* **1243**: 15-29.
- Lee, I., Hunsaker, M. R. & Kesner, R. P. (2005). The role of hippocampal subregions in detecting spatial novelty. *Behav Neurosci* **119**(1): 145-153.
- Lee, J.-M., Calkins, M. J., Chan, K., Kan, Y. W. & Johnson, J. A. (2003). Identification of the NF-E2-related Factor-2-dependent Genes Conferring Protection against Oxidative Stress in Primary Cortical Astrocytes Using Oligonucleotide Microarray Analysis. *Journal of Biological Chemistry* **278**(14): 12029-12038.
- Lee, J. K., Schuchman, E. H., Jin, H. K. & Bae, J.-S. (2012a). Soluble CCL5 Derived from Bone Marrow-Derived Mesenchymal Stem Cells and Activated by Amyloid β Ameliorates Alzheimer's Disease in Mice by Recruiting Bone Marrow-Induced Microglia Immune Responses. *STEM CELLS* **30**(7): 1544-1555.
- Lee, J. W., Lee, Y. K., Yuk, D. Y., Choi, D. Y., Ban, S. B., Oh, K. W. & Hong, J. T. (2008). Neuro-inflammation induced by lipopolysaccharide causes cognitive impairment through enhancement of beta-amyloid generation. *J Neuroinflammation* **5**: 37.
- Lee, J. Y., Oh, T. H. & Yune, T. Y. (2011). Ghrelin Inhibits Hydrogen Peroxide-Induced Apoptotic Cell Death of Oligodendrocytes Via ERK and p38MAPK Signaling. *Endocrinology* **152**(6): 2377-2386.
- Lee, Y. J., Choi, D. Y., Choi, I. S., Kim, K. H., Kim, Y. H., Kim, H. M., Lee, K., Cho, W. G., Jung, J. K., Han, S. B., Han, J. Y., Nam, S. Y., Yun, Y. W., Jeong, J. H., Oh, K. W. & Hong, J. T. (2012b). Inhibitory effect of 4-O-methylhonokiol on lipopolysaccharide-induced neuroinflammation, amyloidogenesis and memory impairment via inhibition of nuclear factor-kappaB in vitro and in vivo models. *Journal of Neuroinflammation* **9**.
- Leger, M., Quiedeville, A., Bouet, V., Haelewyn, B., Boulouard, M., Schumann-Bard, P. & Freret, T. (2013). Object recognition test in mice. *Nat. Protocols* **8**(12): 2531-2537.
- Lei, P., Ayton, S., Finkelstein, D. I., Adlard, P. A., Masters, C. L. & Bush, A. I. (2010). Tau protein: Relevance to Parkinson's disease. *The International Journal of Biochemistry & Cell Biology* **42**(11): 1775-1778.
- Lennartz, R. C. (2008). The role of extramaze cues in spontaneous alternation in a plus-maze. *Learning & behavior* **36**(2): 138-144.

- Li, H., Liu, B., Huang, J., Chen, H., Guo, X. & Yuan, Z. (2013). Insulin inhibits lipopolysaccharide-induced nitric oxide synthase expression in rat primary astrocytes. *Brain Research*(0).
- Li, H., Yao, W., Irwin, M. G., Wang, T., Wang, S., Zhang, L. & Xia, Z. (2015). Adiponectin ameliorates hyperglycemia-induced cardiac hypertrophy and dysfunction by concomitantly activating Nrf2 and Brg1. *Free Radical Biology and Medicine* **84**: 311-321.
- Li, J., Ichikawa, T., Villacorta, L., Janicki, J. S., Brower, G. L., Yamamoto, M. & Cui, T. (2009). Nrf2 Protects Against Maladaptive Cardiac Responses to Hemodynamic Stress. *Arteriosclerosis, Thrombosis, and Vascular Biology* **29**(11): 1843-1850.
- Li, M., Pisalyaput, K., Galvan, M. & Tenner, A. J. (2004). Macrophage colony stimulatory factor and interferon- γ trigger distinct mechanisms for augmentation of β -amyloid-induced microglia-mediated neurotoxicity. *Journal of Neurochemistry* **91**(3): 623-633.
- Li, S., Li, J., Shen, C., Zhang, X., Sun, S., Cho, M., Sun, C. & Song, Z. (2014). tert-Butylhydroquinone (tBHQ) protects hepatocytes against lipotoxicity via inducing autophagy independently of Nrf2 activation. *Biochimica et Biophysica Acta (BBA) - Molecular and Cell Biology of Lipids* **1841**(1): 22-33.
- Li, Y., Du, X.-f., Liu, C.-s., Wen, Z.-l. & Du, J.-l. (2012). Reciprocal Regulation between Resting Microglial Dynamics and Neuronal Activity In Vivo. *Developmental Cell* **23**(6): 1189-1202.
- Ling, Y., Morgan, K. & Kalsheker, N. (2003). Amyloid precursor protein (APP) and the biology of proteolytic processing: Relevance to Alzheimer's disease. *International Journal of Biochemistry and Cell Biology* **35**(11): 1505-1535.
- Linker, R. A., Lee, D.-H., Ryan, S., van Dam, A. M., Conrad, R., Bista, P., Zeng, W., Hronowsky, X., Buko, A., Chollate, S., Ellrichmann, G., Brück, W., Dawson, K., Goelz, S., Wiese, S., Scannevin, R. H., Lukashev, M. & Gold, R. (2011). Fumaric acid esters exert neuroprotective effects in neuroinflammation via activation of the Nrf2 antioxidant pathway. *Brain* **134**(3): 678-692.
- Liu, C., Cui, G., Zhu, M., Kang, X. & Guo, H. (2014). Neuroinflammation in Alzheimer's disease: chemokines produced by astrocytes and chemokine receptors. *Int. J. Clin. Exp. Pathol.* **7**(12): 8342-8355.
- Liu, F., Iqbal, K., Grundke-Iqbal, I., Hart, G. W. & Gong, C.-X. (2004). O-GlcNAcylation regulates phosphorylation of tau: A mechanism involved in Alzheimer's disease. *Proceedings of the National Academy of Sciences of the United States of America* **101**(29): 10804-10809.
- Liu, F., Zaidi, T., Iqbal, K., Grundke-Iqbal, I. & Gong, C. X. (2002a). Aberrant glycosylation modulates phosphorylation of tau by protein kinase A and dephosphorylation of tau by protein phosphatase 2A and 5. *Neuroscience* **115**(3): 829-837.
- Liu, F., Zaidi, T., Iqbal, K., Grundke-Iqbal, I., Merkle, R. K. & Gong, C.-X. (2002b). Role of glycosylation in hyperphosphorylation of tau in Alzheimer's disease. *FEBS Letters* **512**(1-3): 101-106.
- Liu, Y., Liu, F., Iqbal, K., Grundke-Iqbal, I. & Gong, C.-X. (2008). Decreased glucose transporters correlate to abnormal hyperphosphorylation of tau in Alzheimer disease. *FEBS Letters* **582**(2): 359-364.
- Loaiza, A., Porras, O. H. & Barros, L. F. (2003). Glutamate triggers rapid glucose transport stimulation in astrocytes as evidenced by real-time confocal microscopy. *Journal of Neuroscience* **23**(19): 7337-7342.
- Loh, K., Deng, H., Fukushima, A., Cai, X., Boivin, B., Galic, S., Bruce, C., Shields, B. J., Skiba, B., Ooms, L. M., Stepto, N., Wu, B., Mitchell, C. A., Tonks, N. K.,

- Watt, M. J., Febbraio, M. A., Crack, P. J., Andrikopoulos, S. & Tiganis, T. (2009). Reactive oxygen species enhance insulin sensitivity. *Cell Metab* **10**(4): 260-272.
- Luo, X. G., Ding, J. Q. & Chen, S. D. (2010). Microglia in the aging brain: relevance to neurodegeneration. *Mol Neurodegener* **5**: 12.
- Luo, Y., Bolon, B., Kahn, S., Bennett, B. D., Babu-Khan, S., Denis, P., Fan, W., Kha, H., Zhang, J., Gong, Y., Martin, L., Louis, J.-C., Yan, Q., Richards, W. G., Citron, M. & Vassar, R. (2001). Mice deficient in BACE1, the Alzheimer's β -secretase, have normal phenotype and abolished β -amyloid generation. *Nat Neurosci* **4**(3): 231-232.
- Maesako, M., Uemura, K., Kubota, M., Kuzuya, A., Sasaki, K., Asada, M., Watanabe, K., Hayashida, N., Ihara, M., Ito, H., Shimohama, S., Kihara, T. & Kinoshita, A. (2012a). Environmental enrichment ameliorated high-fat diet-induced A β deposition and memory deficit in APP transgenic mice. *Neurobiology of Aging* **33**(5): 1011.e1011-1011.e1023.
- Maesako, M., Uemura, K., Kubota, M., Kuzuya, A., Sasaki, K., Hayashida, N., Asada-Utsugi, M., Watanabe, K., Uemura, M., Kihara, T., Takahashi, R., Shimohama, S. & Kinoshita, A. (2012b). Exercise Is More Effective than Diet Control in Preventing High Fat Diet-induced β -Amyloid Deposition and Memory Deficit in Amyloid Precursor Protein Transgenic Mice. *Journal of Biological Chemistry* **287**(27): 23024-23033.
- Magistretti, P. J. (2006). Neuron-glia metabolic coupling and plasticity. *Journal of Experimental Biology* **209**(12): 2304-2311.
- Mallard, C. (2012). Innate Immune Regulation by Toll-Like Receptors in the Brain. *ISRN Neurology* **2012**: 19.
- Mamelak, M. (2012). Sporadic Alzheimer's disease: the starving brain. *J Alzheimers Dis* **31**(3): 459-474.
- Manczak, M., Calkins, M. J. & Reddy, P. H. (2011). Impaired mitochondrial dynamics and abnormal interaction of amyloid beta with mitochondrial protein Drp1 in neurons from patients with Alzheimer's disease: implications for neuronal damage. *Human Molecular Genetics* **20**(13): 2495-2509.
- Manczak, M. & Reddy, P. H. (2012). Abnormal interaction of VDAC1 with amyloid beta and phosphorylated tau causes mitochondrial dysfunction in Alzheimer's disease. *Human Molecular Genetics* **21**(23): 5131-5146.
- Mandelkow, E.-M. & Mandelkow, E. (2012). Biochemistry and Cell Biology of Tau Protein in Neurofibrillary Degeneration. *Cold Spring Harbor Perspectives in Medicine* **2**(7).
- Marchesi, V. T. (2011). Alzheimer's dementia begins as a disease of small blood vessels, damaged by oxidative-induced inflammation and dysregulated amyloid metabolism: Implications for early detection and therapy. *FASEB Journal* **25**(1): 5-13.
- Marchi, S., Patergnani, S. & Pinton, P. (2014). The endoplasmic reticulum–mitochondria connection: One touch, multiple functions. *Biochimica et Biophysica Acta (BBA) - Bioenergetics* **1837**(4): 461-469.
- Maretzky, T., Reiss, K., Ludwig, A., Buchholz, J., Scholz, F., Proksch, E., de Strooper, B., Hartmann, D. & Saftig, P. (2005). ADAM10 mediates E-cadherin shedding and regulates epithelial cell-cell adhesion, migration, and β -catenin translocation. *Proceedings of the National Academy of Sciences of the United States of America* **102**(26): 9182-9187.
- Martinez, F. O. & Gordon, S. (2014). The M1 and M2 paradigm of macrophage activation: time for reassessment. *F1000Prime Reports* **6**: 13.

- Mazzitelli, S., Xu, P., Ferrer, I., Davis, R. J. & Tournier, C. (2011). The Loss of c-Jun N-Terminal Protein Kinase Activity Prevents the Amyloidogenic Cleavage of Amyloid Precursor Protein and the Formation of Amyloid Plaques In Vivo. *Journal of Neuroscience* **31**(47): 16969-16976.
- McGeer, P. L., Schulzer, M. & McGeer, E. G. (1996). Arthritis and anti-inflammatory agents as possible protective factors for Alzheimer's disease: A review of 17 epidemiologic studies. *Neurology* **47**(2): 425-432.
- McLarnon, J. G. (2012). Microglial chemotactic signaling factors in Alzheimer's disease. *American Journal of Neurodegenerative Disease* **1**(3): 199-204.
- McMahon, M., Itoh, K., Yamamoto, M., Chanas, S. A., Henderson, C. J., McLellan, L. I., Wolf, C. R., Cavin, C. & Hayes, J. D. (2001). The Cap'n'Collar basic leucine zipper transcription factor Nrf2 (NF-E2 p45-related factor 2) controls both constitutive and inducible expression of intestinal detoxification and glutathione biosynthetic enzymes. *Cancer Res* **61**(8): 3299-3307.
- McMahon, M., Itoh, K., Yamamoto, M. & Hayes, J. D. (2003). Keap1-dependent proteasomal degradation of transcription factor Nrf2 contributes to the negative regulation of antioxidant response element-driven gene expression. *J Biol Chem* **278**(24): 21592-21600.
- McMahon, M., Lamont, D. J., Beattie, K. A. & Hayes, J. D. (2010). Keap1 perceives stress via three sensors for the endogenous signaling molecules nitric oxide, zinc, and alkenals. *Proceedings of the National Academy of Sciences* **107**(44): 18838-18843.
- McMahon, M., Thomas, N., Itoh, K., Yamamoto, M. & Hayes, J. D. (2004). Redox-regulated turnover of Nrf2 is determined by at least two separate protein domains, the redox-sensitive Neh2 degron and the redox-insensitive Neh6 degron. *J Biol Chem* **279**(30): 31556-31567.
- McMahon, M., Thomas, N., Itoh, K., Yamamoto, M. & Hayes, J. D. (2006). Dimerization of substrate adaptors can facilitate cullin-mediated ubiquitylation of proteins by a "tethering" mechanism: a two-site interaction model for the Nrf2-Keap1 complex. *J Biol Chem* **281**(34): 24756-24768.
- McManus, M. J., Murphy, M. P. & Franklin, J. L. (2011). The Mitochondria-Targeted Antioxidant MitoQ Prevents Loss of Spatial Memory Retention and Early Neuropathology in a Transgenic Mouse Model of Alzheimer's Disease. *Journal of Neuroscience* **31**(44): 15703-15715.
- McNay, E. C., Fries, T. M. & Gold, P. E. (2000). Decreases in rat extracellular hippocampal glucose concentration associated with cognitive demand during a spatial task. *Proceedings of the National Academy of Sciences* **97**(6): 2881-2885.
- McNay, E. C., Ong, C. T., McCrimmon, R. J., Cresswell, J., Bogan, J. S. & Sherwin, R. S. (2010). Hippocampal memory processes are modulated by insulin and high-fat-induced insulin resistance. *Neurobiol Learn Mem* **93**(4): 546-553.
- Meakin, P. J., Chowdhry, S., Sharma, R. S., Ashford, F. B., Walsh, S. V., McCrimmon, R. J., Dinkova-Kostova, A. T., Dillon, J. F., Hayes, J. D. & Ashford, M. L. (2014). Susceptibility of Nrf2-null mice to steatohepatitis and cirrhosis upon consumption of a high-fat diet is associated with oxidative stress, perturbation of the unfolded protein response, and disturbance in the expression of metabolic enzymes but not with insulin resistance. *Mol Cell Biol* **34**(17): 3305-3320.
- Meakin, P. J., Harper, A. J., Hamilton, D. L., Gallagher, J., McNeilly, A. D., Burgess, L. A., Vaanholt, L. M., Bannon, K. A., Latcham, J., Hussain, I., Speakman, J. R., Howlett, D. R. & Ashford, M. L. J. (2012). Reduction in BACE1 decreases body weight, protects against diet-induced obesity and enhances insulin sensitivity in mice. *Biochemical Journal* **441**(1): 285-295.

- Meher, A. K., Sharma, P. R., Lira, V. A., Yamamoto, M., Kensler, T. W., Yan, Z. & Leitinger, N. (2012). Nrf2 deficiency in myeloid cells is not sufficient to protect mice from high-fat diet-induced adipose tissue inflammation and insulin resistance. *Free Radical Biology and Medicine* **52**(9): 1708-1715.
- Mehlhorn, G., Hollborn, M. & Schliebs, R. (2000). Induction of cytokines in glial cells surrounding cortical β -amyloid plaques in transgenic Tg2576 mice with Alzheimer pathology. *International Journal of Developmental Neuroscience* **18**(4-5): 423-431.
- Menting, K. W. & Claassen, J. A. H. R. (2014). β -secretase inhibitor; a promising novel therapeutic drug in AD. *Frontiers in Aging Neuroscience* **6**.
- Miklossy, J., Doudet, D. D., Schwab, C., Yu, S., McGeer, E. G. & McGeer, P. L. (2006). Role of ICAM-1 in persisting inflammation in Parkinson disease and MPTP monkeys. *Experimental Neurology* **197**(2): 275-283.
- Milder, J. & Patel, M. (2012). Modulation of oxidative stress and mitochondrial function by the ketogenic diet. *Epilepsy Research* **100**(3): 295-303.
- Millan Sanchez, M., Heyn, S. N., Das, D., Moghadam, S., Martin, K. J. & Salehi, A. (2012). Neurobiological Elements of Cognitive Dysfunction in Down Syndrome: Exploring the Role of APP. *Biological Psychiatry* **71**(5): 403-409.
- Miller, D. M., Singh, I. N., Wang, J. A. & Hall, E. D. (2013). Administration of the Nrf2-ARE activators sulforaphane and carnosic acid attenuates 4-hydroxy-2-nonenal-induced mitochondrial dysfunction ex vivo. *Free Radical Biology and Medicine* **57**: 1-9.
- Min, S.-W., Chen, X., Tracy, T. E., Li, Y., Zhou, Y., Wang, C., Shirakawa, K., Minami, S. S., Defensor, E., Mok, S. A., Sohn, P. D., Schilling, B., Cong, X., Ellerby, L., Gibson, B. W., Johnson, J., Krogan, N., Shamloo, M., Gestwicki, J., Masliah, E., Verdin, E. & Gan, L. (2015). Critical role of acetylation in tau-mediated neurodegeneration and cognitive deficits. *Nat Med* **21**(10): 1154-1162.
- Mody, N., Agouni, A., McIlroy, G. D., Platt, B. & Delibegovic, M. (2011). Susceptibility to diet-induced obesity and glucose intolerance in the APP SWE/PSEN1 A246E mouse model of Alzheimer's disease is associated with increased brain levels of protein tyrosine phosphatase 1B (PTP1B) and retinol-binding protein 4 (RBP4), and basal phosphorylation of S6 ribosomal protein. *Diabetologia* **54**(8): 2143-2151.
- Mohammad Abdul, H., Sultana, R., Keller, J. N., St. Clair, D. K., Markesbery, W. R. & Butterfield, D. A. (2006). Mutations in amyloid precursor protein and presenilin-1 genes increase the basal oxidative stress in murine neuronal cells and lead to increased sensitivity to oxidative stress mediated by amyloid β -peptide (1-42), H_2O_2 and kainic acid: implications for Alzheimer's disease. *Journal of Neurochemistry* **96**(5): 1322-1335.
- Moi, P., Chan, K., Aunis, I., Cao, A. & Kan, Y. W. (1994). Isolation of NF-E2-related factor 2 (Nrf2), a NF-E2-like basic leucine zipper transcriptional activator that binds to the tandem NF-E2/AP1 repeat of the β -globin locus control region. *Proceedings of the National Academy of Sciences of the United States of America* **91**(21): 9926-9930.
- Moloney, A. M., Griffin, R. J., Timmons, S., O'Connor, R., Ravid, R. & O'Neill, C. (2010). Defects in IGF-1 receptor, insulin receptor and IRS-1/2 in Alzheimer's disease indicate possible resistance to IGF-1 and insulin signalling. *Neurobiology of Aging* **31**(2): 224-243.
- More, V. R., Xu, J., Shimpi, P. C., Belgrave, C., Luyendyk, J. P., Yamamoto, M. & Slitt, A. L. (2013). Keap1 knockdown increases markers of metabolic syndrome after long-term high fat diet feeding. *Free Radic Biol Med* **61**: 85-94.

- Morris, M., Evans, D. A., Bienias, J. L. & et al. (2003). Consumption of fish and n-3 fatty acids and risk of incident alzheimer disease. *Archives of Neurology* **60**(7): 940-946.
- Morris, M. & Li, L. (2012). Molecular Mechanisms and Pathological Consequences of Endotoxin Tolerance and Priming. *Arch. Immunol. Ther. Exp.* **60**(1): 13-18.
- Morrison, C. D., Pistell, P. J., Ingram, D. K., Johnson, W. D., Liu, Y., Fernandez-Kim, S. O., White, C. L., Purpera, M. N., Uranga, R. M., Bruce-Keller, A. J. & Keller, J. N. (2010). High fat diet increases hippocampal oxidative stress and cognitive impairment in aged mice: implications for decreased Nrf2 signaling. *Journal of Neurochemistry* **114**(6): 1581-1589.
- Morroni, F., Tarozzi, A., Sita, G., Bolondi, C., Zolezzi Moraga, J. M., Cantelli-Forti, G. & Hrelia, P. (2013). Neuroprotective effect of sulforaphane in 6-hydroxydopamine-lesioned mouse model of Parkinson's disease. *NeuroToxicology* **36**: 63-71.
- Mosconi, L., De Santi, S., Li, J., Tsui, W. H., Li, Y., Boppana, M., Laska, E., Rusinek, H. & de Leon, M. J. (2008a). Hippocampal hypometabolism predicts cognitive decline from normal aging. *Neurobiology of Aging* **29**(5): 676-692.
- Mosconi, L., Mistur, R., Switalski, R., Tsui, W. H., Glodzik, L., Li, Y., Pirraglia, E., Santi, S., Reisberg, B., Wisniewski, T. & Leon, M. J. (2009). FDG-PET changes in brain glucose metabolism from normal cognition to pathologically verified Alzheimer's disease. *European Journal of Nuclear Medicine and Molecular Imaging* **36**(5): 811-822.
- Mosconi, L., Pupi, A. & De Leon, M. J. (2008b). Brain Glucose Hypometabolism and Oxidative Stress in Preclinical Alzheimer's Disease. *Annals of the New York Academy of Sciences* **1147**(1): 180-195.
- Mosser, D. M. & Edwards, J. P. (2008). Exploring the full spectrum of macrophage activation. *Nature reviews. Immunology* **8**(12): 958-969.
- Mucke, L. (2000). High-level neuronal expression of a β_{1-42} in wild-type human amyloid protein precursor transgenic mice: synaptotoxicity without plaque formation. *J. Neurosci.* **20**: 4050-4058.
- Mullan, M., Crawford, F., Axelman, K., Houlden, H., Lilius, L., Winblad, B. & Lannfelt, L. (1992). A pathogenic mutation for probable Alzheimer's disease in the APP gene at the N-terminus of β -amyloid. *Nat Genet* **1**(5): 345-347.
- Müller, T., Meyer, H. E., Egensperger, R. & Marcus, K. (2008). The amyloid precursor protein intracellular domain (AICD) as modulator of gene expression, apoptosis, and cytoskeletal dynamics—Relevance for Alzheimer's disease. *Progress in Neurobiology* **85**(4): 393-406.
- Müller, U. C. & Zheng, H. (2012). Physiological Functions of APP Family Proteins. *Cold Spring Harbor Perspectives in Medicine* **2**(2).
- Muramatsu, H., Katsuoka, F., Toide, K., Shimizu, Y., Furusako, S. & Yamamoto, M. (2013). Nrf2 deficiency leads to behavioral, neurochemical and transcriptional changes in mice. *Genes to Cells* **18**(10): 899-908.
- Murray, C., Sanderson, D. J., Barkus, C., Deacon, R. M. J., Rawlins, J. N. P., Bannerman, D. M. & Cunningham, C. (2012). Systemic inflammation induces acute working memory deficits in the primed brain: relevance for delirium. *Neurobiology of Aging* **33**(3): 603-616.e603.
- Muthusamy, V. R., Kannan, S., Sadhaasivam, K., Gounder, S. S., Davidson, C. J., Boehme, C., Hoidal, J. R., Wang, L. & Rajasekaran, N. S. (2012). Acute exercise stress activates Nrf2/ARE signaling and promotes antioxidant mechanisms in the myocardium. *Free Radical Biology and Medicine* **52**(2): 366-376.

- Nagai, N., Thimmulappa, R. K., Cano, M., Fujihara, M., Izumi-Nagai, K., Kong, X., Sporn, M. B., Kensler, T. W., Biswal, S. & Handa, J. T. (2009). Nrf2 is a critical modulator of the innate immune response in a model of uveitis. *Free Radical Biology and Medicine* **47**(3): 300-306.
- Nakamura, M., Shishido, N., Nunomura, A., Smith, M. A., Perry, G., Hayashi, Y., Nakayama, K. & Hayashi, T. (2007). Three Histidine Residues of Amyloid- β Peptide Control the Redox Activity of Copper and Iron. *Biochemistry* **46**(44): 12737-12743.
- Nakanishi, H., Hayashi, Y. & Wu, Z. (2011). The role of microglial mtDNA damage in age-dependent prolonged LPS-induced sickness behavior. *Neuron Glia Biology* **7**(Special Issue 01): 17-23.
- Nakarai, H., Yamashita, A., Nagayasu, S., Iwashita, M., Kumamoto, S., Ohyama, H., Hata, M., Soga, Y., Kushiya, A., Asano, T., Abiko, Y. & Nishimura, F. (2012). Adipocyte-macrophage interaction may mediate LPS-induced low-grade inflammation: Potential link with metabolic complications. *Innate Immunity* **18**(1): 164-170.
- Nakaso, K., Yano, H., Fukuhara, Y., Takeshima, T., Wada-Isoe, K. & Nakashima, K. (2003). PI3K is a key molecule in the Nrf2-mediated regulation of antioxidative proteins by hemin in human neuroblastoma cells. *Febs Letters* **546**(2, 3): 181-184.
- Needham, B. E., Wlodek, M. E., Ciccotosto, G. D., Fam, B. C., Masters, C. L., Proietto, J., Andrikopoulos, S. & Cappai, R. (2008). Identification of the Alzheimer's disease amyloid precursor protein (APP) and its homologue APLP2 as essential modulators of glucose and insulin homeostasis and growth. *The Journal of Pathology* **215**(2): 155-163.
- Newman, A. B., Fitzpatrick, A. L., Lopez, O., Jackson, S., Lyketsos, C., Jagust, W., Ives, D., DeKosky, S. T. & Kuller, L. H. (2005). Dementia and Alzheimer's Disease Incidence in Relationship to Cardiovascular Disease in the Cardiovascular Health Study Cohort. *Journal of the American Geriatrics Society* **53**(7): 1101-1107.
- Nicholas, S. A., Coughlan, K., Yasinska, I., Lall, G. S., Gibbs, B. F., Calzolari, L. & Sumbayev, V. V. (2011). Dysfunctional mitochondria contain endogenous high-affinity human Toll-like receptor 4 (TLR4) ligands and induce TLR4-mediated inflammatory reactions. *The International Journal of Biochemistry & Cell Biology* **43**(4): 674-681.
- Niedowicz, D., Reeves, V., Platt, T., Kohler, K., Beckett, T., Powell, D., Lee, T., Sexton, T., Song, E., Brewer, L., Latimer, C., Kraner, S., Larson, K., Ozcan, S., Norris, C., Hersh, L., Porter, N., Wilcock, D. & Murphy, M. (2014). Obesity and diabetes cause cognitive dysfunction in the absence of accelerated beta-amyloid deposition in a novel murine model of mixed or vascular dementia. *Acta Neuropathologica Communications* **2**(1): 64.
- Nielsen, H. M., Mulder, S. D., Beliën, J. A. M., Musters, R. J. P., Eikelenboom, P. & Veerhuis, R. (2010). Astrocytic A β 1-42 uptake is determined by A β -aggregation state and the presence of amyloid-associated proteins. *Glia* **58**(10): 1235-1246.
- Nimmerjahn, A., Kirchhoff, F. & Helmchen, F. (2005). Resting Microglial Cells Are Highly Dynamic Surveillants of Brain Parenchyma in Vivo. *Science* **308**(5726): 1314-1318.
- Nioi, P., Nguyen, T., Sherratt, P. J. & Pickett, C. B. (2005). The carboxy-terminal Neh3 domain of Nrf2 is required for transcriptional activation. *Mol Cell Biol* **25**(24): 10895-10906.
- Noris, M. & Remuzzi, G. (2013). Overview of Complement Activation and Regulation. *Seminars in Nephrology* **33**(6): 479-492.

- Nunomura, A., Tamaoki, T., Tanaka, K., Motohashi, N., Nakamura, M., Hayashi, T., Yamaguchi, H., Shimohama, S., Lee, H.-g., Zhu, X., Smith, M. A. & Perry, G. (2010). Intraneuronal amyloid β accumulation and oxidative damage to nucleic acids in Alzheimer disease. *Neurobiology of Disease* **37**(3): 731-737.
- O'Connor, J. C., Lawson, M. A., Andre, C., Moreau, M., Lestage, J., Castanon, N., Kelley, K. W. & Dantzer, R. (2008). Lipopolysaccharide-induced depressive-like behavior is mediated by indoleamine 2,3-dioxygenase activation in mice. *Mol Psychiatry* **14**(5): 511-522.
- Oddo, S., Caccamo, A., Shepherd, J. D., Murphy, M. P., Golde, T. E., Kaye, R., Metherate, R., Mattson, M. P., Akbari, Y. & LaFerla, F. M. (2003). Triple-Transgenic Model of Alzheimer's Disease with Plaques and Tangles: Intracellular A β and Synaptic Dysfunction. *Neuron* **39**(3): 409-421.
- Okada, K., Warabi, E., Sugimoto, H., Horie, M., Gotoh, N., Tokushige, K., Hashimoto, E., Utsunomiya, H., Takahashi, H., Ishii, T., Yamamoto, M. & Shoda, J. (2013). Deletion of Nrf2 leads to rapid progression of steatohepatitis in mice fed atherogenic plus high-fat diet. *J Gastroenterol* **48**(5): 620-632.
- Olarte-Sanchez, C. M., Kinnavane, L., Amin, E. & Aggleton, J. P. (2014). Contrasting networks for recognition memory and recency memory revealed by immediate-early gene imaging in the rat. *Behav Neurosci* **128**(4): 504-522.
- Oliveira, A. G., Carvalho, B. M., Tobar, N., Ropelle, E. R., Pauli, J. R., Bagarolli, R. A., Guadagnini, D., Carvalheira, J. B. C. & Saad, M. J. A. (2011). Physical Exercise Reduces Circulating Lipopolysaccharide and TLR4 Activation and Improves Insulin Signaling in Tissues of DIO Rats. *Diabetes* **60**(3): 784-796.
- Olmos-Alonso, A., Schettters, S. T. T., Sri, S., Askew, K., Mancuso, R., Vargas-Caballero, M., Holscher, C., Perry, V. H. & Gomez-Nicola, D. (2016). Pharmacological targeting of CSF1R inhibits microglial proliferation and prevents the progression of Alzheimer's-like pathology. *Brain*.
- Ortuño-Sahagún, D., González, R., Verdaguer, E., Huerta, V., Torres-Mendoza, B., Lemus, L., Rivera-Cervantes, M., Camins, A. & Zárate, C. B. (2014). Glutamate Excitotoxicity Activates the MAPK/ERK Signaling Pathway and Induces the Survival of Rat Hippocampal Neurons In Vivo. *Journal of Molecular Neuroscience* **52**(3): 366-377.
- Pallanck, L. (2013). Mitophagy: Mitofusin Recruits a Mitochondrial Killer. *Current Biology* **23**(13): R570-R572.
- Palomo, J., Dietrich, D., Martin, P., Palmer, G. & Gabay, C. (2015). The interleukin (IL)-1 cytokine family - Balance between agonists and antagonists in inflammatory diseases. *Cytokine*.
- Pan, H., Wang, H., Wang, X., Zhu, L. & Mao, L. (2012). The Absence of Nrf2 Enhances NF- κ B-Dependent Inflammation following Scratch Injury in Mouse Primary Cultured Astrocytes. *Mediators of Inflammation* **2012**: 9.
- Pardossi-Piquard, R., Petit, A., Kawarai, T., Sunyach, C., Alves da Costa, C., Vincent, B., Ring, S., D'Adamio, L., Shen, J., Müller, U., Hyslop, P. S. G. & Checler, F. (2005). Presenilin-Dependent Transcriptional Control of the A β -Degrading Enzyme Neprilysin by Intracellular Domains of β APP and APLP. *Neuron* **46**(4): 541-554.
- Park, C. R., Seeley, R. J., Craft, S. & Woods, S. C. (2000). Intracerebroventricular insulin enhances memory in a passive-avoidance task. *Physiology & Behavior* **68**(4): 509-514.
- Park, L., Wang, G., Zhou, P., Zhou, J., Pitstick, R., Previti, M. L., Younkin, L., Younkin, S. G., Van Nostrand, W. E., Cho, S., Anrather, J., Carlson, G. A. & Iadecola, C. (2011). Scavenger receptor CD36 is essential for the cerebrovascular oxidative stress and neurovascular dysfunction induced by

- amyloid- β . *Proceedings of the National Academy of Sciences* **108**(12): 5063-5068.
- Parkin, J. & Cohen, B. (2001). An overview of the immune system. *The Lancet* **357**(9270): 1777-1789.
- Patel, H. C., Boutin, H. & Allan, S. M. (2003). Interleukin-1 in the Brain. *Annals of the New York Academy of Sciences* **992**(1): 39-47.
- Peake, B. F., Nicholson, C. K., Lambert, J. P., Hood, R. L., Amin, H., Amin, S. & Calvert, J. W. (2013). Hydrogen sulfide preconditions the db/db diabetic mouse heart against ischemia-reperfusion injury by activating Nrf2 signaling in an Erk-dependent manner. *American Journal of Physiology - Heart and Circulatory Physiology* **304**(9): H1215-H1224.
- Peng, B., Zhao, P., Lu, Y.-P., Chen, M.-M., Sun, H., Wu, X.-M. & Zhu, L. (2013). Z-ligustilide activates the Nrf2/HO-1 pathway and protects against cerebral ischemia-reperfusion injury in vivo and in vitro. *Brain Research* **1520**: 168-177.
- Perez-Gonzalez, R., Alvira-Botero, M. X., Robayo, O., Antequera, D., Garzon, M., Martin-Moreno, A. M., Brera, B., de Ceballos, M. L. & Carro, E. (2014). Leptin gene therapy attenuates neuronal damages evoked by amyloid-[beta] and rescues memory deficits in APP/PS1 mice. *Gene Ther* **21**(3): 298-308.
- Pérez-González, R., Antequera, D., Vargas, T., Spuch, C., Bolós, M. & Carro, E. (2011). Leptin induces proliferation of neuronal progenitors and neuroprotection in a mouse model of alzheimer's disease. *Journal of Alzheimer's Disease* **24**(SUPPL. 2): 17-25.
- Perez Nievas, B. G., Hammerschmidt, T., Kummer, M. P., Terwel, D., Leza, J. C. & Heneka, M. T. (2011). Restraint stress increases neuroinflammation independently of amyloid β levels in amyloid precursor protein/PS1 transgenic mice. *Journal of Neurochemistry* **116**(1): 43-52.
- Pi, J., Leung, L., Xue, P., Wang, W., Hou, Y., Liu, D., Yehuda-Shnaidman, E., Lee, C., Lau, J., Kurtz, T. W. & Chan, J. Y. (2010). Deficiency in the nuclear factor E2-related factor-2 transcription factor results in impaired adipogenesis and protects against diet-induced obesity. *J Biol Chem* **285**(12): 9292-9300.
- Piantadosi, C. A., Withers, C. M., Bartz, R. R., MacGarvey, N. C., Fu, P., Sweeney, T. E., Welty-Wolf, K. E. & Suliman, H. B. (2011). Heme Oxygenase-1 Couples Activation of Mitochondrial Biogenesis to Anti-inflammatory Cytokine Expression. *Journal of Biological Chemistry* **286**(18): 16374-16385.
- Pihlaja, R., Koistinaho, J., Kauppinen, R., Sandholm, J., Tanila, H. & Koistinaho, M. (2011). Multiple cellular and molecular mechanisms Are involved in human A β clearance by transplanted adult astrocytes. *Glia* **59**(11): 1643-1657.
- Pinho, C. M., Teixeira, P. F. & Glaser, E. (2014). Mitochondrial import and degradation of amyloid- β peptide. *Biochimica et Biophysica Acta (BBA) - Bioenergetics* **1837**(7): 1069-1074.
- Pistell, P. J., Morrison, C. D., Gupta, S., Knight, A. G., Keller, J. N., Ingram, D. K. & Bruce-Keller, A. J. (2010). Cognitive impairment following high fat diet consumption is associated with brain inflammation. *J Neuroimmunol* **219**(1-2): 25-32.
- Postina, R., Schroeder, A., Dewachter, I., Bohl, J., Schmitt, U., Kojro, E., Prinzen, C., Endres, K., Hiemke, C., Blessing, M., Flamez, P., Dequenue, A., Godaux, E., van Leuven, F. & Fahrenholz, F. (2004). A disintegrin-metalloproteinase prevents amyloid plaque formation and hippocampal defects in an Alzheimer disease mouse model. *The Journal of Clinical Investigation* **113**(10): 1456-1464.
- Prasher, V. P., Farrer, M. J., Kessling, A. M., Fisher, E. M. C., West, R. J., Barber, P. C. & Butler, A. C. (1998). Molecular mapping of alzheimer-type dementia in Down's syndrome. *Annals of Neurology* **43**(3): 380-383.

- Priestley, J. R. C., Kautenburg, K. E., Casati, M. C., Endres, B. T., Geurts, A. M. & Lombard, J. H. (2015). THE NRF2 KNOCKOUT RAT: A NEW ANIMAL MODEL TO STUDY ENDOTHELIAL DYSFUNCTION, OXIDANT STRESS, AND MICROVASCULAR RAREFACTION. *American Journal of Physiology - Heart and Circulatory Physiology*.
- Puig, K. L., Floden, A. M., Adhikari, R., Golovko, M. Y. & Combs, C. K. (2012). Amyloid Precursor Protein and Proinflammatory Changes Are Regulated in Brain and Adipose Tissue in a Murine Model of High Fat Diet-Induced Obesity. *PLoS ONE* **7**(1): e30378.
- Purisai, M. G., McCormack, A. L., Cumine, S., Li, J., Isla, M. Z. & Di Monte, D. A. (2007). Microglial activation as a priming event leading to paraquat-induced dopaminergic cell degeneration. *Neurobiology of Disease* **25**(2): 392-400.
- Purushothaman, S., Renuka Nair, R., Harikrishnan, V. S. & Fernandez, A. C. (2011). Temporal relation of cardiac hypertrophy, oxidative stress, and fatty acid metabolism in spontaneously hypertensive rat. *Mol Cell Biochem* **351**(1-2): 59-64.
- Pussinen, P. J., Havulinna, A. S., Lehto, M., Sundvall, J. & Salomaa, V. (2011). Endotoxemia Is Associated With an Increased Risk of Incident Diabetes. *Diabetes Care* **34**(2): 392-397.
- Puzzo, D., Lee, L., Palmeri, A., Calabrese, G. & Arancio, O. (2014). Behavioral assays with mouse models of Alzheimer's disease: Practical considerations and guidelines. *Biochemical Pharmacology* **88**(4): 450-467.
- Qiao, X., Cummins, D. J. & Paul, S. M. (2001). Neuroinflammation-induced acceleration of amyloid deposition in the APPV717F transgenic mouse. *European Journal of Neuroscience* **14**(3): 474-482.
- Qin, S., Du, R., Yin, S., Liu, X., Xu, G. & Cao, W. (2015). Nrf2 is essential for the anti-inflammatory effect of carbon monoxide in LPS-induced inflammation. *Inflamm. Res.* **64**(7): 537-548.
- Qiu, C., Kivipelto, M. & von Strauss, E. (2009). Epidemiology of Alzheimer's disease: occurrence, determinants, and strategies toward intervention. *Dialogues Clin Neurosci* **11**(2): 111-128.
- Qizilbash, N., Gregson, J., Johnson, M. E., Pearce, N., Douglas, I., Wing, K., Evans, S. J. W. & Pocock, S. J. (2015). BMI and risk of dementia in two million people over two decades: a retrospective cohort study. *The Lancet Diabetes & Endocrinology* **3**(6): 431-436.
- Quiroz-Baez, R., Rojas, E. & Arias, C. (2009). Oxidative stress promotes JNK-dependent amyloidogenic processing of normally expressed human APP by differential modification of α -, β - and γ -secretase expression. *Neurochemistry International* **55**(7): 662-670.
- Rada, P., Rojo, A. I., Chowdhry, S., McMahon, M., Hayes, J. D. & Cuadrado, A. (2011). SCF/ β -TrCP promotes glycogen synthase kinase 3-dependent degradation of the Nrf2 transcription factor in a Keap1-independent manner. *Mol Cell Biol* **31**(6): 1121-1133.
- Rada, P., Rojo, A. I., Evrard-Todeschi, N., Innamorato, N. G., Cotte, A., Jaworski, T., Tobon-Velasco, J. C., Devijver, H., Garcia-Mayoral, M. F., Van Leuven, F., Hayes, J. D., Bertho, G. & Cuadrado, A. (2012). Structural and functional characterization of Nrf2 degradation by the glycogen synthase kinase 3/ β -TrCP axis. *Mol Cell Biol* **32**(17): 3486-3499.
- Rainbolt, T. K., Saunders, J. M. & Wiseman, R. L. (2014). Stress-responsive regulation of mitochondria through the ER unfolded protein response. *Trends in Endocrinology & Metabolism* **25**(10): 528-537.

- Ramaglia, V., Hughes, T. R., Donev, R. M., Ruseva, M. M., Wu, X., Huitinga, I., Baas, F., Neal, J. W. & Morgan, B. P. (2012). C3-dependent mechanism of microglial priming relevant to multiple sclerosis. *Proceedings of the National Academy of Sciences* **109**(3): 965-970.
- Ransohoff, R. M. (2009). Chemokines and Chemokine Receptors: Standing at the Crossroads of Immunobiology and Neurobiology. *Immunity* **31**(5): 711-721.
- Reaume, A. G., Howland, D. S., Trusko, S. P., Savage, M. J., Lang, D. M., Greenberg, B. D., Siman, R. & Scott, R. W. (1996). Enhanced Amyloidogenic Processing of the β -Amyloid Precursor Protein in Gene-targeted Mice Bearing the Swedish Familial Alzheimer's Disease Mutations and a "Humanized" A β Sequence. *Journal of Biological Chemistry* **271**(38): 23380-23388.
- Refolo, L. M., Pappolla, M. A., Malester, B., LaFrancois, J., Bryant-Thomas, T., Wang, R., Tint, G. S., Sambamurti, K. & Duff, K. (2000). Hypercholesterolemia Accelerates the Alzheimer's Amyloid Pathology in a Transgenic Mouse Model. *Neurobiology of Disease* **7**(4): 321-331.
- Reger, M. L., Hovda, D. A. & Giza, C. C. (2009). Ontogeny of Rat Recognition Memory measured by the novel object recognition task. *Developmental Psychobiology* **51**(8): 672-678.
- Reichwald, J., Danner, S., Wiederhold, K. H. & Staufenbiel, M. (2009). Expression of complement system components during aging and amyloid deposition in APP transgenic mice. *J Neuroinflammation* **6**: 35.
- Roses, A. D. (1996). Apolipoprotein E alleles as risk factors in Alzheimer's disease. *Annu Rev Med* **47**: 387-400.
- Roßner, S., Lange-Dohna, C., Zeitschel, U. & Perez-Polo, J. R. (2005). Alzheimer's disease β -secretase BACE1 is not a neuron-specific enzyme. *Journal of Neurochemistry* **92**(2): 226-234.
- Rostène, W., Dansereau, M.-A., Godefroy, D., Van Steenwinckel, J., Goazigo, A. R.-L., Mélik-Parsadaniantz, S., Apartis, E., Hunot, S., Beaudet, N. & Sarret, P. (2011). Neurochemokines: a menage a trois providing new insights on the functions of chemokines in the central nervous system. *Journal of Neurochemistry* **118**(5): 680-694.
- Roubaud-Baudron, C., Krolak-Salmon, P., Quadrio, I., Mégraud, F. & Salles, N. (2012). Impact of chronic *Helicobacter pylori* infection on Alzheimer's disease: preliminary results. *Neurobiology of Aging* **33**(5): 1009.e1011-1009.e1019.
- Rzepecka, J., Pineda, M. A., Al-Riyami, L., Rodgers, D. T., Huggan, J. K., Lumb, F. E., Khalaf, A. I., Meakin, P. J., Corbet, M., Ashford, M. L., Suckling, C. J., Harnett, M. M. & Harnett, W. (2015). Prophylactic and therapeutic treatment with a synthetic analogue of a parasitic worm product prevents experimental arthritis and inhibits IL-1 β production via NRF2-mediated counter-regulation of the inflammasome. *Journal of Autoimmunity* **60**: 59-73.
- Salminen, A., Ojala, J., Suuronen, T., Kaarniranta, K. & Kauppinen, A. (2008). Amyloid- β oligomers set fire to inflammasomes and induce Alzheimer's pathology. *Journal of Cellular and Molecular Medicine* **12**(6a): 2255-2262.
- Salomone, S., Caraci, F., Leggio, G. M., Fedotova, J. & Drago, F. (2011). New pharmacological strategies for treatment of Alzheimer's disease: focus on disease-modifying drugs. *British Journal of Clinical Pharmacology*: no-no.
- Saraiva, M. & O'Garra, A. (2010). The regulation of IL-10 production by immune cells. *Nat Rev Immunol* **10**(3): 170-181.
- Sastre, M., Dewachter, I., Rossner, S., Bogdanovic, N., Rosen, E., Borghgraef, P., Evert, B. O., Dumitrescu-Ozimek, L., Thal, D. R., Landreth, G., Walter, J., Klockgether, T., van Leuven, F. & Heneka, M. T. (2006). Nonsteroidal anti-inflammatory drugs repress β -secretase gene promoter activity by the activation

- of PPAR γ . *Proceedings of the National Academy of Sciences of the United States of America* **103**(2): 443-448.
- Schaefer, E. J., Bongard, V., Beiser, A. S. & et al. (2006). Plasma phosphatidylcholine docosahexaenoic acid content and risk of dementia and alzheimer disease: The framingham heart study. *Archives of Neurology* **63**(11): 1545-1550.
- Schilling, T. & Eder, C. (2011). Amyloid-beta-induced reactive oxygen species production and priming are differentially regulated by ion channels in microglia. *J Cell Physiol* **226**(12): 3295-3302.
- Schuessel, K., Schäfer, S., Bayer, T. A., Czech, C., Pradier, L., Müller-Spahn, F., Müller, W. E. & Eckert, A. (2005). Impaired Cu/Zn-SOD activity contributes to increased oxidative damage in APP transgenic mice. *Neurobiology of Disease* **18**(1): 89-99.
- Seijkens, T., Kusters, P., Chatzigeorgiou, A., Chavakis, T. & Lutgens, E. (2014). Immune Cell Crosstalk in Obesity: A Key Role for Costimulation? *Diabetes* **63**(12): 3982-3991.
- Selfridge, J. E., E, L., Lu, J. & Swerdlow, R. H. (2013). Role of mitochondrial homeostasis and dynamics in Alzheimer's disease. *Neurobiology of Disease* **51**(0): 3-12.
- Seo, H.-A. & Lee, I.-K. (2013). The Role of Nrf2: Adipocyte Differentiation, Obesity, and Insulin Resistance. *Oxidative Medicine and Cellular Longevity* **2013**: 7.
- Serres, S., Bezancon, E., Franconi, J. M. & Merle, M. (2004). Ex vivo analysis of lactate and glucose metabolism in the rat brain under different states of depressed activity. *Journal of Biological Chemistry* **279**(46): 47881-47889.
- Shankar, G. M. & Walsh, D. M. (2009). Alzheimer's disease: synaptic dysfunction and A β . *Mol Neurodegener* **4**: 48.
- Shariati, S. A. M. & De Strooper, B. (2013). Redundancy and divergence in the amyloid precursor protein family. *FEBS Letters* **587**(13): 2036-2045.
- Sheedy, F. J., Grebe, A., Rayner, K. J., Kalantari, P., Ramkhelawon, B., Carpenter, S. B., Becker, C. E., Ediriweera, H. N., Mullick, A. E., Golenbock, D. T., Stuart, L. M., Latz, E., Fitzgerald, K. A. & Moore, K. J. (2013). CD36 coordinates NLRP3 inflammasome activation by facilitating intracellular nucleation of soluble ligands into particulate ligands in sterile inflammation. *Nat Immunol* **14**(8): 812-820.
- Shen, C., Chen, Y., Liu, H., Zhang, K., Zhang, T., Lin, A. & Jing, N. (2008). Hydrogen peroxide promotes A β production through JNK-dependent activation of γ -secretase. *Journal of Biological Chemistry* **283**(25): 17721-17730.
- Sheng, J. G., Bora, S. H., Xu, G., Borchelt, D. R., Price, D. L. & Koliatsos, V. E. (2003). Lipopolysaccharide-induced-neuroinflammation increases intracellular accumulation of amyloid precursor protein and amyloid β peptide in APP_{swe} transgenic mice. *Neurobiology of Disease* **14**(1): 133-145.
- Sherrington, R., Rogaev, E. I., Liang, Y., Rogaeva, E. A., Levesque, G., Ikeda, M., Chi, H., Lin, C., Li, G., Holman, K., Tsuda, T., Mar, L., Foncin, J. F., Bruni, A. C., Montesi, M. P., Sorbi, S., Rainero, I., Pinessi, L., Nee, L., Chumakov, I., Pollen, D., Brookes, A., Sanseau, P., Polinsky, R. J., Wasco, W., Da Silva, H. A. R., Haines, J. L., Pericak-Vance, M. A., Tanzi, R. E., Roses, A. D., Fraser, P. E., Rommens, J. M. & St George-Hyslop, P. H. (1995). Cloning of a gene bearing missense mutations in early-onset familial Alzheimer's disease. *Nature* **375**(6534): 754-760.
- Shih, A. Y., Imbeault, S., Barakauskas, V., Erb, H., Jiang, L., Li, P. & Murphy, T. H. (2005). Induction of the Nrf2-driven antioxidant response confers neuroprotection during mitochondrial stress in vivo. *Journal of Biological Chemistry* **280**(24): 22925-22936.

- Shih, A. Y., Johnson, D. A., Wong, G., Kraft, A. D., Jiang, L., Erb, H., Johnson, J. A. & Murphy, T. H. (2003). Coordinate Regulation of Glutathione Biosynthesis and Release by Nrf2-Expressing Glia Potently Protects Neurons from Oxidative Stress. *The Journal of Neuroscience* **23**(8): 3394-3406.
- Shimizu, E., Kawahara, K., Kajizono, M., Sawada, M. & Nakayama, H. (2008). IL-4-Induced Selective Clearance of Oligomeric β -Amyloid Peptide1–42 by Rat Primary Type 2 Microglia. *The Journal of Immunology* **181**(9): 6503-6513.
- Shin, S., Wakabayashi, J., Yates, M. S., Wakabayashi, N., Dolan, P. M., Aja, S., Liby, K. T., Sporn, M. B., Yamamoto, M. & Kensler, T. W. (2009). Role of Nrf2 in prevention of high-fat diet-induced obesity by synthetic triterpenoid CDDO-imidazolide. *Eur J Pharmacol* **620**(1-3): 138-144.
- Six, E., Ndiaye, D., Laâbi, Y., Brou, C., Gupta-Rossi, N., Israël, A. & Logeat, F. (2003). The Notch ligand Delta1 is sequentially cleaved by an ADAM protease and γ -secretase. *Proceedings of the National Academy of Sciences* **100**(13): 7638-7643.
- Sly, L. M., Krzesicki, R. F., Brashler, J. R., Buhl, A. E., McKinley, D. D., Carter, D. B. & Chin, J. E. (2001). Endogenous brain cytokine mRNA and inflammatory responses to lipopolysaccharide are elevated in the Tg2576 transgenic mouse model of Alzheimer's disease. *Brain Research Bulletin* **56**(6): 581-588.
- Smith, E., Hay, P., Campbell, L. & Trollor, J. N. (2011). A review of the association between obesity and cognitive function across the lifespan: implications for novel approaches to prevention and treatment. *Obesity Reviews* **12**(9): 740-755.
- Smith, E. E. & Greenberg, S. M. (2009). β -Amyloid, Blood Vessels, and Brain Function. *Stroke* **40**(7): 2601-2606.
- Smith, M. A., Casadesus, G., Joseph, J. A. & Perry, G. (2002). Amyloid- β and τ serve antioxidant functions in the aging and Alzheimer brain. *Free Radical Biology and Medicine* **33**(9): 1194-1199.
- Smith, R. A. J. & Murphy, M. P. (2010). Animal and human studies with the mitochondria-targeted antioxidant MitoQ. *Annals of the New York Academy of Sciences* **1201**(1): 96-103.
- Sofroniew, M. V. (2009). Molecular dissection of reactive astrogliosis and glial scar formation. *Trends Neurosci* **32**(12): 638-647.
- Sokolova, A., Hill, M. D., Rahimi, F., Warden, L. A., Halliday, G. M. & Shepherd, C. E. (2009). Monocyte Chemoattractant Protein-1 Plays a Dominant Role in the Chronic Inflammation Observed in Alzheimer's Disease. *Brain Pathology* **19**(3): 392-398.
- Song, M., Jin, J., Lim, J. E., Kou, J., Pattanayak, A., Rehman, J. A., Kim, H. D., Tahara, K., Lalonde, R. & Fukuchi, K. (2011). TLR4 mutation reduces microglial activation, increases A β deposits and exacerbates cognitive deficits in a mouse model of Alzheimer's disease. *J Neuroinflammation* **8**: 92.
- Sosa-Ortiz, A. L., Acosta-Castillo, I. & Prince, M. J. (2012). Epidemiology of Dementias and Alzheimer's Disease. *Archives of Medical Research* **43**(8): 600-608.
- Spires-Jones, T. L., Stoothoff, W. H., de Calignon, A., Jones, P. B. & Hyman, B. T. (2009). Tau pathophysiology in neurodegeneration: a tangled issue. *Trends in Neurosciences* **32**(3): 150-159.
- Spitzer, P., Herrmann, M., Klafki, H. W., Smirnov, A., Lewczuk, P., Kornhuber, J., Wiltfang, J. & Maler, J. M. (2010). Phagocytosis and LPS alter the maturation state of beta-amyloid precursor protein and induce different Abeta peptide release signatures in human mononuclear phagocytes. *J Neuroinflammation* **7**: 59.

- Stack, C., Jainuddin, S., Elipenahli, C., Gerges, M., Starkova, N., Starkov, A. A., Jové, M., Portero-Otin, M., Launay, N., Pujol, A., Kaidery, N. A., Thomas, B., Tampellini, D., Beal, M. F. & Dumont, M. (2014). Methylene blue upregulates Nrf2/ARE genes and prevents tau-related neurotoxicity. *Human Molecular Genetics* **23**(14): 3716-3732.
- Stienstra, R., van Diepen, J. A., Tack, C. J., Zaki, M. H., van de Veerdonk, F. L., Perera, D., Neale, G. A., Hooiveld, G. J., Hijmans, A., Vroegrijk, I., van den Berg, S., Romijn, J., Rensen, P. C. N., Joosten, L. A. B., Netea, M. G. & Kanneganti, T.-D. (2011). Inflammasome is a central player in the induction of obesity and insulin resistance. *Proceedings of the National Academy of Sciences* **108**(37): 15324-15329.
- Strohmeyer, R., Shen, Y. & Rogers, J. (2000). Detection of complement alternative pathway mRNA and proteins in the Alzheimer's disease brain. *Molecular Brain Research* **81**(1-2): 7-18.
- Subaiea, G. M., Adwan, L. I., Ahmed, A. H., Stevens, K. E. & Zawia, N. H. (2013). Short-term treatment with tolfenamic acid improves cognitive functions in Alzheimer's disease mice. *Neurobiology of Aging* **34**(10): 2421-2430.
- Sugimoto, H., Okada, K., Shoda, J., Warabi, E., Ishige, K., Ueda, T., Taguchi, K., Yanagawa, T., Nakahara, A., Hyodo, I., Ishii, T. & Yamamoto, M. (2010). Deletion of nuclear factor-E2-related factor-2 leads to rapid onset and progression of nutritional steatohepatitis in mice. *Am J Physiol Gastrointest Liver Physiol* **298**(2): G283-294.
- Sutherland, L. N., Capozzi, L. C., Turchinsky, N. J., Bell, R. C. & Wright, D. C. (2008). Time course of high-fat diet-induced reductions in adipose tissue mitochondrial proteins: potential mechanisms and the relationship to glucose intolerance. *American Journal of Physiology - Endocrinology and Metabolism* **295**(5): E1076-E1083.
- Swerdlow, R. H. (2011). Brain aging, Alzheimer's disease, and mitochondria. *Biochimica et Biophysica Acta - Molecular Basis of Disease* **1812**(12): 1630-1639.
- Sy, M., Kitazawa, M., Medeiros, R., Whitman, L., Cheng, D., Lane, T. E. & Laferla, F. M. (2011). Inflammation induced by infection potentiates tau pathological features in transgenic mice. *Am J Pathol* **178**(6): 2811-2822.
- Takeda, S., Sato, N., Uchio-Yamada, K., Sawada, K., Kunieda, T., Takeuchi, D., Kurinami, H., Shinohara, M., Rakugi, H. & Morishita, R. (2010). Diabetes-accelerated memory dysfunction via cerebrovascular inflammation and A β deposition in an Alzheimer mouse model with diabetes. *Proceedings of the National Academy of Sciences* **107**(15): 7036-7041.
- Takeuchi, O. & Akira, S. (2010). Pattern Recognition Receptors and Inflammation. *Cell* **140**(6): 805-820.
- Tamagno, E., Guglielmotto, M., Giliberto, L., Vitali, A., Borghi, R., Autelli, R., Danni, O. & Tabaton, M. (2009). JNK and ERK1/2 pathways have a dual opposite effect on the expression of BACE1. *Neurobiology of Aging* **30**(10): 1563-1573.
- Tamagno, E., Parola, M., Bardini, P., Piccini, A., Borghi, R., Guglielmotto, M., Santoro, G., Davit, A., Danni, O., Smith, M. A., Perry, G. & Tabaton, M. (2005). β -site APP cleaving enzyme up-regulation induced by 4-hydroxynonenal is mediated by stress-activated protein kinases pathways. *Journal of Neurochemistry* **92**(3): 628-636.
- Tanaka, N., Ikeda, Y., Ohta, Y., Deguchi, K., Tian, F., Shang, J., Matsuura, T. & Abe, K. (2011). Expression of Keap1-Nrf2 system and antioxidative proteins in mouse brain after transient middle cerebral artery occlusion. *Brain Research* **1370**: 246-253.

- Tanaka, Y., Aleksunes, L. M., Yeager, R. L., Gyamfi, M. A., Esterly, N., Guo, G. L. & Klaassen, C. D. (2008). NF-E2-Related Factor 2 Inhibits Lipid Accumulation and Oxidative Stress in Mice Fed a High-Fat Diet. *Journal of Pharmacology and Experimental Therapeutics* **325**(2): 655-664.
- Tarr, A. J., McLinden, K. A., Kranjac, D., Kohman, R. A., Amaral, W. & Boehm, G. W. (2011). The effects of age on lipopolysaccharide-induced cognitive deficits and interleukin-1beta expression. *Behav Brain Res* **217**(2): 481-485.
- Tateda, K., Matsumoto, T., Miyazaki, S. & Yamaguchi, K. (1996). Lipopolysaccharide-induced lethality and cytokine production in aged mice. *Infect Immun* **64**(3): 769-774.
- Tebay, L. E., Robertson, H., Durant, S. T., Vitale, S. R., Penning, T. M., Dinkova-Kostova, A. T. & Hayes, J. D. (2015). Mechanisms of activation of the transcription factor Nrf2 by redox stressors, nutrient cues, and energy status and the pathways through which it attenuates degenerative disease. *Free Radical Biology and Medicine* **88, Part B**: 108-146.
- Thal, D. R., Griffin, W. S. T. & Braak, H. (2008). Parenchymal and vascular A β -deposition and its effects on the degeneration of neurons and cognition in Alzheimer's disease. *Journal of Cellular and Molecular Medicine* **12**(5b): 1848-1862.
- Thaler, J. P., Yi, C.-X., Schur, E. A., Guyenet, S. J., Hwang, B. H., Dietrich, M. O., Zhao, X., Sarruf, D. A., Izgur, V., Maravilla, K. R., Nguyen, H. T., Fischer, J. D., Matsen, M. E., Wisse, B. E., Morton, G. J., Horvath, T. L., Baskin, D. G., Tsch, xF, p, M. H. & Schwartz, M. W. (2012). Obesity is associated with hypothalamic injury in rodents and humans. *The Journal of Clinical Investigation* **122**(1): 153-162.
- Thimmulappa, R. K., Mai, K. H., Srisuma, S., Kensler, T. W., Yamamoto, M. & Biswal, S. (2002). Identification of Nrf2-regulated genes induced by the chemopreventive agent sulforaphane by oligonucleotide microarray. *Cancer Res* **62**(18): 5196-5203.
- Thimmulappa, R. K., Scollick, C., Traore, K., Yates, M., Trush, M. A., Liby, K. T., Sporn, M. B., Yamamoto, M., Kensler, T. W. & Biswal, S. (2006). Nrf2-dependent protection from LPS induced inflammatory response and mortality by CDDO-Imidazolide. *Biochemical and Biophysical Research Communications* **351**(4): 883-889.
- Thinakaran, G. & Koo, E. H. (2008). Amyloid precursor protein trafficking, processing, and function. *Journal of Biological Chemistry* **283**(44): 29615-29619.
- Thirumangalakudi, L., Prakasam, A., Zhang, R., Bimonte-Nelson, H., Sambamurti, K., Kindy, M. S. & Bhat, N. R. (2008). High cholesterol-induced neuroinflammation and amyloid precursor protein processing correlate with loss of working memory in mice. *Journal of Neurochemistry* **106**(1): 475-485.
- Thomson, C. A., McColl, A., Cavanagh, J. & Graham, G. J. (2014). Peripheral inflammation is associated with remote global gene expression changes in the brain. *J Neuroinflammation* **11**: 73.
- Togo, T., Akiyama, H., Iseki, E., Kondo, H., Ikeda, K., Kato, M., Oda, T., Tsuchiya, K. & Kosaka, K. (2002). Occurrence of T cells in the brain of Alzheimer's disease and other neurological diseases. *Journal of Neuroimmunology* **124**(1-2): 83-92.
- Tomobe, K., Shinozuka, T., Kuroiwa, M. & Nomura, Y. (2012). Age-related changes of Nrf2 and phosphorylated GSK-3 β in a mouse model of accelerated aging (SAMP8). *Archives of Gerontology and Geriatrics* **54**(2): e1-e7.
- Tremblay, M.-È., Lowery, R. L. & Majewska, A. K. (2010). Microglial Interactions with Synapses Are Modulated by Visual Experience. *PLoS Biol* **8**(11): e1000527.

- Tremblay, M. E., Stevens, B., Sierra, A., Wake, H., Bessis, A. & Nimmerjahn, A. (2011). The Role of Microglia in the Healthy Brain. *Journal of Neuroscience* **31**(45): 16064-16069.
- Trimmer, P. A., Keeney, P. M., Borland, M. K., Simon, F. A., Almeida, J., Swerdlow, R. H., Parks, J. P., Parker Jr, W. D. & Bennett Jr, J. P. (2004). Mitochondrial abnormalities in cybrid cell models of sporadic Alzheimer's disease worsen with passage in culture. *Neurobiology of Disease* **15**(1): 29-39.
- Tucsek, Z., Toth, P., Tarantini, S., Sosnowska, D., Gautam, T., Warrington, J. P., Giles, C. B., Wren, J. D., Koller, A., Ballabh, P., Sonntag, W. E., Ungvari, Z. & Csiszar, A. (2014). Aging Exacerbates Obesity-induced Cerebromicrovascular Rarefaction, Neurovascular Uncoupling, and Cognitive Decline in Mice. *The Journals of Gerontology Series A: Biological Sciences and Medical Sciences* **69**(11): 1339-1352.
- Turner, P. R., O'Connor, K., Tate, W. P. & Abraham, W. C. (2003). Roles of amyloid precursor protein and its fragments in regulating neural activity, plasticity and memory. *Progress in Neurobiology* **70**(1): 1-32.
- Ulbrich, F., Kaufmann, K. B., Coburn, M., Lagrèze, W. A., Roesslein, M., Biermann, J., Buerkle, H., Loop, T. & Goebel, U. (2015). Neuroprotective effects of Argon are mediated via an ERK-1/2 dependent regulation of heme-oxygenase-1 in retinal ganglion cells. *Journal of Neurochemistry* **134**(4): 717-727.
- Unno, K., Yamamoto, H., Maeda, K.-i., Takabayashi, F., Yoshida, H., Kikunaga, N., Takamori, N., Asahina, S., Iguchi, K., Sayama, K. & Hoshino, M. (2009). Protection of brain and pancreas from high-fat diet: Effects of catechin and caffeine. *Physiology & Behavior* **96**(2): 262-269.
- Valerio, A., Cardile, A., Cozzi, V., Bracale, R., Tedesco, L., Pisconti, A., Palomba, L., Cantoni, O., Clementi, E., Moncada, S., Carruba, M. O. & Nisoli, E. (2006). TNF- α downregulates eNOS expression and mitochondrial biogenesis in fat and muscle of obese rodents. *The Journal of Clinical Investigation* **116**(10): 2791-2798.
- Valladolid-Acebes, I., Stucchi, P., Cano, V., Fernández-Alfonso, M. S., Merino, B., Gil-Ortega, M., Fole, A., Morales, L., Ruiz-Gayo, M. & Olmo, N. D. (2011). High-fat diets impair spatial learning in the radial-arm maze in mice. *Neurobiology of Learning and Memory* **95**(1): 80-85.
- van den Berg, T. K. & Kraal, G. (2005). A function for the macrophage F4/80 molecule in tolerance induction. *Trends in Immunology* **26**(10): 506-509.
- van der Heide, L. P., Ramakers, G. M. J. & Smidt, M. P. (2006). Insulin signaling in the central nervous system: Learning to survive. *Progress in Neurobiology* **79**(4): 205-221.
- Van Leuven, F. (2013). Alzheimer's Disease. <https://gbiomed.kuleuven.be/english/research/50000622/50525540/alzheimers-disease>.
- Vandal, M., White, P. J., Tremblay, C., St-Amour, I., Chevrier, G., Emond, V., Lefrançois, D., Virgili, J., Planel, E., Giguere, Y., Marette, A. & Calon, F. (2014). Insulin Reverses the High-Fat Diet-Induced Increase in Brain A β and Improves Memory in an Animal Model of Alzheimer Disease. *Diabetes* **63**(12): 4291-4301.
- Vandanmagsar, B., Youm, Y.-H., Ravussin, A., Galgani, J. E., Stadler, K., Mynatt, R. L., Ravussin, E., Stephens, J. M. & Dixit, V. D. (2011). The NLRP3 inflammasome instigates obesity-induced inflammation and insulin resistance. *Nat Med* **17**(2): 179-188.
- Vassar, R. (2001). The β -secretase, BACE. *Journal of Molecular Neuroscience* **17**(2): 157-170.

- Vassar, R., Bennett, B. D., Babu-Khan, S., Kahn, S., Mendiaz, E. A., Denis, P., Teplow, D. B., Ross, S., Amarante, P., Loeloff, R., Luo, Y., Fisher, S., Fuller, J., Edenson, S., Lile, J., Jarosinski, M. A., Biere, A. L., Curran, E., Burgess, T., Louis, J.-C., Collins, F., Treanor, J., Rogers, G. & Citron, M. (1999). β -Secretase Cleavage of Alzheimer's Amyloid Precursor Protein by the Transmembrane Aspartic Protease BACE. *Science* **286**(5440): 735-741.
- Vázquez-Vela, M. E. F., Torres, N. & Tovar, A. R. (2008). White Adipose Tissue as Endocrine Organ and Its Role in Obesity. *Archives of Medical Research* **39**(8): 715-728.
- Veerhuis, R., Nielsen, H. M. & Tenner, A. J. (2011). Complement in the brain. *Molecular Immunology* **48**(14): 1592-1603.
- Velliquette, R. A., O'Connor, T. & Vassar, R. (2005). Energy inhibition elevates β -secretase levels and activity and is potentially amyloidogenic in APP transgenic mice: Possible early events in Alzheimer's disease pathogenesis. *Journal of Neuroscience* **25**(47): 10874-10883.
- Velmurugan, G. V., Sundaresan, N. R., Gupta, M. P. & White, C. (2013). Defective Nrf2-dependent redox signalling contributes to microvascular dysfunction in type 2 diabetes. *Cardiovascular Research* **100**(1): 143-150.
- Venci, J. V. & Gandhi, M. A. (2013). Dimethyl Fumarate (Tecfidera): A New Oral Agent for Multiple Sclerosis. *Annals of Pharmacotherapy* **47**(12): 1697-1702.
- Venugopal, R. & Jaiswal, A. K. (1996). Nrf1 and Nrf2 positively and c-Fos and Fra1 negatively regulate the human antioxidant response element-mediated expression of NAD(P)H:quinone oxidoreductase 1 gene. *Proceedings of the National Academy of Sciences of the United States of America* **93**(25): 14960-14965.
- Verkhatsky, A., Olabarria, M., Noristani, H. N., Yeh, C. Y. & Rodriguez, J. J. (2010). Astrocytes in Alzheimer's Disease. *Neurotherapeutics* **7**(4): 399-412.
- Verret, L., Krezymon, A., Halley, H., Trouche, S., Zerwas, M., Lazouret, M., Lassalle, J.-M. & Rampon, C. (2013). Transient enriched housing before amyloidosis onset sustains cognitive improvement in Tg2576 mice. *Neurobiology of Aging* **34**(1): 211-225.
- Vingtdeux, V. & Marambaud, P. (2012). Identification and biology of α -secretase. *Journal of Neurochemistry* **120**: 34-45.
- Viswanathan, A. & Greenberg, S. M. (2011). Cerebral amyloid angiopathy in the elderly. *Annals of Neurology* **70**(6): 871-880.
- Vorhees, C. V. & Williams, M. T. (2014). Assessing Spatial Learning and Memory in Rodents. *ILAR Journal* **55**(2): 310-332.
- Wang, H.-Q., Xu, Y.-X. & Zhu, C.-Q. (2012). Upregulation of Heme Oxygenase-1 by Acteoside Through ERK and PI3 K/Akt Pathway Confer Neuroprotection Against Beta-Amyloid-Induced Neurotoxicity. *Neurotoxicity Research* **21**(4): 368-378.
- Wang, H., Khor, T. O., Saw, C. L., Lin, W., Wu, T., Huang, Y. & Kong, A. N. (2010). Role of Nrf2 in suppressing LPS-induced inflammation in mouse peritoneal macrophages by polyunsaturated fatty acids docosahexaenoic acid and eicosapentaenoic acid. *Mol Pharm* **7**(6): 2185-2193.
- Wang, H., Liu, K., Geng, M., Gao, P., Wu, X., Hai, Y., Li, Y., Li, Y., Luo, L., Hayes, J. D., Wang, X. J. & Tang, X. (2013a). RXR α Inhibits the NRF2-ARE Signaling Pathway through a Direct Interaction with the Neh7 Domain of NRF2. *Cancer Research* **73**(10): 3097-3108.
- Wang, J., Ho, L., Qin, W., Rocher, A. B., Seror, I., Humala, N., Maniar, K., Dolios, G., Wang, R., Hof, P. R. & Pasinetti, G. M. (2005). Caloric restriction attenuates β -

- amyloid neuropathology in a mouse model of Alzheimer's disease. *The FASEB Journal*.
- Wang, L., Colodner, K. J. & Feany, M. B. (2011). Protein misfolding and oxidative stress promote glial-mediated neurodegeneration in an Alexander disease model. *Journal of Neuroscience* **31**(8): 2868-2877.
- Wang, R., Li, Jing J., Diao, S., Kwak, Y.-D., Liu, L., Zhi, L., Büeler, H., Bhat, Narayan R., Williams, Robert W., Park, Edwards A. & Liao, F.-F. (2013b). Metabolic Stress Modulates Alzheimer's β -Secretase Gene Transcription via SIRT1-PPAR γ -PGC-1 in Neurons. *Cell Metabolism* **17**(5): 685-694.
- Wang, X. J., Sun, Z., Villeneuve, N. F., Zhang, S., Zhao, F., Li, Y., Chen, W., Yi, X., Zheng, W., Wondrak, G. T., Wong, P. K. & Zhang, D. D. (2008). Nrf2 enhances resistance of cancer cells to chemotherapeutic drugs, the dark side of Nrf2. *Carcinogenesis* **29**(6): 1235-1243.
- Wang, Y., Sun, W., Du, B., Miao, X., Bai, Y., Xin, Y., Tan, Y., Cui, W., Liu, B., Cui, T., Epstein, P. N., Fu, Y. & Cai, L. (2013c). Therapeutic effect of MG-132 on diabetic cardiomyopathy is associated with its suppression of proteasomal activities: roles of Nrf2 and NF- κ B. *American Journal of Physiology - Heart and Circulatory Physiology* **304**(4): H567-H578.
- Wang, Z., Wu, D. & Vinters, H. V. (2002). Hypoxia and reoxygenation of brain microvascular smooth muscle cells in vitro: cellular responses and expression of cerebral amyloid angiopathy-associated proteins. *APMIS* **110**(5): 423-434.
- Webster, S. J., Bachstetter, A. D., Nelson, P. T., Schmitt, F. A. & Van Eldik, L. J. (2014). Using mice to model Alzheimer's dementia: an overview of the clinical disease and the preclinical behavioral changes in 10 mouse models. *Frontiers in Genetics* **5**: 88.
- Wegen, S. & Beher, D. (2012). Molecular consequences of amyloid precursor protein and presenilin mutations causing autosomal-dominant Alzheimer's disease. *Alzheimers Res Ther* **4**(2): 9.
- Weldon, D. T., Rogers, S. D., Ghilardi, J. R., Finke, M. P., Cleary, J. P., O'Hare, E., Esler, W. P., Maggio, J. E. & Mantyh, P. W. (1998). Fibrillar beta-amyloid induces microglial phagocytosis, expression of inducible nitric oxide synthase, and loss of a select population of neurons in the rat CNS in vivo. *J Neurosci* **18**(6): 2161-2173.
- Westerman, M. A., Cooper-Blacketer, D., Mariash, A., Kotilinek, L., Kawarabayashi, T., Younkin, L. H., Carlson, G. A., Younkin, S. G. & Ashe, K. H. (2002). The Relationship between A β and Memory in the Tg2576 Mouse Model of Alzheimer's Disease. *The Journal of Neuroscience* **22**(5): 1858-1867.
- Westermann, B. (2012). Bioenergetic role of mitochondrial fusion and fission. *Biochimica et Biophysica Acta (BBA) - Bioenergetics* **1817**(10): 1833-1838.
- White, C. L., Pistell, P. J., Purpera, M. N., Gupta, S., Fernandez-Kim, S. O., Hise, T. L., Keller, J. N., Ingram, D. K., Morrison, C. D. & Bruce-Keller, A. J. (2009). Effects of high fat diet on Morris maze performance, oxidative stress, and inflammation in rats: contributions of maternal diet. *Neurobiol Dis* **35**(1): 3-13.
- WHO (2015a). Dementia (Fact Sheet N°362).
<http://www.who.int/mediacentre/factsheets/fs362/en/>.
- WHO (2015b). Obesity and overweight (Fact Sheet N°311).
<http://www.who.int/mediacentre/factsheets/fs311/en/>.
- Williamson, L. L., Chao, A. & Bilbo, S. D. (2012). Environmental enrichment alters glial antigen expression and neuroimmune function in the adult rat hippocampus. *Brain, Behavior, and Immunity* **26**(3): 500-510.

- Wilson, D. I. G., Watanabe, S., Milner, H. & Ainge, J. A. (2013). Lateral entorhinal cortex is necessary for associative but not nonassociative recognition memory. *Hippocampus* **23**(12): 1280-1290.
- Winters, B. D., Forwood, S. E., Cowell, R. A., Saksida, L. M. & Bussey, T. J. (2004). Double Dissociation between the Effects of Peri-Postrhinal Cortex and Hippocampal Lesions on Tests of Object Recognition and Spatial Memory: Heterogeneity of Function within the Temporal Lobe. *The Journal of Neuroscience* **24**(26): 5901-5908.
- Winzell, M. S. & Ahrén, B. (2004). The High-Fat Diet–Fed Mouse: A Model for Studying Mechanisms and Treatment of Impaired Glucose Tolerance and Type 2 Diabetes. *Diabetes* **53**(suppl 3): S215-S219.
- Wu, G., Xu, G., Schulman, B. A., Jeffrey, P. D., Harper, J. W. & Pavletich, N. P. (2003). Structure of a β -TrCP1-Skp1- β -catenin complex: destruction motif binding and lysine specificity of the SCF(β -TrCP1) ubiquitin ligase. *Mol Cell* **11**(6): 1445-1456.
- Wu, Z., Zhu, Y., Cao, X., Sun, S. & Zhao, B. (2014). Mitochondrial Toxic Effects of A β Through Mitofusins in the Early Pathogenesis of Alzheimer's Disease. *Mol Neurobiol* **50**(3): 986-996.
- Wurtman, R. (2015). Biomarkers in the diagnosis and management of Alzheimer's disease. *Metabolism* **64**(3, Supplement 1): S47-S50.
- Wynne, A. M., Henry, C. J. & Godbout, J. P. (2009). Immune and behavioral consequences of microglial reactivity in the aged brain. *Integrative and Comparative Biology* **49**(3): 254-266.
- Wyss-Coray, T., Loike, J. D., Brionne, T. C., Lu, E., Anankov, R., Yan, F., Silverstein, S. C. & Husemann, J. (2003). Adult mouse astrocytes degrade amyloid- β in vitro and in situ. *Nature Medicine* **9**(4): 453-457.
- Wyss, M. T., Jolivet, R., Buck, A., Magistretti, P. J. & Weber, B. (2011). In Vivo Evidence for Lactate as a Neuronal Energy Source. *Journal of Neuroscience* **31**(20): 7477-7485.
- Xia, M. Q., Bacskai, B. J., Knowles, R. B., Qin, S. X. & Hyman, B. T. (2000). Expression of the chemokine receptor CXCR3 on neurons and the elevated expression of its ligand IP-10 in reactive astrocytes: in vitro ERK1/2 activation and role in Alzheimer's disease. *Journal of Neuroimmunology* **108**(1–2): 227-235.
- Xie, L., Helmerhorst, E., Taddei, K., Plewright, B., Van Bronswijk, W. & Martins, R. (2002). Alzheimer's beta-amyloid peptides compete for insulin binding to the insulin receptor. *J Neurosci* **22**(10): RC221.
- Yamamoto, T., Suzuki, T., Kobayashi, A., Wakabayashi, J., Maher, J., Motohashi, H. & Yamamoto, M. (2008). Physiological Significance of Reactive Cysteine Residues of Keap1 in Determining Nrf2 Activity. *Molecular and Cellular Biology* **28**(8): 2758-2770.
- Yan, Y., Jiang, W., Liu, L., Wang, X., Ding, C., Tian, Z. & Zhou, R. (2015). Dopamine Controls Systemic Inflammation through Inhibition of NLRP3 Inflammasome. *Cell* **160**(1–2): 62-73.
- Yao, J., Irwin, R. W., Zhao, L., Nilsen, J., Hamilton, R. T. & Brinton, R. D. (2009). Mitochondrial bioenergetic deficit precedes Alzheimer's pathology in female mouse model of Alzheimer's disease. *Proceedings of the National Academy of Sciences* **106**(34): 14670-14675.
- Yasojima, K., Schwab, C., McGeer, E. G. & McGeer, P. L. (1999). Up-Regulated Production and Activation of the Complement System in Alzheimer's Disease Brain. *The American Journal of Pathology* **154**(3): 927-936.

- Yeang, H. X. A., Hamdam, J. M., Al-Huseini, L. M. A., Sethu, S., Djouhri, L., Walsh, J., Kitteringham, N., Park, B. K., Goldring, C. E. & Sathish, J. G. (2012). Loss of Transcription Factor Nuclear Factor-Erythroid 2 (NF-E2) p45-related Factor-2 (Nrf2) Leads to Dysregulation of Immune Functions, Redox Homeostasis, and Intracellular Signaling in Dendritic Cells. *The Journal of Biological Chemistry* **287**(13): 10556-10564.
- Yoshida, T. & Nakagawa, M. (2012). Clinical aspects and pathology of Alexander disease, and morphological and functional alteration of astrocytes induced by GFAP mutation. *Neuropathology* **32**(4): 440-446.
- Yoshiike, Y., Chui, D.-H., Akagi, T., Tanaka, N. & Takashima, A. (2003). Specific Compositions of Amyloid- β Peptides as the Determinant of Toxic β -Aggregation. *Journal of Biological Chemistry* **278**(26): 23648-23655.
- Yuzwa, S. A., Shan, X., Macauley, M. S., Clark, T., Skorobogatko, Y., Vosseller, K. & Vocadlo, D. J. (2012). Increasing O-GlcNAc slows neurodegeneration and stabilizes tau against aggregation. *Nat Chem Biol* **8**(4): 393-399.
- Zenaro, E., Pietronigro, E., Bianca, V. D., Piacentino, G., Marongiu, L., Budui, S., Turano, E., Rossi, B., Angiari, S., Dusi, S., Montresor, A., Carlucci, T., Nani, S., Tosadori, G., Calciano, L., Catalucci, D., Berton, G., Bonetti, B. & Constantin, G. (2015). Neutrophils promote Alzheimer's disease-like pathology and cognitive decline via LFA-1 integrin. *Nat Med* **21**(8): 880-886.
- Zhang, C., Zhu, J., Zhang, J., Li, H., Zhao, Z., Liao, Y., Wang, X., Su, J., Sang, S., Yuan, X. & Liu, Q. (2014). Neuroprotective and anti-apoptotic effects of valproic acid on adult rat cerebral cortex through ERK and Akt signaling pathway at acute phase of traumatic brain injury. *Brain Research* **1555**: 1-9.
- Zhang, D. D., Lo, S. C., Cross, J. V., Templeton, D. J. & Hannink, M. (2004). Keap1 is a redox-regulated substrate adaptor protein for a Cul3-dependent ubiquitin ligase complex. *Mol Cell Biol* **24**(24): 10941-10953.
- Zhang, L., Fang, Y., Xu, Y., Lian, Y., Xie, N., Wu, T., Zhang, H., Sun, L., Zhang, R. & Wang, Z. (2015). Curcumin Improves Amyloid β -Peptide (1-42) Induced Spatial Memory Deficits through BDNF-ERK Signaling Pathway. *PLoS ONE* **10**(6): e0131525.
- Zhang, R., Miller, R. G., Gascon, R., Champion, S., Katz, J., Lancero, M., Narvaez, A., Honrada, R., Ruvalcaba, D. & McGrath, M. S. (2009). Circulating endotoxin and systemic immune activation in sporadic Amyotrophic Lateral Sclerosis (sALS). *Journal of neuroimmunology* **206**(1-2): 121-124.
- Zhang, R., Miller, R. G., Madison, C., Jin, X., Honrada, R., Harris, W., Katz, J., Forshe, D. A. & McGrath, M. S. (2013). Systemic immune system alterations in early stages of Alzheimer's disease. *Journal of Neuroimmunology* **256**(1-2): 38-42.
- Zhang, X., Zhou, K., Wang, R., Cui, J., Lipton, S. A., Liao, F.-F., Xu, H. & Zhang, Y.-w. (2007). Hypoxia-inducible Factor 1 α (HIF-1 α)-mediated Hypoxia Increases BACE1 Expression and β -Amyloid Generation. *Journal of Biological Chemistry* **282**(15): 10873-10880.
- Zhang, Y.-K. J., Yeager, R. L., Tanaka, Y. & Klaassen, C. D. (2010). Enhanced expression of Nrf2 in mice attenuates the fatty liver produced by a methionine- and choline-deficient diet. *Toxicology and Applied Pharmacology* **245**(3): 326-334.
- Zhang, Y. W., Thompson, R., Zhang, H. & Xu, H. (2011). APP processing in Alzheimer's disease. *Mol Brain* **4**: 3.
- Zhao, W.-Q. & Townsend, M. (2009). Insulin resistance and amyloidogenesis as common molecular foundation for type 2 diabetes and Alzheimer's disease.

- Biochimica et Biophysica Acta (BBA) - Molecular Basis of Disease* **1792**(5): 482-496.
- Zhao, W. Q., Chen, H., Quon, M. J. & Alkon, D. L. (2004). Insulin and the insulin receptor in experimental models of learning and memory. *Eur J Pharmacol* **490**(1-3): 71-81.
- Zhou, R., Yazdi, A. S., Menu, P. & Tschopp, J. (2011). A role for mitochondria in NLRP3 inflammasome activation. *Nature* **469**(7329): 221-225.
- Zipper, L. M. & Timothy Mulcahy, R. (2002). The Keap1 BTB/POZ dimerization function is required to sequester Nrf2 in cytoplasm. *Journal of Biological Chemistry* **277**(39): 36544-36552.
- Zlokovic, B. V. (2005). Neurovascular mechanisms of Alzheimer's neurodegeneration. *Trends in Neurosciences* **28**(4): 202-208.

7 APPENDICES

7.1 APPENDIX I - SOLUTIONS

Protein Analysis		
Solution	Ingredients	
OxyBlock	PBS-T 0.05% BSA	100 ml 1 g
PBS-T 0.05% (Oxyblot™)	PBS Tween 20	500 ml 0.05% (v/v)
SDS-containing tris-glycine sample buffer	0.5 M Tris HCl 100% Glycerol 20% SDS β-mercaptoethanol Bromophenol blue	4 ml 3.2 ml 3.2 ml 1.6 ml pinch
TAE buffer (1x)	dH ₂ O 10x TAE buffer	450 ml 50 ml
TBS-T (Western blot)	4 M NaCl 1 M Tris/HCl (pH 7.4) Tween-20 dH ₂ O	40 ml 74 ml 1 ml to 2 L
Transfer Buffer	Glycine Tris Base Methanol dH ₂ O	2.93 g 5.81 g 200 ml 800 ml
Tris/glycine running buffer (1x)	dH ₂ O 10x Running Buffer (National Diagnostics; 25 mM Tris, 192 mM Glycine, 0.1% SDS)	900 ml 100 ml
Triton X-100 Lysis buffer stock solution	1 M Tris/HCl 750 mM NaF 5 M NaCl 0.5 M EDTA 0.2 M EGTA 0.5 M NaPPi Triton X-100 dH ₂ O	12.5 ml 33.5 ml 10.0 ml 10.0 ml 12.5 ml 10.0 ml 5% (v/v) To 500 ml
Working Triton X-100 Lysis buffer solution	1 mM Na ₃ VO ₄ * 1 mM Benzamidine 0.1 mM PMSF β-mercaptoethanol Sucrose /ml of Triton X-100 Lysis buffer stock solution	2 μl 1 μl 1 μl 0.1% (v/v) 92 mg

Table 7.1 Table of content of common solutions used for protein elucidation

* Denotes heated to 95°C and left to cool to room temperature prior to addition

SDS-PAGE tris-glycine gel composition (2 gels)			
Ingredient	Resolution		Stacking
	Gel (10%)	Gel (15%)	Gel (4%)
d.H ₂ O	4.15 ml	2.3 ml	2.8 ml
0.5 M Tris, pH 6.8	3.15 ml	3.15 ml	1.25 ml
Bis-Acrylamide	3.75 ml	5.5 ml	0.85 ml
10% SDS	110 µl	110 µl	50 µl
TEMED	11 µl	11 µl	5.4 µl
20% APS	55.4 µl	55.4 µl	50 µl

Table 7.2 Constituents of self-poured Acrylamide gels

Immunohistochemistry Solutions		
Solutions	Ingredients	
10 mM Citric Acid, pH 6.0	Citric Acid dH ₂ O	0.96 g To 500 ml
Blocking Solution	PBST donkey serum	As required 10% (v/v)
Cryoprotectant Solution	Sucrose Polyvinyl-pyrrolidone (PVP-40) Ethylene Glycol 0.1 M PB	75 g 2.5 g 75 ml To 250 ml
Permeabilisation Solution (PBST)	PBS Triton-X 100	500ml 0.1% (v/v)
0.1 M Phosphate buffer (PB)	Na ₂ HPO ₄ (anhydrous) NaH ₂ PO ₄ (anhydrous) dH ₂ O	10.9 g 3.2 g To 1 L

Table 7.3 Table of content of common solutions used for immunohistochemistry

PCR Solutions		
Solutions	Ingredients	
TAE buffer (1x)	dH ₂ O 10x TAE buffer	450 ml 50 ml
Agarose gel (1%)	Agarose 1x TAE buffer Ethidium bromide	1.125 g 112.5 ml 5.6 µl
Agarose gel (2%)	Agarose 1x TAE buffer Ethidium bromide	2.5 g 112.5 ml 5.6 µl

Table.7.4 Table of content of other frequently used solutions.

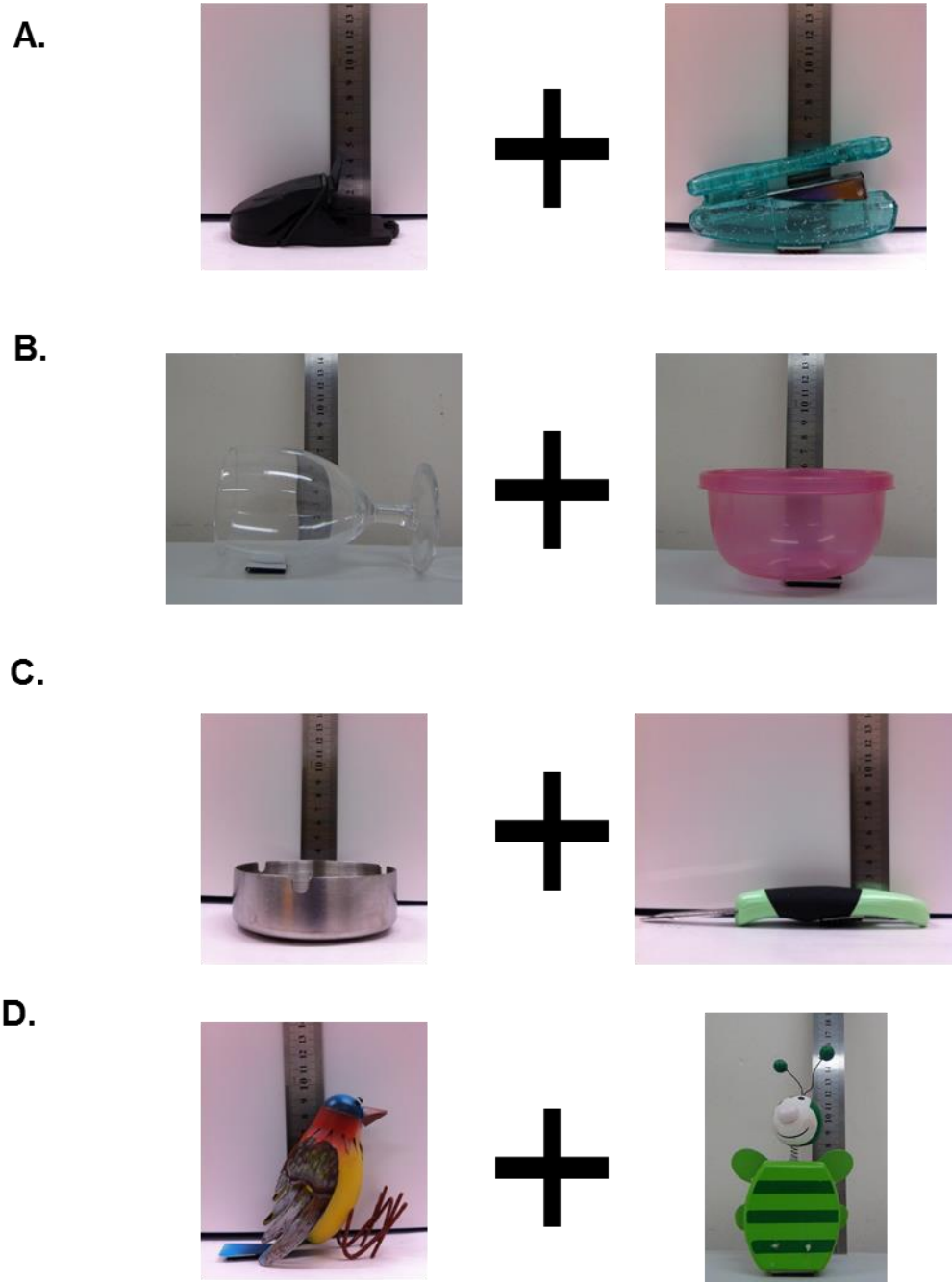
7.2 APPENDIX II – BEHAVIOURAL TASK OBJECTS

Figure 7.1 Pictorial representation and pairing of objects used in behavioural tasks.

Where **A + B** were used for OL tasks and **C + D** were used for NOR tasks. Pictures are provided against the backdrop of a ruler to provide a scaling factor for the objects.

7.3 APPENDIX III – TAQMAN PROBES

NAME	REACTIVITY	CODE
β -Actin	Mouse	4352933E
APP	Mouse	Mm01344172_m1
APP	Human	Hs00169098_m1
Arg1	Mouse	Mm00475988_m1
BACE1	Mouse	Mm00478664_m1
C3	Mouse	Mm00437838_m1
CCL2 (MCP-1)	Mouse	Mm00421242_m1
CCL5 (RANTES)	Mouse	Mm01302427_m1
CCR2	Mouse	Mm00438270_m1
CCR5	Mouse	Mm01963251_s1
EMR1 (F4/80)	Mouse	Mm00802529_m1
IL-1 β	Mouse	Mm00434228_m1
IL-6	Mouse	Mm00446190_m1
MRC1	Mouse	Mm00485148_m1
NOS2 (iNOS)	Mouse	Mm00440488_m1
Nrf2	Mouse	Mm00477786_m1
TNF- α	Mouse	Mm00443260_g1
YM1	Mouse	Mm00657889_mH

Table 7.5 List of RT-PCR TaqMan probes – Prof. M.L.J. Ashford lab

NAME	REACTIVITY	CODE
β -Actin	Mouse	Mm00607939_s1
DUSP1	Mouse	Mm00457274_g1
DUSP2	Mouse	Mm00839675_g1
DUSP4	Mouse	Mm00723761_m1
DUSP5	Mouse	Mm01266104_m1
DUSP6	Mouse	Mm00518185_m1
DUSP7	Mouse	Mm01232570_m1

Table 7.6 List of RT-PCR TaqMan probes – Prof. S.M. Keyse lab

7.4 APPENDIX IV – WESTERN BLOTTING ANTIBODIES

Antibody	Supplier Product ID	Host	MW	Dilution	Blocking Agent
Actin	Sigma Aldrich A2066	Rabbit	42	1:10000	4% BSA
APP (Ab54)	GSK* N/A	Rabbit	~110	1:4000	4% BSA
Akt	Cell Signalling 9272	Rabbit	60	1:1000	4% BSA
BACE1	Sigma Aldrich B0681	Rabbit	60- 75	1:1000	4% BSA
COX IV (G-20)	Santa Cruz Biotechnology sc-69360	Rabbit	17	1:1000	4% BSA
GCLC	Prof. John D. Hayes* N/A	Sheep	73	1:2000	5% milk
GFAP	Millipore AB5541	Chicken	55	1:1000	4% BSA
IκBα (C21)	Santa Cruz Biotechnology Sc-371	Rabbit	35- 41	1:1000	4 % BSA
Mitofusin 1	AbCam ab57602	Mouse	84	1:200	4% BSA
Mitofusin 2	AbCam ab56889	Mouse	86	1:100	4% BSA
ERK1/2 MAPK	Cell Signalling 9102	Rabbit	44, 42	1:2000	4% BSA
p-Akt (Ser473)	Cell Signalling 9271	Rabbit	60	1:1000	4% BSA
p-Akt (Thr308)	Cell Signalling 9275	Rabbit	60	1:1000	4% BSA
p-ERK1/2 MAPK (Thr202/Tyr204)	Cell Signalling 9101	Rabbit	44, 42	1:2000	4% BSA
p-JNK (Thr183/Tyr185)	Cell Signalling 9102	Rabbit	46, 54	1:1000	4% BSA
p-TAU (s396)	Cell Signalling 9632	Mouse	~50- 60	1:1000	4% BSA
JNK	Cell Signalling 9258	Rabbit	46, 54	1:1000	4% BSA

Antibody	Supplier Product ID	Host	MW	Dilution	Blocking Agent
SYP (D-4)	Santa Cruz Biotechnology Sc-17750	Mouse	38- 48	1:2000	4% BSA
TAU-5	Millipore MAB361	Mouse	~50- 60	1:1000	4% BSA
VDAC1	AbCam ab15895	Rabbit	31	1:1000	4% BSA

Table.7.7 List of primary antibodies used for protein elucidation by Western blotting – Prof. M.L.J. Ashford Lab (*denotes gifts)

Antibody	Supplier Product ID	Host	MW	Dilution	Blocking Agent
DUSP4 (S18)	Santa Cruz Sc-1200	Rabbit	43	1:100	5% Milk
DUSP5	In house N/A	Sheep	42	1:2,000	5% BSA
DUSP6	AbCam Ab76310	Rabbit	42/44	1:1,000	5% Milk
DUSP9	In house N/A	Sheep	42	1:2,000	5% Milk
p-MEK (Ser217/221)	Cell Signalling 9154	Rabbit	45	1 ; 1,000	5% BSA
MEK	Cell Signalling 9122	Rabbit	45	1 ; 1,000	5% BSA
β -Tubulin	Sigma T8328	Mouse	51	1:10,000	5% Milk or 5% BSA

Table 7.8 List of primary antibodies used for protein elucidation by Western blotting – Keyse Lab

7.5 APPENDIX V – PRELIMINARY DATA

Preliminary work has been completed with regards to obtaining quantifiable data from the confocal microscopy work performed. Detailed below are the astrocyte cell counts for two regions of the hippocampus as reported by IF with GFAP.

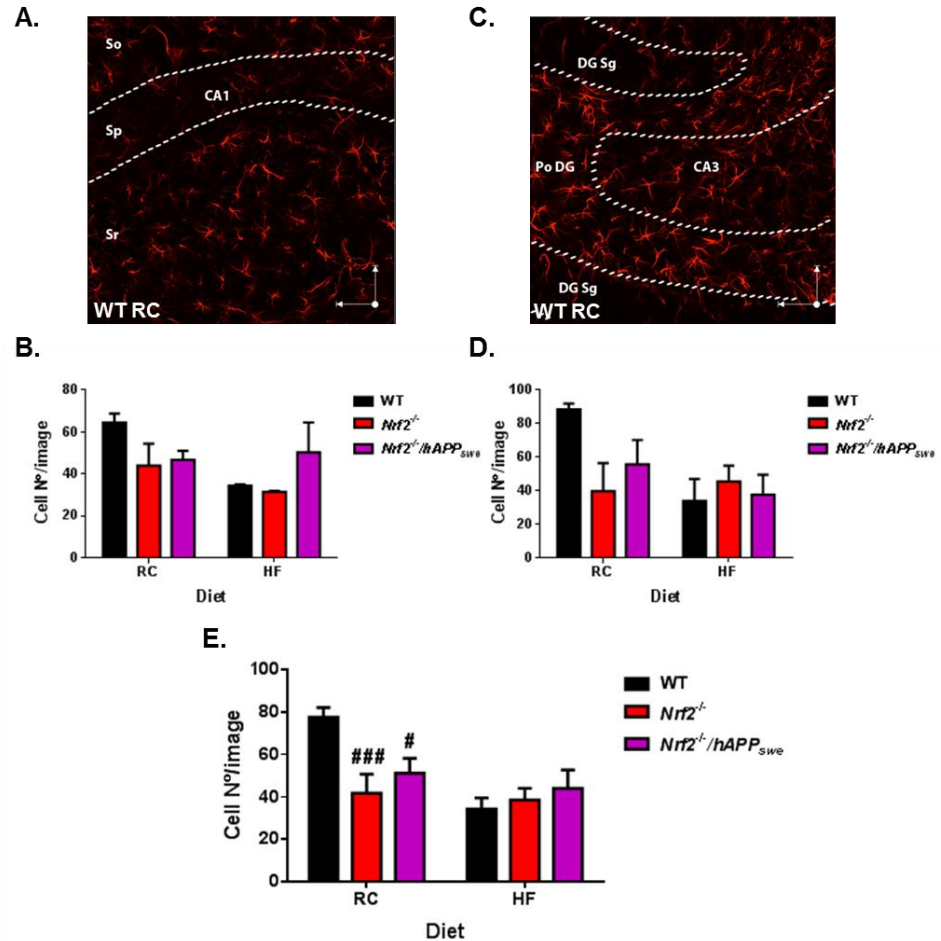


Figure 7.2 Portrayal of changes in astrocyte number resulting from genotype or dietary intervention as depicted by GFAP staining in the hippocampus

All counts were performed on images taken ~0.6 mm from the mid-line of sagittally cut mouse brains with 2-3 animals in each grouping and cell counting was blinded and performed by a summer student (B.M. Pais). The number of cell bodies present within the image stack taken from a 30 μ m brain section was quantified using non-compressed reference files. If branches were seen but the cell body was not included in the slice then the cell was not counted to prevent miscounting of cells from branches that may not have come from the same cell. At this time there are too few numbers to analyse the individual brain regions. Example images from WT mice are provided for the CA1 (A) and CA3/DG (C), with cell counts beneath (B and D respectively). All counts were then combined in (E) to provide a larger overview of astrocyte cell number within the hippocampus and analysed by two-way ANOVA with post hoc Bonferroni. Section numbers CA1: WT = 2-5, *Nrf2*^{-/-} = 2-3, *Nrf2*^{-/-}/*hAPP*_{swe} = 3; CA3/DG: WT = 2-6, *Nrf2*^{-/-} = 2-3, *Nrf2*^{-/-}/*hAPP*_{swe} = 3; CA1 and CA3/DG: WT = 4-11, *Nrf2*^{-/-} = 4-6, *Nrf2*^{-/-}/*hAPP*_{swe} = 6.

